

Dwarf spider species diversity, phylogeny and the evolution of sexually selected traits

Inauguraldissertation
zur
Erlangung des akademischen Grades eines
Doktors der Naturwissenschaften
(Dr. rer. nat.)
der
Mathematisch-Naturwissenschaftlichen Fakultät
der
Universität Greifswald

Vorgelegt von
Shou-Wang Lin

Greifswald, 17.1.2022

Dekan: Prof. Dr. Gerald Kerth

1. Gutachter: Prof. Dr. Gabriele Uhl

2. Gutachter: **Prof. Dr. Dimitar Dimitrov**

Tag der Promotion: **15.07.2022**

Table of contents

Summary	5
1. Introduction	9
1.1. Speciation and species delimitation	9
1.1.1. The origin of species.....	9
1.1.2. How are species delimited?	9
1.1.3. The application of DNA-barcoding in biodiversity studies.....	11
1.2. Sexual selection and speciation	13
1.2.1. Sexual selection.....	13
1.2.2. Effects of sexual selection on speciation.....	14
1.2.3. Sexual dimorphism.....	15
1.2.4. Nuptial gift and gustatory courtship.....	15
1.3. Dwarf spiders as study organism	17
1.3.1. Spider morphology.....	17
1.3.2. Dwarf spider systematics and diversity.....	18
1.3.3. Dwarf spider mating behavior and male prosomal modifications.....	18
1.4. Study aims	20
1.4.1. Complex species history: the case of the dwarf spider genus <i>Shaanxinus</i>	20
1.4.2. Evolution of dwarf spider gustatory-courtship-related prosomal structures.....	21
1.4.3. Evolution of gustatory-courtship-related glandular tissue.....	23
2. References	25
3. Manuscripts	37
2.1. Contribution to manuscripts.....	37
2.2. Taxonomic revision of the dwarf spider genus <i>Shaanxinus</i> Tanasevitch, 2006 (Araneae, Linyphiidae, Erigoninae), with new species from Taiwan and Vietnam (published in <i>Organism Diversity & Evolution</i> , 2019, 19: 211-276)	39

2.3. Evolution of nuptial-gift-related male prosomal structures: taxonomic revision and cladistic analysis of the genus <i>Oedothorax</i> Bertkau, 1883 (Araneae, Linyphiidae, Erigoninae) (published in Zoological Journal of the Linnean Society, 2021, XX: 1-168).....	107
2.4. Diversification through sexual selection on gustatory courtship traits in dwarf spiders (published in Frontiers of Zoology, 2021, 18: 51)	277
4. Eigenständigkeitserklärung.....	313
5. Curriculum Vitae.....	315
6. Other scientific contributions.....	317
7. Acknowledgements.....	319

Summary

Species are the basic units of evolution and biodiversity, and the process of speciation has been one of the most important questions in biology. The evolution of species with common descent is considered to be mainly driven by natural and sexual selection. The material basis and mechanical cause of organismic evolution were recognized during the formation of the modern synthesis of the evolutionary theory in the early 20th century, providing the framework for speciation studies. During this period, the biological species concept was developed in the frame of population genetics, putting emphasis on the reproductive isolation between populations. The phylogenetic species concept developed in the 1980s, on the other hand, does not make any particular assumption about evolutionary or speciation processes. It defines species via their unique combination of character states which are compatible with phylogenetic practices. However, the aforementioned two species concepts are difficult to apply in alpha-taxonomy, where newly discovered species are largely described by the morphological (typological) species concept for practical reasons. Nevertheless, the description of morphological species provides the basis for further assessments of species delimitation via other species concepts and approaches. One of the tools for assisting the identification and discovery of animal species is DNA barcoding, which uses a standard region of mitochondrial DNA sequence as a universal DNA barcode. However, its assumption of intraspecific genetic distances being smaller than interspecific genetic distances does not always hold. Species-level poly-/paraphyly is prevalent due to the discrepancy between the phylogenies of mitochondrial DNA and species. This suggests that the application of DNA barcodes must be combined with an integrative taxonomic approach. Beside the application as a tool for assisting species identification, the information from mitochondrial DNA sequences opens up a window for looking into the complex history of species.

Sexual selection is a potential mechanism driving the evolution of species. It favors traits that increase mating probability and mating success. It can result from intrasexual competition, female preference or sexual conflict. However, previous comparative studies using the degree of sexual dimorphism as a proxy for the strength of sexual selection have yielded inconsistent results as to the relationship between sexual selection and species richness. A possible cause of the inferred low association are factors other than sexual selection, which can also lead to the evolution of sexual dimorphism, such as selection for increased female fecundity. In order to assess the effect of sexual selection on speciation, the lability and evolvability of traits need to be studied that are clearly under sexual selection.

The aim of this thesis is to improve the knowledge about dwarf spider (Erigoninae, Linyphiidae) diversity and taxonomy, and to assess the evolutionary patterns of dimorphic traits that are under sexual selection. I focused on the abundant and diverse male prosomal modifications in dwarf spiders that are linked to the transfer of secretions from the male to the female during courtship and mating (gustatory courtship). This approach explores the process of speciation and the role of sexual selection on species diversification. I described new erigonine species and revised the classification of known species based on phylogenetic analyses. I also applied X-ray micro-computed tomography (micro-CT) to investigate the distribution and evolutionary pattern of the gustatory glands to tease apart the evolution of prosomal shape and glandular equipment.

This cumulative thesis consists of three publications:

Publication 1: This publication aimed at contributing to the knowledge of erigonine diversity. The genus *Shaanxinus* previously contained only two species from China. I collected dwarf spiders from multiple locations in Taiwan from above-ground vegetations with a seldom applied collecting method. Inspection of the collected material resulted in the discovery of 13 *Shaanxinus* species. An additional species from Vietnam was described from a museum collection. I provided a revision of the genus *Shaanxinus*. A phylogenetic analysis using morphological characters was conducted for determining the possible generic synapomorphies. I also reconstructed the glandular distribution associated with male prosomal modifications, as well as the detailed structure of a male secondary sexual organ (pedipalp) by micro-CT. Furthermore, I conducted phylogenetic analyses based on sequences from two mitochondrial and one nuclear loci, and assessed the efficacy of different criteria in species identification using DNA barcoding. Distinction of morphologically similar species have been assisted by molecular data. The species level poly-/paraphyly found in mitochondrial DNA sequences caused the low efficacy of many distance- and tree-based species identification methods, while the nearest neighbor method showed high identification success. The non-monophyly is likely caused by instances of interspecific hybridization and recent parapatric speciation. The genus *Shaanxinus* thus lends itself as an ideal group for congeneric phylogeographic studies addressing the interactions between closely related species.

Published in: Lin, S.-W., Lopardo, L., Haase, M. & Uhl, G. 2019. Taxonomic revision of the dwarf spider genus *Shaanxinus* Tanasevitch, 2006 (Araneae, Linyphiidae, Erigoninae), with new species from Taiwan and Vietnam. *Organism Diversity & Evolution*, 19, 211-276.

Publication 2: Sexually dimorphic prosomal modifications that are related to gustatory courtship occur in many dwarf spider species. These features evolved in the context of sexual selection, which has a potential effect on species diversification. In

contrast to many erigonine genera which present little variability in male prosomal traits, the genus *Oedothorax* presents higher diversity in male prosomal structures among species not only in the position and shapes of the modifications, but also in the degree of modification, ranging from absent to highly elaborated. This genus thus lends itself as a suitable target group for studying the effect of gustatory-courtship-related traits on species diversification. I conducted a revision of the 82 species previously belonging to this genus. Based on the result of a phylogenetic analysis, this genus was re-delimited with 10 species as *Oedothorax sensu stricto*, while taxonomic decisions were made for other species including synonymization with species from other genera and transferring species to other existing and newly defined genera. 25 species were deemed as “*Oedothorax*” *incertae sedis*. The reconstruction of character state evolution suggested multiple origins of specific prosomal modification types. Convergent evolution of these traits among different lineages suggests that sexual selection has played an important role in the species diversification of dwarf spiders.

Published in: Lin, S.-W., Lopardo, L. & Uhl, G. 2021. Evolution of nuptial-gift-related male prosomal structures: taxonomic revision and cladistic analysis of the genus *Oedothorax* (Araneae: Linyphiidae: Erigoninae). *Zoological Journal of the Linnean Society*, XX, 1-168.

Publication 3: Although sexually dimorphic traits have inspired the concept of sexual selection as the driving force of their evolution, they might also have evolved due to other ecological factors. These factors include the sexual signal adaptation to the environment as well as sexual differences in ecological relations and parental investment. In contrast, the gustatory courtship in dwarf spiders is associated with sexually dimorphic male prosomal modifications, which have clearly evolved in the context of sexual selection. Multiple origins of various external prosomal modifications have been shown in erigonine phylogeny, but the evolutionary pattern of the associated glands has not been investigated. Our phylogenetic analysis incorporated the characters related to the glandular distribution in the male prosoma as well as the external shapes yielded from X-ray micro-computed-tomography showed a single origin of gland among the investigated erigonine taxa. The internal anatomy revealed previously undetected trait lability in attachments of muscles to the cuticular structures, as well as the presence/absence and differences in glandular distribution even in species without external modification. Our finding further supports that erigonine male prosomal traits are under divergent selection, and corroborates the argument that erigonines are a suitable group for investigating the effect of sexual selection on speciation.

Published in: Lin, S.-W., Lopardo, L. & Uhl, G. 2021. Diversification through gustatory courtship: an X-ray micro-computed tomography study on dwarf spiders. *Frontiers in Zoology*, 18: 51.

The results of this thesis corroborate the importance of applying phylogenetic methods and an integrative approach in the description of new species, as well as in revising taxa which might not be monophyletic. Overall, the studies contributed to a more comprehensive knowledge about erigonine species diversity, phylogeny and the possible diversifying effect of sexual selection on male traits associated with gustatory courtship.

1. Introduction

1.1. Speciation and species delimitation

1.1.1. *The origin of species*

The magnificent diversity in the organismal world and the discrepancy in species numbers between different taxa have stimulated questions about the underlying processes, which have led to the current patterns of species diversity. Inspired by the relatedness between the geographical distributions of fossil and modern species, as well as the distributional pattern of extant species, Darwin conceived a genealogical tree of a single origin (Darwin 1859, p.116/117). He proposed the concept of natural selection on heritable variations among individuals of the same species, which has led to the evolution of novel species. While natural selection is used to explain how the morphological and ecological divergence of populations occurred as they adapt to local ecological conditions, Darwin (1871) proposed sexual selection as the driving force of the evolution of sexually dimorphic features such as lion's manes and the plumage of some male birds. However, since the genetic basis of heritability and reproductive isolation had not been developed at Darwin's time, his theory could not be tested. In the early 20th century, biologists have started to show how Mendelian genetics is consistent with evolution driven by natural selection (Bateson 1902; Fisher 1919; Haldane 1932; Wright 1931; Yule 1902). Subsequently, theories about the material basis of evolution and the mechanical causes of evolutionary change were further developed starting in the 1930s, provided a framework for studying speciation. This reconciliation of Darwin's theory of evolution and Mendelian genetics was coined by Huxley (1942) as the modern synthesis of evolution, represented by the work of Dobzhansky (1937, 1951) and Mayr (1942). The biological species concept of Mayr and Dobzhansky defined species as interbreeding populations that are reproductively isolated from other such populations. Although different classifications of modes of speciation have been proposed, they are generally based on three main sets of variables: 1) genetic mechanisms generating genetic variability, 2) genetic isolating mechanisms leading to reproductive isolation, and 3) geographic barrier ranging from complete (allopatry) to absent (sympatry) (Singh 2012; White 1978).

1.1.2. *How are species delimited?*

Before Darwin, the ways of classifying kinds of organisms can be regarded as typological or essentialistic. Linnaeus (1707-1778), the founder of the principle of binomial nomenclature, thought that species reflect the existence of fixed, unchangeable type (essence); nearly all of the older definitions of the species, like those applied by Buffon, Lamarck and Cuvier, refer to the morphological similarities shared by conspecific

individuals (Singh 2012; Zachos 2016). It was Mayr and Dobzhansky who clearly formulated the biological species concept, emphasizing the aspect of reproductive isolation (Dobzhansky 1937; Mayr 1942). Although the biological species concept is most widely accepted, there are certain empirical difficulties in its application. For instance, since species delimitation under this concept relies on whether individuals from different populations can produce viable offspring, the concept is not applicable to museum specimens or organisms reproducing non-biparentally. Furthermore, the biological species concept is difficult to apply in situations where incipient speciation takes place and complete reproductive barriers do not occur. When populations have a complete allopatric pattern of distribution, the biological species concept becomes impractical (Cronquist 1978; Stace 1989). Taxonomists face numerous difficulties for such cases of ambiguous phases with gene flow. This spatial-temporal limitation of the biological species concept has been explained by Mayr (1982) that this concept applies when populations belonging to different species occur sympatrically at the same time; its function is to determine the status of co-existing individuals and populations.

Alpha-taxonomy (Mayr et al. 1953) stands for the process of species discovery, description and naming (Luc et al. 2010). In its practice, an approach close to the morphological species concept is usually applied, which defines species as “a community, or a number of related communities, whose distinctive morphological characters are, in the opinion of a competent systematist, sufficiently definite to entitle it, or them, to a specific name” (Regan 1926). Since the vast majority of species have been described from museum collections, the biological species concept cannot be applied (Wheeler 1999). Within the biodiversity knowledge system, the morphological species concept has its utility in general public education and the broad scientific community (Mayo et al. 2008).

The biological species concept emphasizes the process leading to reproductive isolation and is thus restricted to sympatric, sexually reproducing populations. Proponents of the phylogenetic species concept, on the other hand, argue that we do not need to know or understand the speciation process in order to recognize species; instead, they advocate recognizing species based on patterns of character state distributions (Nelson and Platnick 1981; Wheeler 1999). The phylogenetic species concept, which is consistent with phylogenetic theory, but independent of phylogenetic analysis, was developed independently by Eldredge and Cracraft (1980) and Nelson and Platnick (1981). The definition of the phylogenetic species concept is “the smallest aggregation of (sexual) populations or (asexual) lineages diagnosable by a unique combination of character states” (Wheeler and Platnick 2000). Therefore, it can be applied to asexual and allopatric populations.

Both the phylogenetic and the morphological species concepts use a set of characteristics for defining and diagnosing species. The difference between the two concepts is that in phylogenetic species concept, the character states are hypotheses of homology, which can be subject to scrutiny by phylogenetic analysis, while the unique set of diagnostic characteristics by morphological species concept is based on subjective opinions of specialists. However, the subjectivity in alpha-taxonomy is inevitable, since it is a process of building initial empirical hypotheses from an easily observed set of characteristics (Mayo et al. 2008). During this process little is known about homologies. The arbitrary property of any alpha-species concept can lead to a more substantial theory with increasing evidence such as geography, ecology and genetics (Hennig 1966; Lipscomb et al. 2003), as exemplified by the morphological species delimitation of *Shaanxinus* dwarf spiders refined by DNA sequence data (Lin et al. 2019, publication 1 of this thesis). The diagnostic characteristics and generic affinity of species originally determined in alpha-taxonomy can be reassessed via a phylogenetic analysis with a more thorough sampling of intra- and intergeneric variation, making them compatible with the phylogenetic species concept, as exemplified by the revision of the dwarf spider genus *Oedothorax* (Lin et al. 2021, publication 2 of this thesis). This improvement of the knowledge about genealogical relationships among species is crucial for comparative studies aiming at answering questions about patterns in evolution.

In summary, under the unified theory of common descent of species, different species concepts with their epistemologies have their limits, as well as their utilities in different phases and aspects in the pursuit of understanding the patterns of biodiversity. The morphological species concept, as the first step in the exploration of natural kinds, provides knowledge about variations among organisms. This knowledge forms the basis for scrutiny by the phylogenetic species concept to determine the set of defining characters of species compatible with phylogenetics. The biological species concept, on the other hand, aids in answering questions about the species status of sympatric populations that are difficult to be diagnosed morphologically.

1.1.3. The application of DNA-barcoding in biodiversity studies

A standard region of the mitochondrial cytochrome c oxidase (COI) gene has been proposed as an universal “barcode” sequence for global bioidentification system for animals (Hebert et al. 2003). This locus has been shown to generally have interspecific variation exceeding intraspecific variation by one order of magnitude. This thus allows establishing a “barcode gap” for distance-based approaches, or showing reciprocal monophyletic pattern when applying tree-based methods (Barrett and Hebert 2005; Hebert, Stoeckle, et al. 2004). Based on this assumption, the development of a comprehensive DNA barcode database was intended for 1) assigning unknown individuals to species

(Hebert et al. 2003), and 2) enhancing discovery of morphologically cryptic species (Hebert et al. 2004; Mutanen et al. 2012; Smith et al. 2006).

Despite the momentum DNA barcoding has gained among biodiversity research community, evidence from studies on closely related species and sampling of larger geographical scale showed large overlap between intra- and interspecific divergences (Johnson and Cicero 2004; Lin et al. 2019, publication 1 of this thesis; Wiemers and Fiedler 2007) and thus a lack of a barcode gap. Surveys of animal studies have demonstrated high proportions of animal species showing para- or polyphyletic patterns in their mitochondrial sequences, which amounted to 23% in Funk and Omland (2003) and 19% in Ross (2014). This deviation from the premise of using DNA barcode to assist species identification and to improve taxonomic work is largely due to the discrepancy between the evolutionary history of the species and that of mitochondrial DNA (mtDNA), which can cause significant bias when inferring demographic properties of populations and interspecific relationships (Ballard and Whitlock 2004).

The prevalent species-level poly-/paraphyly inferred from mtDNA can be caused by imperfect taxonomy, inadequate phylogenetic information, as well as introgression and incomplete lineage sorting (Funk and Omland 2003). The latter two are influenced by the biology of mtDNA, which is substantially different from the nuclear genome, and this essentially affects its evolutionary pattern. Compared to the nuclear genome, the mitochondrial genome is much smaller, haploid, maternally inherited in most animals, with low to no recombination, etc. (Scheffler 1999). Since animal mtDNA is a single chromatid which does not usually undergo recombination, selection on one part of the chromatid directly affects the spread of other parts of the chromatid in the population (Birky 2001). Due to the maternal inheritance of its haploid genome, the effective population size of mtDNA is about one-quarter of that of the nuclear DNA. Assuming no other influencing factors, lineage sorting by drift is expected to progress more rapidly for mtDNA. Therefore, Incomplete lineage sorting is less likely a cause of species-level para-/polyphyly for mitochondrial than for nuclear loci, except for species that have diverged recently. On the other hand, in case of introgression of heterospecific loci, since mtDNA is a single molecule with low or no recombination, and the lineage sorting is completed more rapidly, a heterospecific mtDNA haplotype has a higher probability to fix after its introgression into the population/species, resulting in the observed species-level para-/polyphyly. Therefore, as a means for species identification and delimitation, DNA barcoding needs to be combined with morphological observation and/or nuclear sequences (Dupuis et al. 2012; Yassin et al. 2010). Since the reduction of costs of sequencing a large number of nuclear markers is a continuing trend, several studies have assessed the application of a nuclear multimarker system for DNA taxonomy across a wide range of animal species (Ješovnik

et al. 2017; Liu et al. 2017; Zarza et al. 2018). Recently, a set of nearly universal single-copy nuclear protein-coding genes have been proposed as standardized nuclear markers in animal DNA taxonomy (Eberle et al. 2020), which has the potential to replace the use of mitochondrial COI gene. On the other hand, mtDNA sequence provides a tool for looking into the complex evolutionary history of closely related species (Monaghan et al. 2006). For this purpose, sequence data of multiple individuals of each of the closely related species need to be acquired at a larger geographical scale. This combination of the sampling conventions of phylogenetics and phylogeography was proposed by Funk and Omland (2003) as congeneric phylogeography. I demonstrated the utility of this concept in the description of closely related dwarf spider species in the genus *Shaanxinus* (Lin et al. 2019, publication 1 of this thesis).

1.2. Sexual selection and speciation

1.2.1. Sexual selection

The concept of sexual selection was introduced by Darwin (1859, p. 116-118) to explain certain aspects of animal reproductive biology that could not be explained by natural selection. While traits that enhance the survival of individuals are supported by natural selection, sexual selection favors traits that increase mating probability and mating success (Darwin 1871). In many cases, natural and sexual selection can operate in the same direction, when individuals adapted to certain environmental circumstances are able to produce the highest number of offspring. However, many traits that are advantageous under sexual selection have deleterious effect under natural selection. Most such costly traits are found in the so-called male secondary sexual traits, which are not directly connected with the act of reproduction, although the distinction between primary and secondary sexual traits can be difficult in some cases (Darwin 1871, p. 112). These traits, like the elaborate weapons and ornaments mostly found in males (Emlen 2008), often reduce the survival probability of the trait bearer. Selection on these traits originates from the reduced investment in gametes and parental care by males, which increases their potential rate of reproduction (Clutton-Brock and Parker 1992). This results in higher numbers of ready-to-mate males related to receptive females at any given time (the operational sex ratio) (Emlen and Oring 1977). The biased operational sex ratios lead to increased intrasexual competition, higher variance in reproductive success and stronger selection for competitive ability in males than in females (Clutton-Brock 2007). Since females invest more in their gametes, female choice on male traits that display their quality as breeding partners is more obvious and prevalent (Tregenza and Wedell 2000). On the other hand, when the selective optima of male and female traits are not reached simultaneously, sexual conflict can occur (Parker 2006). While a monogamous mating

system results in low level of conflict, any deviation from monogamy increases the potential of sexual conflict (Hosken et al. 2001). Such intersexual conflict of interest may lead to antagonistic coevolution between males and females, generating evolutionary divergence of traits involved in reproduction and possibly promoting speciation (Arnqvist et al. 2000).

1.2.2. Effects of sexual selection on speciation

Sexual selection has long been thought to drive speciation (Darwin 1871; Panhuis et al. 2001; Ritchie 2007; West-Eberhard 1983) since the preferences of females for differences in secondary male sexual traits between populations have the potential to result in reproductive isolation (Servedio and Boughman 2017). Among allopatric populations, independent episodes of male-female coevolution under sexual selection may result in divergence of traits in both males and females (Lande 1981). This intersexual coevolution can be caused either by female choice on male traits, or by male manipulation of the female and female counteradaptations (Andersson and Simmons 2006). Several studies suggested divergent male-female coevolution in sexually selected traits in animals, including the courtship signals of jumping spiders (Masta and Maddison 2002), the bower architectures in bowerbirds (Uy and Borgia 2000) and the mating calls of Amazonian frogs (Boul et al. 2007). However, disagreements exist around whether sexual selection can be the sole cause of reproductive isolation, or whether it mostly acts alongside or in the shadow of natural selection (Ritchie 2007; Safran et al. 2013; Servedio and Boughman 2017). Divergence in sexual traits and preferences are often driven by ecological factors, like the divergent evolution of nuptial coloration of male cichlid fish under different underwater light conditions (Allender et al. 2003), and the vibrational signal divergence in treehoppers associated with host plant shift (McNett and Cocroft 2008).

Comparative studies that correlate estimates of sexual selection and species richness by controlling for phylogenetic relatedness do not generally support the supposed association (Ritchie, 2007). In the meta-analysis of Kraaijeveld et al. (2011), a small but significant overall correlation between sexual selection and speciation rate was found, but the divergent effect of sexual selection was strongly dependent on methodological choices and chosen proxies. 40 among the 64 studies reviewed in the meta-analysis by Kraaijeveld et al. (2011) used various kinds of sexual dimorphism as the proxy for the strength of sexual selection, with inconsistent results. Among the reviewed studies by Kraaijeveld et al. (2011), the meta-analysis by Gage et al. (2002) on mammals, butterflies and spiders focusing on sexually dimorphic body size showed no correlation between the degree of sexual dimorphism and the variance in species richness. This might be due to the fact that the evolution of sexual dimorphism is not strongly driven by sexual selection, but by ecological factors (see the next section). For assessing the impact of sexual selection on speciation, traits are required that are under sexual selection with little effect of various

other sources of selection in generating trait diversity (Kraaijeveld et al. 2011). Such sexual selection-based trait lability (Badyaev and Hill 2000; Cardoso and Mota 2008) in sexual traits and mate selectivity are needed for assessing the effect of sexual selection on speciation (Kraaijeveld et al. 2011).

1.2.3. Sexual dimorphism

The abundant diversity of the secondary sexual characters in the animal world has been the primary inspiration for Darwin's hypothesis of sexual selection (Darwin 1859, 1871). These dimorphic traits come in the form of coloration, ornamentation, behavior, size and shape (Berns 2013). Examples of sexually dimorphic male traits evolved under mate choice or intrasexual competition include the enlarged mandibles of stag beetles (Mathieu 1969), the feather ornaments of peacocks (Loyau et al. 2005), the antlers of deer (Goss 1983), and the male prosomal modifications of the dwarf spiders (Lin et al. 2021, publication 2 of this thesis). Alternatively, sexual dimorphism may also have evolved from niche divergence between sexes (Shine 1989) or reproductive role division (Hedrick and Temeles 1989). An example of niche divergence is the larger posterior salivary glands in male octopod *Eledonella pygmaea* due to intersexual vertical habitat partitioning in the water column (Voight 1995); an example of reproductive role division is the female gigantism in many orb-weaving spiders selected for increased fecundity (Head 1995; Hormiga et al. 2000).

1.2.4. Nuptial gift and gustatory courtship

The behavior of transferring non-gametic materials from males to females during courtship and mating occurs in various species across the animal kingdom, including birds, insects, amphibians, crustaceans etc. (Andersson 1994; Lewis et al. 2011; Mann 1984; Vahed 1998, 2007). This nuptial-gift-giving behavior usually increases the donor's reproductive success (Brockmann 2012; Lewis et al. 2011; Lewis and South 2012). The transferred material can consist of objects collected by males (exogenous) or produced by males (endogenous) (e.g., dead insects collected by male scorpionflies or secretions from their enlarged salivary glands, respectively) (Liu and Hua 2010; Thornhill 1976). Nuptial gifts are taken up by females orally or transferred into females' reproductive tracts along with the sperms. They increase a male's chance to mate, prolong copulation time, or result in larger amounts of sperm transferred. This can result in a higher paternity share when females are polyandrous, as was established in studies on insects, in which the nuptial gift types and mechanisms are most diverse (Gwynne 2008; Lewis et al. 2011; Vahed 1998). When the transferred substances contain nutrients, they can increase the longevity and egg production of females, and thus improve the lifetime reproductive success of both the females and the males (Lewis and South 2012).

In spiders, exogenous nuptial gifts have been observed in Pisauridae and Trechaleidae, in which prey wrapped in silk are transferred by the males to the females during courtship (Costa-Schmidt et al. 2008; Stålhandske 2001; van Hasselt 1884). More common in spiders are the endogenous gifts, which are composed of glandular products released from the male prosomal region and taken up by the female during courtship and mating (Austad 1984). This so-called gustatory courtship has been found in some cobweb spiders (Theridiidae, e.g. Vollrath 1977; Knoflach 2004), in one daddy-long-legs spider species (Pholcidae, Huber and Eberhard 1997) and in the dwarf spiders (Linyphiidae, Erigoninae), which seem to have the highest diversity both in species having gustatory courtship and the male morphology related to this behavior (Hormiga et al. 2000; Kunz et al. 2012; Uhl and Maelfait 2008; Vanacker, et al. 2003). These male modifications include elevations, grooves and lateral pits in various prosomal regions with diverse morphologies (Fig. 1). Considering the scattered occurrence of gustatory courtship among spider families, it has most likely evolved several times independently under sexual selection (e.g., Arnedo et al. 2009; Kunz et al. 2012; Michalik and Uhl 2011; Uhl and Maelfait 2008). By studying the distribution of these traits in erigonine phylogeny, we may gain insights into how gustatory courtship and its associated features may have evolved.

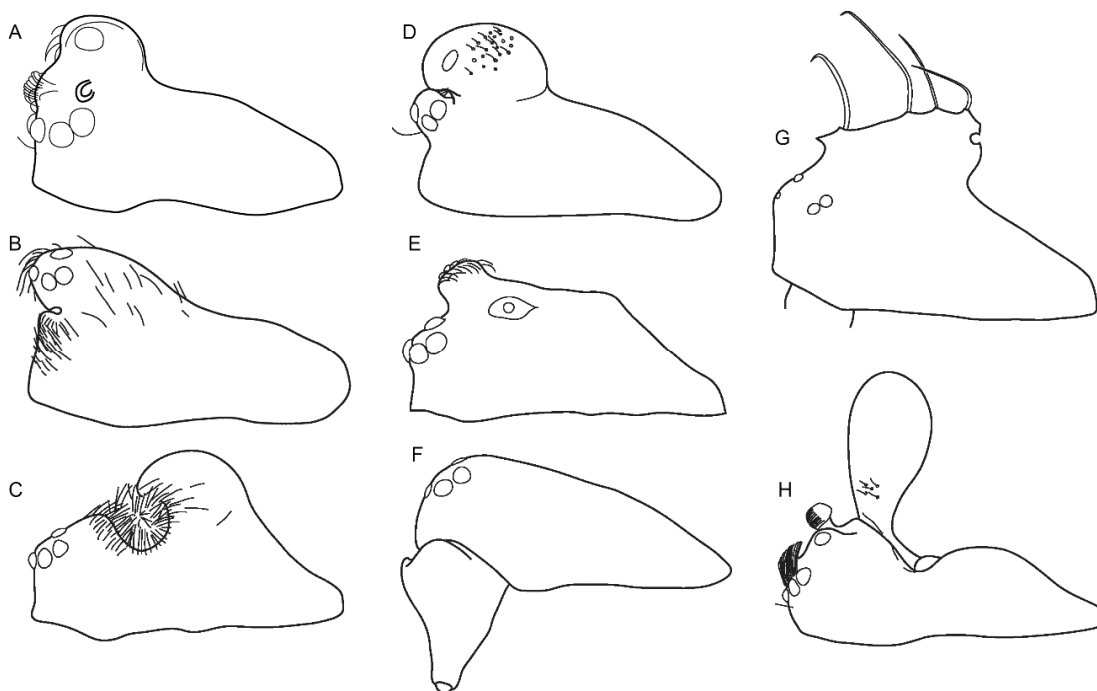


Fig. 1 Lateral view of prosomata of male dwarf spiders (Erigoninae) with prosomal modifications (extracted from Lin et. al. 2021, publication 2 of this thesis). A. *Atypena cirrifrons*. B. *Shaanxinus mingchihensis*. C. *Oedothorax gibbosus*. D. *Callitrichia convector*. E. *O. apicatus*. F. *Mitragrer clypeellum*. G. *Nasoona setifera*. H. *M. noordami*.

1.3. Dwarf spiders as study organism

1.3.1. Spider morphology

Spiders belong to the class Arachnida, and are a monophyletic group based on synapomorphies like cheliceral fangs with venom glands, silk glands and modified male pedipalps for sperm transfer (Coddington and Levi 1991). The spider body is tagmatized into two main regions: the anterior prosoma and the posterior opisthosoma that are connected via the pedicel (Foelix 2011, p. 3). The prosoma has the primary functions of feeding (chelicerae and venom glands) and locomotion (four pairs of walking legs), and contains the central nervous system. The pair of appendages following the chelicerae are the pedipalps (Figs. 3A, B, C). Their primary function is inspecting the environment or prey (Foelix 2011, p. 24). The pedipalps in male spiders are modified into secondary sperm transfer organs. For charging the pedipalps with sperm, the male builds a small horizontal web, deposits a sperm drop from the testes onto it, and then takes up the sperm droplet from the emboli (intromittent organs) into the storage compartments (spermophores) inside the pedipalps; the spermophore is located inside the genital bulb, a modified structure of the terminal part of the pedipalp (Foelix 2011, pp. 226, 227). The opisthosoma contains the organs for respiration, digestion, excretion, reproduction, as well as the spinnerets and silk glands for silk production (Foelix 2011, p. 3). In the Entelegynae spiders, which includes the dwarf spiders, female possess a copulatory organ called epigyne, which is located in front of the genital opening, which is in turn in the middle of the epigastric furrow. This slightly raised plate has cuticular infoldings that form the copulatory ducts and the spermathecae (seminal receptacle) (Figs. 3B, D) (Foelix 2011, p. 230).

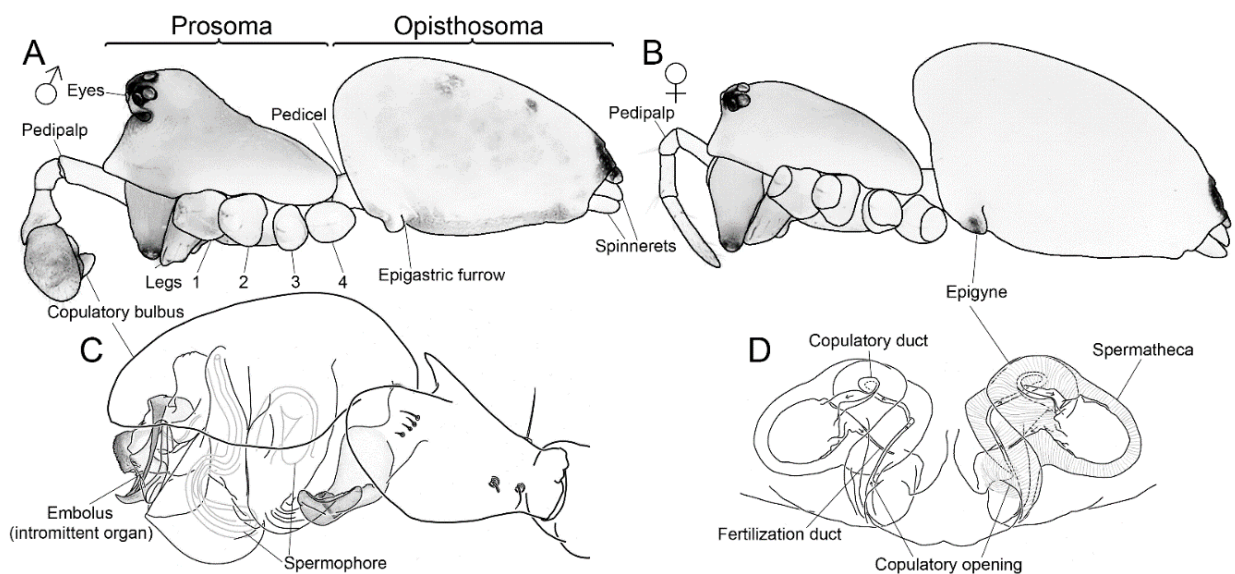


Fig. 3. Spider morphology, with *Shaanxinus shoukaensis* Lin, 2019 as an example. A, B, Lateral view, with the left pedipalp and legs removed at the coxa-trochanter joint. A. Male. B. Female. C. Male copulatory bulb. D. Female genital organ (epigyne). Drawings modified from Lin et al. 2019.

1.3.2. Dwarf spider systematics and diversity

Erigoninae, also called dwarf spiders (over 2600 species, Tanasevitch 2021), is the largest subfamily in Linyphiidae, which in turn is the second most speciose spider family after the jumping spiders (Salticidae) (World Spider Catalog 2021). Currently, the Linyphiidae comprises over 4600 described species in 624 genera (World Spider Catalog 2021), which are classified either into four (Stemonyphantinae, Mynogleninae, Erigoninae, and Linyphiinae, Frick and Scharff 2014) or seven subfamilies (the latter four plus Micronetinae, Dubiaraneinae and Ipaina, Tanasevitch, 2021). The number of described linyphiid species shows a geographical distribution concentrated in the Palaearctic (2549 spp.) and Nearctic (967 spp.) region, while the number of described species in the tropical regions is low (Oriental: 204 spp.; Afrotropical: 423 spp.; Neotropical: 578 spp.) (Tanasevitch 2021). This pattern suggests that tropical regions are generally understudied, where more collecting effort is required for the linyphiid diversity research.

Among the linyphiid subfamilies, prosomal modifications occur in both sexes of a few linyphiines (*Bathyphantes*, *Diplostyla* and *Vesicapalpus*, Hormiga 1999, 2000), both sexes of all mynoglenines (Frick and Scharff 2014) and many erigonine males (e.g., Hormiga 2000). Given the current phylogenetic inference of this family, these modifications have originated independently in each of these subfamilies (Hormiga 2000; Miller and Hormiga 2004; Arnedo et al. 2009). Erigonines (1-3 mm in length) mostly build sheet webs in the leaf litter (Hormiga 2000). They show a rich diversity of sexually dimorphic prosomal modifications. The monophyly of erigonines has been recovered by morphological phylogenetic analyses (Hormiga 2000; Miller and Hormiga 2004) and the higher-level molecular phylogenetic analysis of Linyphiidae by Arnedo et al. (2009). However, the latest analyses based on Arnedo et al. (2009) with increased taxon sampling (Wang et al. 2015; Bao et al. 2017) showed some micronetines nested within the erigonines, resulting in the polyphyly of the latter.

1.3.3. Dwarf spider mating behavior and male prosomal modifications

Like other species in the family Linyphiidae, erigonines build horizontal webs and live on the underside of the web. Courtship and mating take place under the females' web. The typical erigonine male courtship behavior includes moving up and down the palps at the coxal joint, trembling of the first one or two pairs of legs, quivering of the opisthosoma and plucking on the female's web (Bristowe 1931; Kunz et al. 2012; Schlegelmilch 1974). A receptive female turns towards the male. The mating position is antiparallel with the ventral side facing upwards (von Helversen 1976). In most cases of mating behavior observations on species with prosomal modification, the female mouthparts are in contact with or sink into the male prosomal structures (Bristowe 1931; Schlegelmilch 1974; Vanacker et al.

2003; Uhl and Maelfait 2008; Kunz et al. 2012). The female often releases saliva onto the area and reingests it (Kunz et al. 2012, 2013). Behavioral experiments demonstrated that the secretion produced in the prosomal region functions as mating effort through gustatory courtship. Females take up the secretion during mating and are reluctant to mate when no gift is offered (Kunz et al. 2013). The secretion was also shown to affect female fecundity (Uhl and Maelfait 2008; Kunz et al. 2012). In mating position, the male inserts the embolus into one of the two female copulatory openings (Kunz et al. 2012). Copulation can consist of one insertion (with one pedipalp) or two sequential insertions (with both pedipalps) (Kunz et al. 2015; Schlegelmilch 1974). In some species like *Oedothorax retusus* (Westring, 1851), the male produces an amorphous mating plug that covers the female copulatory opening and thereby prevents the female from remating (Uhl and Busch 2009).

Male dwarf spiders show a high diversity of structures on the dorsal and frontal surface of the prosoma (e.g., Hormiga 2000; Lin et al. 2021, publication 2 of this thesis). These modifications include grooves, humps, lobes, a pair of pits (deep invaginations of the cuticle), modified setae and peculiar slender spires, located from the clypeus (the region below the eyes) to the region behind the eyes (Hormiga 2000; Lin et al. 2021, publication 2 of this thesis; Miller 2007; Wiehle 1960). Among the 411 genera currently assigned to erigonines (Tanasevitch 2021), over half of the genera contain species showing sexually dimorphic prosomal features (Lin et al. 2021, publication 2 of this thesis). The variability of these structures strongly differs among genera. For example, there is low variability in *Shaanxinus* Tanasevitch, 2006 (Lin et al. 2019, publication 1 of this thesis), and high variability in *Oedothorax* Bertkau, Förster & Bertkau, 1883, (Wunderlich 1974, Tanasevitch 1998 and 2015). Glandular tissues have been found associated with prosomal structures in almost all histologically examined species (Blest and Taylor 1977; Lin et al. 2019, publication 1 of this thesis; Lopez 1976; Lopez and Emerit 1981; Michalik and Uhl 2011; Schaible et al. 1986; Schaible and Gack 1987). An exception is *Erigone*, which has prosomal modification but no glands and no prosomal contact with the female during copulation. Given the functions of the prosomal secretions during copulation and mating, the diverse prosomal modifications in erigonines strongly suggest evolution under sexual selection (Vanacker et al. 2003).

1.4. Study aims

Erigoninae is a specious group expressing high diversity in their gustatory-courtship-related prosomal modifications. This makes them suitable for addressing questions about the processes and mechanisms of sexual selection, as well as about the effects of sexual selection on speciation. Nevertheless, most erigonines have been described by the morphological species concept, and the monophyly of most of the taxa above species level have not been scrutinized by phylogenetic analyses. This impedes comparative studies aiming at answering questions about the evolution of their sexually dimorphic traits, as well as how selection on these traits might have influenced speciation. The objectives of this thesis are to improve the knowledge about dwarf spider (Erigoninae, Linyphiidae) diversity and taxonomy, as well as to assess the evolutionary pattern of their male traits related to gustatory courtship. These objectives are crucial for studies aiming at answering interesting questions in evolution, including the process of speciation and how sexual selection might have played a role in erigonine species diversification. I applied a phylogenetic approach in describing new species and revising the classification of known species of dwarf spiders. I also investigated the distribution and evolutionary pattern of the gustatory gland using X-ray micro-computed tomography (micro-CT), which presents an important aspect in the lability of the sexually selected erigonine male traits.

1.4.1. Complex species history exemplified by the dwarf spider genus *Shaanxinus* (Publication 1)

Among the current 411 erigonine genera, 166 are monotypic and 74 consist only two species (Tanasevitch 2021). The discrepancy in species richness between genera might be due to either a lack of thorough sampling, or the excessive splitting of some species groups into genera. The genus *Shaanxinus* contained previously only two species, both from China: *S. rufus* Tanasevitch, 2006 and *S. anguilliformis* (Xia et al. 2001). The aim of this study was to describe 13 new *Shaanxinus* species from Taiwan and one new species from Vietnam, and provide a revision of this genus with a morphological phylogenetic analysis for determining the generic synapomorphies. These species resemble the previously described two species in the elevated male prosoma ocular region with a hirsute groove below the anterior median eyes, and possess similar morphology of the male palp. These clearly congeneric species currently show a discontinuity in distribution. Compared to the high *Shaanxinus* species density in Taiwan, the disproportionate scarce records of this genus in continental Asia suggests that the species diversity of this genus is much higher than currently known. This discrepancy might be due to the collecting method I applied in Taiwan for collecting spiders from above-ground vegetation.

I also reconstructed the glandular distribution associated with male prosomal modifications, as well as the detailed structure of pedipalp by micro-computer tomography (micro-CT). We conducted phylogenetic analyses based on sequences from two mitochondrial and one nuclear loci, and assessed the efficacy of different criteria in species identification using DNA barcoding. Molecular data assisted the distinction between morphologically similar species. The species level poly-/paraphyly found in mitochondrial DNA sequences rendered many distance- and tree-based species identification methods ineffective, while the nearest neighbor method showed high efficacy. This non-monophyly implies instances of interspecific hybridization and recent parapatric speciation. Therefore, *Shaanxinus* is an ideal group for applying the concept of congeneric phylogeography in investigating the interaction between closely related species (See introduction, p. 12-13).

Original publication: “Lin, S.-W., Lopardo, L., Haase, M. & Uhl, G. (2019). Taxonomic revision of the dwarf spider genus *Shaanxinus* Tanasevitch, 2006 (Araneae, Linyphiidae, Erigoninae), with new species from Taiwan and Vietnam. *Organism Diversity & Evolution*, 19: 211-276” (p. 39).

1.4.2. Evolution of dwarf spider gustatory-courtship-related prosomal structures (Publication 2)

Nuptial-feeding related sexually dimorphic prosomal modifications occur in many dwarf spider species. These features evolved in the context of sexual selection, which has a potential positive effect on speciation rates. In contrast to many erigonine genera which present little variability in male prosomal traits, *Oedothorax* shows high diversity among species not only in the position and shapes of various modifications, but also in the degree of modification, ranging from absent to elaborated. It was established by Förster and Bertkau (1883) based on the hump behind the eyes in males, with *Oedothorax gibbosus* as the type species. This genus has been the focus of several studies dealing with sexual selection, mating strategies, dimorphic morphology, and comparative analysis aimed at elucidating the functional context and the anatomy of the prosomal structures (e.g., de Keer and Maelfait 1987; Heinemann and Uhl 2000; Vanacker et al. 2004; Maes et al. 2004; Uhl and Busch 2009; Michalik and Uhl 2011; Kunz et al. 2012). With high structural and species diversity, *Oedothorax* lends itself as a suitable target group for studying the effect of gustatory-courtship-related traits on diversification and eventually on speciation rate.

Previously this genus comprised 82 described species distributed across the Northern Hemisphere and Africa (World Spider Catalog 2021), which are mostly 2-3 mm in body length, live in leaf litter, grasslands and other humid habitats. Based on five *Oedothorax* species of European distribution, Wiehle (1960) proposed the diagnostic characters of this

genus based on seta formula on the tibia of the walking legs (chaetotaxy), the locations of trichobothria on metatarsi, the number of teeth on the sides of the cheliceral fang furrow, the female genital morphology, and features in the male copulatory bulb. However, this combination of features is not unique to *Oedothorax*, as later pointed out by several taxonomists, who proposed close relationships or synonymization of it with other genera, including *Callitrichia* and *Toschia* (Bosmans 1985; Holm 1962; Wunderlich 1978). The synonymization of these genera was based on a number of symplesiomorphic features, which are also found in many other erigonines (Scharff 1990). Many species have been described from the Himalaya region, Oriental region and Africa (Bosmans 1988; Jocqué 1985; Jocqué and Scharff 1986; Locket and Russell-Smith 1980; Scharff 1989; Tanasevitch 1998, 2014, 2015, 2016, 2017a, 2017b, 2017c, 2020a, 2020b; Wunderlich 1974) based on the abovementioned shared features. As for most North American *Oedothorax* species (Banks 1900, 1901; Chamberlin 1949; Crosby 1905; Emerton 1882; Petrunkevitch 1925; Strand 1906), their taxonomic placements are dubious. In most cases only females are known, and the descriptions of their male copulatory bulb are not detailed enough for comparative purposes. All in all, A major revision of the genus *Oedothorax* with the application of a phylogenetic method is crucial for studies that aim at addressing the evolutionary pattern of their male prosomal modifications, with the long-term goal in answering whether sexual selection on these traits has facilitated speciation in erigonines.

Our taxonomic revision based on a phylogenetic analysis re-delimited 10 species as *Oedothorax sensu stricto*, while taxonomic decisions were made for other species including synonymization with species from other genera and transferring to other existing and newly defined genera. 25 species were deemed as "*Oedothorax*" *incertae sedis*, awaiting future studies to determine their relationship with other erigonines. The character optimization suggested multiple origins of different prosomal modification types. Convergent evolution in these traits suggests that sexual selection has played an important role in the species diversification of dwarf spiders.

Original publication: "Lin, S.-W., Lopardo, L. & Uhl, G. (2021). Evolution of nuptial-gift-related male prosomal structures: taxonomic revision and cladistic analysis of the genus *Oedothorax* Bertkau, 1883 (Araneae, Linyphiidae, Erigoninae). *Zoological Journal of the Linnean Society*, XX: 1-168" (p. 107).

1.4.3. Evolution of gustatory-courtship-related glandular tissue (Publication 3)

Sexually dimorphic traits have inspired the concept of sexual selection as the driving force of their evolution. However, they can also be due to other ecological factors, like the adaptation of sexual signal to the environment, as well as sexual differences in ecological niche and parental investment. In contrast, the gustatory courtship in dwarf spiders are associated with sexually dimorphic male prosomal modifications, which have clearly evolved in the context of sexual selection. Previous phylogenetic analyses have repeatedly shown multiple origins of various external prosomal modifications in erigonine males, but the evolutionary pattern of the associated glands has not been investigated. Our results of phylogenetic analyses incorporating glandular distributional character yielded from micro-CT showed a single origin of gland among the investigated erigonine taxa; internal anatomy revealed previously undetected trait lability in attachments of muscles to the cuticular structures, as well as differences in glandular distribution even in species without external modification. This further supported that erigonine male prosomal traits are under divergent selection, and suggested erigonine spiders as a suitable target group for investigating the effect of sexual selection on speciation.

Original publication: “Lin, S.-W., Lopardo, L. & Uhl, G. (2021). Diversification through gustatory courtship: an X-ray micro-computed tomography study on dwarf spiders. *Frontiers in Zoology*, 18: 51” (p. 277).

2. References

- Allender, C. J., Seehausen, O., Knight, M. E., Turner, G. F., & Maclean, N. (2003). Divergent selection during speciation of Lake Malawi cichlid fishes inferred from parallel radiations in nuptial coloration. *Proceedings of the National Academy of Sciences of the United States of America*, *100*, 14074–14079.
- Andersson, M. (1994). *Sexual selection*. Princeton, New Jersey: Princeton University Press.
- Andersson, M., & Simmons, L. W. (2006). Sexual selection and mate choice. *Trends in Ecology & Evolution*, *21*, 296–302.
- Arnedo, M. A., Hormiga, G., & Scharff, N. (2009). Higher-level phylogenetics of linyphiid spiders (Araneae, Linyphiidae) based on morphological and molecular evidence. *Cladistics*, *25*, 231–262.
- Arnqvist, G., Edvardsson, M., Friberg, U., & Nilsson, T. (2000). Sexual conflict promotes speciation in insects. *Proceedings of the National Academy of Sciences of the United States of America*, *97*, 10460–10464.
- Austad, S. N. (1984). Evolution of sperm priority patterns in spiders. In R. L. Smith (Ed.), *Sperm Competition and the Evolution of Animal Mating Systems* (pp. 223–249). London: Academic Press.
- Badyaev, A. V., & Hill, G. E. (2000). Evolution of sexual dichromatism: contribution of carotenoids-versus melanin-based coloration. *Biological Journal of the Linnean Society*, *69*, 153–172.
- Ballard, J. W. O., & Whitlock, M. C. (2004). The incomplete natural history of mitochondria. *Molecular Ecology*, *13*, 729–744.
- Banks, N. (1900). Arachnida of the Expedition. In: Papers from the Harriman Alaska Expedition. XI. Entomological Results: 5 Arachnida. *Proceedings of the Washington Academy of Sciences*, *2*, 477–486.
- Banks, N. (1901). Some Arachnida from New Mexico. *Proceedings of the Academy of natural Sciences of Philadelphia*, *53*, 568–597.
- Bao, M., Bai, Z., & Tu, L. H. (2017). On a desmitracheate “micronetine” *Nippononeta alpina* (Li & Zhu, 1993), comb. n. (Araneae, Linyphiidae). *Zookeys*, *645*, 133–146.
- Barrett, R. D. H., & Hebert, P. D. N. (2005). Identifying spiders through DNA barcodes. *Canadian Journal of Zoology*, *83*, 481–491.
- Bateson, W. (1902). *Mendel's Principles of Heredity; a Defense*. Cambridge: University Press.
- Berns, C. M. (2013). The evolution of sexual dimorphism: understanding mechanisms of sexual shape differences. In H. Moriyama (Ed.), *Sexual Dimorphism* (pp. 1–16). Rijeka: InTech.

- Birky, C. W. (2001). The inheritance of genes in mitochondria and chloroplasts: laws, mechanisms, and models. *Annual Review of Genetics*, 35, 125–148.
- Blest, A. D., & Taylor, H. H. (1977). The clypeal glands of *Mynoglenes* and of some other linyphiid spiders. *Journal of Zoology*, 183, 473–493.
- Bosmans, R. (1985). Études sur les Linyphiidae nord-africains. II. Le genre *Oedothorax* Bertkau en Africa du Nord, avec une révision des caractères diagnostiques des mâles des espèces ouest-paléarctiques. *Biologisch Jaarboek Dodonaea*, 53, 58–75.
- Bosmans, R. (1988). Scientific report of the Belgian Cameroon expeditions 1981 and 1983. No. 18. Further Erigoninae and Mynogleninae (Araneae: Linyphiidae) from Cameroonian highlands. *Revue Zoologique Africaine*, 102, 5–32.
- Boul, K. E., Funk, W. C., Darst, C. R., Cannatella, D. C., & Ryan, M. J. (2007). Sexual selection drives speciation in an Amazonian frog. *Proceedings of the Royal Society B*, 274, 399–406.
- Bristowe, W. S. (1931). The mating habits of spiders: a second supplement, with the description of a new thomisid from Krakatau. *Proceedings of the Zoological Society of London*, 4, 1401–1412.
- Brockmann, H. J. (2012). *Advances in the study of behavior*. Amsterdam; Boston: Elsevier.
- Cardoso, G. C., & Mota, P. G. (2008). Speciation evolution of coloration in the genus *Carduelis*. *Evolution*, 62, 753–762.
- Chamberlin, R. V. (1949). On some American spiders of the family Erigonidae. *Annals of the Entomological Society of America*, 41, 483–562.
- Clutton-Brock, T. (2007). Sexual selection in males and females. *Science*, 318, 1882–1885.
- Clutton-Brock, T. H., & Parker, G. A. (1992). Potential reproductive rates and the operation of sexual selection. *Quarterly Review of Biology*, 67, 437–456.
- Coddington, J. A., & Levi, H. W. (1991). Systematics and evolution of spiders (Araneae). *Annual Review of Ecology and Systematics*, 22, 565–592.
- Costa-Schmidt, L. E., Carico, J. E., & de Araújo, A. M. (2008). Nuptial gifts and sexual behavior in two species of spider (Araneae, Trechaleidae, *Paratrechalea*). *Naturwissenschaften*, 95, 731–739.
- Cronquist, A. (1978). Once again, what is a species? In L. V. Knutson (Ed.), *Biosystematics in Agriculture* (pp. 3–20). Montclair, New Jersey, U.S.A: Allenheld Osmin.
- Crosby, C. R. (1905). A catalogue of the Erigoneae of North America, with notes and descriptions of new species. *Proceedings of the Academy of Natural Sciences of Philadelphia*, 301–343.
- Darwin, C. (1859). *On the Origin of Species by Means of Natural Selection*. London: Murray.
- Darwin, C. (1871). *The Descent of Man and Selection in Relation to Sex*. London: Murray.

- de Keer, R., & Maelfait, J. P. (1987). Laboratory observations on the development and reproduction of *Oedothorax fuscus* (Blackwall, 1834) (Araneida, Linyphiidae) under different conditions of temperature and food supply. *Revue d'Ecologie et de Biologie du Sol*, 24, 63–73.
- Dobzhansky, T. (1937). *Genetics and the origin of species*. New York: Columbia University Press.
- Dobzhansky, T. (1951). *Genetics and the origin of species*. 3rd ed. New York: Columbia University Press.
- Dupuis, J. R., Roe, A. D., & Sperling, F. A. H. (2012). Multi-locus species delimitation in closely related animals and fungi: one marker is not enough. *Molecular Ecology*, 21, 4422–4436.
- Eberle, J., Ahrens, D., Mayer, C., Niehuis, O., & Misof, B. (2020). A plea for standardized nuclear markers in metazoan DNA taxonomy. *Trends in Ecology & Evolution*, 35, 336–345.
- Eldredge, N., & Cracraft, J. (1980). *Phylogenetic patterns and the evolutionary process*. New York: Columbia University Press.
- Emerton, J. H. (1882). New England spiders of the family Theridiidae. *Transactions of the Connecticut Academy of Arts and Sciences*, 6, 1–86.
- Emlen, D. J. (2008). The evolution of animal weapons. *Annual Review of Ecology, Evolution, and Systematics*, 39, 387–413.
- Emlen, S. T., & Oring, L. W. (1977). Ecology, sexual selection, and the evolution of mating systems. *Science*, 197, 215–223.
- Fisher, R. A. (1919). XV.—The Correlation between Relatives on the Supposition of Mendelian Inheritance. *Transactions of the Royal Society of Edinburgh*, 52, 399–433.
- Foelix, R. F. (2011). *Biology of Spiders, third edition*. New York: Oxford University Press.
- Förster, A., & Bertkau, P. (1883). Beiträge zur Kenntniss der Spinnenfauna der Rheinprovinz. *Verhandlungen des naturhistorischen Vereins der preussischen Rheinlande und Westfalens*, 40, 205–278.
- Frick, H., & Scharff, N. (2014). Phantoms of Gondwana?—phylogeny of the spider subfamily Mynogleninae (Araneae: Linyphiidae). *Cladistics*, 30, 67–106.
- Funk, D. J., & Omland, K. E. (2003). Species-level paraphyly and polyphyly: frequency, causes, and consequences, with insights from animal mitochondrial DNA. *Annual Review of Ecology, Evolution, and Systematics*, 34, 397–423.
- Gage, M. J. G., Parker, G. A., Nylin, S., & Wiklund, C. (2002). Sexual selection and speciation in mammals, butterflies and spiders. *Proceedings of the Royal Society of London B*, 269, 2309–2316.
- Goss, R. J. (1983). *Deer Antlers: Regeneration, Function, and Evolution*. New York: Academic Press.

- Gwynne, D. T. (2008). Sexual conflict over nuptial gifts in insects. *Annual Review of Entomology*, *53*, 83–101.
- Haldane, J. B. S. (1932). *The Causes of Evolution*. London: Longmans.
- Head, G. (1995). Selection on fecundity and variation in the degree of sexual size dimorphism among spider species (Class Araneae). *Evolution*, *49*, 776–781.
- Hebert, P. D., Cywinska, A., Ball, S. L., & deWaard, J. R. (2003). Biological identifications through DNA barcodes. *Proceedings of the Royal Society of London B: Biological Sciences*, *270*, 313–21.
- Hebert, P. D., Penton, E. H., Burns, J. M., Janzen, D. H., & Hallwachs, W. (2004). Ten species in one: DNA barcoding reveals cryptic species in the neotropical skipper butterfly *Astraptes fulgerator*. *Proceedings of the National Academy of Sciences of the United States of America*, *101*, 14812–14817.
- Hebert, P. D., Stoeckle, M. Y., Zemlak, T. S., & Francis, C. M. (2004). Identification of Birds through DNA Barcodes. *PLOS Biology*, *2*, e312.
- Hedrick, A. V., & Temeles, E. J. (1989). The evolution of sexual dimorphism in animals: hypotheses and tests. *Trends in Ecology & Evolution*, *4*, 136–138.
- Heinemann, S., & Uhl, G. (2000). Male dimorphism in *Oedothorax gibbosus* (Araneae, Linyphiidae): A morphometric analysis. *Journal of Arachnology*, *28*, 23–28.
- Hennig, W. (1966). *Phylogenetic systematics*. Urbana, Illinois: University of Illinois Press.
- Holm, Å. (1962). The spider fauna of the East African mountains. Part I: Fam. Erigonidae. *Zoologiska bidrag från Uppsala*, *35*, 19–204.
- Hormiga, G. (1999). Cephalothoracic sulci in linyphiine spiders (Araneae, Linyphiidae, Linyphiinae). *Journal of Arachnology*, *27*, 94–102.
- Hormiga, G. (2000). Higher level phylogenetics of erigonine spiders (Araneae, Linyphiidae, Erigoninae). *Smithsonian Contributions to Zoology*, *609*, 1–160.
- Hormiga, G., Scharff, N., & Coddington, J. A. (2000). The phylogenetic basis of sexual size dimorphism in orb-weaving spiders (Araneae, Orbiculariae). *Systematic Biology*, *49*, 435–462.
- Hosken, D. J., Garner, T. W. J., & Ward, P. I. (2001). Sexual conflict selects for male and female reproductive characters. *Current Biology*, *11*, 489–493.
- Huber, B. A., & Eberhard, W. G. (1997). Courtship, copulation, and genital mechanics in *Physocyclus globosus* (Araneae, Pholcidae). *Canadian Journal of Zoology*, *75*, 905–918.
- Huxley, J. (1942). *Evolution: The Modern Synthesis*. London: Allen & Unwin.

- Ješovnik, A., Sosa-Calvo, J., Lloyd, M. W., Branstetter, M. G., Fernández, F., & Schultz, T. R. (2017). Phylogenomic species delimitation and host-symbiont coevolution in the fungus-farming ant genus *Sericomyrmex* Mayr (Hymenoptera: Formicidae): ultraconserved elements (UCEs) resolve a recent radiation. *Systematic Entomology*, *42*, 523–542.
- Jocqué, R. (1985). Linyphiidae (Araneae) from the Comoro Islands. *Revue de Zoologie africaine*, *99*, 197–230.
- Jocqué, R., & Scharff, N. (1986). Spiders (Araneae) of the family Linyphiidae from the Tanzanian mountain areas Usambara, Uluguru and Rungwe. *Annalen Zoologische Wissenschaften*, *248*, 1–61.
- Johnson, N. K., & Cicero, C. (2004). New mitochondrial DNA data affirm the importance of Pleistocene speciation in North American birds. *Evolution*, *58*, 1122–1130.
- Knoflach, B. (2004). Diversity in the copulatory behaviour of comb-footed spiders (Araneae, Theridiidae). In K. Thaler (Ed.), *Diversity and Biology of Spiders, Scorpions and other Arachnids* (Vol. 12, pp. 161–256). Linz: Denisia.
- Kraaijeveld, K., Kraaijeveld-Smit, F. J. L., & Maan, M. E. (2011). Sexual selection and speciation: the comparative evidence revisited. *Biological Reviews*, *86*, 367–377.
- Kunz, K., Garbe, S., & Uhl, G. (2012). The function of the secretory cephalic hump in males of the dwarf spider *Oedothorax retusus* (Linyphiidae: Erigoninae). *Animal Behaviour*, *83*, 511–517.
- Kunz, K., Michalik, P., & Uhl, G. (2013). Cephalic secretion release in the male dwarf spider *Oedothorax retusus* (Linyphiidae: Erigoninae): an ultrastructural analysis. *Arthropod Structure & Development*, *42*, 477–482.
- Kunz, K., Witthuhn, M., & Uhl, G. (2015). Paired and complex copulatory organs: do they really impede flexible use? *Journal of Zoology*, *297*, 278–285.
- Lande, R. (1981). Models of speciation by sexual selection on polygenic traits. *Proceedings of the National Academy of Sciences of the United States of America*, *78*, 3721–3725.
- Lewis, S., & South, A. (2012). The evolution of animal nuptial gifts. *Advances in the Study of Behavior*, *44*, 53–97.
- Lewis, S., South, A., Burns, R., & Al-Wathiqui, N. (2011). Nuptial gifts. *Current Biology*, *21*, R644–R645.
- Lin, S.-W., Lopardo, L., Haase, M., & Uhl, G. (2019). Taxonomic revision of the dwarf spider genus *Shaanxinus* Tanasevitch, 2006 (Araneae, Linyphiidae, Erigoninae), with new species from Taiwan and Vietnam. *Organisms Diversity & Evolution*, *19*, 211–276.

- Lin, S.-W., Lopardo, L., & Uhl, G. (2021). Evolution of nuptial-gift-related male prosomal structures: taxonomic revision and cladistic analysis of the dwarf spider genus *Oedothorax* Bertkau, 1883 (Araneae, Linyphiidae, Erigoninae). *Zoological Journal of the Linnean Society*, *XX*, 1-168.
- Lipscomb, D., Platnick, N., & Wheeler, Q. (2003). The intellectual content of taxonomy: a comment on DNA taxonomy. *Trends in Ecology & Evolution*, *18*, 65–66.
- Liu, J., Jiang, J., Song, S., Tornabene, L., Chabbarria, R., Naylor, G. J. P., & Li, C. (2017). Multilocus DNA barcoding – species identification with multilocus data. *Scientific Reports*, *7*, 1–12.
- Liu, S., & Hua, B. (2010). Histology and ultrastructure of the salivary glands and salivary pumps in the scorpionfly *Panorpa obtusa* (Mecoptera: Panorpidae). *Acta Zoologica*, *91*, 457–465.
- Locket, G. H., & Russell-Smith, A. (1980). Spiders of the family Linyphiidae from Nigeria. *Bulletin of the British Arachnological Society*, *5*, 54–90.
- Lopez, A. (1976). Présence de glandes tégumentaires prosomatiques chez les mâles de deux Erigonidae (Araneae). *Compte Rendu Hebdomadaire des Séances de l'Académie des Sciences, Paris*, *282*, 365–367.
- Lopez, A., & Emerit, M. (1981). Le dimorphisme sexuel prosomatique de *Walckenaeria acuminata* BLACKWALL, 1833 (Araneae, Erigonidae). *Bulletin de la Société zoologique de France*, *106*, 125–131.
- Loyau, A., Saint Jalme, M., Cagniant, C., & Sorci, G. (2005). Multiple sexual advertisements honestly reflect health status in peacocks. *Behavioral Ecology and Sociobiology*, *58*, 552–557.
- Luc, M., Doucet, M. E., Fortuner, R., Castillo, P., Decraemer, W., & Lax, P. (2010). Usefulness of morphological data for the study of nematode biodiversity. *Nematology*, *12*, 495–504.
- Maes, L., Vanacker, D., Sylvia, P., & Maelfait, J. P. (2004). Comparative study of courtship and copulation in five *Oedothorax* species. *Belgian Journal of Zoology*, *134*, 29–35.
- Mann, T. (1984). *Spermatophores: Development, Structure, Biochemical Attributes and Role in the Transfer of Spermatozoa*. Berlin: Springer.
- Masta, S. E., & Maddison, W. P. (2002). Sexual selection driving diversification in jumping spiders. *Proceedings of the National Academy of Sciences*, *99*, 4442–4447.
- Mathieu, J. M. (1969). Mating behavior of five species of Lucanidae (Coleoptera: Insecta). *Canadian Entomologist*, *101*, 1054–1062.
- Mayo, S. J., Allkin, R., Baker, W., Blagoderov, V., Brake, I., Clark, B., et al. (2008). Alpha e-taxonomy: responses from the systematics community to the biodiversity crisis. *Kew Bulletin*, *63*, 1–16.
- Mayr, E. (1942). *Systematics and the Origin of Species, from the Viewpoint of a Zoologist*. New York: Columbia University Press.

- Mayr, E. (1982). *The Growth of Biological Thoughts*. Cambridge, MA: Harvard University Press.
- Mayr, E., Linsley, E. G., & Usinger, R. L. (1953). *Methods and Principles of Systematic Zoology*. New York: McGraw-Hill.
- McNett, G. D., & Cocroft, R. B. (2008). Host shifts favor vibrational signal divergence in *Enchenopa binotata* treehoppers. *Behavioral Ecology*, *19*, 650–656.
- Michalik, P., & Uhl, G. (2011). Cephalic modifications in dimorphic dwarf spiders of the genus *Oedothorax* (Erigoninae, Linyphiidae, Araneae) and their evolutionary implications. *Journal of Morphology*, *272*, 814–832.
- Miller, J. A. (2007). Review of erigonine spider genera in the neotropics (Araneae: Linyphiidae, Erigoninae). *Zoological Journal of the Linnean Society*, *149*, 1–263.
- Miller, J. A., & Hormiga, G. (2004). Clade stability and the addition of data: A case study from erigonine spiders (Araneae : Linyphiidae, Erigoninae). *Cladistics*, *20*, 385–442.
- Monaghan, M. T., Balke, M., Pons, J., & Vogler, A. P. (2006). Beyond barcodes: complex DNA taxonomy of a South Pacific Island radiation. *Proceedings of the Royal Society B*, *273*, 887–893.
- Mutanen, M., Aarvik, L., Huemer, P., Kaila, L., Karsholt, O., & Tuck, K. (2012). DNA barcodes reveal that the widespread European tortricid moth *Phalonidia manniana* (Lepidoptera: Tortricidae) is a mixture of two species. *Zootaxa*, *3262*, 1–21.
- Nelson, G., & Platnick, N. I. (1981). *Systematics and Biogeography: Cladistics and Vicariance*. New York: Columbia University Press.
- Panhuis, T. M., Butlin, R., Zuk, M., & Tregenza, T. (2001). Sexual selection and speciation. *Trends in Ecology & Evolution*, *16*, 364–371.
- Parker, G. A. (2006). Sexual conflict over mating and fertilization: an overview. *Philosophical Transactions of the Royal Society B*, *361*, 235–259.
- Petrunkévitch, A. (1925). New Erigoninae from Tennessee. *Journal of the New York Entomological Society*, *33*, 170–176.
- Regan, C. T. (1926). Organic evolution. *Report of the British Association for the Advancement of Science, 1925*, 75–86.
- Ritchie, M. G. (2007). Sexual selection and speciation. *Annual Review of Ecology, Evolution, and Systematics*, *38*, 79–102.
- Ross, H. A. (2014). The incidence of species-level paraphyly in animals: a re-assessment. *Molecular Phylogenetics and Evolution*, *76*, 10–17.
- Safran, R. J., Scordato, E. S. C., Symes, L. B., Rodríguez, R. L., & Mendelson, T. C. (2013). Contributions of natural and sexual selection to the evolution of premating reproductive isolation: a research agenda. *Trends in Ecology & Evolution*, *28*, 643–650.

- Schaible, U., & Gack, C. (1987). Zur Morphologie, Histologie und biologischen Bedeutung der Kopfstrukturen einiger Arten der Gattung *Diplocephalus* (Araneida, Linyphiidae, Erigoninae). *Verhandlungen des naturwissenschaftlichen Vereins in Hamburg*, 29, 171–180.
- Schaible, U., Gack, C., & Paulus, H. F. (1986). Zur Morphologie, Histologie und biologischen Bedeutung der Kopfstrukturen männlicher Zwergspinnen (Linyphiidae: Erigoninae). *Zoologische Jahrbücher. Abteilung für Systematik, Ökologie und Geographie der Tiere*, 113, 389–408.
- Scharff, N. (1989). New species and records of Afrotropical Linyphiidae (Araneae). *Bulletin of the British Arachnological Society*, 8, 13–20.
- Scharff, N. (1990). Spider of the family Linyphiidae from the Uzungwa mountains, Tanzania (Araneae). *Entomologica Scandinavica, Supplement 36*, 1–95.
- Scheffler, I. E. (1999). *Mitochondria*. New York: John Wiley & Sons, Inc.
- Schlegelmilch, B. (1974). *Zur biologischen Bedeutung der Kopffortsätze bei Zwergspinnenmännchen (Microphantidae)*. Diplomarbeit, Universität Freiburg.
- Servedio, M. R., & Boughman, J. W. (2017). The role of sexual selection in local adaptation and speciation. *Annual Review of Ecology, Evolution, and Systematics*, 48, 85–109.
- Shine, R. (1989). Ecological causes for the evolution of sexual dimorphism: a review of the evidence. *Quarterly Review of Biology*, 64, 419–461.
- Singh, B. N. (2012). Concepts of species and modes of speciation. *Current Science*, 103, 784–790.
- Smith, M. A., Woodley, N. E., Janzen, D. H., Hallwachs, W., & Hebert, P. D. (2006). DNA barcodes reveal cryptic host-specificity within the presumed polyphagous members of a genus of parasitoid flies (Diptera: Tachinidae). *Proceedings of the National Academy of Sciences of the United States of America*, 103, 3657–3662.
- Stace, C. A. (1989). *Plant Taxonomy and Biosystematics, second ed.* London: Edward Arnold, a division of Hodder and Stoughton.
- Stålhandske, P. (2001). Nuptial gift in the spider *Pisaura mirabilis* maintained by sexual selection. *Behavioral Ecology*, 12, 691–697.
- Strand, E. (1906). Die arktischen Araneae, Opiliones und Chernetes. In F. Römer & F. Schaudinn (Eds.), *Fauna Arctica* (Vol. 4, pp. 431–478). Jena: Verlag von Gustav Fischer.
- Tanasevitch, A. V. (1998). New *Oedothorax* Bertkau, 1883, from Nepal (Arachnida, Araneae, Linyphiidae). *Bonner Zoologische Beiträge*, 47, 429–441.
- Tanasevitch, A. V. (2014). On the linyphiid spiders from Thailand and West Malaysia (Arachnida: Aranei: Linyphiidae). *Arthropoda Selecta*, 23, 393–414.

- Tanasevitch, A. V. (2015). Notes on the spider genus *Oedothorax* Bertkau, 1883 with description of eleven new species from India (Linyphiidae: Erigoninae). *Revue suisse de Zoologie*, *122*, 381–398.
- Tanasevitch, A. V. (2016). A case of disjunct montane linyphiid species (Araneae) in the Palaetropics, with notes on synonymy and the description of a new species. *Revue Suisse de Zoologie*, *123*, 235–240.
- Tanasevitch, A. V. (2017a). New genera and new species of the family Linyphiidae from Borneo, Sumatra and Java (Arachnida, Araneae). *Revue suisse de Zoologie*, *124*, 141–155.
- Tanasevitch, A. V. (2017b). Another new species of *Oedothorax* Bertkau, 1883 from India (Araneae, Linyphiidae). *Revue Suisse de Zoologie*, *124*, 331–333.
- Tanasevitch, A. V. (2017c). New species and new records of linyphiid spiders from the Indo-Malayan Region (Araneae, Linyphiidae). *Zootaxa*, *4227*, 325–346.
- Tanasevitch, A. V. (2020a). Two new *Oedothorax* Bertkau, 1883 from eastern India (Aranei: Linyphiidae). *Arthropoda Selecta*, *29*, 127–131.
- Tanasevitch, A. V. (2020b). The genus *Oedothorax* Bertkau, 1883 in the Himalayas, with descriptions of four new species from Nepal (Aranei: Linyphiidae). *Arthropoda Selecta*, *29*, 283–291.
- Tanasevitch, A. V. (2021). Linyphiid spiders of the world.
<http://old.cepl.rssi.ru/bio/tan/linyphiidae/>. Accessed 21 April 2021
- Thornhill, R. (1976). Sexual selection and nuptial feeding behaviour in *Bittacus apicalis* (Insecta: Mecoptera). *American Naturalist*, *110*, 529–548.
- Tregenza, T., & Wedell, N. (2000). Genetic compatibility, mate choice and patterns of parentage: Invited review. *Molecular Ecology*, *9*, 1013–1027.
- Uhl, G., & Busch, M. (2009). Securing paternity: mating plugs in the dwarf spider *Oedothorax retusus* (Araneae: Erigoninae). *Biological Journal of the Linnean Society*, *96*, 574–583.
- Uhl, G., & Maelfait, J.-P. (2008). Male head secretion triggers copulation in the dwarf spider *Diplocephalus permixtus*. *Ethology*, *114*, 760–767.
- Uy, J. A. C., & Borgia, G. (2000). Sexual selection drives rapid divergence in bowerbird display traits. *Evolution*, *54*, 273–278.
- Vahed, K. (1998). The function of nuptial feeding in insects: a review of empirical studies. *Biological Reviews*, *73*, 43–78.
- Vahed, K. (2007). All that glitters is not gold: sensory bias, sexual conflict and nuptial feeding in insects and spiders. *Ethology*, *113*, 105–127.
- van Hasselt, A. W. M. (1884). Waarnemingen omtrent anomalieën van de geslachtsdrift bij spinnen-mares. *Tijdschrift voor Entomologie*, *27*, 197–206.

- Vanacker, D., Borre, J. V., Jonckheere, A., Maes, L., Pardo, S., Hendrickx, F., & Maelfait, J. P. (2003). Dwarf spiders (Erigoninae, Linyphiidae, Araneae): good candidates for evolutionary research. *Belgian Journal of Zoology*, *133*, 143–149.
- Vanacker, D., Hendrickx, F., Maes, L., Verraes, P., & Maelfait, J. P. (2004). Can multiple mating compensate for slower development and shorter adult life in a male dimorphic dwarf spider? *Biological Journal of the Linnean Society*, *82*, 269–273.
- Vanacker, D., Maes, L., Pardo, S., Hendrickx, F., & Maelfait, J. P. (2003). Is the hairy groove in the *gibbosus* male morph of *Oedothorax gibbosus* (Blackwall 1841) a nuptial feeding device? *Journal of Arachnology*, *31*, 309–315.
- Voight, J. R. (1995). Sexual dimorphism and niche divergence in a mid-water octopod (Cephalopoda: Bolitaenidae). *Biological Bulletin*, *189*, 113–119.
- Vollrath, F. (1977). *Zur Ökologie und Biologie von kleptoparasitischen Argyrodes elevatus und synöken Argyrodes-Arten (Araneae, Theridiidae)* (Doctoral Thesis). University of Freiburg.
- von Helversen, O. (1976). Gedanken zur Evolution der Paarungsstellung bei den Spinnen. *Entomologica Germanica*, *3*, 13–28.
- Wang, F., Ballesteros, J. A., Hormiga, G., Chesters, D., Zhan, Y., Sun, N., et al. (2015). Resolving the phylogeny of a speciose spider group, the family Linyphiidae (Araneae). *Molecular Phylogenetics and Evolution*, *91*, 135–149.
- West-Eberhard, M. J. (1983). Sexual selection, social competition and speciation. *Quarterly Review of Biology*, *58*, 155–183.
- Wheeler, Q. D. (1999). Why the phylogenetic species concept?—elementary. *Journal of Nematology*, *31*, 134–141.
- Wheeler, Q. D., & Platnick, N. I. (2000). The phylogenetic species concept (sensu Wheeler and Platnick). In Q. D. Wheeler & R. Meier (Eds.), *Species Concepts and Phylogenetic Theory: A Debate*. New York: Columbia University Press.
- White, M. J. D. (1978). *Modes of Speciation*. San Francisco: W. H. Freeman and Company.
- Wiehle, H. (1960). Spinnentiere oder Arachnoidea, XI: Micryphantidae-Zwergspinnen. *Tierwelt Deutschlands*, *47*, 1–620.
- Wiemers, M., & Fiedler, K. (2007). Does the DNA barcoding gap exist? – a case study in blue butterflies (Lepidoptera: Lycaenidae). *Frontiers in Zoology*, *4*, 8.
- World Spider Catalog. (2021). World Spider Catalog Version 22.0. <http://wsc.nmbe.ch>. Accessed 10 April 2021
- Wright, S. (1931). Evolution in Mendelian Populations. *Genetics*, *16*, 97–159.
- Wunderlich, J. (1974). Ein Beitrag zur Synonymie einheimischer Spinnen (Arachnida: Araneae). *Zoologische Beiträge*, *20*, 159–176.

- Wunderlich, J. (1978). Zur Kenntnis der Gattung *Oedothorax* Bertkau 1883, *Callitrichia* Fage 1936 und *Toschia* Caporiacco 1949. *Senckenbergiana Biologica*, 58, 257–260.
- Yassin, A., Markow, T. A., Narechania, A., O’Grady, P. M., & DeSalle, R. (2010). The genus *Drosophila* as a model for testing tree- and character-based methods of species identification using DNA barcoding. *Molecular Phylogenetics and Evolution*, 57, 509–517.
- Yule, G. U. (1902). Mendel’s Laws and their probable relations to inter-racial heredity. *New Phytologist*, 1, 226–227.
- Zachos, F. E. (2016). *Species Concepts in Biology*. Berlin: Springer.
- Zarza, E., Connors, E. M., Maley, J. M., Tsai, W. L. E., Heimes, P., Kaplan, M., & McCormack, J. E. (2017). Bridging multilocus species delimitation and DNA barcoding through target enrichment of UCEs: a case study with Mexican highland frogs. *BioRxiv*, 153601.

3. Manuscripts

3.1. Contribution to manuscripts

Lin, S.-W., Lopardo, L. Haase, M. & Uhl, G. (2019). Taxonomic revision of the dwarf spider genus *Shaanxinus* Tanasevitch, 2006 (Araneae, Linyphiidae, Erigoninae), with new species from Taiwan and Vietnam.

Organism Diversity & Evolution, 19, 211-276.

Data acquisition: 90%, phylogenetic analysis: 90%, figures/tables: 100%, Text: 75%

Lin, S.-W., Lopardo, L. & Uhl, G. (2021). Evolution of nuptial-gift-related male prosomal structures: taxonomic revision and cladistic analysis of the genus *Oedothorax* Bertkau, 1883 (Araneae, Linyphiidae, Erigoninae).

Zoological Journal of the Linnean Society, XX,1-168.

Data acquisition: 100%, phylogenetic analysis: 90%, figures/tables: 100%, Text: 75%

Lin, S.-W., Lopardo, L. & Uhl, G. (2021). Diversification through sexual selection on gustatory courtship traits in dwarf spiders.

Frontiers in Zoology, 18, 51.

Data acquisition: 90%, phylogenetic analysis: 90%, figures/tables: 100%, Text: 75%

Supervisor: Prof. Dr. Gabriele Uhl

Student: Shou-Wang Lin

**3.2. Taxonomic revision of the dwarf spider genus *Shaanxinus* Tanasevitch, 2006
(Araneae, Linyphiidae, Erigoninae), with new species from Taiwan and Vietnam**

Shou-Wang Lin, Lara Lopardo, Martin Haase and Gabriele Uhl

Manuscript published in *Organism Diversity & Evolution* (2019) 19: 211-276



Taxonomic revision of the dwarf spider genus *Shaanxinus* Tanasevitch, 2006 (Araneae, Linyphiidae, Erigoninae), with new species from Taiwan and Vietnam

Shou-Wang Lin¹ · Lara Lopardo¹ · Martin Haase¹ · Gabriele Uhl¹

Received: 16 July 2018 / Accepted: 20 December 2018
© Gesellschaft für Biologische Systematik 2019

Abstract

Dwarf spiders are of special interest due to their sexually dimorphic prosomal structures in males. Glandular secretions within these structures serve as nuptial gifts, and thus sexual selection may have contributed to their high species richness. However, species diversity of dwarf spiders in East Asia is yet understudied. Here, we review the erigonine genus *Shaanxinus* Tanasevitch, 2006, and describe 13 new species from Taiwan: *S. magniclypeus* sp. n. (♂♀), *S. shihchoensis* sp. n. (♂♀), *S. shoukaensis* sp. n. (♂♀), *S. hirticephalus* sp. n. (♂♀), *S. mingchihensis* sp. n. (♂♀), *S. makauyensis* sp. n. (♂♀), *S. lixiangae* sp. n. (♂♀), *S. curviductus* sp. n. (♂♀), *S. tsou* sp. n. (♂♀), *S. hehuanensis* sp. n. (♂♀), *S. seediq* sp. n. (♂♀), *S. meifengensis* sp. n. (♂♀), and *S. atayal* sp. n. (♂♀). In addition, one new species from Vietnam, *S. tamdaoensis* sp. n. (♂), is described from museum material. We reconstructed the dimension of glandular tissues associated with male prosoma modifications in *Shaanxinus*, as well as the detailed palpal structure by micro-computer tomography. Placement within *Shaanxinus* and intrageneric relationships were inferred by means of a cladistic analysis based on morphological characters. Sequences of COI, 16S, and 28S genetic markers corroborated the monophyly of some species, as well as male-female matching. Poly-/paraphyly of morphologically delimited species in the mitochondrial DNA (mtDNA) trees led to the discovery of two seemingly identical species, for which diagnostic morphological features could then be further identified. We discuss incomplete lineage sorting and introgression as possible causes of mtDNA poly-/paraphyly in morphologically indistinguishable specimens.

Keywords Erigonines · Phylogeny · Arboreal spiders · Gustatorial courtship · Sexual selection

Introduction

With more than 4500 described species, Linyphiidae is the second largest spider family worldwide, and the most diverse spider family in the northern hemisphere, with many new species described every year. Among linyphiids, the dwarf spiders (Erigoninae) are the largest subfamily, comprising over 50% of linyphiid species (World Spider Catalog 2018). Erigonines are of particular interest to evolutionary biology due to their sexually

dimorphic prosomal structures. Modifications of the prosoma of males contain glandular tissues that produce secretions, which function as nuptial gifts. The secretions are transferred to the female during gustatorial courtship and affect male mating success (Uhl and Maelfait 2008; Vanacker et al. 2003; Kunz et al. 2012). Since taxa with stronger sexual selection operating on males were found to have higher species richness (Janicke et al. 2018), the erigonines are ideal to test the impact of sexual selection on species diversification, particularly since genera differ in the presence and variability of male prosomal structures (Hormiga 2000). However, such a test requires sound taxonomic and phylogenetic knowledge that yet has to be built up. Some genera of the erigonines are only composed of a few known species, like *Shaanxinus*, of which only two species are known from China, *S. rufus* Tanasevitch, 2006, and *S. anguilliformis* (Xia et al. 2001). The discrepancy in species richness between genera might be due to a lack of thorough sampling, which

✉ Shou-Wang Lin
shouwanglintaiwan@gmail.com

Gabriele Uhl
gabriele.uhl@uni-greifswald.de

¹ Zoological Institute and Museum, Department of General and Systematic Zoology, University of Greifswald, Loitzer Straße 26, 17489 Greifswald, Germany

impedes comparative studies for understanding the effect of sexual selection on species diversity.

According to the data of the Taiwan Biodiversity Information Facility (Shao 2018) (Karsch 1879; Bösenberg and Strand 1906; Oi 1977, 1960; Crosby et al. 1928; Tanasevitch 2011; Schenkel 1963) and Tanasevitch (2018b), currently only 23 linyphiid species are reported from Taiwan, among which 15 belong to the subfamily Erigoninae. In contrast, the Araneidae, the third largest spider family in the world, is represented by 84 species in this database. This discrepancy might be due to the larger body size of Araneidae, which makes them easier to find. If that were the case, this suggests that linyphiid diversity in Taiwan is seriously understudied. Likewise in Vietnam, with an area over nine times larger than Taiwan, only 19 linyphiid species have been recorded until today (Tanasevitch 2018a), indicating a considerable gap of knowledge about the Vietnamese linyphiid species diversity as well.

Shaanxinus males have a prominent prosomal modification. Its configuration is distinct from other erigonines, consisting of an elevated ocular region and a hairy clypeal groove (Fig. 1a, b). The clypeal groove is located horizontally below the eyes, formed by a depression of cuticle. The distances between the upper and the lower margin of the groove differ between species, varying from contacting each other to a broader groove. Besides their prosomal modifications, the male secondary genital organs on the pedipalps represent a second set of sexually dimorphic features. In linyphiids and other major spider families, male palps and female genitalia features are the most useful morphological characters for species and genus discrimination (Comstock 1910; Eberhard 1985; Eberhard and Huber 2010). The highly modified palps of male spiders are presumably subject to sexual selection more than to environmental factors, based on the fact that these genital organs do not appear until the final molt (Bristowe 1938; Jackson 1932). While the form of the male palp is similar in all erigonines, the embolic division (ED) is very variable (Millidge 1977). Understanding how the palpal structures, especially the ED, function during mating may provide insights into the mechanism of sexual selection on these organs.

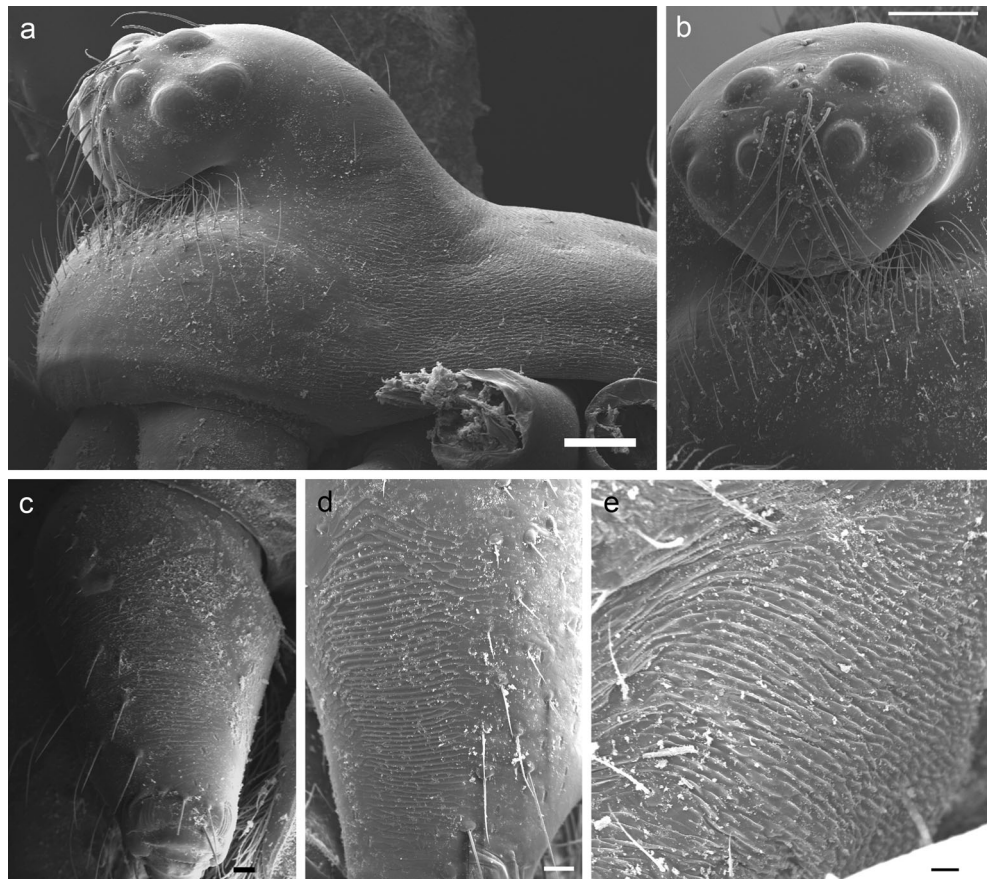
X-ray micro-computed tomography (micro-CT) has been applied as a tool to study arthropod anatomy since in the early twenty-first century (e.g., Fanenbruck et al. 2001; Hörnschemeyer et al. 2002), and it has been employed in studies on various organ systems such as the musculature, the digestive system, and the nervous system of arthropods (e.g., Tanisako et al. 2005; Betz et al. 2007; Mizutani et al. 2007, 2008; Beutel et al. 2008; Friedrich and Beutel 2008; Metscher 2009; Sombke et al. 2015). When dealing with type material, micro-CT offers a non-destructive way of scrutinizing and visualizing morphological features (e.g., Friedrich et al. 2013; Steinhoff and Uhl 2015). Its application also allows reconstruction of glandular tissues, e.g., glands

associated with the spermophore in a spider palp (Sentenská et al. 2017). Here, we explore whether micro-CT allows visualization of the distribution of amorphous glandular tissues associated with male prosomal modifications in erigonines. In addition, we also applied micro-CT to inspect the detailed cuticular structures of an artificially expanded male palp from a holotype, in order to understand the possible interactions between the sclerites on the palp.

Preliminary observation of Taiwanese *Shaanxinus* specimens indicated a paucity of useful somatic characters for species discrimination, and a high similarity of genital organs among congeners. However, traditional typological alpha-level description of species based on morphology alone may sometimes either overestimate or underestimate the number of actual species, by not identifying possible polymorphisms within species, or overlooking subtle morphological differences between species, respectively (Mayr 2000). To complement morphological means of classification, we incorporated phylogenetic analyses of DNA sequences (such as DNA barcodes, see below). The use of DNA barcoding provides an approach for molecular species identification based on sequence differences at short orthologous gene fragments (Hebert et al. 2003). The identification success of this method depends on genetic diversity being markedly lower within than between species, that is, it depends on the members of the same species being each other's closest relatives. This is operationally similar as basing the method on the assumption of species monophyly. Therefore, the tree-based methods for testing barcode efficacy all aim at the highest recovery of species monophyly, as implemented in the SPIDER package (Brown et al. 2012). DNA barcoding has the potential in assisting difficult morphological identification, as well as in revealing cryptic species (Hebert et al. 2004). In animals, barcoding relies on a short standard region of a single mitochondrial genetic marker, the cytochrome c oxidase subunit I gene (COI). It was shown effective in spider species delimitation and identification (e.g., Barrett and Hebert 2005; Robinson et al. 2009; Wang et al. 2017). Nevertheless, in some other taxa, the mitochondrial large subunit rRNA gene (16S) seems more effective in separating taxa compared to COI (Astrin et al. 2006 for pholcid spiders; Lopardo and Uhl 2014 for the erigonine genus *Oedothorax*). It is necessary to keep in mind, however, that species are not necessarily monophyletic. In particular, species paraphyly has been demonstrated to be a prevalent phenomenon (Funk and Omland 2003; Ross 2014), compromising the efficacy of species identification using DNA barcoding.

In the present work, the first author describes 13 new dwarf spider species collected in Taiwan plus one Vietnamese species from the spider collection of the Senckenberg Museum Frankfurt (SMF). These species are assigned to the genus *Shaanxinus*, based on their shared characteristics with the type species *S. rufus*. Micro-CT was applied for assessing the

Fig. 1 *Shaanxinus curviductus* sp. n. **a, b** Male prosoma. **a** Lateral view. **b** Frontal view. **c** Female right chelicera, lateral view. **d** Male right chelicera, lateral view. **e** Male book lung cover. Scale bars 100 μm in **a, b**; 20 μm in **c, d**; and 10 μm in **e**



dimension of glandular tissues associated with the prosomal structures in *S. rufus*, *S. mingchihensis* sp. n., and *S. tamdaoensis* sp. n., as well as the configuration of palpal structures in an expanded palp of the latter species. In addition, we tested the species' generic placement and inferred their interspecific relationships by means of a phylogenetic analysis based on morphological traits. Furthermore, hypotheses of morphology-based species delimitation and sex matching were compared and complemented with analyses of three of the conventional genetic markers in spider phylogenetics, including two fast-evolving mitochondrial genes, COI and 16S, and the more conservative large subunit nuclear 28S rRNA locus. The latter provided resolution in deeper phylogenies of jumping spiders (Maddison and Hedin 2003; Bodner and Maddison 2012). Intra- and interspecific genetic variation was calculated to assess the efficacy of these markers in species delimitation.

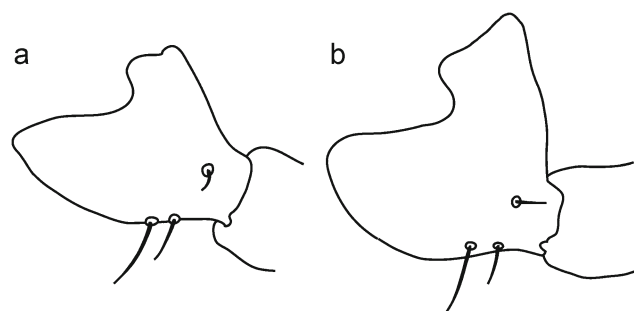
Material and methods

Specimen collection, examination, and description

Spiders were collected in Taiwan in 2014 and 2015 by beating tree branches and catching falling spiders with an umbrella.

Sampling locations were recorded manually at collecting sites according to kilometer markers on the roadside. Coordinates were subsequently assessed by using Google Earth. Specimens were preserved in 80% ethanol and stored at $-20\text{ }^{\circ}\text{C}$ for 1 to 6 months at the Department of Entomology, National Taiwan University, then transported at ambient temperature to the Department of General and Systematic Zoology, University of Greifswald. Specimens were then examined, sorted morphologically, and stored in 70% ethanol at room temperature. Part of the non-type specimens was stored at $-40\text{ }^{\circ}\text{C}$ for preservation of DNA for molecular work. Specimens were studied using a Zeiss Discovery V20 stereo microscope, equipped with a Zeiss AxioCam MRc Digital camera and AxioVision 4.8 software. Measurements were taken with the AxioVision 4.8 software. Photos were produced with a Visionary Digital BK Plus Lab System (duninc.com/bk-plus-lab-system.html) equipped with a Canon EOS 6D and a customized Canon MP-E 651-5 \times Macro Lens for habitus photos, and Mitutoyo M Plan Apo $\times 10$ lens for images of genital features. Female genitalia (epigynes) were excised and macerated with a KOH solution (0.5 g KOH crystals in 8 ml distilled water) heated on a hot plate with double-boiler arrangement for 25 to 40 min in order to lighten the color of sclerotized parts. We mounted macerated epigynes on shallow depression microscope slides equipped with a drop of

Fig. 2 Palpal tibia of **a** *Shaanxinus magniclypeus* sp. n. and **b** *S. hehuanensis* sp. n., dorsal view



Eugenol. Each sample was overlaid with a coverslip, observed, and illustrated with an Olympus CX40 compound microscope connected to a camera lucida. Male palps were dissected at the femur-patella joint and mounted in Eugenol. Drawings were performed by hand. Scanned drawings were edited in Adobe Illustrator and Adobe Photoshop.

For scanning electron microscopy (SEM), one male and one female of *S. curviductus* sp. n. (collected in Litungshan) were cleaned in 5% KOH following the protocol by Schneeberg et al. (2017). An additional pair of male and female was processed but not subjected to KOH. Specimens were dehydrated in an ascending alcohol series and critical point dried with a Leica EM CPD300, mounted on aluminum stubs equipped with sticky copper tape and additionally glued with conductive silver (ACHESON Silver DAG (4-Methylpentan-2-on)). Specimens were sputter-coated with gold-palladium (ratio 80/20; Polaron SC7640, Fisons Instruments) and photographed with a Zeiss EVO LS 10 at an accelerating voltage of 10 kV.

For micro-CT scans, one *S. rufus* paratype, one *S. mingchihensis* sp. n. male paratype, and the *S. tamdaoensis* sp. n. holotype were dehydrated through a graded ethanol series (70, 80, 90, 95, 99% ethanol). To enhance tissue contrast, specimens were transferred to a 1% iodine solution (iodine, resublimated [Carl Roth GmbH & Co. KG, Karlsruhe, Germany; cat. #X864.1] in 99.8% ethanol) for 48 h (Sombke et al. 2015). Samples were washed in 99% ethanol twice, at 24-h interval. Samples were subsequently mounted in modified plastic pipette tips as follows. Tips were modified with heat from a candle flame to adjust the internal diameter to the size of the specimens. The tips were sealed at the narrower end by pressing the heated wall with forceps, and filled with 99% ethanol. After transfer of the specimens into the tips, the open ends were sealed by hot-melt adhesive. Micro-CT scans were performed using an optical laboratory-scale X-ray microscope (Zeiss XradiaXCT-200), which entails a two-stage magnification (geometric and optical magnification) (Sombke et al. 2015). For *S. rufus* and *S. mingchihensis* sp. n., scans were performed with a $\times 20$ objective lens unit using the following settings: 40 kV voltage/ 8 W power and an exposure time of 3 s. These settings resulted in scan times of about 2 h and a pixel size between 1 and

1.5 μm . Tomography projections were reconstructed using XMReconstructor (Carl Zeiss Microscopy GmbH), resulting in image stacks (TIFF format). All scans were performed using Binning 2 (Camera Binning) for noise reduction and subsequently reconstructed with full resolution (using Binning 1). The 3D visualization of image stacks was performed using AMIRA 6.0.1 (Visualization Science Group, FEI). For *S. tamdaoensis*, the setting was the same, except the scan time of about 4 h.

Abbreviations used in the text or figures are given in Table 1. Abbreviations of morphological structures follow mostly Hormiga (2000) and Tanasevitch (2006). References to figures in the cited papers are listed in lower case (fig. or figs.); figures from this paper are noted with an initial capital (Fig. or Figs.).

Measurements

The following morphological measurements were taken. Males: groove height: distance between upper and lower margins of clypeal groove; groove-clypeal margin: distance between upper margin of clypeal groove and lower margin of clypeus; groove-AME: distance between upper margin of clypeal groove and lower margin of AME; ALE-ALE: distance between mesal margins of the ALEs; patella length/height: ratio between length and height of palpal patella; femur/patella: relative length of palpal femur, i.e., as ratio between femur and patella lengths. Females: spermathecae width: distance between lateral-most margins of spermathecae. Males and females: total length: distance between lower margin of clypeus and posterior edge of opisthosoma, in lateral view; carapace length: distance between lower edge of clypeus and posterior edge of carapace, i.e. posterior rim; carapace width: distance at the widest part of carapace; length of opisthosoma: distance between anterior ventral edge of pedicellar tube and posterior edge of opisthosoma excluding spinnerets; lengths of femur, patella, tibia, metatarsus, and tarsus of walking legs; Tm I: ratio between distance from proximal end of metatarsus I to metatarsal trichobothrium and length of metatarsus I. All measurements are in millimeters, with arithmetic means in brackets.

Table 1 List of abbreviations used in the text or figures

Male: pedipalp	
ARP	Anterior radical process
ARS	Anterior radical scaly part
BH	Basal haematodocha
C	Cymbium
E	Embolus
ED	Embolus division
MM	Median membrane
F	Fundus
LER	Lateral extension of radix
MSA	Marginal suprathegular apophysis
PC	Paracymbium
PT	Protegulum
R	Radix
SPT	Suprathegulum
ST	Subtegulum
T	Tegulum
TP	Radical tailpiece
Female: epigyne	
CD	Copulatory duct
FD	Fertilization duct
S	Spermatheca
Ocular area	
ALE	anterior lateral eye(s)
AME	anterior median eye(s)
Spinneret	
AC	Aciniform gland spigot(s)
AG	Aggregate gland spigot(s)
ALS	Anterior lateral spinneret
CY	Cylindrical gland spigot(s)
FL	Flagelliform gland spigot(s)
mAP	Minor ampullate gland spigot(s)
PLS	Posterior lateral spinneret
PMS	Posterior median spinneret
Institutions	
NMNS	National Museum of Natural Science, Taichung, Taiwan
SMF	Senckenberg Museum, Frankfurt am Main, Germany
ZIMG	Zoological Institute and Museum, University Greifswald, Germany
ZMUC	Zoological Museum, University of Copenhagen, Denmark

Morphological phylogenetic analyses

The character matrix for phylogenetic analyses based on 30 discrete and 6 continuous characters was edited and managed using Mesquite 3.10 (Maddison and Maddison 2017). Phylogenetic analyses were carried out using TNT

(Goloboff et al. 2008) with random seed 1, 500 replications, 1000 trees saved per replication, branch swapping by TBR algorithm. Character optimization and tree editing were performed in WinClada version 1.00.08. (Nixon 2002). Morphological continuous characters in this data set were treated as ordered, and analyzed as such (Goloboff et al. 2006). Continuous characters carry phylogenetic information (e.g., Thiele 1993; Rae 1998; Wiens 2001; Humphries 2002; Goloboff et al. 2006; González-José et al. 2008; Lopardo and Hormiga 2015) and with this treatment, the problems with discretization of continuous characters can be avoided (Farris 1990; Wiens 2001; Humphries 2002; e.g., Clouse et al. 2010; de Bivort et al. 2010). We calculated two clade support measures using TNT: Bremer support (tree suboptimal by 4 steps during TBR retained from existing trees) and Jackknife support (removal probability = 36%).

Selection of outgroup taxa was based on a phylogenetic analysis suggesting close relatedness of *Shaanxinus* to *Oedothorax* Bertkau, 1883, and other erigonines (77 taxa, 157 characters; S-W.L., L.L. and G.U., unpublished). Outgroup taxa include: *Linyphia triangularis* (Clerck, 1758) (1♂, ZMUC), *Erigone atra* (Blackwall, 1833) (1♂, ZIMG), *Oedothorax gibbosus* (Blackwall, 1841) (1♂ 1♀, ZMUC), *Oedothorax coronatus* (Tanasevitch, 1998) (1♂, SMF), and *Nasoonia crucifera* (Thorell, 1895) (1♂ 1♀, ZMUC).

Ingroup taxa include *S. mingchihensis* sp. n. (1♂ 1♀, ZIMG), *S. makauyensis* sp. n. (1♂ 1♀, ZIMG), *S. magniclypeus* sp. n. (1♂ 1♀, ZIMG), *S. hirticephalus* sp. n. (1♂ 1♀, ZIMG), *S. curviductus* sp. n. (1♂ 1♀, ZIMG), *S. tsou* sp. n. (1♂ 1♀, ZIMG), *S. meifengensis* sp. n. (1♂ 1♀, ZIMG), *S. hehuanensis* sp. n. (1♂ 1♀, ZIMG), *S. shihchoensis* sp. n. (1♂ 1♀, ZIMG), *S. lixiangae* sp. n. (1♂ 1♀, ZIMG), *S. seediq* sp. n. (1♂ 1♀, ZIMG), *S. atayal* sp. n. (1♂ 1♀, ZIMG), *S. shoukaensis* sp. n. (1♂ 1♀, ZIMG), *S. tamdaoensis* sp. n. (1♂, SMF), and *S. rufus* Tanasevitch, 2006 (1♂, SMF).

DNA sequencing

DNA sequence data of the three genetic markers (see below) were obtained from all 13 Taiwanese *Shaanxinus* species totaling 75 specimens, plus one male individual of *N. crucifera*. Four legs of each specimen were used for DNA extraction, with the remainder of the specimen preserved as morphological voucher. Genomic DNA was extracted with the Qiagen DNeasy Blood & Tissue Kit (QIAGEN GmbH, Hilden, Germany) following the manufacturer's protocol, with an incubation time of 16 h. Fragments of the COI (ca. 680 bp), 16S (ca. 460 bp), and 28S (ca. 810 bp) markers were amplified (respectively) with primers LCO1490, HCO2198 (Folmer et al. 1994), 16Sa, 16Sb (Palumbi et al. 1991), 28Sa (Whiting et al. 1997), and 28Sgh2F (Lopardo et al. 2011) (biomers.net GmbH, Ulm, Germany). Concentration of primer stock solutions applied in all PCRs: LCO1490 1.

14 nmol, HCO2198 1.14 nmol, 16Sa 1.75 nmol, 16Sb 2.7 nmol, 28Sa 2.52 nmol, and 28Sgh2F 0.8 nmol. Polymerase chain reactions (PCR) contained either BIOTAQ or MyTaq (Bioline GmbH, Germany). PCR protocol using BIOTAQ (most 28S (70/76), part of 16S (21/76) and part of COI (21/76)): reaction mixes (15 μ l) included 1.5 μ l 5 \times reaction buffer, 1.2 μ l 50 mmol MgCl₂, 0.3 μ l 10 mmol dNTP, 0.06 μ l BIOTAQ, 0.4 μ l of each primer, and 1 μ l DNA template. PCR cycle steps for 16S and COI: initial denaturation step (2 min, 94 °C), 35 \times (30 s at 94 °C; 30 s at 42 °C, 90 s at 72 °C), final extension step (5 min, 72 °C). PCRs for 28S differed in the annealing temperature at 44 °C. PCR protocol using MyTaq (several 28S (6/76), larger proportion of 16S (55/76), and larger proportion of COI (55/76)): reaction mixes (10 μ l) included 5 μ l MyTaq HS Red Mix 2 \times , 0.2 μ l of each primer, and 1 μ l DNA template. PCR cycle steps: initial denaturation step (1 min, 95 °C), 35 \times (15 s at 95 °C; 15 s at 42 °C, 40 s at 72 °C), final extension step (5 min, 72 °C). For unsuccessful sequencing, PCRs were repeated with 45 cycles to increase the target yield. PCRs were carried out on an Applied Biosystems Veriti thermal cycler (Applied Biosystems, CA) and visualized with agarose gel electrophoresis (1%) in TAE buffer using RotiGelStain (Carl Roth GmbH, Germany). PCR products were purified using ExoSAP-IT PCR Product Cleanup Reagent (Thermo Fisher) and subsequently sequenced using the PCR primers and the ABI PRISM BigDye Terminator cycle sequencing kit (Applied Biosystems) with an annealing temperature of 48 °C. Cycle sequencing products were purified using HighPrep DTR Dye Terminator Removal Clean Up (MagBio Genomics) prior to being run on an ABI 3130xl Genetic Analyser (Applied Biosystems). All molecular work was carried out in the sequencing facility, ZIMG. Resulting sequences were BLASTed (Altschul et al. (1997) against the GenBank nucleotide database (as of November 11th, 2017). Most similar hits were erigonine species. All new sequences generated in this study are deposited in GenBank (see Table 2). All molecular vouchers are stored in ZIMG.

Alignment and evolutionary model selection

DNA sequences of different lengths were aligned with the program MAFFT v.7 (Katoh et al. 2002; Katoh and Standley 2013). Pairwise alignment followed the E-INS-I strategy with default settings. Best-fit evolutionary models of DNA substitution for each marker were evaluated with the program jModeltest v.2.1.10 (Guindon et al. 2003; Darriba et al. 2012). The following criteria for model selection were explored: the Akaike Information Criterion (AIC) (Akaike 1974), Akaike Information Criterion corrected for small sample sizes (AICc) (Hurvich and Tsai 1989), Bayesian Information Criterion (BIC) (Schwarz 1978), and a decision-theoretic performance-based approach (DT) (Minin et al.

2003). The four criteria were in agreement in all the analyses, and the model selection was straightforward (Table 3).

Molecular phylogenetic analyses

Datasets

As in morphological phylogenetic analysis, we selected outgroup taxa based on close relationships suggested by the result of a phylogenetic analysis (77 taxa, 157 characters; S-W.L., L.L. and G.U., unpublished) and the availability of all three sequences of COI, 16S, and 28S on GenBank, which are *N. crucifera*, *L. triangularis*, *Hylyphantes graminicola* (Sundevall, 1830), *Oedothorax apicatus* (Blackwall, 1850), and *Ummeliata insecticeps* (Bösenberg & Strand, 1906). For an additional non-erigonine linyphiid representative, of which sequences are available in GenBank, *Tenuiphantes tenuis* Blackwall, 1852 was selected. In addition, *Pimoa rupicola* (Simon, 1884) was incorporated based on the sister relationship between Pimoidae and Linyphiidae. Individuals with unsuccessful sequences for at least one marker were not considered and therefore, as stated above, the ingroup consisted of 76 individuals.

Parsimony analyses

COI, 16S, 28S, and the combined dataset of these three markers were analyzed performing heuristic searches with parsimony under equal weights using the program TNTv.1.1 (Goloboff et al. 2008). The most parsimonious trees were found using heuristic searches that consisted of 500 replicates, using tree bisection-reconnection branch swapping (TBR), saving 1000 trees per replication. Gaps were treated as fifth state. Bremer support (BS, Bremer 1988, 1994) and relative Bremer support (relative fit difference, RFD, Goloboff and Farris 2001) were calculated. Jackknife frequencies were calculated in TNT by computing 4000 pseudoreplicates.

Bayesian analyses

Bayesian analyses were carried out for each marker and the combined dataset in MrBayes ver.3.2.6 (Ronquist et al. 2012). Two independent runs of 4,000,000 generations using four Markov Chain Monte-Carlo (MCMC) chains and sampling trees every 500 generations were performed. The standard deviation of split frequencies lower than 0.01 ensured convergence of the runs. The first 25% samples were discarded as *burnin*. Effective sample sizes (ESSs) were analyzed with the program Tracer v1.7 (Rambaut et al. 2018). In all analyses, ESSs were higher or much higher than 200, indicating that a large number of independent samples were drawn from the posterior distribution, minimizing correlation among the samples. Posterior probabilities were calculated and reported as a

Table 2 List of *Shaanxinus* specimens from Taiwan that were analyzed in this study, including outgroup taxa for the phylogenetic analyses. Locality, source (if sequence not generated in this study), GenBank accession numbers, and ZIMG museum voucher numbers are given

Specimen	Sex	Population	16S	COI	28S	Voucher/source
<i>Hyllyphantes graminicola</i>			JN816487.1 (AY078664.1)	KY270332.1 KY270457.1	JN816917.1 (EU003410.1)	16S and 28S: Jang (2012); COI: Astrin et al. (2016) 16S: Homrighaus et al. (2003); COI: Astrin et al. (2016); 28S: Alvarez-Padilla et al. (2009)
<i>Linyphia triangularis</i>			KF906727.1	KY270268.1	KT003057.1+ FJ838734.1	16S: Lopardo and Uhl (2014); COI: Astrin et al. (2016); 28S: Wang et al. (2015) and Arnedo et al. (2009)
<i>Oedothorax apicatus</i>			MG201051.1	MG201051.1	MG200876.1	Ballarin and Li (2018)
<i>Pimoa rupicola</i>			FJ838693.1	KC244266.1	FJ838739.1	16S and 28S: Arnedo et al. (2009); COI: Vink and Kean (2013)
<i>Tenuiphantes tenuis</i>			JN816490.1	JN817123.1	JN816921.1; GU338552.1	16S, COI, 28S: Jang and Hwang (2011); 28S: Wang, Q., Li, S., and Murphy, R.W. (2009), unpublished
<i>Ummeliata insecticeps</i>						
<i>Nasoona crucifera</i> _Taiwan_92	M	Shimianshan	MHI68430	MHI73176	MHI65401	
<i>S._curviductus</i> _m_TA_7	M	Taian	MHI68431	MHI73177	MHI65402	
<i>S._curviductus</i> _m_TA_8	M	Taian	MHI68432	MHI73178	MHI65403	
<i>S._curviductus</i> _m_TA_9	M	Taian	MHI68433	MHI73179	MHI65404	
<i>S._curviductus</i> _m_TA_10	M	Taian	MHI68434	MHI73180	MHI65405	
<i>S._curviductus</i> _m_TA_11	M	Taian	MHI68435	MHI73181	MHI65406	
<i>S._curviductus</i> _m_TA_12	M	Taian	MHI68436	MHI73182	MHI65407	
<i>S._curviductus</i> _m_TA_26	M	Taian	MHI68450	MHI73196	MHI65421	
<i>S._curviductus</i> _m_BP_27	M	Wujhishan	MHI68451	MHI73197	MHI65422	
<i>S._curviductus</i> _f_BP_28	F	Wujhishan	MHI68452	MHI73198	MHI65423	
<i>S._curviductus</i> _f_CSLDMt_32	F	Litungshan	MHI68455	MHI73201	MHI65426	
<i>S._curviductus</i> _m_CSLDMt_70	M	Litungshan	MHI68488	MHI73234	MHI65459	
<i>S._curviductus</i> _f_CSLDMt_71	F	Litungshan	MHI68489	MHI73235	MHI65460	
<i>S._curviductus</i> _f_CSLDMt_72	F	Litungshan	MHI68490	MHI73236	MHI65461	
<i>S._curviductus</i> _m_TA_73	M	Taian	MHI68491	MHI73237	MHI65462	
<i>S._curviductus</i> _m_BP_74	M	Beipu	MHI68492	MHI73238	MHI65463	
<i>S._curviductus</i> _m_BP_75	M	Beipu	MHI68493	MHI73239	MHI65464	
<i>S._curviductus</i> _f_BP_76	F	Beipu	MHI68494	MHI73240	MHI65465	
<i>S._curviductus</i> _f_BP_77	F	Beipu	MHI68495	MHI73241	MHI65466	
<i>S._mingchiensis</i> _m_QL_13	M	Qilan	MHI68437	MHI73183	MHI65408	
<i>S._mingchiensis</i> _f_MC_16	F	Mingchih	MHI68440	MHI73186	MHI65411	
<i>S._makauyensis</i> _f_MC_84	F	Mingchih	MHI68499	MHI73245	MHI65470	
<i>S._makauyensis</i> _m_MC_14	M	Mingchih	MHI68438	MHI73184	MHI65409	
<i>S._makauyensis</i> _f_QL_15	F	Qilan	MHI68439	MHI73185	MHI65410	
<i>S._makauyensis</i> _f_MC_83	F	Mingchih	MHI68498	MHI73244	MHI65469	
<i>S._magnichlypeus</i> _eastern_m_TTSMMt_17	M	Shimianshan	MHI68441	MHI73187	MHI65412	
<i>S._magnichlypeus</i> _eastern_f_TTSMMt_18	F	Shimianshan	MHI68442	MHI73188	MHI65413	
<i>S._magnichlypeus</i> _eastern_m_HLCKMt_19	M	Chikeshan	MHI68443	MHI73189	MHI65414	
<i>S._magnichlypeus</i> _eastern_f_HLCKMt_20	F	Chikeshan	MHI68444	MHI73190	MHI65415	
<i>S._magnichlypeus</i> _eastern_m_TTSK_21	M	Shouka	MHI68445	MHI73191	MHI65416	
<i>S._magnichlypeus</i> _northern_m_TPPL_54	M	Pinglin	MHI68472	MHI73218	MHI65443	
<i>S._magnichlypeus</i> _northern_f_TPPL_55	F	Pinglin	MHI68473	MHI73219	MHI65444	
<i>S._magnichlypeus</i> _northern_f_TPYMMt_56	F	Lujiaokan Creek	MHI68474	MHI73220	MHI65445	
<i>S._magnichlypeus</i> _northern_f_TPSZ_57	F	Sanzhi	MHI68475	MHI73221	MHI65446	
<i>S._magnichlypeus</i> _northern_m_TPWL_58	M	Wanli	MHI68476	MHI73222	MHI65447	
<i>S._hirticephalus</i> _m_TTSK_22	M	Shouka	MHI68446	MHI73192	MHI65417	
<i>S._hirticephalus</i> _m_HLCKMt_23	M	Chikeshan	MHI68447	MHI73193	MHI65418	

Table 2 (continued)

Specimen	Sex	Population	16S	COI	28S	Voucher/source
<i>S. hirticephalus</i> _m_TTSK_24	M	Shouka	MHI 68448	MHI73194	MHI65419	
<i>S. hirticephalus</i> _f_TTSK_25	F	Shouka	MHI 68449	MHI73195	MHI65420	
<i>S. hirticephalus</i> _f_SK_67	F	Shouka	MHI 68485	MHI73231	MHI65456	
<i>S._sou_m_CYSC_30</i>	M	Shihcho	MHI 68453	MHI73199	MHI65424	
<i>S._sou_f_CYSC_31</i>	F	Shihcho	MHI 68454	MHI73200	MHI65425	
<i>S._sou_f_CYSC_78</i>		Shihcho	MHI 68496	MHI73242	MHI65467	
<i>S._sou_f_CYSC_79</i>		Shihcho	MHI 68497	MHI73243	MHI65468	
<i>S._meifengensis_m_MF_33</i>	M	Meifeng	MHI 68456	MHI73202	MHI65427	
<i>S._meifengensis_m_MF_34</i>	M	Meifeng	MHI 68457	MHI73203	MHI65428	
<i>S._meifengensis_f_MF_35</i>	F	Meifeng	MHI 68458	MHI73204	MHI65429	
<i>S._meifengensis_f_MF_36</i>	F	Meifeng	MHI 68459	MHI73205	MHI65430	
<i>S._hehuanensis_f_YF_37</i>	F	Yuanfeng	MHI 68460	MHI73206	MHI65431	
<i>S._hehuanensis_f_HH_38</i>	F	Mount Hehuan	MHI 68461	MHI73207	MHI65432	
<i>S._hehuanensis_m_HH_39</i>	M	Mount Hehuan	MHI 68462	MHI73208	MHI65433	
<i>S._hehuanensis_m_YF_40</i>	M	Yuanfeng	MHI 68463	MHI73209	MHI65434	
<i>S._hehuanensis_f_HH_85</i>	F	Mount Hehuan	MHI 68500	MHI73246	MHI65471	
<i>S._hehuanensis_m_YF_86</i>	M	Yuanfeng	MHI 68501	MHI73247	MHI65472	
<i>S._hehuanensis_m_YF_87</i>	M	Yuanfeng	MHI 68502	MHI73248	MHI65473	
<i>S._hehuanensis_f_YF_88</i>	F	Yuanfeng	MHI 68503	MHI73249	MHI65474	
<i>S._hehuanensis_f_YF_89</i>	F	Yuanfeng	MHI 68504	MHI73250	MHI65475	
<i>S._shihchouensis_f_CYSC_41</i>	F	Shihcho	MHI 68464	MHI73210	MHI65435	
<i>S._shihchouensis_m_CYSC_42</i>	M	Shihcho	MHI 68465	MHI73211	MHI65436	
<i>S._shihchouensis_m_CYSC_43</i>	M	Shihcho	MHI 68466	MHI73212	MHI65437	
<i>S._lixiangae_f_QL_49</i>	F	Mingchih	MHI 68467	MHI73213	MHI65438	
<i>S._lixiangae_m_MC_50</i>	M	Qilan	MHI 68468	MHI73214	MHI65439	
<i>S._seediq_m_MF_51</i>	M	Meifeng	MHI 68469	MHI73215	MHI65440	
<i>S._seediq_f_MF_52</i>	M	Meifeng	MHI 68470	MHI73216	MHI65441	
<i>S._seediq_f_MF_53</i>	F	Meifeng	MHI 68471	MHI73217	MHI65442	
<i>S._seediq_f_CSLDMt_68</i>	F	Litungshan	MHI 68486	MHI73232	MHI65457	
<i>S._seediq_f_CSLDMt_69</i>	F	Litungshan	MHI 68487	MHI73233	MHI65458	
<i>S._atayal_m_CSLDMt_59</i>	M	Litungshan	MHI 68477	MHI73223	MHI65448	
<i>S._atayal_f_CSLDMt_60</i>	F	Litungshan	MHI 68478	MHI73224	MHI65449	
<i>S._atayal_f_CSLDMt_61</i>	F	Litungshan	MHI 68479	MHI73225	MHI65450	
<i>S._atayal_m_CSLDMt_90</i>	M	Litungshan	MHI 68505	MHI73251	MHI65476	
<i>S._shoukaensis_f_SK_62</i>	F	Shouka	MHI 68480	MHI73226	MHI65451	
<i>S._shoukaensis_f_SK_63</i>	F	Shouka	MHI 68481	MHI73227	MHI65452	
<i>S._shoukaensis_m_SK_64</i>	M	Shouka	MHI 68482	MHI73228	MHI65453	
<i>S._shoukaensis_m_SK_65</i>	M	Shouka	MHI 68483	MHI73229	MHI65454	
<i>S._shoukaensis_m_SK_66</i>	M	Shouka	MHI 68484	MHI73230	MHI65455	

Table 3 Phylogenetic analyses dataset information for molecular markers

Datasets	Sequence length (in bp)	Sequence length with gap characters	Model selected by jModeltest (criteria)
16S	332–448	453	GTR + I + G (AIC, AICc, BIC, DT)
COI	583–685	685	GTR + I + G (AIC, AICc, BIC, DT)
28S	470–807	819	GTR + G (AIC, AICc, BIC, DT)

majority-rule consensus of the saved trees. Tree visualization was done using FigTree 1.4.3 (Rambaut 2016).

Efficacy of mitochondrial markers as DNA barcode

Mitochondrial marker efficacy was tested applying operational approaches based on sequence similarity, which require measuring identification accuracy and inter-/intraspecific sequence variation (Ward 2009; Brown et al. 2012). *N. crucifera* was used as the only outgroup taxon for both COI and 16S, as well as their combined dataset, each with a total of 76 terminals. Species delimitation efficacy was assessed by distance- and tree-based measures as implemented in the SPIDER package (Brown et al. 2012) in the R environment developed by R Core Team (2011). Intra- and interspecific estimates of evolutionary divergence (pairwise uncorrected distances) were also calculated in SPIDER, and used for both distance and tree-based measures. The substitution model proposed by Hebert et al. (2003) for calculating genetic distance for species identification was the Kimura-2-parameter model (K2P), and has been widely applied in barcoding studies. Nevertheless, Srivathsan and Meier (2012) demonstrated that for closely related COI sequences, the use of uncorrected distances yields higher or similar identification success rates for both tree-based and distance-based identification techniques than the K2P distance. The optimal genetic distance suitable as threshold for species delimitation for each dataset, by the criterion of lowest cumulative error, was assessed using the function “threshOpt” in SPIDER (Brown et al. 2012) (Table 4). Distance measures include Nearest Neighbor (NN) (Austerlitz et al. 2009), Barcode of Life Data Systems (BOLD) identification criterion (Brown et al. 2012), and Meier’s best close match (MBCM) (Meier et al. 2006). Tree-based measures using the neighbor-joining algorithm (Saitou and Nei 1987) include species monophyly, bootstrap monophyly (10,000 replicates), and Rosenberg’s probability of reciprocal monophyly (Rosenberg

2007). The only singleton, *N. crucifera*, was excluded from the calculations. Maximum intraspecific and minimum interspecific variations were calculated. The presence/absence of a Barcode Gap for each dataset and the combined dataset was assessed by examining whether there was an overlap between the maximum intraspecific and minimum interspecific variations.

To check for substitution saturation in COI sequences, identical sequences were excluded, resulting in 57 unique sequences. Numbers of transition and transversions versus Kimura’s two-parameter distance were plotted using DAMBE (Xia 2013, 2017), with the options of pairwise deletion and genetic distance model F84.

Results

Taxonomy

Family Linyphiidae Blackwall, 1859
Subfamily Erigoninae Emerton, 1882
Genus *Shaanxinus* Tanasevitch, 2006

Type species. *Shaanxinus rufus* Tanasevitch, 2006 by original designation

Diagnosis. The genus is characterized by a configuration of male prosomal modifications that is unique among known erigonines: Males have prosoma elevated at ocular region, hirsute clypeal groove, and hirsute clypeus (Fig. 1a, b). Additionally, male can be distinguished by the palpal tibia with an apical hollow varying in depth on the dorsoretrolateral side (Fig. 2), the suprategulum apophysis short, the distal part of PC scaly (Fig. 3c, g), and ED with characteristic configuration (see below). Despite the unique male prosomal features of *Shaanxinus*, this genus shares some similarities of male

Table 4 Efficacy analyses, dataset information, and optimum threshold values from cumulative error estimation

Partition	Length (aligned)	Base composition				SPIDER optimum threshold
		A	C	G	T	
16S	458	0.388	0.139	0.121	0.352	0.006
COI	685	0.403	0.239	0.143	0.214	0.008–0.01
Combined	1143	0.397	0.199	0.134	0.269	0.007–0.01

genitalia with *Nasoona* Locket, 1982, but the PC tip of *Nasoona* has no scaly region like in *Shaanxinus*. Females are similar to males in somatic features (but without prosomal modification) and also resemble *Nasoona* species. Females differ from the latter genus by a simpler epigynum, not projecting externally. Diagnostic features for species are mostly limited to shape of epigyne and body size.

Description. Rather large, yellowish-, brownish- to reddish-colored erigonines. Males: total length 2.03–3.95. Prosoma: yellow, red, or brown; darker around carapace furrow (thoracic furrow in Miller and Hormiga (2004)) in some species (e.g., *S. tsou* sp. n.); broad oval; carapace 0.97–1.62 long, 0.74–1.25 wide; prosoma sexually dimorphic, ocular region elevated; with hairy clypeal groove, upper and lower groove margins separated or in contact with each other (but not fused; e.g., in contact: *S. curviductus* sp. n.; separated: *S. hirticephalus* sp. n.); glandular tissues distributed around clypeal groove and part of the ocular region (Fig. 5b, c, e, f, h, i) clypeus directed obliquely backwards toward the ocular area (Fig. 1a); area in and below clypeal groove covered largely by short fine setae, in some species clypeus covered entirely by setae (e.g., *S. magniclypeus* sp. n.), in others central lower half region glabrous (e.g. *S. curviductus* sp. n., Fig. 1a); ventrolaterally pointing long setae distributed from the interocular region down to the groove in some species (Fig. 1b). Chelicerae: promargin with five teeth; retromargin with four teeth; numerous striae on lateral sides, compressed and evenly spaced (Fig. 1d). Legs: yellow to red; leg formula differs among species; tibial macrosetae quite robust, longer than diameter of tibia; all metatarsi with one trichobothrium (Tm I 0.79–0.91). Pedipalps: patella short, ratio length/height = 1.38–1.80; tibia with one prolateral and two retrolateral trichobothria; dorso-retrolaterally enlarged margin with dense setae and prolateral flat extension; a hollow between the two structures; PC with anteriorly oriented angle near junction with cymbium (e.g., Fig. 3b, pointed by arrow), distal part scaly, with/without mesal and retrolateral apophyses in addition to PC tip (e.g., with both: *S. curviductus* sp. n., Fig. 3f; with retrolateral: *S. shihchoensis* sp. n.; without either: *S. tamdaoensis* sp. n., Fig. 6) PC distal setae short or absent, four to eight basal setae; protegulum without papillae; tegular sac absent; suprattegulum semi-circular and short, MSA absent (*S. rufus*, Fig. 7) or present (e.g. *S. magniclypeus* sp. n., Fig. 8a); DSA short, inconspicuous; no visible MM in unexpanded palps, except *S. rufus* and *S. tamdaoensis* sp. n.; radix complex, with rather short, triangular radical tailpiece (Fig. 3d) and anterior radical process (Fig. 3a, d), distal part with outgrowth (LER, Fig. 3c, d), with folded edge hosting distal part of embolus in resting position; middle part of radix scaly; embolus slender and long, thin at tip, base connected to radix via joint (Fig. 3d); E with subterminal opening (Fig. 3e). Opisthosoma with intraspecifically variable stripe patterns on

beige background; PLS with two AG, one FL and several AC; PMS with two AC and one mAP (Fig. 4d–e).

Females: somatic features as in males, without prosomal modifications. Epigyne without prominent outgrowth (Fig. 4f); spermathecae one pair; copulatory openings as slits between ventral and dorsal plates of epigyne (Fig. 8f, h, indicated by arrows), posterior to spermathecae in all species with known females (e.g. *S. magniclypeus* sp. n., Fig. 8f–h) except *S. anguilliformis* (see original species description); copulatory ducts strongly sclerotized, length and trajectory differ among species, correlated to embolus length of conspecific male. In addition to spigots arrangement as in males, females possess two CY on PLS and one on PMS (Fig. 4a, c).

Remarks. Embolic length among species in this genus can be roughly divided into two groups: longer or shorter than width of cymbium (e.g., Figs. 3e and 8e, respectively). Species with long embolus: *S. hirticephalus* sp. n., *S. curviductus* sp. n., *S. meifengensis* sp. n., *S. hehuanensis* sp. n., *S. lixiangae* sp. n., *S. seediq* sp. n., *S. atayal* sp. n., *S. tamdaoensis* sp. n., *S. anguilliformis*, and *S. rufus*. Species with short embolus: *S. mingchihensis* sp. n., *S. magniclypeus* sp. n., *S. shihchoensis* sp. n., and *S. shoukaensis* sp. n.

Regarding curvature of spermophore within tegulum of pedipalp (from retrolateral view), species with more curved spermophore present a medium turn upward: *S. shihchoensis* sp. n., *S. shoukaensis* sp. n., *S. curviductus* sp. n., *S. tsou* sp. n., *S. hehuanensis* sp. n., *S. seediq* sp. n., *S. meifengensis* sp. n., and *S. atayal* sp. n. In species with less curved spermophore, the angle between medium turn and longitudinal axis of cymbium is larger than 45°: *S. magniclypeus* sp. n., *S. hirticephalus* sp. n., and *S. tamdaoensis* sp. n. *S. mingchihensis* sp. n., *S. makauyensis* sp. n., and *S. lixiangae* sp. n. have intermediate curvature, with a medium turn relatively parallel to the longitudinal axis of cymbium. *S. rufus* has no medium turn of spermophore (Fig. 7b).

Natural history. The Taiwanese species are arboreal spiders from low to middle-altitude forests, habitats range from underbrush formed by ferns or low bushes, vines rich of leaves, to high tree branches with or without leaf litter accumulated on them. Larger amount of individuals are more often found on branches on which litter has accumulated. *S. tamdaoensis* sp. n. was also collected in forests (800–1100 m amsl), but no information exists regarding its particular habitat. *S. rufus* from Shaanxi Province in China was collected from herbal vegetation at the roadside in secondary broadleaved forest, 1300–1700 m amsl (Peter Jäger, Frankfurt am Main, 2017, personal communication). No habitat data are available for *S. anguilliformis*.

Distribution. Shaanxi Province and Hebei Province in Northern China, Taiwan, and Vietnam.

Table 5 Morphological characters

Characters of males, discrete:

- Ch 1: E length: 0, long; 1, short
 Ch 2: ARS: 0, absent; 1, present (Fig. 3c)
 Ch 3: MM papillae: 0, absent; 1, present (Fig. 37a). Character 41 in Miller and Hormiga (2004)
 Ch 4: radix-embolus connection: 0, continuous; 1, membranous. Character 51 in Miller and Hormiga (2004)
 Ch 5: ARP: 0, absent; 1, present. Character 23 in Hormiga (2000); 55 in Miller and Hormiga (2004)
 Ch 6: LER: 0, absent; 1, present
 Ch 7: LER, marginal groove hosting distal part of embolus: 0, absent; 1, present
 Ch 8: spermophore in T: 0, with similar/slightly smaller diameter comparing to spermophore in ST; 1, much thinner than spermophore in ST
 Ch 9: spermophore curvature in T: 0, not particularly curved; 1, particularly curved (Fig. 25a)
 Ch 10: TS: 0, absent; 1, present. Character 10 in Hormiga (2000); 19 in Miller and Hormiga (2004)
 Ch 11: MSA: 0, absent; 1, present. Character 6 in Miller (1999); 14 in Hormiga (2000); 34 in Miller and Hormiga (2004)
 Ch 12: SPT junction with tegulum: 0, continuous; 2, with membrane. Character 12 in (Hormiga 2000); 12 in Zujko-Miller (1999); 25 in Miller and Hormiga (2004)
 Ch 13: PC base anterior protuberance: 0, absent; 1, present (Fig. 8a, indicated by arrow)
 Ch 14: PC distal part scaly: 0, absent; 1, present (Fig. 3f)
 Ch 15: PC distal setae: 0, absent; 1, present
 Ch 16: PC distal setae number: 0, more or equal to three; 1, fewer than three
 Ch 17: PC retrolateral apophysis: 0, absent (Fig. 8a, c); 1, present (Figs. 13c, 23c, indicated by arrow)
 Ch 18: PC retrolateral apophysis size: 0, small (Fig. 13c, indicated by arrow); 1, large (Fig. 29c, indicated by arrow)
 Ch 19: palpal tibia, retrolateral area with short and thick setae: 0, absent; 1, present (Fig. 15d, indicated by arrow)
 Ch 20: Palpal tibia prolateral extension: 0, pointed (Fig. 2a); 1, flat and prolaterally extended (Fig. 2b)
 Ch 21: clypeal groove: 0, absent; 1, present
 Ch 22: clypeal groove, laterally pointed setae: 0, absent (Fig. 9d); 1, present (Fig. 1b)
 Ch 23: clypeus hirsute: 0, absent; 1, present
 Ch 24: clypeus, lower half bald: 0, absent (Fig. 9d); 1, present (Fig. 1a)
 Ch 25: chelicerae, mastidia: 0, absent; 1, present
 Ch 26: length of first and second pair of legs: 0, second pair longer; 1, first pair longer or as long as second pair
 Ch 27: tibia III distal dorsal macrosetae: 0, absent; 1, present. Character 141 in Miller and Hormiga (2004)
 Ch 28: tibia IV distal dorsal macrosetae: 0, absent; 1, present. Character 143 in Miller and Hormiga (2004)
 Ch 29: metatarsus IV trichobothrium: 0, absent; 1, present Character 65 in Hormiga (2000); 152 in Miller and Hormiga (2004)

Character of females, discrete:

- Ch 30: copulatory opening direction: 0, laterally entering (Fig. 8h); 1, mesally entering (Fig. 29h)

Characters of males, continuous:

- Ch 31: ALE-ALE/carapace width
 Ch 32: groove-clypeal margin/carapace width
 Ch 33: AME-groove/carapace width
 Ch 34: carapace width/length
 Ch 35: carapace width/tibia IV length

Character of females, continuous:

- Ch 36: spermathecae width/carapace width

Shaanxinus rufus Tanasevitch, 2006

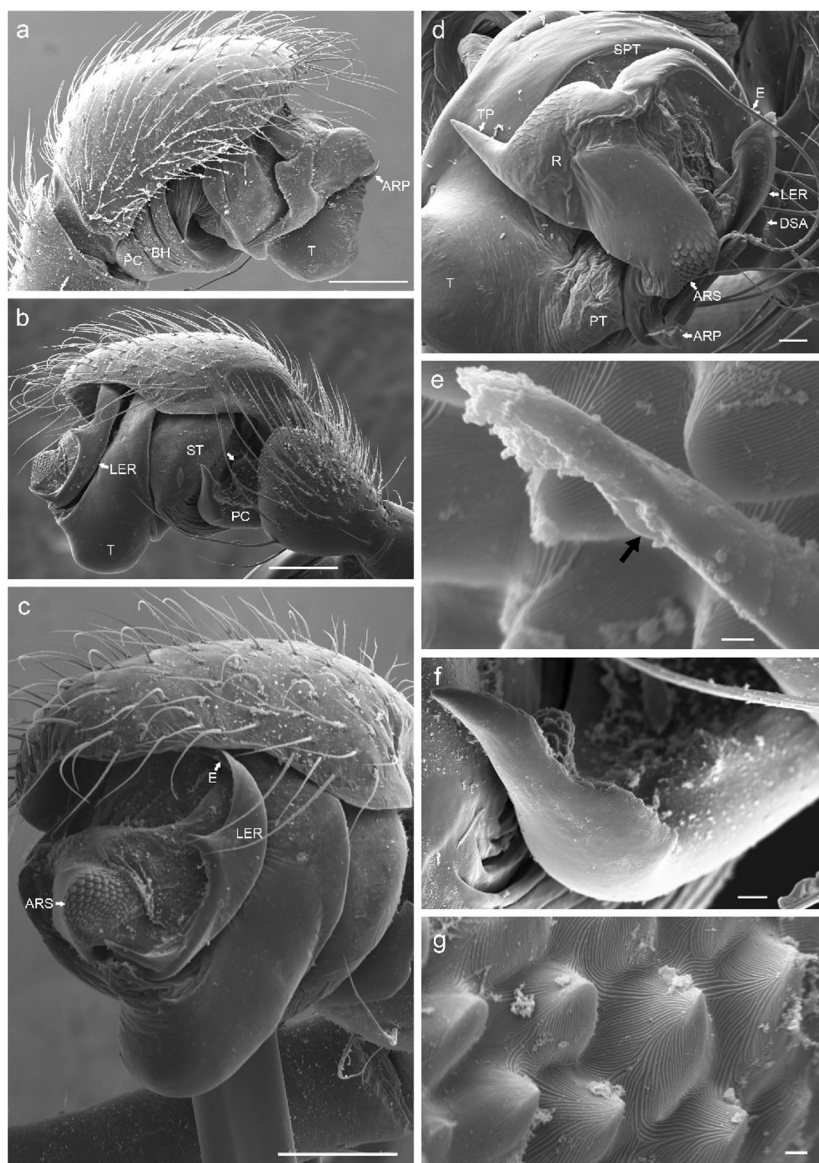
Figs. 5a–c and 7

Shaanxinus rufus Tanasevitch, 2006: 293, fig. 51–56 (Dm)

Type material. Holotype: ♂ (SMF), China, Shaanxi Prov., S flanks of Taibai Shan, above Houshenzi, secondary

broadleaved forest, 1300–1700 m, 23.VI.1997, leg. J. Martens & P. Jäger, examined. Paratypes: 2♂ (SMF), same, above Houshenzi, secondary broadleaved forest, 1300–1700 m, 19.VI.1997, leg. J. Martens & P. Jäger, examined; ♂ (ZMMU), same locality, 20.VI.1997, leg. J. Martens & P. Jäger, not examined.

Fig. 3 Left palp of *Shaanxinus curviductus* sp. n. male. **a–c, f, g** Unexpanded palp. **d, e** Expanded palp. **a** Prolateral. **b** Retrolateral. **c** Apical. **d** ED. **e** Embolic tip view. **f** PC, distal part. **g** Fine structure of ARS. Scale bars 100 μ m in **a, b, c**; 20 μ m in **d**; 10 μ m in **f**; and 1 μ m in **e, g**



Diagnosis. Males are distinguished from other *Shaanxinus* species by the anteriorly extended prosomal modification bearing eyes, less extended in other species. The Taiwanese and Vietnamese species share the following features and are distinct from *S. rufus*: chelicerae with a pair of mastidia (Fig. 5d, indicated by arrows; absent in *S. rufus*, Fig. 5a); tibia chaetotaxy 2-2-1-1 (*S. rufus* 2-2-2-2); PC distal setae 0–2 (five in *S. rufus*, Fig. 7b); strongly sclerotized scaly sclerite on radix (ARS, Fig. 8a; absent in *S. rufus*, Fig. 7c).

Description. See Tanasevitch (2006)

Distribution. Shaanxi Province, China.

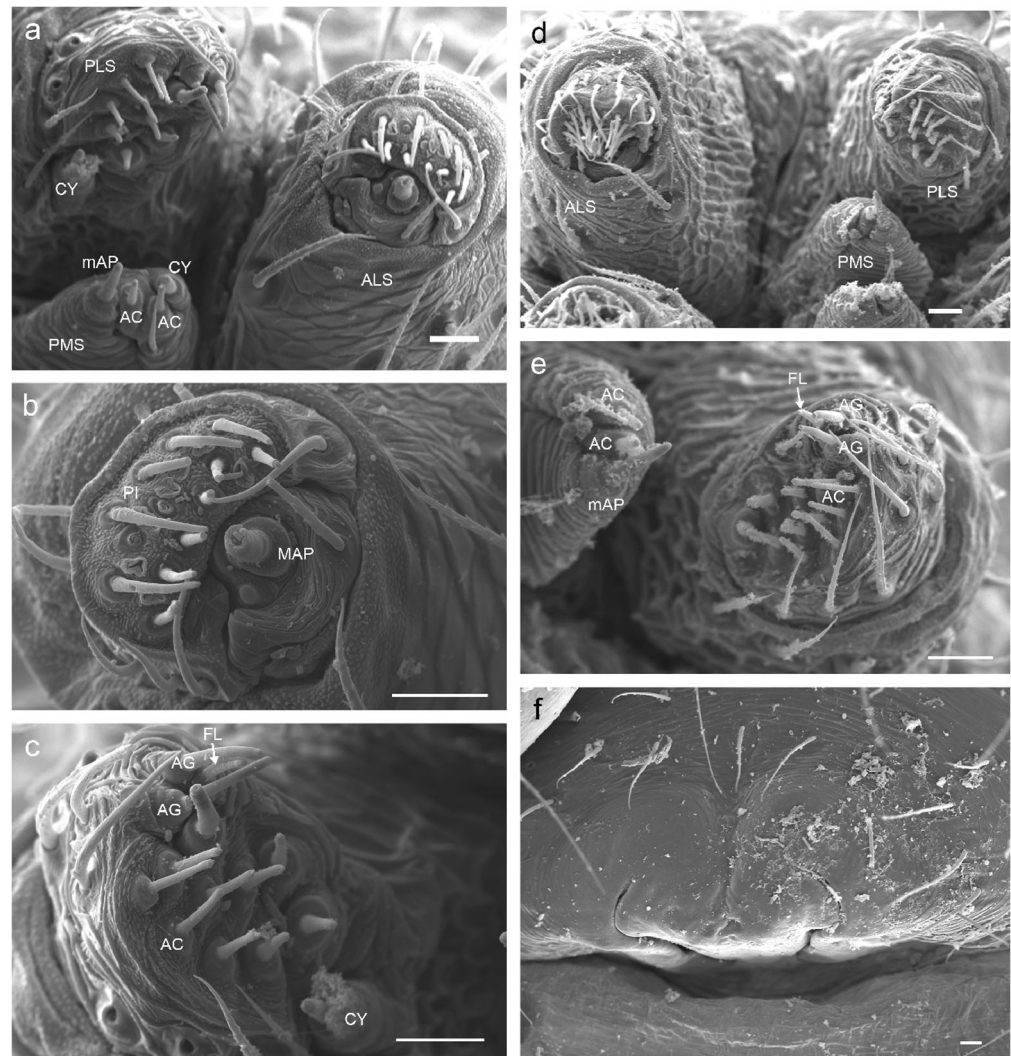
Shaanxinus anguilliformis (Xia, Zhang, Gao, Fei & Kim, 2001)
Walckenaeria anguilliformis Xia et al., 2001: 161 figs. 1–7 (Dmf)

Shaanxinus anguilliformis Tanasevitch, 2006: 296 (transfer from *Walckenaeria*).

Type material. >Holotype: ♂, 15.VI.1986 Zhangshiguan (38.0° N, 114.5° E), Shijiazhuang, Hebei Province, collected by Zhu, Mingsheng, not examined. Paratypes: 3 ♂ 6 ♀, same locality and date as holotype, not examined. Deposited in the Department of Cellular Biology, Norman Bethune University of Medical Science, Changchun, China.

Remarks. According to Shuqiang Li (Beijing, personal communication, 2017), all specimens of this species have been lost, along with all other spider specimens previously stored in the Department of Cellular Biology, Norman Bethune University of Medical Sciences, Changchun, China (now Norman Bethune Health Science Center of Jilin University). Consequently, the

Fig. 4 *Shaanxinus tsou* sp. n. photos. **a–d** Male habitus. **e–h** Female habitus. **a, e** Dorsal view. **b, f** Lateral view. **c, g** Ventral view. **d, h** Frontal view. Scale bars 1 mm



only available morphological reference for this species is the original description by Xia et al. (2001). For the purpose of interspecific comparison and diagnosis, the morphological content of the aforementioned article is rather incomplete and therefore this species was not included in our phylogenetic analysis. For example, there is no statement about male cheliceral mastidia, nor whether the clypeus is hirsute. One of the drawings, however, suggests a rather glabrous clypeus and clypeal groove (figs. 3–4 in Xia et al. 2001: 168). Unless the lack of setae is due to omission, this would be a substantial difference from all other congeners. Moreover, tibial chaetotaxy was also not stated. On the other hand, the drawings of the male palp (although with low resolution) suggest a similar congeneric configuration of the ED. The embolus seems to be thicker than in all other species. The epigyne drawings in figs. 6–7 in Xia et al. (2001): 168 indicate copulatory openings situated anterior to spermathecae, and the dorsal plate seems to have a middle ridge or scape, which are significantly different from all other *Shaanxinus* species with known females. Several features

indicate a close relationship between *S. rufus* and *S. anguilliformis* in comparison to other species. In both species, the legs II are much longer than the first pair. The species also share a similar shape of the PC tip. In addition, if the interpretation of the spermophore is correct (a dark band in retrolateral view of tegulum in fig. 2, Xia et al. 2001: 168), then the curvature is similar to that in *S. rufus*. The ARS is also not depicted, and it is here interpreted as absent. Absence of ARS also occurs in *S. rufus*. Despite difficulties impeding interspecific comparison, according to the shared features of *S. anguilliformis* with congeners and lack of evidence indicating closer relationship with other taxa, this species remains in the current classification.

Description. See Xia et al. (2001)

Distribution. Hebei Province, China

Shaanxinus magniclypeus Lin sp. n.
Figs. 2a, 8, 9, 10, 11 and 12

Fig. 5 Micro-CT reconstruction of *Shaanxinus* prosoma, based on scans conducted on samples in 99% ethanol. **a, d, g** External morphology. **b, e, h** Glandular tissues associated with prosomal modifications. **c, f, i** Virtual sections with glandular tissues outlined. **a–c** *S. rufus*. **d–f** *S. mingchihensis* sp. n. **g–i** *S. tamdaoensis* sp. n.

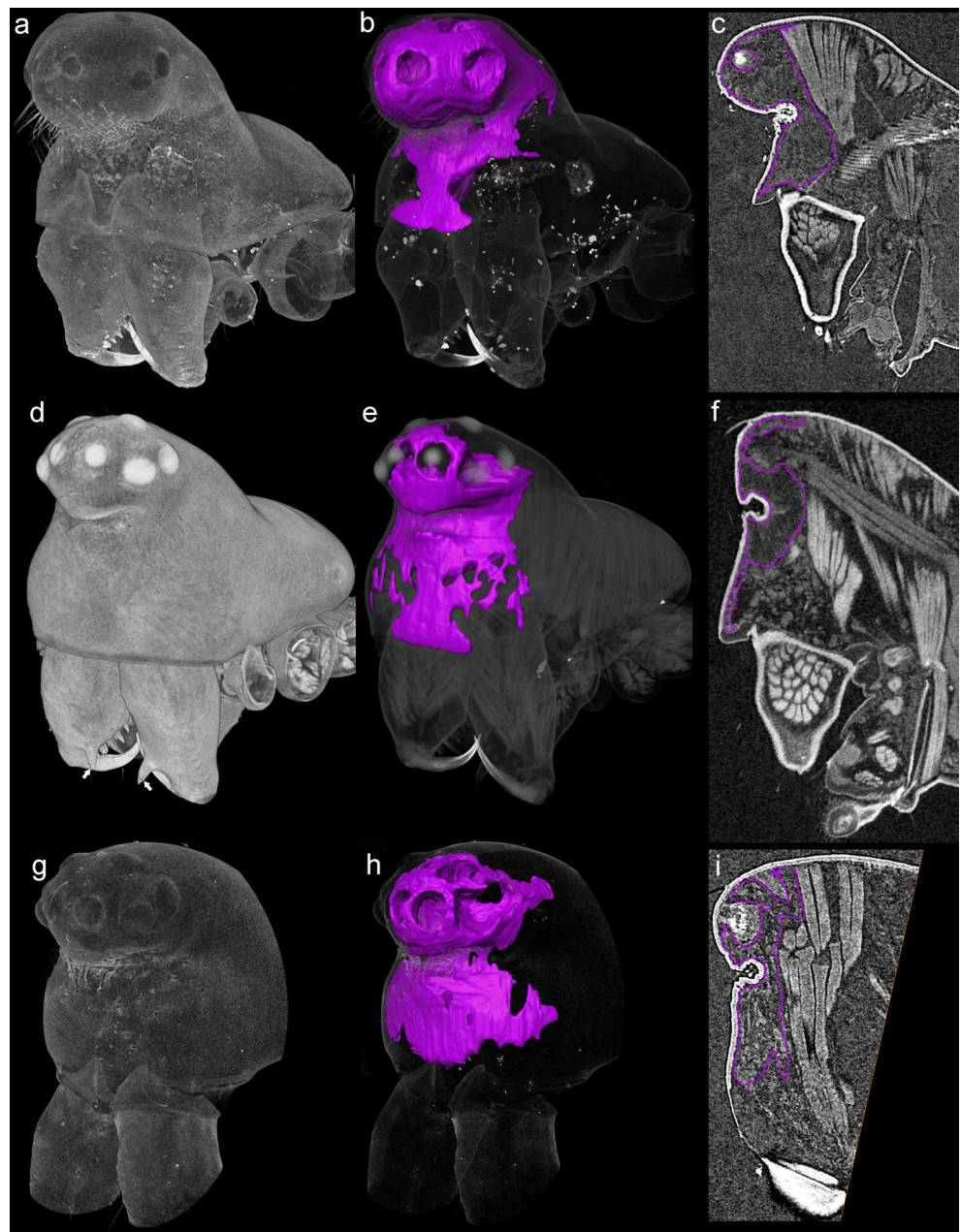


Fig. 6 Micro-CT reconstruction of the expended right palp of *S. tamdaoensis* sp. n. Sample in 99% ethanol during the scan. Green: PC; yellow: LER; blue: TP; purple: ARS; red: E

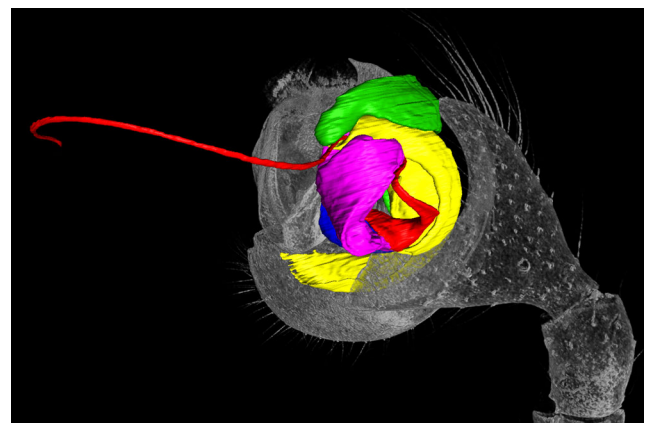
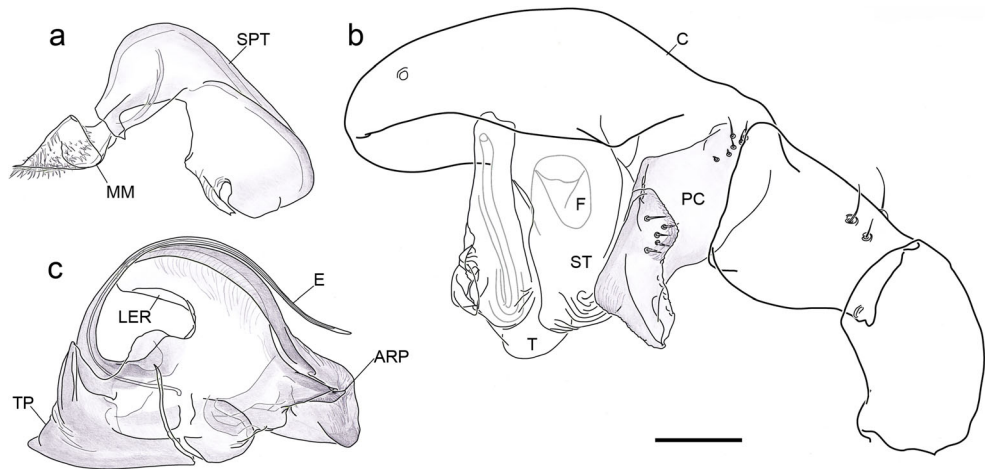


Fig. 7 Male right palp of *Shaanxinus rufus* (inverted). **a** Supratégulum and median membrane. **b** Retrolateral view, supratégulum and embolic division excised. **c** Embolic division. Scale bar 0.10 mm



Material: see below, as listed for the two geographical populations.

Derivatio nominis. The specific name is derived from the Latin “magnus,” meaning tall, and clypeus, referring to the especially tall clypeal region. The name is a noun in apposition.

Diagnosis. Males: Clypeus completely hirsute, central lower region not glabrous (Figs. 9d and 11d), a feature only shared with *S. hirticephalus* sp. n.; clypeal groove upper and lower margins not in contact, setae in groove short and thin, vertically oriented, which distinguishes this species from *S. mingchihensis* sp. n., *S. makauyensis* sp. n., *S. curviductus* sp. n., *S. tsou* sp. n., *S. meifengensis* sp. n., *S. hehuanensis* sp. n., *S. lixiangae* sp. n., *S. seediq* sp. n., and *S. atayal* sp. n.; PC tip simple, spoon-shaped; distal seta absent, mesal apophysis present, retrolateral apophysis absent (Figs. 8a, c and 10a, c), a combination of features only shared with *S. tamdaoensis* sp. n. Spermophore in retrolateral tegulum relatively weakly curved (Figs. 8d and 10d) (see generic description). Embolus short (Figs. 8e and 10e) (see generic description).

Females: general appearance of epigyne similar to *S. shihchoensis* sp. n. and *S. shoukaensis* sp. n., with dorsal and ventral plates not extended posteriorly; copulatory duct length shorter than these two species; shape of copulatory opening different from *S. shihchoensis* sp. n. by having less laterally extended dorsal plate; different from *S. shoukaensis* sp. n. because the latter has ventral plate extended ventrally over the dorsal plate at copulatory opening (Figs. 8g, h and 10g, h; see description and figures of *S. shihchoensis* sp. n. and *S. shoukaensis* sp. n.).

Remarks. Individuals collected from Hualien County and Pingtung County (Eastern population) showed morphological differences from those collected from Taipei City and New Taipei City (Northern population), and are described here separately.

Shaanxinus magniclypeus Lin sp. n., Eastern population
Figs. 2a, 8, 9 and 12

Type material. Holotype: ♂, Taitung County, Shimianshan, 396 m (22° 55' 53" N; 121° 10' 41" E), 19.VI.2014, tree branch beating, in subtropical broad-leaved forest, leg. S.-W. Lin (ZIMG-II-28404). Paratypes: 4♂ 6♀, same locality and date as holotype, tree branch beating, leg. S.-W. Lin (ZIMG-II-28405~28,414); 1♂, Pingtung County, Shizi Township, close to Shouka Cyclist Rest House, 458 m (22° 14' 34" N; 120° 50' 42" E), 20.VI.2014, tree branch beating, in subtropical secondary broad-leaved forest, leg. S.-W. Lin (ZIMG-II-28415). 4♂ 5♀, Hualien County, Yuli Township, close to Chikeshan, 750 m (23° 23' 13" N; 121° 22' 53" E), 19.VI.2014, tree branch beating, in subtropical secondary broad-leaved forest, leg. S.-W. Lin (2♂ 3♀ NMNS-7927-001~005; 2♂ 2♀ SMF).

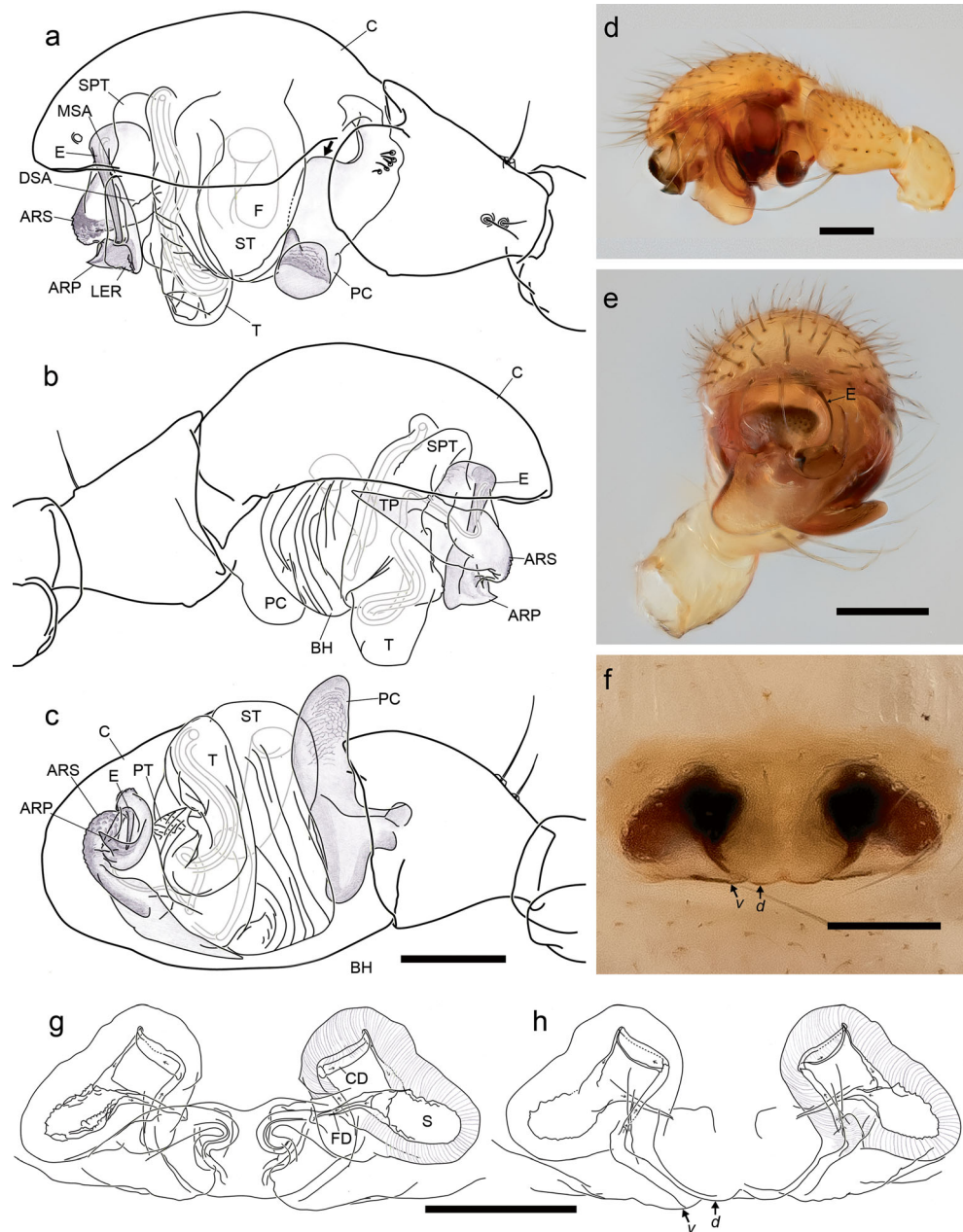
Other material. Same locality and date as holotype, tree branch beating, leg. S.-W. Lin 4♂ 6♀ (ZIMG-II-28416, 28418, 28419, 28421, 28423); Hualien County, Yuli Township, close to Chikeshan, 750 m (23° 23' 13" N; 121° 22' 53" E), 19.VI.2014, tree branch beating, in subtropical secondary broad-leaved forest, leg. S.-W. Lin 2♂ 5♀ (ZIMG-II-28417, 28420, 28422, 28424).

Diagnosis. Males: distance between clypeal groove upper and lower margins large, also significantly larger than Northern population (*t* test, $n_1 = 10$, $n_2 = 10$, $t = 4.4074$, $p < 0.001$). PC gradually decreases in width from middle part toward tip.

Females: Posterior margin of dorsal plate slightly sclerotized (Fig. 8f).

Description. Male (Holotype, ZIMG): total length: 2.47. Carapace 1.15 long, 0.87 wide. Opisthosoma 1.34 long, 0.81 wide. ALE-ALE: 0.141. Clypeal groove height: 0.031; groove-clypeal margin: 0.46; AME-groove: 0.077. Leg

Fig. 8 *Shaanxinus magniclypeus* sp. n., Eastern population, **a–e** Male left palp, drawings and photos. **a, d** Retrolateral view. **b** Prolateral view. **c** Ventral view. **e** Apical view. **f–h** Epigyne, photo and drawings. **f, h** Ventral view, “*d*” dorsal plate, “*v*”: ventral plate. **g** Dorsal view. Scale bars 0.10 mm



formula $2 > 4 > 1 > 3$; leg measurements see Appendix Table 10; Tm I: 0.86. Pedipalp: patella length/height = 1.39; femur/patella = 3.89. Palpal features and prosomal modifications as in diagnosis and generic description.

Female (Paratype, ZIMG): total length: 2.77. Carapace 1.08 long, 0.85 wide. Leg formula $2 = 1 > 4 > 3$; leg measurements see Appendix Table 10; Tm I: 0.83. Opisthosoma 1.68 long, 1.13 wide. Spermathecae width: 0.3. See diagnosis and generic description for somatic features and epigyne morphology.

Variation. Measurements based on type material (10♂, 10♀).

Males ($n = 10$): total length: 0.2–0.25 (2.38). Carapace 0.97–1.21 (1.13) long, 0.74–0.93 (0.85) wide. ALE-ALE:

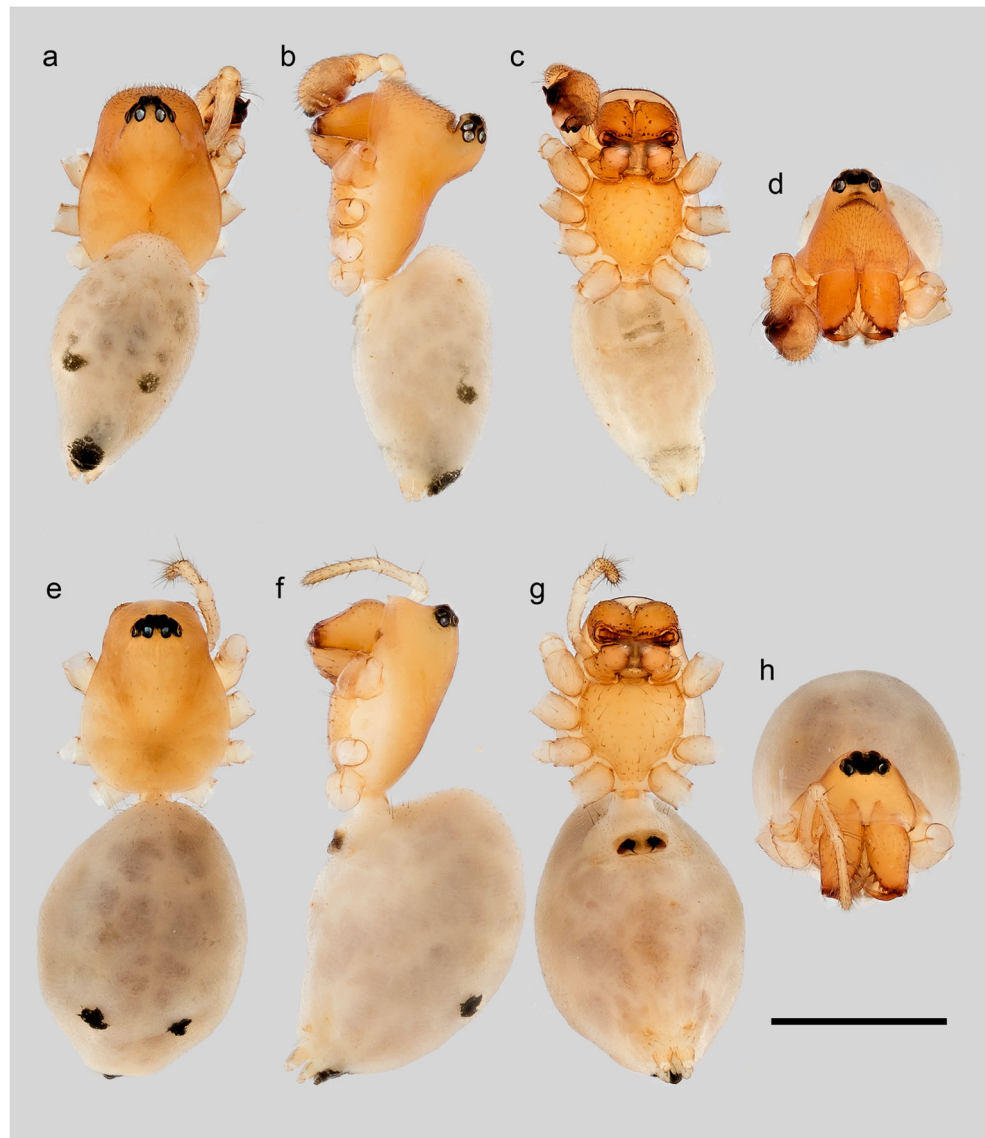
0.114–0.159 (0.14). Groove height: 0.013–0.054 (0.03). Groove-clypeal margin: 0.37–0.49 (0.45). AME-groove: 0.068–0.09 (0.078). Tm I: 0.81–0.88 (0.83).

Females ($n = 10$): total length: 2.6–3.05 (2.8). Carapace 1.08–1.33 (1.15) long, 0.82–0.97 (0.87) wide. Spermathecae width: 0.27–0.3 (0.28); distance between two copulatory openings: 0.13–0.154 (0.143). Tm I: 0.81–0.9 (0.86).

Distribution. Taiwan, Hualien County, Pingtung County.

Shaanxinus magniclypeus Lin sp. n., Northern population Figs. 10, 11 and 12

Fig. 9 *Shaanxinus magniclypeus* sp. n., Eastern population, photos. **a–d** Male habitus. **e–h** Female habitus. **a, e** Dorsal view. **b, f** Lateral view. **c, g** Ventral view. **d, h** Frontal view. Scale bars 1 mm

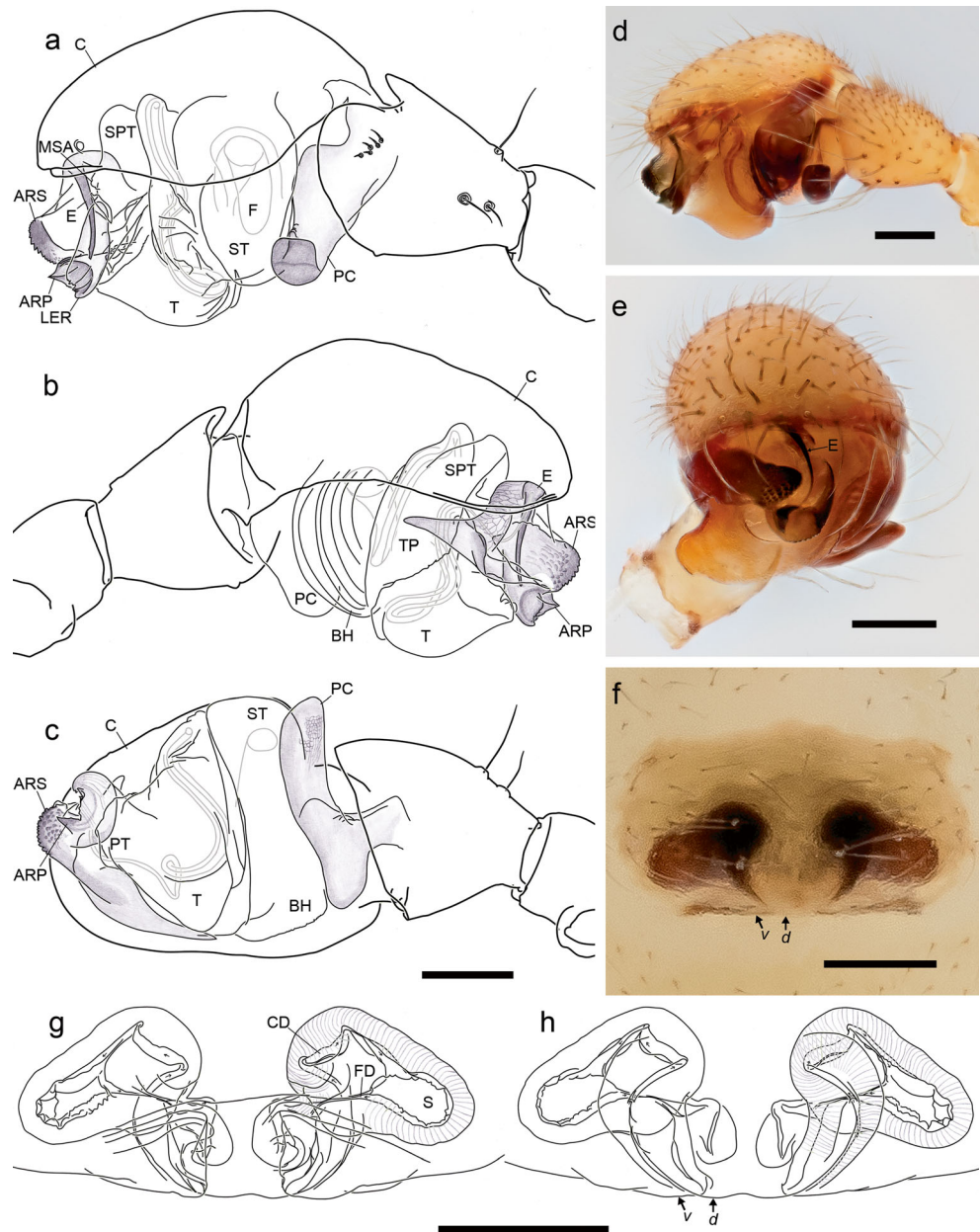


Type material. Paratypes: 1♂ 1♀, Taipei City, close to Lujiaoken Creek, 350 m (25° 11' 26" N; 121° 34' 32" E), 15.V.2014, tree branch beating, in subtropical broad-leaved forest, leg. S.-W. Lin (ZIMG-II-28425, 28431); 1♀, same locality, 29.IV.2014, leg. S.-W. Lin (ZIMG-II-28432); 2♂, New Taipei City, Wanli District, close to Masu creek, 290 m (25° 09' 34" N; 121° 37' 25" E), 21.IV.2014, tree branch beating, in subtropical secondary broad-leaved forest, leg. S.-W. Lin (ZIMG-II-28426, 28427); 1♂ 1♀, New Taipei City, Sanzhi District, 222 m (25° 13' 39" N; 121° 31' 28" E), 21.IV.2014, tree branch beating, in subtropical secondary broad-leaved forest, leg. S.-W. Lin (ZIMG-II-28428, 28,433); 3♂ 5♀, New Taipei City, Pinglin District, 371 m (24° 58' 01" N; 121° 44' 25" E), 24.IV.2014, tree branch beating, in subtropical secondary broad-leaved forest, leg. S.-W. Lin (SMF); 3♂ 2♀, New Taipei City, Pinglin District, close to Pinglin Elementary School Yuguang, 397 m (24° 57' 43" N; 121° 44' 13" E), 16.V.2014, tree branch beating, in

subtropical secondary broad-leaved forest, leg. S.-W. Lin (NMNS-7927-006~010).

Other material. Taipei City, close to Lujiaoken Creek, 350 m (25° 11' 26" N; 121° 34' 32" E), 15.V.2014, tree branch beating, in subtropical broad-leaved forest, leg. S.-W. Lin 1♀ (ZIMG-II-28434); same locality, 29.IV.2014, leg. S.-W. Lin 1♀ (ZIMG-II-28435); New Taipei City, Pinglin District, 371 m (24° 58' 01" N; 121° 44' 25" E), 24.IV.2014, tree branch beating, in subtropical secondary broad-leaved forest, leg. S.-W. Lin 1♂ 4♀ (ZIMG-II-28429, 28,436, 28,437); New Taipei City, Wanli District, close to Masu creek, 290 m (25° 09' 34" N; 121° 37' 25" E), 21.IV.2014, tree branch beating, in subtropical secondary broad-leaved forest, leg. S.-W. Lin 1♂ (ZIMG-II-28430); New Taipei City, Pinglin District, close to Pinglin Elementary School Yuguang, 397 m (24° 57' 43" N; 121° 44' 13" E), 16.V.2014, tree branch beating, in subtropical

Fig. 10 *Shaanxinus magniclypeus* sp. n., Northern population, **a–e** Male left palp, drawings and photos. **a, d** Retrolateral view. **b** Prolateral view. **c** Ventral view. **e** Apical view. **f–h** Epigyne, photo and drawings. **f, h** Ventral view, “*d*” dorsal plate, “*v*” ventral plate. **g** Dorsal view. Scale bars 0.10 mm



secondary broad-leaved forest, leg. S.-W. Lin 1♂ 1♀ (ZMUC); New Taipei City, Sanzhi District, 222 m (25° 13' 39" N; 121° 31' 28" E), 21.IV.2014, tree branch beating, in subtropical secondary broad-leaved forest, leg. S.-W. Lin 1♀ (ZIMG-II-28438).

Diagnosis. Clypeal groove upper and lower margins slightly away from each other in most examined specimens (9/10), in contrast to larger distance in Eastern population (see description of the latter); PC middle part as wide as distal part. Other diagnostic features refer to generic description and Eastern population.

Females differ from Eastern population in the weaker sclerotization on the posterior margin of dorsal epigynal

plate. See generic description and diagnosis of Eastern population.

Description. Male (paratype, ZIMG): total length: 2.4. Carapace 1.11 long, 0.85 wide. Opisthosoma 1.29 long, 0.86 wide. ALE-ALE: 0.149. Clypeal groove height: 0.007; groove-clypeal margin: 0.41. AME-groove: 0.078. Leg formula 2 > 1 > 4 > 3; leg measurements see Appendix Table 10; Tm I: 0.83. Pedipalp: patella length/height = 1.62; femur/patella = 4.16. Palpal features and prosomal modifications as in diagnosis and generic description.

Female (Paratype, ZIMG): total length: 2.79. Carapace 1.08 long, 0.83 wide. Opisthosoma 1.68 long, 1.21 wide. Leg

Fig. 11 *Shaanxinus magniclypeus* sp. n., Northern population, photos. **a–d** Male habitus. **e–h** Female habitus. **a, e** Dorsal view. **b, f** Lateral view. **c, g** Ventral view. **d, h** Frontal view. Scale bars 1 mm



formula 1 = 2 > 4 > 3; leg measurements see Appendix Table 10; Tm I: 0.84. Spermathecae width: 0.29. See diagnosis and generic description for somatic features and epigyne morphology.

Variation. Measurements based on type material (10♂, 10♀).

Males ($n = 10$): total length: 2.33–2.57 (2.45). Carapace 1.1–1.17 (1.13) long, 0.81–0.87 (0.84) wide. AME-groove: 0.078–0.096 (0.086). ALE-ALE: 0.136–0.152 (0.145). Groove-clypeal margin: 0.36–0.44 (0.41). Groove height: 0–0.019 (0.011). Tm I: 0.79–0.85 (0.82).

Females ($n = 10$): total length: 2.52–3.33 (2.79). Carapace 1.05–1.25 (1.13) long, 0.81–0.93 (0.85) wide. Spermathecae width: 0.25–0.32 (0.28); distance between two copulatory openings: 0.096–0.134 (0.114). Tm I: 0.81–0.88 (0.84).

Distribution. Taiwan, Taipei City, New Taipei City.

Shaanxinus shihchoensis Lin sp. n.

Figs. 12, 13 and 14

Type material. Holotype: ♂, Chiayi County, Zhushi Township, close to Shihcho Mountain, 1181 m (23° 28' 22" N; 120° 41' 33" E), 5.V.2014, tree branch beating, in subtropical secondary broad-leaved forest, leg. S.-W. Lin (ZIMG-II-28439). Paratypes: 9♂ 10♀, same locality and date as holotype, tree branch beating, leg. S.-W. Lin (3♂ 4♀, ZIMG-II-28440, 28441, 28442; 3♂ 3♀, SMF; 3♂ 3♀, NMNS-7927-011~016).

Other material. Same locality and date as holotype, tree branch beating, leg. S.-W. Lin (10♂ 20♀, ZIMG-II-28452, 28443~28445, 28447, 28454, 28455; 9♂ 7♀, ZMUC); Chiayi County, Fanlu Township, 324 m (23° 27' 38" N; 120° 35' 25" E), 5.V.2014, tree branch beating, in subtropical secondary broad-leaved forest, leg. S.-W. Lin, 1♂ 2♀ (ZIMG-II-28446, 28453).

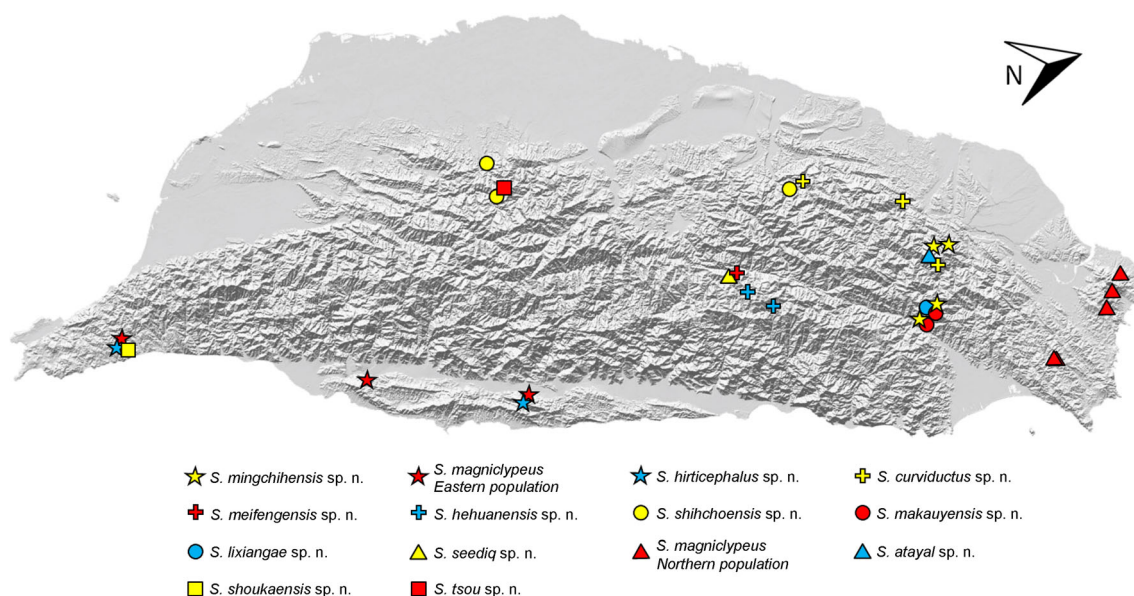


Fig. 12 Collecting sites of *Shaanxinus* in Taiwan. Two or more symbols next to each other represent sites where multiple species were collected; the location is at the center between symbols

Derivatio nominis. The specific name is an adjective derived from the mountain “Shihcho” near the collecting site of the holotype.

Diagnosis. Males: clypeal groove upper and lower margins contacting at the middle; setae on upper and lower margins nearly vertically oriented (Fig. 14d), a feature differentiating this species from *S. mingchihensis* sp. n., *S. makauyensis* sp. n., *S. curviductus* sp. n., *S. tsou* sp. n., *S. meifengensis* sp. n., *S. hehuanensis* sp. n., *S. lixiangae* sp. n., *S. seediq* sp. n., and *S. atayal* sp. n. Retrolateral apical palpal tibia without short stout setae, which distinguish this species from its similar species *S. shoukaensis* sp. n. PC with 1–2 distal setae; tip simple, spoon-shaped; mesal apophysis absent, retrolateral apophysis present, basally situated (Fig. 13a, c), a combination of PC features shared only with *S. shoukaensis* sp. n. Spermophore in retrolateral tegulum relatively strongly curved, S-shaped (Fig. 13d) (see generic remarks). Embolus relatively short (Fig. 13e) (see generic remarks). *S. shihchoensis* sp. n. can be distinguished from the morphologically similar *S. shoukaensis* sp. n. by the shape of PC, the ratio of AME-groove to carapace width, significantly larger in *S. shihchoensis* sp. n. (t test, $n_1 = 10$, $n_2 = 7$, $t = 6.8512$, $p < 0.001$), and the significantly smaller ratio of groove-clypeal margin to carapace width (t test, $n_1 = 10$, $n_2 = 7$, $t = -6.2378$, $p < 0.01$).

Females: epigynal dorsal and ventral plates not extended posteriorly; dorsal plate at copulatory openings extends laterally over ventral plate; copulatory ducts relatively short (Fig. 13g, h). Epigyne similar to *S. shoukaensis* sp. n.; in the latter the ventral plate extends ventrally over dorsal plate at copulatory opening, and posterior margin of dorsal plate less heavily sclerotized (Fig. 13f).

Description. Male (Holotype, ZIMG): total length: 2.52. Carapace 1.16 long, 0.91 wide. Opisthosoma 1.35 long, 0.85 wide. ALE-ALE: 0.239. Clypeus hirsute, central distal region glabrous; groove height: 0; groove-clypeal margin: 0.27. AME-groove: 0.161. Leg formula 1 = 2 > 4 > 3; leg measurements see Appendix Table 10; Tm I: 0.86. Pedipalp: patella length/height = 1.62; femur/patella = 4.57. Palpal features and prosomal modifications as described in diagnosis and generic description.

Female (Paratype, ZIMG): total length: 2.62. Carapace 1.1 long, 0.88 wide. Opisthosoma 1.45 long, 0.96 wide. Leg formula 1 = 2 > 4 > 3; leg measurements see Appendix Table 10; Tm I: 0.84. Spermathecae width: 0.263. See diagnosis and generic description for somatic features and epigyne morphology.

Variation. Measurements based on type material (10♂, 10♀).

Males ($n = 10$): total length: 2.26–2.76 (2.48). Carapace 1.05–1.28 (1.17) long, 0.82–0.96 (0.9) wide. ALE-ALE: 0.205–0.255 (0.236). Groove height: 0–0 (0). Groove-clypeal margin: 0.25–0.3 (0.29). AME-groove: 0.14–0.17 (0.157). Tm I: 0.82–0.89 (0.85).

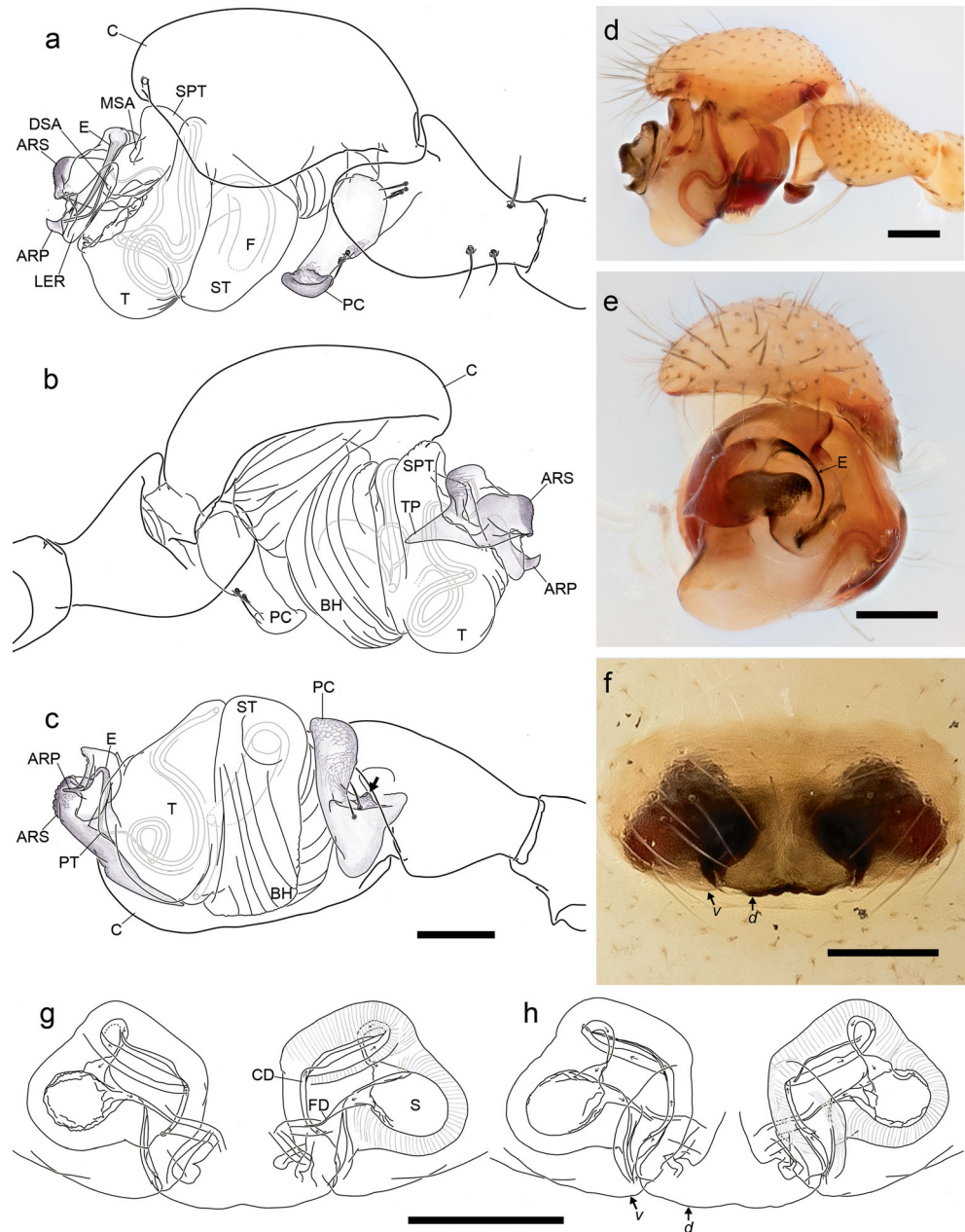
Females ($n = 10$): total length 2.5–3.04 (2.7). Carapace 1.05–1.19 (1.12) long, 0.81–0.93 (0.87) wide. Spermathecae width: 0.25–0.29 (0.27); Tm I: 0.82–0.89 (0.86).

Distribution. Taiwan, Chiayi County.

Shaanxinus shoukaensis Lin sp. n.
Figs. 12, 15 and 16

Type material. Holotype: ♂, Pingtung County, Shizi Township, close to Shouka cyclist rest house, 458 m (22°

Fig. 13 *Shaanxinus shihchoensis* sp. n., **a–e** Male left palp, drawings and photos. **a, d** Retrolateral view. **b** Proateral view. **c** Ventral view. **e** Apical view. **f–h** Epigyne, photo and drawings. **f, h** Ventral view, “*d*” dorsal plate, “*v*” ventral plate. **g** Dorsal view. Scale bars 0.10 mm



14° 34' N; 120° 50' 42' E), 20.VI.2014, tree branch beating, in subtropical secondary broad-leaved forest, leg. S.-W. Lin (ZIMG-II-28456). Paratypes: 6♂, same locality and date as holotype, leg. S.-W. Lin (ZIMG-II-28457~28,462); 7♀, same locality as holotype, 20.VI.2014, leg. S.-W. Lin (ZIMG-II-28463~28,469).

Derivatio nominis. The specific name is an adjective derived from Shouka Cyclist Rest House (Japanese: Kotobukidouge), a near the collecting site of the type specimens.

Diagnosis. Males: middle part of clypeal groove upper and lower margins contacting each other, setae on upper and lower groove vertically oriented (Fig. 16d), which distinguishes this

species from *S. mingchihensis* sp. n., *S. makuyensis* sp. n., *S. curviductus* sp. n., *S. tsou* sp. n., *S. meifengensis* sp. n., *S. hehuanensis* sp. n., *S. lixiangae* sp. n., *S. seediq* sp. n., and *S. atayal* sp. n. PC with one distal seta; tip simple, spoon-shaped; mesal apophysis absent; retrolateral apophysis present, basally situated (Fig. 15a, c), a combination of PC features shared only with *S. shihchoensis* sp. n. Spermophore in retrolateral tegulum relatively strongly curved, S-shaped (Fig. 15a) (see generic remarks). Embolus relatively short (Fig. 15e) (see generic remarks). *S. shoukaensis* sp. n. can be distinguished from the morphologically similar *S. shihchoensis* sp. n. by the shape of PC, the significantly smaller ratio of AME-groove to carapace width, and the significantly larger ratio of groove-clypeal margin to

Fig. 14 *Shaanxinus shihchoensis* sp. n. photos. **a–d** Male habitus. **e–h** Female habitus. **a, e** Dorsal view. **b, f** Lateral view. **c, g** Ventral view. **d, h** Frontal view. Scale bars 1 mm



carapace width (see significance values in *S. shihchoensis* sp. n. diagnosis).

Females: epigynal dorsal and ventral plates not extended posteriorly; margins of copulatory openings formed by ventral plate extend mesally (Fig. 15h). See also generic description and diagnosis of *S. shihchoensis* sp. n. female.

Description. Male (holotype, ZIMG): total length: 2.45. Carapace 1.14 long, 0.86 wide. Opisthosoma 1.35 long, 0.85 wide. ALE-ALE: 0.228. Clypeus hirsute, central distal region glabrous; groove height: 0; groove-clypeal margin: 0.32; AME-groove: 0.126; Leg formula 1 = 2 > 4 > 3; leg measurements see Appendix Table 10; Tm I: 0.82. Pedipalp: patella length/height = 1.72; femur/patella = 4.87. Palpal features and prosomal modifications as generic description.

Female (Paratype, ZIMG): total length: 2.44. Carapace 1.02 long, 0.81 wide. Opisthosoma 1.37 long, 0.88 wide. Leg formula 1 = 2 > 4 > 3; leg measurements see Appendix Table 10;

Tm I: 0.87. Spermathecae width: 0.25. See diagnosis and generic description for somatic features and epigyne morphology.

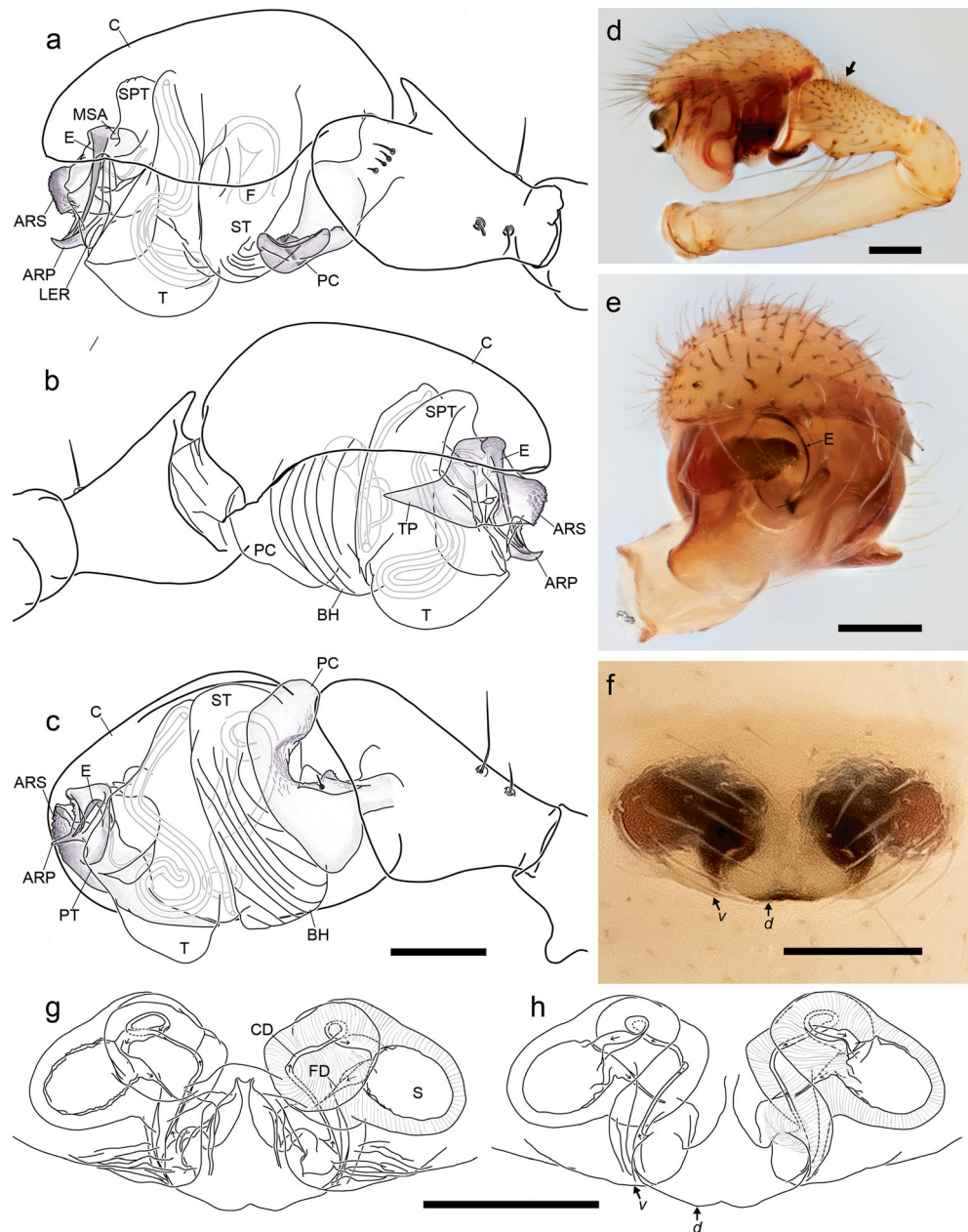
Variation. Measurements based on type material (7♂ 7♀).

Males ($n = 7$): total length: 2.15–2.49 (2.29). Carapace 1–1.14 (1.07) long, 0.76–0.86 (0.8) wide. ALE-ALE: 0.189–0.228 (0.205). Groove height: 0–0 (0). Groove-clypeal margin: 0.28–0.32 (0.3). AME-groove: 0.098–0.126 (0.114). Tm I: 0.82–0.89 (0.84).

Females ($n = 7$): total length: 2.42–2.66 (2.44). Carapace 0.89–1.04 (0.99) long, 0.75–0.83 (0.79) wide. Spermathecae width: 0.21–0.26 (0.24). Tm I: 0.84–0.88 (0.86).

Remarks. At the collecting site of the male specimens of this new species, male specimens of *S. hirticephalus* sp. n. and *S. magniclypeus* sp. n. were also found. Due to the close morphological similarity between males of *S. shihchoensis* sp. n. and *S. shoukaensis* sp. n., and the confidence in the matching of sexes of the former species. The tentative matching of the

Fig. 15 *Shaanxinus shoukaensis* sp. n., **a–e** Male left palp, drawings and photos. **a** Retrolateral view. **b** Proteralateral view. **c** Ventral view. **d** Retrolateral view. **e** Apical view. **f–h** Epigyne, photo and drawings. **f, h** Ventral view, “*d*” dorsal plate, “*v*” ventral plate. **g** Dorsal view. Scale bars 0.10 mm



five female specimens at this location with males of *S. shoukaensis* sp. n. was based on similarity of epigyne morphology and ratio between lengths of legs I and II to females of closely related species *S. shihchoensis* sp. n. This matching has been corroborated by mtDNA data.

Distribution. Taiwan, Pingtung County

Shaanxinus hirticephalus Lin sp. n.

Figs. 12, 17 and 18

Type material. Holotype: ♂, Hualien County, Fuli Township, 22.III.2015, tree branch beating, in subtropical broad-

leaved forest, leg. S.-W. Lin (ZIMG-II-28470). Paratypes: 1♂, Pingtung County, Shizi Township, close to Shouka cyclist rest house, 458 m (22° 14' 34" N; 120° 50' 42" E), 20.VI.2014, tree branch beating, in subtropical broad-leaved forest, leg. S.-W. Lin (ZIMG-II-28471); 2♂ 2♀, Pingtung County, Shizi Township, close to Shouka cyclist rest house, 458 m (22° 14' 34" N; 120° 50' 42" E), 22.III.2015, tree branch beating, in subtropical broad-leaved forest, leg. S.-W. Lin (ZIMG-II-28472, 28474–28,476); 1♂, Hualien County, Yuli Township, close to Chikeshan, 750 m (23° 23' 13" N; 121° 22' 53" E), 19.VI.2014, tree branch beating, in subtropical secondary broad-leaved forest, leg. S.-W. Lin (ZIMG-II-28473).

Fig. 16 *Shaanxinus shoukaensis* sp. n. photos. **a–d** Male habitus. **e–h** Female habitus. **a, e** Dorsal view. **b, f** Lateral view. **c, g** Ventral view. **d, h** Frontal view. Scale bars 1 mm



Derivatio nominis. The specific name is derived from the Latin “hirtus,” meaning hairy, and cephalic, referring to the unique long-haired region on the prosoma behind the ocular region. This name is a noun in apposition.

Diagnosis. Males: clypeal groove upper and lower margins not contacting each other; setae in groove vertically oriented, which distinguishes this species from *S. mingchihensis* sp. n., *S. makauyensis* sp. n., *S. curviductus* sp. n., *S. tsou* sp. n., *S. meifengensis* sp. n., *S. hehuanensis* sp. n., *S. lixiangae* sp. n., *S. seediq* sp. n., and *S. atayal* sp. n. Area between ocular region and carapace furrow with long setae, a unique feature among *Shaanxinus* species (Fig. 18a). PC with one distal seta; tip narrow; mesal apophysis present; retrolateral apophysis absent (Fig. 17a, c), a unique combination of PC features. Spermophore in retrolateral tegulum relatively weakly curved (Fig. 17a) (see generic remarks). Embolus long (Fig. 17e) (see generic remarks).

Females: longer setae also present on respective region on prosoma as in males, but not as long (Fig. 17e). Epigynal

dorsal and ventral plates not extended posteriorly; copulatory ducts relatively long (Fig. 28g, h) (see generic description).

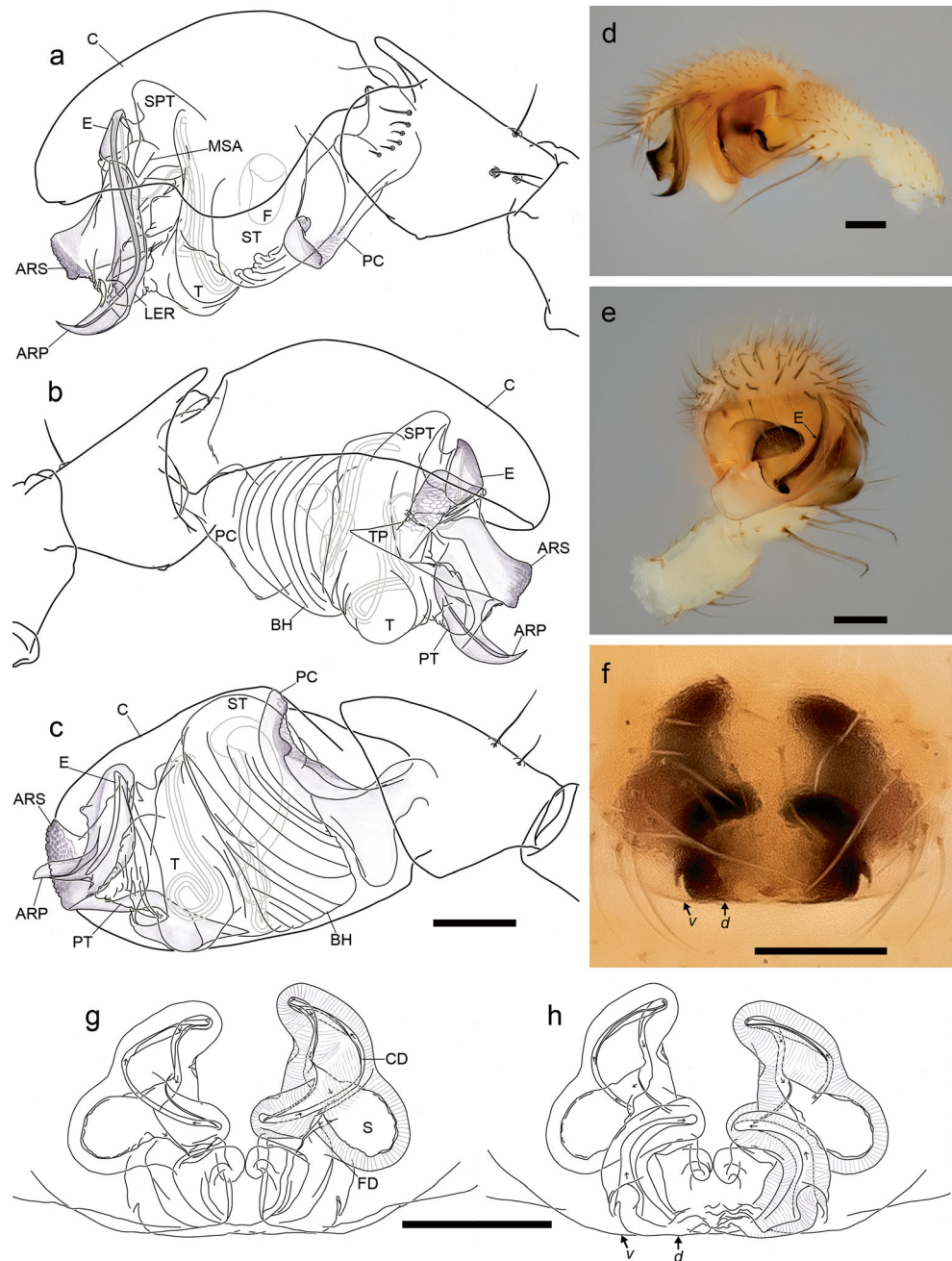
Description. Male (Holotype, ZIMG): total length: 2.53. Carapace 1.17 long, 0.96 wide. Opisthosoma 1.37 long, 1.04 wide. ALE-ALE: 0.176. Clypeus hirsute, no central anterior glabrous region; groove height: 0.123; groove-clypeal margin: 0.35; AME-groove: 0.123. Leg formula $2 > 4 > 1 > 3$; leg measurements see Appendix Table 10; Tm I: 0.88. Pedipalp: patella length/height = 1.8; femur/patella = 4.95. Palpal features and prosomal modifications as diagnosis and generic description.

Female (Paratype, ZIMG): total length: 3.36. Carapace 1.22 long, 0.97 wide. Opisthosoma 2.14 long, 1.5 wide. Leg formula $2 > 1 > 4 > 3$; leg measurements see Appendix Table 10; Tm I: 0.89. Spermathecae width: 0.23. See diagnosis and generic description for somatic features and epigyne morphology.

Variation. Measurements based on type material (5♂).

Males ($n = 5$): total length: 2.49–2.85 (2.6). Carapace 1.12–1.31 (1.2) long, 0.93–1.06 (0.98) wide. ALE-ALE: 0.169–

Fig. 17 *Shaanxinus hirticephalus* sp. n., a–e Male left palp, drawings and photos. **a** retrolateral view. **b** Prolateral view. **c** Ventral view. **d** Retrolateral view. **e** Apical view. **f–h** Epigyne, photo and drawings. **f, h** Ventral view, “*d*” dorsal plate, “*v*” ventral plate. **g** Dorsal view. Scale bars 0.10 mm



0.197 (0.179). Groove height: 0.054–0.123 (0.075). Groove-clypeal margin: 0.34–0.44 (0.39). AME-groove: 0.123–0.141 (0.133). Tm I: 0.82–0.88 (0.86).

Distribution. Taiwan, Hualien County, Pingtung County.

Shaanxinus mingchihensis Lin sp. n.

Figs. 5d–f, 12, 19 and 20

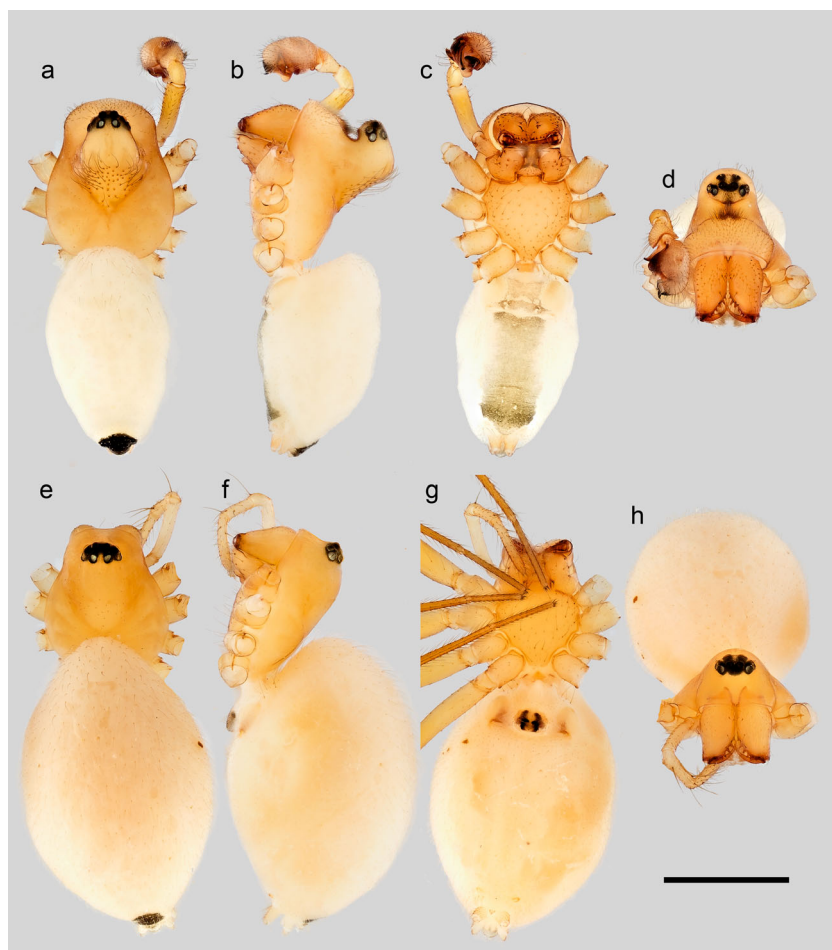
Type material. Holotype: ♂, Yilan County, close to Minchih Forest Recreation Area, 1112 m (24° 38'46" N, 121° 27' 44" E), 17.IV.2014, tree branch beating, in temperate broad-leaved forest, leg. S.-W. Lin (ZIMG-II-28477). Paratypes: 4♀, same

locality and date as holotype, tree branch beating, in temperate broad-leaved forest, leg. S.-W. Lin (ZIMG-II-28483–28486); 3♂ 2♀, Yilan County, Qilan, 893 m (24° 36' 37" N; 121° 29' 15" E), 17.IV.2014, tree branch beating, in temperate broad-leaved forest, leg. S.-W. Lin (ZIMG-II-28478–28482).

Derivatio nominis. The specific name is an adjective referring to the locality wherefrom the type material of this species was collected.

Diagnosis. Males: clypeal groove upper and lower margins contacting at the middle in most specimens examined (5/6);

Fig. 18 *Shaanxinus hirticephalus* sp. n. photos. **a–d** Male habitus. **e–h** Female habitus. **a, e** Dorsal view. **b, f** Lateral view. **c, g** Ventral view. **d, h** Frontal view. Scale bars 1 mm



setae on upper and lower groove laterally oriented, which distinguishes this species from *S. rufus*, *S. magnichypeus* sp. n., *S. hirticephalus* sp. n., *S. shihchoensis* sp. n., *S. shoukaensis* sp. n., and *S. tamdaoensis* sp. n. PC with one distal seta; tip narrow; mesal apophysis present; retrolateral apophysis in middle position of PC (see Fig. 19c), a combination of PC features shared only with *S. makauyensis* sp. n. Spermophore in retrolateral tegulum strongly curved, S-shaped (Fig. 19d) (see generic remarks). Embolus relatively short (Fig. 19e) (see generic remarks). See diagnosis of *S. makauyensis* sp. n.

Females: epigyne dorsal and ventral plates not extended posteriorly; copulatory ducts relatively short (Fig. 19g, h) (see generic description and diagnosis of *S. makauyensis* sp. n.).

Description. Male (Holotype, ZIMG): total length: 2.67. Carapace 1.14 long, 0.93 wide. Opisthosoma 1.54 long, 0.91 wide. ALE-ALE: 0.17. Clypeus hirsute, central distal region glabrous; groove height: 0; groove-clypeal margin: 0.32; AME-groove: 0.11. Leg formula 1 > 2 > 4 > 3; leg measurements see Appendix Table 10; Tm I: 0.87. Pedipalp: patella length/height = 1.63; femur/patella = 4.69. Palpal features and prosomal modifications as in diagnosis and generic description.

Female (Paratype, ZIMG): total length: 2.77. Prosoma: 1.08 long, 0.85 wide. Leg formula 1 > 2 > 4 > 3; leg measurements see Appendix Table 10; Tm I: 0.85. Opisthosoma 1.77 long, 1.01 wide. Spermathecae width: 0.26. See diagnosis and generic description for somatic features and epigyne morphology.

Variation. Measurements based on type material (4♂, 6♀) plus two non-type male specimens.

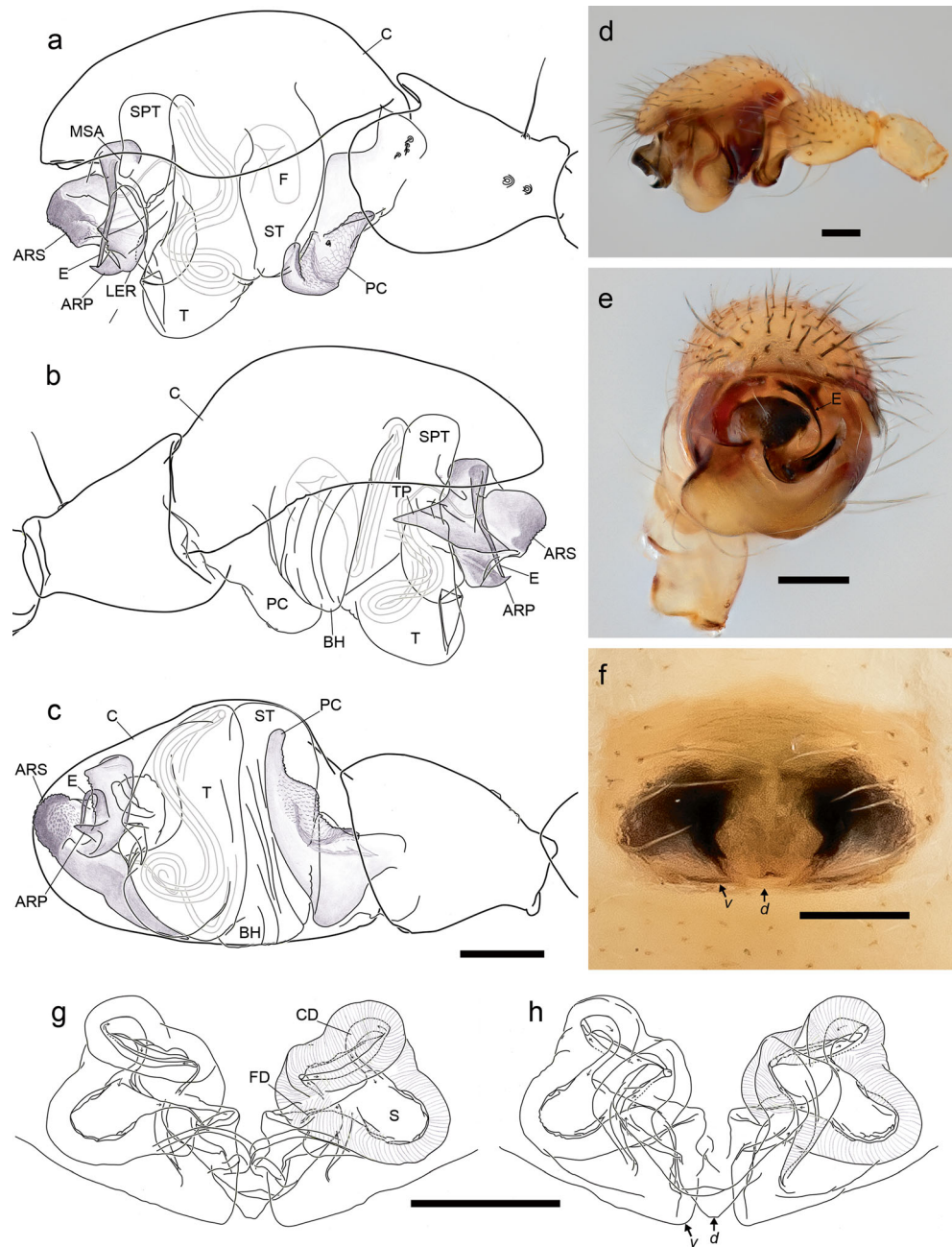
Males ($n = 4$): total length: 2.7–2.78 (2.74). Carapace 1.14–1.22 (1.18) long, 0.92–0.94 (0.93) wide. ALE-ALE: 0.167–0.195 (0.186). Groove height: 0–0.011 (0.003). Groove-clypeal margin: 0.29–0.33 (0.31). AME-groove: 0.105–0.127 (0.117). Tm I: 0.85–0.88 (0.87).

Females ($n = 6$): total length: 2.85–3.29 (3.01). Prosoma: 1.1–1.25 (1.16) long, 0.83–0.93 (0.88) wide. Spermathecae width: 0.25–0.3 (0.27). Tm I: 0.82–0.89 (0.86).

Distribution. Taiwan, Yilan County, close to Mingchih and Qilan.

Shaanxinus makauyensis Lin sp. n.
Figs. 12, 21 and 22

Fig. 19 *Shaanxinus mingchihensis* sp. n., **a–e** Male left palp, drawings and photos. **a**, **d** Retrolateral view. **b** Prolateral view. **c** Ventral view. **e** Apical view. **f–h** Epigyne, photo and drawings. **f**, **h** Ventral view, “*v*” dorsal plate, “*d*” ventral plate. **g** Dorsal view. Scale bars 0.10 mm



Type material. Holotype: ♂, Yilan County, Qilan, 893 m (24° 36' 37" N; 121° 29' 15" E), 17.IV.2014, tree branch beating, in temperate broad-leaved forest, leg. S.-W. Lin (ZIMG-II-28487). Paratypes: 1♀, same locality and date as holotype, leg. S.-W. Lin (ZIMG-II-28490); 1♂ 1♀, Yilan County, close to Minchih Forest Recreation Area, 1112 m (24°38' 46" N, 121°27' 44" E), 17.IV.2014, tree branch beating, in temperate broad-leaved forest, leg. S.-W. Lin (ZIMG-II-28488, 28,489).

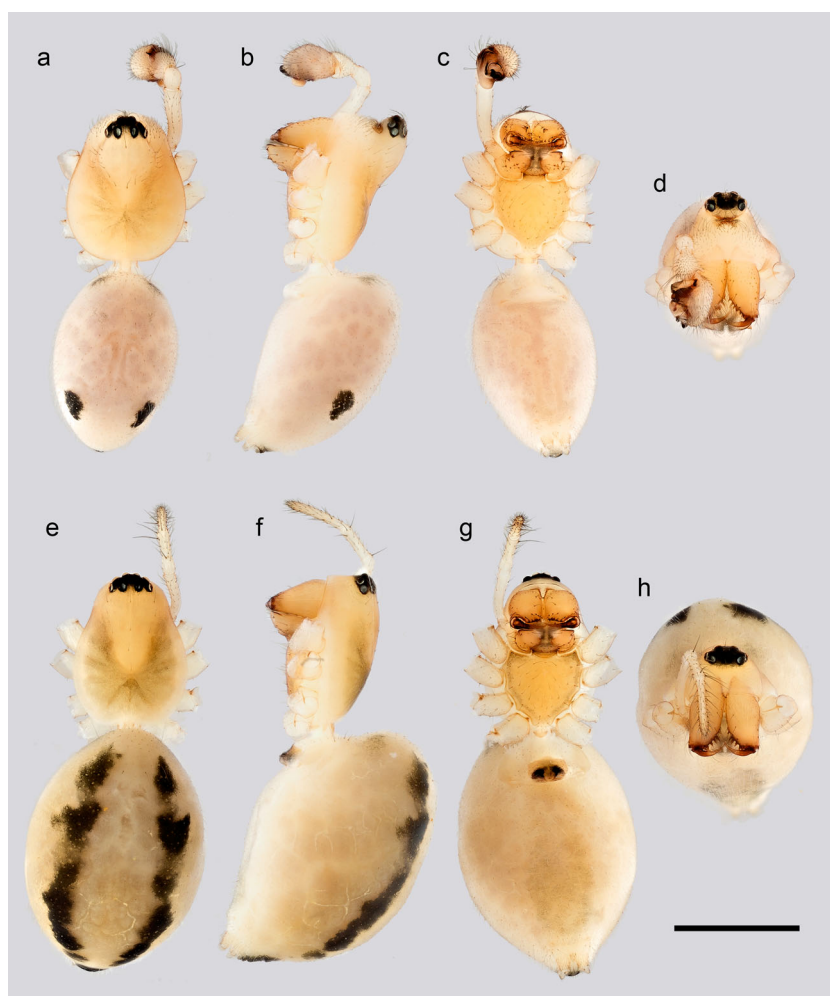
Derivatio nominis. The specific name is an adjective formed after the Makauy Ecological Park, whence the holotype of this species was collected.

Diagnosis. Males: morphologically nearly identical to *S. mingchihensis* sp. n., but with two distal setae on PC, and the tip of PC slightly broader (Fig. 21a, c; refer to diagnosis of *S. mingchihensis* sp. n.).

Females: morphologically almost identical to *S. mingchihensis* sp. n., but with CD extending more laterally (Fig. 21g, h).

Description. Male (Holotype, ZIMG): total length: 2.55. Carapace 1.11 long, 0.87 wide. Opisthosoma 1.43 long, 0.87 wide. ALE-ALE: 0.175. Clypeus hirsute, central distal region glabrous; groove height: 0; groove-clypeal margin: 0.27; AME-groove: 0.105. Leg formula 1 > 2 > 4 > 3; leg

Fig. 20 *Shaanxinus mingchihensis* sp. n. photos. **a–d** Male habitus. **e–h** Female habitus. **a, e** Dorsal view. **b, f** Lateral view. **c, g** Ventral view. **d, h** Frontal view. Scale bars 1 mm



measurements see Appendix Table 10; Tm I: 0.87. Pedipalp: patella length/height = 1.67; femur/patella = 4.72. Palpal features and prosomal modifications as in diagnosis and generic description.

Female (Paratype, ZIMG): total length: 3.29. Prosoma: 1.15 long, 0.9 wide. Leg formula 1 > 2 > 4 > 3; leg measurements see Appendix Table 10; Tm I: 0.87. Opisthosoma 2.2 long, 1.5 wide. Spermathecae width: 0.27.

Variation. Measurements based on type material (2♂, 2♀).

Males ($n = 2$): total length as holotype, while the second male specimen lacks opisthosoma. Carapace 1.05; 1.11 long, 0.87; 0.88 wide. ALE-ALE: 0.175; 0.181. Groove height: 0; 0. Groove-clypeal margin: 0.27; 0.27. AME-groove: 0.105; 0.111. Tm I: 0.85; 0.90.

Females ($n = 2$): total length: 2.84; 3.29. Prosoma: 1.05; 1.15 long, 0.81; 0.9 wide. Spermathecae width: 0.24; 0.27. Tm I: 0.87; 0.89.

Distribution. Taiwan, Yilan County, close to Mingchih and Qilan.

Shaanxinus lixiangae Lin sp. n.

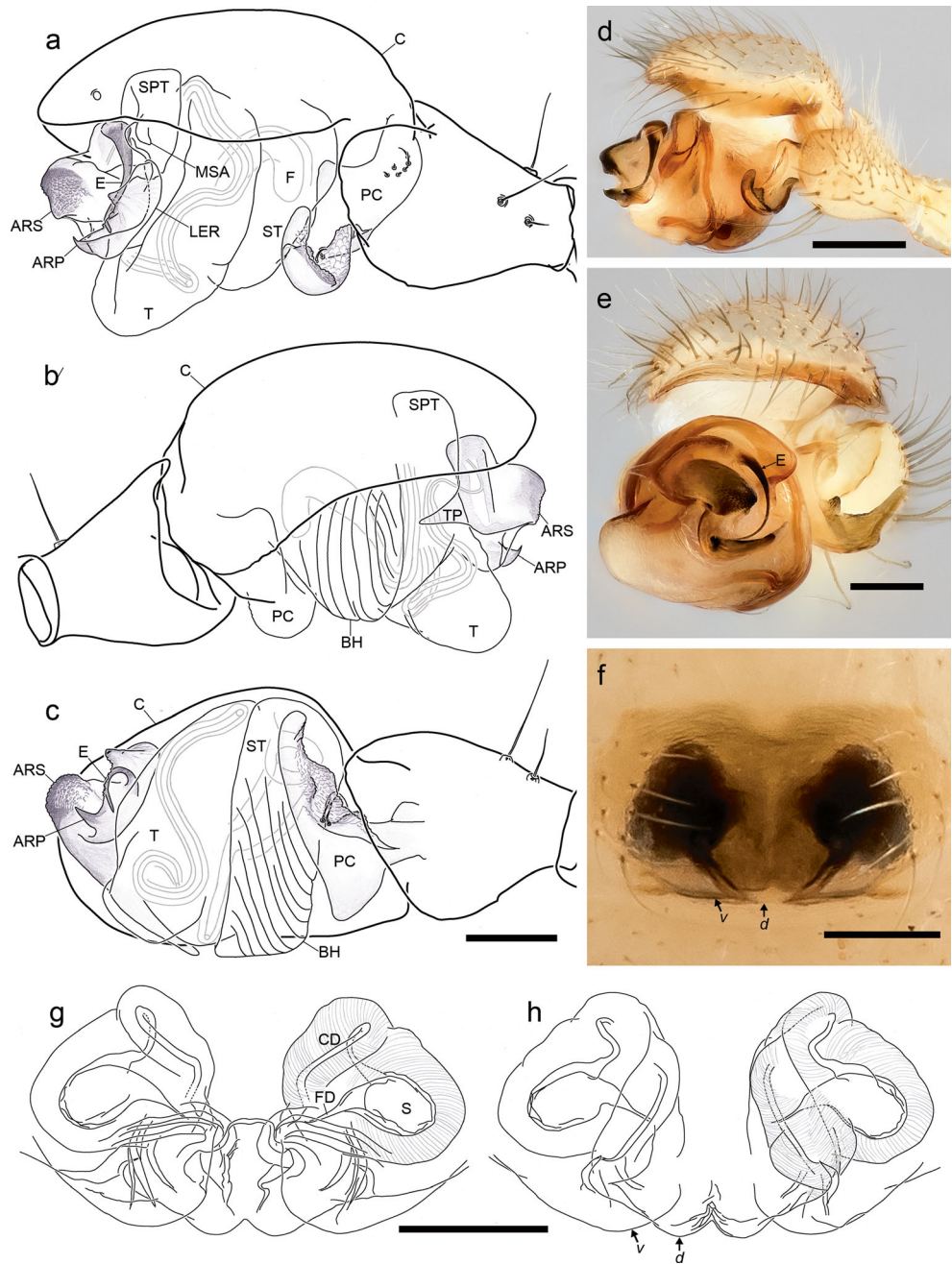
Figs. 12, 23 and 24

Type material. Holotype: ♂, Yilan County, close to Minchih Forest Recreation Area, 1112 m (24° 38' 46" N; 121° 27' 44" E), 17.IV.2014, tree branch beating, in temperate broad-leaved forest, leg. S.-W. Lin (ZIMG-II-28491). Paratype: 1♀, Yilan County, Qilan, (22° 55' 53" N; 121° 10' 41" E) 17.IV.2014, tree branch beating, in temperate broad-leaved forest, leg. S.-W. Lin (ZIMG-II-28492).

Derivatio nominis. The specific name is formed from the name of S.-W. Lin's mother, Li-Xiang Huang, who helped with collecting.

Diagnosis. Males: Clypeal groove upper and lower margins contacting each other, setae on upper and lower groove laterally oriented, which distinguishes this species from *S. rufus*, *S. magniclypeus* sp. n., *S. hirticephalus* sp. n., *S. shihchoensis* sp. n., *S. shoukaensis* sp. n. and *S. tamdaensis* sp. n. PC distal seta absent; tip narrow; mesal apophysis distally situated, these

Fig. 21 *Shaanxinus makauyensis* sp. n., **a–e** Male left palp, drawings and photos. **a, d** Retrolateral view. **b** Proateral view. **c** Ventral view. **e** Apical view. **f–h** Epigyne, photo and drawings. **f, h** Ventral view, “*v*” dorsal plate, “*d*” ventral plate. **g** Dorsal view. Scale bars 0.10 mm



two PC features distinguish this species from *S. mingchihensis* sp. n. and *S. makauyensis* sp. n.; retrolateral apophysis present, located in middle-distal position of PC (Fig. 23a, c). Spermophore in retrolateral tegulum curved, S-shaped (Fig. 23d) (see generic remarks). Embolus relatively long (Fig. 23e) (see generic remarks).

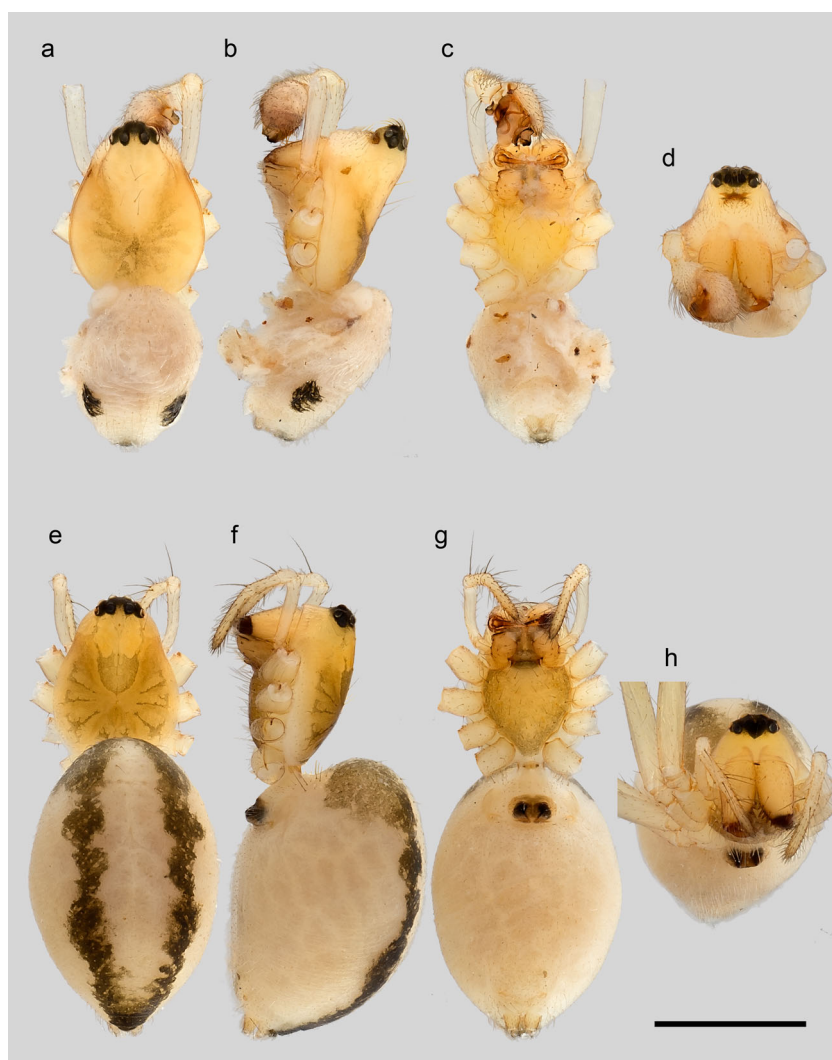
Females: epigyne dorsal and ventral plates slightly extended posteriorly; copulatory duct relatively long (Fig. 23g, h) (see generic description).

Description. Male (Holotype, ZIMG): total length: 2.58. Carapace 1.17 long, 0.91 wide. Opisthosoma 1.40 long, 0.8 wide. ALE-ALE: 0.194. Clypeus hirsute, central distal region

glabrous; groove height: 0; groove-clypeal margin: 0.34; AME-groove: 0.116. Leg formula 1-2-4-3; leg measurements see Appendix Table 10; Tm I: 0.84. Pedipalp: patella length/height = 1.67; femur/patella = 4.55. Palpal features and prosomal modifications as in diagnosis and generic description.

Female (Paratype, ZIMG): total length: 3.17. Carapace 1.23 long, 0.95 wide. Opisthosoma 1.92 long, 1.37 wide. Leg formula 1-2-4-3; leg measurements see Appendix Table 10; Tm I: 0.89. Spermathecae width: 0.27. See diagnosis and generic description for somatic features and epigyne morphology.

Fig. 22 *Shaanxinus makauyensis* sp. n. photos. **a–d** Male habitus. **e–h** Female habitus. **a, e** Dorsal view. **b, f** Lateral view. **c, g** Ventral view. **d, h** Frontal view. Scale bars 1 mm



Distribution. Taiwan, Yilan County, close to Mingchih and Qilan.

Shaanxinus curviductus Lin sp. n.

Figs. 1, 3, 4, 12, 25 and 26

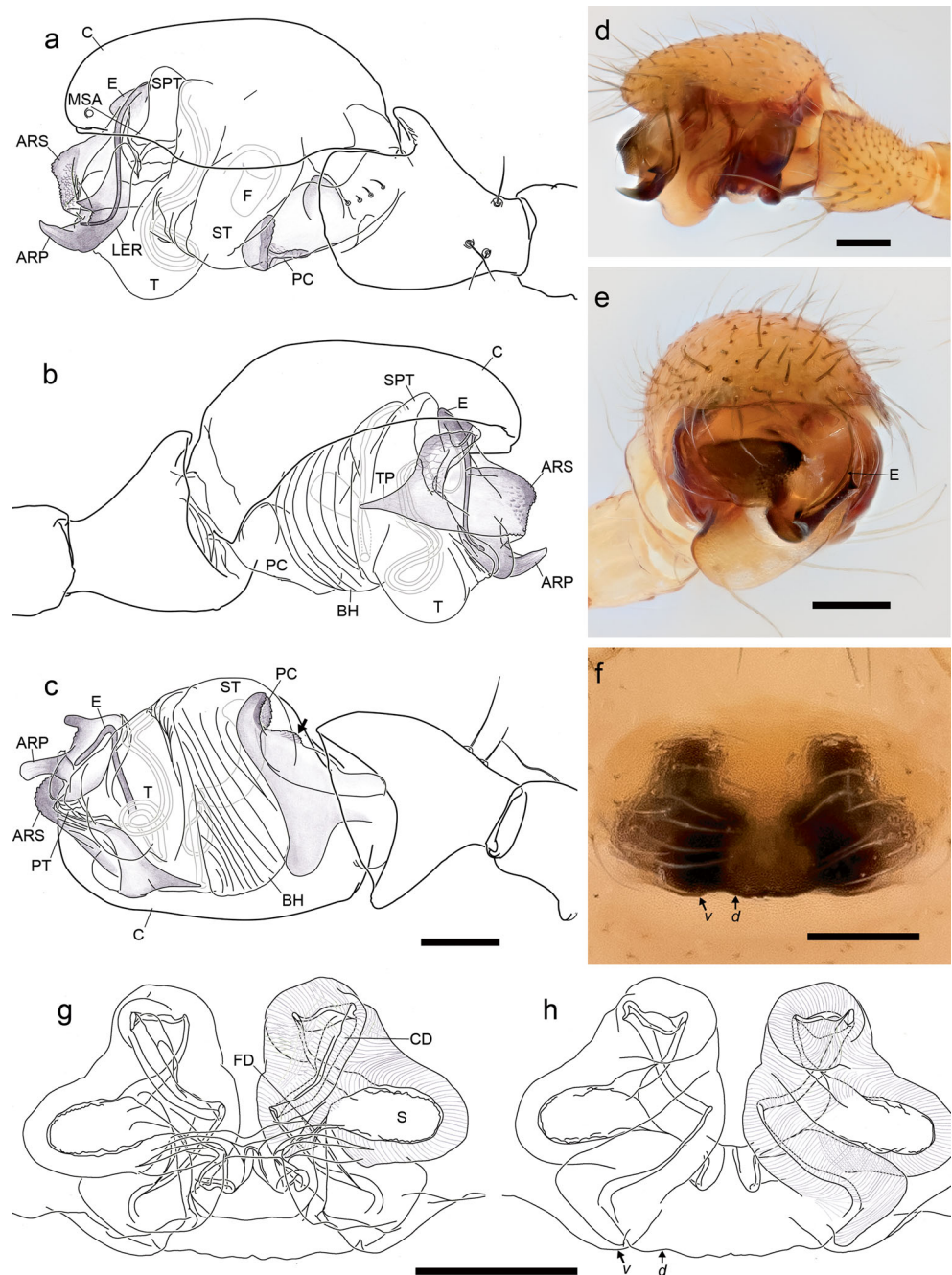
Type material. Holotype: ♂, Hsinchu County, Beipu Township, near Wujhishan, 517 m (24° 39' 01" N; 121° 05' 24" E), 17.VI.2014, tree branch beating, in subtropical secondary broad-leaved forest, leg. S.-W. Lin (ZIMG-II-28493). Paratypes: 7♂ 8♀, same locality and date as holotype, leg. S.-W. Lin (ZIMG-II-28494~28500, 28521~28,528); 2♂ 3♀, Miaoli County, Taian Township, 1004 m (24° 22' 17" N; 120° 56' 09" E), 10.VII.2014, tree branch beating, in subtropical secondary broad-leaved forest, leg. S.-W. Lin (ZMUC); 5♂ 2♀, same locality, 21.VII.2014, leg. S.-W. Lin (5♂ 1♀, NMNS-7927-017~021, 023; 1♀, SMF). 1♂, Hsinchu County, Chienshih Township, close to Litungshan, 1523 m (24° 41' 20" N; 121° 18' 35" E), 15.V.2014, tree branch beating, in subtropical broad-leaved forest, leg. S.-W. Lin (SMF); 2♂

4♀, same locality, 23.VII.2017, leg. S.-W. Lin (ZIMG-II-28501, 28,502, 28,530~28,533); 1♀, same locality, 20.V.2014, leg. S.-W. Lin (ZIMG-II-28529).

Other material. Miaoli County, Taian Township, 1004 m (24° 22' 17" N; 120° 56' 09" E), 21.VII.2014, tree branch beating, in subtropical secondary broad-leaved forest, leg. S.-W. Lin, 28♂ 32♀ (13♂ 9♀, ZIMG-II-28508~28,519, 28,503, 28,537; 5♂ 8♀, SMF; 5♂ 8♀, ZMUC; 5♂ 7♀, NMNS-7927-022, 024); same locality, 10.VII.2014, leg. S.-W. Lin, 8♂ 16♀ (ZIMG-II-28504~28,507, 28,536); Hsinchu County, Chienshih Township, close to Litungshan, 1523 m (24° 41' 20" N; 121° 18' 35" E), 23.VII.2017, tree branch beating, in subtropical broad-leaved forest, leg. S.-W. Lin, 1♂ 2♀ (ZIMG-II-28520, 28,538).

Derivatio nominis. The specific name is derived from the Latin “curvus,” meaning curved, and duct, referring to the especially sinuous spermophore in male palps. This name is a noun in apposition.

Fig. 23 *Shaanxinus lixiangae* sp. n., **a–e** Male left palp, drawings and photos. **a, d** Retrolateral view. **b** Prolateral view. **c** Ventral view. **e** Apical view. **f–h** Epigyne, photo and drawings. **f, h** Ventral view, “*d*” dorsal plate, “*v*” ventral plate. **g** Dorsal view. Scale bars 0.10 mm

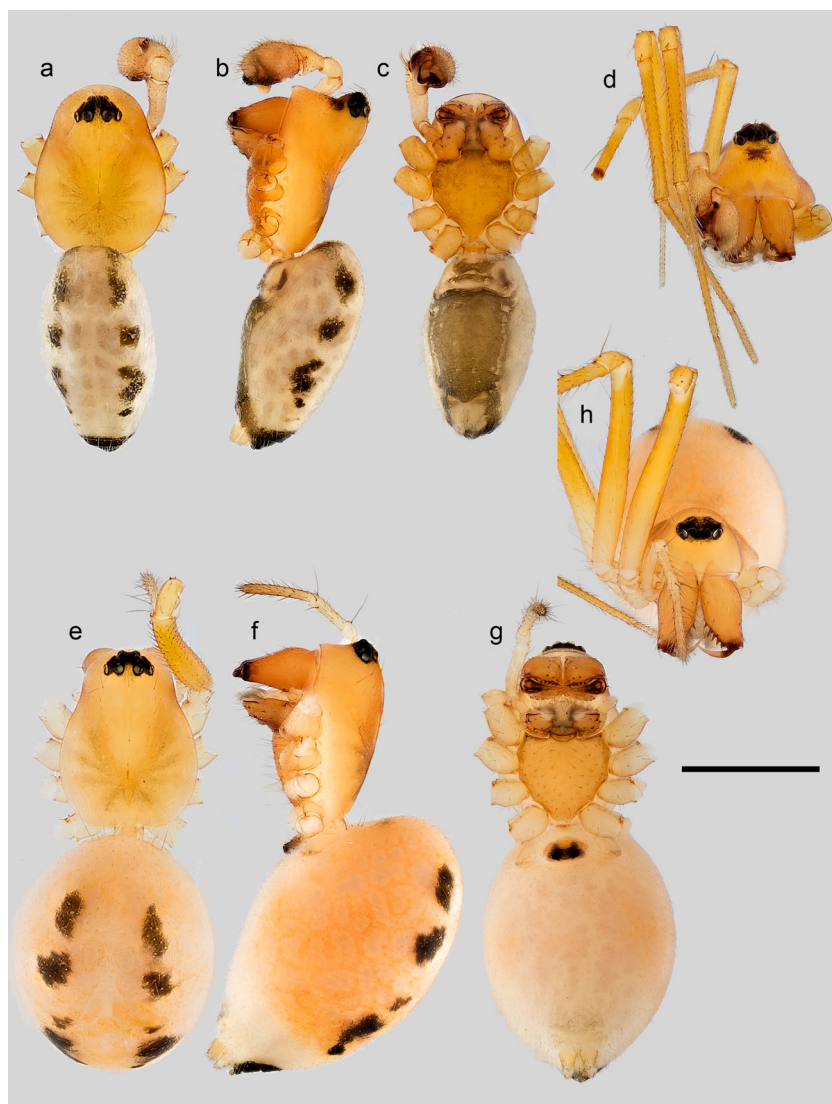


Diagnosis. Males: clypeal groove upper and lower margins close to or contacting each other, setae on the upper part of the groove laterally oriented, which distinguishes this species from *S. rufus*, *S. magniclpeus* sp. n., *S. hirticephalus* sp. n., *S. shihchoensis* sp. n., *S. shoukaensis* sp. n. and *S. tamdaoensis* sp. n. PC distal seta absent, mesal apophysis present; retrolateral apophysis situated in the middle of PC (Fig. 25a, c). Spermophore in tegulum on retrolateral side strongly curved, S-shaped (Fig. 25d) (see generic remarks). Embolus relatively long (Fig. 25e) (see generic remarks). Differences to the similar species *S. tsou* sp. n. see diagnosis of the latter.

Females: epigyne dorsal and ventral plates extended posteriorly; copulatory ducts relatively long, trajectory similar to *S. hehuanensis* sp. n., can be distinguished from the latter species by its lesser curvature and the wider distance between ducts on both sides (Fig. 25f–h). Carapace width significantly smaller than *S. hehuanensis* sp. n. (t test, $n_1 = 10$, $n_2 = 10$, $t = -10.658$, $p < 0.001$, see data below). Morphology indistinguishable from *S. tsou* sp. n. (see diagnosis of the latter).

Description. Male (holotype, ZIMG): total length: 2.61. Carapace 1.16 long, 0.91 wide. Opisthosoma 1.43 long, 0.89 wide. ALE-ALE: 0.198. Clypeus hirsute, central distal region

Fig. 24 *Shaanxinus lixiangae* sp. n. photos. **a–d** Male habitus. **e–h** Female habitus. **a, e** Dorsal view. **b, f** Lateral view. **c, g** Ventral view. **d, h** Frontal view. Scale bars 1 mm



glabrous; groove height: 0.006; groove-clypeal margin: 0.26; AME-groove: 0.13. Leg formula 1 = 2 > 4 > 3; leg measurements see Appendix Table 10; Tm I: 0.86. Pedipalp: patella length/height = 1.62; femur/patella = 4.3. Palpal features and prosomal modifications as in diagnosis and generic description.

Female (paratype, ZIMG): total length: 2.93. Carapace 1.12 long, 0.86 wide. Opisthosoma 1.85 long, 1.22 wide. Leg formula 1 = 2 > 4 > 3; leg measurements see Appendix Table 10; Tm I: 0.89. Spermathecae width: 0.26. See diagnosis and generic description for somatic features and epigyne morphology.

Variation. Measurements based on type material (18♂, 18♀).

Males ($n = 18$): total length: 2.35–2.8 (2.61). Carapace 1.12–1.26 (1.2) long, 0.87–0.97 (0.93) wide. ALE-ALE: 0.186–0.216 (0.198). Groove height: 0–0.01 (0.002). Groove-clypeal margin: 0.26–0.35 (0.31). AME-groove: 0.111–0.16 (0.137). Tm I: 0.79–0.89 (0.86).

Females ($n = 18$): total length: 2.4–3.02 (2.76). Carapace 1.08–1.16 (1.13) long, 0.82–0.95 (0.86) wide. Spermathecae width: 0.26–0.3 (0.28); Tm I: 0.79–0.9 (0.86).

Distribution. Taiwan, Hsinchu County, Miaoli County.

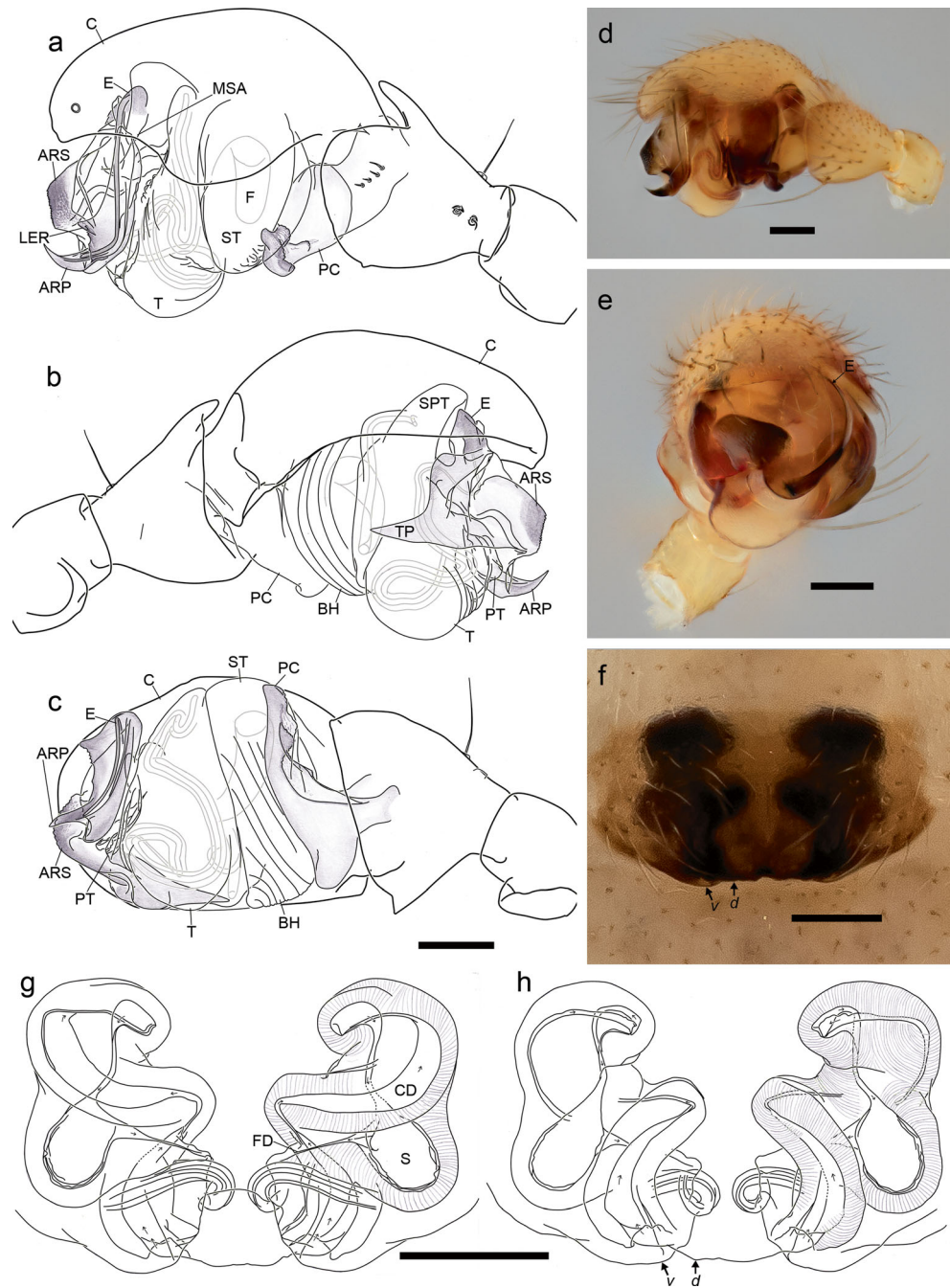
Shaanxinus tsou Lin sp. n.

Figs. 12, 27 and 28

Type material. Holotype: ♂, Chiayi County, Zhushi Township, close to Shihcho Mountain, 1181 m (23° 28' 22" N; 120° 41' 33" E), 5.V.2014, tree branch beating, in subtropical secondary broad-leaved forest, leg. S.-W. Lin (ZIMG-II-28539). Paratypes: 1♂ 7♀, same location and date as holotype, leg. S.-W. Lin (ZIMG-II-28540–28547).

Derivatio nominis. The specific name is derived from Tsou, a Taiwanese aboriginal tribe living in the collecting area of the holotype. This is a noun in apposition.

Fig. 25 *Shaanxinus curviductus* sp. n., **a–e** Male left palp, drawings and photos. **a, d** Retrolateral view. **b** Proteral view. **c** Ventral view. **e** Apical view. **f–h** Epigyne, photo and drawings. **f, h** Ventral view, “*d*” dorsal plate, “*v*” ventral plate. **g** Dorsal view. Scale bars 0.10 mm



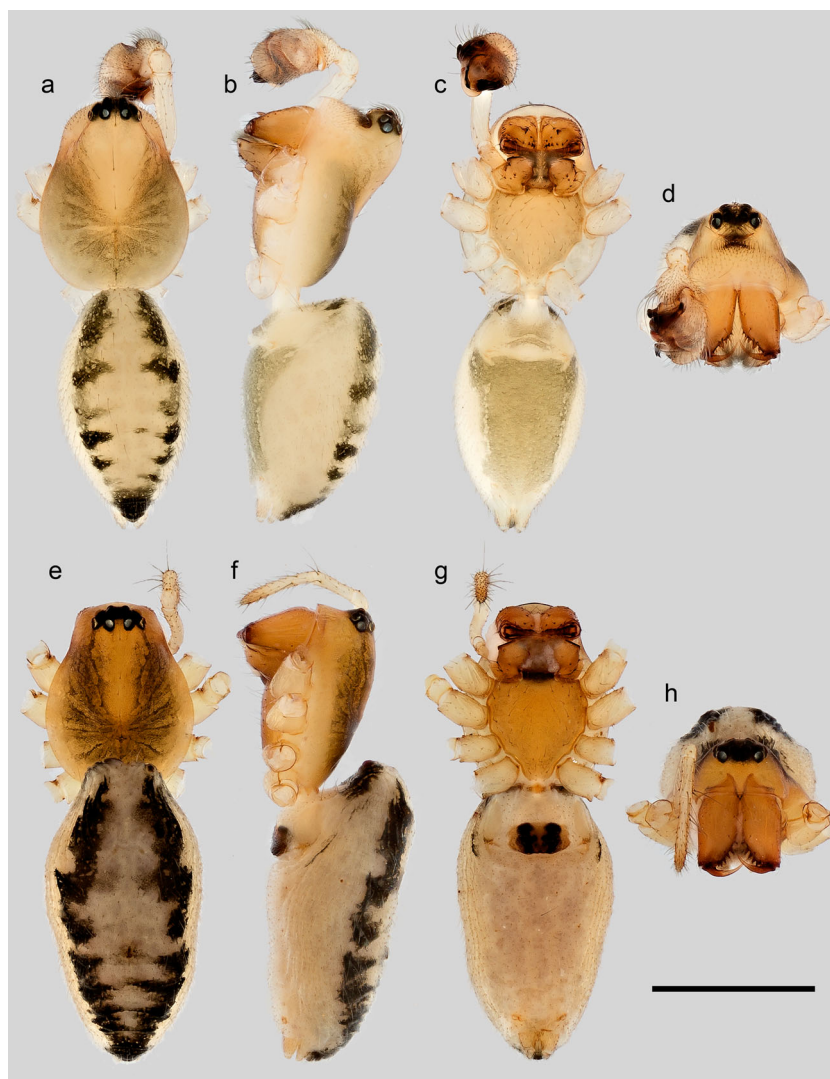
Diagnosis. Males: this species is morphologically similar to *S. curviductus* sp. n., but they differ in the shape of PC tip (Fig. 27a, c), and the distance between the tooth on LER and ARP, longer in *S. tsou* sp. n. (0.15; 0.16) than in *S. curviductus* sp. n. (0.11–0.13 (0.12), SD < 0.01).

Females: morphologically indistinguishable from *S. curviductus* sp. n., but phylogenetic inferences from both 28S and COI sequence data grouped the three sequenced females from near Shihcho Mountain with the male of *S. tsou* sp. n., forming a monophyletic group distinct from the clades comprising *S. curviductus* sp. n. representatives. Therefore,

females collected from this site are all regarded as conspecific to *S. tsou* sp. n. males.

Description. Male (Holotype, ZIMG): total length: 2.59. Carapace 1.19 long, 0.93 wide. Opisthosoma 1.42 long, 1 wide. ALE-ALE: 0.22. Clypeus hirsute, central distal region glabrous; groove height: 0; groove-clypeal margin: 0.29. AME-groove: 0.16; Leg formula 1 > 2 > 4 > 3; leg measurements see Appendix Table 10; Tm I: 0.9. Pedipalp: patella length/height = 1.54; femur/patella = 4.65. Palpal features and prosomal modifications as in diagnosis and generic description.

Fig. 26 *Shaanxinus curviductus* sp. n. photos. **a–d** Male habitus. **e–h** Female habitus. **a, e** Dorsal view. **b, f** Lateral view. **c, g** Ventral view. **d, h** Frontal view. Scale bars 1 mm



Female (Paratype, ZIMG): total length: 2.93. Carapace 1.2 long, 0.98 wide. Opisthosoma 1.72 long, 1.13 wide. Leg formula 1 > 2 > 4 > 3; leg measurements see Appendix Table 10; Tm I: 0.85. Spermathecae width: 0.29. See diagnosis and generic description for somatic features and epigyne morphology.

Variation. Measurements based on type material (2♂, 7♀)

Males ($n = 2$): total length: 2.59; 2.63. Carapace 1.19; 1.26 long, 0.93; 0.96 wide. ALE-ALE: 0.22; 0.24. Groove height: 0; 0. Groove-clypeal margin: 0.29; 0.29. AME-groove: 0.158; 0.161. Tm I: 0.86; 0.9.

Females ($n = 7$): total length: 2.6–3.25 (2.85). Carapace 1.06–1.24 (1.15) long, 0.84–0.97 (0.91) wide. Spermathecae width: 0.27–0.3 (0.29). Tm I: 0.85–0.9 (0.87).

Distribution. Taiwan, Chiayi County.

Shaanxinus hehuanensis Lin sp. n.
Figs. 2b, 12, 29 and 30

Type material. Holotype: ♂, Nantou County, Ren-ai Township, next to Yuanfeng parking lot, 2763 m (24° 07' 04" N; 121° 14' 13' E), 18.VI.2014, bush branch beating, in alpine grassland close to coniferous forest, leg. S.-W. Lin (ZIMG-II-28562). Paratypes: 8♂ 8♀, same locality and date as holotype, bush branch beating, leg. S.-W. Lin (2♂ 2♀, ZIMG-II-28563, 28564, 28570, 28571; 2♂ 2♀, SMF; 2♂ 2♀, ZMUC; 2♂ 2♀, NMNS-7927-033~036). 1♂ 2♀, Hualien County, Xiulin Township, close to Mount Hehuan, 2674 m (24° 10' 42" N; 121° 18' 14" E), 18.VI.2014, tree branch beating, on lower broad-leaved tree in coniferous forest, leg. S.-W. Lin (ZIMG-II-28565, 28572, 28573).

Other material. Same locality and date as holotype, 18.VI.2014, bush branch beating, leg. S.-W. Lin, 3♂ 3♀ (ZIMG-II-28566–28568, 28574, 28575, 28577). Hualien County, Xiulin Township, close to Mount Hehuan, 2674 m (24° 10' 42" N; 121° 18' 14" E), 18.VI.2014, tree branch beating, on lower broad-leaved tree in coniferous forest, leg. S.-W. Lin, 1♂ 1♀ (ZIMG-II-28569, 28576).

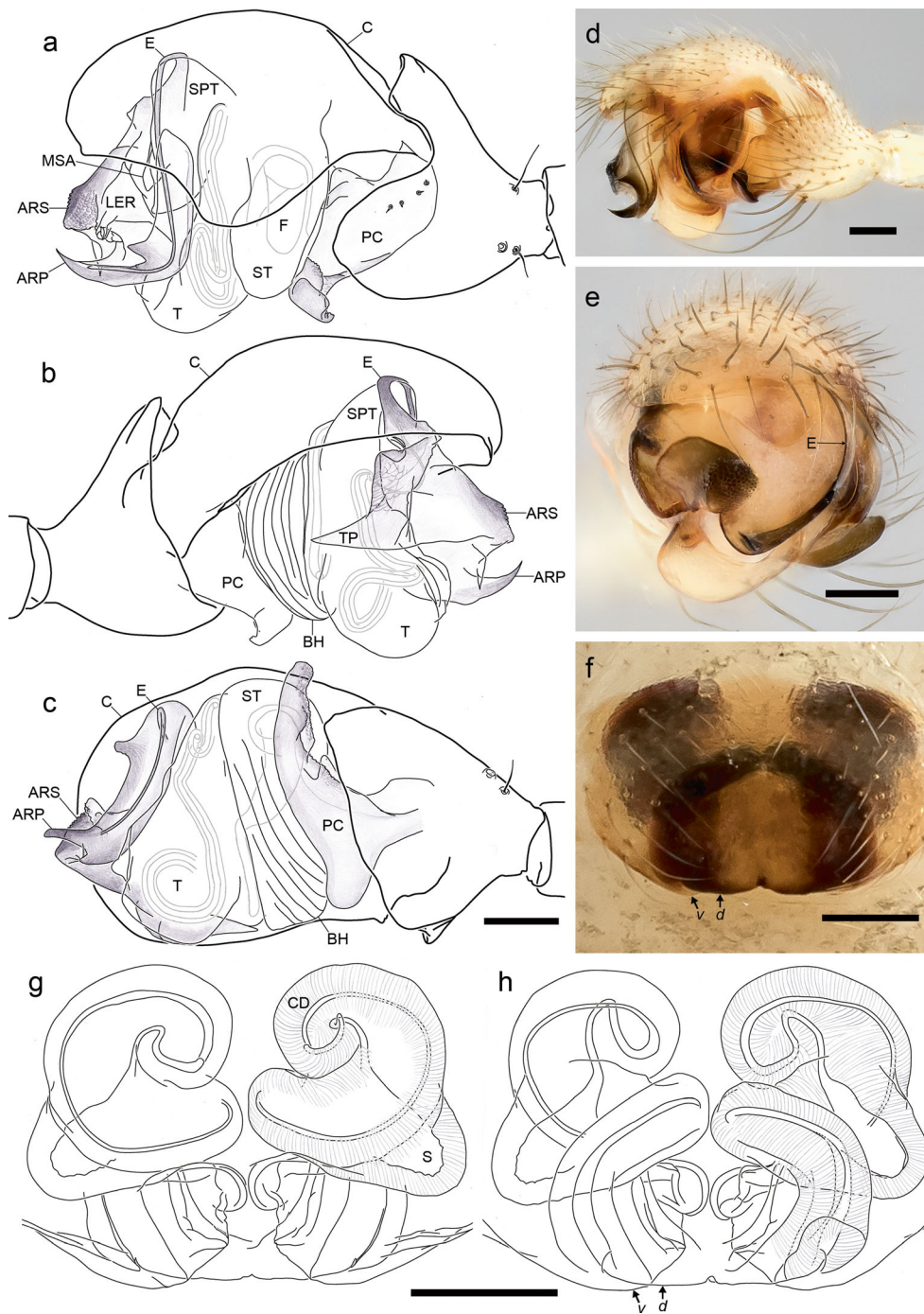


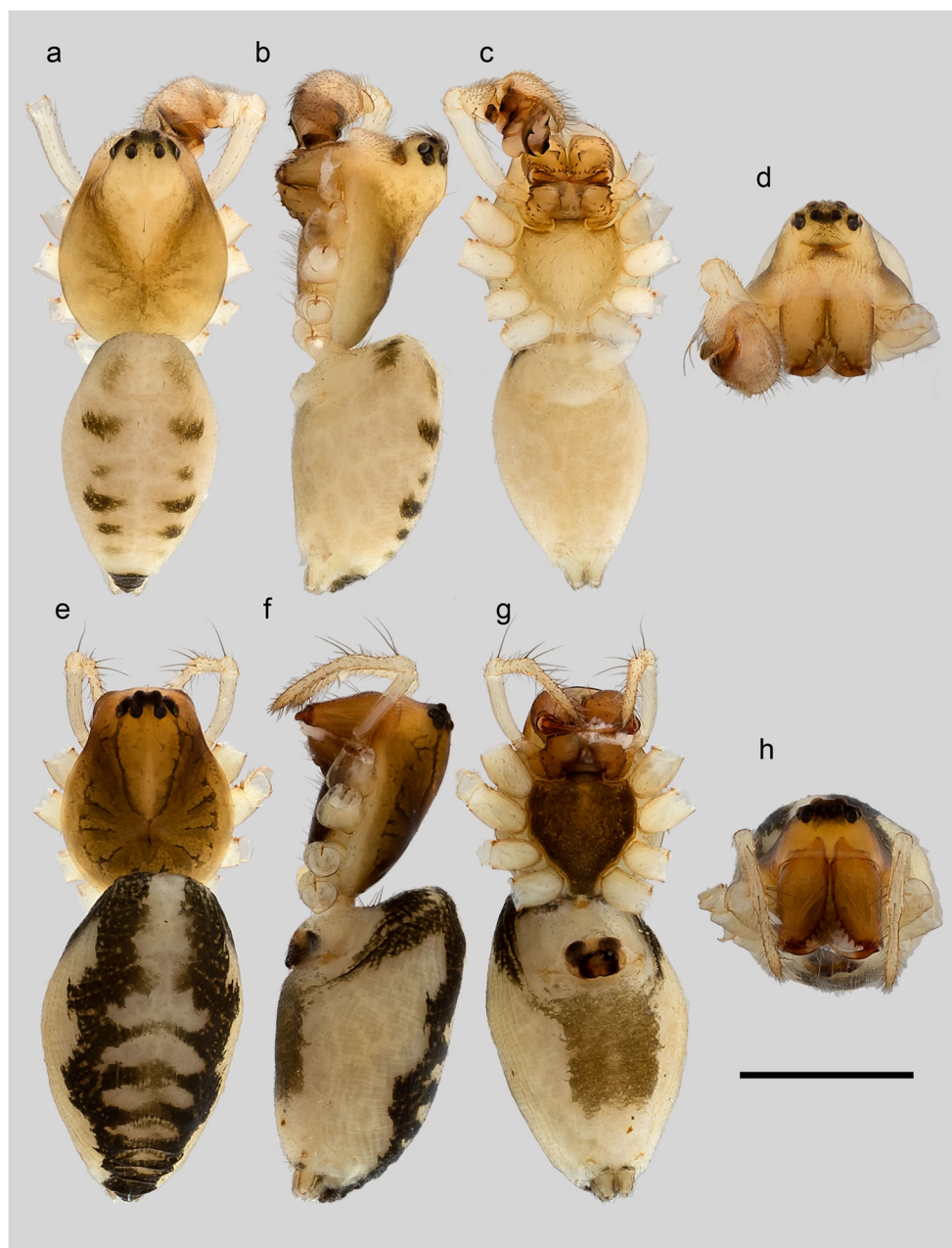
Fig. 27 *Shaanxinus tsou* sp. n., **a–e** Male left palp, drawings and photos. **a, d** Retrolateral view. **b** Prolateral view. **c** Ventral view. **e** Apical view. **f–h** Epigyne, photo and drawings. **f, h** Ventral view, “d” dorsal plate, “v” ventral plate. **g** Dorsal view. Scale bars 0.10 mm

Derivatio nominis. The specific name is an adjective derived from Mount Hehuan, a mountain near the collecting site of the holotype specimen.

Diagnosis. Males: carapace size similar to *S. meifengensis* sp. n., both species significantly larger than remaining species described here. Clypeal groove upper and lower margins close to or contacting each other, setae on upper and lower part of

groove laterally oriented, which distinguishes this species from *S. rufus*, *S. magniclypeus* sp. n., *S. hirticephalus* sp. n., *S. shihchoensis* sp. n., *S. shoukaensis* sp. n. and *S. tamdaoensis* sp. n. PC distal setae absent; retrolateral apophysis prominent, smaller than *S. atayal* sp. n., close to PC tip but less distal than in *S. meifengensis* sp. n. (Fig. 29a, c; see description and figures of *S. atayal* sp. n. and *S. meifengensis* sp. n.). Spermatheca in retrolateral tegulum

Fig. 28 *Shaanxinus tsou* sp. n. photos. **a–d** Male habitus. **e–h** Female habitus. **a, e** Dorsal view. **b, f** Lateral view. **c, g** Ventral view. **d, h** Frontal view. Scale bars 1 mm



strongly curved, S-shaped (Fig. 29d) (see generic remarks). Embolus relatively long (Fig. 29e) (see generic remarks).

Females: epigyne dorsal and ventral plates extended posteriorly; copulatory ducts trajectory similar to *S. curviductus* sp. n., can be distinguished from the latter by its proximity in the middle of the vulva (Fig. 29f–h).

Description. Male (Holotype, ZIMG): total length: 3.15. Carapace 1.49 long, 1.2 wide. Opisthosoma 1.72 long, 1.2 wide. ALE-ALE: 0.206. Clypeus hirsute, central distal region glabrous; groove height: 0.006; groove-clypeal margin: 0.4. AME-groove: 0.159; Leg formula 1 = 2 > 4 > 3; leg measurements see Appendix Table 10; Tm I: 0.88. Pedipalp: patella

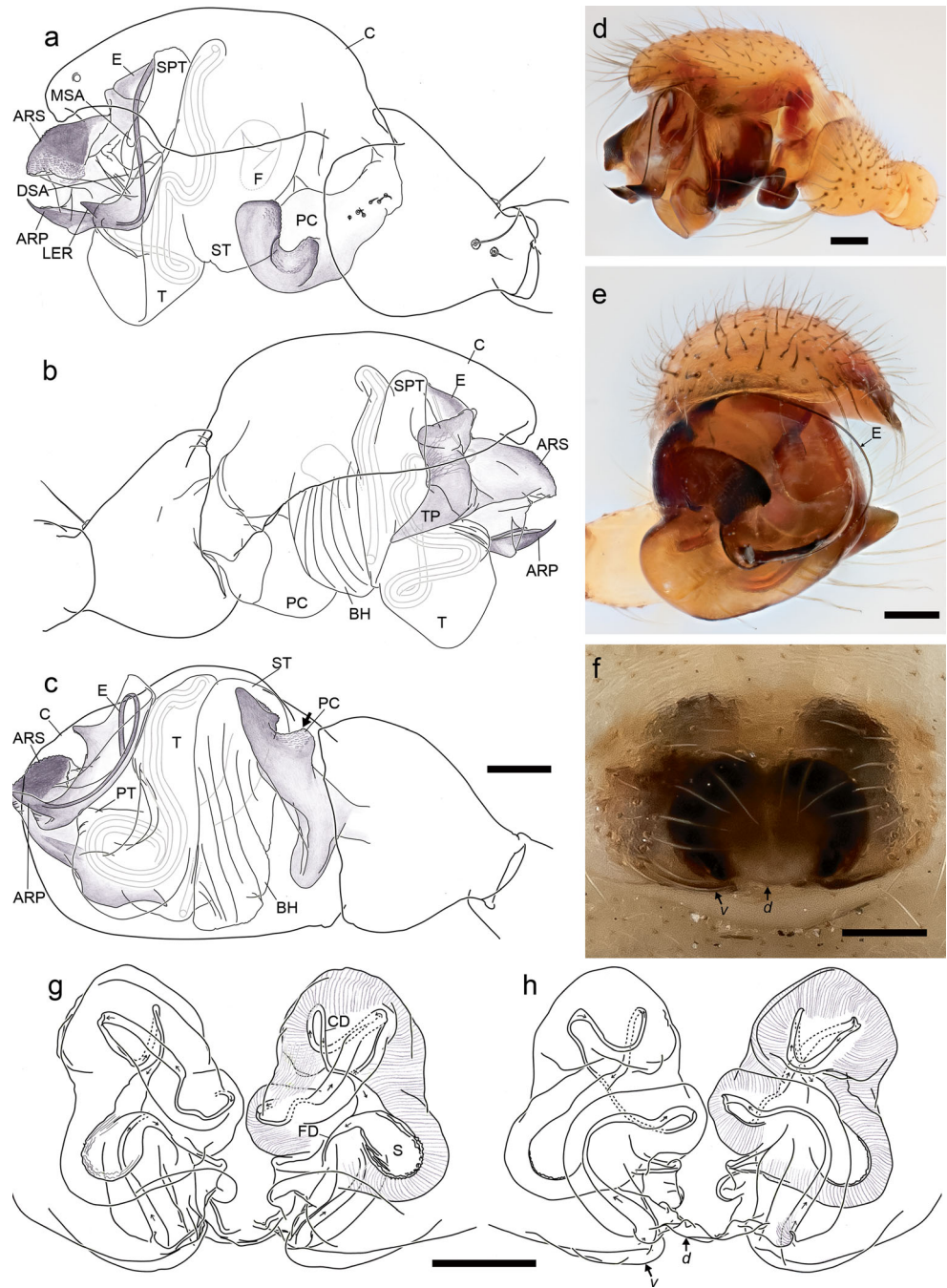
length/height = 1.78; femur/patella = 4.85. Palpal features and prosomal modifications as in diagnosis and generic description.

Female (Paratype, ZIMG): total length: 3.49. Carapace 1.47 long, 1.16 wide. Opisthosoma 1.96 long, 1.51 wide. Leg formula 1 = 2 > 4 > 3; leg measurements see Appendix Table 10; Tm I: 0.9. Spermathecae width: 0.35. See diagnosis and generic description for somatic features and epigyne morphology.

Variation. Measurements based on type material (10♂, 10♀).

Males ($n = 10$): total length: 3.05–3.42 (3.23). Carapace 1.4–1.6 (1.51) long, 1.1–1.25 (1.2) wide. ALE-ALE: 0.195–

Fig. 29 *Shaanxinus hehuanensis* sp. n., **a–e** Male left palp, drawings and photos. **a, d** Retrolateral view. **b** Proateral view. **c** Ventral view. **e** Apical view. **f–h** Epigyne, photo and drawings. **f, h** Ventral view, “*d*” dorsal plate, “*v*” ventral plate. **g** Dorsal view. Scale bars 0.10 mm



0.227 (0.209). Groove height: 0–0.021 (0.004). Groove-clypeal margin: 0.38–0.42 (0.4). AME-groove: 0.141–0.185 (0.16). Tm I: 0.82–0.91 (0.88).

Females (n = 10): total length: 3.27–3.95 (3.53). Carapace 1.31–1.62 (1.47) long, 1–1.22 (1.14) wide. Spermathecae width: 0.32–0.4 (0.35). Tm I: 0.87–0.92 (0.9).

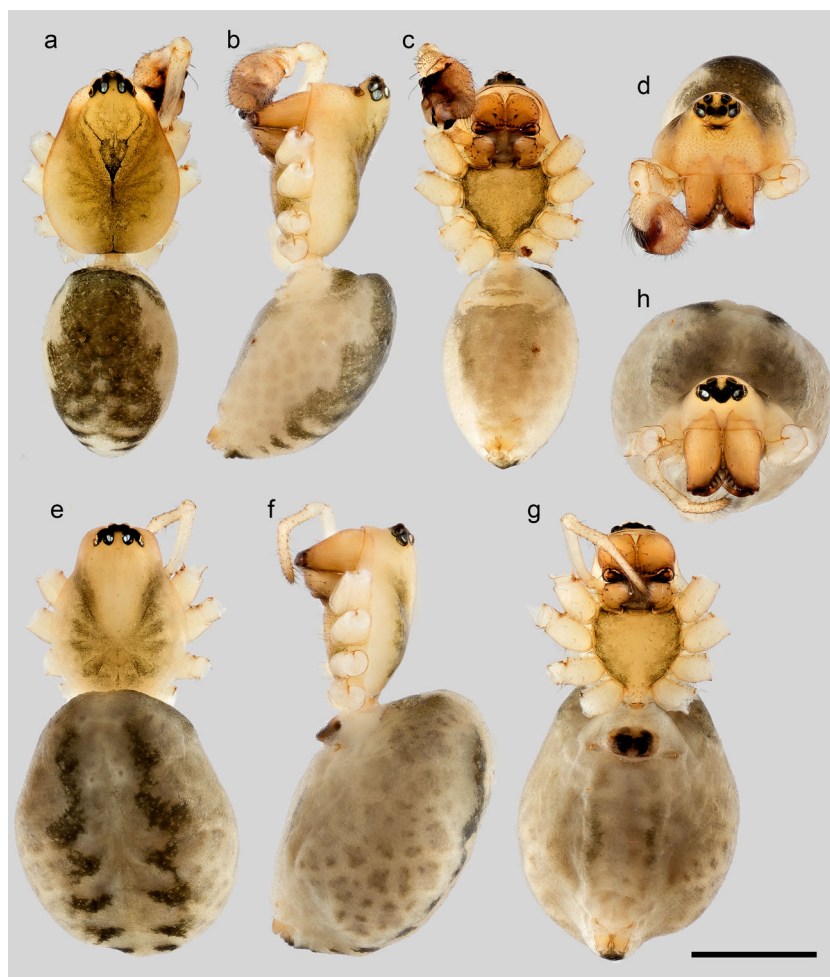
Distribution. Taiwan, Nantou County, Hualien County, close to Mount Hehuan.

Shaanxinus seediq Lin sp. n.

Figs. 12, 31 and 32

Type material. Holotype: ♂, Nantou County, Ren-ai Township, next to Highland Experimental Farm, National Taiwan University, 2151 m (24° 05' 18" N; 121° 10' 23" E), 19.II.2017, tree branch beating, in temperate broad-leaved forest, leg. S.-W. Lin (ZIMG-II-28578). Paratype: 1♂ 1♀, same locality as holotype, 18.VI.2014, tree branch beating,

Fig. 30 *Shaanxinus hehuanensis* sp. n. photos. **a–d** Male habitus. **e–h** Female habitus. **a, e** Dorsal view. **b, f** Lateral view. **c, g** Ventral view. **d, h** Frontal view. Scale bars 1 mm



leg. S.-W. Lin (ZIMG-II-28579, 28,580); 1♀, Hsinchu County, Chienshih Township, close to Litungshan, 1523 m (24° 41' 20" N; 121° 18' 35" E), 15.V.2014, tree branch beating, in subtropical broad-leaved forest, leg. S.-W. Lin (ZIMG-II-28581); 1♀, same location and collecting method, 20.V.2014, leg. S.-W. Lin (ZIMG-II-28582).

Derivatio nominis. The specific name is derived from Seediq, a Taiwanese aboriginal tribe living in the collecting area of the holotype. This is a noun in apposition.

Diagnosis. Males: clypeal groove upper and lower margins not contacting each other, setae on upper and lower groove laterally oriented, which distinguishes this species from *S. rufus*, *S. magniclypeus* sp. n., *S. hirticephalus* sp. n., *S. shihchoensis* sp. n., *S. shoukaensis* sp. n. and *S. tamdaoensis* sp. n. PC distal seta absent; tip narrow; mesal apophysis present; retrolateral apophysis prominent, distally situated, parallel to PC tip (Fig. 31a, c), which is unique among congeners. Spermophore in retrolateral tegulum strongly curved, S-shaped (Fig. 31d) (see generic remarks). Embolus relatively long (Fig. 31e) (see generic remarks).

Females: epigyne dorsal and ventral plates extending posteriorly; posterior area of ventral plate elevated more than dorsal plate; dorsal plate contrastingly lighter (Fig. 31f).

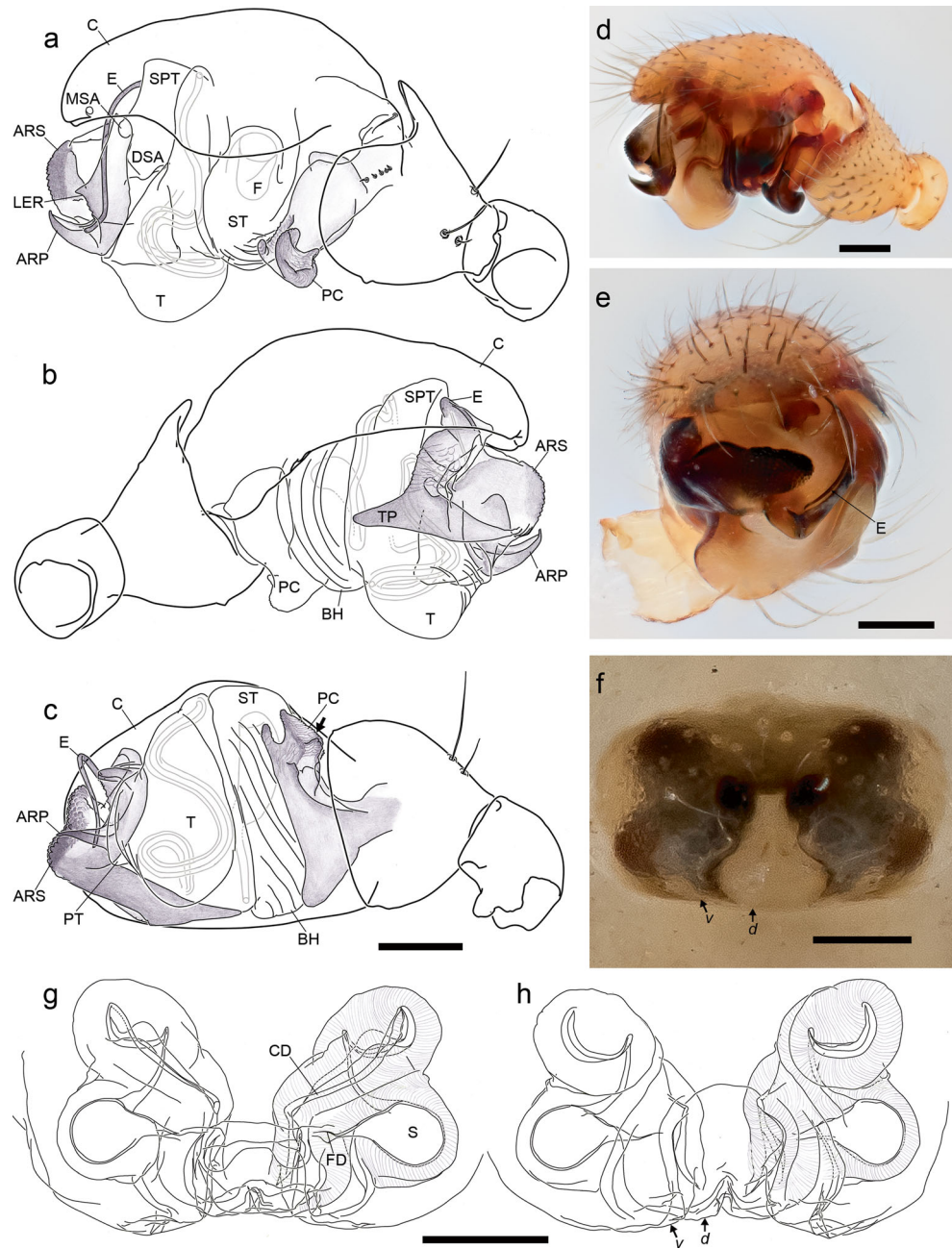
Description. Male (Holotype, ZIMG): total length: 2.3. Carapace 1 long, 0.81 wide. Opisthosoma 1.37 long, 0.77 wide. ALE-ALE: 0.14. Clypeus hirsute, central distal region glabrous; groove height: 0.02; groove-clypeal margin: 0.25; AME-groove: 0.10. Leg formula 1 > 2 > 4 > 3; leg measurements see Appendix Table 10; Tm I: 0.82. Pedipalp: patella length/height = 1.54; femur/patella = 4.23. Palpal features and prosomal modifications as in diagnosis and generic description.

Female (Paratype, ZIMG): total length: 2.7. Carapace 1.09 long, 0.85 wide. Opisthosoma 1.68 long, 1.08 wide. Leg formula 1 = 2 > 4 > 3; leg measurements see Appendix Table 10; Tm I: 0.87. Spermathecae width: 0.33. See diagnosis and generic description for somatic features and epigyne morphology.

Variation. Measurements based on male and female type material (2♂3♀).

Males (n = 2): total length: 2.3; 2.58. Carapace 1; 1.11 long, 0.81; 0.88 wide. ALE-ALE: 0.144; 0.172. Groove height:

Fig. 31 *Shaanxinus seediq* sp. n., **a–e** Male left palp, drawings and photos. **a, d** Retrolateral view. **b** Prolateral view. **c** Ventral view. **e** Apical view. **f–h** Epigyne, photo and drawings. **f, h** Ventral view, “*d*” dorsal plate, “*v*” ventral plate. **g** Dorsal view. Scale bars 0.10 mm



0.012; 0.017. Groove-clypeal margin: 0.25; 0.31. AME-groove: 0.101; 0.102. Tm I: 0.82; 0.85.

Females ($n = 3$): total length: 2.7–2.86 (2.77). Carapace 1.02–1.09 (1.06) long, 0.81–0.84 (0.83) wide. Spermathecae width: 0.3–0.33 (0.31). Tm I: 0.87–0.88 (0.88).

Distribution. Taiwan, Nantou County, Hsinchu County.

Shaanxinus meifengensis Lin sp. n.

Figs. 12, 33 and 34

Type material. Holotype: ♂, Nantou County, Ren-ai Township, next to Highland Experimental Farm, National

Taiwan University, 2151 m (24° 05' 18" N; 121° 10' 23" E), 3.V.2014, tree branch beating, in temperate broad-leaved forest, leg. S.-W. Lin (ZIMG-II-28548). Paratypes: 4♂ 5♀, same locality and date as holotype, tree branch beating, leg. S.-W. Lin (2♂ 3♀, ZIMG-II-28549, 28550, 28555–28557; 2♂ 2♀, SMF); 5♂ 5♀, same locality as holotype, 18.VI.2014, tree branch beating, leg. S.-W. Lin (2♂ 2♀, ZMUC; 3♂ 3♀, NMNS-7927-025–027, 029–031).

Other material. Same locality and date as holotype, tree branch beating, leg. S.-W. Lin, 7♂ 8♀ (ZIMG-II-28551, 28553, 28554, 28558–28561); same locality as holotype,

Fig. 32 *Shaanxinus seediq* sp. n. photos. **a–d** Male habitus. **e–h** Female habitus. **a, e** Dorsal view. **b, f** Lateral view. **c, g** Ventral view. **d, h** Frontal view. Scale bars 1 mm



18.VI.2014, tree branch beating, leg. S.-W. Lin, 17♂ 23♀ (1♂, ZIMG-II-28552; 6♂ 8♀, SMF; 5♂ 7♀, ZMUC; 5♂ 8♀, NMNS-7927-028, 032).

Derivatio nominis. The specific name is an adjective derived from “Mei-Feng,” the Chinese name of Highland Experimental Farm, National Taiwan University.

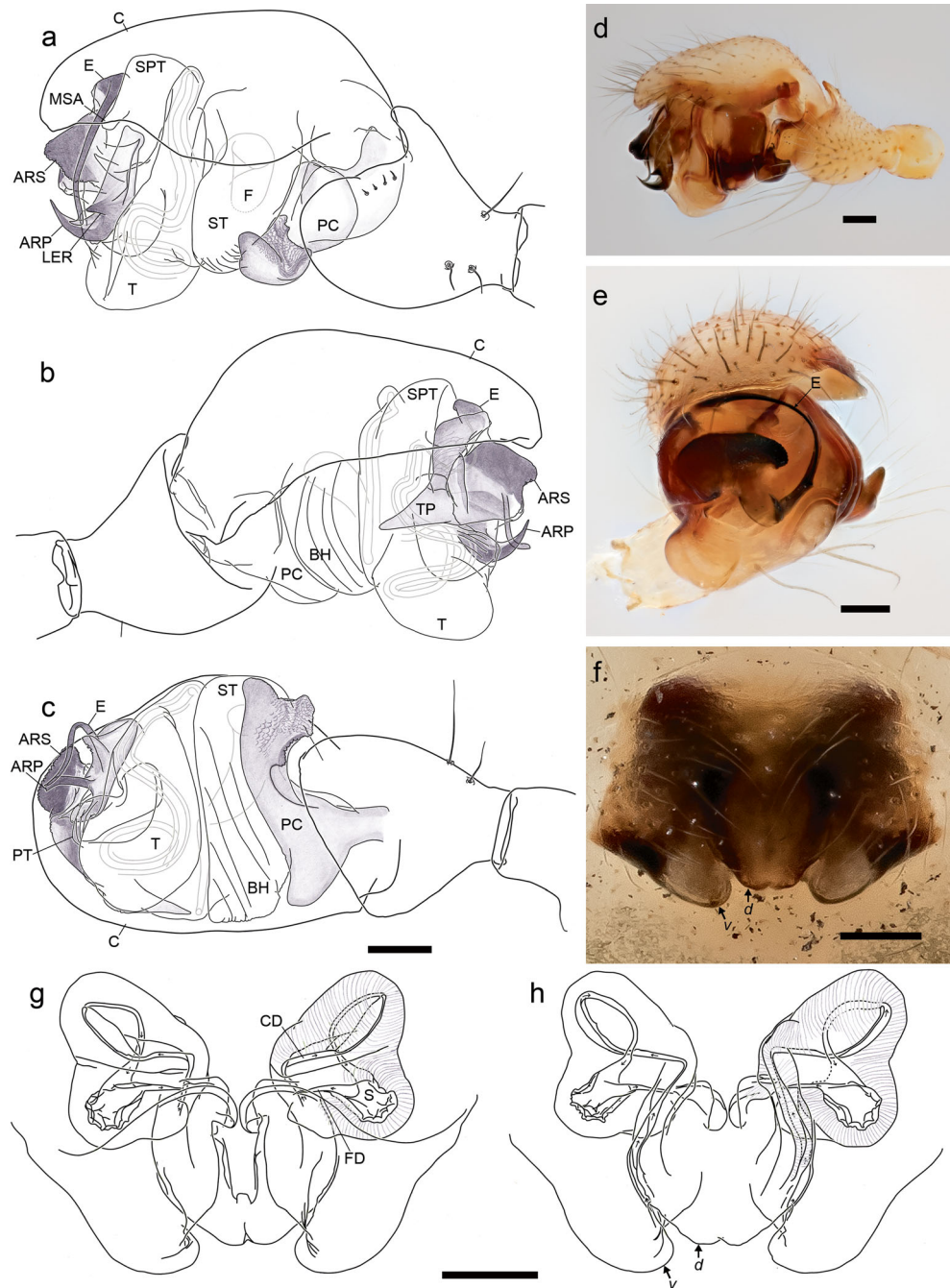
Diagnosis. Males: carapace size similar to *S. hehuanensis* sp. n., both significantly larger than remaining species described here. Clypeal groove upper and lower margins close to or contacting each other, setae on upper and lower groove laterally oriented, which distinguishes this species from *S. rufus*, *S. magniclypeus* sp. n., *S. hirticephalus* sp. n., *S. shihchoensis* sp. n., *S. shoukaensis* sp. n., and *S. tamdaoensis* sp. n. PC distal setae absent; tip wide; mesal apophysis present; retrolateral apophysis

prominent, distally situated (Fig. 33a, c; see also diagnoses of *S. hehuanensis* sp. n. and *S. atayal* sp. n.). Spermophore in retrolateral tegulum relatively strongly curved, S-shaped (Fig. 33d) (see generic remarks). Embolus relatively long (Fig. 33e) (see generic remarks).

Females: epigyne dorsal and ventral plates greatly extending posteriorly, unique among congeners (Fig. 33f–h).

Description. Male (Holotype, ZIMG): total length: 3.17. Carapace 1.46 long, 1.17 wide. Opisthosoma 1.77 long, 1.14 wide. ALE-ALE: 0.189. Clypeus hirsute, central distal region glabrous; groove height 0.003; groove-clypeal margin: 0.37; AME-groove: 0.14. Leg formula 1 > 2 > 4 > 3; leg measurements see Appendix Table 10; Tm I: 0.87. Pedipalp: patella length/height = 1.77; femur/patella = 4.66. Palpal features and prosomal modifications as in diagnosis and generic description.

Fig. 33 *Shaanxinus meifengensis* sp. n., **a–e** Male left palp, drawings and photos. **a, d** Retrolateral view. **b** Prolateral view. **c** Ventral view. **e** Apical view. **f–h** Epigyne, photo and drawings. **f, h** Ventral view, “*d*” dorsal plate, “*v*” ventral plate. **g** Dorsal view. Scale bars 0.10 mm



Female (Paratype, ZIMG): total length: 3.19. Carapace 1.23 long, 0.97 wide. Opisthosoma 1.88 long, 1.74 wide. Leg formula 1 > 2 > 4 > 3; leg measurements see Appendix Table 10; Tm I: 0.89. Spermathecae width: 0.35. See diagnosis and generic description for somatic features and epigyne morphology.

Variation. Measurements based on type material (10♂, 10♀).

Males (*n* = 10): total length: 2.87–3.25 (3.07). Carapace 1.37–1.53 (1.43) long, 1.12–1.2 (1.15) wide. ALE-ALE: 0.175–0.195 (0.185). Groove height: 0–0.013 (0.003).

Groove-clypeal margin: 0.32–0.38 (0.36). AME-groove: 0.12–0.15 (0.13). Tm I: 0.86–0.91 (0.88).

Females (*n* = 10): total length: 2.94–3.47 (3.18). Carapace 1.23–1.47 (1.33) long, 0.97–1.1 (1.05) wide. Spermathecae width: 0.34–0.39 (0.36). Tm I: 0.87–0.92 (0.9).

Distribution. Taiwan, Nantou County.

Shaanxinus atayal Lin sp. n.

Figs. 12, 35 and 36

Fig. 34 *Shaanxinus meifengensis* sp. n. photos. **a–d** Male habitus. **e–h** Female habitus. **a, e** Dorsal view. **b, f** Lateral view. **c, g** Ventral view. **d, h** Frontal view. Scale bars 1 mm



Type material. Holotype: ♂, Hsinchu County, Chiensih Township, close to Litungshan, 1523 m (24° 41' 20" N; 121° 18' 35" E), 20.V.2014, tree branch beating, in subtropical broad-leaved forest, leg. S.-W. Lin (ZIMG-II-28583). Paratypes: 7♀, same locality and date as holotype, leg. S.-W. Lin (ZIMG-II-28587~28,593); 3♂ 1♀, same locality, 23.VII.2017, leg. S.-W. Lin (ZIMG-II-28584~28,586, 28,594).

Derivatio nominis. The specific name is a noun in apposition, derived from Atayal, a Taiwanese aboriginal tribe living in the collecting area of the type specimens.

Diagnosis. Males: carapace size relatively large, smaller than *S. meifengensis* sp. n. and *S. hehuanensis* sp. n. Clypeal groove upper and lower margins contacting each other, setae on upper and lower groove laterally oriented, which distinguishes this species from *S. rufus*, *S. magniclypeus* sp. n., *S. hirticephalus* sp. n., *S. shihchoensis* sp. n., *S. shoukaensis* sp. n., and *S. tamdaoensis* sp. n. PC distal setae absent; tip wide; mesal apophysis present; retrolateral apophysis

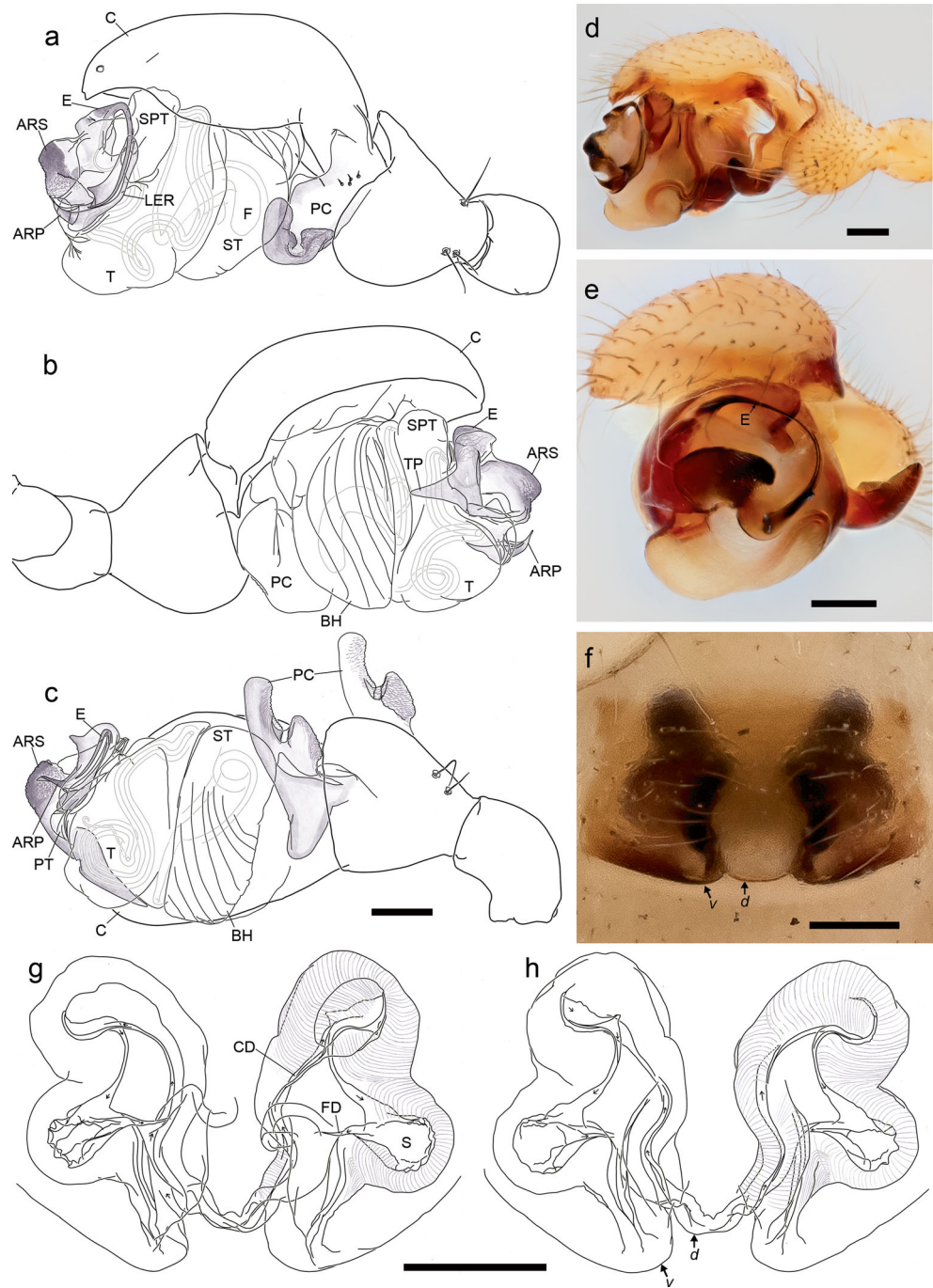
prominent, larger than *S. hehuanensis* sp. n., distally situated, but less distal than *S. meifengensis* sp. n. Figs. 29a, c, 33a, c and 35a, c; see also diagnoses of *S. hehuanensis* sp. n. and *S. meifengensis* sp. n.). Spermophore in retrolateral tegulum relatively strongly curved, S-shaped (Fig. 35d) (see generic remarks). Embolus relatively long (Fig. 35e) (see generic remarks).

Females: epigyne dorsal and ventral plates extended posteriorly (Fig. 35f–h), but less than *S. meifengensis* sp. n. (Fig. 33f–h).

Description. Male (Holotype, ZIMG): total length: 3. Carapace 1.32 long, 1.04 wide. Opisthosoma 1.7 long, 1.04 wide. ALE-ALE: 0.198. Clypeus hirsute, central distal region glabrous; groove height: 0; groove-clypeal margin: 0.33; AME-groove: 0.138. Leg formula 1 > 2 > 4 > 3; leg measurements see Appendix Table 10; Tm I: 0.88. Pedipalp: patella length/height = 1.6; femur/patella = 4.55. Palpal features and prosomal modifications as in diagnosis and generic description.

Female (Paratype, ZIMG): total length: 2.89. Carapace 1.22 long, 0.96 wide. Opisthosoma 1.69 long, 1.27 wide.

Fig. 35 *Shaanxinus atayal* sp. n., **a–e** Male left palp, drawings and photos. **a, d** Retrolateral view. **b** Prolateral view. **c** Ventral view. **e** Apical view. **f–h** Epigyne, photo and drawings. **f, h** Ventral view, “*d*” dorsal plate, “*v*” ventral plate. **g** Dorsal view. Scale bars 0.10 mm



Leg formula 1 > 2 > 4 > 3; leg measurements see Appendix Table 10; Tm I: 0.89. Spermathecae width: 0.31. See diagnosis and generic description for somatic features and epigyne morphology.

Variation. Measurements based on 4 male and 7 female paratypes.

Males ($n = 4$): total length: 2.34–3 (2.6). Carapace 1.21–1.32 (1.29) long, 0.98–1.04 (1.02) wide. ALE–ALE: 0.187–0.201 (0.196). Groove height: 0–0.004 (0.001). Groove–

clypeal margin: 0.33–0.37 (0.34). AME–groove: 0.106–0.141 (0.13). Tm I: 0.85–0.88 (0.87).

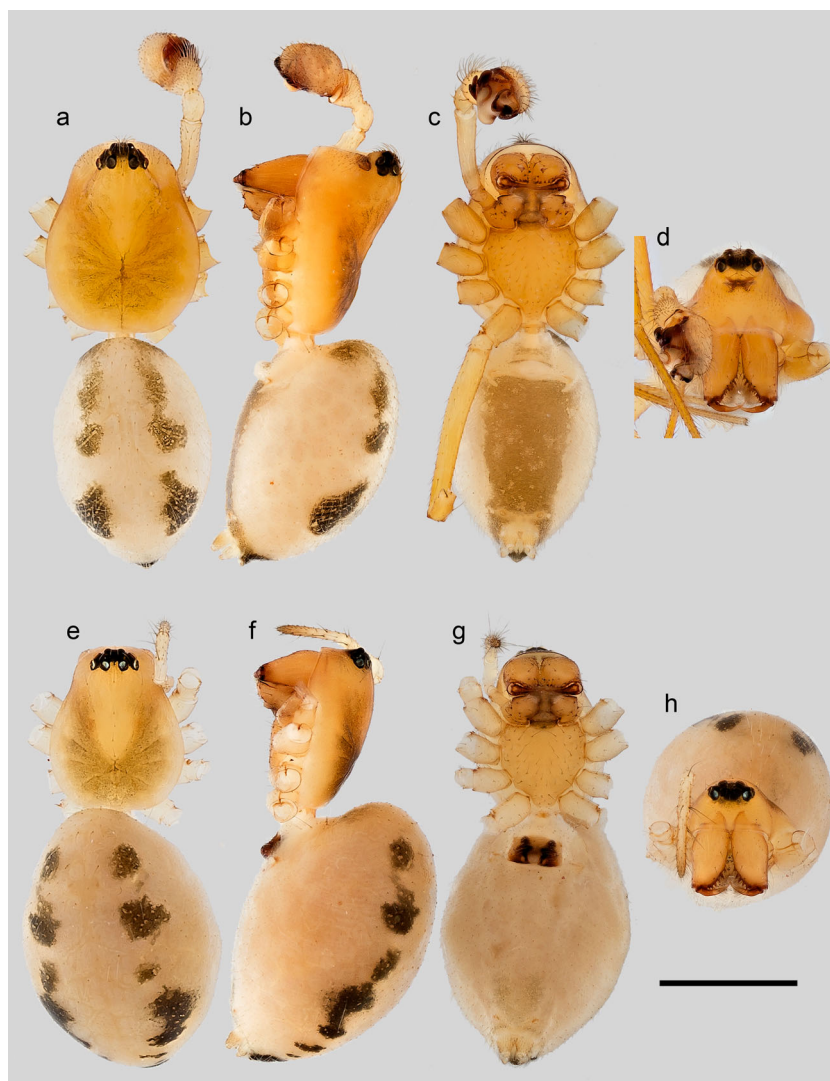
Females ($n = 8$): total length: 2.72–3.16 (2.93). Carapace 1.14–1.22 (1.18) long, 0.9–0.95 (0.92) wide. Spermathecae width: 0.28–0.33 (0.3). Tm I: 0.84–0.9 (0.88).

Distribution. Taiwan, Hsinchu County.

Shaanxinus tamdaoensis Lin sp. n.

Figs. 5g–i, 6, 37 and 38

Fig. 36 *Shaanxinus atayal* sp. n. photos. **a–d** Male habitus. **e–h** Female habitus. **a, e** Dorsal view. **b, f** Lateral view. **c, g** Ventral view. **d, h** Frontal view. Scale bars 1 mm



Type material. Holotype: ♂, Vietnam, Vin Phuc Province, Tam Dao National Park, 800–1100 m (21° 28' N; 105° 38' E), H. Malicky leg. 19.V-13.VI.1995, J. Wunderlich vend. 2008 (SMF).

Derivatio nominis. The specific name is an adjective, derived from Tam Dao National Park, the collecting site of the holotype.

Diagnosis. Male: clypeal groove upper and lower margins not contacting each other; setae on upper and lower groove slightly laterally oriented. PC distal seta absent, tip simple, not widened; mesal and retrolateral apophyses absent (Fig. 37d), a combination of PC features unique among congeners. Spermophore in retrolateral tegulum slightly curved (Fig. 37a) (see generic remarks). Embolus extremely long (Fig. 37e; see generic remarks).

Description. Male (Holotype, SMF): total length: 2.76. Carapace 1.19 long, 0.9 wide. Opisthosoma 1.6 long, 1.11

wide. ALE-ALE: 0.194. Clypeus hirsute, central distal region glabrous; groove height: 0.012; groove-clypeal margin: 0.25; AME-groove: 0.1. Leg formula 1 = 2 > 4 > 3; leg measurements see Appendix Table 10; Tm I: 0.91. Pedipalp: patella length/height = 1.78; femur/patella = 5.45. Median membrane present, with long papillae (Fig. 37a, b). Palpal features and prosomal modifications as in diagnosis and generic description.

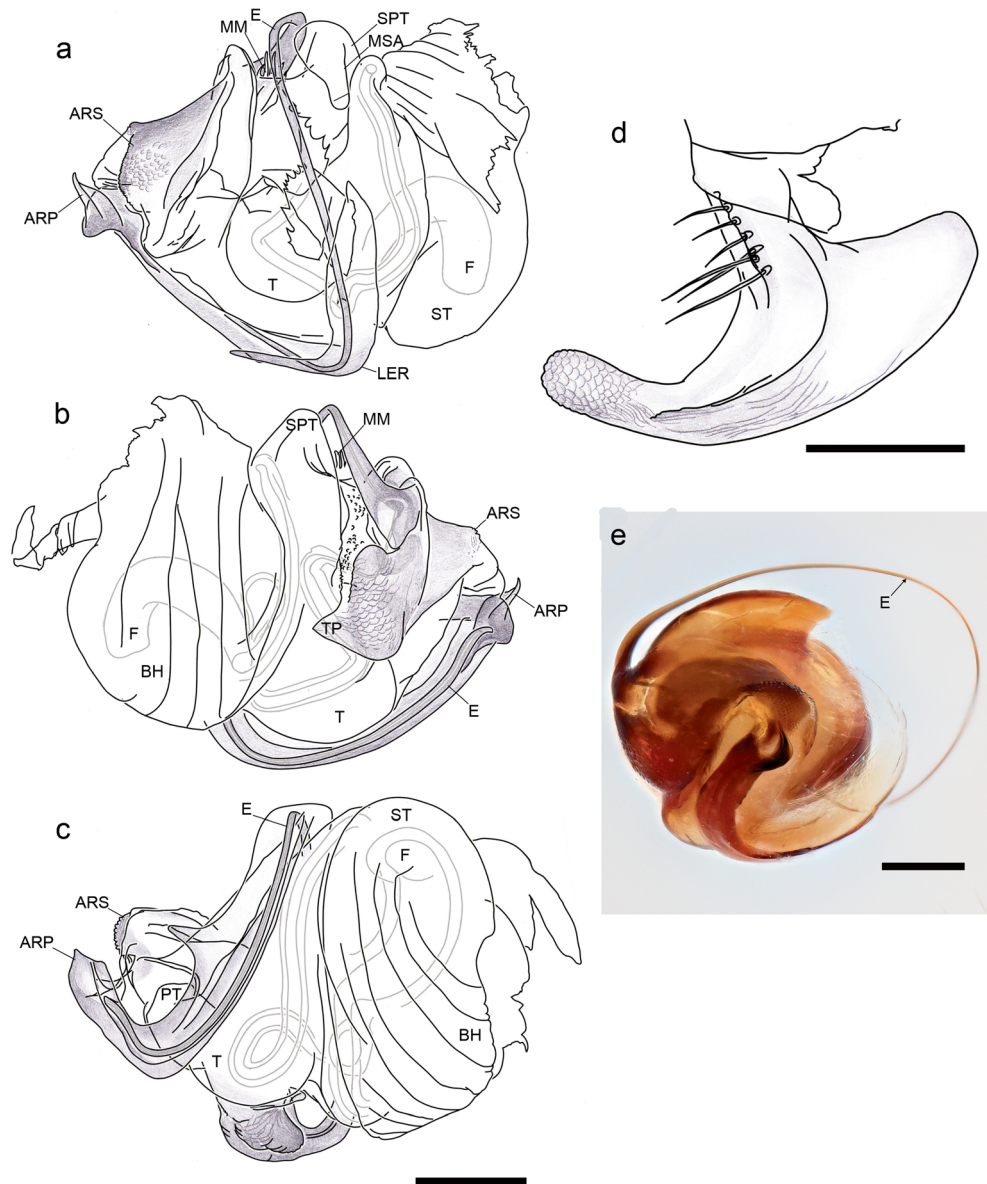
Female: unknown.

Distribution. Vietnam.

Micro-CT investigation on male prosomal modification and palp

In all three inspected species, relatively homogenous grey areas were found on virtual sections, adjacent to the cuticle and clearly distinguishable from muscle tissues and eye-

Fig. 37 *Shaanxinus tamdaoensis* sp. n., male left palp. **a–c** Bulbus drawings. **a** Retrolateral view. **b** Prolateral view. **c** Ventral view. **d** PC, prolateral view. **e** *bulbus*, apical view. Scale bars 0.10 mm



related structures (Fig. 5c, f, i). Similar structures were not found in the corresponding area in other dwarf spider species without prosomal modifications (S-W.L., L.L., and G.U., unpublished). The distribution of these tissues resembles that of some *Oedothorax* species, of which the nuptial-gift-producing glands have been identified through histological sections and transmissive electron microscopy (Michalik and Uhl 2011). Therefore, we assume that the tissues found here produce nuptial gifts. The distribution of these tissues seems correlated with surface areas of dense setae (compare Fig. 5a, d, g with Fig. 5b, e, h). Canals penetrating the cuticle are visible on the clypeal area, which connect the setae and the secretory tissue, in especially high density at the clypeal groove (Fig. 5c, f, i). In the *S. tamdaoensis* sp. n. sample collected in 1995 and the *S. rufus* sample collected in 1997, slight disconnection was observed between the cuticle and muscle tissues, but the

glandular tissues remain tightly connected to the cuticle, probably due to their robust structural continuity through the cuticular canals (Fig. 5c, i).

Configuration of *S. tamdaoensis* sp. n. male palpal structures in an artificially expanded palp is shown in Fig. 6. Dorsal part of lateral extension of radix was fitted into distal margin of palpal tibia; ventral part was fitted to paracymbium; anterior scaly part of radix, anterior radical process and paracymbium tip held the embolus, with the distal part of embolus protruded. Embolus is presumably held by LER in an unexpanded palp, like the case in other *Shaanxinus* species (see discussion below).

Intragenetic relationships

Characters applied for the morphological phylogenetic analysis is shown in Table 5. The most parsimonious tree

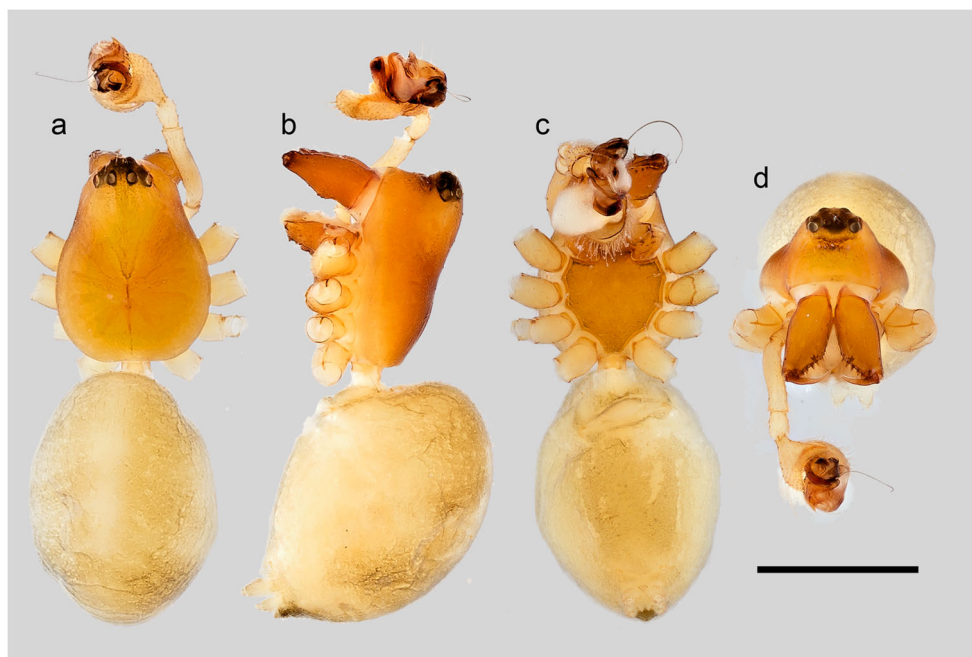


Fig. 38 *Shaanxinus tamdaoensis* sp. n., male habitus photos. **a** Dorsal view. **b** Lateral view. **c** Ventral view. **d** Frontal view. Scale bars 1 mm

($L = 53.806$, $CI = 0.605$, $RI = 0.802$) (Fig. 39) recovered *Shaanxinus* monophyletic (Clade 5), with *N. crucifera* as sister taxon, and *S. rufus* as the ingroup species splitting off first. Three synapomorphies supported *Shaanxinus*: LER groove hosting the distal part of the embolus (Ch 7), PC distal part scaly (Ch 14), and the presence of a clypeal groove (Ch 21). Two characters supported the monophyly of the clade containing the 14 species described here (Clade 6): spermophore in tegulum curved (Ch 9, homoplastic) and the presence of mastidia on male chelicerae (Ch 25, synapomorphic). The branch containing the Taiwanese species (Clade 7) was supported by the absence of papillae on the median membrane (Ch 3, synapomorphic). Clade 8 was supported by a completely hirsute clypeus (Ch 23, homoplastic since shared with *L. triangularis*), in contrast to all other *Shaanxinus* species, which have a glabrous distal region of the clypeus, and by the longer second pair of legs (Ch 26, homoplastic, due to shared character state with *S. rufus*). For the resolution of the interspecific relationships of the Taiwanese *Shaanxinus* species, the combination of both discrete and continuous characters was important; most branches were weakly supported, with Jackknife values below 50, except Clade 11 (Jackknife value = 50).

Molecular phylogenetic analyses

Test of morphological species delimitation and sex matching

As expected, 28S gave only limited phylogenetic resolution; only the monophyly of *S. hirticephalus* sp. n., *S. magniclypeus* sp. n.,

and *S. tsou* sp. n. were supported (Fig. 40). The two mtDNA markers generated similar overall tree topologies, while COI (685 bp) performed slightly better than 16S (458 bp) in recovering species monophyly and resolving interspecific branches. COI recovered 10 monophyletic species (*S. seediq* sp. n., *S. tsou* sp. n., *S. mingchihensis* sp. n., *S. makauyensis* sp. n., *S. lixiangae* sp. n., *S. magniclypeus* sp. n., *S. hirticephalus* sp. n., *S. shihchouensis* sp. n., *S. shoukaensis* sp. n., and *S. meifengensis* sp. n.), whereas 16S recovered the monophyly of eight of those 10 species (compare Figs. 41 and 42).

Two species, *S. tsou* sp. n. and *S. makauyensis* sp. n., were not recognized in the morphological examination, and were reevaluated after the molecular phylogenetic analyses. Morphological differences between these latter two species and *S. curviductus* sp. n. and *S. mingchihensis* sp. n. were subsequently discovered in a reciprocal illumination approach. However, we found no morphological differences among specimens comprising the polyphyletic *S. curviductus* sp. n. (Figs. 41, 42 and 43). As to the two geographical populations of *S. magniclypeus* sp. n., they were considered at first two distinct species since morphological differences are minor (see species diagnosis). Due to their position on a single branch, and the absence of monophyly in all molecular datasets (Figs. 40, 41, 42 and 43) but allopatric distribution, we consider it more appropriate to describe them as one species.

Since all species included male and female specimens, species rendered as monophyletic by the genetic data also supported their sex matching. Based on the hypotheses from 16S, COI, and the combined dataset, the monophyletic *S. meifengensis* sp. n. was nested within *S. hehuanensis* sp.

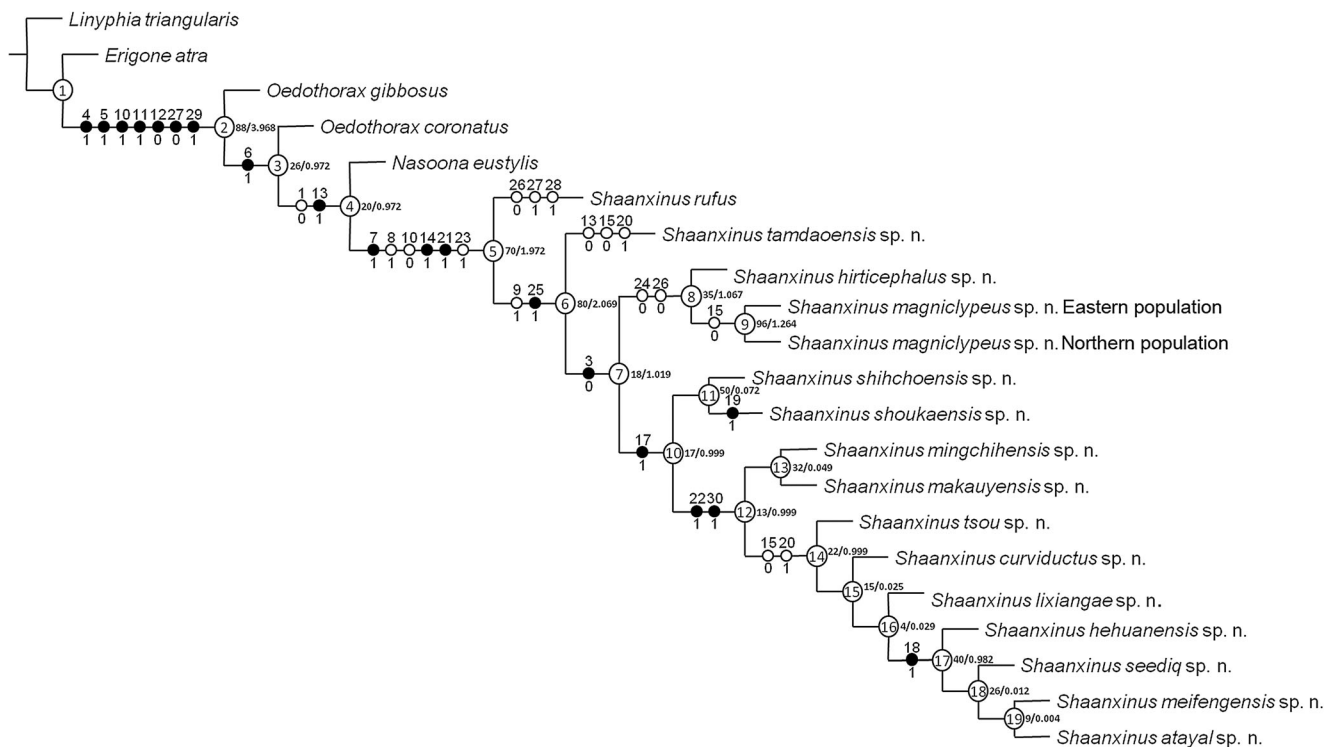


Fig. 39 Morphological phylogeny of *Shaanxinus*, single most parsimonious tree ($L = 53.806$, $CI = 0.605$, $RI = 0.802$), from the analysis of 30 discrete and six continuous morphological characters. Unambiguous character optimizations are shown for every branch in

the tree. Non-homoplastic character transformations are marked in black. Branches without depicted unambiguous character transformations are supported by continuous characters (not shown). Jackknife/Bremer support values are shown right to the node of each branch

n., rendering the latter paraphyletic (Figs. 41, 42 and 43). On both 16S and COI hypotheses, *O. apicatus* was sister to *Shaanxinus*, whereas 28S and the combined dataset supported a close relatedness of *Shaanxinus* with *N. crucifera*.

Efficacy of mitochondrial markers as DNA barcode

Intra- and interspecific uncorrected sequence divergences for the 16S, COI and combined datasets are reported in Tables 6, 7 and 8 and boxplots in Figs. 41, 42, and 43, respectively. 16S generally gave the lowest divergence values. The mean intraspecific divergence ranged from 0% (*S. mingchihensis* sp. n.) to 2.44% (*S. curviductus* sp. n.), while the mean interspecific divergence ranged from 0.18% (*S. shihchoensis* sp. n. - *S. shoukaensis* sp. n.) to 7.58% (*S. magniclypeus* sp. n. - *S. meifengensis* sp. n.). The COI marker showed a mean intraspecific divergence ranging from 0 to 5.21% (*S. curviductus* sp. n.), and a mean interspecific divergence ranging from 3.30% (*S. shihchoensis* sp. n. - *S. shoukaensis* sp. n.) to 13.08% (*S. meifengensis* sp. n. - *S. shoukaensis* sp. n.). Finally, the combination of markers showed a mean intraspecific divergence ranging from 0% (*S. makauyensis* sp. n.) to 4.14% (*S. curviductus* sp. n.), and a mean interspecific divergence ranging from 2.00% (*S. shihchoensis* sp. n. - *S. shoukaensis* sp. n.) to 10.72% (*S. magniclypeus* sp. n. - *S. meifengensis* sp. n.). Both markers and their combination showed overlaps

between the intra- and interspecific mean divergences (Figs. 41, 42 and 43), and a large proportion of individuals had maximum intraspecific divergence higher than minimum interspecific divergence (Fig. 44). In other words, no Barcode Gap seems to exist for *Shaanxinus* for this dataset.

Operational approach

Results from distance-based measures using the Nearest Neighbor and Meier's best close match gave similar identification success rates for COI, 16S, and their combination, suggesting similar marker efficiencies (Table 9). However, the BOLD identification criterion produced a much lower success rate in 16S than COI and the combined dataset. In the three tree-based measures, both markers failed to recover part of the species, with COI performing better than 16S and the combined dataset. Finally, only a few species had their monophyly recovered by COI and the combined dataset with significant probability according to the criterion of Rosenberg's probability of reciprocal monophyly, while 16S recovered none of them.

Test for COI substitution saturation

Among *Shaanxinus* species (left side of Fig. 45), both transitions and transversions did not show signs of saturation, indicating that the COI sequences were appropriate for

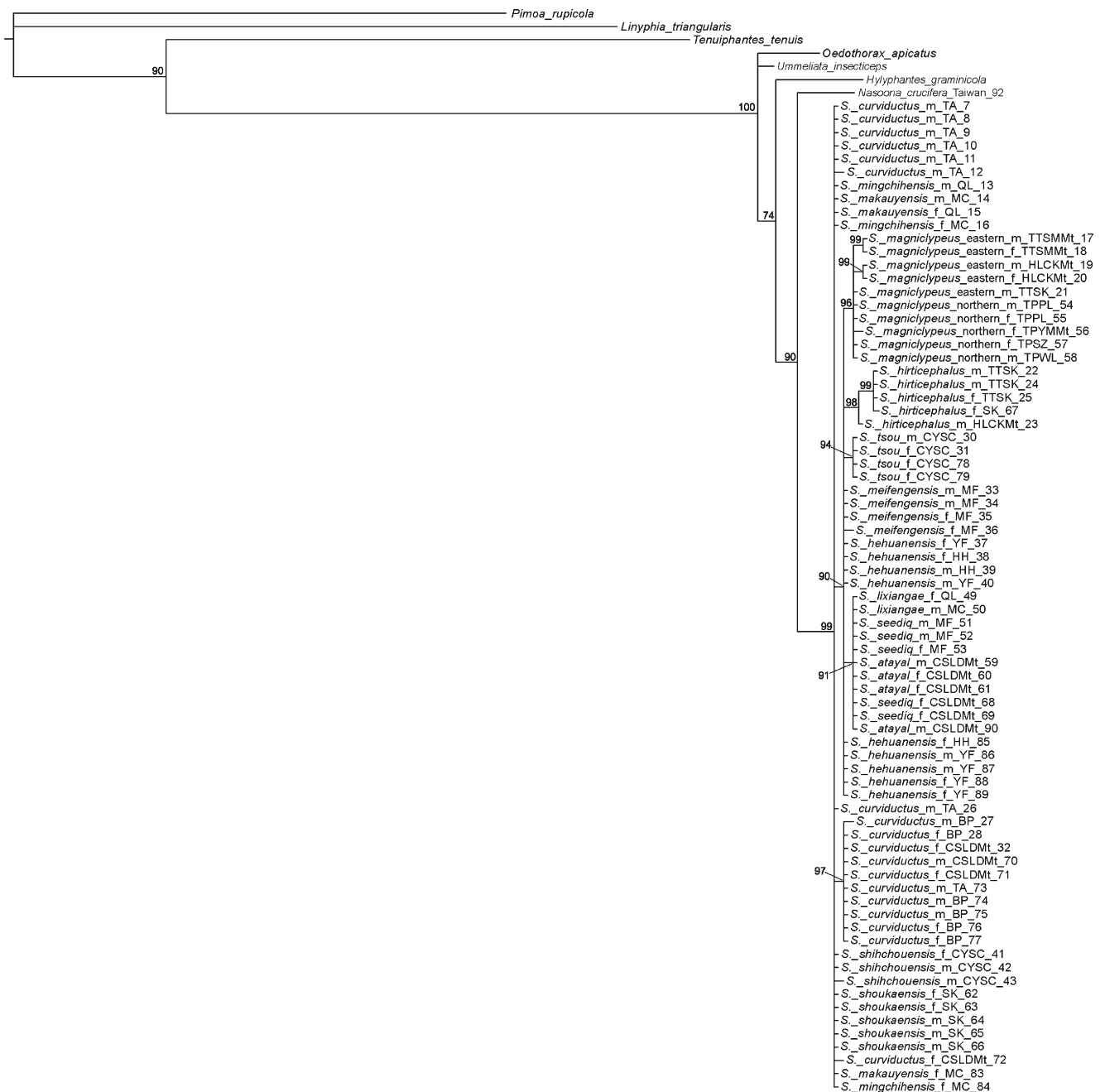


Fig. 40 Tree topology from the Bayesian analysis of the 28S dataset. Numbers below nodes indicate posterior probabilities. Nodes with posterior probability lower than 50% are collapsed

intra-generic phylogenetic analysis. In contrast, the intergeneric comparison with the *N. crucifera* sequence (right side of Fig. 45) suggested that saturation had been reached, rendering deeper phylogenetic analyses problematic.

Discussion

Our study on Taiwanese *Shaanxinus* species has brought attention to issues about exploring prosomal structures using

micro-CT technique, functions of male palpal structures, species diversity, efficacy of different markers in DNA barcoding, and possible reasons for species poly-/paraphyly in mtDNA gene trees.

Exploration of erigonine male prosomal glandular tissues and palpal structures using micro-CT

Previously, several studies have employed histological methods for determining the presence and ultrastructure

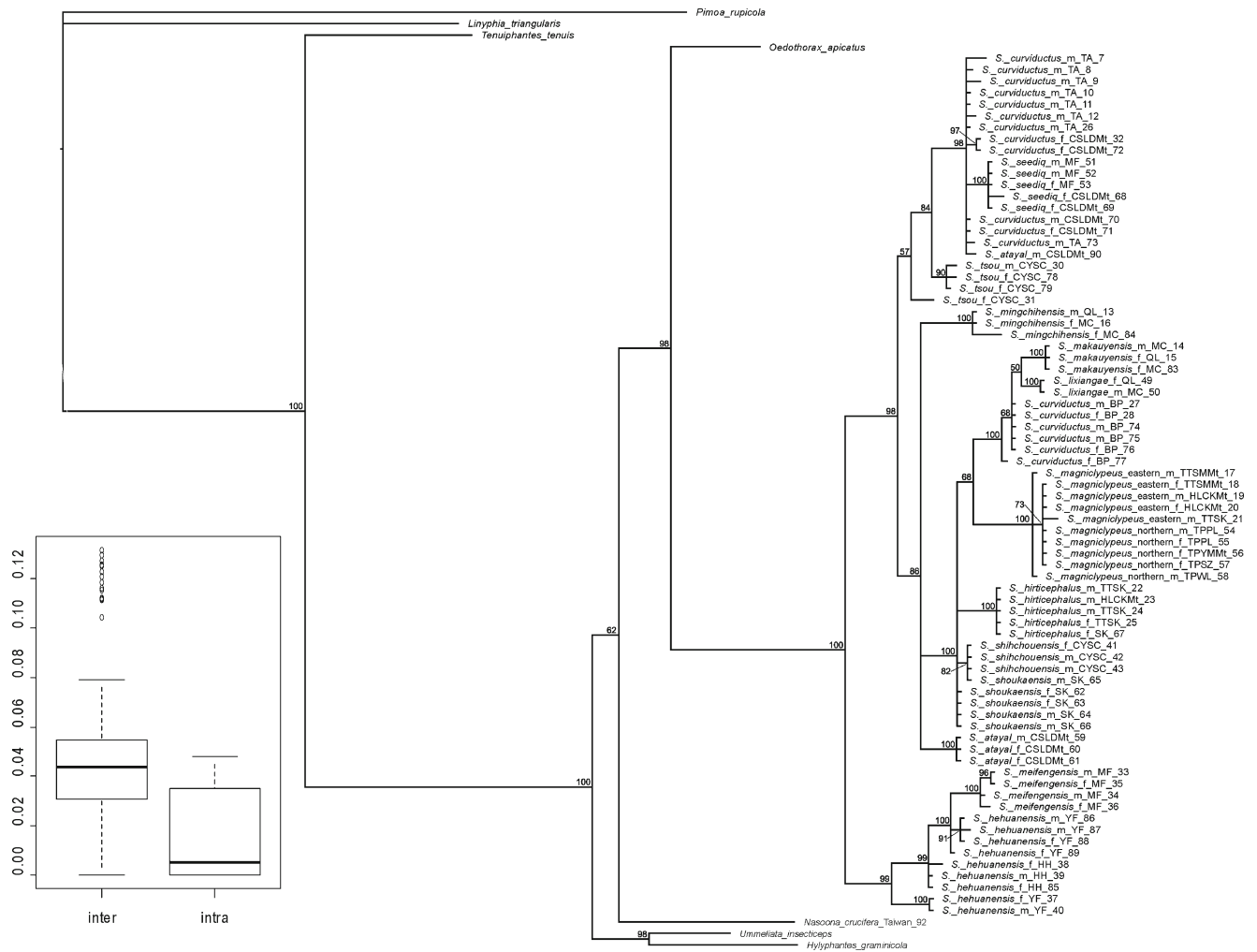


Fig. 41 Tree topology from the Bayesian analysis of the 16S dataset. Numbers below nodes indicate posterior probabilities. Nodes with posterior probability lower than 50% are collapsed. Lower left: Box plot showing p-distances for the 16S dataset between sequences of

Shaanxinus specimens. Boxes represent first (bottom) and third (top) quartiles. Black horizontal bar within boxes indicate median values. Whiskers show values within 1.5 times the interquartile range. Outlying data are represented with circles

of gland cells in linyphiids (Schaible and Gack 1987; Michalik and Uhl 2011; de Causmaecker 2004; Schaible et al. 1986; Blest and Taylor 1977) and theridiids (Legendre and Lopez 1974; Juberthie and Lopez 1980). Our study represents the first endeavor to reconstruct the extent of glandular tissues associated with erigonine prosomal modifications by means of micro-CT. Although the technique does not allow for determination of gland cell types as given in Michalik and Uhl (2011), our results show that the areas of glandular tissues are distinguishable from surrounding muscular tissues in virtual sections. Instead of using critical-point-dried samples, like in Sentenská et al. (2017), we scanned the samples in alcohol, whereby we achieved sufficient contrast in the reconstructed images for delineating the glandular tissues. Due to its non-destructive nature, this method can be applied in cases where dehydrating or sectioning the

samples are not permitted, e.g., when only the type material is available. In addition, this method further allows for volume calculation of the marked tissue. The extent and volume of glandular tissues may show species- or group-specific patterns, and thus might provide further characters for species identification and phylogenetic analyses in erigonines and other animal groups.

Functions of male palpal structures

The male spider copulatory organs have drawn much interest of research on the functioning of these complex species specific organs, as well as on the factors that could have driven their evolution (Huber 1993, 1994a, 1995a, b, c; Huber and Eberhard 1997; Barrantes et al. 2013; Uhl et al. 2007; Burger et al. 2010; Burger 2008). In all the investigated spider species, mechanistic functions of male

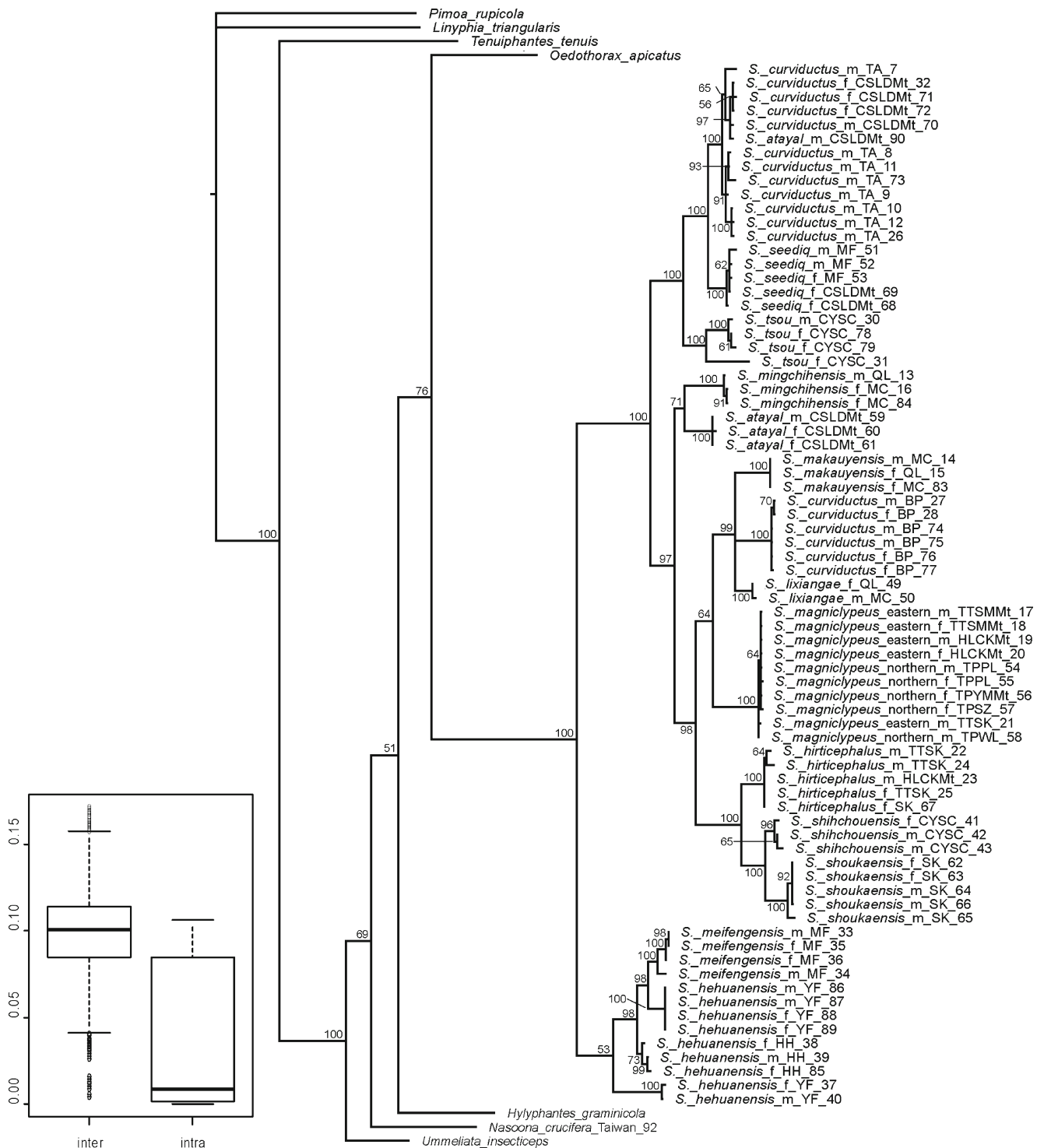


Fig. 42 Tree topology from the Bayesian analysis of the COI dataset. Numbers below nodes indicate posterior probabilities. Nodes with posterior probability lower than 50% are collapsed. Lower left: Box plot showing p-distances for the COI dataset between sequences of

Shaanxinus specimens. Boxes represent first (bottom) and third (top) quartiles. Black horizontal bar within boxes indicate median values. Whiskers show values within 1.5 times the interquartile range. Outlying data are represented with circles

palpal structures belong almost exclusively to intersexual interaction, with male appendages pressing against female genital structures, e.g., scapes, atria, and furrows. Interestingly, in four pholcid species, interactions between

male basal palpal segments (coxa, trochanter, and femur) and cheliceral structures help holding the palp in the rotated position (Huber and Eberhard 1997; Huber 1995a; Uhl et al. 1995)

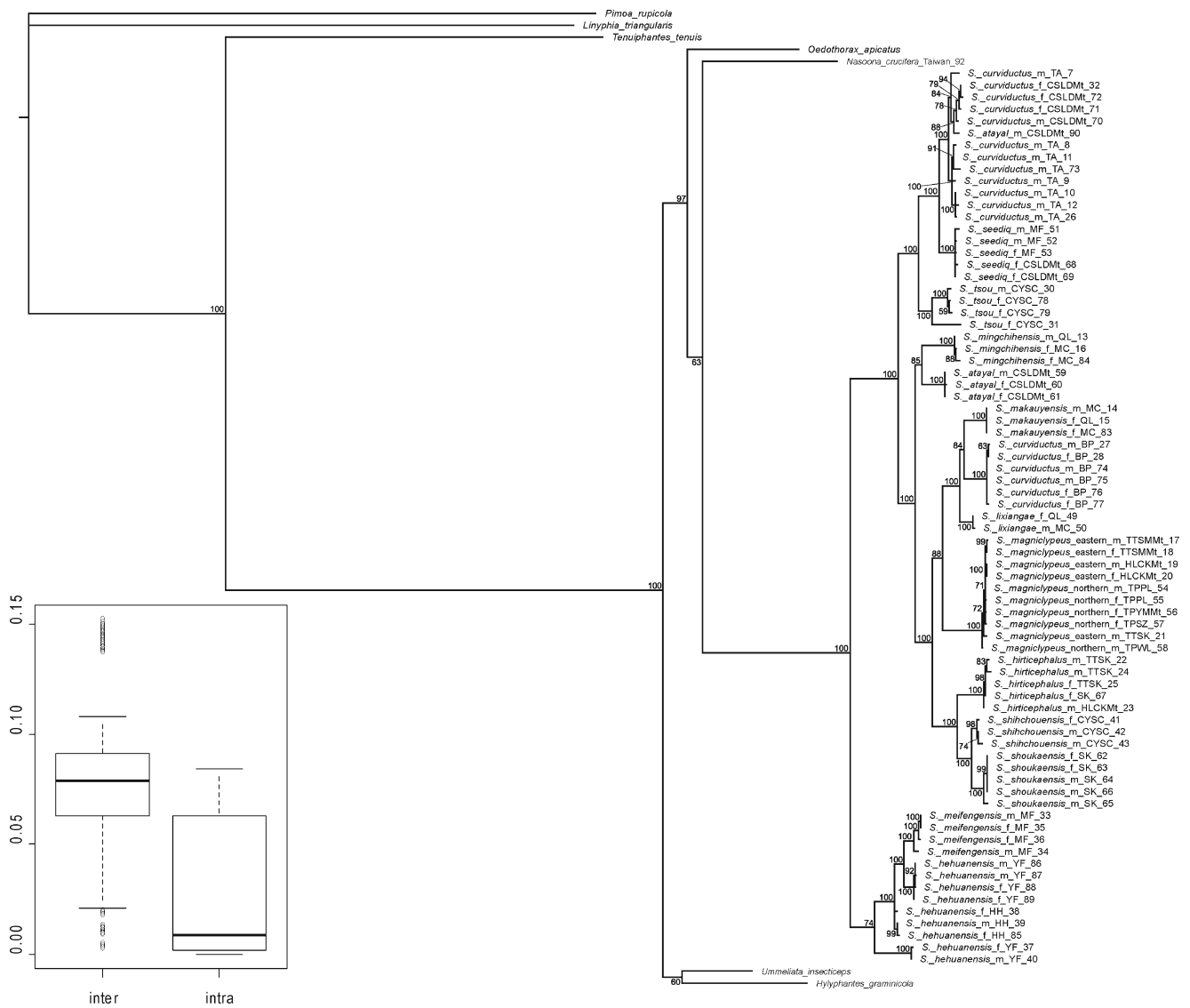


Fig. 43 Tree topology from the Bayesian analysis of the combined dataset of 16S, COI, and 28S. Numbers below nodes indicate posterior probabilities. Nodes with posterior probability lower than 50% are collapsed. Lower left: Box plot showing p-distances for the combined dataset of 16S and COI between sequences of *Shaanxinus* specimens.

Boxes represent first (bottom) and third (top) quartiles. Black horizontal bar within boxes indicate median values. Whiskers show values within 1.5 times the interquartile range. Outlying data are represented with circles

To our knowledge, only four linyphiid species have been investigated for their male palpal sclerite functions during copulation, including *Lepthyphantes leprosus* (Micronetinae) (van Helsdingen 1965) and three species of *Haplunis* (Mynogleninae) (Blest and Pomeroy 1978). In these studies, the only tentative description of an interaction between male palpal sclerites is the distal offshoot of the paracymbium of *L. leprosus* pressing against the median membrane, which in its turn lies against the embolus (van Helsdingen 1965). All the other male structures in these linyphiid species function by pressing against female structures during mating. Different from the complex structures in female spiders described in the abovementioned studies, *Shaanxinus* species have much

simpler female external genitalia, without any external projecting structures (Fig. 4f), which provides hardly any anchoring point for male structures other than the embolus. Therefore, the most probable function of *Shaanxinus* male palpal sclerites may be locking the palp in the rotated position during palpal expansion, as seen in the expanded *S. tamdaoensis* sp. n. palp (Fig. 6). Artificially expanding genital bulbs, however, may result in completely different spatial relations of the bulbal sclerites compared to natural expansions during mating, as was shown in *Nesticus cellulanus* (Huber 1994b, 1995c). In contrast to *N. cellulanus*, the palpal sclerites of *S. tamdaoensis* sp. n. do interact. Considering the complex morphology of *Shaanxinus* palp, the structural affinity between palpal sclerites and the absence of

Table 7 Mean and range (in brackets) of pairwise uncorrected distances between sequences of *Shaanxinus* specimens for the COI dataset

	1	2	3	4	5	6	7	8	9	10	11	12	13
1 <i>curviductus</i>	5.21 (0–10.66)												
2 <i>minchiensis</i>	8.98 (8.33–9.41)	0.10 (0–0.15)											
3 <i>makayensis</i>	8.22 (5.69–10.07)	8.63 (8.47–8.80)	0.00										
4 <i>magnicypeus</i>	8.96 (6.42–10.59)	8.11 (7.74–8.52)	7.29 (7.08–7.47)	0.14 (0–0.44)									
5 <i>hiricephalus</i>	8.58 (7.45–9.97)	8.87 (8.47–9.51)	8.11 (7.88–8.59)	8.95 (8.95–9.51)	0.46 (0–0.93)								
6 <i>tsou</i>	8.00 (6.18–11.21)	9.39 (8.91–9.86)	10.40 (10.22–10.51)	10.40 (9.88–11.09)	10.31 (9.78–11.50)	2.99 (0.44–5.55)							
7 <i>meifengensis</i>	11.57 (10.80–12.70)	11.59 (11.09–11.99)	12.52 (12.41–12.55)	12.81 (12.54–13.03)	11.98 (11.09–12.73)	12.12 (11.68–12.85)	0.83 (0–1.61)						
8 <i>hehuanensis</i>	11.37 (10.36–12.83)	10.90 (10.36–11.53)	11.87 (11.24–12.85)	12.26 (11.65–12.99)	11.67 (11.24–12.73)	11.80 (11.09–12.55)	3.95 (2.77–7.88)	3.78 (0–7.45)					
9 <i>shihchoensis</i>	8.97 (7.15–10.46)	9.09 (8.47–9.95)	8.74 (8.18–9.43)	9.80 (9.20–10.63)	4.83 (4.23–5.67)	9.42 (8.76–10.81)	12.65 (11.53–13.89)	12.20 (11.24–13.89)	0.66 (0.44–1.03)				
10 <i>lixiangae</i>	8.28 (4.09–10.66)	7.89 (7.59–8.19)	4.38 (4.23–4.53)	6.26 (5.99–6.57)	7.93 (7.59–8.44)	10.68 (10.51–10.80)	12.59 (12.41–12.70)	11.82 (11.39–13.14)	8.09 (7.45–8.75)	0.29			
11 <i>seediq</i>	5.77 (2.63–10.95)	8.63 (8.18–9.10)	9.50 (9.20–9.93)	9.65 (9.14–10.25)	10.65 (10.07–11.66)	6.39 (5.55–7.59)	11.95 (11.53–12.41)	11.79 (10.51–12.99)	10.33 (9.64–11.15)	10.47 (10.22–10.66)	0.41 (0.15–0.74)		
12 <i>atayal</i>	7.47 (0.44–10.36)	6.40 (5.40–8.80)	8.32 (7.88–9.34)	8.13 (7.23–10.10)	8.67 (8.18–9.51)	8.71 (8.18–9.51)	11.61 (10.95–11.97)	11.27 (10.51–11.97)	9.11 (8.32–10.29)	8.65 (7.88–10.36)	7.02 (2.77–8.76)	4.33 (0–8.47)	
13 <i>shoukaensis</i>	9.82 (8.03–11.32)	8.04 (7.88–8.35)	8.58 (8.47–9.05)	9.19 (8.91–9.81)	5.82 (5.40–6.75)	10.28 (5.40–6.75)	13.08 (12.26–13.72)	12.23 (11.97–12.99)	3.30 (2.92–4.12)	7.71 (7.45–8.32)	10.85 (10.51–11.39)	9.53 (8.91–10.95)	0.35 (0–0.88)

Lower left: interspecific distances. Diagonal (bold): intraspecific distances

Table 8 Mean and range (in brackets) of pairwise uncorrected distances between sequences of *Sitonaiximus* specimens for the combined dataset

	1	2	3	4	5	6	7	8	9	10	11	12	13
1 <i>curviductus</i>	4.14 (0-8.45)												
2 <i>minchiensis</i>	6.95 (6.57-7.31)	0.06 (0-0.09)											
3 <i>makauyensis</i>	6.32 (3.77-8.06)	6.63 (6.49-7.04)	0.00										
4 <i>magnitclypeus</i>	7.20 (5.00-8.52)	6.79 (6.49-7.04)	5.69 (5.52-5.79)	0.15 (0-0.44)									
5 <i>hiritecephalus</i>	6.66 (5.52-7.67)	6.90 (6.66-7.31)	6.07 (5.96-6.32)	6.56 (6.30-6.85)	0.27 (0-0.54)								
6 <i>tsou</i>	5.94 (4.47-8.91)	7.01 (6.66-7.31)	7.90 (7.62-8.36)	8.16 (7.71-8.75)	7.73 (7.19-8.94)	2.36 (0.44-4.33)							
7 <i>meifengensis</i>	9.27 (8.59-10.25)	9.48 (9.11-9.81)	10.30 (10.17-10.34)	10.72 (10.67-10.80)	9.73 (9.20-10.11)	9.44 (8.94-10.52)	0.60 (0-1.05)						
8 <i>hehuanensis</i>	9.10 (8.15-10.23)	9.06 (9.71-8.59)	9.87 (9.38-10.43)	10.32 (9.96-10.77)	9.48 (9.11-10.10)	9.17 (8.33-10.32)	3.13 (2.02-6.05)	2.88 (0-5.87)					
9 <i>shihchoensis</i>	6.52 (5.08-7.76)	6.75 (6.40-7.16)	6.03 (5.78-6.26)	7.01 (6.66-7.51)	3.55 (3.24-4.06)	6.69 (6.13-7.87)	9.88 (9.29-10.39)	9.54 (8.94-10.30)	0.38 (0.26-0.58)				
10 <i>lixiangae</i>	6.39 (2.72-8.64)	6.28 (6.05-6.57)	3.07 (2.98-3.16)	5.25 (5.00-5.47)	6.05 (5.87-6.32)	8.05 (10.17-10.34)	10.25 (10.17-10.34)	9.76 (9.38-10.52)	5.65 (5.35-5.87)	0.18 (0.18-0.18)			
11 <i>seediq</i>	4.44 (2.02-8.33)	6.85 (6.57-7.22)	7.58 (7.45-7.80)	7.98 (7.58-8.34)	8.15 (7.89-8.66)	4.88 (9.20-9.55)	9.33 (9.20-9.55)	9.05 (8.15-9.64)	7.72 (7.45-7.99)	8.25 (8.15-8.33)	0.32 (0.09-0.61)		
12 <i>atayal</i>	5.62 (0.35-8.06)	5.15 (4.38-7.12)	6.46 (6.05-8.34)	6.76 (6.05-8.34)	6.62 (6.22-7.49)	6.25 (8.68-9.29)	9.04 (8.68-9.29)	8.79 (8.15-9.20)	6.54 (6.05-7.41)	6.62 (8.24-5.96)	5.34 (2.19-6.57)	3.21 (0-6.31)	
13 <i>shoukaensis</i>	7.14 (5.52-8.35)	6.12 (5.96-6.48)	5.96 (5.87-6.31)	6.67 (6.40-7.23)	4.10 (3.86-4.69)	7.39 (9.64-10.60)	10.17 (9.64-10.60)	9.58 (9.29-10.08)	2.00 (1.84-2.31)	5.43 (5.26-5.87)	8.05 (7.89-8.41)	6.85 (6.31-8.06)	0.25 (0-0.61)

Lower left: interspecific distances. Diagonal (bold): intraspecific distances

Table 9 Summary of results from the six operational criteria for marker efficacy used in this study across datasets, reported as identification success rates (in percent) or number of species recovered

Partition	Distance-based measures			Tree-based measures		
	NN (%)	BOLD i.c. (%)	MBCM (%)	Sp. monophyly	Boot. monophyly	Rosenberg
16S	96	53	91	8/13 (62%)	6/13 (46%)	0/13
COI	99	88	95	10/13 (77%)	10/13 (77%)	4/13 (31%)
Combined	99	89	96	10/13 (77%)	10/13 (77%)	3/13 (23%)

NN nearest neighbor, *BOLD i.c.* BOLD identification criterion, *MBCM* Meier's best close match, *Sp. monophyly* Species monophyly, *Boot. monophyly* Bootstrap monophyly, *Rosenberg* Rosenberg's probability of reciprocal monophyly

corresponding outer structures on female epigyne, the spatial relations of the bulbal sclerites on the expanded *S. tamdaensis* sp. n. palp very likely represents the natural interactions between bulbal sclerites. This situation is similar to the simple-shaped epigyne of *Oedothorax retusus* (see fig. 2 in Kunz et al. 2015), in which the males also possess complex copulatory organs. Possibly, the interaction between bulbal sclerites during mating is more important than the coupling to the surface of the epigyne, which may explain why palps can be inserted into both sides of female genitalia in *O. retusus* (Kunz et al. 2015).

Effect of collecting method on assessed erigonine diversity

Until today, no comprehensive report and knowledge about habitats of erigonines exists. When mentioned, they are considered to be leaf-litter dwellers and build tiny sheet webs (Hormiga 2000). Erigonines are indeed mostly found in leaf litter; however, occasionally they are found in other habitats like under bark, in rotting logs, in vegetation, and in forest canopy (Miller 2007). Several studies of tropical lowland forest canopies have shown dominance of Theridiidae,

Salticidae, and Araneidae (e.g., Sørensen 2004; Majer and Recher 1988; Stork 1991; Basset and Arthington 1992; Guilbert et al. 1994; Höfer et al. 1994; Majer et al. 1994; Russell-Smith and Stork 1995; Silva 1996), but in the study of Sørensen (2004) in montane forest in Tanzania, Linyphiidae was shown to be the most abundant spider family, and was the second most diverse in terms of species richness. Most studies on the diet of erigonines were carried out in agroecosystems, which showed that collembolans are a major component of their prey (Chapman et al. 2013; Agustí et al. 2003; Nyffeler and Benz 1981; Sunderland 1986). Our survey of Taiwanese dwarf spiders also included extensive leaf litter sifting (Lin, unpublished). However, the *Shaanxinus* species described in the present study are only found on vegetation above ground, where small invertebrate prey like collembola occur as well, especially at certain positions among tree branches and in between entangled vines, where leaf litter has accumulated. Although high above the ground, these microenvironments resemble the conditions of traditionally recognized erigonine habitats in the soil or under bark. We assume that the diversity of erigonines is much higher than currently anticipated, since habitats above ground have not been scrutinized but are important to complement our understanding of erigonine diversity.

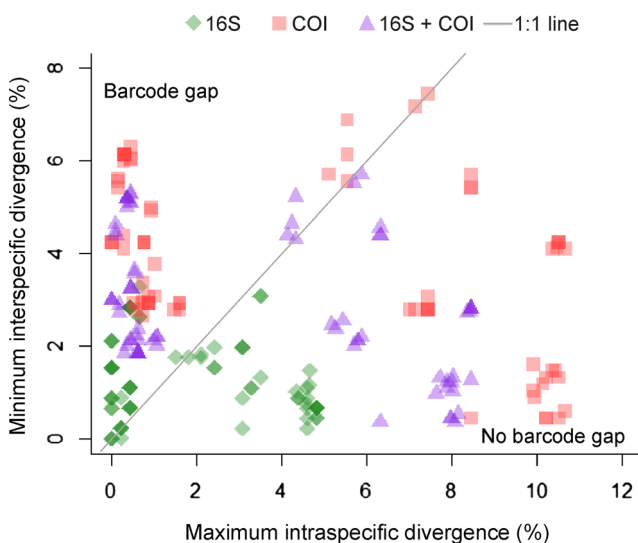


Fig. 44 Graphic representation of the presence/absence of a barcode gap for all datasets, calculated from species pairs using uncorrected p-distances

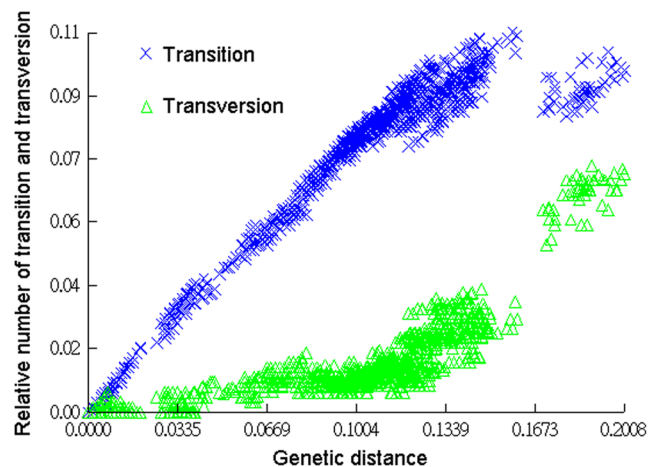


Fig. 45 Number of transitions and transversions in COI sequences of 56 individuals of 13 species of *Shaanxinus* and one individual of *Nasoona crucifera*, plotted against F84 genetic distance

Implication of the discovery of Taiwanese *Shaanxinus* species

Taxonomic affinity of the species described in this study to the type species of *Shaanxinus* was supported by synapomorphies inferred from morphological phylogenetic analysis. Previously, *Shaanxinus* was only recorded from Shaanxi (Tanasevitch 2006) and Hebei Provinces (Xia et al. 2001) in mainland China. Comparing the species density of *Shaanxinus* discovered in Taiwan with the disproportionate scarce records of this genus in continental East Asia, we assume that the species diversity in Vietnam, China, and other adjacent countries is much higher than currently known. More intensive collecting effort, as well as the application of the tree beating method applied here, could significantly increase the detection of new species.

Possible causes of Taiwanese *Shaanxinus* diversity

Our survey in Taiwan covered a large geographical range including different latitudes, altitudes, and both sides of the Central Mountain Range, the major water shed of the island (Fig. 12). Many sites have relatively high numbers of collected individuals. Some locally abundant species, like *S. shihchoensis* sp. n., *S. meifengensis* sp. n., and *S. hehuanensis* sp. n., were not found on other sites where other species like *S. curviductus* sp. n. and *S. magnichypeus* sp. n. were abundantly collected. This could be explained either by their low capacity/propensity to disperse, or by local adaptation to e.g. high altitudes for *S. meifengensis* sp. n. and *S. hehuanensis* sp. n. and might increase the level of inbreeding. According to Kimura and Ohta (1969), when population size is smaller, it will take fewer generations until the fixation of selectively neutral genes, which is here suggested for the two distinct groups of haplotypes found in different local populations of *S. curviductus* sp. n. Low dispersal rates and the resulting reduced gene flow between original populations as well as founder effects may have accelerated differentiation (Mayr 1942). Taiwan Island has diverse environmental conditions including alpine forest, cloud forest, temperate deciduous forest, and sub-tropical/tropical forest. In these diverse environments, natural selection may have accelerated divergence and promoted adaptive radiation (Schluter 2000).

On the other hand, characters useful in species discrimination almost only occur in male prosomal structures and secondary sexual organs of both sexes. Species with longer male emboli also have longer female copulatory ducts, indicating sexual coevolution. It may be a consequence of sexual conflict (Chapman et al. 2003) resulting from a coevolutionary arms race over the control of fertilization. As a consequence of a more sinuous copulatory duct, the male embolus might need more time to reach the spermathecae; hence, mating is prolonged and females might increase the time during which they consume the nuptial gift secretions. In this context, it is

worth noting the strikingly diverse shapes of paracymbium and embolic division among *Shaanxinus* species. According to the observation of an artificially expanded *S. tamdaoensis* sp. n. male palp, the paracymbium and embolic division work together to hold the embolus in a certain position. The micro-CT reconstruction provided the details of the parts of sclerites which overlapped with each other, and could not be observed with light microscopy or SEM (Table 9). It demonstrated a high structural compatibility between the male palpal sclerites, which potentially function for holding the intromittent organ in position. These observations suggest that sexual selection on these features may as well have increased the differences among populations and eventually led to a species radiation (Sauer and Hausdorf 2009). Therefore, both natural and sexual selection together may have driven the high species diversity of *Shaanxinus* in Taiwan. In order to understand the extent of influence of these factors on Taiwanese *Shaanxinus* diversity, and to infer the speciation rate, it is necessary to obtain *Shaanxinus* from continental East Asia for DNA sequencing and phylogenetic analyses.

Morphological phylogenetic analysis

The species discovered in this study, though morphologically similar, are distinctive from each other mostly in the male secondary genital organs, the pedipalps, and in details of the prosomal modifications. As a result of their similarity and concomitant lack of informative characters, intrageneric branches on the morphological phylogenetic hypothesis are generally weakly supported. The resolution of the interspecific relationships is mainly due to the six continuous characters. Nevertheless, close relationships between the two geographical populations of *S. magnichypeus* sp. n. inferred from morphology were also corroborated by the molecular phylogenetic analyses of mtDNA markers (Fig. 39).

DNA barcoding assisted discovery of new species

DNA barcoding has been demonstrated to be useful in disclosing hidden diversity when coupled with morphological and behavioral data (Hebert et al. 2004). According to the concept of reciprocal illumination in phylogenetic systematics (Hennig 1966), the hypothesis of synapomorphy of one character and the indicated relationship is compared to those of other characters. Re-examining conflicting hypotheses may then correct mistaken observations or interpretations (Williams et al. 2016). In the course of the present study, the morphology of specimens originally assigned to *S. curviductus* sp. n. and *S. mingchihensis* sp. n. was re-examined in light of the relationships indicated by mtDNA loci, which led to the discovery of two species, *S. tsou* sp. n. and *S. makauyensis* sp. n. Our collecting efforts yielded only

two male and three female specimens of *S. tsou* sp. n. from Shihcho. While the *S. tsou* sp. n. male morphology is distinct from *S. curviductus* sp. n., no morphological difference seems to exist among their females. Nevertheless, the placement of such females collected in Shihcho in the same clade with *S. tsou* sp. n. males in the COI tree and the combined dataset corroborates the matching of these females with these males. Although it was found for spiders (Lopardo and Uhl 2014; Astrin et al. 2006) and non-spider taxa (Steinke et al. 2005; Vences et al. 2005; Lindsay et al. 2015) that 16S outperforms COI in recovering species monophyly, we found the opposite as by Wang et al. (2017). In the case of *Shaanxinus*, COI and 16S had the same topology except for *S. tsou* sp. n. and *S. shoukaensis* sp. n., which were rendered paraphyletic or remained unresolved in the 16S tree. This was probably due to the lower phylogenetic signal of 16S.

Efficacy of different criteria in species identification using DNA barcoding

Among the distance-based criteria we tested, the NN gave the highest identification rate, while the MCBM analysis provided a slightly lower success rate, and the BOLD identification criterion gave the least identification success (Table 9). The inferiority of the MCBM identification criterion to NN was due to the application of a set threshold, which rejected the identification of individuals to their nearest neighbor when their genetic difference was over 1%. Since the BOLD identification criterion does not aim at finding the closest neighbor, but instead considers all specimens within the threshold of the query, it yields ambiguous outcomes when two species have individuals between which genetic distances were within the threshold. This was the case of COI sequences between several individuals of *S. curviductus* sp. n. and one individual of *S. atayal* sp. n. (see also below), and between many species pairs for 16S, and thus its success rate of species identification was lower than for NN and MBCM. Although NN performed well in species identification, incidences of misidentification were still caused by the close clustering of one *S. atayal* sp. n. specimen with some *S. curviductus* sp. n. individuals. In such cases, identification by DNA barcoding must be aided by a morphological analysis.

In contrast to the high identification success by distance-based methods, especially when the nearest neighbor was searched for and no threshold was applied, the performance of tree-based methods in recovering species monophyly was compromised by the cases of species poly-/paraphyly. Similar results were presented in the study on *Oedothorax* by Lopardo and Uhl (2014), where the recovery of species monophyly was unsuccessful (48%) for both COI and the combined dataset of COI and 16S, while the identification rate by distance-based methods was high (98%).

Species poly-/paraphyly and possible causes

mtDNA sequences have been widely applied as DNA barcodes for identification or assessing species diversity, and as a tool for testing species delimitation based on morphological scrutiny. Nevertheless, mtDNA sequences may lead to erroneous interpretation of the absence of a Barcode Gap or the deviation from species-level monophyly in the resulting phylogeny, due to the special nature of mitochondrial DNA acting as a single locus with little/no recombination (reviewed by Ballard and Whitlock 2004). Surveys of cases of species poly-/paraphyly demonstrated these phenomena to be common among various taxonomic groups (Funk and Omland 2003; Ross 2014). They were most likely in closely related species where speciation rates were rapid and effective population sizes large (Elias et al. 2007). In the present study, species polyphyly and paraphyly on mtDNA trees were also detected and resulted in the absence of a Barcode Gap. Possible causes of species-level poly-/paraphyly have been proposed by Funk and Omland (2003). These include imperfect taxonomy, inadequate phylogenetic information, gene paralogy, interspecific hybridization, and incomplete lineage sorting.

The specimens of *S. curviductus* sp. n. are distributed on two separated branches, one grouping the individuals from Mount Litungshan and Taian, the second comprising individuals from Beipu. Since most of the interspecific branches are well supported in the COI and 16S trees, inadequate phylogenetic information sensu Funk and Omland (2003) is not a likely explanation for species-level polyphyly. Furthermore, the re-inspection of morphology did not lead to the discovery of differences among individuals from the three local populations, so misidentification was also ruled out. The possibility of gene paralogy can be excluded as well, due to the following two reasons. First, since mitochondrial loci are single-copy genes, orthology of alleles is safe to be assumed. Secondly, instead of a mixture of true mtDNA and nuclear mitochondrial pseudogenes (numts) among individuals from the same local population, no sign of numts has been detected, since *S. curviductus* sp. n. presented a pattern of two clear groups of haplotypes, one from Beipu and the other from Litungshan and Taian, and the COI sequences do not contain stop codons. The two remaining possible explanations are incomplete lineage sorting and interspecific hybridization. In general, incomplete lineage sorting is less of a concern for mitochondrial than for nuclear loci, except for very recently diverged species, due to the haploidy and maternal inheritance of mitochondria (Funk and Omland 2003). Furthermore, the two haplotype groups of *S. curviductus* sp. n. (one from Beipu, the other from Litungshan and Taian) locate distantly on the trees, each being sister to other morphologically relatively dissimilar species. The likelihood that *S. curviductus* sp. n. maintained this ancient haplotype polymorphism in the course of speciation seems low. Therefore,

incomplete lineage sorting is unlikely in this case. Consequently, interspecific hybridization and introgression seems to be the most probable scenario (see below), although currently the possible source of the introgressed mtDNA has not been found. Introgression and the subsequent sweeps of heterospecific mtDNA in local populations could lead to species-paraphyly in gene-trees, a phenomenon seen among recently diverged species with sympatric or parapatric distributions in various animal groups, including birds (Grant et al. 2005; Drovetski et al. 2018), crickets (Shaw 2002), freshwater crabs (Barber et al. 2012), locusts (Hawlitschek et al. 2017), and also in spiders (Leduc-Robert and Maddison 2018).

Throughout the history of adaptive radiation, introgressive hybridization may have been a persistent feature (Grant et al. 2005), and thus must be cautioned when interpreting non-monophyly in molecular phylogenies of closely related species. The incidence of one sample of *S. atayal* sp. n. clustering within *S. curviductus* sp. n. populations from Taian and Mount Litungshan might also represent a case of mtDNA introgression. Since all samples of *S. curviductus* sp. n. from the two localities share similar haplotypes, and all but one of the four *S. atayal* sp. n. occurred on a distant branch, the direction of introgression is likely to be from *S. curviductus* sp. n. into *S. atayal* sp. n. In order to determine the contact zone of the distribution of these two species, and the frequency of introgressed mtDNA, a wider geographical coverage of sampling with a larger sample size of *S. atayal* sp. n. is needed.

Distant positions of morphologically similar species *S. makauyensis* and *S. mingchihensis* on mtDNA trees

In contrast to the allopatric distribution of morphologically identical *S. curviductus* sp. n. populations with two distinct mtDNA haplotype groups, the morphological similarity and distinct genetic difference in mtDNA in the sympatric species *S. makauyensis* sp. n. and *S. mingchihensis* sp. n. is an intriguing case. Two alternative hypotheses may be proposed for the observed pattern: first, the minor differences in detailed PC and epigyne shape may represent intraspecific variation, and the species-level polyphyly indicates a recent introgression of heterospecific mtDNA, which has affected only part of the population. Second, both genetic and morphological differences are indications of heterospecificity. If the first hypothesis is true, there must be a third species of which the mtDNA has introgressed into the *S. makauyensis* sp. n. - *S. mingchihensis* sp. n. population, but in the current analyses no heterospecific haplotypes clustered with either taxa (as seen in the case of *S. atayal* sp. n.). Assuming that the hypothesis of heterospecificity is true, and the morphological features in male and female genitalia assumed to be sexually selected, their similarity is more likely due to synapomorphy than plesiomorphy or convergence due to natural or

sexual selection, since reinforcement of reproductive isolation at the contact zone would have caused increased differences in these structures (Wallace 1912). If their similarity represents synapomorphy, then their distant positions on the mtDNA tree is likely a result of heterospecific mtDNA introgression into one of the ancestral population of these species. Hybridization has the potential to induce instantaneous species diversification in animals by causing allopolyploidy or through conversion to a unisexual mode of reproduction. Repeated asymmetric hybridization might also explain the pattern (Dowling and Secor 1997). In the case of *S. makauyensis* sp. n. and *S. mingchihensis* sp. n., instantaneous speciation through conversion to unisexuality can be excluded, since both sexes were found for both species. An increased geographical coverage of sampling and higher number of individuals will help to evaluate the heterospecificity hypothesis, and might reveal the source of introgressed mtDNA.

Paraphyly of *S. hehuanensis* and its basal position on the mtDNA trees

The nesting of *S. meifengensis* sp. n. within *S. hehuanensis* sp. n. represents a plausible incidence of incomplete lineage sorting which resulted from rapid species radiation (Funk and Omland 2003). The higher genetic variation in 16S and COI in *S. hehuanensis* sp. n. and its paraphyly with respect to *S. meifengensis* sp. n. may be a result of peripatric speciation. The high intraspecific genetic variation of *S. hehuanensis* sp. n. shown in trees in Figs. 41, 42, and 43 indicates a longer population history of this species compared to other congeners.

Since Taiwan was connected to the East Asian continent during the last glacial period, and the sea level rose and formed the Taiwan Strait about 13,000 to 11,000 years ago (Voris 2000), many endemic animal and plant species represent descendants of relic species of the past fauna shared between continental East Asia and Taiwan. *S. meifengensis* sp. n. and *S. hehuanensis* sp. n. are genetically distant to other Taiwanese *Shaanxinus* species and occur at the highest altitudes among their congeners, which might indicate a retained ancestral state of adaptation to colder climate during glacial periods.

Incongruence between mtDNA trees and 28S tree

Despite limited resolution of interspecific relationships in the 28S tree, some incongruence with the mtDNA trees are notable. Due to their identical sequence, all four specimens of *S. atayal* sp. n. formed a clade with all specimens of *S. lixiangae* sp. n. and *S. seediq* sp. n. in the 28S tree, suggesting a close relationship. However, in the mtDNA tree, these species were not close. If the identical 28S

sequence of these three species was not due to convergence or symplesiomorphy, but a result of common descent, an assumption according to *Hennig's auxiliary principle* (Hennig 1966), then the incongruence would imply difference in the evolutionary history between mitochondrial and nuclear DNA sequences in the studied taxa. There are two possible sources of substantial error using mtDNA in inferring phylogeny of species. One is the error of inferring the gene genealogy from the data, the second the error of inferring the species genealogy from that of a single molecule (Ballard and Whitlock 2004). Since the interspecific branches in the trees of two mtDNA markers were mostly well supported, high accuracy of gene tree inferences can be assumed. Therefore, the incongruence between morphological species delimitation, mtDNA trees, and the 28S tree suggests that most likely the mtDNA tree in this case may not represent the true evolutionary history of the species. Incomplete lineage sorting and introgression, as discussed above, may have caused the conflicting signals from different character sets in *Shaanxinus*. Compared to nuclear loci, mitochondrial alleles usually introgress easier, since mitochondrial alleles are less linked to or co-adapted with many nuclear genes that may be selected against heterospecific hybridization (Barton and Jones 1983; Shaw 2002; Barber et al. 2012). Furthermore, mitochondria are maternally inherited, and thus the effective population size of mitochondrial alleles is smaller than that of nuclear alleles, which, when genetic drift has more influence on allele frequency than natural selection, causes fixation of introgressed mitochondrial alleles in the population on average four times faster than in the case of nuclear alleles (Harrison 1989; Moore 1995). The fixation rate might even be higher when maternally inherited symbionts like *Wolbachia*, highly prevalent among arthropod taxa, cause indirect selection on mtDNA due to linkage disequilibrium (Hurst and Jiggins 2005). Due to the prevalence of mtDNA introgression, many studies demonstrated the advantage of using nuclear markers over mitochondrial markers in inferring species genealogy (Shaw 2002; Drovetski et al. 2018). Given the incidences of possible mtDNA introgression seen in the present study, it might be necessary to draw evidence from multi-locus nDNA analyses, in order to resolve *Shaanxinus* interspecific relationships, and give insights into interspecific interactions in the past and present.

Conclusions and outlook

As exemplified by the *Shaanxinus* mtDNA phylogeny, the prevalence of biological processes causing species-level poly-/paraphyly on mtDNA trees cautions against the tendency of implicitly assuming monophyly of alleles of nominal species at the study locus. Due to the widespread phenomena

of introgression and incomplete lineage sorting, especially in groups of closely related species, setting an arbitrary threshold of genetic divergence does not contribute to species identification success, nor does the endeavor in looking for a Barcode Gap. Instead, we appeal for enriching the sequence database with multiple individuals from different populations of each species, and identifying specimens using the nearest neighbor criterion, while being alert to cases of possible introgression by carefully inspecting the morphology. For the same reason, the recovery of species monophyly is not necessarily a good measure for marker efficacy in species identification, but is one of several tools or criteria for unraveling the evolutionary history of species, which may include incongruence among different character sets. In the face of frequently discovered species-level poly-/paraphyly in phylogenetic studies of congeneric animal species, Funk and Omland (2003) proposed the concept of congeneric phylogeography, by which they stress the importance of integrating the sampling conventions of systematic studies above species level with that of population genetics for more accurate insights into the evolutionary biology of a taxon. By sampling comprehensively at the phylogeographical scale when studying relationships among congeners, inference of species delimitations and historical events can be improved to give less-biased understanding about their biology. Our newly discovered Taiwanese *Shaanxinus* species showed a high diversity in a relatively small and isolated area, in contrast to the scarce record on continental East Asia. Furthermore, the mtDNA tree implied a complex history of their interspecific gene flows. The group lends itself as an ideal candidate taxon for in-depth congeneric phylogeographical sampling in Taiwan and on the continent, together with multi-locus phylogenetic analyses. Thereby, it would be possible to investigate *Shaanxinus* species diversity and address questions about the origin of Taiwanese species, speciation rate, population-level processes relevant to micro- and macroevolution, and eventually the role of sexual selection for speciation.

Acknowledgements We are very grateful to Theo Michael Schmitt, Anja Junghanns, and Pierick Mougino for suggestions on the manuscript. For kindly loaning material, we would like to thank Julia Altmann, Peter Jäger (both Senckenberg Museum Frankfurt, DE; SMF) and Nikolaj Scharff (Zoological Museum, University of Copenhagen, DK; ZMUC). We also thank the University of Greifswald (International Office) for a stipend to visit the aforementioned two museums. For providing facility for preserving and identifying newly collected material, we would like to thank Shih-Feng Shiao (National Taiwan University, Taiwan). For support in collecting specimen, we sincerely thank Li-Xiang Huang, the first author's mother. For support in molecular lab work, we thank Silke Fregin; for imaging assistance, we thank Peter Michalik and Tim Dederichs (all Zoological Institut and Museum, Greifswald, DE; ZIMG). For micro-CT imaging and reconstruction, we cordially thank Stefan Bock. The SEM images were taken by Carsten Müller at the Image Center of Biology, Greifswald. For critical reviews and constructive advice, we thank Andrei D. Tanasevitch and Gustavo Hormiga.

Appendix 1

Table 10 Leg measurements of male holotype and one female paratype of the new species described in the text. All measurements in millimeters

<i>Shaanxinus magniclypeus</i> sp. n.								
	Male				Female			
	I	II	III	IV	I	II	III	IV
Femur	1.05	1.12	0.84	1.04	1.16	1.17	0.91	1.1
Patella	0.28	0.29	0.25	0.25	0.3	0.3	0.25	0.27
Tibia	0.92	0.96	0.6	0.86	1.06	1.06	0.67	0.92
Metatarsus	0.82	0.93	0.73	0.99	1.03	1.04	0.79	1.04
Tarsus	0.5	0.49	0.37	0.48	0.54	0.53	0.42	0.51
Total	3.57	3.8	2.79	3.62	4.08	4.1	3.03	3.84
<i>Shaanxinus shihchoensis</i> sp. n.								
	Male				Female			
	I	II	III	IV	I	II	III	IV
Femur	1.26	1.28	0.91	1.11	1.26	1.29	0.95	1.14
Patella	0.29	0.3	0.26	0.26	0.32	0.33	0.27	0.27
Tibia	1.1	1.09	0.68	0.96	1.19	1.16	0.71	0.95
Metatarsus	1.08	1.09	0.81	1.08	1.2	1.2	0.86	1.13
Tarsus	0.61	0.59	0.42	0.5	0.62	0.61	0.42	0.51
Total	4.35	4.34	3.08	3.91	4.58	4.59	3.22	3.99
<i>Shaanxinus shoukaensis</i> sp. n.								
	Male				Female			
	I	II	III	IV	I	II	III	IV
Femur	1.16	1.17	0.87	1.02	1.19	1.17	0.86	1.05
Patella	0.3	0.3	0.25	0.26	0.31	0.29	0.27	0.27
Tibia	0.98	0.98	0.65	0.87	1.07	1.05	0.62	0.87
Metatarsus	0.97	0.99	0.76	1.03	1.08	1.08	0.8	1.04
Tarsus	0.51	0.49	0.38	0.46	0.53	0.52	0.38	0.45
Total	3.93	3.93	2.9	3.64	4.17	4.11	2.92	3.67
<i>Shaanxinus hirticephalus</i> sp. n.								
	Male				Female			
	I	II	III	IV	I	II	III	IV
Femur	1.4	1.64	1.18	1.5	1.3	1.37	1.03	1.26
Patella	0.33	0.33	0.31	0.31	0.36	0.36	0.31	0.32
Tibia	1.18	1.47	0.88	1.27	1.18	1.22	0.76	1.03
Metatarsus	1.16	1.5	1.07	1.49	1.23	1.26	0.93	1.21
Tarsus	0.63	0.64	0.45	0.57	0.58	0.59	0.42	0.52
Total	4.7	5.58	3.89	5.13	4.64	4.8	3.46	4.33
<i>Shaanxinus mingchihensis</i> sp. n.								
	Male				Female			
	I	II	III	IV	I	II	III	IV
Femur	1.47	1.47	1.04	1.27	1.69	1.64	1.2	1.45
Patella	0.32	0.31	0.27	0.29	0.36	0.36	0.31	0.32
Tibia	1.33	1.28	0.77	1.06	1.55	1.49	0.93	1.22
Metatarsus	1.29	1.28	0.92	1.2	1.49	1.44	1.07	1.36
Tarsus	0.64	0.65	0.44	0.55	0.72	0.9	0.49	0.59
Total	5.06	4.99	3.44	4.37	5.81	5.62	4	4.94
<i>Shaanxinus makauyensis</i> sp. n.								

Table 10 (continued)

	Male				Female			
	I	II	III	IV	I	II	III	IV
Femur	1.45	1.42	1.03	1.26	1.56	1.52	1.09	1.32
Patella	0.31	0.3	0.26	0.27	0.34	0.34	0.29	0.29
Tibia	1.32	1.3	0.78	1.06	1.52	1.48	0.85	1.16
Metatarsus	1.34	1.31	0.95	1.26	1.44	1.42	1.01	1.33
Tarsus	0.69	0.655	0.47	0.54	0.73	0.7	0.48	0.59
Total	5.11	4.99	3.5	4.38	5.59	5.45	3.72	4.69
<i>Shaanxinus lixiangae</i> sp. n.								
	Male				Female			
	I	II	III	IV	I	II	III	IV
Femur	1.3	1.02	0.93	1.12	1.5	1.48	1.09	1.35
Patella	0.32	0.27	0.26	0.27	0.33	0.34	0.3	0.31
Tibia	1.19	1.02	0.71	0.94	1.38	1.34	0.86	1.12
Metatarsus	1.14	1	0.79	1.04	1.33	1.29	0.93	1.24
Tarsus	0.62	0.57	0.44	0.5	0.69	0.66	0.48	0.57
Total	4.56	3.88	3.13	3.87	5.23	5.11	3.67	4.58
<i>Shaanxinus curviductus</i> sp. n.								
	Male				Female			
	I	II	III	IV	I	II	III	IV
Femur	1.19	1.2	0.86	1.05	1.31	1.34	0.97	1.2
Patella	0.29	0.29	0.25	0.27	0.31	0.3	0.27	0.28
Tibia	1.04	1.02	0.63	0.87	1.22	1.16	0.73	0.99
Metatarsus	1.04	1.04	0.78	1.02	1.21	1.21	0.88	1.15
Tarsus	0.53	0.55	0.41	0.47	0.61	0.61	0.43	0.55
Total	4.1	4.09	2.92	3.68	4.67	4.61	3.27	4.18
<i>Shaanxinus tsou</i> sp. n.								
	Male				Female			
	I	II	III	IV	I	II	III	IV
Femur	1.34	1.31	0.93	1.16	1.5	1.47	1.02	1.3
Patella	0.31	0.31	0.26	0.26	0.34	0.34	0.29	0.3
Tibia	1.17	1.17	0.73	1.01	1.35	1.31	0.78	1.06
Metatarsus	1.21	1.21	0.89	1.17	1.32	1.31	0.93	1.23
Tarsus	0.63	0.62	0.43	0.54	0.67	0.65	0.47	0.56
Total	4.66	4.61	3.23	4.15	5.19	5.09	3.48	4.45
<i>Shaanxinus hehuanensis</i> sp. n.								
	Male				Female			
	I	II	III	IV	I	II	III	IV
Femur	1.65	1.63	1.16	1.43	1.78	1.78	1.31	1.52
Patella	0.4	0.38	0.33	0.34	0.44	0.43	0.38	0.38
Tibia	1.57	1.53	0.61	1.22	1.72	1.69	1.11	1.42
Metatarsus	1.54	1.55	1.17	1.48	1.68	1.68	1.2	1.57
Tarsus	0.76	0.74	0.53	0.52	0.79	0.8	0.53	0.67
Total	5.93	5.84	3.8	4.98	6.41	6.37	4.52	5.56
<i>Shaanxinus seediq</i> sp. n.								
	Male				Female			
	I	II	III	IV	I	II	III	IV
Femur	1.29	1.24	0.86	1.09	1.36	1.33	0.94	1.14
Patella	0.28	0.28	0.24	0.24	0.3	0.31	0.26	0.26
Tibia	1.17	1.13	0.65	0.91	1.23	1.19	0.69	0.98
Metatarsus	1.14	1.12	0.78	1.03	1.21	1.20	0.81	1.12
Tarsus	0.59	0.56	0.39	0.46	0.58	0.56	0.4	0.47
Total	4.47	4.32	2.93	3.73	4.68	4.6	3.09	3.97
<i>Shaanxinus meifengensis</i> sp. n.								
	Male				Female			
	I	II	III	IV	I	II	III	IV
Femur	1.78	1.75	1.24	1.47	1.77	1.69	1.21	1.51
Patella	0.39	0.37	0.32	0.33	0.36	0.36	0.33	0.33
Tibia	1.69	1.64	1.01	1.31	1.61	1.56	0.92	1.22
Metatarsus	1.69	1.65	1.17	1.51	1.61	1.56	1.11	1.45
Tarsus	0.84	0.8	0.55	0.66	0.76	0.74	0.5	0.61
Total	6.4	6.21	4.28	5.28	6.12	5.91	4.07	5.12
<i>Shaanxinus atayal</i> sp. n.								
	Male				Female			

Table 10 (continued)

	I	II	III	IV	I	II	III	IV
Femur	1.51	1.5	1.09	1.33	1.47	1.41	1.02	1.25
Patella	0.35	0.33	0.29	0.3	0.35	0.34	0.29	0.3
Tibia	1.42	1.39	0.88	1.17	1.32	1.28	0.81	1.07
Metatarsus	1.41	1.38	1	1.3	1.32	1.26	0.94	1.23
Tarsus	0.68	0.66	0.44	0.53	0.63	0.65	0.42	0.54
Total	5.37	5.27	3.71	4.63	5.09	4.95	3.48	4.39
<i>Shaanxinus tamdaoensis</i> sp. n.								
	Male							
	I	II			III		IV	
Femur	1.3	1.3			0.96		1.14	
Patella	0.31	0.31			0.27		0.27	
Tibia	1.19	1.18			0.73		0.97	
Metatarsus	1.17	1.14			0.84		1.11	
Tarsus	0.63	0.62			0.43		0.52	
Total	4.59	4.54			3.23		4.01	

References

- Agustí, N., Shayler, S. P., Harwood, J. D., Vaughan, I. P., Sunderland, K., & Symondson, W. O. C. (2003). Collembola as alternative prey sustaining spiders in arable ecosystems: prey detection within predators using molecular markers. *Molecular Ecology*, *12*, 3467–3475.
- Akaike, H. (1974). A new look at the statistical model identification. *IEEE Transactions on Automatic Control*, *19*, 716–723.
- Altschul, S. F., Madden, T. L., Schaffer, A. A., Zhang, J., Zhang, Z., Miller, W., et al. (1997). Gapped BLAST and PSI-BLAST: A new generation of protein database search programs. *Nucleic Acids Research*, *25*, 3389–3402.
- Álvarez-Padilla, F., Dimitrov, D., Giribet, G., & Hormiga, G. (2009). Phylogenetic relationships of the spider family Tetragnathidae (Araneae, Araneoidea) based on morphological and DNA sequence data. *Cladistics*, *25*, 109–146.
- Amedo, M. A., Hormiga, G., & Scharff, N. (2009). Higher-level phylogenetics of linyphiid spiders (Araneae, Linyphiidae) based on morphological and molecular evidence. *Cladistics*, *25*, 231–262.
- Astrin, J. J., Huber, B. A., Misof, B., & Klütsch, C. F. C. (2006). Molecular taxonomy in pholcid spiders (Pholcidae, Araneae): evaluation of species identification methods using CO1 and 16S rRNA. *Zoologica Scripta*, *35*, 441–457.
- Astrin, J. J., Höfer, H., Spelda, J., Holstein, J., Bayer, S., Hendrich, L., et al. (2016). Towards a DNA barcode reference database for spiders and harvestmen of Germany. *PLoS One*, *11*, e0162624.
- Austerlitz, F., David, O., Schaeffer, B., Bleakley, K., Olteanu, M., Leblois, R., et al. (2009). DNA barcode analysis: a comparison of phylogenetic and statistical classification methods. *BMC Bioinformatics*, *10*, S10.
- Ballard, J. W. O., & Whitlock, M. C. (2004). The incomplete natural history of mitochondria. *Molecular Ecology*, *13*, 729–744.
- Ballarin, F., & Li, S. (2018). Diversification in tropics and subtropics following the mid-Miocene climate change: a case study of the spider genus *Nesticella*. *Global Change Biology*, *24*, e577–e591.
- Barber, B. R., Xu, J., Pérez-Losada, M., Jara, C. G., & Crandall, K. A. (2012). Conflicting evolutionary patterns due to mitochondrial introgression and multilocus phylogeography of the Patagonian freshwater crab *Aegla neuquensis*. *PLoS One*, *7*, e37105.
- Barrantes, G., Aisenberg, A., & Eberhard, W. G. (2013). Functional aspects of genital differences in *Leucauge argyra* and *L. mariana* (Araneae: Tetragnathidae). *The Journal of Arachnology*, *41*, 59–69.
- Barrett, R. D. H., & Hebert, P. D. N. (2005). Identifying spiders through DNA barcodes. *Canadian Journal of Zoology*, *83*, 481–491.
- Barton, N., & Jones, J. (1983). Evolutionary biology: Mitochondrial DNA: new clues about evolution. *Nature*, *306*, 317.
- Basset, Y., & Arthington, A. (1992). The arthropod community of an Australian rainforest tree: abundance of component taxa, species richness and guild structure. *Australian Journal of Ecology*, *17*, 89–98.
- Betz, O., Wegst, U., Weide, D., Heethoff, M., Helfen, L., Lee, W. K., et al. (2007). Imaging applications of synchrotron X-ray phase-contrast microtomography in biological morphology and biomaterials science. I. General aspects of the technique and its advantages in the analysis of millimetre-sized arthropod structure. *Journal of Microscopy*, *227*, 51–71.
- Beutel, R. G., Friedrich, F., & Whiting, M. F. (2008). Head morphology of *Caurinus* (Boreidae, Mecoptera) and its phylogenetic implications. *Arthropod Structure & Development*, *37*, 418–433.
- Blest, A. D., & Pomeroy, G. (1978). The sexual behaviour and genital mechanics of three species of *Mynoglenes* (Araneae: Linyphiidae). *Journal of Zoology*, *185*, 319–340.
- Blest, A. D., & Taylor, H. H. (1977). The clypeal glands of *Mynoglenes* and of some other linyphiid spiders. *Journal of Zoology*, *183*, 473–493.
- Bodner, M. R., & Maddison, W. P. (2012). The biogeography and age of salticid spider radiations (Araneae: Salticidae). *Molecular Phylogenetics and Evolution*, *65*, 213–240.
- Bösenberg, W., & Strand, E. (1906). Japanische Spinnen. *Abhandlungen der Senckenbergischen Naturforschenden Gesellschaft*, *30*, 93–422.
- Bremer, K. (1988). The limits of amino acid sequence data in angiosperm phylogenetic reconstruction. *Evolution*, *42*, 795–803.
- Bremer, K. (1994). Branch support and tree stability. *Cladistics*, *10*, 295–304.
- Bristowe, W. S. (1938). The classification of spiders. *Proceedings of the Zoological Society of London (B)*, *108*, 285–322.
- Brown, S. D. J., Collins, R. A., Boyer, S., Lefort, M.-C., Malumbres-Olarte, J., Vink, C. J., et al. (2012). Spider: an R package for the analysis of species identity and evolution, with particular reference to DNA barcoding. *Molecular Ecology Resources*, *12*, 562–565.
- Burger, M. (2008). Functional genital morphology of armored spiders (Arachnida: Araneae: Tetrablemmidae). *Journal of Morphology*, *269*, 1073–1094.
- Burger, M., Izquierdo, M., & Carrera, P. (2010). Female genital morphology and mating behavior of *Orchestina* (Arachnida: Araneae: Oonopidae). *Zoology*, *113*, 100–109.
- Chapman, T., Armqvist, G., Bangham, J., & Rowe, L. (2003). Sexual conflict. *Trends in Ecology & Evolution*, *18*, 41–47.

- Chapman, E. G., Schmidt, J. M., Welch, K. D., & Harwood, J. D. (2013). Molecular evidence for dietary selectivity and pest suppression potential in an epigeal spider community in winter wheat. *Biological Control*, *65*, 72–86.
- Clouse, R. M., de Bivort, B. L., & Giribet, G. (2010). A phylogenetic analysis for the South-east Asian mite harvestman family Stylocellidae (Opiliones: Cyphophthalmi)—a combined analysis using morphometric and molecular data. *Invertebrate Systematics*, *23*, 515–529.
- Comstock, J. H. (1910). The palpi of male spiders. *Annals of the Entomological Society of America*, *3*, 161–185.
- Crosby, C. R., Bishop, S. C., & Seeley, R. M. (1928). Revision of the spider genera *Erigone*, *Eperigone* and *Catabrithorax* (Erigoneae). *New York State Museum Bulletin*, *278*, 1–73.
- Darriba, D., Taboada, G. L., Doallo, R., & Posada, D. (2012). jModelTest 2: more models, new heuristics and parallel computing. *Nature Methods*, *9*, 772–772. <https://doi.org/10.1038/nmeth.2109>.
- de Bivort, B. L., Clouse, R. M., & Giribet, G. (2010). A morphometrics-based phylogeny of the temperate Gondwanan mite harvestmen (Opiliones, Cyphophthalmi, Pettalidae). *Journal of Zoological Systematics and Evolutionary Research*, *48*, 294–309.
- de Causmaecker, B. (2004). Morfologie en histologie van de mannelijke kopstructuren bij *Oedothorax* dwergspinnen en zaadcompetitie bij de mannelijk dimorfe *Oedothorax gibbosus* (Blackwall, 1814)(Erigoninae, Linyphiidae, Araneae). *Master's thesis, Faculty of Biology*, University of Gent, Belgium.
- Dowling, T. E., & Secor, C. L. (1997). The role of hybridization and introgression in the diversification of animals. *Annual Review of Ecology and Systematics*, *28*, 593–619.
- Drovetski, S. V., Reeves, A. B., Red'kin, Y. A., Fadeev, I. V., Koblik, E. A., Sotnikov, V. N., et al. (2018). Multi-locus reassessment of a striking discord between mtDNA gene trees and taxonomy across two congeneric species complexes. *Molecular Phylogenetics and Evolution*, *120*, 43–52.
- Eberhard, W. G. (1985). *Sexual selection and animal genitalia* (Vol. 244). Cambridge: Harvard University Press.
- Eberhard, W. G., & Huber, B. A. (2010). Spider genitalia: precise maneuvers with a numb structure in a complex lock. In J. L. Leonard & A. Córdoba-Aguilar (Eds.), *Evolution of primary sexual characters in animals* (pp. 249–284). Oxford: Oxford University Press.
- Elias, M., Hill, R. I., Willmott, K. R., Dasmahapatra, K. K., Brower, A. V., Mallet, J., et al. (2007). Limited performance of DNA barcoding in a diverse community of tropical butterflies. *Proceedings of the Royal Society of London B: Biological Sciences*, *274*, 2881–2889.
- Fanenbruck, M., De Carlo, F., & Mancini, D. (2001). Evaluating the Advantage of X-ray Microtomography in Microanatomical Studies of Small Arthropods. APS Activity Reports. Argonne, Illinois: Argonne National Laboratory.
- Farris, J. S. (1990). Phenetics in camouflage. *Cladistics*, *6*, 91–100.
- Folmer, O., Black, M., Hoeh, W., Lutz, R., & Vrijenhoek, R. (1994). DNA primers for amplification of mitochondrial cytochrome c oxidase subunit I from diverse metazoan invertebrates. *Molecular Marine Biology and Biotechnology*, *3*, 294–299.
- Friedrich, F., & Beutel, R. G. (2008). Micro-computer tomography and a renaissance of insect morphology. *Proceedings of SPIE*, *7078*, 70781U1–70781U6.
- Friedrich, F., Pohl, H., Beckmann, F., & Beutel, R. G. (2013). The head of *Merope tuber* (Meropeidae) and the phylogeny of Mecoptera (Hexapoda). *Arthropod Structure & Development*, *42*, 69–88.
- Funk, D. J., & Omland, K. E. (2003). Species-level parphyly and polyphyly: frequency, causes, and consequences, with insights from animal mitochondrial DNA. *Annual Review of Ecology, Evolution, and Systematics*, *34*, 397–423.
- Goloboff, P. A., & Farris, J. S. (2001). Methods for quick consensus estimation. *Cladistics*, *17*, S26–S34.
- Goloboff, P. A., Mattoni, C. I., & Quinteros, A. S. (2006). Continuous characters analyzed as such. *Cladistics*, *22*, 589–601.
- Goloboff, P. A., Farris, J. S., & Nixon, K. C. (2008). TNT, a free program for phylogenetic analysis. *Cladistics*, *24*, 774–786.
- González-José, R., Escapa, I., Neves, W. A., Cúneo, R., & Pucciarelli, H. M. (2008). Cladistic analysis of continuous modularized traits provides phylogenetic signals in *Homo* evolution. *Nature*, *453*, 775.
- Grant, P. R., Grant, B. R., & Petren, K. (2005). Hybridization in the recent past. *The American Naturalist*, *166*, 56–67.
- Guilbert, E., Chazeau, J., & Larbogne, L. D. (1994). Canopy arthropod diversity of New Caledonian forests sampled by fogging: preliminary results. *Memoirs of the Queensland Museum*, *36*, 77–85.
- Guindon, S., Gascuel, O., & Rannala, B. (2003). A simple, fast, and accurate algorithm to estimate large phylogenies by maximum likelihood. *Systematic Biology*, *52*, 696–704.
- Harrison, R. G. (1989). Animal mitochondrial DNA as a genetic marker in population and evolutionary biology. *Trends in Ecology & Evolution*, *4*, 6–11.
- Hawlitshcek, O., Morinière, J., Lehmann, G., Lehmann, A., Kropf, M., Dunz, A., et al. (2017). DNA barcoding of crickets, katydids and grasshoppers (Orthoptera) from Central Europe with focus on Austria, Germany and Switzerland. *Molecular Ecology Resources*, *17*, 1037–1053.
- Hebert, P. D., Cywinska, A., Ball, S. L., & deWaard, J. R. (2003). Biological identifications through DNA barcodes. *Proceedings of the Royal Society of London B: Biological Sciences*, *270*, 313–321.
- Hebert, P. D., Penton, E. H., Burns, J. M., Janzen, D. H., & Hallwachs, W. (2004). Ten species in one: DNA barcoding reveals cryptic species in the neotropical skipper butterfly *Astraptes fulgerator*. *Proceedings of the National Academy of Sciences of the United States of America*, *101*, 14812–14817.
- Hennig, W. (1966). *Phylogenetic systematics*. Urbana, Illinois: University of Illinois Press.
- Höfer, H., Brescovit, A. D., Adis, J., & Paarmann, W. (1994). The spider fauna of neotropical tree canopies in Central Amazonia: first results. *Studies on Neotropical Fauna and Environment*, *29*, 23–32.
- Hormiga, G. (2000). Higher level phylogenetics of erigonine spiders (Araneae, Linyphiidae, Erigoninae). *Smithsonian Contributions to Zoology*, *609*, 1–160.
- Hormiga, G., Arnedo, M., & Gillespie, R. G. (2003). Speciation on a conveyor belt: sequential colonization of the Hawaiian Islands by *Orsonwelles* spiders (Araneae, Linyphiidae). *Systematic Biology*, *52*, 70–88.
- Hörschemeyer, T., Beutel, R. G., & Pasop, F. (2002). Head structures of *Priacma serrata* Leconte (Coleoptera, Archostemata) inferred from X-ray tomography. *Journal of Morphology*, *252*, 298–314.
- Huber, B. A. (1993). Genital mechanics and sexual selection in the spider *Nesticus cellulanus* (Araneae: Nesticidae). *Canadian Journal of Zoology*, *71*, 2437–2447.
- Huber, B. A. (1994a). Copulatory mechanics in the funnel-web spiders *Histopona torpida* and *Textrix denticulata* (Agelenidae, Araneae). *Acta Zoologica*, *75*, 379–384.
- Huber, B. A. (1994b). Funktion und evolution komplexer Kopulationsorgane. Eine Analyse von Schnittserien durch in copula schockfixierte Spinnen. *Mitteilungen der Deutschen Gesellschaft für Allgemeine und Angewandte Entomologie*, *9*, 247–250.
- Huber, B. A. (1995a). Copulatory mechanism in *Holocnemus pluchi* and *Pholcus opilionoides*, with notes on male cheliceral apophyses and stridulatory organs in Pholcidae (Araneae). *Acta Zoologica*, *76*, 291–300.
- Huber, B. A. (1995b). Genital morphology and copulatory mechanics in *Anyphaena accentuata* (Anyphaenidae) and *Clubiona pallidula* (Clubionidae: Araneae). *Journal of Zoology*, *235*, 689–702.
- Huber, B. A. (1995c). The retrolateral tibial apophysis in spiders—shaped by sexual selection? *Zoological Journal of the Linnean Society*, *113*, 151–163.

- Huber, B. A., & Eberhard, W. G. (1997). Courtship, copulation, and genital mechanics in *Physocyclus globosus* (Araneae, Pholcidae). *Canadian Journal of Zoology*, *75*, 905–918.
- Humphries, C. J. (2002). Homology, characters and continuous variables. In N. Macleod & P. Forey (Eds.), *Morphology, shape and phylogeny* (pp. 8–26). London: Taylor and Francis.
- Hurst, G. D., & Jiggins, F. M. (2005). Problems with mitochondrial DNA as a marker in population, phylogeographic and phylogenetic studies: the effects of inherited symbionts. *Proceedings of the Royal Society of London B*, *272*, 1525–1534.
- Hurvich, C. M., & Tsai, C.-L. (1989). Regression and time series model selection in small samples. *Biometrika*, *76*, 297–307.
- Jackson, A. R. (1932). On new and rare British spiders. *Proceedings of the Dorset Natural History and Antiquarian Field Club*, *53*, 200–214.
- Jang, K. H. (2012). *Molecular Phylogeny of Spiders (Arachnida, Araneae)*. Doctoral thesis, Kyungpook National University, South Korea.
- Janicke, T., Ritchie, M. G., Morrow, E. H., & Marie-Orleach, L. (2018). Sexual selection predicts species richness across the animal kingdom. *Proceedings of the Royal Society B*, *285*, 20180173.
- Juberthie, C., & Lopez, A. (1980). La glande clypéale d'*Argyrodes argyrodes* (Walck.): nouvelles précisions sur son ultrastructure. *Revue Arachnologique*, *3*, 1–11.
- Karsch, F. (1879). Baustoffe zu einer Spinnenfauna von Japan. *Verhandlungen des naturhistorischen Vereins der preussischen Rheinlande und Westfalens*, *36*, 57–105.
- Katoh, K., & Standley, D. M. (2013). MAFFT multiple sequence alignment software version 7: improvements in performance and usability. *Molecular Biology and Evolution*, *30*, 772–780.
- Katoh, K., Misawa, K., Kuma, K., & Miyata, T. (2002). MAFFT: a novel method for rapid multiple sequence alignment based on fast Fourier transform. *Nucleic Acids Research*, *30*, 3059–3066.
- Kimura, M., & Ohta, T. (1969). The average number of generations until fixation of a mutant gene in a finite population. *Genetics*, *61*, 763–771.
- Kunz, K., Garbe, S., & Uhl, G. (2012). The function of the secretory cephalic hump in males of the dwarf spider *Oedothorax retusus* (Linyphiidae: Erigoninae). *Animal Behaviour*, *83*, 511–517.
- Kunz, K., Witthuhn, M., & Uhl, G. (2015). Paired and complex copulatory organs: do they really impede flexible use? *Journal of Zoology*, *297*, 278–285.
- Leduc-Robert, G., & Maddison, W. P. (2018). Phylogeny with introgression in *Habronattus* jumping spiders (Araneae: Salticidae). *BMC Evolutionary Biology*, *18*, 24.
- Legendre, R., & Lopez, A. (1974). Étude histologique de quelques formations glandulaires chez les Araignées du genre *Argyrodes* (Theridiidae) et description d'un nouveau type de glande: la glande clypéale des mâles. *Bulletin de la Société Zoologique de France*, *99*, 453–460.
- Lindsay, D. J., Grossmann, M. M., Nishikawa, J., Bentlage, B., & Collins, A. G. (2015). DNA barcoding of pelagic cnidarians: current status and future prospects. *Bulletin of Plankton Society of Japan*, *62*, 39–43.
- Lopardo, L., & Hormiga, G. (2015). Out of the twilight zone: phylogeny and evolutionary morphology of the orb-weaving spider family Mysmenidae, with a focus on spinneret spigot morphology in symphytognathoids (Araneae, Araneoidea). *Zoological Journal of the Linnean Society*, *173*, 527–786.
- Lopardo, L., & Uhl, G. (2014). Testing mitochondrial marker efficacy for DNA barcoding in spiders: a test case using the dwarf spider genus *Oedothorax* (Araneae: Linyphiidae: Erigoninae). *Invertebrate Systematics*, *28*, 501–521.
- Lopardo, L., Giribet, G., & Hormiga, G. (2011). Morphology to the rescue: molecular data and the signal of morphological characters in combined phylogenetic analyses—a case study from mysmenid spiders (Araneae, Mysmenidae), with comments on the evolution of web architecture. *Cladistics*, *27*, 278–330.
- Maddison, W. P., & Hedin, M. C. (2003). Jumping spider phylogeny (Araneae: Salticidae). *Invertebrate Systematics*, *17*, 529–549.
- Maddison, W. P., & Maddison, D. R. (2017). Mesquite: a modular system for evolutionary analysis. Version 3.10 <http://www.mesquiteproject.org>. Accessed 2 Jan 2018.
- Majer, J., & Recher, H. (1988). Invertebrate communities on Western Australian eucalypts: a comparison of branch clipping and chemical knockdown procedures. *Australian Journal of Ecology*, *13*, 269–278.
- Majer, J. D., Recher, H. F., & Postle, A. C. (1994). Comparison of arthropod species richness in eastern and western Australian canopies: a contribution to the species number debate. *Memoirs of the Queensland Museum*, *36*, 121–131.
- Mayr, E. (1942). *Systematics and the origin of species, from the viewpoint of a zoologist*. New York: Columbia University Press.
- Mayr, E. (2000). The biological species concept. In Q. Wheeler & R. Meier (Eds.), *Species concepts and phylogenetic theory: a debate* (pp. 17–29). New York: Columbia University Press.
- Meier, R., Shiyang, K., Vaidya, G., & Ng, P. K. (2006). DNA barcoding and taxonomy in Diptera: a tale of high intraspecific variability and low identification success. *Systematic Biology*, *55*, 715–728.
- Metscher, B. D. (2009). MicroCT for comparative morphology: simple staining methods allow high-contrast 3D imaging of diverse non-mineralized animal tissues. *BMC Physiology*, *9*, 11.
- Michalik, P., & Uhl, G. (2011). Cephalic modifications in dimorphic dwarf spiders of the genus *Oedothorax* (Erigoninae, Linyphiidae, Araneae) and their evolutionary implications. *Journal of Morphology*, *272*, 814–832.
- Miller, J. A. (1999). Revision and cladistic analysis of the erigonine spider genus *Sisicottus* (Araneae, Linyphiidae, Erigoninae). *The Journal of Arachnology*, *27*, 553–603.
- Miller, J. A. (2007). Review of erigonine spider genera in the neotropics (Araneae: Linyphiidae, Erigoninae). *Zoological Journal of the Linnean Society*, *149*, 1–263.
- Miller, J. A., & Hormiga, G. (2004). Clade stability and the addition of data: a case study from erigonine spiders (Araneae: Linyphiidae, Erigoninae). *Cladistics*, *20*, 385–442.
- Millidge, A. F. (1977). The conformation of the male palpal organs of linyphiid spiders, and its application to the taxonomic and phylogenetic analysis of the family (Araneae: Linyphiidae). *Bulletin of the British Arachnological Society*, *4*, 1–60.
- Minin, V., Abdo, Z., Joyce, P., & Sullivan, J. (2003). Performance-based selection of likelihood models for phylogeny estimation. *Systematic Biology*, *52*, 674–683.
- Mizutani, R., Takeuchi, A., Hara, T., Uesugi, K., & Suzuki, Y. (2007). Computed tomography imaging of the neuronal structure of *Drosophila* brain. *Journal of Synchrotron Radiation*, *14*, 282–287.
- Mizutani, R., Takeuchi, A., Akamatsu, G., Uesugi, K., & Suzuki, Y. (2008). Element-specific microtomographic imaging of *Drosophila* brain stained with high-Z probes. *Journal of Synchrotron Radiation*, *15*, 374–377.
- Moore, W. S. (1995). Inferring phylogenies from mtDNA variation: mitochondrial-gene trees versus nuclear-gene trees. *Evolution*, *49*, 718–726.
- Nixon, K. C. 2002. WINKLADA, program and documentation. (1.00.08 ed.). Accessed 25 Sep 2014.
- Nyffeler, M., & Benz, G. (1981). Field studies on the feeding ecology of spiders: observations in the region of Zurich (Switzerland). *Anzeiger für Schädlingskunde, Pflanzen und Umweltschutz*, *54*, 33–39.
- Oi, R. (1960). Linyphiid spiders of Japan. *Journal of the Institute of Polytechnics Osaka City University*, *11*, 137–244.
- Oi, R. (1977). A new erigonid spider from Formosa. *Acta Arachnologica*, *27*, 23–26.

- Palumbi, S. R., Martin, A. P., Romano, S., Mcmilan, W. O., Stice, L., & Grabowski, G. (1991). *The simple fool's guide to PCR*. Honolulu: University of Hawaii.
- R Development Core Team. (2011). *R: a language and environment for statistical computing*. R Core Team. Vienna: The R Foundation for Statistical Computing.
- Rae, T. C. (1998). The logical basis for the use of continuous characters in phylogenetic systematics. *Cladistics*, *14*, 221–228.
- Rambaut, A. (2016). FigTree 1.4.3. <http://tree.bio.ed.ac.uk/software/figtree/>. Accessed 2 Jan 2018.
- Rambaut, A., Drummond, A. J., Xie, D., Baele, G., & Suchard, M. A. (2018). Posterior summarisation in Bayesian phylogenetics using Tracer 1.7. *Systematic Biology*, *67*, 901–904.
- Robinson, E. A., Blagoev, G. A., Hebert, P. D., & Adamowicz, S. J. (2009). Prospects for using DNA barcoding to identify spiders in species-rich genera. *ZooKeys*, *16*, 27–46.
- Ronquist, F., Teslenko, M., van der Mark, P., Ayres, D. L., Darling, A., Höhna, S., et al. (2012). MrBayes 3.2: efficient Bayesian phylogenetic inference and model choice across a large model space. *Systematic Biology*, *61*, 539–542.
- Rosenberg, N. A. (2007). Statistical tests for taxonomic distinctiveness from observations of monophyly. *Evolution*, *61*, 317–323.
- Ross, H. A. (2014). The incidence of species-level paraphyly in animals: a re-assessment. *Molecular Phylogenetics and Evolution*, *76*, 10–17.
- Russell-Smith, A., & Stork, N. (1995). Composition of spider communities in the canopies of rainforest trees in Borneo. *Journal of Tropical Ecology*, *11*, 223–235.
- Saitou, N., & Nei, M. (1987). The neighbor-joining method: a new method for reconstructing phylogenetic trees. *Molecular Biology and Evolution*, *4*, 406–425.
- Sauer, J., & Hausdorf, B. (2009). Sexual selection is involved in speciation in a land snail radiation on Crete. *Evolution*, *63*, 2535–2546.
- Schaible, U., & Gack, C. (1987). Zur Morphologie, Histologie und biologischen Bedeutung der Kopfstrukturen einiger Arten der Gattung *Diplocephalus* (Araneida, Linyphiidae, Erigoninae). *Verhandlungen des naturwissenschaftlichen Vereins in Hamburg*, *29*, 171–180.
- Schaible, U., Gack, C., & Paulus, H. F. (1986). Zur Morphologie, Histologie und biologischen Bedeutung der Kopfstrukturen männlicher Zwergspinnen (Linyphiidae: Erigoninae). *Zoologische Jahrbücher. Abteilung für Systematik, Ökologie und Geographie der Tiere*, *113*, 389–408.
- Schenkel, E. (1963). Ostasiatische Opilioniden aus dem Museum d'Histoire Naturelle de Paris. *Mémoires du Muséum National d'Histoire Naturelle, Série A, Zoologie*, *25*, 483–494.
- Schluter, D. (2000). *The ecology of adaptive radiation*. Oxford: OUP Oxford.
- Schneeberg, K., Bauernfeind, R., & Pohl, H. (2017). Comparison of cleaning methods for delicate insect specimens for scanning electron microscopy. *Microscopy Research and Technique*, *80*, 1199–1204.
- Schwarz, G. (1978). Estimating the dimension of a model. *Annals of Statistics*, *6*, 461–464.
- Sentenská, L., Müller, C. H., Pekár, S., & Uhl, G. (2017). Neurons and a sensory organ in the pedipalps of male spiders reveal that it is not a numb structure. *Scientific Reports*, *7*, 12209.
- Shao, K. T. (2018). Catalogue of life in Taiwan. Web electronic publication. version 2009. <http://taibnet.sinica.edu.tw>. Accessed 22 Oct 2018.
- Shaw, K. L. (2002). Conflict between nuclear and mitochondrial DNA phylogenies of a recent species radiation: what mtDNA reveals and conceals about modes of speciation in Hawaiian crickets. *Proceedings of the National Academy of Sciences of the United States of America*, *99*, 16122–16127.
- Silva, D. (1996). Species composition and community structure of Peruvian rainforest spiders: a case study from a seasonally inundated forest along the Samiria river. *Revue Suisse de Zoologie*, *2*, 597–610.
- Sombke, A., Lipke, E., Michalik, P., Uhl, G., & Harzsch, S. (2015). Potential and limitations of X-Ray micro-computed tomography in arthropod neuroanatomy: a methodological and comparative survey. *Journal of Comparative Neurology*, *523*, 1281–1295.
- Sørensen, L. L. (2004). Composition and diversity of the spider fauna in the canopy of a montane forest in Tanzania. *Biodiversity and Conservation*, *13*, 437–452.
- Srivathsan, A., & Meier, R. (2012). On the inappropriate use of Kimura-2-parameter (K2P) divergences in the DNA-barcoding literature. *Cladistics*, *28*, 190–194.
- Steinhoff, P. O. M., & Uhl, G. (2015). Taxonomy and nomenclature of some mainland SE-Asian *Coeliccia* species (Odonata, Platycnemididae) using micro-CT analysis. *Zootaxa*, *4059*, 257–276.
- Steinke, D., Vences, M., Salzburger, W., & Meyer, A. (2005). TaxI: a software tool for DNA barcoding using distance methods. *Philosophical Transactions of the Royal Society B*, *360*, 1975–1980.
- Stork, N. (1991). The composition of the arthropod fauna of Bornean lowland rain forest trees. *Journal of Tropical Ecology*, *7*, 161–180.
- Sunderland, K. D. (1986). Distribution of linyphiid spiders in relation to capture of prey in cereal fields. *Pedobiologia*, *29*, 367–375.
- Tanasevitch, A. V. (2006). On some Linyphiidae of China, mainly from Taibai Shan, Qinling Mountains, Shaanxi Province (Arachnida: Araneae). *Zootaxa*, *1325*, 277–311.
- Tanasevitch, A. V. (2011). On some linyphiid spiders from Taiwan (Araneae: Linyphiidae). *Zootaxa*, *3114*, 31–39.
- Tanasevitch, A. V. (2018a). Linyphiid spiders of the world. <http://old.cepl.rssi.ru/bio/tan/linyphiidae/>. Accessed 23 May 2018.
- Tanasevitch, A. V. (2018b). A survey of the genus *Nasoona* Locket, 1982 with the description of six new species (Araneae, Linyphiidae). *Revue Suisse de Zoologie*, *125*, 87–100.
- Tanisako, A., Hori, A., Okumura, A., Miyata, C., Kuzuryu, C., Obi, T., et al. (2005). Micro-CT of *Pseudocneorhinus bifasciatus* by projection X-ray microscopy. *Journal of Electron Microscopy*, *54*, 379–383.
- Thiele, K. (1993). The holy grail of the perfect character: the cladistic treatment of morphometric data. *Cladistics*, *9*, 275–304.
- Uhl, G., & Maelfait, J.-P. (2008). Male head secretion triggers copulation in the dwarf spider *Diplocephalus permixtus*. *Ethology*, *114*, 760–767.
- Uhl, G., Huber, B. A., & Rose, W. (1995). Male pedipalp morphology and copulatory mechanism in *Pholcus phalangioides* (Fuesslin, 1775) (Araneae, Pholcidae). *Bulletin of the British Arachnological Society*, *10*, 1–9.
- Uhl, G., Nessler, S. H., & Schneider, J. (2007). Copulatory mechanism in a sexually cannibalistic spider with genital mutilation (Araneae: Araneidae: *Argiope bruennichi*). *Zoology*, *110*, 398–408.
- van Helsdingen, P. J. (1965). Sexual behaviour of *Lepthyphantes leprosus* (Ohlert) (Araneida, Linyphiidae), with notes on the function of the genital organs. *Zoologische Mededelingen*, *41*, 15–42.
- Vanacker, D., Borre, J. V., Jonckheere, A., Maes, L., Pardo, S., Hendrickx, F., et al. (2003). Dwarf spiders (Erigoninae, Linyphiidae, Araneae): good candidates for evolutionary research. *Belgian Journal of Zoology*, *133*, 143–149.
- Vences, M., Thomas, M., van der Meijden, A., Chiari, Y., & Vieites, D. R. (2005). Comparative performance of the 16S rRNA gene in DNA barcoding of amphibians. *Frontiers in Zoology*, *2*, 5.
- Vink, C. J., & Kean, J. M. (2013). PCR gut analysis reveals that *Tenuiphantes tenuis* (Araneae: Linyphiidae) is a potentially significant predator of Argentine stem weevil, *Listronotus bonariensis* (Coleoptera: Curculionidae), in New Zealand pastures. *New Zealand Journal of Zoology*, *40*, 304–313.
- Voris, H. K. (2000). Maps of Pleistocene sea levels in Southeast Asia: shorelines, river systems and time durations. *Journal of Biogeography*, *27*, 1153–1167.

- Wallace, A. (1912). Influence of natural selection upon sterility and fertility. In A. Wallace (Ed.), *Darwinsim: an exposition of the theory of natural selection with some of its applications* (3rd. ed., pp. 173–179). London: Macmillan.
- Wang, Q., Li, S., & Murphy, R. W. 2009. Higher-level phylogeny of linyphiid spiders (Araneae: Linyphiidae) based on mitochondrial and nuclear gene sequences. Unpublished.
- Wang, F., Ballesteros, J. A., Hormiga, G., Chesters, D., Zhan, Y., Sun, N., et al. (2015). Resolving the phylogeny of a speciose spider group, the family Linyphiidae (Araneae). *Molecular Phylogenetics and Evolution*, *91*, 135–149.
- Wang, Z. L., Yang, X. Q., Wang, T. Z., & Yu, X. (2017). Assessing the effectiveness of mitochondrial COI and 16S rRNA genes for DNA barcoding of farmland spiders in China. *Mitochondrial DNA Part A*, *29*, 695–702.
- Ward, R. D. (2009). DNA barcode divergence among species and genera of birds and fishes. *Molecular Ecology Resources*, *9*, 1077–1085.
- Whiting, M. F., Carpenter, J. C., Wheeler, Q. D., & Wheeler, W. C. (1997). The Strepsiptera problem: phylogeny of the holometabolous insect orders inferred from 18S and 28S ribosomal DNA sequences and morphology. *Systematic Biology*, *46*, 1–68.
- Wiens, J. J. (2001). Character analysis in morphological phylogenetics: problems and solutions. *Systematic Biology*, *50*, 689–699.
- Williams, D., Schmitt, M., & Wheeler, Q. (2016). *The future of phylogenetic systematics: the legacy of Willi Hennig* (Vol. 86). Cambridge: Cambridge University Press.
- World Spider Catalog (2018). World Spider Catalog. <http://wsc.nmbe.ch>, version 19.5. Accessed 22 Oct 2018.
- Xia, X. (2013). DAMBE5: a comprehensive software package for data analysis in molecular biology and evolution. *Molecular Biology and Evolution*, *30*, 1720–1728.
- Xia, X. (2017). DAMBE6: new tools for microbial genomics, phylogenetics, and molecular evolution. *Journal of Heredity*, *108*, 431–437.
- Xia, Q., Zhang, G. R., Gao, J. C., Fei, R., & Kim, J. P. (2001). Three new species of spiders of Erigoninae (Araneae: Linyphiidae) from China. *Korean Arachnology*, *17*, 161–168.
- Zujko-Miller, J. (1999). On the phylogenetic relationships of *Sisicottus hibernus* (Araneae, Linyphiidae, Erigoninae). *The Journal of Arachnology*, *27*, 44–52.

Publisher's note Springer Nature remains neutral with regard to jurisdictional claims in published maps and institutional affiliations.

3.3. Evolution of nuptial-gift-related male prosomal structures:

taxonomic revision and cladistic analysis of the genus *Oedothorax* Bertkau, 1883

(Araneae, Linyphiidae, Erigoninae)

Shou-Wang Lin, Lara Lopardo and Gabriele Uhl

Manuscript published in *Zoological Journal of the Linnean Society* (2021) XX: 1-168

(Volume number not yet assigned)

Evolution of nuptial-gift-related male prosomal structures: taxonomic revision and cladistic analysis of the genus *Oedothorax* (Araneae: Linyphiidae: Erigoninae)

SHOU-WANG LIN,* LARA LOPARDO and GABRIELE UHL^o

Department of General and Systematic Zoology, University of Greifswald, Germany

Received 19 December 2019; revised 28 February 2021; accepted for publication 20 April 2021

Sexual selection has been shown to drive speciation. In dwarf spiders (erigonines), males possess diverse, sexually selected prosomal structures with nuptial-gift-producing glands. The genus *Oedothorax* is suitable for investigating the evolution of these features due to high structural variation. We have re-delimited this genus based on a phylogenetic analysis. Ten species are *Oedothorax* s.s.; five are transferred back to their original generic placement; 25 remain unplaced as '*Oedothorax*'. Four junior synonymies are proposed: *Callitrichia simplex* to *Ca. holmi* comb. nov.; *Gongylidioides kougianensis* to *G. insulanus* comb. nov.; *Ummeliata ziaowutai* to *U. esyunini* comb. nov.; *Oe. kathmandu* to *Mitrager unicolor* comb. nov. *Oedothorax seminolus* is a junior synonym of *Soulgas corticarius* and the transfer of *Oe. alascensis* to *Halorates* is confirmed. The replacement name *Ca. hirsuta* is proposed for *Ca. pilosa*. The male of *Callitrichia longiducta* comb. nov. and the female of '*Oedothorax*' *nazareti* are newly described. Thirty-eight *Oedothorax* species are transferred to other genera. *Callitrichia spinosa* is transferred to *Holmelgonia*. Three genera are erected: ***Cornitibia***, ***Emertongone*** and ***Jilinus***. *Ophrynia* and *Toschia* are synonymized with *Callitrichia*. Character optimization suggests multiple origins of different prosomal modification types. Convergent evolution in these traits suggests that sexual selection has played an important role in erigonine diversification.

ADDITIONAL KEYWORDS: gustatorial courtship – mate choice – parallel evolution – prosomal modification – sexual selection – spiders.

INTRODUCTION

NUPTIAL GIFTS IN SPIDERS AND THE CASE OF GLANDULAR SECRETIONS IN THE FAMILY LINYPHIIDAE

A nuptial gift is material apart from sperm that is usually offered by the male to the female during courtship and mating. Although not part of the definition by Lewis & South (2012) (modified from South *et al.*, 2010), such gift-giving behaviour often increases the reproductive success of the donor. Nuptial gifts have evolved independently in many animal taxa, from birds to insects (Andersson, 1994; Vahed, 1998, 2007; Lewis *et al.*, 2011). Gifts can consist

of objects collected by the male (exogenous gifts) or produced by the male (endogenous gifts). Gifts can be taken in orally by the female or are transferred along with the gametes into the reproductive tract of the female. Males that offer a nuptial gift to the female are more likely to mate, or copulate longer and transfer more sperm, which results in a higher paternity share when females are promiscuous, as was established for insects in which the most diverse nuptial gift types and mechanisms occur (Vahed, 1998; Gwynee, 2008; Lewis *et al.*, 2011). As paternal investment, transferred nutrients can increase the lifespan and egg production of females, and thus improve the lifetime reproductive success of both the givers and the recipients (Lewis & South, 2012). In addition, it has been shown that a nuptial gift can protect males from sexual cannibalism ('shield effect'), as was established for *Pisaura mirabilis* (Clerck, 1757) (Toft & Albo, 2016).

*Corresponding author. E-mail: shouwanglintaiwan@gmail.com

[Version of record, published online 20 November 2021; <http://zoobank.org/> urn:lsid:zoobank.org:pub:BE2B3859-8F6A-4543-8A69-91840F82377B]

In spiders, exogenous nuptial gifts have been found in a few species in Pisauridae (Van Hasselt, 1884; Stålhandske, 2001) and Trechaleidae (Costa-Schmidt *et al.*, 2008), in which the males deliver prey packed in silk when courting. As for endogenous gifts, glandular products released from the male prosomal region and taken up by the female during courtship are particularly common in spiders (Austad, 1984). This so-called gustatory courtship behaviour has been reported in several species of Theridiidae ('cobweb spiders'; e.g. Vollrath, 1977; Knoflach, 2004), in a pholcid ('daddy-longleg spiders'; Huber, 1997) and in the linyphiid subfamily Erigoninae – which seems to be the champion of endogenous gustatory gifts (e.g. Vanacker *et al.*, 2003; Uhl & Maelfait, 2008; Kunz *et al.*, 2012). Gustatory courtship behaviour in spiders is associated with a sexual dimorphism of the prosoma, with male prosomata being more elevated than those of females (see below). Given the scattered occurrence among families, it seems that male traits related to gustatory courtship have evolved several times independently and in the context of sexual selection in spiders (e.g. Uhl & Maelfait 2008; Michalik & Uhl, 2011; Kunz *et al.*, 2012). Detailed studies have started to explore the exact functions of these features during courtship and copulation, as well as their occurrence and evolution within erigonine spiders (Vanacker *et al.*, 2004; Uhl & Maelfait 2008; Arnedo *et al.*, 2009; Michalik & Uhl, 2011; Kunz *et al.*, 2012).

Linyphiidae is the second-most diverse spider family (World Spider Catalog, 2020). It currently consists of four (Stemonyphantinae, Mynogleninae, Erigoninae and Linyphiinae; Frick & Scharff, 2014) or seven (the latter four plus Micronetinae, Dubiaraneinae and Ipainae; Tanasevitch, 2021) subfamilies, with a total of 606 genera (Tanasevitch, 2021). Within these subfamilies, prosomal modifications occur in many Erigoninae (see below), all Mynogleninae (Frick & Scharff, 2014) and a few Linyphiinae (*Bathyphantes* Menge, 1866, *Diplostyla* Emerton 1882 and *Vesicapalpus* Millidge 1991; Hormiga, 1999, 2000). The current phylogenetic pattern of linyphiid relationships implies that these modifications have originated independently in each of these subfamilies (Hormiga, 2000; Miller & Hormiga, 2004; Arnedo *et al.*, 2009). Here, we focus on the Erigoninae, the so-called dwarf spiders or money spiders (1–3 mm in length), representing the most species-rich subfamily of the Linyphiidae, of which most species build tiny sheet webs in the leaf litter (Hormiga, 2000). Erigonines show a wealth of sexually dimorphic prosomal modifications (Frick *et al.*, 2010) and have been consistently recovered as a monophyletic group (Hormiga, 2000; Miller & Hormiga, 2004; Arnedo *et al.*, 2009). Based on morphological data, the phylogenetic analyses of Miller & Hormiga (2004) and Frick *et al.* (2010) provide the latest information on the evolutionary

patterns of Erigoninae (with up to 80 genera). On the foundation of their character matrix, further studies on the placement of single genera were carried out by adding additional taxa and characters (e.g. *Solenysa* Simon, 1894; Tu & Hormiga, 2011). The higher level molecular phylogenetic analysis of linyphiids by Arnedo *et al.* (2009) has been expanded with an increased taxon sampling (Wang *et al.*, 2015; Bao *et al.*, 2017), providing the latest and largest molecular phylogenetic dataset of linyphiids, including 81 linyphiid genera (111 spp.), among which 25 genera are erigonines (30 spp.).

BIZARRE PROSOMA SHAPES IN A PHYLOGENETIC CONTEXT

Erigonines are unique in the diversity of male structures on the dorsal surface of the prosoma, from simple elevations to bizzare turrets (Hormiga, 2000). Modifications of the region behind the eyes (or the entire ocular region) can consist of grooves, humps, lobes, pits (deep invaginations of the cuticle), modified setae and peculiar slender spires [e.g. *Oedothorax gibbosus* (Blackwall, 1841), *Callitrichia sellafontis* Scharff, 1990, *Caracladus aviculus* (L. Koch, 1896), *Trichopterna thorelli* (Westring, 1861), *Mitrager noordami* van Helsdingen, 1985 and *Walckenaeria acuminata* Blackwall, 1833, respectively] (Wiehle, 1960a; Hormiga, 2000; Miller, 2007). Among the 402 linyphiid genera currently belonging to erigonines (Tanasevitch, 2019), sexually dimorphic features are present in at least 223 genera (estimated by Lin from descriptions in previous studies; e.g. Simon, 1884; Roberts, 1987; Chamberlin, 1949; Holm, 1962; Millidge, 1991; Eskov & Marusik, 1994; Hormiga, 2000; Paquin & Dupérré, 2003; Miller & Hormiga, 2004; Miller, 2007; Ono *et al.*, 2009; Frick *et al.*, 2010; Zhao & Li, 2014). Also, the diversity of the prosomal structures in males strongly differs among genera [e.g. low in *Shaanxinus* Tanasevitch, 2006 (Lin *et al.*, 2019); high in *Oedothorax* Bertkau, 1883; e.g. Wunderlich, 1974; Tanasevitch, 1998, 2015]. In about 20 species examined, the modified prosomal regions are associated with extensive secretory glandular tissue, except *Erigone atra* Blackwall, 1833 (Lopez, 1976; Blest & Taylor, 1977; Lopez & Emerit, 1981; Schaible *et al.*, 1986; Schaible & Gack, 1987; Michalik & Uhl, 2011; Lin *et al.*, 2019). So far, only ten species with prosomal modifications have been observed for their mating behaviour [*Diplocephalus latifrons* (O. Pickard-Cambridge, 1863), *Di. permixtus* (O. Pickard-Cambridge, 1871), *Erigone atra* Blackwall, 1833, *Er. dentipalpis* (Wider, 1834), *Er. longipalpis* (Sundevall, 1830), *Hypomma bituberculatum* (Wider, 1834), *Oe. gibbosus*, *Oe. retusus* (Westring, 1851) and *Walckenaeria corniculans* (O. Pickard-Cambridge, 1875), *W. cuspidata* Blackwall, 1833], and in all cases, except the three *Erigone*

Audouin, 1826 species, the female mouthparts are in contact with, or sink into, the male prosomal structures (Bristowe, 1931; Schlegelmilch, 1974; Vanacker *et al.*, 2003; Uhl & Maelfait, 2008; Kunz *et al.*, 2012). Among the above-mentioned species, only the two *Oedothorax* species have been investigated for both their mating behaviour and their glandular tissues (Vanacker *et al.*, 2003; Kunz *et al.*, 2012). Behavioural experiments have demonstrated that the functional context of the secretion that is produced in the prosomal region is mating effort through gustatory courtship. Females take up the secretion during mating and are reluctant to mate when no gift is offered (Kunz *et al.*, 2013). The secretion was also shown to affect female fecundity (Uhl & Maelfait, 2008; Kunz *et al.*, 2012). Consequently, it seems highly likely that the male prosomal structures of erigonine spiders have evolved under sexual selection (Vanacker *et al.*, 2003).

Among the many erigonine genera, the genus *Oedothorax* has been the focus of several studies dealing with sexual selection, mating strategies, dimorphic morphology and comparative analysis aimed at elucidating the functional context and the anatomy of the prosomal structures (e.g. De Keer & Maelfait, 1987; Heinemann & Uhl, 2000; Maes *et al.*, 2004; Vanacker *et al.*, 2004; Uhl & Busch, 2009; Michalik & Uhl, 2011; Kunz *et al.*, 2012). These studies on *Oedothorax* are based on the six most common European species, whose male prosomal morphology varies from absence of modifications to highly complex structures. All European *Oedothorax* males possess glandular tissue and produce secretions for gustatorial courtship (Michalik & Uhl, 2011). In one species, *Oe. gibbosus*, there are two male morphs that differ in prosomal shape and glandular tissues. Each male morph shows different mating strategies and life-history patterns (Vanacker *et al.*, 2004). We focused on the genus *Oedothorax* due to the available background knowledge on the reproductive biology and to explore the phylogenetic relationships as a necessary step to assess the evolutionary history of prosomal modifications and gustatorial courtship and their potential for speciation.

TAXONOMIC HISTORY OF THE GENUS *OEDOTHORAX*

The genus *Oedothorax* was established by Förster & Bertkau (1883) based on the hump behind the eyes in males, with the type species *Oe. gibbosus*. Currently, this genus comprises 82 described species distributed across the Northern Hemisphere and Africa (World Spider Catalog, 2020), which are mostly 2–3 mm in body length, and live in leaf litter, grasslands and other humid habitats. Diagnostic characteristics for the genus *Oedothorax* were proposed by Wiehle (1960a) based on tibial chaetotaxy, location of metatarsal

trichobothria, number of teeth on the anterior and posterior sides of the cheliceral fang furrow, epigyne and vulva morphology, and a particular coexistence between a heavily sclerotized embolus and a conductor ('radix' in the current study) in the male copulatory bulb. Holm (1962) proposed a close relationship between *Oedothorax* and the African genus *Callitrichia* Fage, 1936, given their resemblance in chaetotaxy and the similarity of their copulatory bulbs. Wunderlich (1974) described ten new *Oedothorax* species from Nepal [two of which were subsequently transferred to *Nasooona* Locket, 1982 by Tanasevitch (2014b)], thereby adding to, and modifying, the diagnosis of *Oedothorax*. Later, he described two African *Oedothorax* species, and proposed *Callitrichia* and *Toschia* Caporiacco, 1949 as junior synonyms of *Oedothorax* (Wunderlich, 1978), a view supported by Bosmans (1985). In the 1970s and 1980s, several additional African *Oedothorax* species were described by Locket & Russell-Smith (1980), Jocqué (1985), Bosmans (1988), Jocqué & Scharff (1986) and Scharff (1989). As pointed out by Scharff (1990a), the arguments supporting the previous synonymization of *Callitrichia* and *Toschia* with *Oedothorax* were based on a number of symplesiomorphic features also present in many other linyphiids. Contrary to Wunderlich's opinion, Tanasevitch (1998) held the view that *Callitrichia* and *Toschia* may actually belong to other genera, and that all the Himalayan *Oedothorax* species were clearly congeneric with the type species *Oe. gibbosus*. However, in his latest publication, Tanasevitch (2020b) regarded Afrotropical *Oedothorax* species, including *Callitrichia* and *Toschia*, to be more closely related to the Himalayan and Oriental *Oedothorax* species than to the Palaearctic representatives. Neither Wunderlich's nor Tanasevitch's views were based on synapomorphic features, and their proposed diagnostic characteristics are not unique to *Oedothorax*. As for most North American *Oedothorax* species, their taxonomic placement is dubious, as in most cases only females are known. Lately, several newly described species from Asia were assigned to *Oedothorax* based on the same potentially plesiomorphic features (Tanasevitch, 2016, 2017a, b, c, 2018, 2020a, b). Taken together, *Oedothorax* requires a comprehensive phylogenetic analysis in which the genus is delimited and diagnosed with synapomorphic features, and its composition, pattern of relationships as well as the taxonomic placement of its current species are determined.

THE GOAL OF THIS REVISION

In this study, we explore the phylogenetic relationships within the genus *Oedothorax*. We conduct a comprehensive phylogenetic analysis with 64% of the currently known and accepted *Oedothorax*

species, as well as other closely related erigonine taxa. With the inferred phylogeny and synapomorphies of species congeneric to the type species, we test the monophyly of the genus *Oedothorax*, and assess the taxonomic status of species currently assigned to it. Understanding the pattern of relationships among these taxa serves to reconstruct the evolution of their dimorphic gustatorial structures and, finally, to assess the role of sexual selection in species diversification.

MATERIAL AND METHODS

In this section, taxa are referred to according to original names (i.e. as in [World Spider Catalog, 2020](#)); in the Results and Discussion sections below, revised names are applied.

STUDY DESIGN

We took a two-step approach. First, in order to determine the phylogenetic position of *Oedothorax* (and several morphologically similar taxa), we expanded the data matrix of [Frick et al. \(2010\)](#), the currently most comprehensive erigonine phylogeny, originally based on the matrix of [Miller & Hormiga \(2004\)](#). In addition to *Oe. gibbosus* already included in the matrix of [Miller & Hormiga \(2004\)](#) and [Frick et al. \(2010\)](#), we appended two additional *Oedothorax* species to the character matrix (see below). Moreover, seven erigonine species were added due to observed similarity with *Oedothorax* in their male and female genitalia. In addition, *Ummeliata insecticeps* (Bösenberg & Strand, 1906) was included due to its close relationship with *Hylyphantes* Simon, 1884 and *Oedothorax* in the molecular phylogenetic hypothesis of [Wang et al. \(2015\)](#). This resulted in our Matrix I consisting of 121 taxa and 176 discrete characters ([Supplementary Information, Matrix I](#)).

Second, for further investigating the intra- and intergeneric relationships of *Oedothorax* and their closely related taxa, as well as inferring the evolution of their male prosomal features, we constructed Matrix II based on the results of the analysis of Matrix I. Criteria for outgroup selection for Matrix II are given in parentheses after each species in the 'Specimens' section below. Thirteen species were taken from the matrix of [Miller & Hormiga \(2004\)](#) and [Frick et al. \(2010\)](#). Based on similar genital and somatic morphology, seven African species and seven Asian species were also included. The ingroup in Matrix II consists of 53 *Oedothorax* species for which male specimens were available. For a total of 79 taxa in Matrix II (instead of 80, due to the synonymization of *Ca. simplex* ([Jocqué & Scharff, 1986](#)) with *Oe. holmi*

syn. nov.), 128 discrete and four continuous characters were scored (see Appendix 1), of which 55 discrete characters were taken from [Miller & Hormiga \(2004\)](#) (see [Supplementary Information, Matrix II](#)).

The taxonomic status of species for which specimens were unavailable during this study are discussed based on descriptions from the literature.

SPECIMENS

Matrix I

In addition to taxa included in [Frick et al. \(2010\)](#): *Ca. sellafontis*, *Ca. simplex* ([Jocqué & Scharff, 1986](#)), *Holmelgonia basalis* ([Jocqué & Scharff, 1986](#)), *Nasoona crucifera* ([Thorell, 1895](#)), *Oe. apicatus* ([Blackwall, 1850](#)) and *Oe. nazareti* [Scharff, 1989](#), *Ophrynia uncata* [Jocqué & Scharff, 1986](#), *Op. juguma* [Scharff, 1990](#), *Shaanxinus mingchihensis* [Lin, 2019](#) and *Ummeliata insecticeps*.

Matrix II

Outgroup taxa: Selected from matrix of [Frick et al. \(2010\)](#): *Pimosa altiocolata* ([Keyserling, 1886](#)) (sister-group of Linyphiidae, root for the phylogenetic hypotheses), *Stemonyphantes lineatus* ([Linnaeus, 1758](#)) (sister-group to all other linyphiids), *Linyphia triangularis* ([Clerck, 1757](#)) (representing Linyphiinae), *Gongylidiellum latebricola* ([O. Pickard-Cambridge, 1871](#)), [replacing *Gongylidiellum vivum* ([O. Pickard-Cambridge, 1875](#)) due to sample availability, representing 'basal-most erigonines'], *Erigone atra* (replacing *Erigone psychrophila* [Thorell, 1871](#) due to sample availability), *Diplocentria bidentata* ([Emerton, 1882](#)), *Lophomma punctatum* ([Blackwall, 1841](#)), *Walckenaeria acuminata* [replacing *Walckenaeria directa* ([O. Pickard-Cambridge, 1874](#)) due to sample availability], *Gonatium rubellum* ([Blackwall, 1841](#)) [replacing *Gonatium rubens* ([Blackwall, 1833](#)) due to sample availability], *Araeoncus humilis* ([Blackwall, 1841](#)) [these six species were sampled from branches of 'distal erigonines' in [Frick et al. \(2010\)](#)], *Gongylidium rufipes* ([Linnaeus, 1758](#)), *Hylyphantes graminicola* ([Sundevall, 1830](#)) and *Tmeticus tolli* [Kulczyński, 1908](#) [these three species together formed a branch sister to *Oe. gibbosus* on the tree of [Frick et al. \(2010\)](#), and are selected in this study as potential sister-taxa of *Oedothorax*]; selected based on similarity of genitalia: *Atypena cirrifrons* ([Heimer, 1984](#)), *Ca. formosana* [Oi, 1977](#), *Ca. sellafontis*, *Ca. simplex*, *Ho. basalis*, *Op. juguma*, *Op. uncata*, *Ho. basalis*, *Mitrager noordami*, *Na. crucifera*, *Na. setifera* ([Tanasevitch, 1998](#)), *S. mingchihensis* [Lin, 2019](#), *Toschia picta* ([Caporiacco, 1949](#)), *Typhistes gloriosus* [Jocqué, 1984](#) and *U. insecticeps*.

Ingroup taxa: *Oedothorax agrestis* ([Blackwall, 1853](#)), *Oe. angelus* [Tanasevitch, 1998](#), *Oe. apicatus*,

Oe. assuetus Tanasevitch, 1998, *Oe. clypeellum* Tanasevitch, 1998, *Oe. convector* Tanasevitch, 2014, *Oe. cornutus* Tanasevitch, 2015, *Oe. coronatus* Tanasevitch, 1998, *Oe. cunur* Tanasevitch, 2015, *Oe. dismodicoides* Tanasevitch, 1998, *Oe. elongatus* Wunderlich, 1974, *Oe. esyunini* Zhang, Zhang & Yu, 2003, *Oe. falcifer* Tanasevitch, 1998, *Oe. falciferoides* Tanasevitch, 2015, *Oe. fuscus* (Blackwall, 1834), *Oe. gibbifer* (Kulczyński, 1882a), *Oe. gibbosus*, *Oe. globiceps* Thaler, 1987, *Oe. hirsutus* Wunderlich, 1974, *Oe. holmi* Wunderlich, 1978, *Oe. hulongsensis* Zhu & Wen, 1980, *Oe. kodaikanal* Tanasevitch, 2015, *Oe. latitibialis* Bosmans, 1988, *Oe. legrandi* Jocqué, 1985, *Oe. lineatus* Wunderlich, 1974, *Oe. longiductus* Bosmans, 1988, *Oe. lopchu* Tanasevitch, 2015, *Oe. lucidus* Wunderlich, 1974, *Oe. macrophthalmus* Lockett & Russell-Smith, 1980, *Oe. malearmatus* Tanasevitch, 1998, *Oe. meghalaya* Tanasevitch, 2015, *Oe. meridionalis* Tanasevitch, 1987, *Oe. modestus* Tanasevitch, 1998, *Oe. montifer* (Emerton, 1882), *Oe. muscicola* Bosmans, 1988, *Oe. nazareti* Scharff, 1989, *Oe. paludigena* Simon, 1926, *Oe. paracymbialis* Tanasevitch, 2015, *Oe. pilosus* Wunderlich, 1978, *Oe. retusus*, *Oe. rusticus* Tanasevitch, 2015, *Oe. savigniformis* Tanasevitch, 1998, *Oe. sexoculatus* Wunderlich, 1974, *Oe. sexoculorum* Tanasevitch, 1998, *Oe. simplicithorax* Tanasevitch, 1998, *Oe. stylus* Tanasevitch, 2015, *Oe. tholusus* Tanasevitch, 1998, *Oe. tingitanus* (Simon, 1884), *Oe. trilobatus* (Banks, 1896), *Oe. uncus* Tanasevitch, 2015, *Oe. unicolor* Wunderlich, 1974, *Oe. usitatus* Jocqué & Scharff, 1986 and *Oe. villosus* Tanasevitch, 2015.

SPECIMENS EXAMINATION AND DESCRIPTION

Alcohol-preserved specimens (70%) were scored and photographs were taken using a Zeiss Discovery V20 stereomicroscope, equipped with a Zeiss AxioCam MRc Digital camera and AxioVision 4.8 software. Measurements were taken with AxioVision 4.8 software, as well as images of male palps in the [Supplementary Information, Figs S1–S5](#) in the online version of this paper. Additional photos were produced with a Visionary Digital BK Plus Lab System (duninc.com/bk-plus-lab-system.html) equipped with a Canon EOS 6D and a customized Canon MP-E 651–5× Macro Lens for habitus photos, and Mitutoyo M Plan Apo 10× lens for images of genital features. Depending on the availability of specimens and the degree of sclerotization of the vulva, observation of female genitalia (epigyne) were either conducted on the animal without excision, or excised and digested with pancreatin solution for one day, or processed in KOH solution (0.5 g KOH crystals in 8 mL distilled water) heated on a hot plate with double-boiler arrangement for 25 to 40 min in order to lighten the colour of sclerotized parts. The pancreatin

solution was prepared using SIGMA Pancreatin P7545 enzyme complex, in a solution of sodium borate prepared using the concentrations described by [Dingerkus & Uhler \(1977\)](#), as modified by [Alvarez-Padilla & Hormiga \(2008\)](#). Macerated epigynes were mounted on excavated microscope slides with a drop of Eugenol. For specimens with a relatively pale opisthosomal coloration, the entire female was submerged in Eugenol on a cavity microscope slide, with the epigyne facing upwards. Previous studies of erigonine phylogenetics used scanning electron microscopy (SEM) and analysed ultrastructural details such as cuticular pores and modified setae (e.g. [Hormiga, 2000](#); [Miller & Hormiga, 2004](#)). The majority of species examined in this study are only represented by type specimens and, therefore, a comprehensive comparative SEM approach was not feasible. Accordingly, we focused on comparative morphological data from light microscopy. Internal anatomical data on the presence and distribution of glandular tissue, as well as their spatial relationship with muscular tissue, will be published in a follow-up paper (Lin *et al.*, unpublished).

The investigation of spinnerets was performed by placing the specimens in Eugenol on a cavity slide. The specimens were positioned by putting them into small rings that were cut off from the tips of plastic pipettes, aided by additional plastic pieces to finely adjust the angles of the specimens. Each sample was overlaid with a coverslip, observed and illustrated with an Olympus CX40 compound microscope connected to a camera lucida. Male pedipalps were mounted in Eugenol. Drawings were performed by hand. Scanned drawings were edited in Adobe Illustrator and Adobe Photoshop. Measurements are given in mm. Arithmetic means are calculated for the interspecific variation. Distribution data and taxonomic reference of species are from the [World Spider Catalog \(2020\)](#).

MORPHOLOGICAL PHYLOGENETIC ANALYSES

Matrices I and II were edited and managed using MESQUITE 3.10 ([Maddison & Maddison, 2017](#)). Parsimony analyses were conducted with TNT v.1.1 ([Goloboff *et al.*, 2008](#)) using a traditional search with random seed 1500 replications, 1000 trees saved per replication, branch-swapping by TBR algorithm. Character optimization and tree editing were performed in WinClada v.1.00.08 ([Nixon, 2002](#)). Morphological continuous characters in Matrix II were treated as ordered, and analysed as such ([Goloboff *et al.*, 2006](#)). We calculated two clade-support measures using TNT: Bremer support (tree suboptimal by 17 steps during TBR retained from existing trees) and Jackknife support (removal probability = 36%).

Additionally, we conducted implied weighting schemes for Matrix II with and without continuous characters (same settings as above). The constant of concavity k varied from relatively high to relatively low cost (1–6, 10, 15, 20, 30, 100, 1000) set to homoplasies (Goloboff, 1993).

RESULTS

PHYLOGENETIC ANALYSES

Matrix I: The result of the analysis of the expanded matrix of Miller & Hormiga (2004) and Frick *et al.* (2010) resulted in 296 most-parsimonious trees [tree length (L) = 1149, consistency index (CI) = 0.187, retention index (RI) 0.589]. The consensus tree has a topology identical to that of Frick *et al.* (2010) except for the ‘distal erigonine’ clade (Fig. 1). All ten additional species group together with *Oe. gibbosus*, *Gongylidium rufipes*, *Tm. tolli* and *Hylyphantes graminicola*, supporting the suspected close relationship of these species to *Oedothorax* based on preliminary observation of similarities in male and female genitalia.

Matrix II: The analysis of this matrix resulted in three most-parsimonious trees (Figs 2, 3; L = 489.848, CI = 0.322, RI = 0.643, only unambiguous character transformations are shown). Standard statistics of characters are given in Appendix 1. The monophyly of the 53 species of *Oedothorax* included in this study is not recovered. The tree topology was strongly influenced by the inclusion of the four continuous characters in the analysis. When only discrete characters were used (2472 most-parsimonious trees, L = 461), several branches collapsed on the consensus tree, except 37 branches: Clades 1, 2, 3, 5, 8, 9, 10, 11, 12, 13, 17–19, 23–26, 27–34, 45, 46, 50, 52, 54, 58, 59, 61, 66–68, 77.

The following clades relevant to *Oedothorax* were obtained from the analysis of the complete Matrix II (see also Taxonomy below):

Clade 13: This clade includes *Oedothorax s.s.*, *Callitrichia* (including *Ophrynia* Jocqué, 1981, *Toschia* and most of the previous Afrotropical *Oedothorax* species), *Holmelgonia* Jocqué & Scharff, 2007, *Nasoonia*, *Shaanxinus*, *Ummeliata* Strand, 1942, *Gongylidium* Menge, 1868, *Hylyphantes* and *Tmeticus* Menge, 1868, and the Oriental/Indomalayan taxa, including *Mitrager* van Helsdingen, 1985, *Atypena* Simon, 1894 and some ‘*Oedothorax*’ incertae sedis. This clade is supported by the presence of membranous region between radix and embolus (Ch 24, synapomorphic), the absence of small setae at retrolateral margin of cymbium (Ch 1, homoplastic), the presence of tegular sac (Ch 41, homoplastic) and the separated pedicel sternite and pleurites (Ch 111, homoplastic). In addition, these

taxa also share the following combination of features: tibial chaetotaxy 2-2-1-1, each metatarsus with one trichobothrium; palpal tibia with two retrolateral trichobothria, one prolateral trichobothrium [except *M. lucida* (Wunderlich, 1974) **comb. nov.**, *M. sexoculata* (Wunderlich, 1974) **comb. nov.** and *Ca. convector* (Tanasevitch, 2014) **comb. nov.**]; paracymbium spiral form, with basal and distal groups of setae (except in *Oe. apicatus*, *Oe. gibbifer* and *Oe. retusus*, where the distal setal group cannot be recognized); radical tail piece (except *Ca. convector*) and anterior radical process (except *Hylyphantes graminicola* and ‘*Oe.*’ *meghalaya*) present. The epigynal morphology within this clade is relatively simple and constant across taxa, slightly convex [except *Nasoonia*, see generic taxonomic remarks in Tanasevitch (2018)], with a dorsal plate extending anteriorly, fused with ventral plate, the receptacles (spermathecae) located at the anterior end of the lateral borders between the ventral and dorsal plates.

Clade 27 (Oedothorax s.s.): This clade includes *Oe. gibbosus*, the type species of *Oedothorax*, and it is therefore regarded here as *Oedothorax s.s.* The synapomorphies supporting the monophyly of the ten *Oedothorax* species in Clade 27 are listed below (see generic description). Within *Oedothorax s.s.*, Clade 28 (the ‘*gibbosus*-like species group’) is supported by two characters: male post-PME thin setae laterally directed (Ch 88, synapomorphic), and the post-PME lobe in male (Ch 92, homoplastic). The sister-relationship of *Oe. gibbosus* and *Oe. trilobatus* is supported by the presence of post-PME groove (Ch 91, homoplastic). The monophyly of *Oe. gibbifer*, *Oe. apicatus* and *Oe. retusus* is supported by four characters: embolic membrane small, proximally directed (Ch 35, synapomorphic), paracymbium distal setae absent (Ch 6, homoplastic), palpal tibia basal thorn present (Ch 51, homoplastic) and male carapace sulci and pits (Ch 93, homoplastic). Sister-relationship of *Oe. apicatus* and *Oe. retusus* is supported by the broad embolus base (Ch 13, synapomorphic). The monophyly of Clade 26 is supported by the presence of distal small protuberances on radical tailpiece (Ch 32, synapomorphic). Clade 27 is supported by two synapomorphies: male palpal tibia prolateral small apophysis present (Ch 54), and two sub-AME setae (Ch 77). The monophyly of *Oe. fuscus* and *Oe. tingitanus* is supported by bifurcate protegulum (Ch 37, synapomorphic) and absence of tegular papillae (Ch 42, homoplastic).

Clade 39 (Holmelgonia + Callitrichia): Except ‘*Oedothorax*’ *nazareti*, all the original Afrotropical *Oedothorax* species are placed within Clade 39, which now comprises the African genera *Callitrichia* (with one species from Thailand, *Ca. convector*) and *Holmelgonia*. This group is supported by two homoplastic characters: the presence of radical papillae (Ch 27) and the entry of copulatory duct into



Downloaded from https://academic.oup.com/zoolinnean/advance-article/doi/10.1093/zoolinnean/zlab033/6432417 by guest on 03 January 2022

Figure 1. The consensus tree of 296 most-parsimonious trees from the analysis of the expanded matrix of Miller & Hormiga (2004) and Frick *et al.* (2010) (Matrix I), with Bremer/Jackknife support values shown beside nodes. Newly appended taxa in bold.

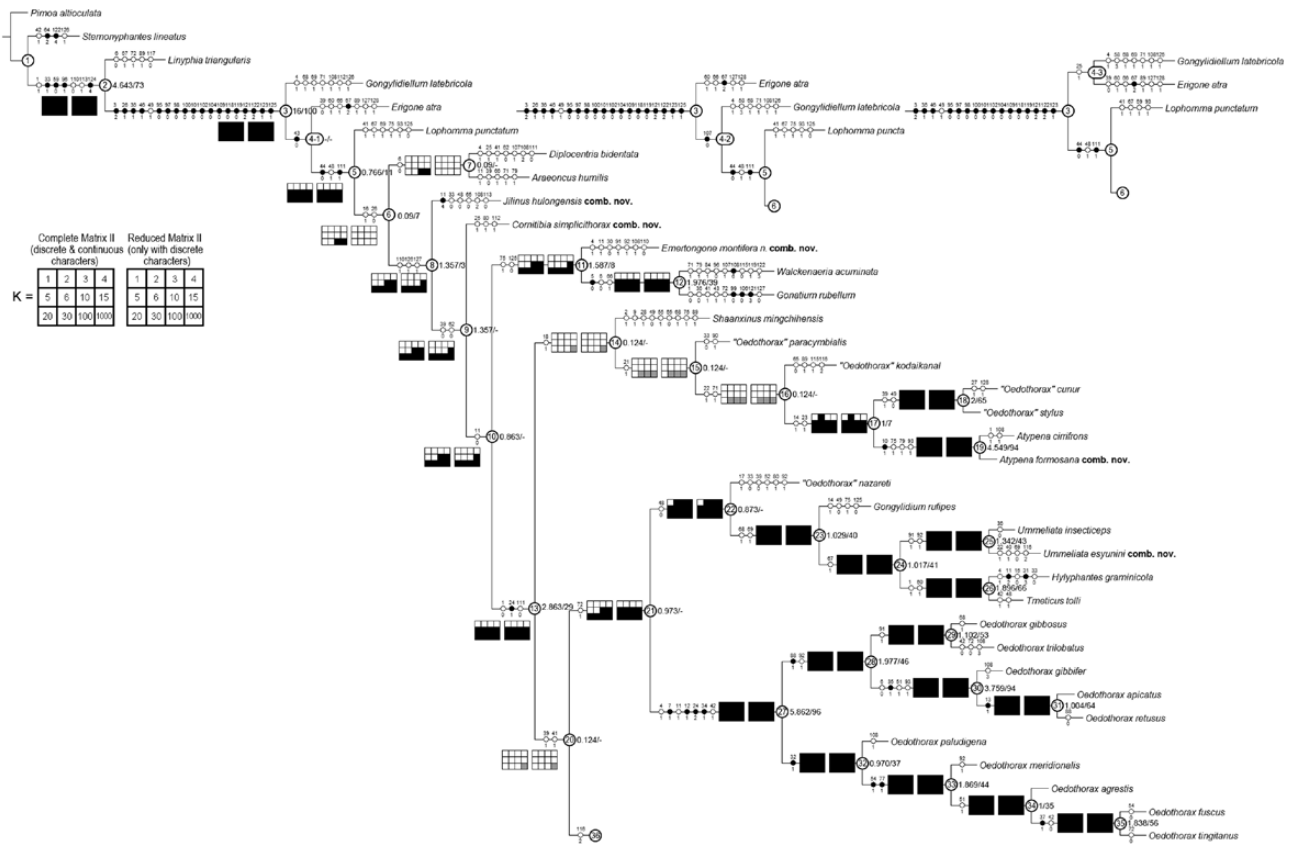


Figure 2. The first part of the three most-parsimonious trees generated from the analysis of Matrix II, with Bremer/Jackknife support values shown beside nodes. The presence/absence of clades in the consensus trees of the most-parsimonious trees of the implied weights analysis with different k values are shown in the box under/on the branches: black for presence when considering all taxa; grey for presence only when *Callitrichia convector* (Tanasevitch, 2014) and *Ca. usitata* (Jocqué & Scharff, 1986) are not considered; white for absence.

the spermatheca ectal to the exit of fertilization duct from the spermatheca (Ch 128). The synapomorphies supporting Clade 40 are listed below (see generic description of *Callitrichia*).

Clade 55 (Mitrager): All Kashmir and Nepalese [except of *Cornitibia simplicithorax* (Tanasevitch, 1998) **comb. nov.**; see Taxonomy below] and half of the Indian *Oedothorax*, together with *M. noordami* constitute a monophyletic group (Clade 55). The synapomorphies supporting this clade are listed below (see generic description of *Mitrager*).

The taxonomic decisions below were made based on the result of our phylogenetic analyses.

IMPLIED WEIGHTING SCHEMES FOR MATRIX II WITH AND WITHOUT CONTINUOUS CHARACTERS

When analysed with discrete characters only, the analyses with implied weights resulted in one to six trees, depending on the k values (tree length is based on the

equally weighted characters calculated in WinClada). The analysis with both discrete and continuous characters found one tree for each k value. The results are listed in Appendix 2, and are summarized in Figures 2 and 3. Independently of the use of continuous characters, all implied weights (IW) analyses, except one (see below), resulted in four major stable clades: *Gongylidium* + *Ummeliata* + *Tmeticus* + *Hylyphantes* (Clade 23), *Oedothorax* s.s. (Clade 27), *Callitrichia* [with or without *Ca. usitata* (Jocqué & Scharff, 1986) **comb. nov.** or *Ca. convector*, Clade 39] and *Mitrager* (with or without *Ca. convector*, ‘*Oe.* meghalaya’ or ‘*Oe.* uncus’). The latter two clades are absent when analysed under $k = 1$, the concavity that penalized homoplasy the highest. When $k = 1000$, the trees of IW analyses of both the complete Matrix II and only discrete characters resulted in the highest numbers of clades shared with the tree from the equal weight (EW) analysis of the complete Matrix II (66 and 62 clades, respectively; when disregarding *Ca. convector* and *Ca. usitata*, the numbers become 70 and 67, respectively).

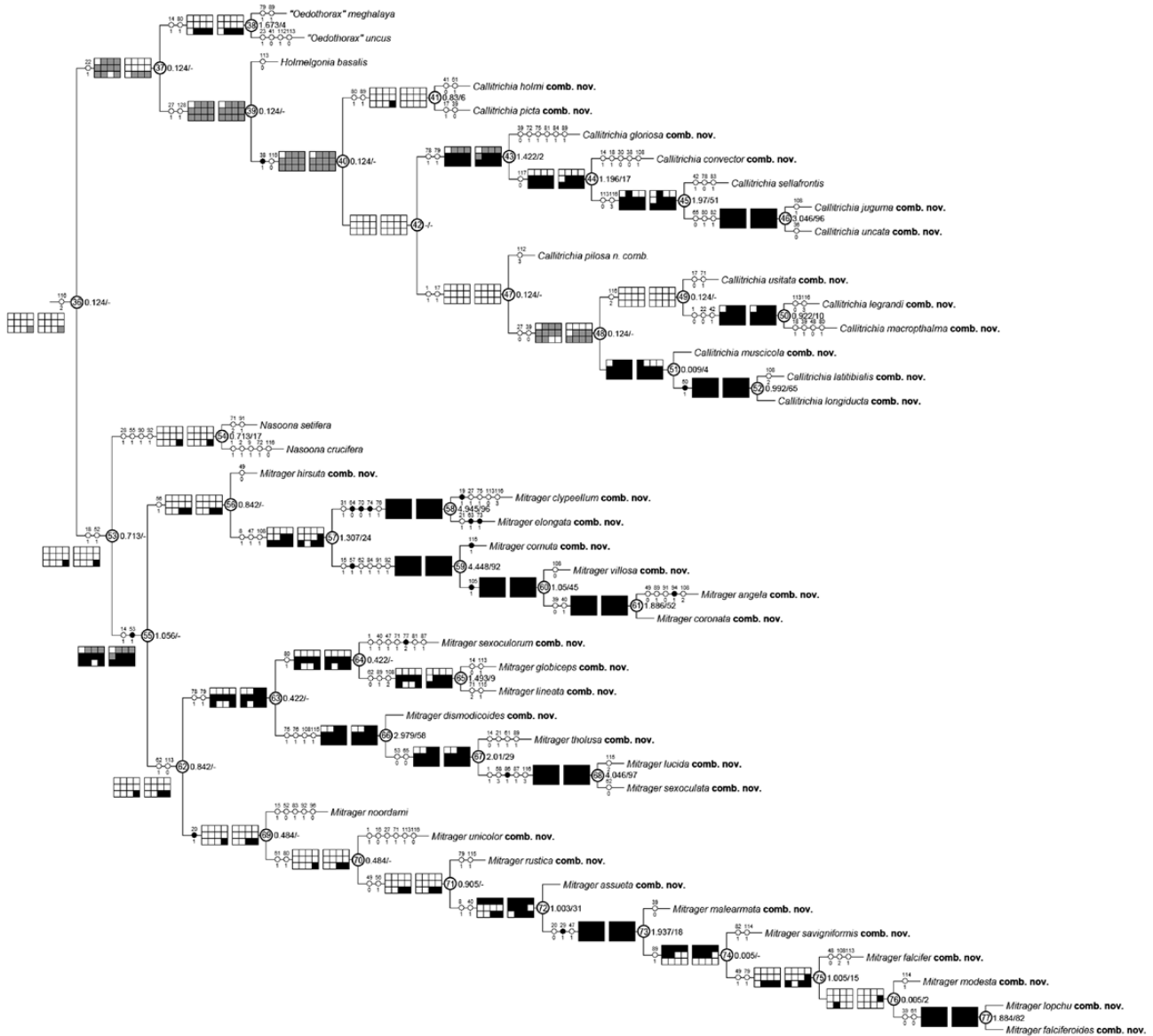


Figure 3. Continuation of [Figure 2](#), showing Clade 36.

CHARACTER TRANSFORMATIONS OF PROSOMAL STRUCTURES

For definitions of characters see Appendix 3. Most of the prosomal modifications defined in the present study showed a pattern of multiple origins on our resulted phylogenetic hypotheses from analysis of Matrix II. Reconstruction of character transformations of eight conspicuous prosomal modifications is visualized on the cladogram in [Figure 4](#). The cheliceral basal apophysis has a single origin. The PME lobe originated eight times independently. The pre-PME groove originated twice and was lost once. The clypeal hump originated twice. The post-PME groove evolved five times independently and was lost once. The lateral sulci and pits have three origins.

The post-PME lobe originated nine/ten times and was lost one/zero times depending on fast or slow optimization, respectively. The inter-AME-PME lobe evolved twice.

TAXONOMY

The taxonomic actions and discussions performed here are relevant to the 53 original *Oedothorax* species studied, as well as to the other 29 species uninspected here. The treatment pertains to and affects the following taxa: *Oedothorax* species (within *Oedothorax s.s.*), ‘*Oedothorax*’ species (unknown taxonomic status, as *Oedothorax incertae sedis*), *Atypena*, *Callitrichia*, *Gongylidioides* Oi, 1960, *Halorates* Hull, 1911,

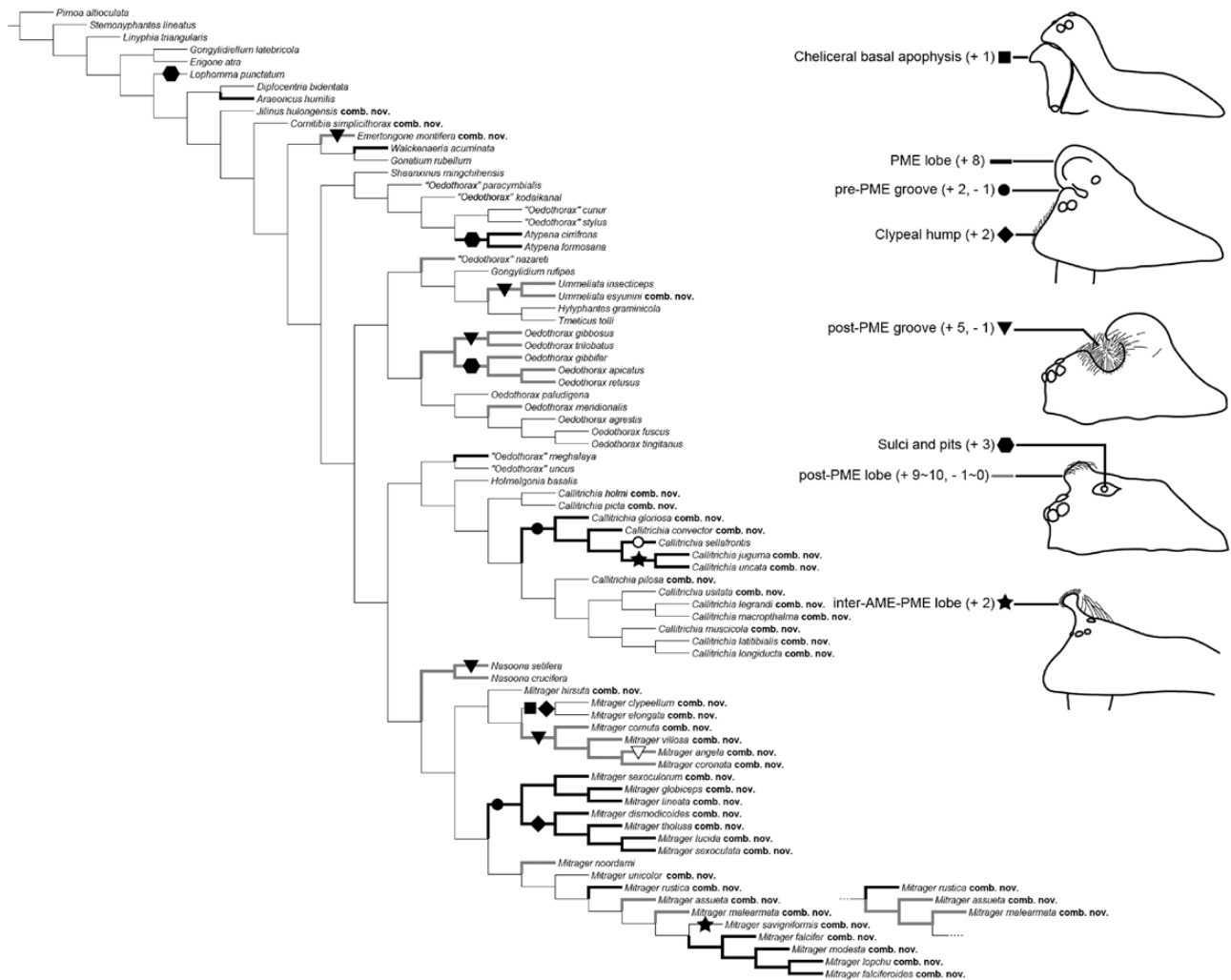


Figure 4. Character transformation of selected prosomal characters reconstructed on the first among the three most-parsimonious trees generated from the analysis of Matrix II.

Holmelgonia, *Hybauchenidium* Holm, 1973, *Mitrager*, *Nasoona*, *Shaanxinus*, *Soulgas* Crosby & Bishop, 1936, *Ummeliata* and the new genera *Cornitibia*, *Emertongone* and *Jilinus*.

OEDOTHORAX S.S. BERTKAU, 1883

Type species: *Neriene gibbosa* Blackwall, 1841.

Monophyly: This group is supported by the following unambiguous character transformations: paracymbium base visible from dorsal view of male pedipalp (Ch 4, homoplastic), median position of distal setae group on paracymbium (Ch 7, synapomorphic), embolus base horn present (Ch 12, synapomorphic) embolic membrane cylindrical (Ch 34, synapomorphic) and tegular papillae present (Ch 42, homoplastic); and

the following ambiguous character transformations: embolus prolaterally spiral (Ch 11, homoplastic, ambiguous transformation), radix-embolus membranous region extend to prolateral side of radix (Ch 24, synapomorphic, ambiguous transformation).

Diagnosis: The newly circumscribed *Oedothorax* s.s. is similar to *Callitrichia*, *Mitrager* and other species in Clade 13 in their configuration of the embolic division, the tibial chaetotaxy and the epigyne morphology. *Oedothorax* s.s. is characterized and can be distinguished from other taxa in Clade 13 by the following features:

1. Paracymbium: small-sized; base visible from dorsal view of male pedipalp (medium- to large-sized in other species in Clade 13; base covered by cymbium from dorsal view); distal part not enlarged (greatly enlarged in most *Callitrichia* species); distal setae group with middle position or indistinguishable

from basal setae group (with distal position in other species in Clade 13); distal clasp distally extended, without striae (retrolaterally extended and/or with striae in many *Mitrager* species).

2. Copulatory bulb: embolus base protuberance present (arrow in Fig. 5B) (absent in other species in Clade 13); embolus prolaterally spiral around pointed, prolaterally spiral anterior radical process (embolus

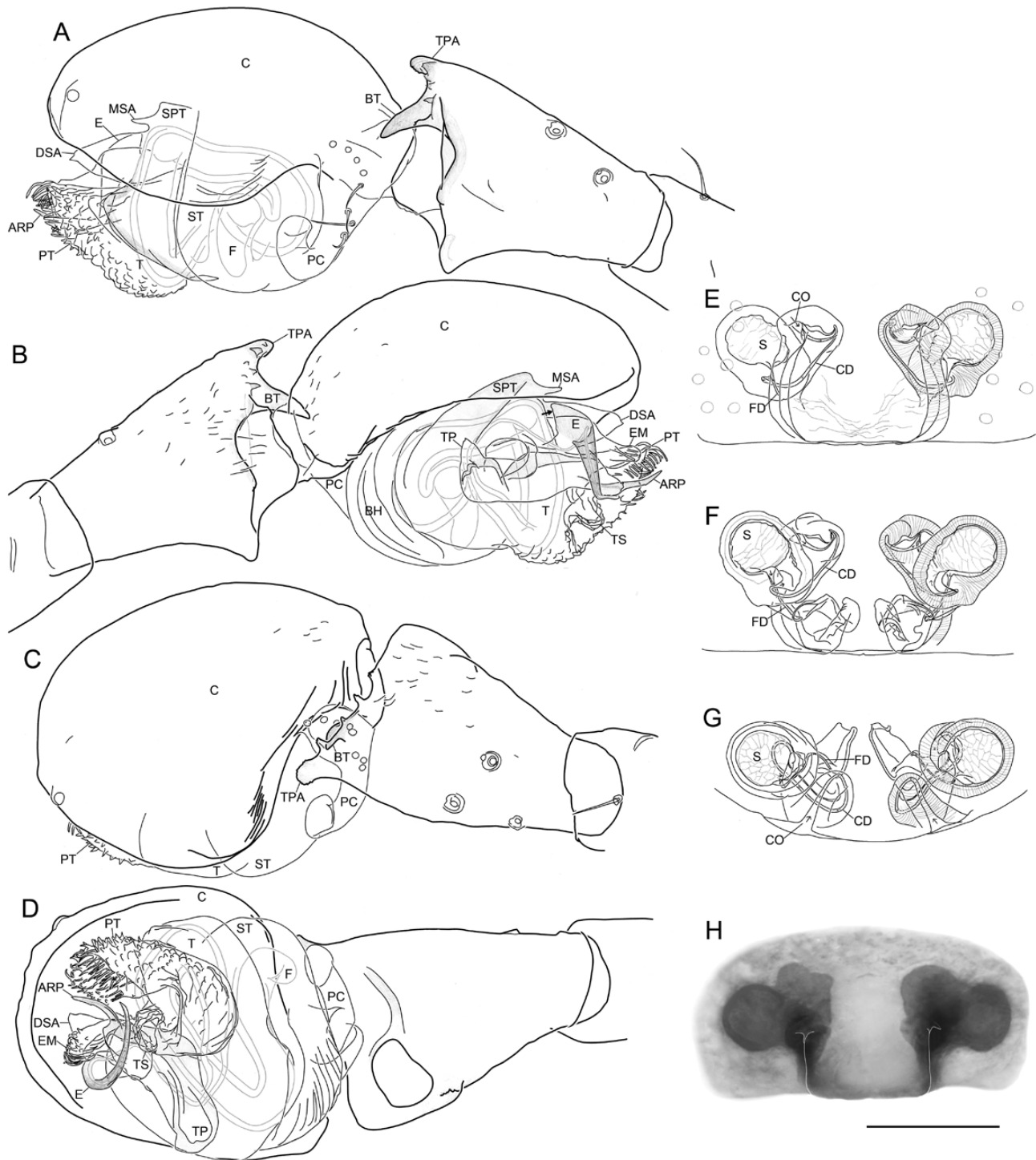


Figure 5. *Oedothorax agrestis* (Blackwall, 1853). A–D, male left palp. A, retrolateral view. B, prolateral view. C, dorsal view. D, ventral view. E–H, epigyne. E, ventral view. F, dorsal view. G, anterior view. H, external morphology. Scale bar 0.1 mm.

retrolaterally spiral in other species in Clade 13); embolic membrane cylindrical (imperceptible in some species in unexpanded pedipalps) (either flat and broad or absent in other species in Clade 13); embolus–radix membranous region extended to prolateral side of radix (not extended to prolateral side of radix in other species in Clade 13); ventral radical process absent (present in most *Callitrichia*, some *Mitrager*, *Atypena* and some ‘*Oedothorax*’ *incertae sedis* species); lateral extension of radix absent (present in all *Mitrager*, *Atypena*, *Ca. convector* and some ‘*Oedothorax*’ *incertae sedis* species); tegular papillae present in some species, protegulum with papillae, tegular sac short; marginal suprategular apophysis present; distal suprategular apophysis straight, distally oriented, mostly narrow and round at tip (except *Oe. gibbosus* and *Oe. trilobatus*, tip broad and smoothly serrated).

3. Tibia: moderately modified; shape of prolateral apophysis varies among species, but never elevated vertically (vertically elevated in many *Callitrichia*, some *Mitrager* and some ‘*Oedothorax*’ *incertae sedis* species); with basal thorn in some species (absent in other species in Clade 13); retrolateral apophysis absent (present in *Mitrager*, *Atypena*, *Ca. convector* and some ‘*Oedothorax*’ *incertae sedis* species); prolateral spike absent (present in most *Mitrager* species).
4. Epigyne: different from *Callitrichia* and *Holmelgonia* in the mesal entrance of copulatory ducts into the spermathecae with respect to the exits of the fertilization ducts.

Description: The genus includes medium-sized (male 1.2–2.5, female 2.1–3.8) erigonines with an evenly coloured opisthosoma from light brown to dark brown. Male and female posterior median spinnerets with one minor ampullate gland spigot, two aciniform gland spigots; posterior lateral spinnerets with triad, more than three aciniform gland spigots; female posterior median spinnerets and posterior lateral spinnerets with one and two cylindrical gland spigots, respectively. Male prosoma varies in the degree of prosomal modifications, ranging from unnoticeable (*Oe. paludigena*, *Oe. agrestis*, *Oe. fuscus* and *Oe. tingitanus*) to prominent post-PME humps, post-PME grooves and lateral sulci and pits. Palpal patella prolateral proximal vertical macrosetae absent. This genus also shares those features defining Clade 13 (see above). For palpal and epigynal features, see description of Clade 13 and diagnosis.

New circumscription: According to our phylogenetic analysis and descriptions from the literature, only ten species are regarded here as ‘true’ *Oedothorax*: *Oe. gibbosus* and its congeners: *agrestis*, *apicatus*, *fuscus*, *gibbifer*, *meridionalis*, *paludigena*, *retusus*, *tingitanus* and *trilobatus*. However, 27 additional species remain

here as ‘*Oedothorax*’ *incertae sedis* (see section below) and are deemed not congeneric with the type species, but await future taxonomic treatment. The remaining 43 species are transferred from *Oedothorax* to other genera (see taxonomic actions below).

Natural history: Most species are found in humid environments like in litter, under bark or stones, in grasslands, marshes or at riversides.

Remarks: Although no types of *Oedothorax* s.s. were examined, detailed descriptions and illustrations in the literature abound, allowing clear identification of the examined specimens.

New distribution: Europe, Turkey, Caucasus, Iran, Russia to Central Asia, China, Azores, North Africa, North America.

OEDOTHORAX GIBBOSUS (BLACKWALL, 1841)

(FIGS 6, 7O, 8A, 9A; SUPPORTING INFORMATION, FIG. S1A)

Neriere gibbosa Blackwall, 1841: 653 (Dmf).

Neriere tuberosa Blackwall, 1841: 654 (Dm).

Argus gibbosus Walckenaer, 1847: 513.

Argus tuberosus Walckenaer, 1847: 514.

Neriere tuberosa Blackwall, 1864: 279, pl. 19, fig. 192 (m).

Erigone tuberosa Thorell, 1873: 447.

Neriere gibbosa O. Pickard-Cambridge, 1873: 455, pl. 34, fig. 20.

Erigone henkingi Dahl, 1883: 49, figs 29, 30 (Dm).

Gongylidium gibbosum Simon, 1884: 489, figs 270–272 (mf).

Gongylidium tuberosum Simon, 1884: 490, figs 273–275 (m, Df).

Neriere henkingi Dahl, 1886: 88.

Neriere gibbosa Simon, 1894: 666, fig. 720 (m).

Kulczynskiellum gibbosum F.O. Pickard-Cambridge, 1895: 39.

Gongylidium gibbosum Becker, 1896: 86, pl. 9, fig. 7K (mf).

Kulczynskiellum tuberosum Bösenberg, 1902: 171, pl. 15, fig. 232 (mf).

Oedothorax gibbosus Bösenberg, 1902: 213, pl. 19, fig. 300 (mf). *Stylothorax gibbosa* Reimoser, 1919: 72.

Stylothorax henkingi Reimoser, 1919: 72.

Stylothorax tuberosa Reimoser, 1919: 73.

Oedothorax gibbosus Simon, 1926: 451, 522, fig. 785 (mf).

Oedothorax tuberosus Simon, 1926: 452, 522.

Oedothorax gibbosus Bishop & Crosby, 1935: 264, pl. 22, figs 70–73 (mf).

Oedothorax gibbosus Denis, 1947: 138, figs 6A, 7A, 8A, 9F, 10G, H, 11F (mf). *Oedothorax tuberosus* Denis, 1947: 138, figs 1A, 6B, C, 7B, 8B, 9G, 10I–K, 11G (mf).

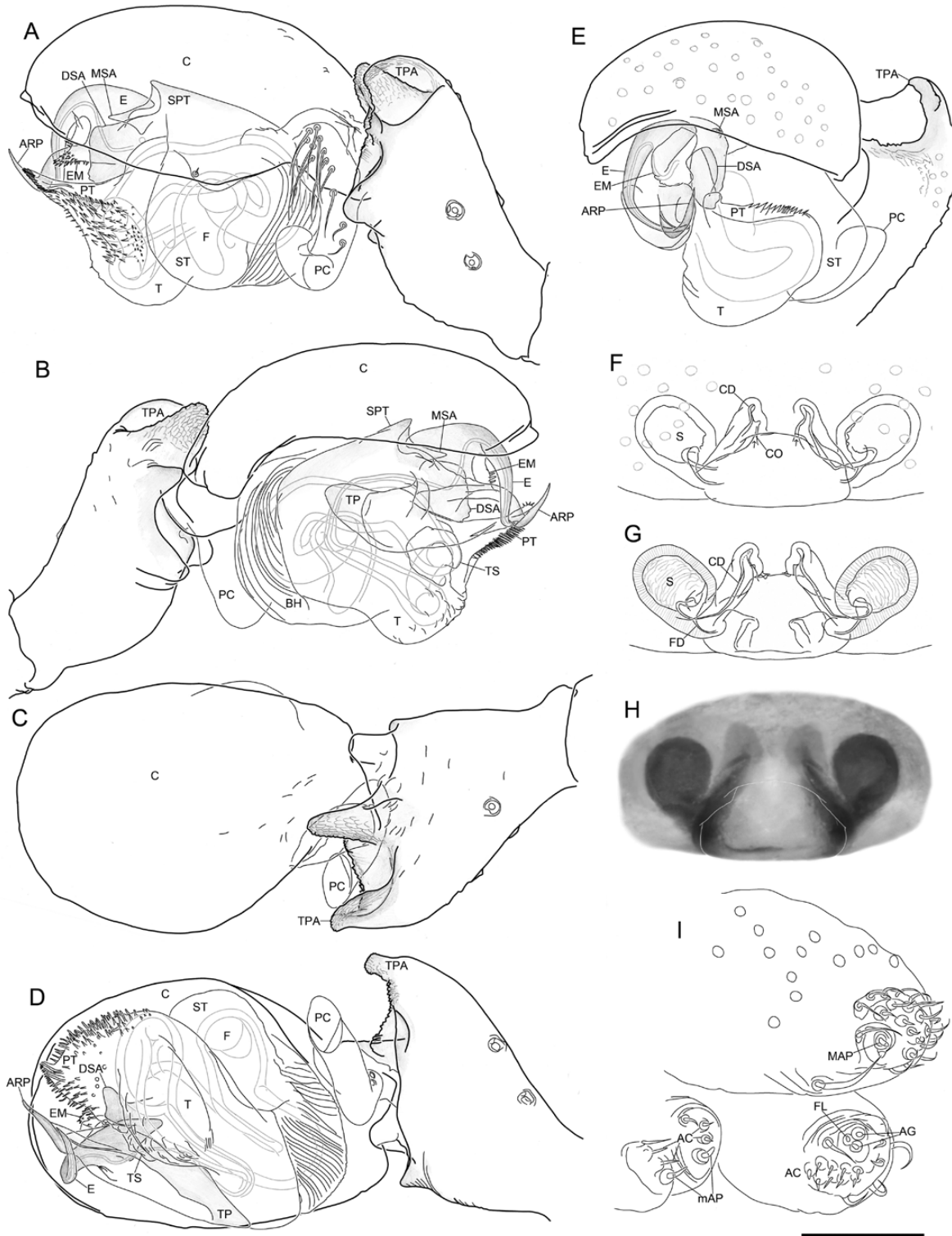


Figure 6. *Oedothorax gibbosus* (Blackwall, 1841). A–E, male left palp. A, retrolateral view. B, prolateral view. C, dorsal view. D, ventral view. E, apical view. F–H, epigyne. F, ventral view. G, dorsal view. H, external morphology. I, male spinnerets. Scale bar 0.1 mm.

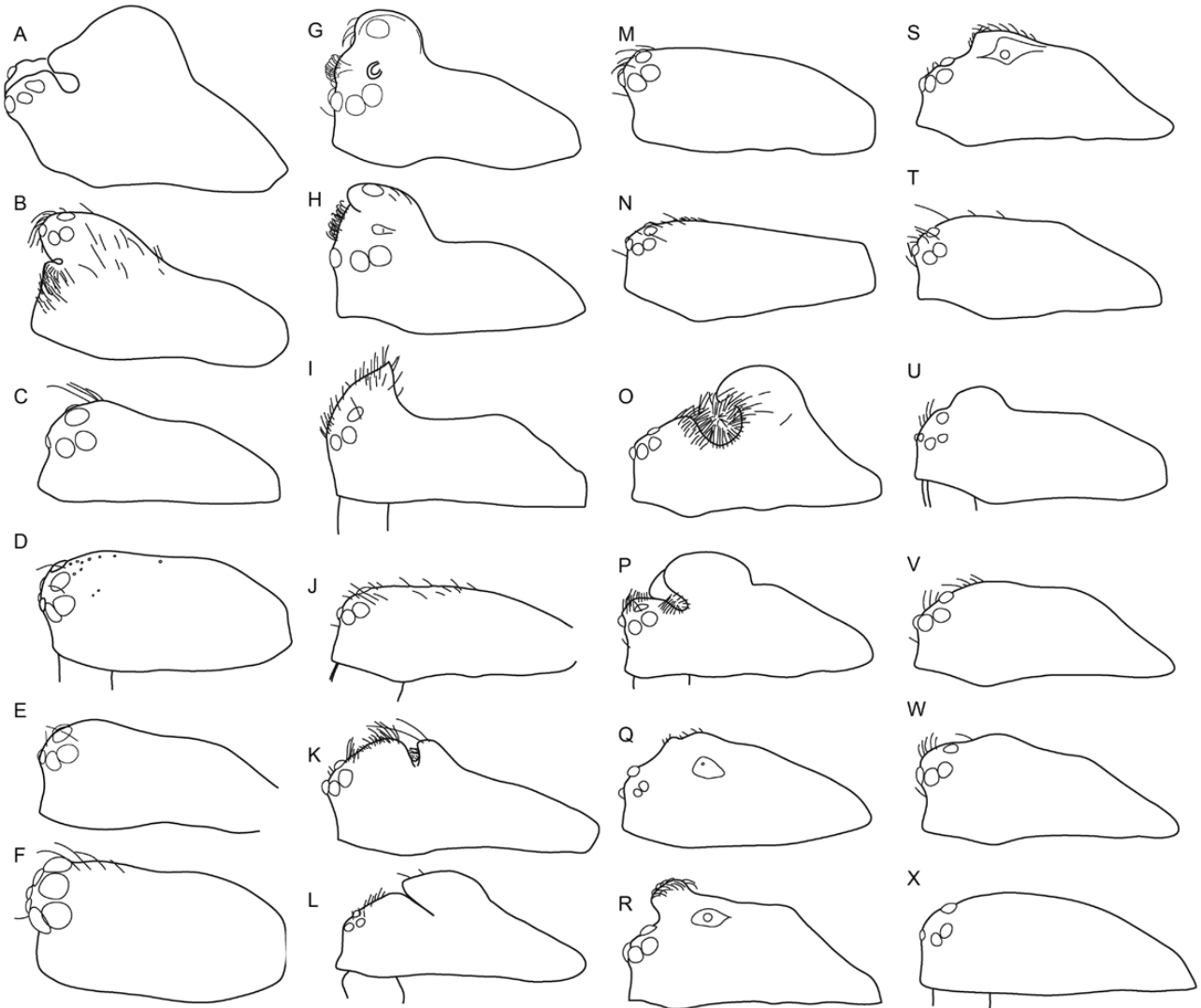


Figure 7. Male prosomal morphology, lateral. A, *Emertongone montifera* (Emerton, 1882) (Paquin & Dupérré, 2003, fig. 1187). B, *Shaanxinus mingchihensis* Lin, 2019 (traced from photograph). C, *Oedothorax paracymbialis* Tanasevitch, 2015 (traced from photograph). D, *Oe. kodaikanal* Tanasevitch, 2015 (traced from photograph). E, *Oe. cunur* Tanasevitch, 2015 (traced from photograph). F, *Oe. stylus* Tanasevitch, 2015 (traced from photograph). G, *Atypena cirrifrons* (Heimer, 1984) (traced from photograph). H, *A. formosana* (Oi, 1977) (Oi, 1977, fig. 2). I, *Oe. nazareti* Scharff, 1989 (Scharff, 1989: fig. 7). J, *Gongylidium rufipes* (Linnaeus, 1758) (traced from photograph). K, *Ummeliata insecticeps* (Bösenberg & Strand, 1906) (Tu & Li 2004: fig. 8A). L, *U. esyunini* (Zhang, Zhang & Yu, 2003) (Zhang et al., 2003, fig. 2A). M, *Hylyphantes graminicola* (Sundevall, 1830) (traced from photograph). N, *Tmeticus tolli* Kulczyński, 1908 (traced from photograph). O, *Oedothorax gibbosus* (Blackwall, 1841) [Roberts, 1987: fig. 21 (e)]. P, *Oe. trilobatus* (Banks, 1896) (Bishop & Crosby, 1935: fig. 79). Q, *Oe. gibbifer* (Kulczyński, 1882) (Heimer & Nentwig, 1991: fig. 604.5). R, *Oe. apicatus* (Blackwall, 1850) [Roberts, 1987: fig. 23 (d)]. S, *Oe. retusus* (Westring, 1851) [Roberts, 1987: fig. 23 (c)]. T, *Oe. paludigena* Simon, 1926 [Millidge, 1975: fig. (5)]. U, *Oe. meridionalis* Tanasevitch, 1987 (Tanasevitch, 1987: fig. 107). V, *Oe. agrestis* (Blackwall, 1853) (Roberts, 1987: fig. 23B). W, *Oe. fuscus* (Blackwall, 1834) (Roberts, 1987: fig. 23A). X, *Oe. tingitanus* (Simon, 1884) (Denis, 1968: fig. 11).

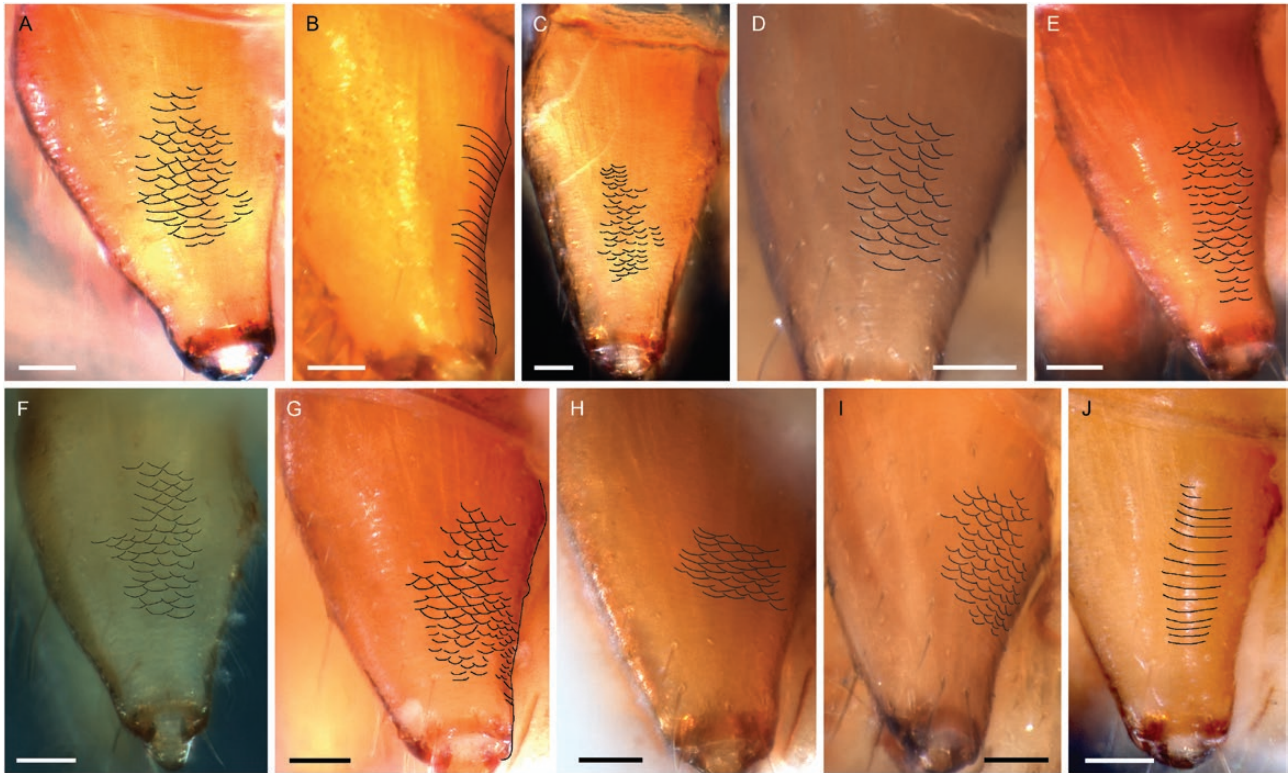


Figure 8. Male chelicerae, stridulatory striae on lateral side. A, *Oedothorax gibbosus* (Blackwall, 1841). B, *Oe. trilobatus* (Banks, 1896). C, *Oe. gibbifer* (Kulczyński, 1882). D, *Oe. apicatus* (Blackwall, 1850). E, *Oe. retusus* (Westring, 1851). F, *Oe. paludigena* Simon, 1926. G, *Oe. meridionalis* Tanasevitch, 1987. H, *Oe. agrestis* (Blackwall, 1853). I, *Oe. fuscus* (Blackwall, 1834). J, *Oe. tingitanus* (Simon, 1884). Scale bars 0.05 mm.

Oedothorax gibbosus Locket & Millidge, 1953: 239, figs 145A, 146A, G, H (mf).

Oedothorax tuberosus Locket & Millidge, 1953: 239, figs 145A, 146B, G, H (mf).

Oedothorax tuberosus Wiehle, 1960a: 454, figs 835–842 (mf).

Oedothorax tuberosus Tystshenko, 1971: 251, fig. 829 (f).

Oedothorax tuberosus Miller, 1971: 262, pl. LIV, figs 4–6 (f).

Oedothorax gibbosus Palmgren, 1976: 89, figs 8.9–12, 14, 15 (mf).

Oedothorax tuberosus Palmgren, 1976: 89, figs 8.9, 13–15 (f).

Oedothorax gibbosus Růžička, 1978: 195, fig. 8H, I (f).

Oedothorax gibbosus Bosmans, 1985: 65, figs 11, 25, 31 (m).

Oedothorax gibbosus Roberts, 1987: 57, figs 21E, 22B (mf).

Oedothorax gibbosus tuberosus Roberts, 1987: 57, fig. 21F–g (downgraded to ‘form’).

Oedothorax gibbosus de Keer & Maelfait, 1988: 3.

Oedothorax gibbosus Heimer & Nentwig, 1991: 224, fig. 601 (mf).

Oedothorax gibbosus Hormiga, 2000: 48, figs 21A–G, pl. 49A–F, 50A–F, 51A–F (mf).

Oedothorax gibbosus Tanasevitch, 2015: 382, figs 1, 2 (m).

Oedothorax gibbosus Russell-Smith, 2016: 22, fig. 1 (f).

Type material: In Blackwall’s description (1841), 2♂ of *gibbosus* morph, 1♂ of *tuberosus* morph and 5♀ were found under stones in a moist pasture in Oakland, United Kingdom, in May 1838 [individual number according to Walckenaer (1847)], but no type designation was made, nor does any reference provide information about where the types might have been deposited. Nevertheless, the unique prosomal modification of the *gibbosus* morph described in the original description makes the identification of specimens in this study unequivocal. Subsequently, the identical palpal morphology confirmed the conspecificity of examined *tuberosus* morph with the *gibbosus* morph (Roberts, 1987).

Examined material: **Denmark:** Øjesø, near Feldballe (56°17’ N, 10°36’ E), 6♂4♀ 19.v.1997, leg. Peter Gejdos (ZMUC 00008860); Ulvshale Skov, toward Skovbund, 3♂6♀ 12.x.2002, leg. J. Peterson, det. N. Scharff, 2002

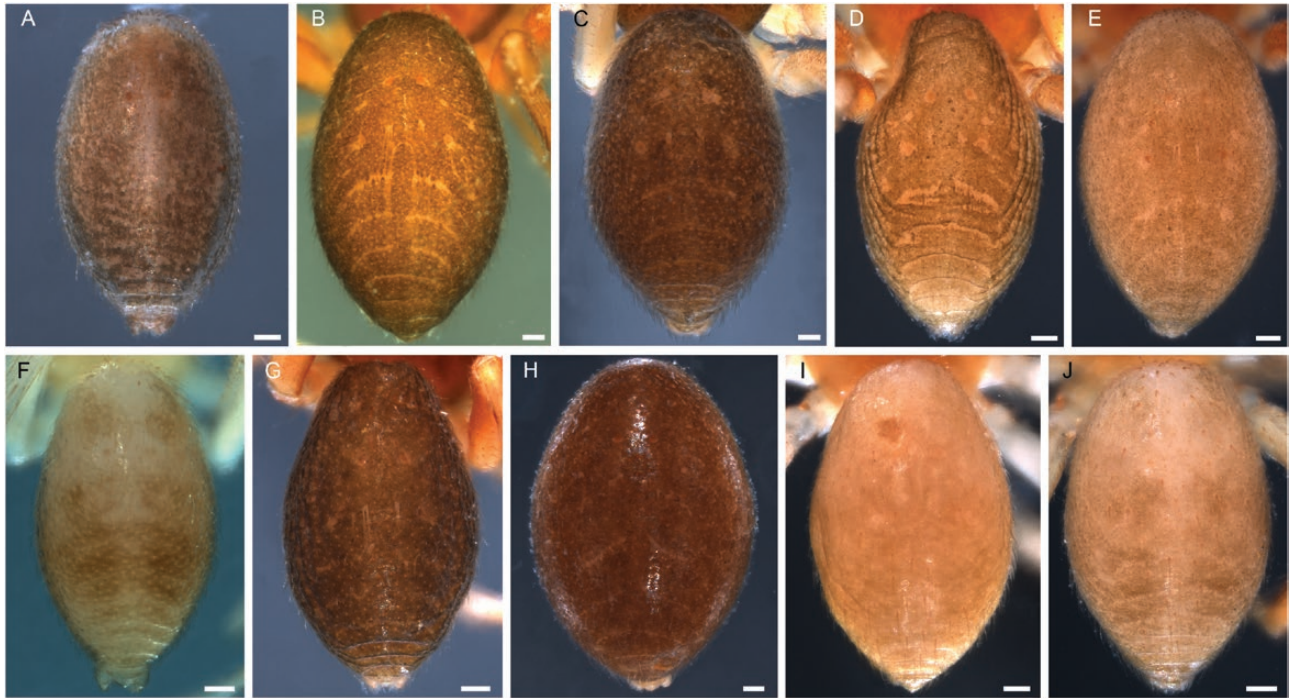


Figure 9. Male opisthosoma, dorsal view. A, *Oedothorax gibbosus* (Blackwall, 1841). B, *Oe. trilobatus* (Banks, 1896). C, *Oe. gibbifer* (Kulczyński, 1882). D, *Oe. apicatus* (Blackwall, 1850). E, *Oe. retusus* (Westring, 1851). F, *Oe. paludigena* Simon, 1926. G, *Oe. meridionalis* Tanasevitch, 1987. H, *Oe. agrestis* (Blackwall, 1853). I, *Oe. fuscus* (Blackwall, 1834). J, *Oe. tingitanus* (Simon, 1884). Scale bars 0.1 mm.

(ZMUS 00007790). **England:** Cambridgeshire, Wicken Fen, 2♂ 18.–22.v.1957, leg. D. J. Clark (NHM). **Wales:** Merionethshire, Dolgelly, 1♂ 8.vi.1954, coll. D. J. Clark, det. G. H. Locket (NHM).

Diagnosis:

Males: This species has two male morphs. The *gibbosus*-morph can be identified by the shape of post-ocular groove and hump, not divided into three lobes on the anterior side as in *Oe. trilobatus*; the groove is equipped with dense setae as in *Oe. trilobatus*, absent in the *Mitrager* species with post-ocular groove. The *tuberosus*-morph does not possess a post-ocular groove, and the prosoma is elevated at the position of the fovea, distinguishing it from other *Oedothorax s.s.* species. The bifid palpal tibial prolateral apophysis and the absence of basal thorn distinguish this species from other *Oedothorax s.s.* species.

Females: Can be distinguished from other *Oedothorax s.s.* species by the epigynal general configuration and number of sub-AME setae (one; two in *Oe. fuscus*, *Oe. agrestis*, *Oe. meridionalis* and *Oe. tingitanus*). Distinguished from *Oe. agrestis*, *Oe. apicatus*, *Oe. fuscus*, *Oe. gibbifer*, *Oe. tingitanus* and *Oe. retusus* by the more convergent ventral plate borders. Distinguished from *Oe. meridionalis* by not having a wide chamber

at the entrances of the copulatory ducts (Fig. 6F, in comparison to Fig. 10F); from *Oe. paludigena* by the narrower posterior margin of the dorsal plate; from *Oe. trilobatus* by the much shorter copulatory ducts.

Description:

Male, tuberosus-morph (ZMUC 00007790): Total length: 2.37. Prosoma: 1.05 long, 0.77 wide, postocular region with a hump posteriorly, without post-ocular groove. Eyes: AME-AME: 0.03, AME width: 0.05, AME-ALE: 0.03, ALE width: 0.07, ALE-PLE: 0, PLE width: 0.07, PLE-PME: 0.04, PME width: 0.07, PME-PME: 0.07. Sternum: 0.61 long, 0.55 wide. Legs: dorsal proximal macroseta on tibia I, II, III and IV 1.20, 1.47, 1.80 and 2.13 times diameter of tibia, respectively; Tm I: 0.62.

Male, gibbosus-morph (ZMUC 00008860): Total length: 2.35. Prosoma: 1.03 long, 0.79 wide, postocular region with wide, transverse, hirsute groove and large hump posteriorly (Fig. 7O). Eyes: AME-AME: 0.04, AME width: 0.05, AME-ALE: 0.03, ALE width: 0.06, ALE-PLE: 0, PLE width: 0.07, PLE-PME: 0.06, PME width: 0.06, PME-PME: 0.08. Sternum: 0.59 long, 0.54 wide. Legs: dorsal proximal macroseta on tibia I, II, III and IV 0.22, 0.17, 0.78 and 0.82 times diameter of tibia, respectively; Tm I: 0.65.

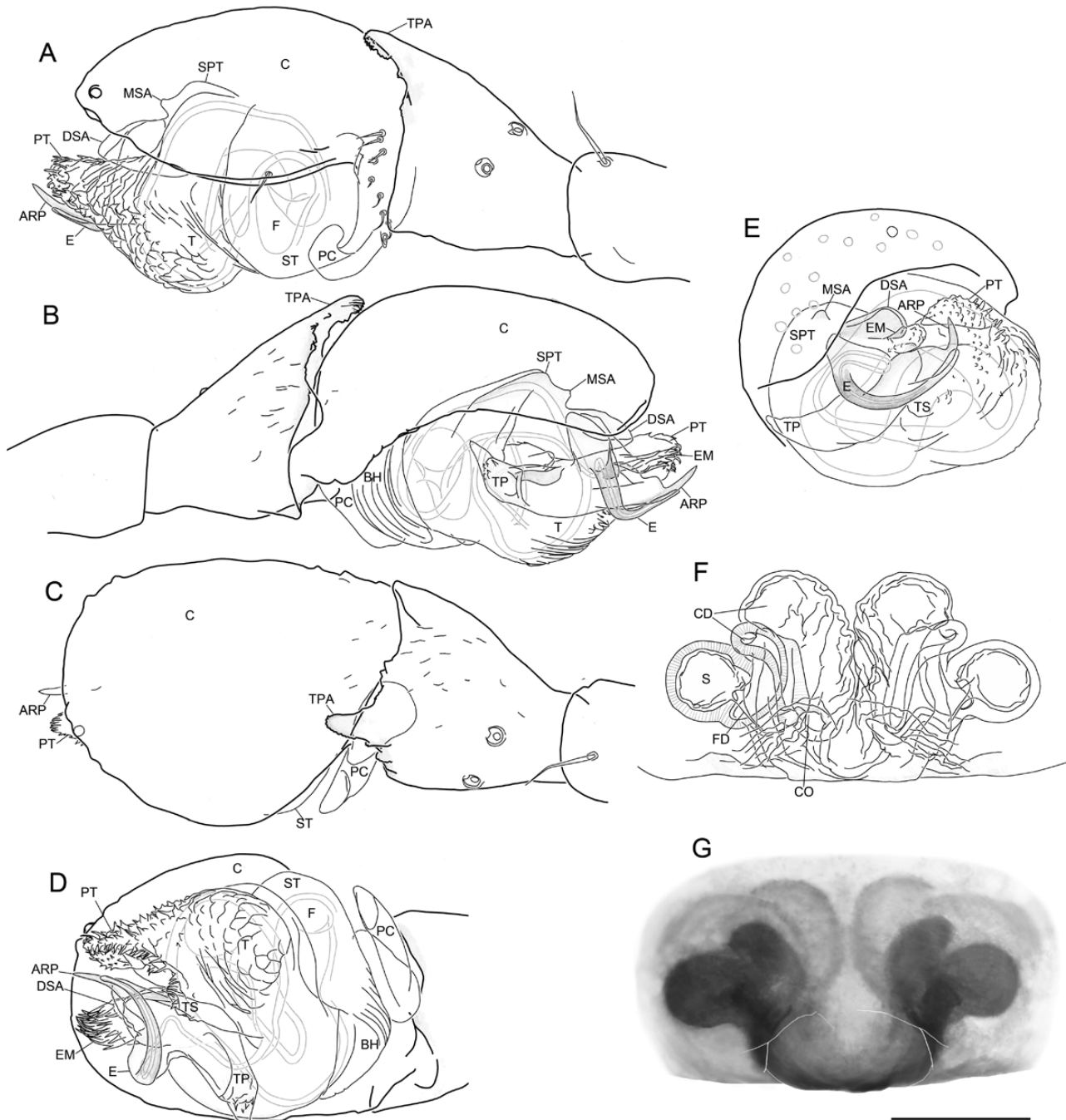


Figure 10. *Oedothorax meridionalis* Tanasevitch, 1987. A–E, male right palp, images flipped horizontally. A, retrolateral view. B, prolateral view. C, dorsal view. D, ventral view. E, apical view. F, G, epigyne. F, ventral view. G, external morphology. Scale bar 0.1 mm.

Male, both morphs: Clypeus: not hirsute, one sub-AME seta. Chelicerae: mastidia present; stridulatory striae scaly, rows widely and evenly spaced (Fig. 8A). Pedipalp: TPA with two scaly lobes, a depressed region in between with scaly distal margin; BT absent (Fig. 6C); PC distal setae at median position (Fig. 6A); T without papillae,

protegulum with long papillae; TS short, without papillae (Fig. 6D); DSA tip broad and smoothly serrated (Fig. 6A); EM short, cylindrical, distally oriented, with papillae; TP without small protuberances; E not broadened at basal part (Fig. 6B). Opisthosoma: brown, evenly coloured (Fig. 9A); spinnerets see Fig. 6I.

Female (ZMUC): Total length: 2.53. Prosoma: 1.13 long, 0.83 wide. Eyes: AME-AME: 0.029, AME width: 0.054, AME-ALE: 0.031, ALE width: 0.074, ALE-PLE: 0.005, PLE width: 0.074, PLE-PME: 0.053, PME width: 0.064, PME-PME: 0.068. Clypeus: not hirsute, one sub-AME seta. Sternum: 0.65 long, 0.58 wide. Legs: dorsal proximal macroseta on tibia II, III and IV 1.76, 2.02 and 2.14 times diameter of tibia, respectively; Tm I: 0.69. Chelicerae: stridulatory striae scale-like. Epigyne: Clade 13 characteristic morphology, ventral plate borders converging anteriorly, copulatory duct short (Fig. 6F–H) Opisthosoma: brown, evenly coloured.

Variation: The measurements are based on examined material.

Males, tuberosus-morph (N = 7, means in parentheses): Total length 2.23–2.37 (2.28). Prosoma: 1.02–1.11 (1.06) long, 0.76–0.85 (0.80) wide. Legs: dorsal proximal macroseta on tibia I, II, III and IV 0.82–1.39 (1.12), 0.87–1.64 (1.31, *N* = 5), 1.48–2.00 (1.75, *N* = 6) and 1.56–2.16 (1.85) times diameter of tibia, respectively; Tm I: 0.60–0.68 (0.65).

Males, gibbosus-morph (N = 5, means in parentheses): Total length 1.94–2.35 (2.22). Prosoma: 0.97–1.06 (1.02) long, 0.76–0.81 (0.79) wide. Legs: dorsal proximal macroseta on tibia I, II, III and IV 0.19–0.60 (0.28), 0.17–0.61 (0.30), 0.41–1.16 (0.70) and 0.45–1.52 (0.83) times diameter of tibia, respectively; Tm I: 0.59–0.71 (0.64).

Females (N = 10, means in parentheses): Total length 2.33–2.83 (2.64). Prosoma: 0.93–1.20 (1.15) long, 0.71–0.87 (0.83) wide. Legs: dorsal proximal macroseta on tibia I, II, III and IV 1.53–1.82 (1.69, *N* = 9), 1.71–1.87 (1.79, *N* = 8), 1.89–2.27 (2.07) and 1.90–2.37 (2.20) times diameter of tibia, respectively; Tm I: 0.59–0.69 (0.65)

Distribution: Europe, Turkey.

Habitat: Open, humid areas.

OEDOTHORAX AGRESTIS (BLACKWALL, 1853)

(FIGS 5, 7V, 8H, 9H; SUPPORTING INFORMATION, FIG. S1G)

Neriene agrestis Blackwall, 1853: 23 (Dmf).

Neriene agrestis Blackwall, 1864: 276, pl. 19, fig. 190, pl. 22, fig. D (mf).

Neriene agrestis O. Pickard-Cambridge, 1882: 4, pl. 1, fig. 2B.

Gongylidium agreste Simon, 1884: 494, figs 280–282 (mf).

Gongylidium agrestis Becker, 1896: 89, pl. 9, fig. 9 (mf).

Kulczynskiellum agreste Bösenberg, 1902: 169, pl. 15, fig. 228 (mf).

Oedothorax agrestis de Lessert, 1910: 193.

Stylothorax agrestis Reimoser, 1919: 72.

Oedothorax agrestis Simon, 1926: 453, 523, fig. 784 (mf).

Oedothorax agrestis Denis, 1947: 140, figs 2D, 6G, 7H, 8H, 9B, 10C, 11B (mf).

Oedothorax agrestis Locket & Millidge, 1953: 241, figs 145C, 146D, 147C, D (mf).

Oedothorax agrestis Wiehle, 1960a: 445, figs 817–826 (mf).

Oedothorax agrestis Merrett, 1963: 386, fig. 46A–F (m).

Oedothorax agrestis Tystshenko, 1971: 251, fig. 827 (f).

Oedothorax agrestis Miller, 1971: 262, pl. LIV, figs 17–19 (mf).

Oedothorax agrestis Palmgren, 1976: 87, figs 7.11, 13–17 (mf).

Oedothorax agrestis Růžička, 1978: 195, fig. 8E, F (f).

Oedothorax agrestis Müller, 1983: 64, fig. 2a–c (m).

Oedothorax agrestis Bosmans, 1985: 65, figs 16, 21, 33 (m).

Oedothorax agrestis Roberts, 1987: 57, figs 22D, 23B (mf).

Oedothorax agrestis Heimer & Nentwig, 1991: 224, fig. 606 (mf).

Oedothorax agrestis Aakra 2000: 81, fig. 3A–E (mf).

Type material: Not examined. According to the original description of Blackwall (1853), individuals were collected in Oakland, United Kingdom, among herbage and under stones in pastures near woods. According to O. Pickard-Cambridge (1882), Blackwall lost all type material of *Oe. agrestis*. The original and subsequent descriptions, nevertheless, make the identification of this species unequivocal.

Examined material: **England:** London, Beckenham, 1♂ 2.ii.1958, coll. D. J. Clark, det. G. H. Locket (NHM); Dorset, River Allen, Noritumb, c. 650 m, 3♂ 1.ix.1965, under stones by river (AMNH, No. 3080); Cumbria, Drumburgh, salt marsh, 1♀ 15.viii.1965 (AMNH). **Wales:** Merionethshire, Dolgellau, Cymmel Abbey, 1♀ 6.vi.56, coll. and det. D. J. Clark (NHM). **Scotland:** Perth, River Tay, under stone by loch, 1♂ 2.ix.1965 (AMNH No.3083). **Switzerland:** Trius, 1♀ det. Schenkel (AMNH). **Sweden:** Öland, Stora Rör, 1♀ 15.vii.1931, leg. Nielsen, 16.ii.1932, det. Seheukel (ZMUC 00011739).

Diagnosis:

Males: The lack of male prosomal modifications and the presence of an embolic base protuberance

distinguishes the males of this species from the 'gibbosus-like species group' (Clade 22). *Oedothorax agrestis* is further distinguished from *Oe. paludigena* by the the palpal tibia prolateral apophysis basal thorn, and from *Oe. fuscus* and *Oe. tingitanus* by the lack of a bifurcated protegulum.

Females: Can be distinguished from other species by the epigynal configuration and number of sub-AME setae (two; one in *Oe. gibbosus*, *Oe. trilobatus*, *Oe. apicatus*, *Oe. retusus*, *Oe. gibbifer* and *Oe. paludigena*). Distinguished from *Oe. apicatus* by the more anteriorly extended copulatory ducts; from *Oe. fuscus* by the less sclerotized epigyne, the dorsal plate bordered by thinner dark stripes and the copulatory ducts less extended anteriorly; from *Oe. gibbosus*, *Oe. retusus*, *Oe. gibbifer* and *Oe. meridionalis* by the more curved and less convergent ventral plate borders; from *Oe. tingitanus* by the lateral copulatory openings (Fig. 5E, G; mesal in *Oe. tingitanus*, Fig. 11F); from *Oe. trilobatus* by the more anteriorly located copulatory openings.

Description:

Male (London): Total length: 2.54. Prosoma: 0.95 long, 0.80 wide, postocular region slightly elevated (Fig. 7V). Eyes: AME-AME: 0.03, AME width: 0.06, AME-ALE: 0.017, ALE width: 0.08, ALE-PLE: 0.01, PLE width: 0.08, PLE-PME: 0.05, PME width: 0.08, PME-PME: 0.06. Clypeus: not hirsute, two sub-AME setae. Sternum: 0.57 long, 0.59 wide. Chelicerae: mastidia absent; stridulatory striae scaly, rows widely and evenly spaced (Fig. 8H). Legs: dorsal proximal macroseta on tibia I, III and IV 0.96, 1.68 and 1.90 times diameter of tibia, respectively; Tm I: 0.64. Pedipalp: TPA short, rod-like, distal part scaly, with several small denticles; basal thorn short, pointed antero-ventrally; PC distal setae at median position (Fig. 5A); T papillae scale-like, PT with long papillae; TS short, without papillae (Fig. 5D); DSA tip narrow, pointed (Fig. 5A); EM median-long, cylindrical, distally oriented, with long papillae at tip; ARP prolaterally spiral; TP with several small protuberances; E not broadened at basal part (Fig. 5B). Opisthosoma: brown, evenly coloured (Fig. 9H).

Female (Wales): Total length: 3.19. Prosoma: 1.20 long, 0.91 wide. Eyes: AME-AME: 0.03, AME width: 0.07, AME-ALE: 0.02, ALE width: 0.10, ALE-PLE: 0.01, PLE width: 0.08, PLE-PME: 0.04, PME width: 0.08, PME-PME: 0.06. Sternum: 0.68 long; 0.65 wide. Legs: dorsal proximal macroseta on tibia I, II and III 1.28, 1.47 and 1.76 times diameter of tibia, respectively; Tm I: 0.63. Chelicerae: stridulatory striae scaly, rows widely and evenly spaced. Epigyne: Clade 13 characteristic

morphology, borders between dorsal and ventral plates parallel, copulatory duct short (Fig. 5E–H).

Variation: The measurements are based on examined material.

Males (N = 6, means in parentheses): Total length 2.21–2.54 (2.3). Prosoma: 0.95–0.99 (0.96) long, 0.76–0.81 (0.79) wide. Legs: dorsal proximal macroseta on tibia I, II, III and IV 0.96–1.13 (1.06), 0.94–1.51 (1.24, N = 5), 1.66–1.88 (1.75) and 1.84–2.14 (1.96) times diameter of tibia, respectively; Tm I: 0.55–0.70 (0.64).

Females (N = 4, means in parentheses): Total length 2.89–3.65 (3.18). Prosoma: 1.02–1.30 (1.17) long, 0.79–0.1.01 (0.90) wide. Legs: dorsal proximal macroseta on tibia I, II, III and IV 1.28–1.55 (1.39, N = 3), 1.2–1.67 (1.44), 1.34–1.94 (1.66) and 1.50–1.85 (1.73, N = 3) times diameter of tibia, respectively; Tm I: 0.60–0.74 (0.65).

Distribution: Europe.

Habitat: Among herbage and under stones in pastures; in swamp litter; stony lakeshores.

OEDOTHORAX APICATUS (BLACKWALL, 1850)

(FIGS 7R, 8D, 9D, 12; SUPPORTING INFORMATION, FIG. S1D)

- Neriere apicata* Blackwall, 1850: 339 (Dm).
Erigone gibbicollis Westring, 1851: 41 (Dm).
Micryphantes tuberculatus Grube, 1859: 469 (Dm).
Erigone gibbicollis Westring, 1861: 223 (Df).
Neriere apicata Blackwall, 1864: 269, pl. 18, f, 183 (m, Df).
Micryphantes gibbus Ohlert, 1867: 65 (Dm).
Phalops gibbicollis Menge, 1871: 220, pl. 43, fig. 119 (mf).
Erigone gibbicollis Thorell, 1871: 112.
Erigone apicata Dahl, 1883: 46.
Gongylidium apicatum Simon, 1884: 487, figs 267–269 (mf).
Neriere apicata Chyzer & Kulczyński, 1894: 93, pl. 4, fig. 1 (mf).
Neriere apicata Simon, 1894: 666, fig. 719 (m).
Kulczynskiellum apicatum F.O. Pickard-Cambridge, 1895: 39.
Gongylidium apicatum Becker, 1896: 86, pl. 11, fig. 2 (mf).
Kulczynskiellum apicatum Bösenberg, 1902: 169, pl. 15, fig. 227 (mf).
Oedothorax apicatus de Lessert, 1910: 191.
Stylothorax apicata Dahl, 1912: 603.

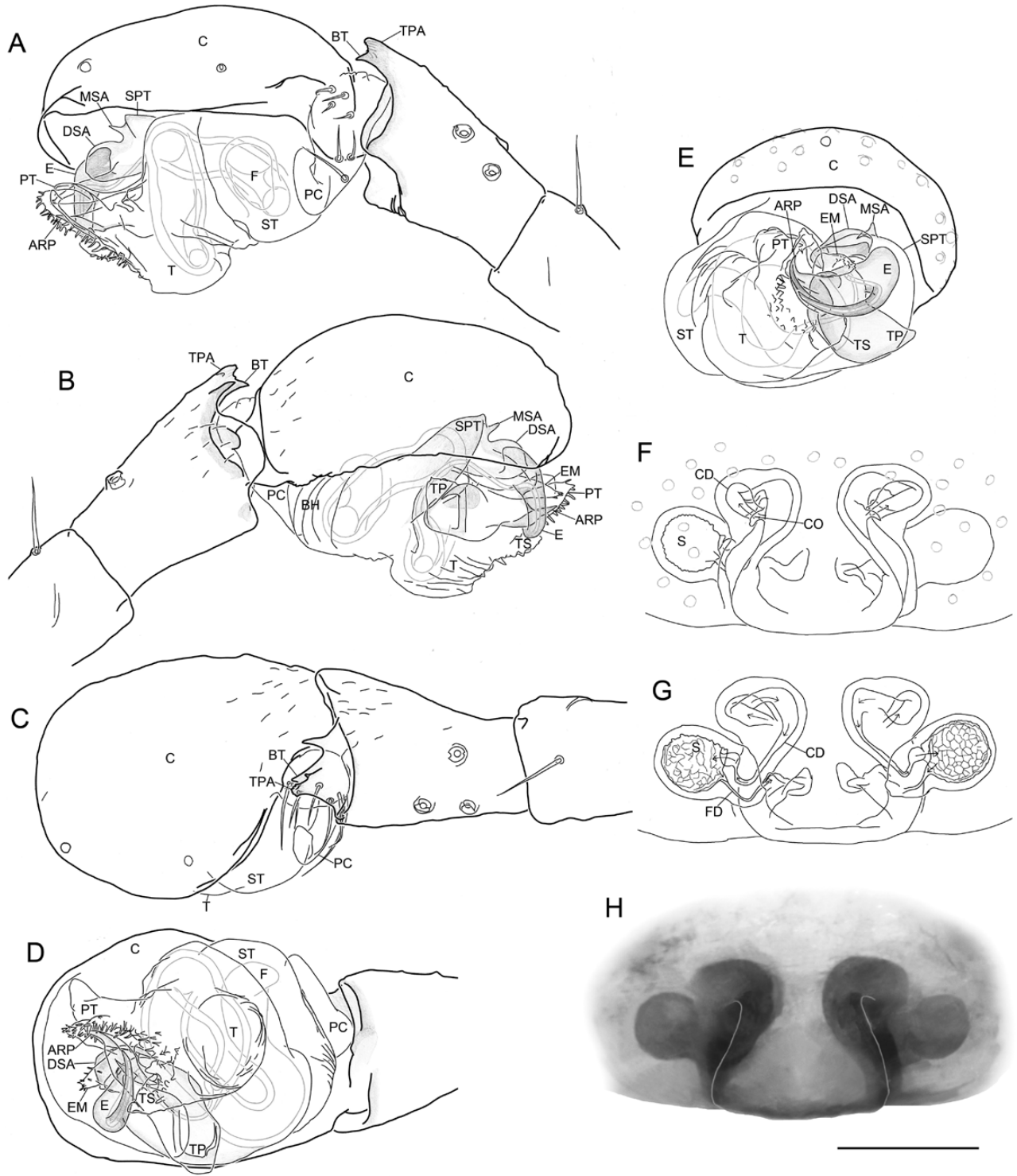


Figure 11. *Oedothorax tingitanus* (Simon, 1884). A–D, male left palp. A, retrolateral view. B, prolateral view. C, dorsal view. D, ventral view. E, distal view. F, G, epigyne. F, ventral view. G, dorsal view. H, external morphology. Scale bar 0.1 mm.

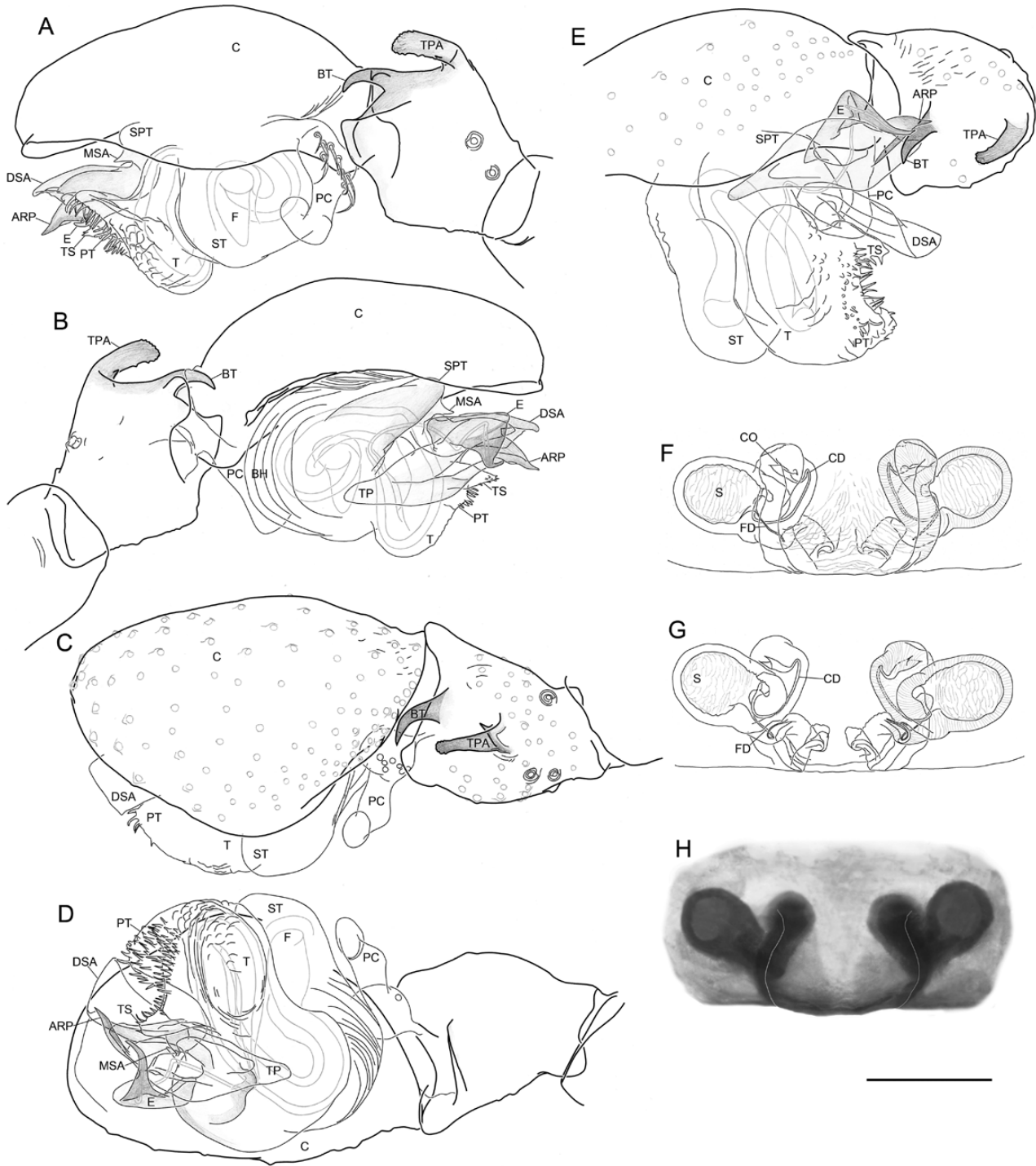


Figure 12. *Oedothorax apicatus* (Blackwall, 1850). A–D, male left palp. A, retrolateral view. B, prolateral view. C, dorsal view. D, ventral view. E, male right palp, expanded, image flipped horizontally. F–H, epigyne. F, ventral view. G, dorsal view. H, external morphology. Scale bar 0.1 mm.

- Oedothorax apicatus* Denis, 1947: 145, figs 2A, 3–5, 6F, 7C, 8C, 9C, 10D, 11C (mf).
Oedothorax apicatus Locket & Millidge, 1953: 241, figs 145F, 146F, 147G, H (mf).
Oedothorax apicatus Wiehle, 1960a: 437, figs 798–806 (mf).
Oedothorax apicatus Wiehle, 1960b: 477, fig. 22a, b (mf).
Oedothorax apicatus Tystshenko, 1971: 251, fig. 830 (f).
Oedothorax apicatus Miller, 1971: 262, pl. LIV, figs 7–9 (f).
Oedothorax apicatus Palmgren, 1976: figs 88, 7.23, 8.3, 8.7, 8.8 (m).
Oedothorax apicatus Millidge, 1977: 11, fig. 24 (m).
Oedothorax apicatus Růžicka, 1978: 195, figs 8A, 9A (f).
Oedothorax apicatus Hu & Wang, 1982: 63, fig. I.1–4 (m).
Oedothorax apicatus Hu, 1984: 196, fig. 206.1–4 (mf).
Oedothorax apicatus Bosmans, 1985: 65, figs 14, 19, 37 (m).
Oedothorax apicatus Song, 1987: 153, fig. 114 (mf).
Oedothorax apicatus Tanasevitch, 1987: 355
Oedothorax apicatus Roberts, 1987: 58, figs 22F, 23D (mf).
Oedothorax apicatus Hu & Wu, 1989: 174, fig. 144.1–6 (mf).
Oedothorax apicatus Tanasevitch, 1990: 102, figs 24.61, 28.4 (f).
Oedothorax apicatus Chen & Gao, 1990: 111, fig. 139a, b (mf).
Oedothorax apicatus Heimer & Nentwig, 1991: 224, fig. 602 (mf).
Oedothorax apicatus Alderweireldt, 1992: 5, fig. 1B (f).
Oedothorax apicatus Zhao, 1993: 191, fig. 86a–d (mf).
Oedothorax apicatus Wunderlich, 1995: 473, fig. 7 (m).
Oedothorax apicatus Song, Zhu & Chen, 1999: 199, fig. 113D, E, H (mf).
Oedothorax apicatus Hu, 2001: 550, fig. 370.1–3 (f).
Oedothorax apicatus Russell-Smith, 2016: 23, fig. 3 (f).

Type material: Not examined. Blackwall (1850) collected one adult male on a rail in Oakland, England, in February 1850, but provided no deposition data. The original and subsequent descriptions, nevertheless, make the identification of this species unequivocal.

Examined material: **Scotland:** Perth, River Tay, drift litter, c. 400 m, 1♂5♀ 2.ix.1965 (AMNH No.3085). **England:** Essex, Crabknowe Spit, tide litter, 1♀ 18.iv.1961 (AMNH No. 3059). **Sweden:** Gotland, Ljugarn, 1♂1♀, det. Schenkel (AMNH). **Germany:** Greifswald, 2♂ 2014 (ZIMG); Hessen, Bad Hersfeld, Obersberg, soil avalanche, pitfall trap, 5♂ 18.ix–18. Xi.1980, leg. V. Puthz, det. S.-W. Lin, 17.xi.2015 (SMF). **China:** Xinjiang, 1♂3♀ 4.vii.1991 (Institute of Zoology, Chinese Academy of Science, IZCSA-Ar 20637).

Diagnosis:

Males: This species resembles *Oe. retusus* and *Oe. gibbifer* in the post-ocular hump and lateral sulci and pits, but it can be distinguished from the latter two by the knob-like shape of the post-ocular hump and its longer palpal tibia prolateral apophysis.

Females: Can be distinguished from other species by the epigynal configuration and the number of sub-AME setae (one; two in *Oe. fuscus*, *Oe. agrestis*, *Oe. meridionalis* and *Oe. tingitanus*). Distinguished from *Oe. agrestis* by the larger spermathecae; from *Oe. gibbifer*, *Oe. retusus* and *Oe. gibbosus* by the more curved and the less convergent ventral plate borders; from *Oe. trilobatus* and *Oe. meridionalis* by the much more anteriorly located copulatory openings; from *Oe. tingitanus* by the lateral copulatory openings (Fig. 12F, in comparison to mesal in the latter species, Fig. 11F); from *Oe. paludigena* by the anteriorly less convergent ventral plate borders (anteriorly more convergent in *Oe. paludigena*, Fig. 13F).

Description:

Male (ZIMG): Total length: 2.11. Prosoma: 0.91 long, 0.73 wide, postocular region elevated, with knob-like hump and lateral sulci and pits (Fig. 7R). Eyes: AME-AME: 0.03, AME width: 0.05, AME-ALE: 0.04, ALE width: 0.07, ALE-PLE: 0.01, PLE width: 0.07, PLE-PME: 0.04, PME width: 0.05, PME-PME: 0.10. Clypeus: not hirsute, one sub-AME seta. Sternum: 0.55 long, 0.55 wide. Chelicerae: mastidia absent; stridulatory striae scale-like, rows widely and evenly spaced (Fig. 8D). Legs: dorsal proximal macroseta on tibia I, II, III and IV 0.41, 0.42, 0.80 and 0.89 times diameter of tibia, respectively; Tm I: 0.67. Pedipalp: TPA rod-like, distal part scaly; BT long, pointed retrolaterally; PC distal setae adjacent to basal setae (Fig. 12A); T with scale-like papillae, PT with long papillae; TS short, with papillae (Fig. 12D); DSA tip broad, margin smooth (Fig. 12A); EM short, cylindrical, proximally oriented; TP without small protuberances; E broad at basal part (Fig. 12B). Opisthosoma: brown, evenly coloured (Fig. 9D).

Female (ZIMG): Total length: 2.95. Prosoma: 1.23 long, 1.03 wide. Eyes: AME-AME: 0.22, AME width: 0.76, AME-ALE: 0.36, ALE width: 0.10, ALE-PLE: 0.01, PLE width: 0.09, PLE-PME: 0.06, PME width: 0.08, PME-PME: 0.09. Clypeus: not hirsute, one sub-AME seta. Sternum: 0.78 long; 0.74 wide. Legs: dorsal proximal macroseta on tibia I, II, III and IV 1.29, 1.30, 1.49 and 1.67 times diameter of tibia, respectively; Tm I: 0.67. Chelicerae: stridulatory striae scaly, widely and evenly spaced. Epigyne: Clade 13 characteristic morphology, borders between dorsal

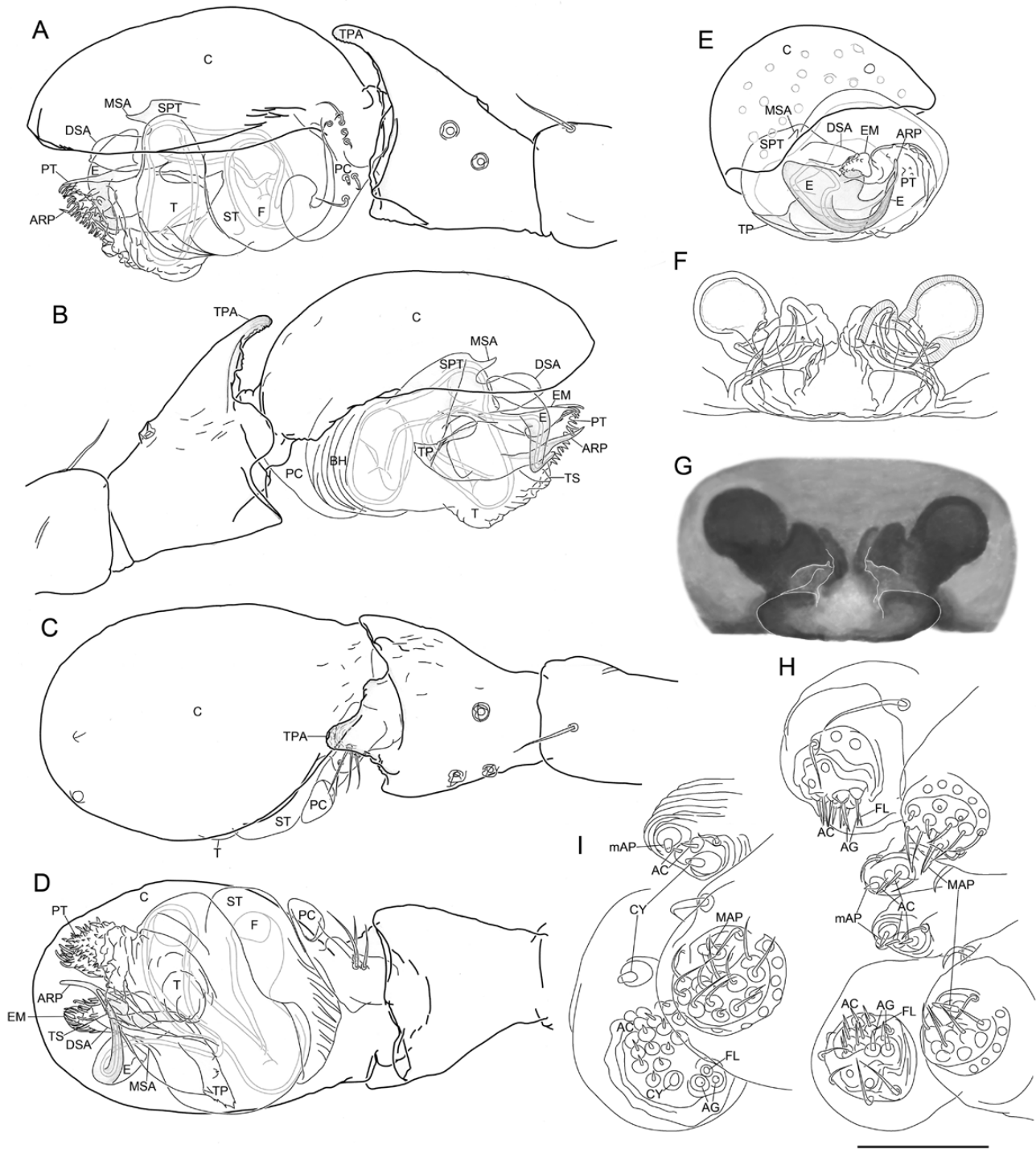


Figure 13. *Oedothorax paludigena* Simon, 1926. A–E, male left palp. A, retrolateral view. B, prolateral view. C, dorsal view. D, ventral view. E, apical view. F, G, epigyne. F, ventral view. G, external morphology. H, male spinnerets. I, female left spinnerets. Scale bar 0.1 mm.

and ventral plates parallel, copulatory duct short (Fig. 12F–H). Opisthosoma: brown, evenly coloured.

Variation: The measurements are based on examined material.

Males (N = 10, means in parentheses): Total length 1.30–2.32 (2.07). Prosoma: 0.87–1.04 (0.93) long, 0.71–0.86 (0.76) wide. Legs: dorsal proximal macroseta on tibia I, II, III and IV 0.34–0.74 (0.51), 0.39–0.59 (0.52), N = 8, 0.61–0.91 (0.74) and 0.78–1.15 (0.91, N = 8) times diameter of tibia, respectively; Tm I: 0.61–0.67 (0.63).

Females (N = 10, means in parentheses): Total length 2.51–3.37 (2.96). Prosoma: 0.98–1.35 (1.19) long, 0.84–1.03 (0.95) wide. Legs: dorsal proximal macroseta on tibia I, II, III and IV 1.11–1.38 (1.27), 1.09–1.68 (1.32), 0.73–1.82 (1.39) and 1.27–1.79 (1.52) times diameter of tibia, respectively; Tm I: 0.61–0.70 (0.66).

Distribution: Europe, Turkey, Caucasus, Russia to Central Asia, China.

Habitat: In moss, grass and sparse vegetation.

OEDOTHORAX FUSCUS (BLACKWALL, 1834)

(FIGS 7W, 8I, 9I, 14; SUPPORTING INFORMATION, FIG. S1H)

Neriere fusca Blackwall, 1834: 382 (Dmf).

Erigone simplex Westring, 1851: 44 (Dmf).

Neriere fusca Blackwall, 1864: 275, pl. 19, fig. 189, pl. 12, fig. 1 (mf).

Microneta tessellate Menge, 1871: 230, pl. 45, fig. 129 (mf, misidentified).

Erigone fusca Thorell, 1871: 125.

Erigone tarsalis Thorell, 1875a: 90 (Dm).

Erigone tarsalis Thorell, 1875b: 43 (Dm).

Neriere agrestis O. Pickard-Cambridge, 1879: 115 (m, misidentified).

Erigone marina L.Koch, 1882: 629, fig. 7 (Df).

Erigone commutabilis Dahl, 1883: 50, fig. 32 (Dm).

Gongylidium retusum Simon, 1884: 481, figs 258–260 (mf, misidentified).

Gongylidium tarsale Simon, 1884: 483.

Neriere tarsalis van Hasselt, 1885: 166.

Neriere fusca Chyzer & Kulczyński, 1894: 94, pl. 4, fig. 4 (mf).

Neriere fusca Simon, 1894: 666, figs 718, 736 (mf).

Kulczynskiellum fuscum F.O. Pickard-Cambridge, 1895: 39.

Gongylidium retusum Becker, 1896: 84, pl. 9, fig. 6 (mf).

Gongylidium gibbum O. Pickard-Cambridge, 1901: 33 (Df).

Kulczynskiellum fuscum Bösenberg, 1902: 170, pl. 15, fig. 229 (mf).

Oedothorax gibbus Smith, 1904: 110.

Stylothorax fusca, Dahl, 1912: 603.

Stylothorax gibba Reimoser, 1919: 72.

Stylothorax tarsalis Reimoser, 1919: 73.

Oedothorax fuscus Simon, 1926: 453, 523, fig. 783 (mf).

Oedothorax fuscus Denis, 1947: 140, figs 1B, 2C, 6H, 7F, 8F, 9A, 10A, B, 11A (mf).

Oedothorax fuscus Millidge, 1951: 551, fig. 2a (f).

Oedothorax fuscus Locket & Millidge, 1953: 240, figs 145B, 146C, 147A, B (mf).

Oedothorax fuscus Wiehle, 1960a: 449, figs 827–834 (mf).

Oedothorax fuscus Tystshenko, 1971: 251, fig. 828 (f).

Oedothorax fuscus Miller, 1971: 262, pl. LIV, figs 13–16 (mf).

Oedothorax fuscus Millidge, 1975: 120, fig. 10 (f).

Oedothorax fuscus Palmgren, 1976: 87, figs 7.12, 18–21 (mf).

Oedothorax fuscus Růžička, 1978: 195, fig. 8G (f).

Oedothorax fuscus van Helsdingen, 1978: 194.

Oedothorax fuscus Bosmans, 1985: 59, figs 13, 23, 30 (m).

Oedothorax fuscus Roberts, 1987: 57, figs 22C, 23A (mf).

Oedothorax fuscus Heimer & Nentwig, 1991: 224, fig. 605 (mf).

Oedothorax fuscus Alderweireldt, 1992: 5, fig. 1a (f).

Oedothorax fuscus Bosmans & Van Keer 2012: 8, figs 4, 5 (f).

Oedothorax fuscus Russell-Smith, 2016: 24, fig. 4 (f).

Type material: No type was designated. Nevertheless, the descriptions in the subsequent studies make the identification of this species unequivocal.

Examined material: **Denmark:** 1♂ 16.–30.vi.1993, leg. S. Langenmark & O. E. Meyer, det. O. Gudik-Sørensen, 1997 (ZMUC); Fyn, Onsebakke, 19.9 km north of Fåborg (55°13'23.6" N, 10°17'17" E), 24 m, 1♂ 20.vi.2009, leg. & det. N. Scharff, 2009 (ZMUC 00012872); Seeland, 1♂ 15.viii.1980 det. N. Scharff (ZMUC); Vesterlyng, NWZ, PG47 Strandeng, opskyl, 3♀ 15.i.2005, leg. H. Liljehult (ZMUC 00009622).

Morocco: Environs de Rabat, estuaire, 2♂2♀ 1973, coll. B. Elkaim, det. R. Jocqué (RMCA 154.376); same data, 2♀ (RMCA 154.371); same data, 1♀ (RMCA 154.375).

England: Cheshire, Red Rocks, 1♂ 2.ix.1961, coll. W. Kirby, det. D. J. Clark (NHM). **Wales:** Whiteford, *Spartina* drift, 4♂1♀ 26.ix.1966 (AMNH No.3243).

Scotland: Calgary, Isle of Mull, 1♀ 2.iv.1994, coll. P. A. Selden (NHM).

Diagnosis:

Males: The lack of prosomal humps, pits or sulci distinguishes this species from the ‘*gibbosus*-like species group’ (Clade 28). It resembles *Oe. tingitanus* in having a bifurcated protégulum, but can be distinguished by its limited distribution of papillae at the distal part of the mesal branch of the protégulum (Fig. 14D) and the absence of a tooth prolateral to the palpal tibia prolateral apophysis (compare Fig. 14C, D with Fig. 11C, D).

Females: Can be distinguished from other species by the epigynal configuration and number of sub-AME setae (two; one in *Oe. gibbosus*, *Oe. trilobatus*, *Oe. apicatus*, *Oe. retusus*, *Oe. gibbifer* and *Oe. paludigena*). Distinguished from *Oe. gibbifer*, *Oe. retusus*, *Oe. paludigena* and *Oe. gibbosus* by the less convergent ventral plate borders; from *Oe. agrestis* by the more anteriorly extended copulatory ducts and the thicker dark stripes at each side of the dorsal plate; from *Oe. trilobatus* and *Oe. meridionalis* by the copulatory

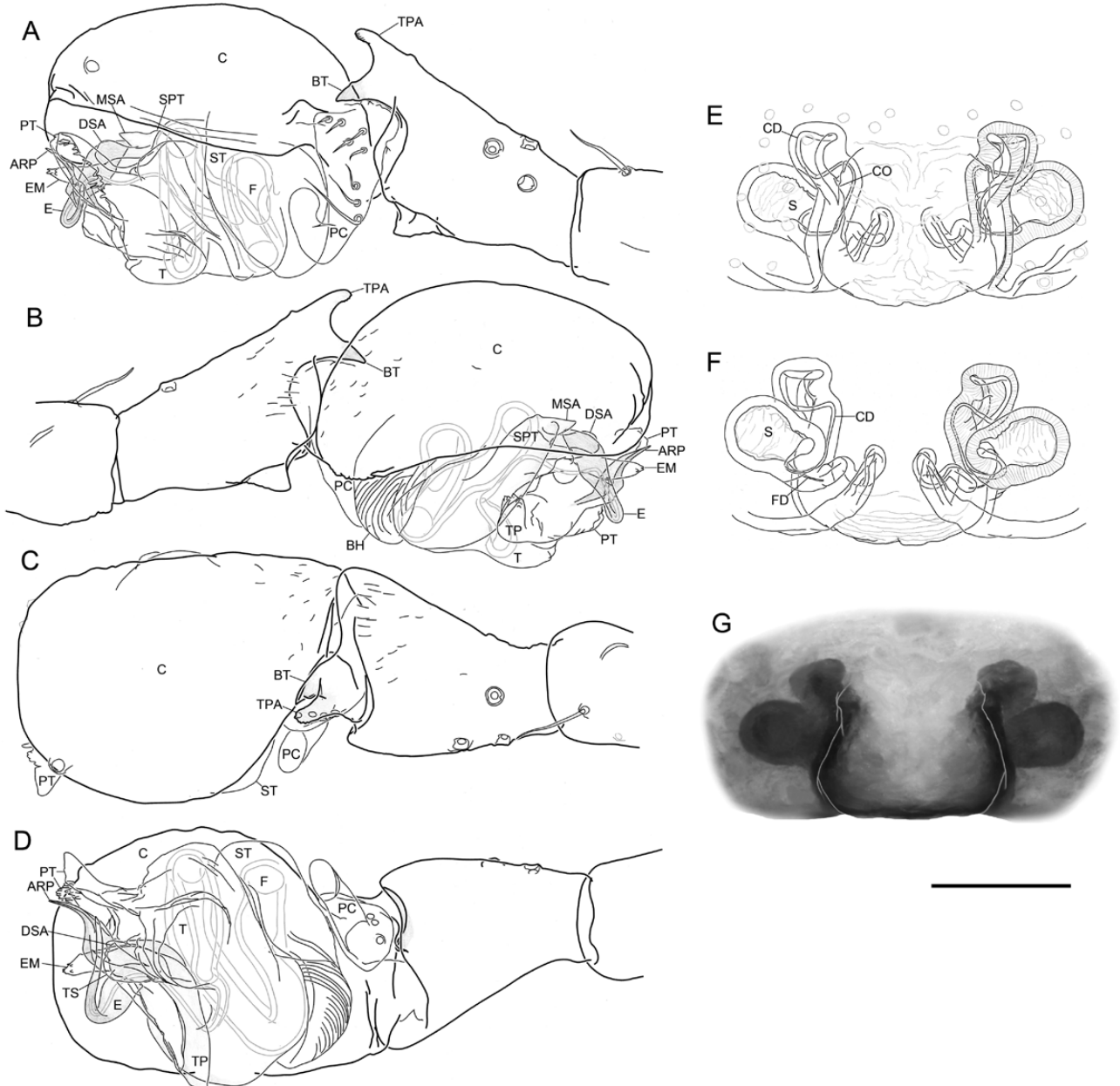


Figure 14. *Oedothorax fuscus* (Blackwall, 1834). A–D, male left palp. A, retrolateral view. B, prolateral view. C, dorsal view. D, ventral view. E–G, epigyne. E, ventral view. F, dorsal view. G, external morphology. Scale bar 0.1 mm.

openings much more anteriorly located; from *Oe. tingitanus* by the more convoluted trajectories of the copulatory ducts (Fig. 14E, F, simpler in the latter species), and a wider separation between both copulatory ducts (narrower in the latter species).

Description:

Male (Denmark, 1993): Total length: 1.99. Prosoma: 0.92 long, 0.73 wide, without external modification (Fig. 7W). Eyes: AME-AME: 0.04, AME width: 0.05, AME-ALE: 0.02, ALE width: 0.07, ALE-PLE: 0.00, PLE width: 0.07, PLE-PME: 0.04, PME width: 0.06, PME-PME: 0.09. Clypeus: not hirsute, two sub-AME setae. Sternum: 0.55 long, 0.53 wide. Chelicerae: mastidia absent; stridulatory striae scaly, widely and evenly spaced (Fig. 8I). Legs: dorsal proximal macroseta on tibia I, II, III and IV 1.18, 1.49, 2.20 and 2.03 times diameter of tibia, respectively; Tm I: 0.61. Pedipalp: TPA rod-like, distal part scaly (Fig. 14A); BT short, pointed retrolaterally (Fig. 14C); PC distal setae at median position (Fig. 14A); T without papillae, PT bifurcate, distal part of mesal branch with long papillae, ectal branch without papillae; TS short, without papillae (Fig. 14D); DSA tip round (Fig. 14A); EM median-long, cylindrical, distally oriented, with small papillae at tip (Fig. 14D); ARP pointed, prolaterally spiral; TP with several small protuberances; E not broadened at basal part (Fig. 14B). Opisthosoma: brown, evenly coloured (Fig. 9I).

Female (ZMUC 00009622): Total length: 2.88. Prosoma: 1.14 long, 0.91 wide. Eyes: AME-AME: 0.03, AME width: 0.06, AME-ALE: 0.02, ALE width: 0.09, ALE-PLE: 0.00, PLE width: 0.08, PLE-PME: 0.04, PME width: 0.08, PME-PME: 0.06. Clypeus: not hirsute, two sub-AME setae. Sternum: 0.68 long; 0.65 wide. Legs: dorsal proximal macroseta on tibia I, II, III and IV 1.56, 1.66, 1.83 and 1.97 times diameter of tibia, respectively; Tm I: 0.64. Chelicerae: stridulatory striae rows broadly and evenly spaced. Epigyne: Clade 13 characteristic morphology, borders between dorsal and ventral plates parallel, copulatory duct of median length (Fig. 14E–G). Opisthosoma: brown, evenly coloured.

Variation: The measurements are based on examined material.

Males (N = 10, means in parentheses): Total length 1.23–2.14 (1.96). Prosoma: 0.85–0.92 (0.90) long, 0.68–0.77 (0.72) wide. Legs: dorsal proximal macroseta on tibia I, II, III and IV 1.00–1.55 (1.26, N = 8), 1.07–1.56 (1.37, N = 9), 1.91–2.20 (2.03, N = 8) and 1.92–2.49 (2.16, N = 8) times diameter of tibia, respectively; Tm I: 0.55–0.65 (0.60).

Females (N = 10, means in parentheses): Total length 2.26–2.91 (2.65). Prosoma: 0.98–1.16 (1.08) long, 0.82–0.91 (0.87) wide. Legs: dorsal proximal macroseta on tibia I, II, III and IV 1.22–1.79 (1.55), 1.19–1.93 (1.60), 1.58–2.39 (2.00) and 1.93–2.67 (2.22) times diameter of tibia, respectively; Tm I: 0.59–0.66 (0.63)

Distribution: Azores, Europe, North Africa.

Habitat: Grasslands, wetlands, saltmarsh.

OEDOTHORAX GIBBIFER (KULCZYŃSKI, 1882)
(FIGS 7Q, 8C, 9C, 15; SUPPORTING INFORMATION, FIG. S1C)

Erigone gibbifera Kulczyński, 1882a: 17 (Dmf).

Erigone gibbifera Kulczyński, 1882b: 21, pl. 2, fig. 13 (Dmf).

Gongylidium cantalicum Simon, 1884: 480, figs 255–257 (Dmf).

Gongylidium gibbiferum Simon, 1884: 499.

Neriene gibbifera Chyzer & Kulczyński, 1894: 94, pl. 4, fig. 3 (mf).

Stylothorax gibbifera Reimoser, 1919: 72.

Stylothorax cantalica Reimoser, 1919: 72.

Oedothorax cantalicus Simon, 1926: 453, 523.

Oedothorax gibbifer Ovsyannikov, 1937: 90, fig. 2 (f).

Oedothorax gibbifer Denis, 1947: 138, figs 2B, 6E, 7E, 8E, 9D, 10F, 11E (mf).

Oedothorax gibbifer Vogelsanger, 1948: 54, figs 6–8 (mf).

Oedothorax gibbifer Miller, 1971: 262, pl. LIV, figs 10–12 (f).

Oedothorax gibbifer Růžička, 1978: 195, figs 8C, D, 9C (f).

Oedothorax gibbifer Thaler, 1978: 186, figs 15–17 (m).

Oedothorax gibbifer Bosmans, 1985: 65, figs 12, 28, 34 (m).

Oedothorax gibbifer Heimer & Nentwig, 1991: 224, fig. 604 (mf).

Type material: No type data in Kulczyński (1882a). Nevertheless, the unique palpal tibia shape and male prosomal modification illustrated in the original description suffice for an identification of this species.

Examined material: **Austria:** Lower Austria, Scheibbs District, Gaming, Seebachlacke, 2♀ 17.vi.1972, leg. F. Ressler, det. J. Wunderlich (SMF 62907). No collecting data: 1♂1♀, leg. Miller, det. Wunderlich xii.1968 (SMF 24213/2); 1♂2♀ (SMF 59615)

Diagnosis:

Males: Can be distinguished from *Oe. retusus* and *Oe. apicatus* by the small palpal tibial prolateral

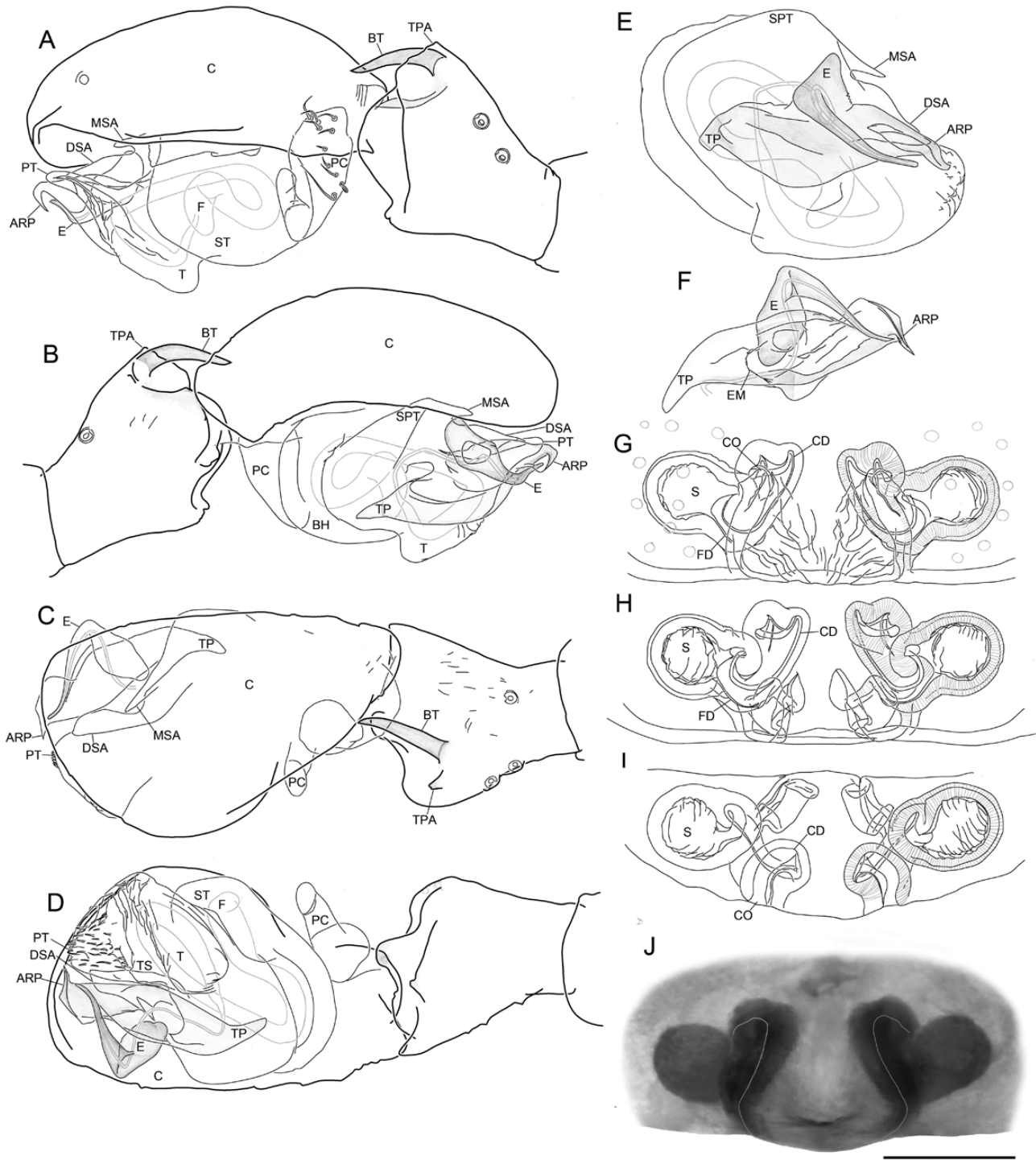


Figure 15. *Oedothorax gibbifer* (Kulczyński, 1882). A–F, male left palp. A, retrolateral view. B, prolateral view. C, dorsal view. D, ventral view. E, copulatory bulb, apical view. F, embolic division, ventral view. G–J, epigyne. G, ventral view. H, dorsal view. I, anterior view. J, external morphology. Scale bar 0.1 mm.

apophysis, the prolaterally oriented basal thorn (Fig. 15C; retrolaterally oriented in the other two species), and the unbroadened basal part of embolus (Fig. 15B; broadened in the two other species).

Females: Can be distinguished from *Oe. meridionalis*, *Oe. agrestis*, *Oe. fuscus* and *Oe. tingitanus* by having one sub-AME seta (two in the latter four species). Distinguished from *Oe. meridionalis* and *Oe. trilobatus* by the more anteriorly located copulatory openings (Fig. 15G); from *Oe. gibbosus* by the less convergent borders between the dorsal and ventral plates and by the lateral copulatory opening (Fig. 15G; posterior in *Oe. gibbosus*, Fig. 6F); from *Oe. apicatus* and *Oe. retusus* by the broader posterior width of the epigynal dorsal plate, and by the dorsal plate surface wrinkles converging towards the center of posterior margin (Fig. 15G; wrinkles diverging towards posterior margin in the latter two species, Figs 12F, 16E).

Description:

Male (SMF 24213/2): Total length: 2.46. Prosoma: 1.15 long, 0.87 wide, postocular region elevated, with lateral sulci and pits (Fig. 7Q). Eyes: AME-AME: 0.04, AME width: 0.04, AME-ALE: 0.05, ALE width: 0.08, ALE-PLE: 0.01, PLE width: 0.08, PLE-PME: 0.07, PME width: 0.06, PME-PME: 0.07. Clypeus: not hirsute, one sub-AME seta. Sternum: 0.68 long, 0.62 wide. Chelicerae: mastidia absent, stridulatory striae scaly, widely and evenly spaced (Fig. 8C). Legs: dorsal proximal macroseta on tibia I and II 1.24 and 1.18 times diameter of tibia, respectively; Tm I: 0.79. Pedipalp: TPA short; basal thorn long, pointed prolaterally (Fig. 15C); PC distal setae adjacent to basal setae (Fig. 15A); T without papillae, PT with long papillae, TS short, without papillae (Fig. 15D); DSA tip narrow (Fig. 15A); EM short, cylindrical, proximally oriented; TP without small protuberances; E not broadened at basal part (Fig. 15B, F). Opisthosoma: brown, evenly coloured (Fig. 9C).

Female (SMF 62907): Total length: 3.02. Prosoma: 1.16 long, 0.90 wide. Eyes: AME-AME: 0.02, AME width: 0.07, AME-ALE: 0.03, ALE width: 0.10, ALE-PLE: 0.01, PLE width: 0.08, PLE-PME: 0.05, PME width: 0.07, PME-PME: 0.08. Clypeus: not hirsute, one sub-AME seta. Sternum: 0.71 long; 0.66 wide. Legs: dorsal proximal macroseta on tibia I, II, III and IV 1.76, 1.90, 2.12 and 2.13 times diameter of tibia, respectively; Tm I: 0.62. Chelicerae: stridulatory striae scale-like, rows widely and evenly spaced. Epigyne: Clade 13 characteristic morphology, borders between dorsal and ventral plates slightly converging anteriorly, copulatory duct short (Fig. 15G–J). Opisthosoma: brown, evenly coloured.

Variation: The measurements are based on examined material.

Males (N = 2, means in parentheses): Total length 2.40–2.46. Prosoma: 1.09–1.15 long, 0.87–0.87 wide. Legs: Tm I: 0.74–0.76.

Females (N = 4, means in parentheses): Total length 3.02–3.86 (3.42). Prosoma: 1.16–1.44 (1.34) long, 0.90–1.09 (1.03) wide. Legs: dorsal proximal macroseta on tibia I, II, III and IV 1.17–1.76 (1.49), 1.54–1.90 (1.69), 1.92–2.12 (2.02, N = 3) and 1.88–2.15 (2.05) times diameter of tibia, respectively; Tm I: 0.62–0.81 (0.75).

Distribution: Poland, France, Russia, Switzerland, Czech Republic, Germany, Austria.

Habitat: Wet habitats, swampy areas, from low areas up to 2450 m.

OEDOTHORAX MERIDIONALIS TANASEVITCH, 1987 (FIGS 7U, 8G, 9G, 10; SUPPORTING INFORMATION, FIG. S1F)

Oedothorax meridionalis Tanasevitch, 1987: 355, figs 107–110 (Dmf).

Oedothorax meridionalis Tanasevitch, 1990: 102, figs 23.6, 24.3, 28.3 (mf).

Oedothorax meridionalis Tanasevitch, 2015: 382, figs 3–6 (m).

Type material: Holotype: **Georgia:** Caucasus, Adjara, Keda District, Magutseti, *Platanus* forest, litter, ♂ 9.x.1981, leg. S. Golovatch (ZMMU, not examined). Paratypes: **Georgia:** Abkhazia, Sukhumi District, Verkhnyaya Kelasuri Village, deciduous forest, 1♀ 27.x.1981 (ZMMU, not examined); Abkhazia, Sukhumi Dim., near Klasuri Cave, litter, 1♀ 11.iv.1983, leg. S. Golovatch (ZMMU, not examined). **Azerbaijan:** Shemakha Dim., Pirkuli State Reserve, bank of river, 1200–1400 m, 1♂4♀ (ZMMU, examined), 1♂2♀ (SMF 33815, not examined), 3♀ (Zoological Institute of the USSR Academy of Science, Leningrad, not examined) 19.ix.1984, leg. D. Logunov.

Additional Examined material: **Georgia:** Caucasus, Algeti National Park, west of Manglisi, Eagus, Picea, acer etc. forest, 1400–1450 m, litter and under bark, 2♂ 16.–18.v.1987, leg. S. Golovatch & K. Eskov, Tanasevitch (Tanasevitch personal collection).

Diagnosis:

Males: Can be identified from all other *Oedothorax* species by the following combination of features: a post-ocular elevation without lateral sulci and pits,

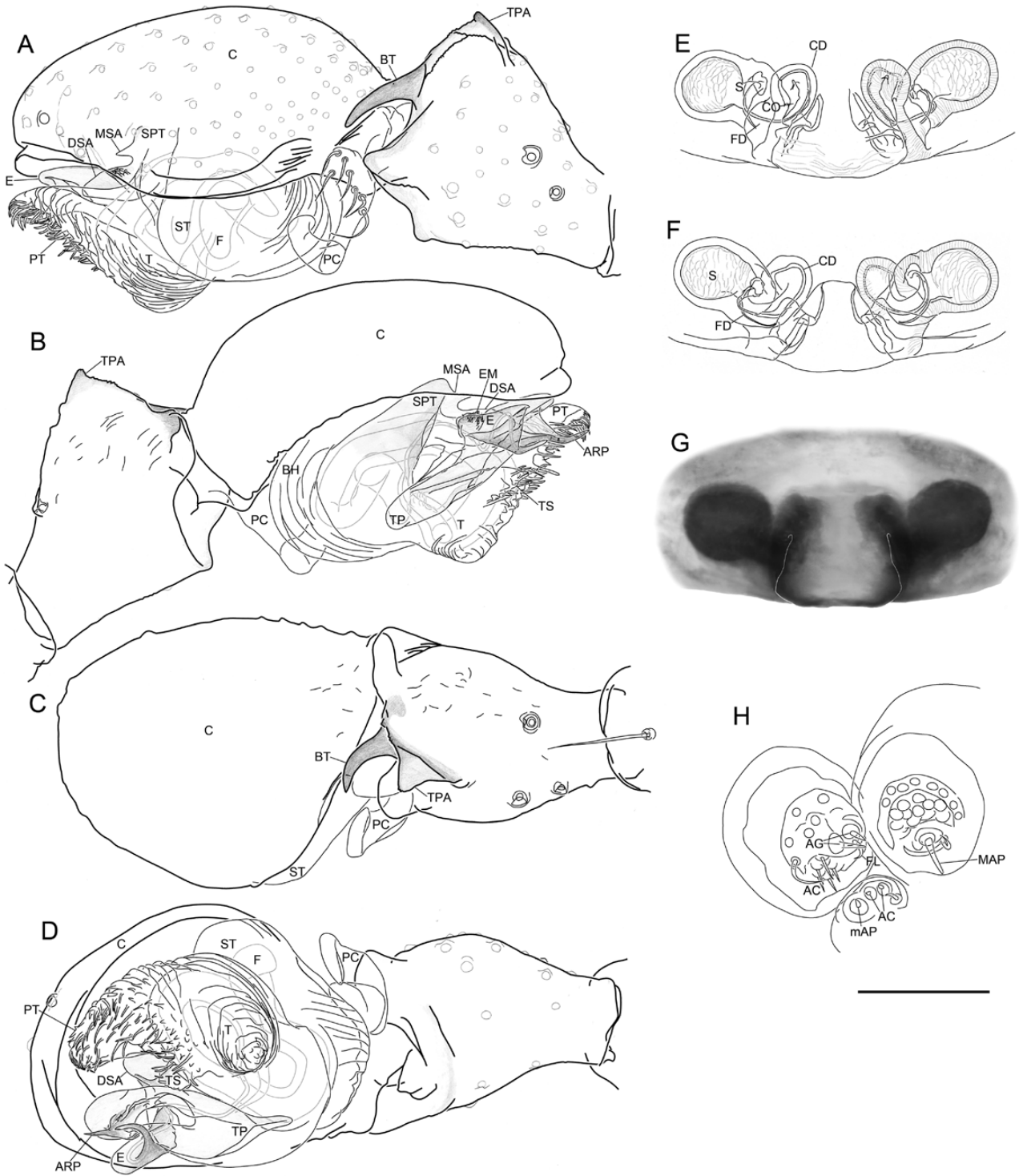


Figure 16. *Oedothorax retusus* (Westring, 1851). A–D, male left palp. A, retrolateral view. B, prolateral view. C, dorsal view. D, ventral view. E–G, epigyne. E, ventral view. F, dorsal view. G, external morphology. H, male right spinnerets. Scale bar 0.1 mm.

and without transverse groove (Fig. 7U); two sub-AME setae (one in *Oe. gibbosus*, *Oe. trilobatus*, *Oe. apicatus*, *Oe. retusus*, *Oe. gibbifer* and *Oe. paludigena*).

Females: Similar to females of other species in the *Oedothorax* s.s., but can be identified by the posterior location of copulatory openings (more anterior in species except *Oe. trilobatus*) and the presence of wide, membranous chambers at the entrance of copulatory ducts (absent in other species).

Description:

Male (Tanasevitch personal collection): Total length: 2.13. Prosoma: 0.90 long, 0.73 wide, postocular region with hump (Fig. 7U). Eyes: AME-AME: 0.03, AME width: 0.05, AME-ALE: 0.02, ALE width: 0.08, ALE-PLE: 0.01, PLE width: 0.07, PLE-PME: 0.05, PME width: 0.07, PME-PME: 0.11. Clypeus: not hirsute, two sub-AME setae. Sternum: 0.53 long, 0.56 wide. Chelicerae: mastidia absent; stridulatory striae scaly, rows widely and evenly spaced (Fig. 8G). Legs: dorsal proximal macroseta on tibia I, II, III and IV 1.23, 1.36, 1.46 and 1.69 times diameter of tibia, respectively; Tm I: 0.47. Pedipalp: TPA rod-like, distal part scaly; BT absent; several tiny denticles retrolateral and prolateral to TPA (Fig. 10C); PC distal setae at median position (Fig. 10A); T papillae scale-like, long-papillae-bearing region extend from protégulum until retrolateral side of TS; TS short (Fig. 10D); DSA tip round (Fig. 10A); EM median-long, cylindrical, distally oriented, with long papillae; TP with several small protuberances (Fig. 10B); E not broadened at basal part. Opisthosoma: brown, evenly coloured (Fig. 9G).

Female (ZMMU): Total length: 2.82. Prosoma: 1.09 long, 0.89 wide. Eyes: AME-AME: 0.03, AME width: 0.05, AME-ALE: 0.02, ALE width: 0.09, ALE-PLE: 0, PLE width: 0.08, PLE-PME: 0.03, PME width: 0.08, PME-PME: 0.07. Clypeus: not hirsute, two sub-AME setae. Sternum: 0.58 long, 0.64 wide. Legs: dorsal proximal macroseta on tibia I, II, III and IV 1.72, 1.81, 2.25 and 2.42 times diameter of tibia, respectively; Tm I: 0.74. Epigyne: Clade 13 characteristic morphology, borders between dorsal and ventral plates converging anteriorly; CO posterior to spermathecae, with membranous chamber; copulatory duct short (Fig. 10F, G). Opisthosoma: brown, evenly coloured.

Variation: The measurements are based on examined material.

Males (N = 3, means in parentheses): Total length 1.83–2.13 (1.95). Prosoma: 0.89–0.95 (0.91) long, 0.71–0.74

(0.73) wide. Legs: dorsal proximal macroseta on tibia I, II, III and IV 0.97–1.64 (1.28), 1.21–1.36 (N = 2), 1.46–2.22 (1.82) and 1.69–2.41 (1.97) times diameter of tibia, respectively; Tm I: 0.65–0.71 (0.69).

Females (N = 4, means in parentheses): Total length 2.36–3.06 (2.76). Prosoma: 1.09–1.16 (1.13) long, 0.89–0.92 (0.90) wide. Legs: dorsal proximal macroseta on tibia I, II, III and IV 1.73–1.94 (1.82), 1.81–1.94 (1.88), 1.95–2.29 (2.16) and 2.28–2.6 (2.44) times diameter of tibia, respectively; Tm I: 0.65–0.74 (0.70).

Distribution: Russia (Caucasus, Central Asia), Iran.

Habitat: See type material and examined material.

Remarks: This species, like other true *Oedothorax* species, does not have a lateral extension of the radix. The lateral extension of convector (termed lateral extension of radix in the current study) illustrated in figs 4–6 in Tanasevitch (2015) might be a misinterpretation of the distal suprategular apophysis.

OEDOTHORAX PALUDIGENA SIMON, 1926

(Figs 7T, 8F, 9F, 13)

Oedothorax fuscus paludigena Simon, 1926: 453, 523 (Dm).

Oedothorax fuscus paludigena Denis, 1947: 142, figs 6I, 7G, 8G (m).

Oedothorax paludigena Millidge, 1975: 120, figs 1–9 (m, Df, elevated from subspecies).

Oedothorax paludigena Bosmans, 1985: 65, figs 17, 24, 35 (m).

Oedothorax paludigenus Canard & Cruveillier, 2016: 44 (proposed correction of gender ending).

Oedothorax paludigena Pantini & Mazzoleni, 2018: 35, fig. 6a–e (mf).

Type material: Lectotype ♂ [designated by Millidge (1975)] and syntype ♀: **France:** Bouches-du-Rhône, Martigues, Alpes-Maritimes, mouth of the Var, leg. de Dalmas, 1918 (Tube No. 4476, MNHN, not examined).

Examined material: **Greece:** Epirus, between Salaora and Arta, at the border of lagoon, 1♀ 28.iii.1978, leg. S. Vit (MHNG). **France:** Corsica, 15 km north of l'Île-Rousse, from humid leaf litter of an alder forest in Ostriconi, 2♂ vi.1984, leg. & det. H. G. Müller (MHNG).

Diagnosis:

Males: The lack of prosomal humps, pits or sulci distinguishes this species from the 'gibbosus-like

species group' (Clade 28) and *Oe. meridionalis*. Distinguished from *Oe. fuscus*, *Oe. agrestis* and *Oe. tingitanus* by having one sub-AME seta (two in the latter three species) and the absence the palpal tibial basal thorn.

Females: Can be distinguished from other species by the epigynal configuration and number of sub-AME setae (one; two in *Oe. fuscus*, *Oe. agrestis*, *Oe. meridionalis* and *Oe. tingitanus*). Distinguished from *Oe. gibbosus*, *Oe. apicatus*, *Oe. retusus* and *Oe. gibbifer* by the more anteriorly situated copulatory openings; from *Oe. trilobatus* by the much shorter copulatory ducts.

Description:

Male (MHNG): Total length: 2.00. Prosoma: 0.83 long, 0.86 wide, unmodified (Fig. 7T). Eyes: AME-AME: 0.04, AME width: 0.05, AME-ALE: 0.02, ALE width: 0.07, ALE-PLE: 0, PLE width: 0.06, PLE-PME: 0.05, PME width: 0.06, PME-PME: 0.06. Clypeus: not hirsute, one sub-AME seta. Sternum: 0.5 long; 0.5 wide. Chelicerae: mastidia absent; stridulatory striae scaly, rows widely and evenly spaced (Fig. 8F). Legs: dorsal proximal macroseta on tibia I, II, III and IV 1.35, 1.27, 1.47 and 1.31 times diameter of tibia, respectively; Tm I: 0.61. Pedipalp: TPA triangular, distal part blunt and scaly, with small protuberances on both sides of tip; BT absent; PC distal setae at median position (Fig. 13A); T papillae scale-like, PT with long-papillae; TS short, without papillae (Fig. 13D); DSA tip round (Fig. 13A); EM long, cylindrical, distally oriented, with long papillae; ARP pointed, prolaterally spiral; TP with several small protuberances; E not broadened at basal part (Fig. 13B). Opisthosoma: brown, evenly coloured (Fig. 9F); spinnerets see Fig. 13H.

Female (MHNG): Total length: 2.85. Prosoma: 1.00 long, 0.80 wide. Eyes: AME-AME: 0.04, AME width: 0.07, AME-ALE: 0.02, ALE width: 0.08, ALE-PLE: 0.01, PLE width: 0.07, PLE-PME: 0.06, PME width: 0.07, PME-PME: 0.06. Clypeus: not hirsute, one sub-AME seta. Sternum: 0.62 long; 0.61 wide. Legs: dorsal proximal macroseta on tibia I, II, III and IV 1.54, 1.55, 1.78 and 1.85 times diameter of tibia, respectively; Tm I: 0.65. Epigyne: Clade 13 characteristic morphology, dorsal plate posterior margin wide, borders between dorsal and ventral plates strongly converging anteriorly, CO posteriorly directed, located posterior to spermathecae, CD of shorter length (Fig. 13F, G). Opisthosoma: brown, evenly coloured; spinnerets see Fig. 13I.

Distribution: France, Corsica, Sardinia, Italy, Greece.

Habitat: Costal marshes in the western Mediterranean.

OEDOTHORAX RETUSUS (WESTRING, 1851)

(FIGS 7S, 8E, 9E, 16; SUPPORTING INFORMATION, FIG. S1E)

- Erigone retusa* Westring, 1851: 41 (Dmf).
Neriere elevata O. Pickard-Cambridge, 1862: 7966 (Dmf).
Tmeticus foveolatus Menge, 1868: 186, pl. 35, fig. 86 (Dmf).
Neriere retusa O. Pickard-Cambridge, 1873: 451.
Gongylidium fuscum Simon, 1884: 478, figs 252–254 (mf, misidentified).
Neriere retusa Chyzer & Kulczyński, 1894: 94, pl. 4, fig. 2 (mf).
Kulczynskiellum retusum F.O. Pickard-Cambridge, 1895: 39.
Gongylidium fuscum Becker, 1896: 82, pl. 9, fig. 5 (mf).
Kulczynskiellum retusum Bösenberg, 1902: 170, pl. 15, fig. 230 (mf).
Oedothorax retusus, de Lessert, 1910: 192.
Kulczynskiellum retusum Fedotov, 1912: 454, pl. 8, fig. 2 (f).
Stylothorax retusa, Dahl, 1912: 603.
Oedothorax retusus Denis, 1947: 145, figs 6D, 7D, 8D, 9E, 10E, 11D (mf).
Oedothorax retusus Vogelsanger, 1948: 53, fig. 9 (f).
Oedothorax retusus Lockett & Millidge, 1953: 241, figs 145D, E, 146E, 147E, F (mf).
Oedothorax retusus Wiehle, 1960a: 440, figs 807–816 (mf).
Oedothorax retusus Holm, 1962: 165, fig. 61C–d (m).
Oedothorax retusus Tystshenko, 1971: 251, figs 820, 831 (mf).
Oedothorax retusus Miller, 1971: 262, pl. LIV, figs 20–22 (f).
Oedothorax retusus Palmgren, 1976: 88, figs 7.22, 8.1–2, 8.4–6.
Oedothorax retusus Růžička, 1978: 195, figs 8B, 9B (f).
Oedothorax retusus Hu & Wang, 1982: 63, fig. II.1–4 (f).
Oedothorax retusus Hu, 1984: 199, fig. 209.1–4 (f).
Oedothorax retusus Bosmans, 1985: 65, figs 15, 20, 32 (m).
Oedothorax retusus Roberts, 1987: 57, figs 22E, 23C (mf).
Oedothorax retusus Heimer & Nentwig, 1991: 224, fig. 603 (mf).
Oedothorax retusus Alderweireldt, 1992: 5, fig. 1c (f).
Oedothorax retusus Zhao, 1993: 199, fig. 90a–c (f).
Oedothorax retusus Uhl, Nessler & Schneider, 2010: 77, fig. 1E, F (f).
Oedothorax retusus Uhl et al., 2014: 348, fig. 1A–F (mf).
Oedothorax retusus Kunz, Witthuhn & Uhl, 2015: 279, figs 1A–h, 2A–j (mf).

Oedothorax retusus Russell-Smith, 2016: 23, fig. 2 (f).
Type material: No type designation nor illustration in Westring (1851). Subsequent studies do not mention the examination of types. Nevertheless, the unique palpal tibia shape and male prosomal modification illustrated in later descriptions suffice for an identification of this species.

Examined material: **Scotland**: Tentsmuir, damp dune slack, 1♂2♀ 8.ix.1965 (No.3114 AMNH). **England**: Yorkschire, Askham Bog, 1♀ 12.vii.53 (AMNH); New Forest, Matley Passage, sand pit, 1♀ 15.viii.1955 (AMNH); Oxford, Noke wood, 1♀ 20.x.1954. **Switzerland**: Basel (47° N, 8° E), 1♂1♀ (AMNH); Westring, 1♂(AMNH); Trius, 1♀ det. Schenkel (received 1946), Schenkel collection (AMNH). **Norway**: 1♂ xiii.1962, N, Svartisen, M, J. O. 40 (AMNH); 2♀ xiii.1960, RO/RO/S J. A. L. O. (AMNH); 1♂ xiii.1962, N, Svartisen, M, J. O. 46 (AMNH). **Germany**: Greifswald, 1♂ 2014, coll. and det. S.-W. Lin. Data unrecognizable: 4♂1♀ (AMNH).

Diagnosis:

Males: This species is similar to *Oe. apicatus* and *Oe. gibbifer*, all three possess post-ocular hump and lateral sulci and pits, but this species can be distinguished from *Oe. apicatus* by not having the knob-like shape of post-ocular hump, and can be distinguished from *Oe. gibbifer* by the retrolaterally bent palpal tibial basal thorn, pointing prolaterally in the latter.

Females: Can be distinguished from other species by the epigynal configuration and number of sub-AME setae (one; two in *Oe. fuscus*, *Oe. agrestis*, *Oe. meridionalis* and *Oe. tingitanus*). Distinguished from *Oe. apicatus* by the more convergent ventral plate borders; from *Oe. gibbosus* by the more curved ventral plate borders; from *Oe. gibbifer* by the wrinkles close to the posterior margin of the central area parallel to the margin; from *Oe. paludigena* by the narrower posterior margin of the dorsal plate; from *Oe. trilobatus* by the much shorter copulatory ducts.

Description:

Male (AMNH): Total length: 2.14. Prosoma: 0.91 long, 0.74 wide, postocular region elevated, with lateral sulci and pits (Fig. 7S). Eyes: AME-AME: 0.02, AME width: 0.05, AME-ALE: 0.03, ALE width: 0.06, ALE-PLE: 0.01, PLE width: 0.06, PLE-PME: 0.04, PME width: 0.06, PME-PME: 0.05. Clypeus: not hirsute, one sub-AME seta. Sternum: 0.57 long, 0.53 wide. Chelicerae: mastidia absent; stridulatory striae scaly, rows widely and evenly spaced (Fig. 8E). Legs: dorsal proximal

macroseta on tibia I, II and IV 1.16, 1.16 and 1.87 times diameter of tibia, respectively; Tm I: 0.69. Pedipalp: TPA broad at base, triangular, distal part scaly; BT long, pointed retrolaterally; PC no recognizable distal setae group (Fig. 16A); T with scale-like papillae, PT with long papillae; TS short, with papillae (Fig. 16D); DSA tip round (Fig. 16A); EM short, cylindrical, proximally oriented; TP without small protuberances (Fig. 16B); E broad at basal part. Opisthosoma: brown, evenly coloured (Fig. 9E); spinnerets see Fig. 16H.

Female (AMNH): Total length: 2.73. Prosoma: 1.07 long, 0.82 wide. Eyes: AME-AME: 0.02, AME width: 0.06, AME-ALE: 0.03, ALE width: 0.08, ALE-PLE: 0.00, PLE width: 0.08, PLE-PME: 0.04, PME width: 0.07, PME-PME: 0.07. Clypeus: not hirsute, one sub-AME seta. Sternum: 0.63 long; 0.62 wide. Legs: dorsal proximal macroseta on tibia I, II, III and IV 1.24, 1.35, 1.72 and 1.82 times diameter of tibia, respectively; Tm I: 0.63. Chelicerae: stridulatory striae similar to male. Epigyne: Clade 13 characteristic morphology, borders between dorsal and ventral plates converging anteriorly, copulatory duct short (Fig. 16E–G). Opisthosoma: brown, evenly coloured.

Variation: The measurements are based on examined material.

Males (N = 10, means in parentheses): Total length 1.88–2.23 (2.06). Prosoma: 0.88–1.04 (0.93) long, 0.69–0.81 (0.75) wide. Legs: dorsal proximal macroseta on tibia I, II, III and IV 0.91–1.47 (1.21), 1.11–1.62 (1.25, N = 9), 1.35–2.24 (1.60, N = 9) and 1.42–2.38 (1.75, N = 8) times diameter of tibia, respectively; Tm I: 0.58–0.69 (0.62).

Females (N = 10, means in parentheses): Total length 2.29–3.02 (2.65). Prosoma: 1.01–1.20 (1.13) long, 0.80–0.91 (0.87) wide. Legs: dorsal proximal macroseta on tibia I, II, III and IV 1.24–1.79 (1.51), 1.35–1.74 (1.53), 1.47–2.25 (1.85) and 1.58–2.35 (1.98) times diameter of tibia, respectively; Tm I: 0.60–0.69 (0.64).

Distribution: Europe, Turkey, Caucasus, Russia to Kazakhstan, China

Habitat: In low vegetation or under stones close to water.

OEDOTHORAX TINGITANUS (SIMON, 1884)

(FIGS 7X, 8J, 9J, 11; SUPPORTING INFORMATION, FIG. S1I)

Gongylidium tingitanum Simon, 1884: 483 (Dm).

Neriene insolens Simon, 1894: 633 (Dm).

Stylothorax tingitana Reimoser, 1919: 73.

Oedothorax tingitanus Denis, 1968: 151, figs 11–15 (mf).

Oedothorax tingitanus Bosmans, 1985: 59, figs 1–3, 22, 36 (mf).

Type material: ♂ Lectotype and 2♀ paralectotypes based on Bosmans (1985): **Morocco**: close to Tanger, 1868, coll. Simon (MNHN 4881, not examined).

Examined material: **Morocco**: Mediterranean coast, salt marsh, west of M'diq (Tekouan), 8♂8♀ 17.v.1977, coll. P. Hillyard, det. A. F. Millidge (NHM); Merdia herga, west coast, salt marsh vegetation, 16♂1♀ 16.v.1977, coll. P. D. Hillyard, det. A. F. Millidge (NHM).

Diagnosis:

Males: The lack of male prosomal modifications and the presence of an embolic base protuberance distinguishes the males of this species from the 'gibbosus-like species group' (Clade 28). Males share with *Oe. fuscus* the bifurcated protogulum, but can be distinguished by the extended distribution of papillae (from the distal part of the mesal branch of protogulum until the base of TS) and the presence of a tooth prolateral to the palpal tibia prolateral apophysis (in *Oe. fuscus* the papillae is limited to the distal part of the mesal branch and the prolateral tooth is absent).

Females: Can be distinguished from other species by the epigynal configuration and number of sub-AME setae (two; one in *Oe. gibbosus*, *Oe. trilobatus*, *Oe. apicatus*, *Oe. retusus*, *Oe. gibbifer* and *Oe. paludigena*). Distinguished from *Oe. trilobatus* and *Oe. meridionalis* by the much more anteriorly located copulatory openings (Fig. 11E); from *Oe. agrestis*, *Oe. apicatus*, *Oe. gibbifer* and *Oe. retusus* by the mesal copulatory openings (Fig. 11E; lateral in the first three species, Figs 5E, 12F, 15G; posterior in *Oe. retusus* Fig. 16E) and the more anteriorly extended copulatory ducts; from *Oe. gibbosus* by the more curved and less convergent borders between the dorsal and ventral plates (Fig. 11E, in contrast to Fig. 6F); from *Oe. fuscus* by the less convoluted copulatory ducts compared to *Oe. fuscus* (Fig. 14E) and the narrower separation between the copulatory ducts (wider in *Oe. fuscus*).

Description:

Male (Merdia herga): Total length: 1.96. Prosoma: 0.90 long, 0.68 wide, unmodified (Fig. 7X). Eyes: AME-AME: 0.06, AME width: 0.07, AME-ALE: 0.04, ALE width: 0.07, ALE-PLE: 0.00, PLE width: 0.08, PLE-PME: 0.02, PME width: 0.05, PME-PME: 0.03. Clypeus:

not hirsute, two sub-AME setae. Sternum: 0.52 long, 0.5 wide. Chelicerae: mastidia absent; stridulatory striae imbricated, rows widely and evenly spaced (Fig. 8J). Legs: dorsal proximal macroseta on tibia I, II, III and IV 1.60, 1.51, 2.02 and 2.34 times diameter of tibia, respectively; Tm I: 0.66. Pedipalp: TPA rod-like, distal part scaly; BT short, situated close to tip of tibial prolateral apophysis, pointed anteriorly; tooth prolateral to TPA; PC distal setae at median position (Fig. 11A); T without papillae, PT bifurcate, papillae-bearing region extending from distal part of mesal branch until base of TS, ectal branch without papillae; TS short (Fig. 11D); DSA tip round (Fig. 11A); EM median-long, cylindrical, distally oriented, with small papillae at tip; TP with several small protuberances (Fig. 11B); E not broadened at basal part. Opisthosoma: brown, evenly coloured (Fig. 9J).

Female (Merdia herga): Total length: 2.30. Prosoma: 0.97 long, 0.77 wide. Eyes: AME-AME: 0.03, AME width: 0.06, AME-ALE: 0.02, ALE width: 0.08, ALE-PLE: 0.01, PLE width: 0.07, PLE-PME: 0.06, PME width: 0.07, PME-PME: 0.05. Clypeus: not hirsute, two sub-AME setae. Sternum: 0.61 long; 0.58 wide. Legs: dorsal proximal macroseta on tibia I, II, III and IV 1.68, 1.59, 2.05 and 2.27 times diameter of tibia, respectively; Tm I: 0.66. Chelicerae: stridulatory striae similar to male. Epigyne: Clade 13 characteristic morphology, borders between dorsal and ventral plates converging anteriorly, copulatory duct of median length (Fig. 11F–H). Opisthosoma: brown, evenly coloured.

Variation: Measurements are based on 10♂1♀ (Merdia herga) and 8♀ (Tekouan).

Males (N = 10, means in parentheses): Total length 1.84–2.06 (1.93). Prosoma: 0.82–0.91 (0.87) long, 0.66–0.73 (0.69) wide. Legs: dorsal proximal macroseta on tibia I, II, III and IV 1.24–1.78 (1.47, N = 9), 1.46–1.76 (1.59), 1.90–2.30 (2.11, N = 9) and 1.98–2.44 (2.21) times diameter of tibia, respectively; Tm I: 0.60–0.68 (0.64).

Females (N = 9, means in parentheses): Total length 2.10–2.69 (2.44). Prosoma: 0.97–1.07 (1.04) long, 0.77–0.88 (0.83) wide. Legs: dorsal proximal macroseta on tibia I, II, III and IV 1.58–1.92 (1.70), 1.41–1.90 (1.71), 1.86–2.20 (2.02) and 1.90–2.37 (2.13) times diameter of tibia, respectively; Tm I: 0.56–0.71 (0.65).

Distribution: Spain, Morocco, Algeria, Tunisia.

Habitat: Marshes, salt meadows, wet meadows, lake shores, riversides.

OEDOTHORAX TRILOBATUS (BANKS, 1896)

(FIGS 7P, 8B, 9B, 17; SUPPORTING INFORMATION, FIG. S1B)

Dicyphus trilobatus Banks, 1896: 64 (Dm).*Hypomma trilobata* Crosby, 1905: 310.*Lophocarenum trilobatum* Emerton, 1909: 191, pl. 3, fig. 1 (m).*Oedothorax trilobatus* Bishop & Crosby, 1935: 268, pl. 22, figs 7, 8 (m, Df).*Oedothorax trilobatus* Paquin & Dupérré, 2003: 115, figs 1190–1193 (mf).*Oedothorax trilobatus* Marusik et al., 2010: 287, figs 3–11 (mf).

Type material: Bishop & Crosby (1935) stated that the type locality was Ithaca, New York, but no type designation data was provided by Banks (1896). The original and subsequent descriptions, nevertheless, make the identification of this species unequivocal.

Examined material: USA: New York, McLean 2♂ 8.v.1919 (AMNH); Laborador Pond, 1♂ 14.v.1921,

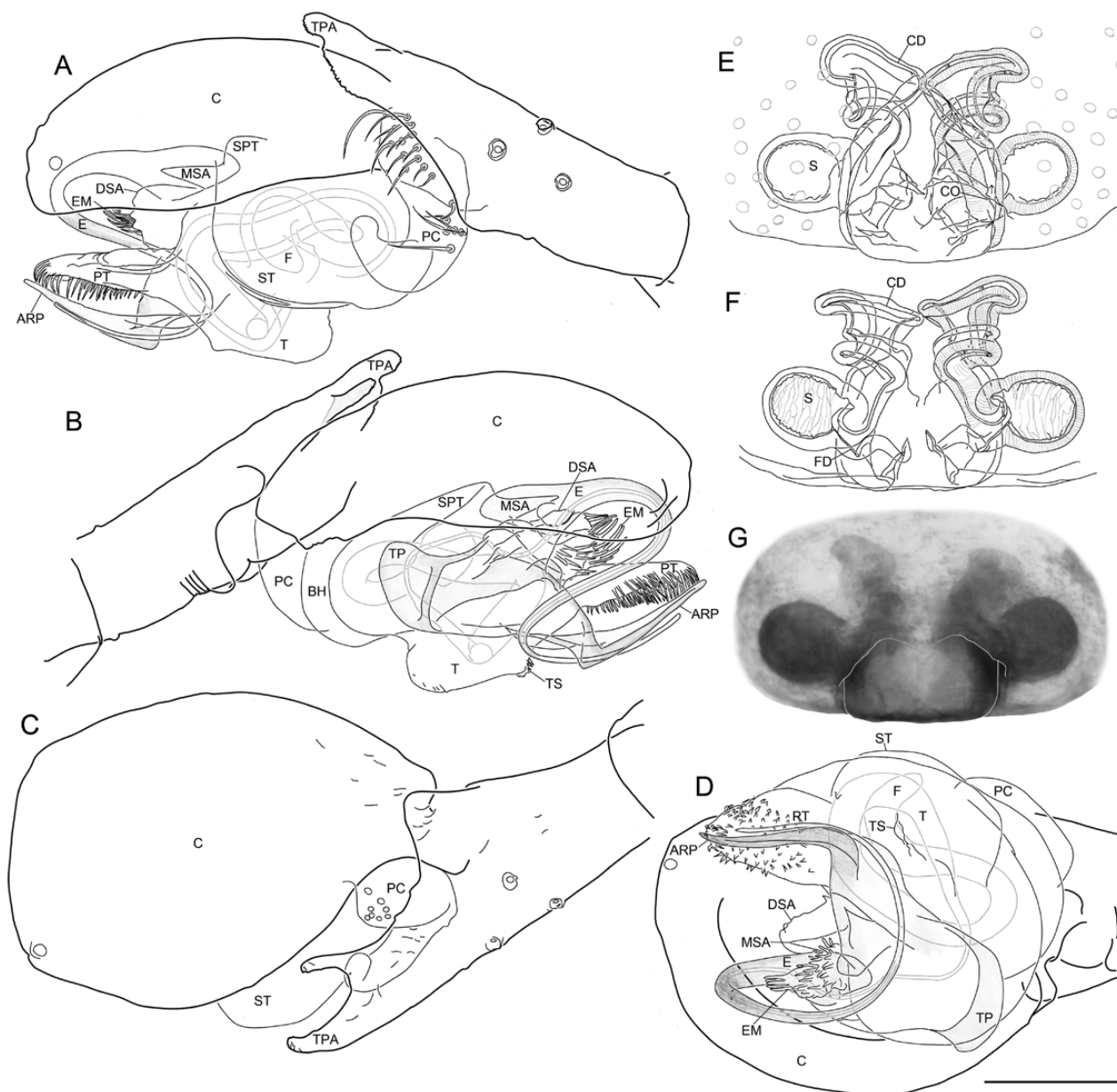


Figure 17. *Oedothorax trilobatus* (Banks, 1896). A–D, male left palp. A, retrolateral view. B, prolateral view. C, dorsal view. D, ventral view. E–G, epigyne. E, ventral view. F, dorsal view. G, external morphology. Scale bar 0.1 mm.

Beside other somatic characteristics mentioned in their description and common to many erigonine genera, the distinctive feature of these three species is the two longitudinal dense clusters of setae with particular morphology at the interocular region of the male. Holm (1962) described a number of new species of *Callitrichia* and added descriptions of the palps, including the enlarged terminal part of paracymbium and the short, stout, curved embolus, which is connected to a 'scaphium' (i.e. radix) with two distal apophyses (i.e. anterior radical process and ventral radical process). Based on similarities in, for example, metatarsal trichobothria, epigyne structure, eye arrangement and embolic division, he suggested that *Callitrichia* has a close relationship with *Oedothorax*, although the embolus is slender and the ventral radical process is absent in the latter genus. He also elaborated on the close relationship between *Toschia* and *Oedothorax*, as previously pointed out by di Caporiacco (1949), and further proposed some differences between them, such as the distally wide paracymbium. However, the similarity between *Callitrichia* and *Toschia* in their embolic division was not mentioned.

Scharff (1990a) briefly addressed the issues about the subsequently proposed synonymies, one among *Oedothorax*, *Callitrichia* and *Toschia* by Wunderlich (1978) and the other between *Callitrichia* and *Atypena* (Jocqué, 1983), and argued in favour of treating all taxa as separate genera until a complete revision of all genera has been done. He also suggested a close relationship of *Ophrynia* with the above-mentioned genera based on resemblance in the shape of the embolic division. However, he stated that the paracymbium of *Ophrynia* differed significantly from that of those genera, although this may only be true for species like *Ca. infecta* (Jocqué & Scharff, 1986) **comb. nov.** (fig. 128 in Jocqué & Scharff, 1986) and *Ca. uncata* (Jocqué & Scharff, 1986) **comb. nov.** (Fig. 18A, arrow), both with the terminal area of the paracymbium ventrodistally extended (pers. obs.). In our view, the distally wide paracymbium of other *Ophrynia* species, including the type species *Ca. superciliosa* (Jocqué, 1981) **comb. nov.**, resembles considerably that of *Callitrichia* and *Toschia*, which in turn is different from the narrow terminal part of the paracymbium of *Oedothorax* species from the Palearctic realm.

Although the type species *Ca. hamifera* was not included in our analysis, we consider *Ca. sellafrontis* a suitable representative due to its many shared features with *Ca. hamifera*, including two cluster of special dense setae at interocular region, posterior median eye lobe (Fig. 19H; fig. 53c, d in Holm, 1962), male palpal tibial apophysis shape (Fig. 20A–C; fig. 53a, b in Holm, 1962), paracymbium shape (Fig. 20A; fig. 54c in Holm, 1962), protégulum morphology (Fig. 20D; fig. 21a in Fage & Simon, 1936), the shape of

embolic division (Fig. 20B; fig. 54a in Holm, 1962), and the shape of epigyne (Fig. 20F; fig. 53e in Holm, 1962). We also consider *Ca. uncata* and *Ca. juguma* (Scharff, 1990) **comb. nov.** valid representatives for *Ophrynia*, since they share the following common male features with the type species of *Ophrynia* (*Ca. superciliosa*): inter-AME-PME groove; palpal tibial prolateral apophysis broad, flat, with a retrolateral branch; embolic division with a moderate, poorly sclerotized ventral radical process and a round tip of radical tail piece. Furthermore, *Ca. juguma* resembles *Ca. superciliosa* especially by the dentate tips of the bifid palpal tibial apophysis (Fig. 21A, C; figs 39, 40 in Jocqué, 1981), enlarged terminal part of paracymbium without extended ventrodistal angle (Fig. 21A; fig. 39 in Jocqué, 1981, in contrast to *Ca. uncata*, Fig. 18A), bifid anterior radical process (Fig. 21B; fig. 41 in Jocqué, 1981), papillae on ventral radical process, and perpendicular lateral setae on metatarsi and tarsi of legs I and II of the male, which is the only proposed synapomorphy of *Ophrynia* (Scharff, 1990a).

The results of our phylogenetic analysis placed the two original *Ophrynia* species as sister to *Ca. sellafrontis*. Features supporting this relationship are related to the reduction of spinnerets gland spigots, including the absence of the aciniform and the minor ampullate gland spigots, as well as the absence of the aggregated gland spigot (also in *Ca. convector*). This high degree of reduction of spigots has not been seen in other studied species so far. This close relationship between the original *Ophrynia* species and *Ca. sellafrontis* renders the remaining *Callitrichia* species a paraphyletic assemblage. The truncated protégulum is a newly proposed synapomorphy of the redefined *Callitricha*.

The original generic description of *Toschia* by di Caporiacco (1949) included two species, and proposed several features that are not unique for the current members described under *Toschia* to date. Holm's (1962) account for this genus also includes diagnostic characteristics not exclusive to *Toschia* (e.g. lack of carapace modification), and states that the cheliceral stridulatory organ of the type species of *Toschia* (namely *Ca. picta* (Caporiacco, 1949) **comb. nov.**) is absent. However, our observations refute this previous statement; the cheliceral stridulatory organ is present in *Toschia* (see Fig. 22D). Jocqué (1984) mentioned the need of a detailed study of the male palp, given the difficulty to place species with certainty to either *Toschia*, *Atypena* [proposed by Jocqué (1983) as a senior synonym of *Callitrichia*] or *Oedothorax*. Interestingly, however, he assigned *Ca. minuta* (Jocqué, 1984) **comb. nov.** to *Toschia* based on the distally wide paracymbium, a common feature shared by many *Callitrichia* species. Additionally, *Ca. minuta* share with *Ca. legrandi* (Jocqué, 1985) **comb. nov.** the vertical palpal tibial apophysis, the small apophysis retrolateral to it, the

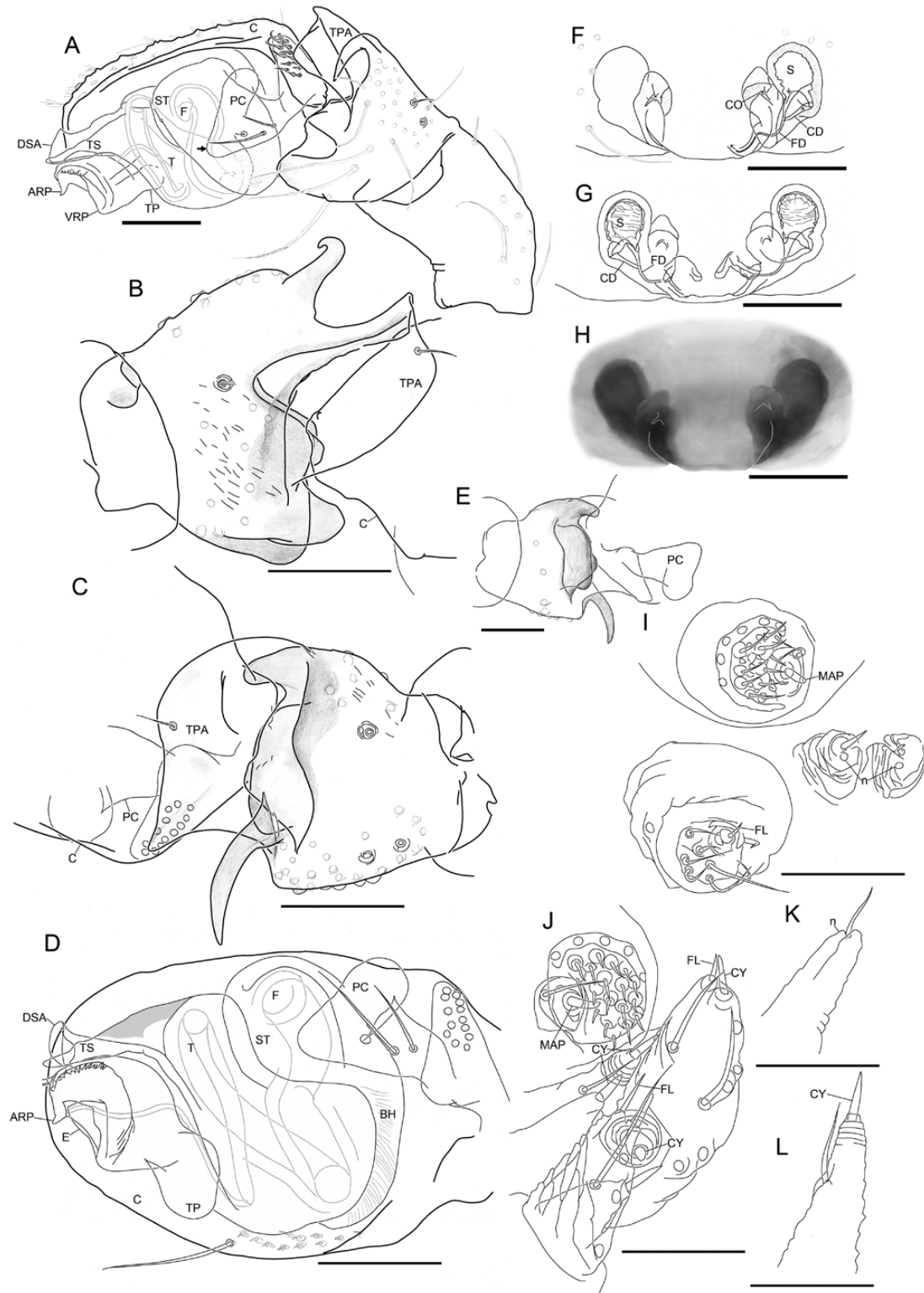


Figure 18. *Callitrichia uncata* (Jocqué & Scharff, 1986). A–E, male right palp, images flipped horizontally. A, ventroretrolateral view. B, ventral view. C, tibia, dorsal view. D, tibia, prolateral view. E, tibia, ventral view. F–H, epigyne. F, ventral view. G, dorsal view. H, external morphology. I, male spinnerets. J, female spinnerets. K, male left posterior median spinneret. L, female left posterior median spinneret. Scale bars 0.1 mm.

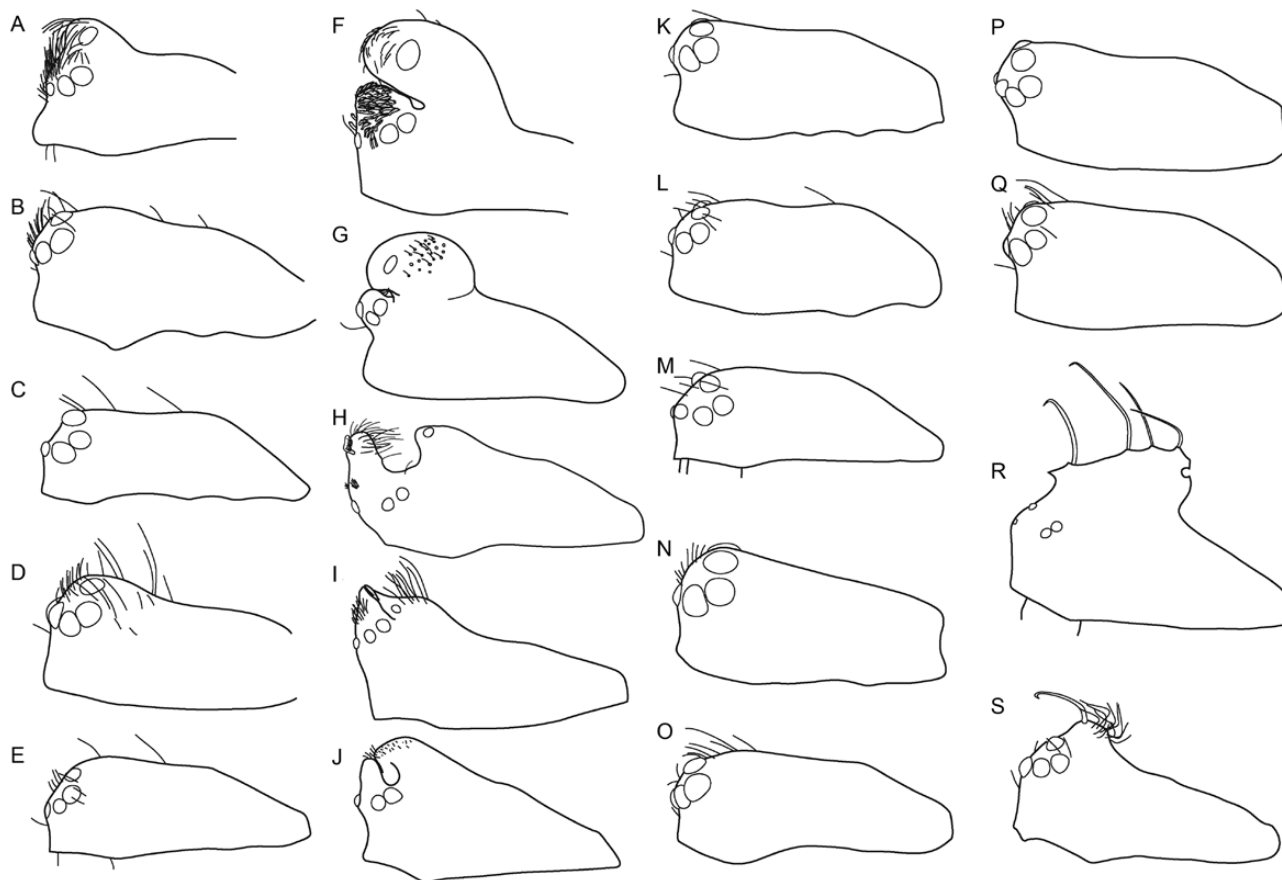


Figure 19. Male prosomal morphology, lateral. A, *Oedothorax meghalaya* Tanasevitch, 2015 (traced from photograph). B, *Oe. uncus* Tanasevitch, 2015 (traced from photograph). C, *Holmelgonia basalis* Jocqué & Scharff, 1986 (Jocqué & Scharff, 1986, fig. 18). D, *Callitrichia holmi* (Wunderlich, 1978) (traced from photograph). E, *Ca. picta* (Caporiacco, 1949) (Holm 1962, fig. 58). F, *Ca. gloriosa* (Jocqué, 1984) (traced from photograph). G, *Ca. convector* Tanasevitch, 2014 (traced from photograph). H, *Ca. sellafrontis* Scharff, 1990 (traced from photograph). I, *Ca. juguma* (Scharff, 1990) (Scharff 1990a, fig. 164). J, *Ca. uncata* (Jocqué & Scharff, 1986) (Jocqué & Scharff, 1986, fig. 130). K, *Ca. pilosa* (Wunderlich, 1978) (traced from photograph). L, *Ca. usitata* (Jocqué & Scharff, 1986) (traced from photograph). M, *Ca. legrandi* (Jocqué, 1985) (Jocqué, 1985, fig. 21). N, *Ca. macrophthalma* (Locket & Russell-Smith, 1980) (traced from photograph). O, *Ca. muscicola* (Bosmans, 1988) (traced from photograph). P, *Ca. latitibialis* (Bosmans, 1988) (traced from photograph). Q, *Ca. longiducta* (Bosmans, 1988) (traced from photograph). R, *Nasoona setifera* (Tanasevitch, 1998) (Tanasevitch, 1998a, fig. 3). S, *N. crucifera* (Thorell, 1895) (Tu & Li, 2004, fig. 6A).

absence of ventral radical process, the less enlarged terminal part of paracymbium, and the smaller body size. We provisionally transfer *Toschia spinosa* Holm, 1968 to *Holmelgonia* (but see below) based on the presence of a central embolar apophysis (fig. 28 in Holm, 1968), a feature shared with the type species *Ho. nemoralis* (Holm, 1962) [fig. 55 in Jocqué & Scharff (1986) and other *Holmelgonia* species, and absent in *Callitrichia*]. In addition, despite the lack of detail in the original palpal drawing of *Toschia celans* Gao et al., 1996, some features can be recognized, such as the embolic division with a radix not connected to the embolus via a membrane, and the paracymbium base covered by the retrolateral apophysis (absent in other species of *Toschia*). Given that these palpal features are

significantly different from the general configuration of *Callitrichia*, and that all type specimens for this species are seemingly lost (therefore, no further inspection is possible), we conclude that this species is most likely misplaced in *Toschia*, and we provisionally transfer it to *Callitrichia* [*Ca. celans* (Gao et al., 1996) **comb. nov. incertae sedis**]. Remaining *Toschia* species can be confidently transferred to *Callitrichia* according to inspection of the figures in their original descriptions by Holm (1962), Jocqué (1981) and Jocqué & Scharff (1986).

Jocqué (1984) questioned the generic position of *Typhistes gloriosus* based on a unique 'long downpointing apophysis' (i.e. the ventral radical process as defined in the present study) among other features. He also proposed that the genus *Typhistes*

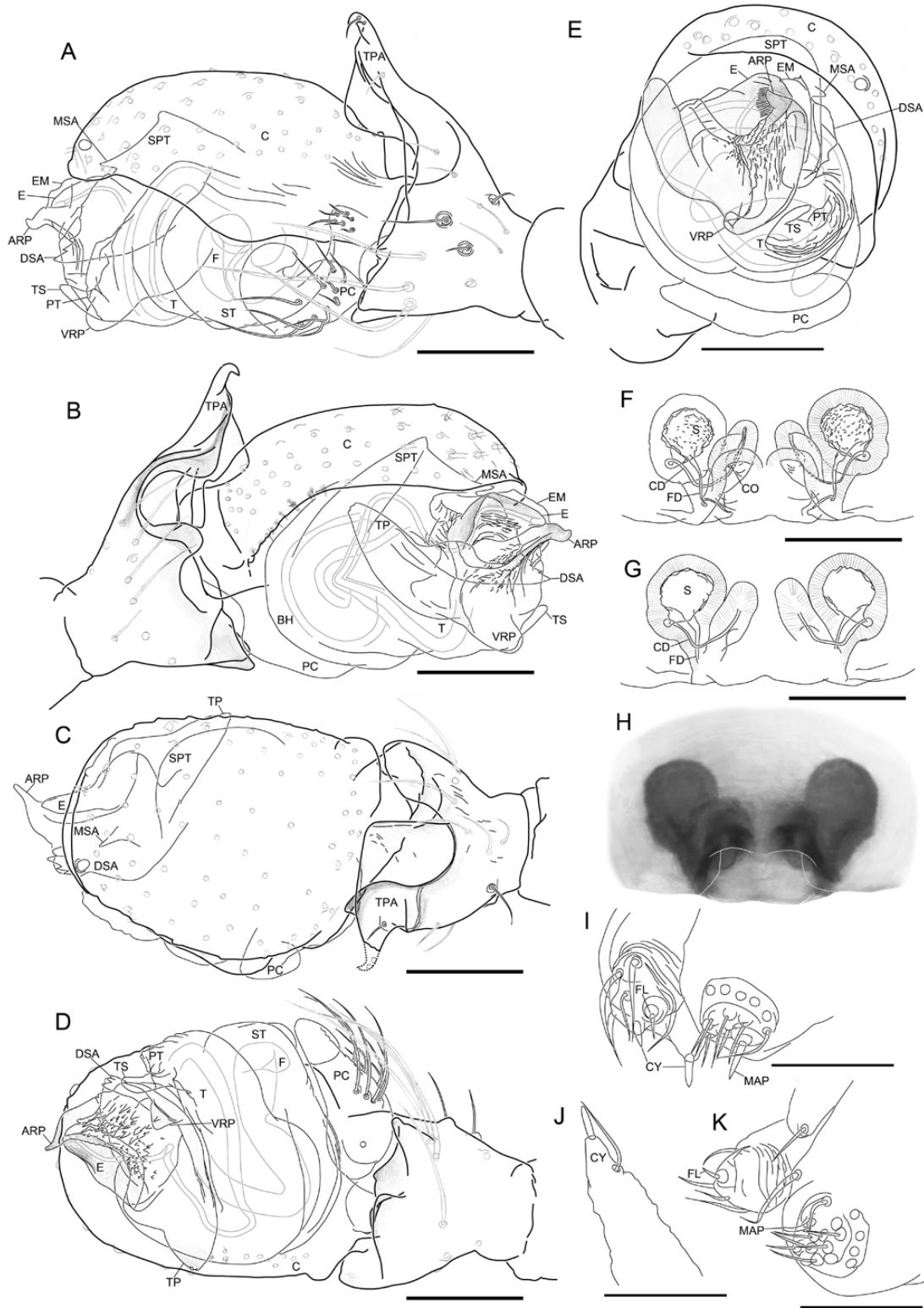


Figure 20. *Callitrichia sellafrontis* Scharff, 1990. A–D, male left palp. A, retrolateral view. B, prolateral view. C, dorsal view. D, ventral view. E, male right palp, apical view, image horizontally flipped. F–H, epigyne. F, ventral view. G, dorsal view. H, external morphology. I, female right anterior lateral spinneret and posterior lateral spinneret. J, female right posterior median spinneret, dorsal view. K, male left spinnerets. Scale bars 0.1 mm.

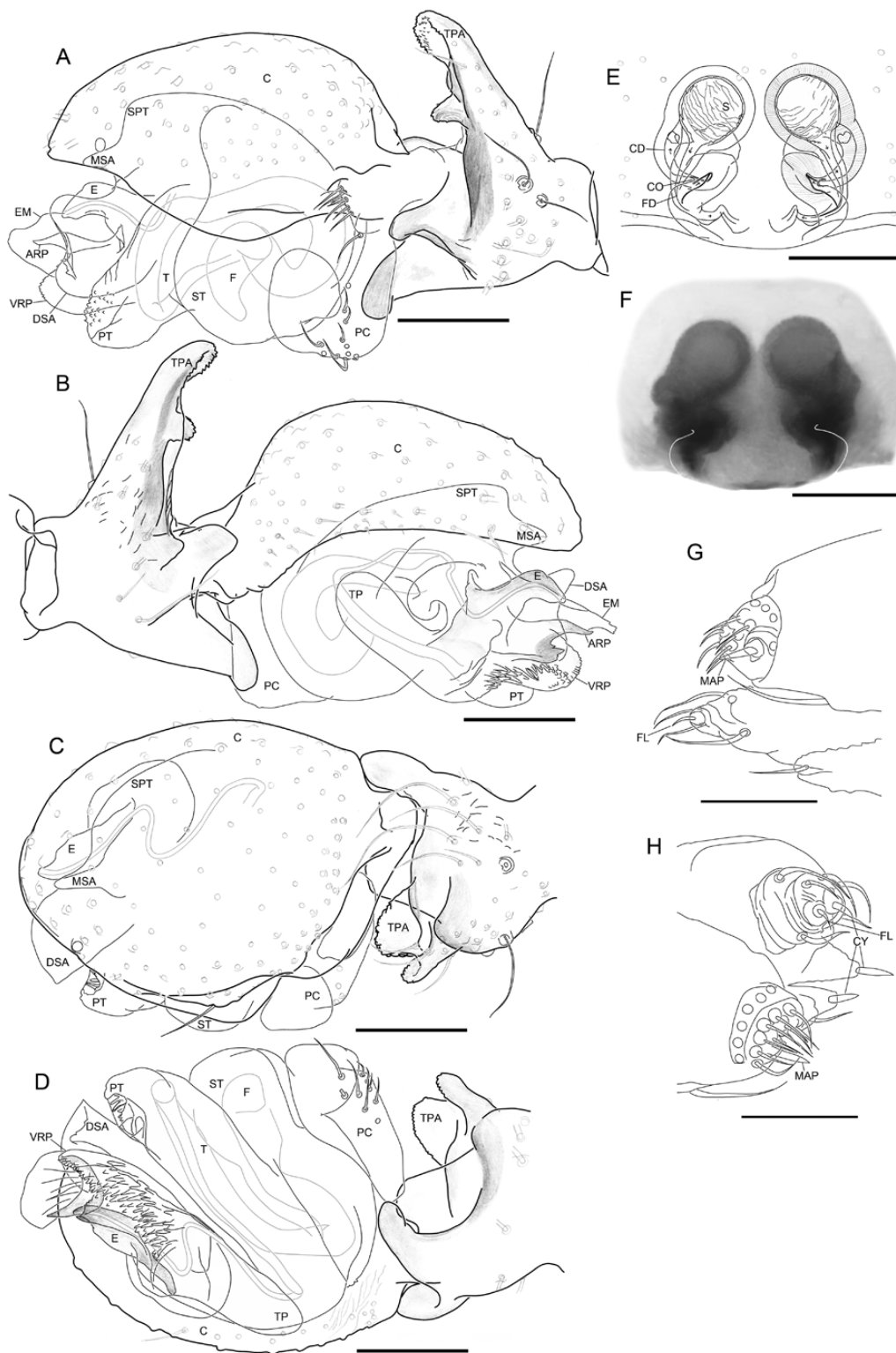


Figure 21. *Callitrichia juguma* (Scharff, 1990). A–D, male left palp. A, retrolateral view. B, prolateral view. C, dorsal view. D, ventral view. E, F, epigyne. E, ventral view. F, external morphology. G, male right spinnerets. H, female left spinnerets. Scale bars 0.1 mm.



Figure 22. Male chelicerae, stridulatory striae on lateral side. A, *'Oedothorax' meghalaya*. B, *'Oe.' uncus*. C, *Holmelgonia basalis*. D, *Callitrichia holmi*. E, *Ca. picta*. F, *Ca. gloriosa*. G, *Ca. convector*. H, *Ca. sellafrontis*. I, *Ca. juguma*. J, *Ca. uncata*. K, *Ca. pilosa*. L, *Ca. usitata*. M, *Ca. legrandi*. N, *Ca. macrophthalma*. O, *Ca. muscicola*. P, *Ca. latitibialis*. Q, *Ca. longiducta*. R, *Nasoona setifera*. S, *N. crucifera*. Scale bars 0.05 mm.

is closely related to *Oedothorax* and *Atypena* (i.e. as *Callitrichia*). The results of our phylogenetic analysis are in agreement with [Jocqué \(1984\)](#), placing *Typhistes gloriosus* within *Callitrichia*; we therefore transfer this species to *Callitrichia* as *Ca. gloriosa* ([Jocqué, 1984](#)) **comb. nov.**

Monophyly: This genus is supported by the following two unambiguous character transformations: the distal part of the protogulum forming a rim (Ch 38, synapomorphic) and the number of aciniform gland spigots on posterior lateral spinneret equal to, or more than, three (Ch 116, homoplastic).

Diagnosis: *Callitrichia* is similar to other taxa in Clade 13 in the palpal morphology and other somatic features, but is characterized and can be distinguished by the following combination of palpal and epigynal features:

1. Paracymbium: median- to large-sized; base covered by cymbial basal retrolateral extension from dorsal view (invisible from dorsal view in *Oedothorax*); terminal part moderately to greatly enlarged (slender in *Oedothorax*; moderately enlarged in *Mitrager*); distal setae group with distal position (with middle position in *Oedothorax*); distal clasp anteriorly extended, without striae (retrolaterally extended and/or with striae in many *Mitrager*).
2. Copulatory bulb: embolus retrolaterally curved, short, usually stout, basal protuberance absent (prolaterally curved, with basal protuberance in *Oedothorax*); embolic membrane flat, with few or no papillae (cylindrical in *Oedothorax*); embolus–radix membranous region not extended to prolateral side of radix (extended to prolateral side in *Oedothorax*); ventral radical process present in most species [except *Ca. macrophthalma* ([Locket & Russell-Smith, 1980](#)) **comb. nov.**, *Ca. legrandi* and *Ca. paralegrandi* ([Tanasevitch, 2016](#)) **comb. nov.**] (absent in *Oedothorax* and most *Mitrager* species), degree of extension varies from low [e.g. *Ca. holmi* ([Wunderlich, 1978](#)) **comb. nov.**, *Ca. uncata*] to high [*Ca. gloriosa*, *Ca. pileata* ([Jocqué & Scharff, 1986](#)) **comb. nov.**]; in many species, radix with papillae in area between anterior radical process and ventral radical process [radical papillae absent in *Oedothorax*, *Atypena* and *Mitrager*, except *M. clypeellum* ([Tanasevitch, 1998](#)) **comb. nov.**]; lateral extension of radix absent (except in *Ca. macrophthalma* and *Ca. convector*); tegular papillae absent; central emboliar apophysis absent (present in *Ho. basalis*); marginal suprategular apophysis present, distal suprategular

apophysis straight, distally oriented, mostly round at tip.

3. Palpal tibia: prolateral apophysis ranges from vertically highly extended (e.g. *Ca. sellafrontis*) to low (e.g. *Ca. legrandi*) (not vertically extended in *Oedothorax* and most *Mitrager*, except *M. noordami*); retrolateral apophysis inconspicuous (conspicuous in *Mitrager*, *Atypena* and some '*Oedothorax*' *incertae sedis*).
4. Epigyne: different from *Oedothorax* in that the entrance of copulatory ducts into the spermathecae are ectal to the exits of fertilization ducts from the spermathecae.

Description: The genus includes medium-sized erigonines with a mostly variegated opisthosoma [except *Ca. latitibialis* ([Bosmans, 1988](#)) **comb. nov.**, *Ca. legrandi*, *Ca. longiducta* ([Bosmans, 1988](#)) **comb. nov.**, *Ca. macrophthalma*, *Ca. monoceros* ([Miller, 1970](#)) **comb. nov.**, *Ca. monticola* ([Tullgren, 1910](#)), *Ca. muscicola* ([Bosmans, 1988](#)) **comb. nov.**, *Ca. obtusifrons* [Miller, 1970](#), *Ca. paralegrandi* and *Ca. pilosa* ([Wunderlich, 1978](#)) **comb. nov.**]. Male prosoma varies in degree of modification, ranging from absent to prominent PME hump, inter-AME-PME groove and inter-AME-PME lobe. One sub-AME seta. Chelicerae of normal form and size, without mastidia. This genus also shares those features defining Clade 13 (see above). For palpal and epigynal feature see diagnosis.

Species included: The genus comprise 55 species and one subspecies as follows. Twenty-two species originally placed in *Callitrichia*: *Ca. afromontana* [Scharff, 1990](#), *Ca. aliena* [Holm, 1962](#), *Ca. cacuminata* [Holm, 1962](#), *Ca. crinigera* [Scharff, 1990](#), *Ca. glabriceps* [Holm, 1962](#), *Ca. hamifera*, *Ca. inacuminata* [Bosmans, 1977](#), *Ca. incerta* [Miller, 1970](#), *Ca. kenya* [Fage, 1936](#), *Ca. marakweti* [Fage, 1936](#), *Ca. meruensis* [Holm, 1962](#), *Ca. mira* ([Jocqué & Scharff, 1986](#)), *Ca. monticola*, *Ca. obtusifrons*, *Ca. paludicola* [Holm, 1962](#), *Ca. pileata* ([Jocqué & Scharff, 1986](#)), *Ca. hirsuta* **nom. nov.** ([Jocqué & Scharff, 1986](#)), *Ca. ruwenzoriensis* [Holm, 1962](#), *Ca. sellafrontis*, *Ca. silvatica* [Holm, 1962](#), *Ca. taeniata* [Holm, 1968](#) and *Ca. turrita* [Holm, 1962](#).

Twelve species (plus one subspecies) here transferred from *Ophrynia*: *Ca. galeata* ([Jocqué & Scharff, 1986](#)) **comb. nov.**, *Ca. galeata lukwangulensis* ([Jocqué & Scharff, 1986](#)) **comb. nov.**, *Ca. infecta* **comb. nov.**, *Ca. insulana* ([Scharff, 1990](#)) **comb. nov.**, *Ca. juguma* **comb. nov.**, *Ca. perspicua* ([Scharff, 1990](#)) **comb. nov.**, *Ca. revelatrix* ([Jocqué & Scharff, 1986](#)) **comb. nov.**, *Ca. rostrata* ([Jocqué & Scharff, 1986](#))

comb. nov., *Ca. summicola* (Jocqué & Scharff, 1986)
comb. nov., *Ca. superciliosa*, *Ca. trituberculata*
 (Bosmans, 1988) **comb. nov.**, *Ca. truncatula*
 (Scharff, 1990) **comb. nov.**, *Ca. uncata*.

Eight species here transferred from *Toschia*: *Ca. aberdarensis* (Holm, 1962) **comb. nov.**, *Ca. casta* (Jocqué & Scharff, 1986) **comb. nov.**, *Ca. concolor* (Caporiacco, 1949) **comb. nov.**, *Ca. cypericola* (Jocqué, 1981) **comb. nov.**, *Ca. minuta*, *Ca. picta*, *Ca. telekii* (Holm, 1962) **comb. nov.** and *Ca. virgo* (Jocqué & Scharff, 1986) **comb. nov.**

Eleven species here transferred from *Oedothorax*: *Ca. convector*, *Ca. holmi* (= *Ca. simplex* (Jocqué & Scharff, 1986), *synon. nov.*), *Ca. latitibialis*, *Ca. legrandi*, *Ca. longiducta*, *Ca. muscicola*, *Ca. pilosa*, *Ca. paralegrandi*, *Ca. monoceros*, *Ca. macrophthalma* and *Ca. usitata*.

One species here transferred from *Toschia celans*: *Ca. gloriosa*.

One species misplaced in *Toschia* (*T. celans*) here transferred as *Ca. celans*.

The following species are here transferred to other genera: *Atypena formosana* (Oi, 1977) from *Callitrichia*; *Holmelgonia spinosa* (Holm, 1968) **comb. nov.** from *Toschia*.

Distribution: Tanzania, Malawi, Cameroon, Algeria, Kenya, Nigeria, Uganda, Angola, South Africa, Congo, Comoros, Ethiopia, India (Himalaya), Thailand.

Natural history: Species of this genus have been found in litter, low vegetations and under stones in habitats like montane rain forests, evergreen forests and gallery forests.

CALLITRICHIA CONVECTOR (TANASEVITCH, 2014)
COMB. NOV.

(FIGS 19G, 22G, 23, 24G)

Oedothorax convector Tanasevitch, 2014a: 408, figs 64–71 (Dm).

Type material: Holotype: **Thailand:** Chiang Mai Province, Chomthong District, Doi Inthanon, 1780 m, ♂ 3.iii.1987, leg. P. Schwendinger (MHNG, examined).

Diagnosis:

Males: This species can be recognized by the shape of prosomal modification with the inter-AME-PME

groove and PME lobe; it can be discriminated from *Oedothorax* s.s., *Mitrager* and other *Callitrichia* species by its palpal features including the presence of tibial retrolateral apophysis with setae (no setae in *Mitrager*), the absence of tibial prolateral trichobothrium, the shape of paracymbium (distal clasp particularly long and slender), and the radix without tail piece.

Description:

Male (holotype, MHN): Total length: 1.68. Prosoma: 0.75 long, 0.55 wide, PME on frontal side of elevated region, short curved setae grouped at both sides of dorsal surface of prosomal elevation behind PME, inter-PME-PLE groove, three pairs of strong setae at groove lower margin, no setae inside groove (Fig. 19G). Eyes: AME-AME: 0.03, AME width: 0.05, AME-ALE: 0.01, ALE width: 0.05, ALE-PLE: 0.01, PLE width: 0.05, PLE-PME: 0.10, PME width: 0.05, PME-PME: 0.18. Clypeus: not hirsute, one sub-AME seta, particularly long. Chelicerae: stridulatory striae rows wide and evenly spaced (Fig. 22G). Sternum: 0.46 long, 0.5 wide. Legs: dorsal proximal macroseta on tibia IV 3.13 times diameter of tibia; Tm I: 0.81. Pedipalp: TPA narrow, slightly curved; TRA extended anteriorly, covering PC base from retrolateral view; PC long, distal-setae-bearing middle part enlarged, distal clasp slender and long (Fig. 23A–C); T without papillae; PT slender and long, with scale-like papillae; TS long, with small papillae; MSA absent; DSA short and wide (Fig. 23H); EM short, without papillae, not exceeding ARP (Fig. 23E); R without TP, scaly region distributed from ARP to VRP; LER present; E prolaterally spiral, between ARP and LER (Fig. 23E, F, G). Opisthosoma: dorsal pattern see Fig. 24G; PMS with mAP, two AC; PLS with one FL, 3+ AC (Fig. 23I–K).

Female: Unknown

Distribution: Only known from the type locality in Thailand.

Habitat: No data.

CALLITRICHIA GLORIOSA (JOCQUÉ, 1984) **COMB. NOV.**
 (FIGS 19F, 22F, 24F, 25, 26E, F; SUPPORTING
 INFORMATION, FIG. S2D)

Typhistes gloriosus Jocqué, 1984: 136, figs 38–45 (Dmf).

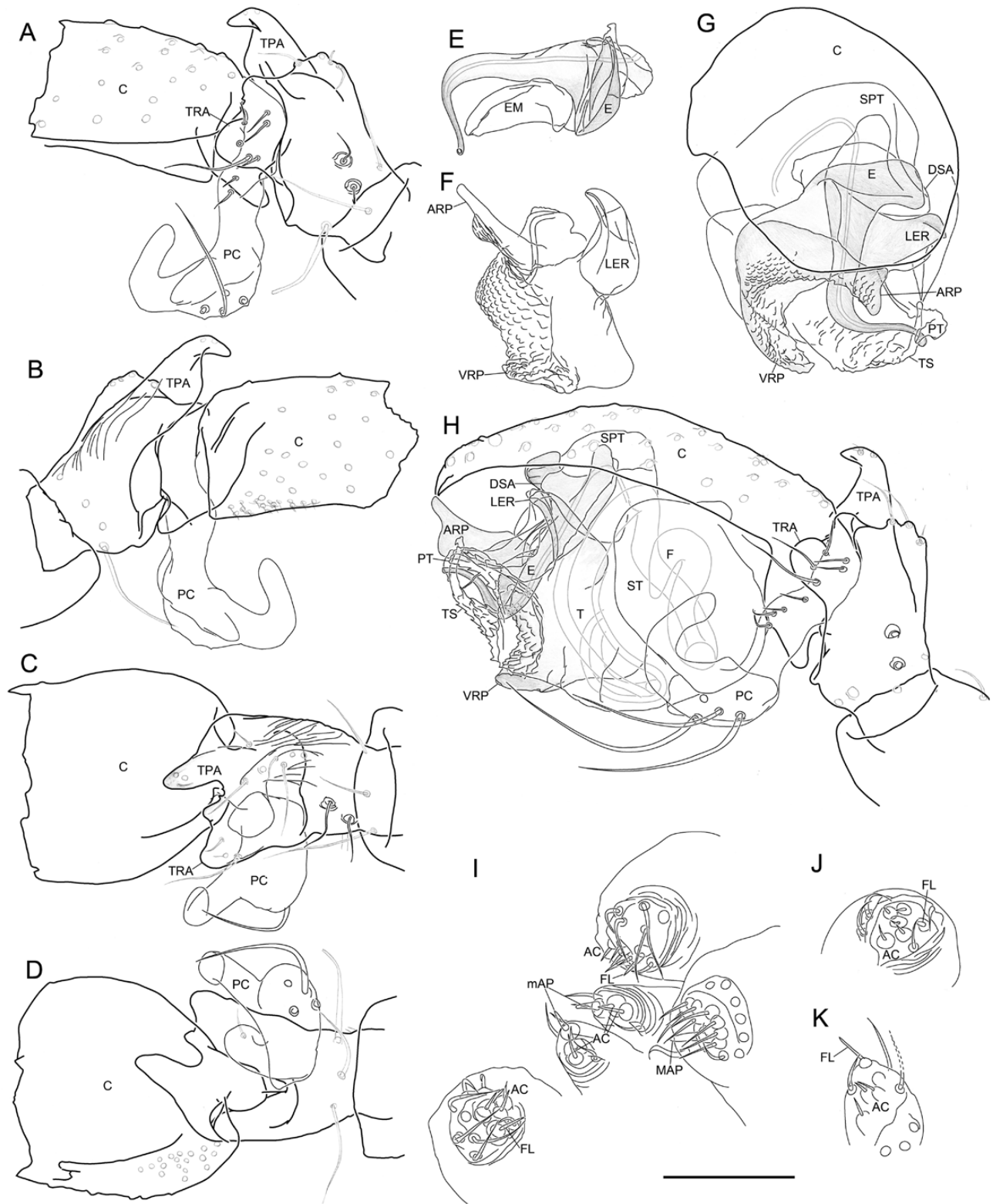


Figure 23. *Callitrichia convector* (Tanasevitch, 2014). A–F, male right palp, images flipped horizontally. A, retrolateral view. B, prolateral view. C, dorsal view. D, ventral view. E, embolus and median membrane, dorsal view. F, radix, apical view. G, H, male left palp. G, apical view. H, retrolateral view. I, male spinnerets. J, male right posterior lateral spinneret. K, male left posterior lateral spinneret. Scale bar 0.1 mm.

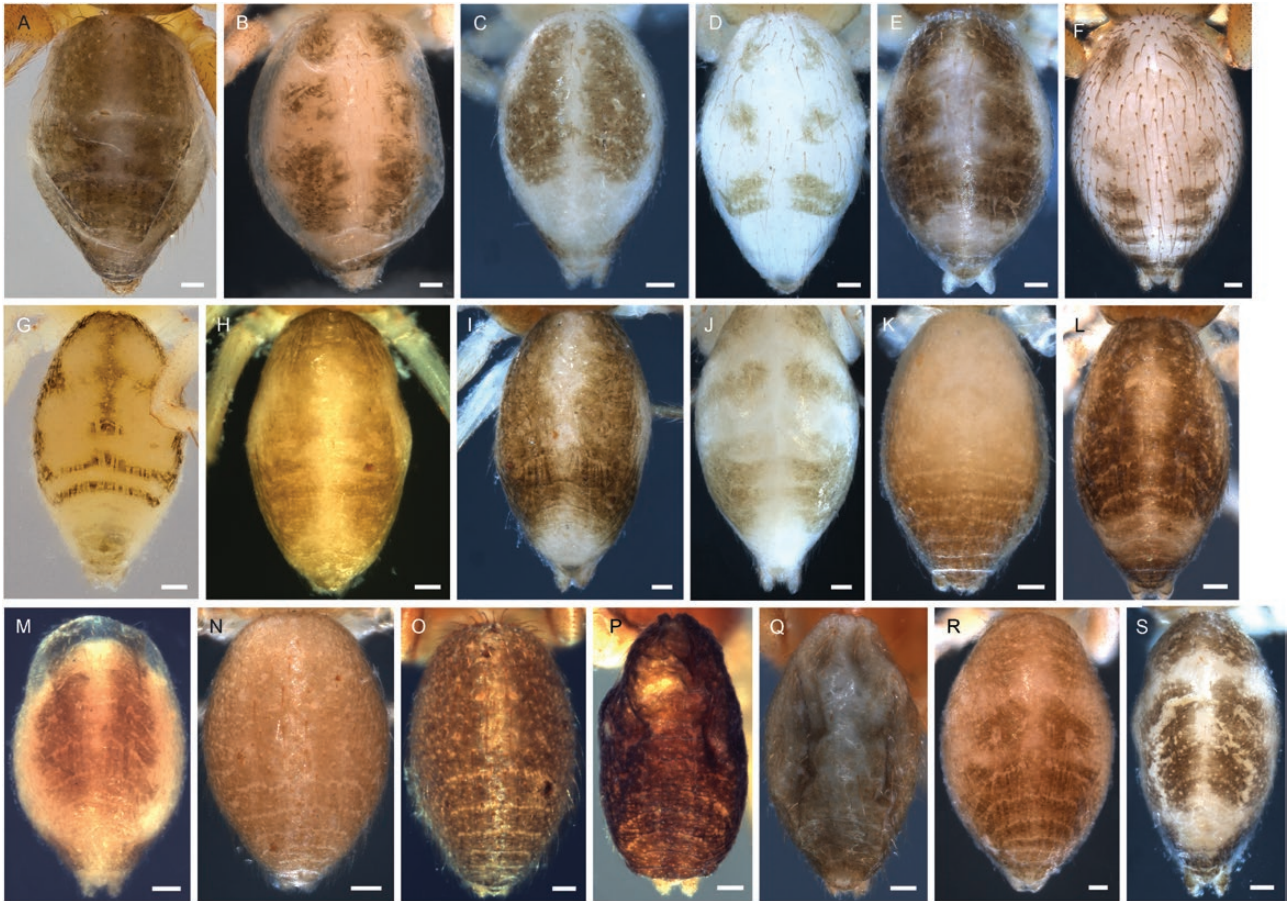


Figure 24. Male opisthosoma, dorsal view. A, '*Oedothorax*' *meghalaya* Tanasevitch, 2015. B, '*Oe.*' *uncus* Tanasevitch, 2015. C, *Holmelgonia basalis* Jocqué & Scharff, 1986. D, *Callitrichia holmi* (Wunderlich, 1978). E, *Ca. picta* (Caporiacco, 1949). F, *Ca. gloriosa* (Jocqué, 1984). G, *Ca. convector* Tanasevitch, 2014. H, *Ca. sellafrontis* Scharff, 1990. I, *Ca. juguma* (Scharff, 1990). J, *Ca. uncatata* (Jocqué & Scharff, 1986). K, *Ca. pilosa* (Wunderlich, 1978). L, *Ca. usitata* (Jocqué & Scharff, 1986). M, *Ca. legrandi* (Jocqué, 1985). N, *Ca. macrophthalma* (Lockett & Russell-Smith, 1980). O, *Ca. muscicola* (Bosmans, 1988). P, *Ca. latitibialis* (Bosmans, 1988). Q, *Ca. longiducta* (Bosmans, 1988). R, *Nasoonia setifera* (Tanasevitch, 1998). S, *N. crucifera* (Thorell, 1895). Scale bars 0.1 mm.

Examined material: South Africa, Eastern Cape Province, Kei Mouth. litter in costal forest, 3♂1♀ 12.xii.2002, Rec. Haddad C. (RMCA).

Diagnosis:

Males: This species, together with *Ca. obtusifrons* and *Ca. trituberculata*, can be distinguished from other *Callitrichia*, *Mitrager* and *Oedothorax* species by their unique palpal tibia prolateral apophysis morphology; this species can be further distinguished from *Ca. trituberculata* by its less externally protruded distal-setae-bearing part of paracymbium (extremely protruded in the latter species, see fig. 7D in Bosmans, 1988) and the position of the posterior median eyes close to the top of the PME lobe (at basal position

directly behind the posterior lateral eyes in the latter species, see fig. 7A in Bosmans, 1988); and from *Ca. obtusifrons* by its less distal distribution of the retrolateral denticles on the palpal tibial prolateral apophysis (distally distributed in the latter species, see plate 25, fig. 4 in Miller, 1970).

Females: Similar to *Ca. obtusifrons* and *Ca. trituberculata* in the epigyne morphology, in which the central part of the dorsal plate is separated from the ventral plate by a transverse ridge [clearly visible in fig. 4, plate 26 in Miller (1970); slightly recognizable in fig. 7G in Bosmans (1988)], but can be distinguished from the latter two by the broad posterior margin of the dorsal plate, which is about as broad as the width of the spermathecae (Fig. 25G, H).

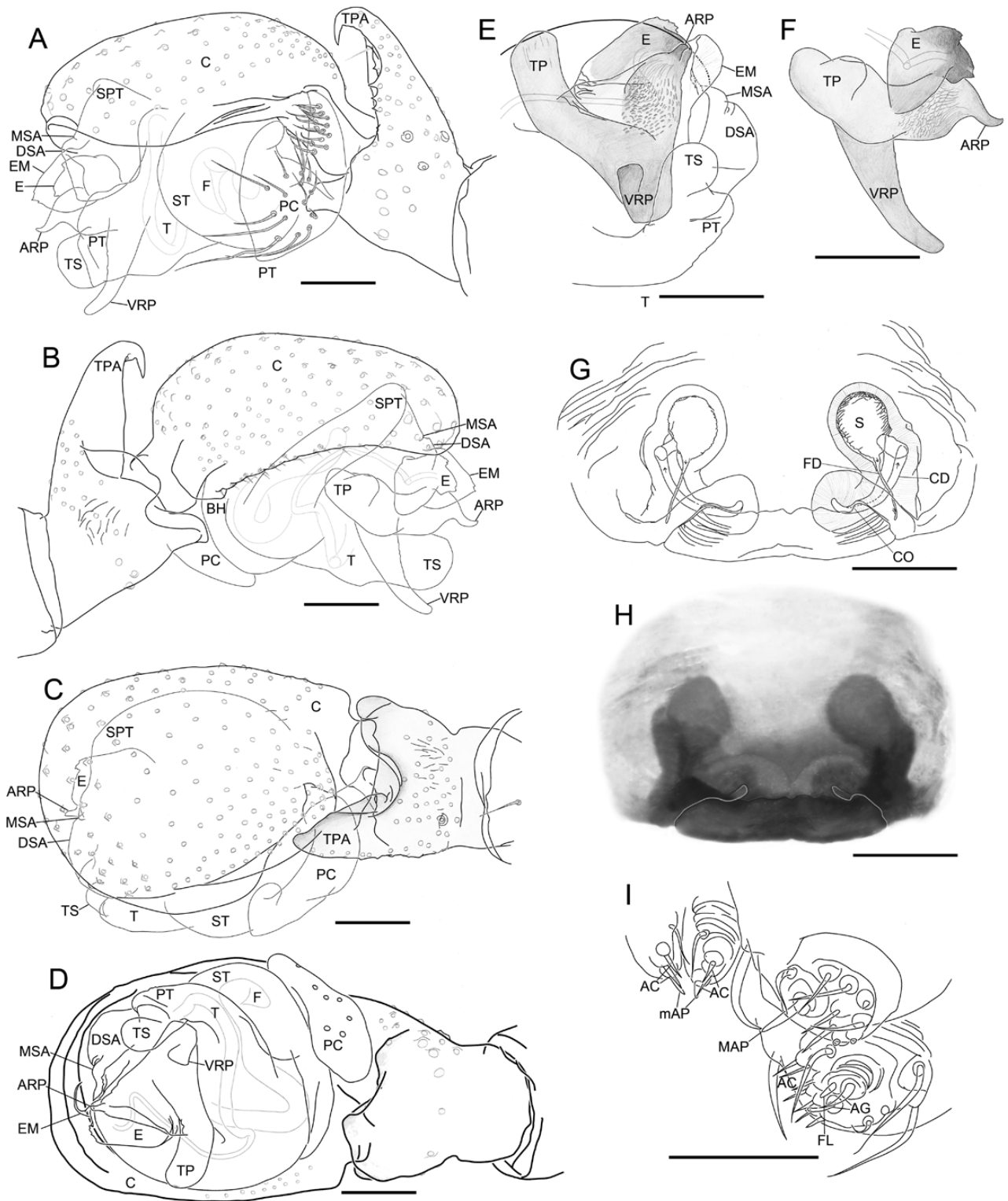


Figure 25. *Callitrichia gloriosa* (Jocqué, 1984). A–F, male left palp. A, retrolateral view. B, proateral view. C, dorsal view. D, ventral view. E, F, embolic division E, ventral view. F, proateral view. G, H, epigyne. G, ventral view. H, external morphology. I, male spinnerets. Scale bars 0.1 mm.

Description:

Male (RMCA): Total length: 2.82. Prosoma: 1.28 long, 0.92 wide, PME area largely elevated, with inter-AME-PME groove, interocular region anterior to inter-AME-PME groove with branched setae laterally oriented (Figs 19F, 26E, F). Eyes: AME-AME: 0.03, AME width: 0.06, AME-ALE: 0.1, ALE width: 0.1, ALE-PLE: 0, PLE width: 0.08, PLE-PME: 0.22, PME width: 0.09, PME-PME: 0.3. Clypeus: hirsute. Sternum: 0.69 long, 0.64 wide. Chelicerae: mastidia absent; stridulatory striae ridged, rows compressed and evenly spaced (Fig. 22F). Legs: dorsal proximal macroseta on tibia I, II, III and IV 0.56, 0.62, 1 and 2.59 times diameter of tibia, respectively; Tm I: 0.58. Pedipalp: TPA large, broad at base, narrow distally, pointed downward at tip, with several denticles on retrolateral side (Fig. 25A, C); PC base not visible from dorsal view, distal setae close to distal clasp, terminal part broad, distal clasp extended apically (Fig. 25A); T without papillae, PT truncated, apical part without papillae; TS short, thick (Fig. 25A, D); MSA small; DSA wide, truncated at tip (Fig. 25A); EM broad and flat, with few small papillae at distal margin, not exceeding ARP; ARP pointed; LER absent; VRP long; scaly papillae at upper half of area between

ARP and VRP; TP round at tip; E short and stout, slightly retrolaterally curved, median part dorsally elevated, with small protuberances (Fig. 25E, F). Opisthosoma: dorsal pattern see Fig. 24F; PMS with mAP, two AC; PLS with triad, 3+ AC (Fig. 25I).

Female (RMCA): Total length: 2.28. Prosoma: 1.20 long, 0.86 wide. Eyes: AME-AME: 0.02, AME width: 0.05, AME-ALE: 0.08, ALE width: 0.09, ALE-PLE: 0, PLE width: 0.09, PLE-PME: 0.8, PME width: 0.08, PME-PME: 0.08. Clypeus: not hirsute, one sub-AME seta. Sternum: 0.7 long, 0.64 wide. Legs: dorsal proximal macroseta on tibia I, II, III and IV 1.96, 2.22, 2.9 and 3.26 times diameter of tibia, respectively; Tm I: . Epigyne: Clade 13 characteristic morphology (Fig. 25G, H). Opisthosoma dorsal pattern same as male; PMS one CY, one mAP, two AC; PLS with triad, two CY, 3+ AC.

Distribution: South Africa.

Remarks: The male tibial apophysis, embolic division and prosomal modification of this species resemble those of *Ca. obtusifrons* and *Ca. trituberculata*. The description of [Bosmans \(1988\)](#) concerning the absence

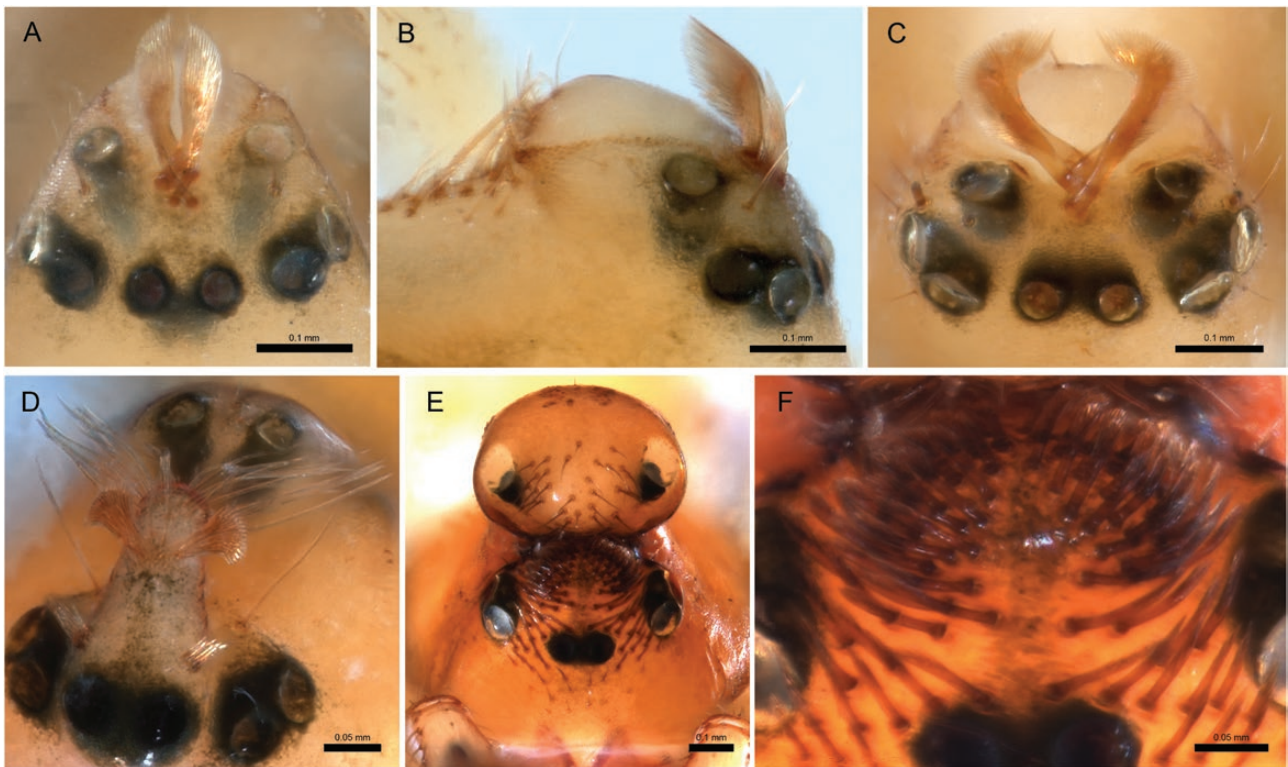


Figure 26. Branched setae at interocular region. A–B, *Mitrager angela* (Tanasevitch, 1998). A, frontal view. B, lateral view. C, *M. coronata* (Tanasevitch, 1998), frontal view. D, *Callitrichia sellafrontis* Scharff, 1990. E–F, *Ca. gloriosa* (Jocqué, 1984). E, overview. F, closer view.

of PME in *Ca. trituberculata* male contradicts his drawing of male prosoma, lateral view, where PME was depicted (fig. 7A in [Bosmans, 1988](#)). Following the results of our phylogenetic analysis, this species is transferred to *Callitrichia*, a placement also consistent with the morphological traits of the species.

CALLITRICHIA HIRSUTA NOM. NOV.

Atypena pilosa [Jocqué & Scharff, 1986](#): 23, figs 62–66 (Dm).

Callitrichia pilosa [Scharff, 1990b](#): 124 (Tm from *Atypena*). Junior secondary homonym of *Callitrichia pilosa* ([Wunderlich, 1978](#))

Zoobank registration: urn:lsid:zoobank.org:act:E74AA2B3-AF77-4220-9439-12C04F97E2EA

Derivatio nominis: The name refers to the setae on the interocular region, from Latin *hirsutus*, hairy.

Remarks: Due to the transfer of the older name *Oedothorax pilosa* to *Callitrichia*, the combination is not available and thus, a replacement name is here provided.

CALLITRICHIA HOLMI (WUNDERLICH, 1978) COMB. NOV.

([FIGS 19D, 22D, 24D, 27](#); [SUPPORTING INFORMATION, FIG. S2B](#))

Oedothorax holmi [Wunderlich, 1978](#): 259, figs 4–7 (Dm).

Atypena simplex [Jocqué & Scharff, 1986](#): 23, figs 67–71 (Dmf). *Callitrichia simplex* [Scharff 1990b](#): 124 (Tmf from *Atypena*) *synon. nov.*

Type material: *Oedothorax holmi*: Holotype: **East Africa**: no further location and collecting data, ♂ leg. Knipper (SMF 29395, examined). *Atypena simplex*: Holotype: **Tanzania**: Uluguru Mts., Lupanga West, montane rain forest 1400 m, ♂ 1.vii.1981, coll. N, Scharff. (ZMUC, not examined). Paratype: **Tanzania**: Uluguru Mts., Kimboza Forest, 250 m, lowland rain forest, 1♀ 18.vii.1981, coll. N, Scharff. (ZMUC, not examined).

Examined material: **Tanzania**: Tanga, Muheza Kwamgumi Forest Reserve (4°57' S, 38°44' E), 170–220 m, 2♂2♀ 18.vii.1995 (ZMUC).

Diagnosis:

Males: This species is characterized by the lack of prosomal modification, the large dorso-retrolaterally extended triangular tibial prolateral apophysis and the

embolic division with papillated area between the stout anterior radical process and the short ventral radical process. For distinctions between this species and the similar species *Ca. criniger* see [Scharff \(1990a: 17\)](#).

Females: Can be distinguished from other *Callitrichia* species by the more oval spermathecae ([Fig. 27G, H](#)).

Description:

Male (measurement ZMUC; feature description for both ZMUC sample and holotype from SMF): Total length: 1.93. Prosoma: 0.87 long, 0.70 wide, carapace unmodified, interocular region with dense setae ([Fig. 19D](#)). Eyes: AME-AME: 0.03, AME width: 0.06, AME-ALE: 0.02, ALE width: 0.07, ALE-PLE: 0, PLE width: 0.08, PLE-PME: 0.04, PME width: 0.07, PME-PME: 0.07. Clypeus: not hirsute, one sub-AME seta. Sternum: 0.48 long, 0.51 wide. Chelicerae: mastidia absent; stridulatory striae rows compressed and evenly spaced ([Fig. 22D](#)). Legs: dorsal proximal macroseta on tibia I, II, III and IV 0.96, 1.29, 3.16 and 3.84 times diameter of tibia, respectively; Tm I: 0.84. Pedipalp: patella prolateral proximal vertical macrosetae present; TPA triangular, sclerotized, largely extended dorsoretrolaterally; PC median-sized, base not visible from dorsal view, distal setae close to distal clasp directed apically; T without papillae; PT with long papillae, surrounded by apical rim; TS short, without papillae; MSA present; DSA tip anteriorly oriented ([Fig. 27A, C](#)); EM flat, anterior margin with few small papillae, not exceeding ARP; ARP thick, sclerotized, angled on retrolateral side; LER absent; VRP short, blunt; papillae-bearing region between ARP, VRP and E base; TP tip pointed; E thick, striated, retrolaterally spiral, anterior margin at base slightly wavy ([Fig. 27B, D](#)). Opisthosoma: dorsal pattern see [Fig. 24D](#); PMS with mAP, two AC; PLS with triad, 3+ AC ([Fig. 27I, J](#)).

Male (holotype, SMF): Total length: 1.88. Prosoma: 0.80 long, 0.65 wide. Eyes: AME-AME: 0.02, AME width: 0.05, AME-ALE: 0.02, ALE width: 0.06, ALE-PLE: 0, PLE width: 0.08, PLE-PME: 0.03, PME width: 0.07, PME-PME: 0.07. Other features same as above.

Female (ZMUC): Total length: 2.07. Prosoma: 0.89 long, 0.69 wide. Eyes: AME-AME: 0.04, AME width: 0.05, AME-ALE: 0.02, ALE width: 0.08, ALE-PLE: 0, PLE width: 0.08, PLE-PME: 0.04, PME width: 0.07, PME-PME: 0.06. Clypeus: not hirsute, one sub-AME seta. Sternum: 0.52 long, 0.56 wide. Legs: dorsal proximal macroseta on tibia I, II, III and IV 3.04, 3.37, 3.54 and 4.28 times diameter of tibia, respectively; Tm I: 0.77. All metatarsi with trichobothrium. Epigyne: Clade 13 characteristic morphology, borders between ventral and dorsal plates converging anteriorly and

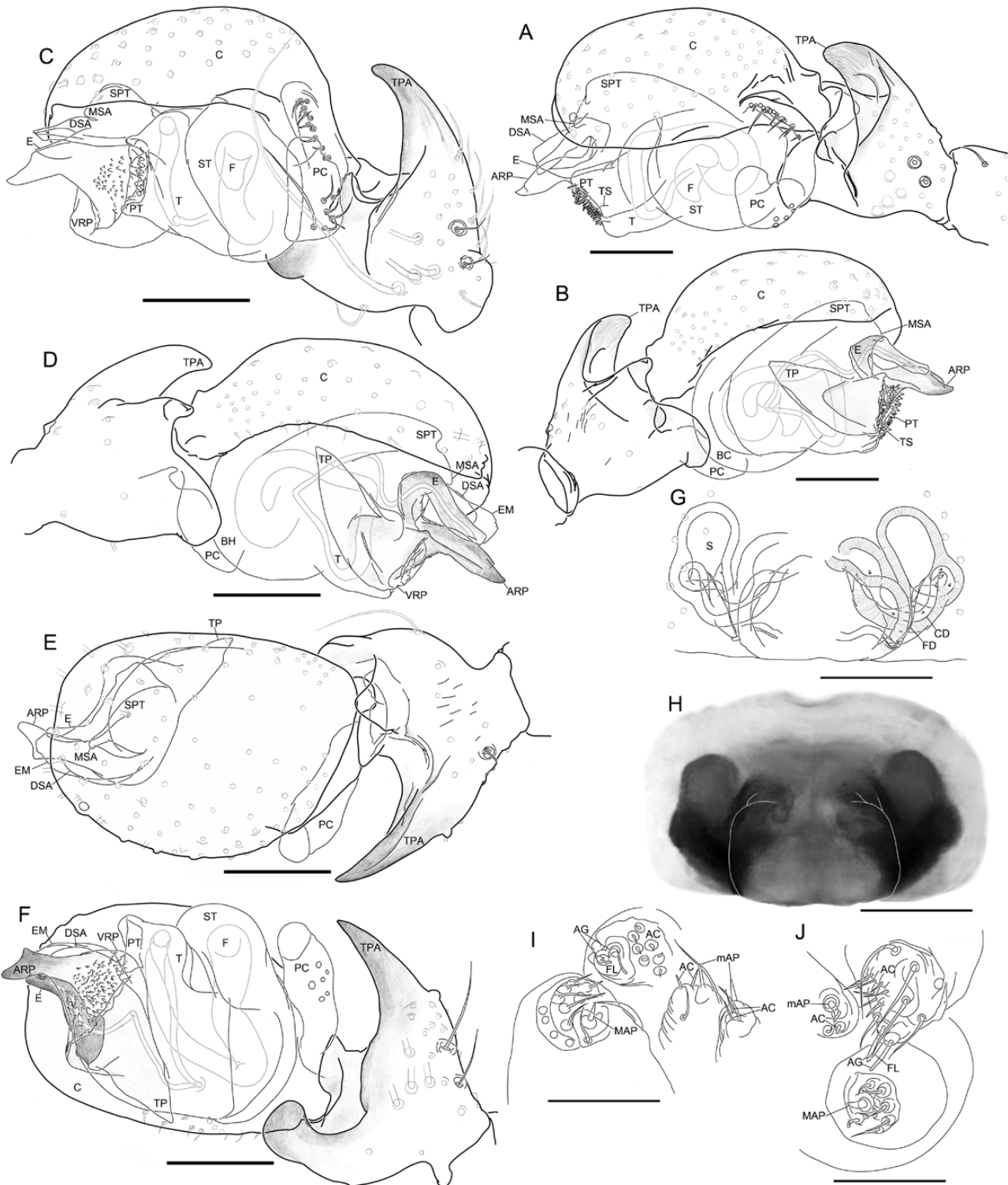


Figure 27. *Callitrichia holmi* (Wunderlich, 1978). A, B, male holotype right palp, images flipped horizontally. A, retrolateral view. B, prolateral view. C–F, ‘*Callitrichia simplex*’, male left palps. C, retrolateral view. D, prolateral view. E, dorsal view. F, ventral view. G, H, epigyne of ‘*Ca. simplex*’. G, ventral view. H, external morphology. I, male holotype spinnerets. J, ‘*Ca. simplex*’, male right spinnerets. Scale bars 0.1 mm.

posteriorly (Fig. 27G, H). Opisthosoma: dorsal pattern same as male; PMS with mAP, two AC, CY; PLS with triad, 3+ AC, two CY.

Variation: The measurements are based on examined material.

Males ($N = 4$, means in parentheses): Total length 1.86–1.95 (1.90). Prosoma: 0.80–0.87 (0.84) long, 0.65–0.70 (0.68) wide. Legs: dorsal proximal macroseta on tibia I, II, III and IV 0.96–1.4 (1.13, $N = 3$), 1.17–1.29 ($N = 2$), 2.94–3.46 (3.19, $N = 3$) and 3.47–3.84 (3.69, $N = 3$) times diameter of tibia, respectively; Tm I: 0.79–0.85 (0.81, $N = 3$).

Females ($N = 2$): Total length 2.07; 2.09. Prosoma: 0.86; 0.89 long, 0.69; 0.70 wide. Legs: dorsal proximal macroseta on tibia II / III / IV 3.37, 4.22 / 3.54, 4.01 / 4.28, 4.83 times diameter of tibia, respectively.

Distribution: East Africa, Tanzania

Habitat: Montane rain forests and lowland rain forests.

Taxonomic remarks: According to the results of our phylogenetic analysis, *Oe. holmi* is placed nested within *Callitrichia*. Since this species also shares the synapomorphic features with the latter genus, its transfer seems justified. In addition, given the identical male palpal structures of *Ca. simplex* and the holotype of *Oe. holmi* (the female is unknown), these species are here synonymized, *Ca. holmi* having priority over *Ca. simplex*.

CALLITRICHIA JUGUMA (SCHARFF, 1990) COMB. NOV.

(FIGS 19I, 21, 22I, 24I; SUPPORTING INFORMATION, FIG. S2F)

Ophrynia juguma Scharff, 1990a: 66, figs 164–172 (Dmf).

Examined material: Tanzania: Uzungwa Mts., Iringa Region, Uzungwa Scarp Forest Reserve, 2♂2♀, leg. N, Scharff (ZMUC).

Diagnosis:

Males: Similar to *Ca. rostrata*, *Ca. perspicua* and *Ca. insulana* in the shapes of the flat PME lobe and inter-AME-PME lobe, forming the narrow inter-AME-PME groove (figs 155, 164 and 173 in Scharff, 1990; fig. 116 in Jocqué & Scharff, 1986), which distinguishes them from other erigonines; this species can be further distinguished from the latter three species by the shape of the palpal tibial apophysis (Fig. 21A–C, in

comparison to figs 157 and 177 in Scharff, 1990a; fig. 118 in Jocqué & Scharff, 1986).

Females: Epigyne morphology similar to other *Callitrichia* species, but can be distinguished by the particularly close distance between the spermathecae (Fig. 21E, F, in comparison to e.g. Fig. 18G, fig. 115 in Jocqué & Scharff, 1986, and fig. 163 in Scharff, 1990a).

Description:

Male (ZMUC): Total length: 2.08. Prosoma: 0.89 long, 0.74 wide, with a narrow and small PME lobe; posterior part with fine, long setae over PME; frontal part ends in a ridge, pointing up and forward, curved inward in the middle, with transversal slit at the peak (Fig. 19I). AME-AME: 0.04, AME width: 0.04, AME-ALE: 0.03, ALE width: 0.07, ALE-PLE: 0.07, PLE width: 0.06, PLE-PME: 0.07, PME width: 0.04, PME-PME: 0.07. Clypeus: not hirsute, one sub-AME seta. Sternum: 0.51 long, 0.49 wide. Chelicerae: mastidia absent; stridulatory striae ridged, rows compressed and evenly spaced (Fig. 22I). Legs: metatarsi and tarsi of legs I and II with perpendicular lateral setae, long and numerous; dorsal proximal macroseta on tibia I, II, III and IV 1.44, 1.57, 2.10 and 2.96 times diameter of tibia, respectively; Tm I: 0.79. Pedipalp: patella prolateral proximal vertical macrosetae absent; tibia with one prolateral, two retrolateral trichobothria; TPA large, broadly rounded, prolateral side straight, retrolateral side with small, round, scaly distal process (Fig. 21C); PC base not visible from dorsal view, distal setae close to distal clasp, distal-setae-bearing area wide, distal clasp extended apically (Fig. 21A); T without papillae, PT truncated, apical part with papillae; TS absent (Fig. 21A); MSA present; DSA wide, median part of tip concave (Fig. 21A); EM broad and flat, without papillae, exceeding ARP; ARP thick, bifid; LER absent; VRP short, with papillae extended to median part of R; TP long, round at tip; E short and stout, slightly retrolaterally curved (Fig. 21B, C). Opisthosoma: dorsal pattern see Fig. 24I; PMS without spigots; PLS with one FL (Fig. 21G).

Female (ZMUC): Total length: 1.87. Prosoma: 0.79 long, 0.66 wide. AME-AME: 0.03, AME width: 0.04, AME-ALE: 0.02, ALE width: 0.07, ALE-PLE: 0.01, PLE width: 0.06, PLE-PME: 0.04, PME width: 0.05, PME-PME: 0.05. Clypeus: not hirsute, one sub-AME seta. Sternum: 0.51 long, 0.49 wide. Legs: dorsal proximal macroseta on tibia I, II, III and IV 2.88, 2.76, 2.67 and 3.21 times diameter of tibia, respectively; Tm I: 0.88. Epigyne of Clade 13 characteristic morphology, borders between ventral and dorsal plates converging anteriorly and posteriorly, CO posterior

to spermathecae (Fig. 21E, F). Opisthosoma: dorsal pattern as male; spigots as in male, PMS with one CY; PLS with two CY (Fig. 21H).

Remarks: Following the results of our phylogenetic analysis, this species is transferred to *Callitrichia*, a placement also consistent with morphological traits of the species.

***CALLITRICHIA LATITIBIALIS* (BOSMANS, 1988) COMB. NOV.**

(FIGS 19P, 22P, 24P, 28; SUPPORTING INFORMATION, FIG. S2M)

Oedothorax latitibialis Bosmans, 1988: 17, fig. 5E–G (Dm).

Type material: Holotype: **Cameroon:** Bambouto Mountains, 2700 m, pitfall in montane grassland, 1♂ 17.i.1983 (RMCA 165.079, examined). Paratypes: 1♂, same data (RMCA 165.087, examined).

Diagnosis:

Males: This species can be identified by the lack of prosomal modification and the conspicuous,

characteristic male palpal tibial apophyses, similar to that of *Ca. longiducta*, but with a different denticle morphology on tibial prolateral apophyses; the body size of this species is larger.

Description:

Male (holotype): Total length: 2.11. Prosoma: 1.09 long, 0.89 wide, unmodified (Fig. 19P). Eyes: AME-AME: 0.02, AME width: 0.06, AME-ALE: 0.03, ALE width: 0.09, ALE-PLE: 0.01, PLE width: 0.08, PLE-PME: 0.05, PME width: 0.09, PME-PME: 0.05. Chelicerae: mastidia absent; stridulatory striae rows widely and evenly spaced (Fig. 22P). Clypeus: not hirsute, one sub-AME seta. Sternum: 0.62 long, 0.61 wide. Legs: dorsal proximal macroseta on tibia I 1.61 times diameter of tibia; Tm I: 0.63. Pedipalp: patella prolateral proximal vertical macrosetae absent; tibia with slender, highly sclerotized, pointed, dorsally situated apophysis bent retrolaterally at tip, base connected with TPA through thin plate; TPA wide, flat, apical ridge with peculiar denticles (Fig. 28C); PC large, base not visible from dorsal view, distal setae close to distal clasp, distal-setae-bearing area wide, distal clasp without striae, clasp extended apically; T without papillae, PT without papillae, distal rim thin and smooth at margin; TS

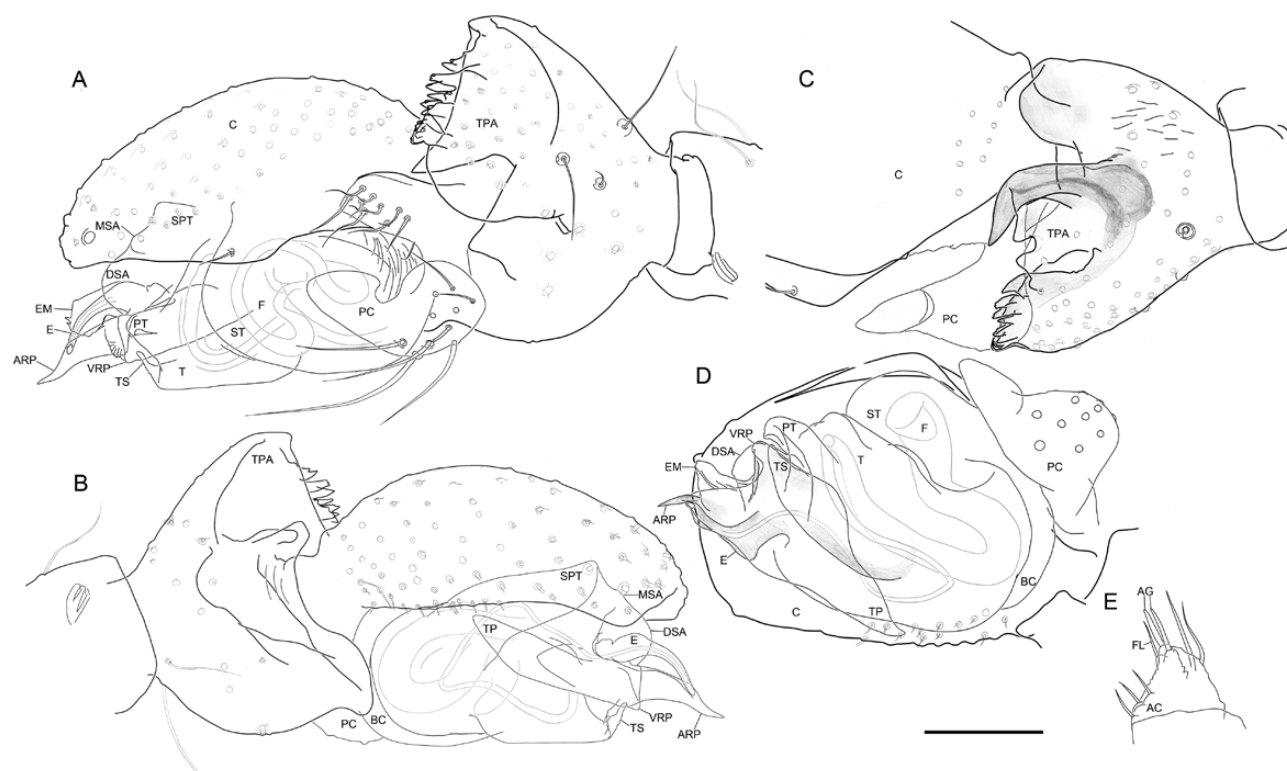


Figure 28. *Callitrichia latitibialis* (Bosmans, 1988). A–D, male right palp, images flipped horizontally. A, retrolateral view. B, prolateral view. C, dorsal view. D, ventral view. E, male left posterior lateral spinneret. Scale bar 0.1 mm.

short, without papillae; MSA inconspicuous; DSA tip straight; EM flat, anterior margin with small papillae, not exceeding ARP (Fig. 28A); ARP pointed; LER absent; VRP present, retrolaterally oriented; TP tip slender; E slightly retrolaterally spiral (Fig. 28B, D). Opisthosoma: single-coloured dark grey (Fig. 24P); PLS with triad, 3+ AC (Fig. 28E).

Male (paratype): Prosoma: 1.10 long, 0.88 wide. Legs: dorsal proximal macroseta on tibia II and III 1.70 and 2.31 times diameter of tibia, respectively; Tm I: 0.63.

Female: Unknown.

Distribution: Cameroon, only known from the type locality.

Habitat: Montane grasslands.

Remarks: According to the results of our phylogenetic analysis this species is transferred to *Callitrichia*, a placement also consistent with morphological traits of the species.

CALLITRICHIA LEGRANDI (JOCQUÉ, 1985) **COMB. NOV.**

(FIGS 19M, 22M, 24M, 29; SUPPORTING INFORMATION, FIG. S2J)

Oedothorax legrandi Jocqué, 1985: 206, figs 21–27 (Dmf).

Type material: Holotype: **Comoros:** Mohéli, Miringoni, Chalet St. Antoine, 700m, rain forest, sieving litter, ♂ 11.xi.1983 (RMCA 161.072, examined). PARATYPES: 5♀, same collecting site as holotype, sweepnet, 7.–8.xi.1984 (RMCA, examined); 1♂2♀, same collecting site as holotype, sweeping by night, 8.xi.1983 (RMCA, examined); 2♂, same location, pitfall, 6.–11.xi.1983 (RMCA, examined).

Diagnosis:

Males: This species can be identified by the lack of prosomal modification and the particular shape of the tibial apophyses, with a vertically elevated TPS and a small TPA with one enlarged, slightly sclerotized setal base at tip.

Females: Can be distinguished from other *Callitrichia* species by the dorsal pattern of the opisthosoma, the shape and position of the spermatheca (e.g. less oval than *Ca. holmi*; less anteriorly situated than *Ca. longiducta*; separation between spermathecae wider than in *Ca. juguma*) and the position of copulatory opening (e.g. more anterior than *Ca. muscicola*).

Description:

Male (paratype, RMCA 161.055): Total length: 1.67. Prosoma: 0.72 long, 0.58 wide, unmodified (Fig. 19M). Eyes: AME-AME: 0.03, AME width: 0.05, AME-ALE: 0.02, ALE width: 0.06, ALE-PLE: 0.01, PLE width: 0.05, PLE-PME: 0.04, PME width: 0.06, PME-PME: 0.04. Clypeus: not hirsute, one sub-AME seta. Sternum: 0.42 long, 0.44 wide. Chelicerae: mastidia absent; stridulatory striae rows widely and evenly spaced (Fig. 22M). Legs: Tm I: 0.62. Pedipalp: patella prolateral proximal vertical macrosetae absent; TPS vertically oriented, tip scaly; TPA small, with one enlarged, slightly sclerotized setal base at tip (Fig. 29C, D); PC large, base not visible from dorsal view, distal setae close to distal clasp, distal-setae-bearing area slightly wide, distal clasp extended apically (Fig. 29A); T without papillae, PT without papillae, distal rim thin and smooth at margin; TS absent (Fig. 29E); MSA present; DSA tip straight; EM absent (Fig. 29A); ARP pointed; LER absent; VRP absent; TP tip slender; E retrolaterally spiral (Fig. 29E). Opisthosoma: dorsal pattern see Fig. 24M; PMS with mAP, AC absent; PLS with triad, AC absent (Fig. 29I).

Female (paratype, RMCA 160.870): Total length: 1.69. Prosoma: 0.66 long, 0.52 wide. Eyes: AME-AME: 0.02, AME width: 0.04, AME-ALE: 0.02, ALE width: 0.04, ALE-PLE: 0.01, PLE width: 0.05, PLE-PME: 0.05, PME width: 0.04, PME-PME: 0.05. Clypeus: not hirsute, one sub-AME seta. Sternum: 0.40 long; 0.41 wide. Legs: dorsal proximal macroseta on tibia I, II, III and IV 2.40, 2.43, 2.89 and 2.81 times diameter of tibia, respectively; Tm I: 0.69. Epigyne: Clade 13 characteristic morphology, borders between ventral and dorsal plates converging anteriorly and posteriorly, entrances of copulatory ducts into spermathecae directly dorsal to the exits of fertilization ducts (Fig. 29G, H). Opisthosoma: dorsal pattern similar to male; PMS with mAP, two AC, CY; PLS with triad, two CY, 3+ AC (Fig. 29J).

Variation: The measurements are based on examined material.

Males (N = 3, means in parentheses): Total length 1.51–1.67 (1.60). Prosoma: 0.63–0.76 (0.70) long, 0.52–0.62 (0.57) wide.

Females (N = 6, means in parentheses): Total length 1.50–1.99 (1.73). Prosoma: 0.65–0.75 (0.69) long, 0.50–0.55 (0.53) wide. Legs: dorsal proximal macroseta on tibia I, II, III and IV 2.04–2.46 (2.30), 2.00–2.64 (2.38, N = 5), 2.32–2.89 (2.66) and 2.52–3.30 (2.95) times diameter of tibia, respectively; Tm I: 0.58–0.69 (0.63).

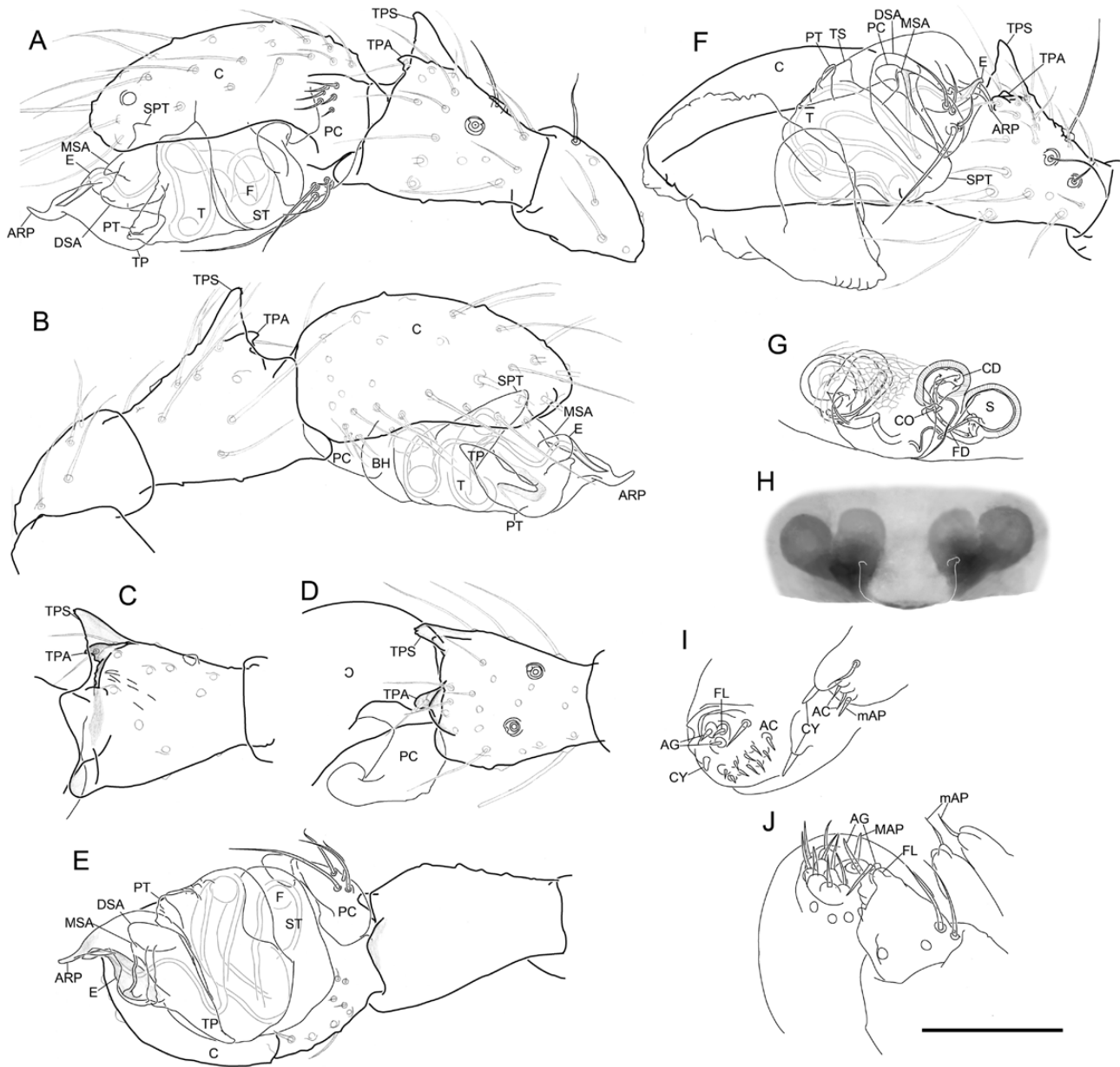


Figure 29. *Callitrichia legrandi* (Jocqué, 1985). A–F, male right palp, images flipped horizontally. A, retrolateral view. B, prolateral view. C, tibia, prolateral view. D, dorsal view. E, ventral view. F, expanded, retrolateral view. G, H, epigyne. G, ventrolateral view. H, external morphology. I, male spinnerets. J, female right posterior median spinneret and posterior lateral spinneret. Scale bar 0.1 mm.

Distribution: Comoros, only known from the type locality.

Habitat: Rain forest litter.

Remarks: Following the results of our phylogenetic analysis, this species is transferred to *Callitrichia*, a placement also consistent with the morphological traits of the species.

***CALLITRICHIA LONGIDUCTA* (BOSMANS, 1988)**

COMB. NOV.; MALE NEW DESCRIPTION

(Figs 19Q, 22Q, 24Q, 30; Supplementary Information, Figs S1–S5)

Oedothorax longiductus Bosmans, 1988: 17, fig. 11C, f (Df, ‘*Oe. longiducta*’ *lapsus calami*).

Type material: Holotype: **Cameroon:** Tchabal Mbabo, 2000 m, among stones and ferns in open grassland, ♀

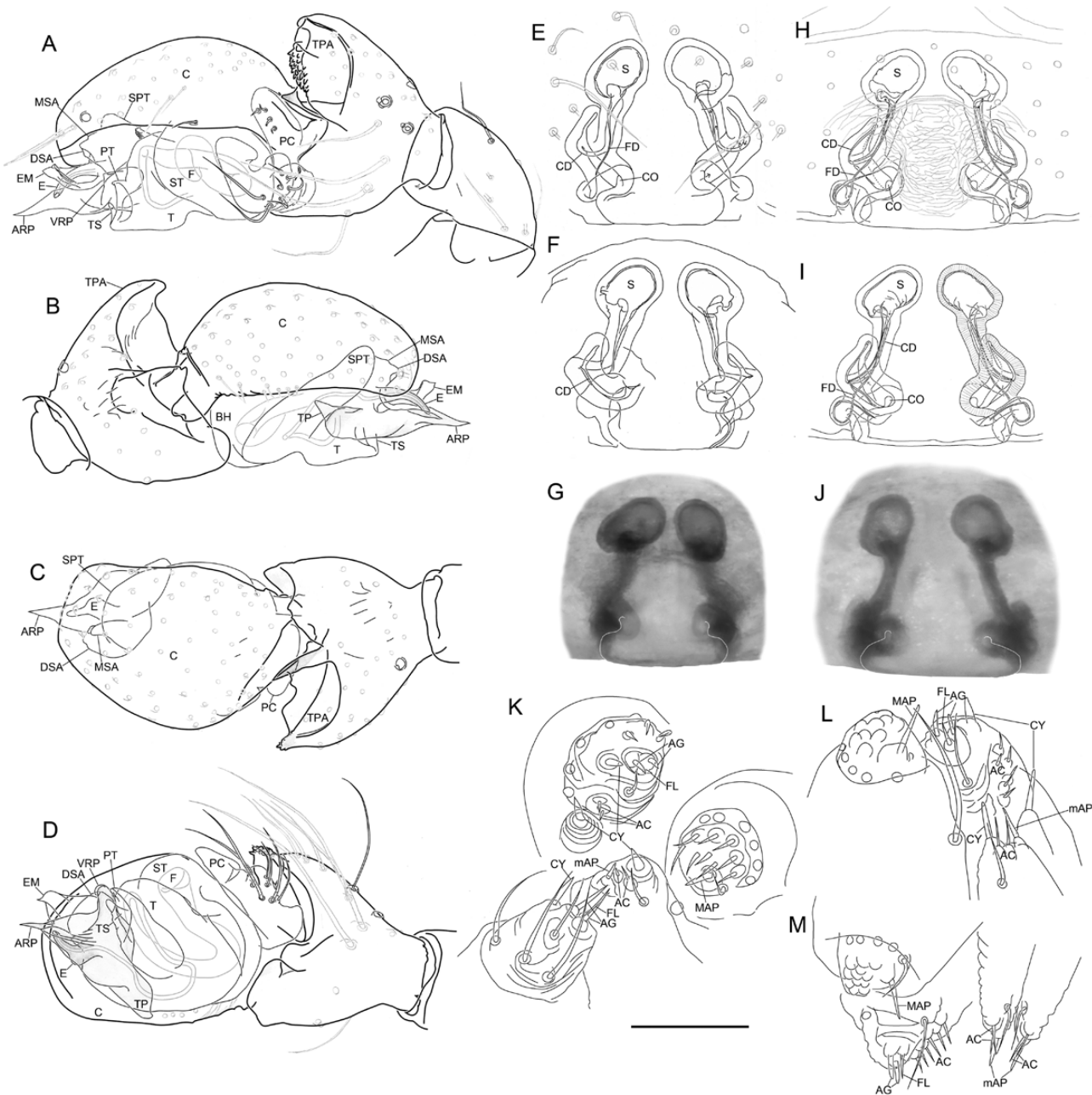


Figure 30. *Callitrichia longiducta* (Bosmans, 1988). A–D, male left palp. A, retrolateral view. B, prolateral view. C, dorsal view. D, ventral view. E–G, female paratype epigyne. E, ventral view. F, dorsal view. G, external morphology. H–J, SMF epigyne. H, ventral view. I, dorsal view. J, external morphology. K, female paratype spinnerets. L, SMF female left spinnerets. M, SMF male spinnerets. Scale bar 0.1 mm.

12.iii.1983 (RMCA 165.870, examined). PARATYPE: 1♀, same data (examined).

Examined material: **Guinea:** Lola Prefecture, Mount Nimba, 1♂16♀ 18.ii.1956 leg. M, Lamotte (SMF).

Diagnosis:

Males: This species can be identified by the lack of prosomal modification and by the conspicuous, characteristic male palpal tibial apophyses, similar to

that of *Ca. latitibialis*, but with a different denticle morphology on the tibial prolateral apophyses and also smaller body size.

Females: Can be distinguished by the spermathecae located much more anteriorly than any other species.

Description:

Male (SMF): Total length: 1.93. Prosoma: 0.91 long, 0.73 wide, unmodified (Fig. 19Q). Eyes: AME-AME: 0.02, AME width: 0.05, AME-ALE: 0.02, ALE width: 0.08, ALE-PLE: 0, PLE width: 0.08, PLE-PME: 0.03, PME width: 0.08, PME-PME: 0.048. Clypeus: not hirsute, one sub-AME seta. Sternum: 0.55 long, 0.51 wide. Chelicerae: without mastidia; stridulatory striae rows compressed and evenly spaced (Fig. 22Q). Legs: dorsal proximal macroseta on tibia I, II and III 2.02, 2.41 and 2.86 times diameter of tibia, respectively; Tm I: 0.71. Pedipalp: patella prolateral proximal vertical macrosetae absent; tibia with a slender, highly sclerotized, pointed, dorsally situated apophysis straight at tip, base connected with TPA through thin plate; TPA wide, flat, apical ridge with small denticles (Fig. 30C); PC large, base not visible from dorsal view, distal setae close to distal clasp, distal-setae-bearing area wide, distal clasp extended apically (Fig. 30A); T without papillae, PT without papillae, distal rim thin and smooth at margin; TS short, without papillae (Fig. 30D); MSA inconspicuous; DSA short; EM flat, anterior margin without papillae, not exceeding ARP (Fig. 30B); ARP pointed; LER absent; VRP retrolaterally oriented; TP tip triangular; E slightly retrolaterally spiral (Fig. 30D). Opisthosoma: single-coloured grey (Fig. 24Q); PMS with mAP, two AC; PLS with triad, two AC (Fig. 30M).

Female (SMF): Total length: 2.40. Prosoma: 1.11 long, 0.84 wide. Eyes: AME-AME: 0.03, AME width: 0.06, AME-ALE: 0.03, ALE width: 0.10, ALE-PLE: 0.01, PLE width: 0.10, PLE-PME: 0.05, PME width: 0.09, PME-PME: 0.07. Clypeus: not hirsute, one sub-AME seta. Sternum: 0.64 long; 0.61 wide. Legs: dorsal proximal macroseta on tibia I, II and III 2.08, 2.35 and 1.45 times diameter of tibia, respectively; Tm I: 0.66. Epigyne: spermathecae exceptionally anteriorly located, borders between dorsal and ventral plates converging anteriorly (Fig. 30H–K). Opisthosoma: single-coloured grey; PMS with mAP, two AC, CY; PLS with triad, two CY, 3+ AC (Fig. 30L).

Female (holotype, RMCA): Total length: 2.03. Prosoma: 0.94 long, 0.72 wide. Eyes: AME-AME: 0.04, AME width: 0.05, AME-ALE: 0.03, ALE width: 0.08, ALE-PLE: 0, PLE width: 0.09, PLE-PME: 0.06, PME width: 0.07, PME-PME: 0.07. Clypeus: not hirsute, one sub-AME seta. Sternum: 0.54 long; 0.57 wide. Legs: dorsal

proximal macroseta on tibia I, II, III and IV 2.21, 2.39, 3.17 and 3.20 times diameter of tibia, respectively; Tm I: 0.64. Epigyne: same as SMF sample (Fig. 30E–G, paratype). Opisthosoma: single-coloured grey; PMS with mAP, two AC, CY; PLS with triad, two CY, two AC (Fig. 30K, paratype).

Variation: The measurements are based on examined material.

Females (N = 12, means in parentheses): Total length 2.03–2.67(2.43). Prosoma: 0.94–1.19 (1.10) long, 0.72–0.90 (0.82) wide. Legs: dorsal proximal macroseta on tibia I, II, III and IV 2.08–2.50 (2.26, N = 7), 2.25–2.75 (2.49, N = 5), 1.45–3.17 (2.62, N = 7) and 2.83–3.63 (3.21, N = 5) times diameter of tibia, respectively; Tm I: 0.56–0.72 (0.66, N = 10).

Distribution: Cameroon, Guinea.

Habitat: Mountain areas, among stones and ferns in open grasslands.

Remarks: The male of *Ca. longiducta* was collected together with 16 females (with identical epigynal morphology to that of the holotype) and shares the same somatic characters of the females, enabling a straightforward assignment to this species. Following the results of our phylogenetic analysis, this species is transferred to *Callitrichia*, a placement also consistent with the morphological traits of the species.

CALLITRICHIA MACROPHTHALMA LOCKET & RUSSELL-SMITH, 1980, **COMB. NOV.**

(FIGS 19N, 22N, 24N, 31; SUPPORTING INFORMATION, FIG. S2K)

Oedothorax macrophthalmus Locket & Russell-Smith, 1980: 69, figs 48–57 (Dmf).

Oedothorax macrophthalmus Bosmans, 1985: 56, figs 18, 26 (m).

Type material: Holotype: **Nigeria**: Iita, Ibadan, in litter in riverine forest, west bank of lake, ♂ 26.iii.1973 (NHM 1979.7.26.5, examined). PARATYPES: Iita, Ibadan, same data as holotype, 1♀; same location, litter in riverine woodland, 1♂ 22.iv.1973; same location, litter in fallow bush, COPR site, 5♀ 3.iii.1973; same location, 1♂2♀ 18.iv.1973; same location, litter in riverine woodland, 2♂5♀ 28.iv.1974; same location, litter in fallow bush, 1♀ 9.ix.1974 (not examined).

Examined material: **Nigeria**: Iita, Ibadan, COPR site, 2♀ 3.ii.1973 (NHM); same location, 1♀ 21.x.1974 (NHM); same location, fallow bush, 2♀ 5.vii.1973,

leg. & det. A. Russell-Smith, 1993 (RMCA 177.475); same location, riverine woodland, 1♂2♀ 7.iii.1974, leg. W. Bank (NHM); same location, riverine wood, 1♀ 9.xi.1974 (NHM); Côte d'Ivoire; Kossou, secondary forest, 17.iii.1975. det. R. Jocqué 1981 (RMCA 153.985).

Diagnosis:

Males: This species can be distinguished from *Oedothorax* s.s., *Mitrager* and other *Callitrichia* species by the scaly structure on the tegulum, the presence of a lateral radical extension of distinct morphology, and the small, scaly palpal tibial prolateral apophysis.

Females: Can be distinguished from all other examined taxa by the especially large, spherical chambers inside the copulatory openings.

Description:

Male (NHM): Total length: 1.61. Prosoma: 0.67 long, 0.51 wide, unmodified (Fig. 19N). Eyes: AME-AME: 0.02, AME width: 0.05, AME-ALE: 0.01, ALE width: 0.07, ALE-PLE: 0.01, PLE width: 0.10, PLE-PME: 0.01, PME width: 0.09, PME-PME: 0.03. Clypeus: not hirsute, one sub-AME seta. Sternum: 0.42 long, 0.43 wide. Chelicerae: mastidia absent; stridulatory striae rows widely and evenly spaced (Fig. 22N). Legs: tibia dorsal proximal macroseta on tibia I, II, III and IV 1.91, 2.12, 2.65 and 2.62 times diameter of tibia, respectively; Tm I: 0.54. Pedipalp: patella prolateral proximal vertical macrosetae absent; TPS absent; TPA short and flat, distal and ventral surfaces scaly (Fig. 31C); PC short, base not visible from dorsal view, distal setae at distal position of PC (Fig. 31A); T papillae scale-like; PT truncated, with small papillae; TS short, without papillae (Fig. 31D); MSA absent; DSA broad (Fig. 31A); EM not exceeding ARP, distally oriented, with long papillae; LER not extended dorsal to E; VRP absent; TP broad, with several small protuberances (Fig. 31B); E retrolaterally spiral, not broadened at basal part, without basal protuberance; ARP with groove fitting E (Fig. 31D). Opisthosoma: evenly coloured, grey (Fig. 24N). PMS with mAP, two AC; PLS with triad, one AC (Fig. 31H–J).

Female (NHM): Total length: 1.59. Prosoma: 0.73 long, 0.57 wide. Eyes: AME-AME: 0.01, AME width: 0.05, AME-ALE: 0.02, ALE width: 0.08, ALE-PLE: 0.01, PLE width: 0.07, PLE-PME: 0.02, PME width: 0.08, PME-PME: 0.03. Clypeus: not hirsute, one sub-AME seta. Sternum: 0.47 long; 0.46 wide. Legs: tibia dorsal proximal macroseta on tibia I, II, III and IV 1.87, 2.12, 2.57 and 2.70 times diameter of tibia, respectively; Tm I: 0.53. Epigyne: area around CO scaly, copulatory ducts wide into chambers at openings, U-curve of copulatory duct ectal to spermathecae (Fig. 31E–G). Opisthosoma: evenly coloured, grey.

Variation: The measurements are based on examined material.

Males (N = 3, means in parentheses): Total length 1.46–1.61. Prosoma: 0.63–0.69 (0.66) long, 0.48–0.59 (0.53) wide. Legs: dorsal proximal macroseta on tibia I and II 1.31–1.91 (N = 2) and 1.74–2.12 (N = 2) times diameter of tibia, respectively; Tm I: 0.48–0.54 (0.51).

Females (N = 8, means in parentheses): Total length 1.59–2.34 (1.96). Prosoma: 0.70–0.88 (0.77) long, 0.53–0.73 (0.61) wide. Legs: dorsal proximal macroseta on tibia I, II, III and IV 1.85–2.79 (2.07, N = 6), 1.98–3.07 (2.32, N = 7), 2.37–4.20 (2.77, N = 7) and 2.57–4.22 (3.16, N = 3) times diameter of tibia, respectively; Tm I: 0.48–0.65 (0.53).

Distribution: Nigeria.

Habitat: Forest litter.

Remarks: Although this species is scored as having LER, its morphology differs significantly from the LER of *Ca. convector*, *Mitrager* and *Atypena*. Following the results of our phylogenetic analysis, this species is transferred to *Callitrichia*, a placement also consistent with morphological traits of the species.

CALLITRICHIA MONOCEROS (MILLER, 1970) COMB. NOV.

Oedothorax monoceros Miller, 1970: 117, pl. XXIV, figs 1–5 (Dm).

Type material: Holotype: **Angola:** Cazombo, bank of Nhá-Bica stream, c. 1200 m (11°53' S, 22°54' E), fallen leaves, ♂ ii.1955, leg. A. de Barros Machado (Ang. 4977.7, not examined).

Diagnosis:

Males: This species can be recognized by the conspicuous, forwardly bent, brown-coloured strong seta between the posterior median eyes, and the smaller, slenderer palpal tibial prolateral apophysis compared to congeners.

Distribution: Angola, only known from the type locality.

Remarks: According to drawings in Miller (1970), the male palpal tibia of this species resembles that of *Ca. pilosa* and *Ca. muscicola*. The unmodified carapace, the distally enlarged paracymbium and the shape of the embolic division are also similar to these two species, as well as to *Ca. longiducta* and *Ca. latitibialis*.

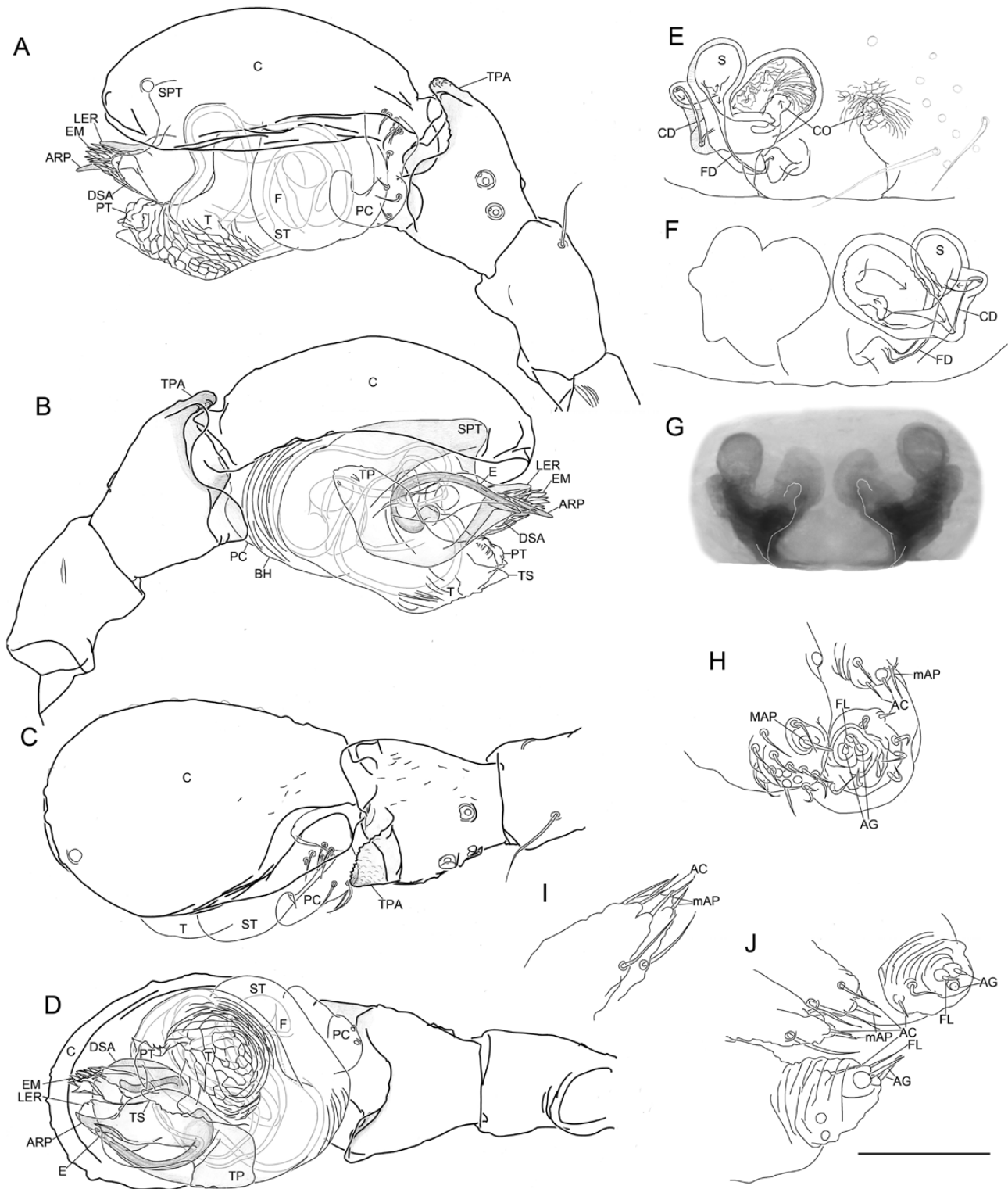


Figure 31. *Callitrichia macrophthalmalpa* (Locket & Russell-Smith, 1980). A–D, male left palp. A, retrolateral view. B, prolateral view. C, dorsal view. D, ventral view. E–G, epigyne. E, ventral view. F, dorsal view. G, external morphology. H, male right spinnerets. I, male posterior median spinnerets. J, male posterior median spinnerets and posterior lateral spinnerets. Scale bar 0.1 mm.

The geographical proximity of the type locality of *Ca. monoceros* (Angola) to that of the latter three species (Cameroon) support the assumption of close relationships between these species. We thus transfer this species, whose morphology does not correspond with the newly delimited *Oedothorax*, to *Callitrichia*.

CALLITRICHIA MUSCICOLA (BOSMANS, 1988) COMB. NOV.

(FIGS 190, 220, 240, 32; SUPPORTING INFORMATION, FIG. S2L)

Oedothorax muscicolus Bosmans, 1988: 18, fig. 6a–g (Dmf; ending of species epithet corrected to ‘icola’, see WSC 2020).

Type material: Holotype: **Cameroon:** Hosséré Vokré, 1400 m, in thick mosses along a fast-flowing rivulet in open landscape, ♂ 21.iv.1983 (RMCA 165.084, not examined). Paratypes: 3♂7♀, same data as holotype (RMCA 165.091, 1♂4♀, examined); Tchabal Mbabo, 1600 m, in litter of moist forest near a fountain, 1♀ 10.iv.1983 (RMCA 165.088, examined).

Diagnosis:

Males: This species can be diagnosed by the lack of prosomal modification and by the particular arrangement of the male palpal features as described below.

Females: The evenly coloured grey opisthosoma distinguishes this species from others with opisthosomal pattern; from *Ca. longiducta* by the less anteriorly situated spermathecae.

Description:

Male (RMCA 165.091): Total length: 2.15. Prosoma: 0.96 long, 0.76 wide, unmodified (Fig. 190). Eyes: AME-AME: 0.02, AME width: 0.05, AME-ALE: 0.02, ALE width: 0.08, ALE-PLE: 0, PLE width: 0.10, PLE-PME: 0.03, PME width: 0.08, PME-PME: 0.06. Clypeus: not hirsute, one sub-AME seta. Sternum: 0.59 long, 0.58 wide. Chelicerae: mastidia absent; stridulatory striae scaly, widely and evenly spaced (Fig. 220). Legs: dorsal proximal macroseta on tibia III and IV 3.07 and 3.37 times diameter of tibia, respectively; Tm I: 0.63. Pedipalp: patella prolateral proximal vertical macrosetae absent; TPS absent; TPA wide, short, flat, apical ridge scaly (Fig. 32C); PC large, base not visible from dorsal view, distal setae close to distal clasp, distal-setae-bearing area wide, distal clasp extended apically (Fig. 32A); T without papillae, PT without papillae, distal rim thin and smooth at margin; TS short, without papillae (Fig. 32E); MSA

present; DSA short, broad; EM flat, without papillae, not exceeding ARP (Fig. 32A); ARP pointed; LER absent; VRP retrolaterally oriented; TP tip slender (Fig. 32E); E retrolaterally spiral (Fig. 32D). Opisthosoma: single-coloured grey (Fig. 240); PMS with mAP, two AC; PLS with triad, 3+ AC (Fig. 32I).

Female (RMCA 165.091): Total length: 2.77. Prosoma: 1.12 long, 0.82 wide. Eyes: AME-AME: 0.03, AME width: 0.06, AME-ALE: 0.02, ALE width: 0.10, ALE-PLE: 0, PLE width: 0.10, PLE-PME: 0.04, PME width: 0.09, PME-PME: 0.06. Clypeus: not hirsute, one sub-AME seta. Sternum: 0.67 long, 0.66 wide. Legs: dorsal proximal macroseta on tibia I, II, III and IV 2.22, 2.50, 2.87 and 3.47 times diameter of tibia, respectively; Tm I: 0.66. Epigyne: CO close to dorsal plate posterior margin (Fig. 32F, G). Opisthosoma: single-coloured grey; PMS with mAP, two AC, CY; PLS with triad, two CY, 3+ AC (Fig. 32H).

Variation: The measurements are based on examined material.

Females (N = 5, means in parentheses): Total length 2.32–2.77 (2.60). Prosoma: 1.09–1.15 (1.12) long, 0.82–0.87 (0.84) wide. Legs: dorsal proximal macroseta on tibia I, II, III and IV 1.70–2.45 (2.23), 2.21–2.68 (2.50), 2.78–3.07 (2.90) and 3.14–3.47 (3.28) times diameter of tibia, respectively; Tm I: 0.65–0.66 (0.65).

Distribution: Cameroon: Tchabal Mbabo.

Habitat: See type specimens data.

Remarks: Following the results of our phylogenetic analysis, this species is transferred to *Callitrichia*, a placement also consistent with morphological traits of the species.

CALLITRICHIA PARALEGRANDI (TANASEVITCH, 2016) COMB. NOV.

Oedothorax paralegrandi Tanasevitch, 2016: 237, figs 2–13 (Dmf).

Type material: Holotype: **India:** Himachal Pradesh, Dalhousie, 1950 m, in soil, ♂ 20.x.1988, leg. S. Vit (MHNG) Paratypes: 2♀, collected together with holotype (MHNG, not examined); Dalhousie, 1950 m, in soil, 2♀ 20.x.1988, leg. S. Vit (MHNG, not examined).

Diagnosis:

Males: This species can be distinguished from congeners by its palpal tibial apophysis with numerous small tubercles.

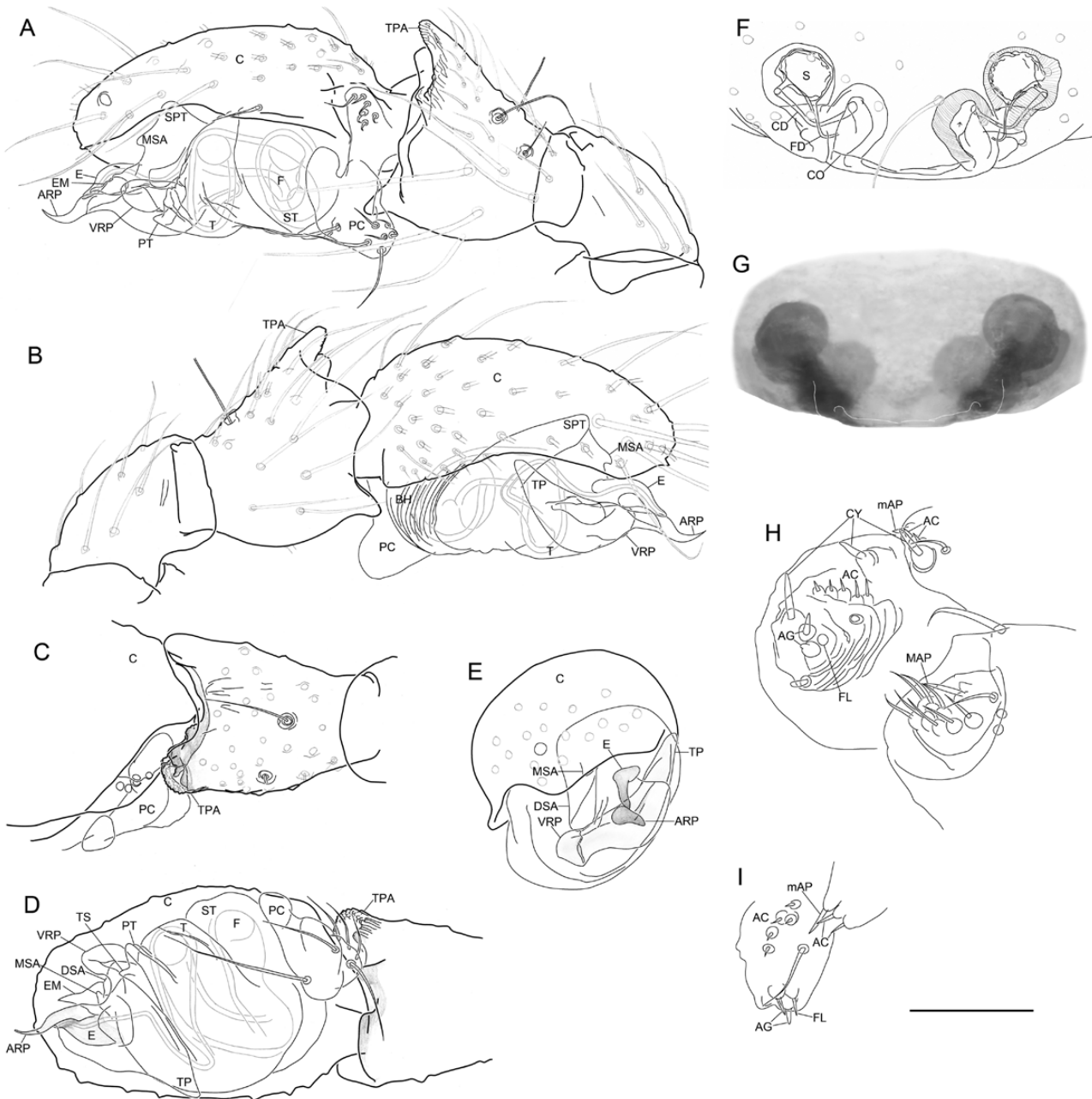


Figure 32. *Callitrichia muscicola* (Bosmans, 1988). A–E, male left palp. A, retrolateral view. B, prolateral view. C, dorsal view. D, apical view. E, ventral view. F, G, epigyne. F, ventral view. G, external morphology. H, female left spinnerets. I, male left posterior median spinneret and posterior lateral spinneret. Scale bar 0.1 mm.

Females: Differ from *Ca. legrandi* by the large size of copulatory opening.

Distribution: This species is only known from a single locality in the highlands of the Indian Himalayas.

Remarks: The palpal features of this species differ greatly from the newly delimited *Oedothorax*. However,

as observed in fig. 13 in [Tanasevitch \(2016\)](#), the entrances of the copulatory ducts into the spermathecae are most probably ectal to the exits of fertilization ducts from the spermathecae, a feature characteristic of *Callitrichia*. In addition, according to [Tanasevitch \(2016\)](#), the species is closely related to *Ca. legrandi*. We thus transfer it to *Callitrichia*, rendering it one of the only two *Callitrichia* species outside Africa.

CALLITRICHIA PICTA (CAPORIACCO, 1949) COMB. NOV.
(FIGS 19E, 22E, 24E, 33; SUPPORTING INFORMATION,
FIG. S2C)

Toschia picta di Caporiacco, 1949: 363, fig. 26a–c (Dmf).
Rhaebothorax hadzji Caporiacco, 1949: 368, fig. 30a–c
(Dm).

Toschia picta Holm, 1962: 157, fig. 58a–e, pl. V, figs 14,
15 (mf).

Toschia picta van Helsdingen, 1982: 178.

Mecynargus hadzji, Brignoli, 1983: 345.

Oedothorax pictus Brignoli, 1983: 350.

Examined material: D. R. Congo, Kivu-N. Province,
Mt. Muleke (00°17' S, 029°15' E), 1820 m, 1♂ 5.vii.1963,
coll. M, J. Celis, det. A. Holm, 1967 (RMCA).

Diagnosis:

Males: This species shows no external prosomal modification, which distinguishes it from the congeners with prosomal modifications; the presence of a long, scaly ventral radical process distinguishes it from other *Callitrichia* species lacking external prosomal modification, except *Ca. casta* and *Ca. hirsuta*; can be further distinguished from the former by its slightly laterally extended distal retrolateral margin of the palpal tibial prolateral apophysis. Males of this species are morphologically identical to *Ca. hirsuta* based on the inspection of figs 62–66 in Jocqué & Scharff (1986).

Females: Can be identified by the following combination of features: opisthosoma dark brownish grey, dorsal with a pale longitudinal stripe like in male; an obvious loop can be seen in the part of copulatory duct ectal to the spermathecae from ventral view of the vulva of epigyne (fig. 58E in Holm 1962); distance between the copulatory openings longer than in other species with the previous feature.

Description:

Male (RMCA): Total length: 2.17. Prosoma: 0.97 long, 0.68 wide, without modification (Fig. 19E). Eyes: AME-AME: 0.04, AME width: 0.02, AME-ALE: 0.07, ALE width: 0.07, ALE-PLE: 0.01, PLE width: 0.07, PLE-PME: 0.05, PME width: 0.07, PME-PME: 0.05. Clypeus not hirsute, one sub-AME seta. Sternum: 0.53 long, 0.53 wide. Chelicerae: mastidia absent; stridulatory striae ridged, rows compressed and evenly spaced (Fig. 22E). Legs: dorsal proximal macroseta on tibia I, II, III and IV 1.74, 2.14, 2.43 and 3.30 times diameter of tibia, respectively; Tm I: 0.70. Pedipalp: patella prolateral proximal vertical macrosetae absent; TPA

large, distal part slightly dilated and truncate at tip (Fig. 33C); PC base not visible from dorsal view, distal setae close to distal clasp, distal-setae-bearing area wide, externally protruded into a high blunt elevation, distal clasp extended apically (Fig. 33A); T without papillae, PT truncated, apical part without papillae; TS absent (Fig. 33D); MSA present; DSA wide, round at tip (Fig. 33A); EM broad and flat, without papillae, not exceeding ARP; ARP pointed, with groove hosting E; LER absent; VRP long, with papillae between ARP and VRP; TP long, triangular; E short and stout, slightly retrolaterally curved, median part dorsally elevated (Fig. 33B). Opisthosoma: dorsal pattern see Fig. 24E; PMS with mAP, two AC; PLS with triad, 3+ AC (Fig. 33G).

Female (RMCA 111987): Total length: 2.61. Prosoma: 1.02 long, 0.77 wide. Eyes: AME-AME: 0.03, AME width: 0.04, AME-ALE: 0.04, ALE width: 0.6, ALE-PLE: 0.02, PLE width: 0.06, PLE-PME: 0.06, PME width: 0.06, PME-PME: 0.07. Clypeus: not hirsute, one sub-AME seta. Sternum: 0.62 long, 0.58 wide. Legs: dorsal proximal macroseta on tibia I, II, III and IV 2.19, 2.36, 2.74 and 3.38 times diameter of tibia, respectively; Tm I: 0.65. Epigyne: (Fig. 33E, F). Opisthosoma: single-coloured grey; PMS with mAP, two AC, CY; PLS with triad, two CY, 3+ AC.

Distribution: Congo, Kenya.

Remarks: Besides structures corresponding to anterior radical process, radical tailpiece and ventral radical process, Holm (1962) described the embolic division of this species as having a short mesal process close to the embolus, probably referring to the embolic membrane (Fig. 33B, D). This species is similar to *Ca. hirsuta* from Tanzania [compare Figs 33 and 19E with figs 62–66 in Jocqué and Scharff (1986)]. It is even possible that *Ca. hirsuta* is a junior synonym of *Ca. picta*, which will require examining the male of *Ca. hirsuta*. Following the results of our phylogenetic analysis, this species is transferred to *Callitrichia*, a placement also consistent with morphological traits of the species.

CALLITRICHIA PILOSA (WUNDERLICH, 1978)
COMB. NOV.

(FIGS 19K, 22K, 24K, 34; SUPPORTING INFORMATION,
FIG. S2H)

Oedothorax pilosus Wunderlich, 1978: 258, figs 1–3
(Dm).

Type material: Holotype: **Ethiopia:** Shewa Province,
det. Wunderlich 1977 (SMF 11353, examined).

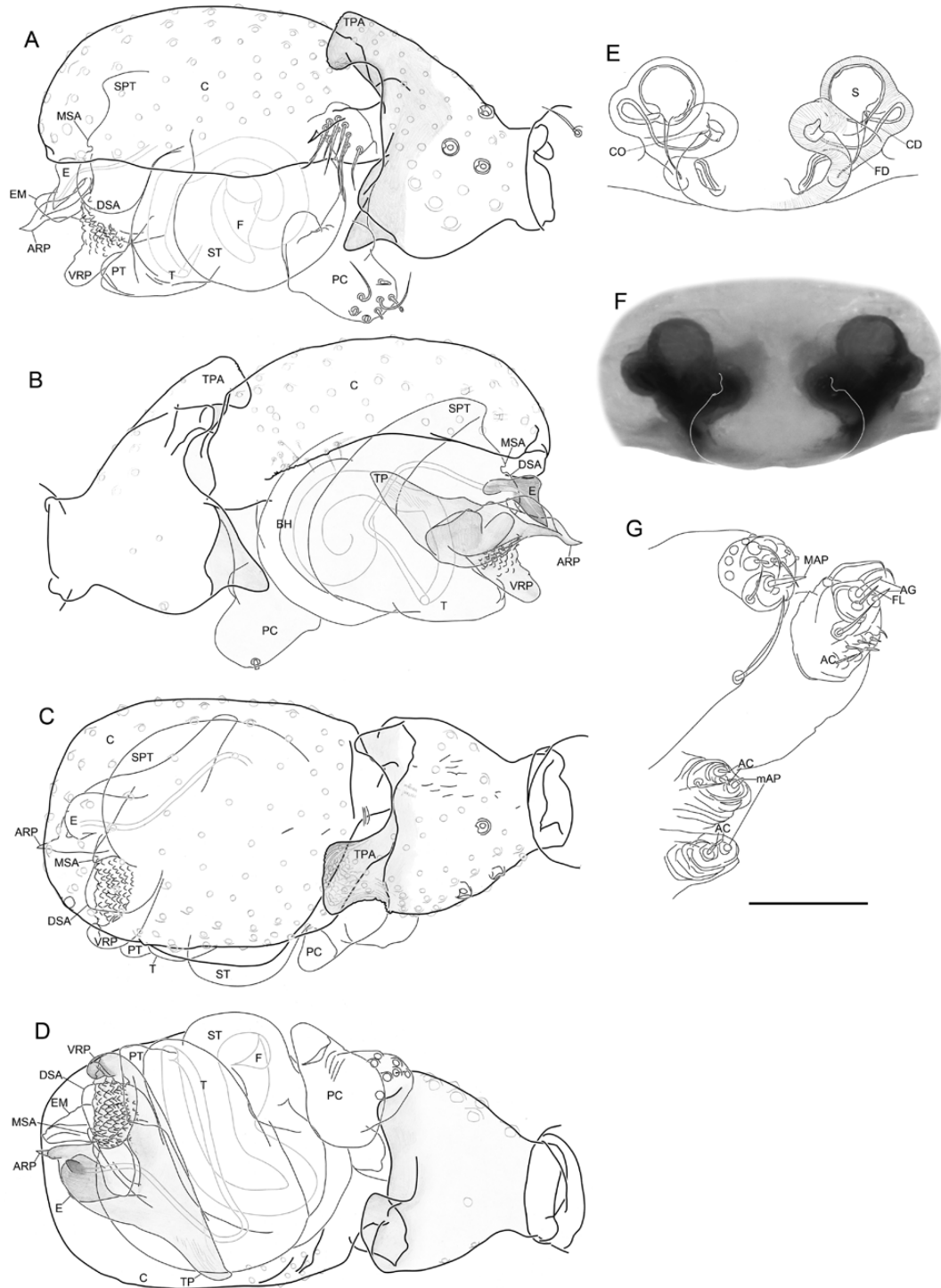


Figure 33. *Callitrichia picta* (Caporiacco, 1949). A–D, male left palp. A, retrolateral view. B, prolateral view. C, dorsal view. D, ventral view. E, F, epigyne. E, ventral view. F, external morphology. G, male spinnerets. Scale bar 0.1 mm.

Diagnosis:

Males: Can be identified by the shape of palpal tibial prolateral apophysis, the embolic division morphology and the lack of prosomal modification.

Description:

Male (holotype, SMF): Total length: 1.85. Prosoma: 0.81 long, 0.64 wide, unmodified (Fig. 19K). Eyes: AME-AME: 0.02, AME width: 0.05, AME-ALE: 0.01, ALE width: 0.09, ALE-PLE: 0, PLE width: 0.08, PLE-PME: 0.03, PME width: 0.06, PME-PME: 0.07. Clypeus: not hirsute, one sub-AME seta. Sternum: 0.52 long, 0.46 wide. Chelicerae: mastidia absent; stridulatory striae rows widely and evenly spaced (Fig. 22K). Legs: Tm I: 0.74. Pedipalp: patella prolateral proximal vertical macrosetae absent; TPA distally with a broader retrolateral lobe and a narrower prolateral lobe, both scaly, with hollow in-between (Fig. 34C); PC base not visible from dorsal view, distal setae close to distal clasp, distal-setae-bearing area wide, distal clasp extended apically (Fig. 34A); T without papillae, PT with longitudinal folds along distal rim; TS short, without papillae (Fig. 34D); MSA present; DSA wide, tip angled at ventral side; EM flat, without papillae, not exceeding ARP; ARP pointed; LER absent; VRP long; radical part close to ARP wrinkled; TP tip pointed; E retrolaterally spiral (Fig. 34E). Opisthosoma: anterior half light-grey, posterior half dark-grey, with continuous transition in the middle (Fig. 24K); PMS with mAP, two AC; PLS with triad, 3+ AC (Fig. 34F).

Female: Unknown.

Distribution: Ethiopia, only known from the type locality.

Habitat: Unknown.

Remarks: Following the results of our phylogenetic analysis, this species is transferred to *Callitrichia*, a placement also consistent with morphological traits of the species. The specific epithet of this species has priority over the later published *Callitrichia pilosa* (Jocqué & Scharff, 1986), the latter is given a new replacement name *Ca. hirsuta* (see above).

CALLITRICHIA SELLAFRONTIS SCHARFF, 1990
(FIGS 19H, 20, 22H, 24H, 26D; SUPPORTING
INFORMATION, FIG. S2F)

Callitrichia sellafontis Scharff, 1990a: 19, figs 22–30 (Dmf).

Type material: Holotype: **Tanzania:** Uzungwa Mts., Iringa Region, Uzungwa Scarp Forest Reserve (= Chita

Forest) above Chita village, montane rain forest, 1600 m, sweepnetted, ♂ 12.xi.1984, leg. N, Scharff (ZMUC, not examined). Paratypes: same locality with holotype 5♂11♀, leg. N, Scharff (ZMUC, not examined); same locality, 1650 m, sweep-netted, 1♂3♀ 12–13.xi.1984, leg. N, Scharff (ZMUC, not examined); same locality, 1600 m, litter, 1♂6♀ 08–12.xi.1984, leg. N, Scharff; same locality, 1500 m, sweep-netted, 9♂16♀ 02–13.xi.1984, leg. N, Scharff (ZMUC, not examined).

Examined material: Tanzania: Iringa. Mufindi Dist. Uzungwa Scarp For. Res. 8°30.05'S, 35°52' E. elev. 1515 m, 2♂3♀ 4.iii.1996. McKamey *et al.* Canopy Fog 35 (ZMUC, 3 vials).

Diagnosis:

Males: This species can be recognized by its unique saddle-shaped prosomal modification and the pair of distinct setal tuft on the interocular lobe.

Females: Somatic features, as well as epygyne morphology, similar to many congeners like *Ca. hamifera*, *Ca. kenya*, *Ca. ruwenzoriensis* etc. Further detailed comparison of epigyne morphologies is needed (beyond the scope of the current study).

Description:

Male (ZMUC): Total length: 1.6. Prosoma: 0.76 long, 0.7 wide, saddle-shaped, with inter-AME-PME lobe and PME lobe; inter-AME-PME-lobe with one pair of setal tufts on frontal surface and thin, long setae on lateral, dorsal and posterior surface (Figs 19H, 26D). Eyes: AME-AME: 0.04, AME width: 0.05, AME-ALE: 0.04, ALE width: 0.05, ALE-PLE: 0.02, PLE width: 0.05, PLE-PME: 0.17, PME width: 0.05, PME-PME: 0.05. Clypeus: not hirsute, one sub-AME seta. Sternum: 0.48 long, 0.52 wide. Chelicerae: mastidia absent; stridulatory striae ridged, rows compressed and evenly spaced (Fig. 22H). Legs: dorsal proximal macroseta on tibia II 1.43 times diameter of tibia; Tm I: 0.80. Pedipalp: patella prolateral proximal vertical macrosetae absent; TPA large, apically hooked and hollow ventrally (Fig. 20C); PC base not visible from dorsal view, distal setae close to distal clasp, distal-setae-bearing area wide, distal clasp extended apically (Fig. 20A); T without papillae, PT truncated, without papillae; TS median-long, slender, without papillae (Fig. 20D); MSA present; DSA wide, tip with with several denticles (Fig. 20A); EM broad and flat, without papillae, not exceeding ARP; ARP thick; LER absent; VRP long; radical part close to ARP wrinkled, with papillae between ARP, VRP and E; TP long; E retrolaterally spiral, flat, with

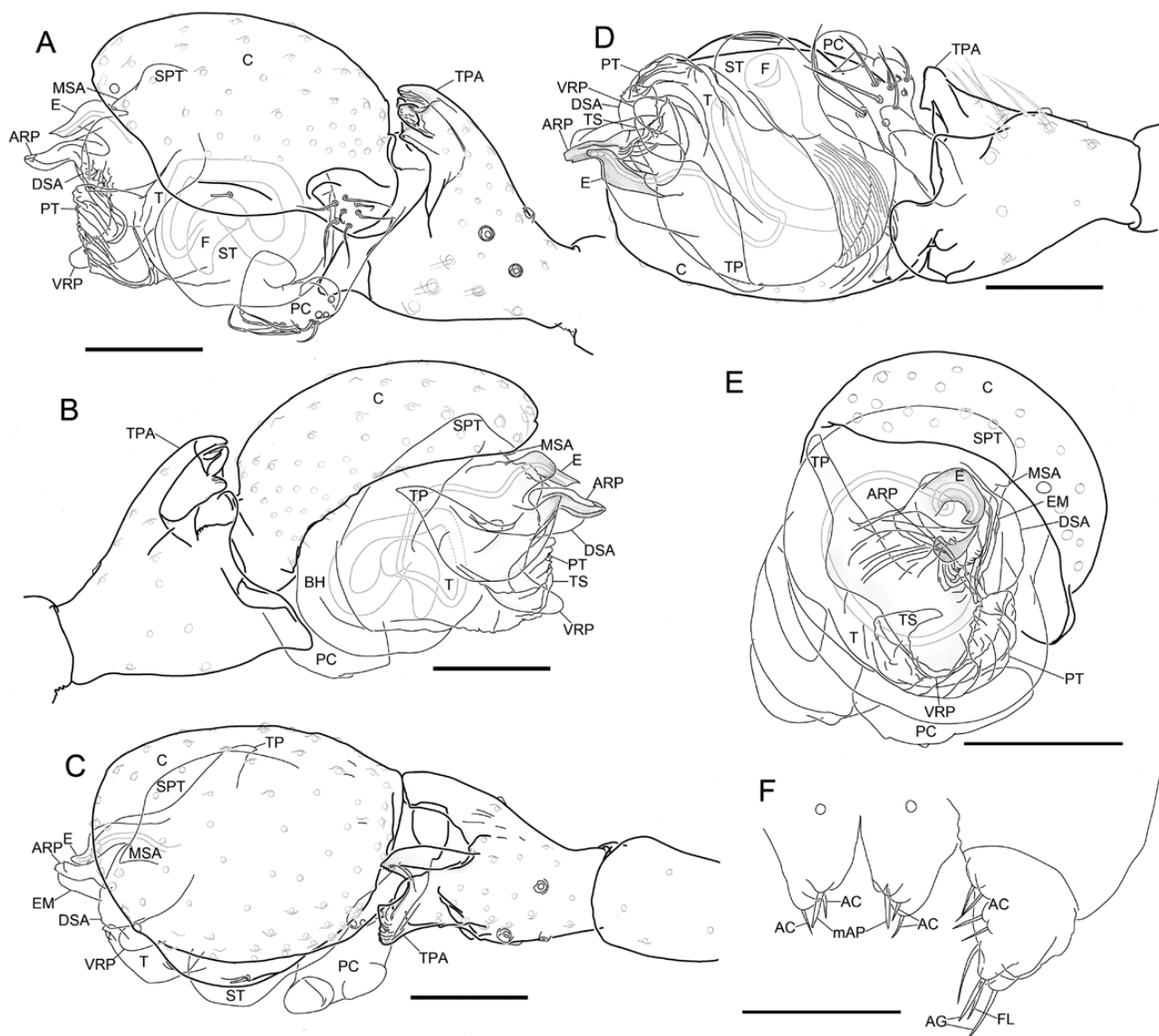


Figure 34. *Callitrichia pilosa* (Wunderlich, 1978). A–E, male right palp, images flipped horizontally. A, retrolateral view. B, prolateral view. C, dorsal view. D, ventral view. E, apical view. F, male posterior median spinnerets and right posterior lateral spinneret. Scale bars 0.1 mm.

papillae and striation (Fig. 20B, E). Opisthosoma: dorsal pattern see Fig. 24H; PMS without spigots; PLS with one FL (Fig. 20K).

Female (ZMUC): Total length: 2.1. Prosoma: 0.82 long, 0.64 wide. Eyes: AME-AME: 0.02, AME width: 0.05, AME-ALE: 0.03, ALE width: 0.06, ALE-PLE: 0.01, PLE width: 0.05, PLE-PME: 0.06, PME width: 0.05, PME-PME: 0.05. Clypeus: not hirsute, one sub-AME seta. Sternum: 0.48 long, 0.48 wide. Legs: dorsal proximal macroseta on tibia I, II, III and IV 3.43, 3.41, 4.11 and 3.75 times diameter of tibia, respectively; Tm I: 0.75.

Epigyne: Clade 13 characteristic morphology (Fig. 20F–H); Opisthosoma: dorsal pattern as male; spigots as in male, PMS with one CY; PLS with two CY (Fig. 20I, J).

Remarks: Males of this species have a pair of feather-like setal tufts at the interocular region, superficially similar to those found in *Mitrager coronata* (Tanasevitch, 1998) **comb. nov.** and related species. However, the structure in this species is formed by many aggregated setae, while each of the two pairs of feather-like setae found in *Mitrager* species are branched single large setae.

CALLITRICHIA UNCATA (JOCQUÉ & SCHARFF, 1986)
COMB. NOV.(FIGS 18, 19J, 22J, 24J; SUPPORTING INFORMATION,
FIG. S2G)*Ophrynia uncata* Jocqué & Scharff, 1986: 41, figs 130–138 (Dmf).*Examined material:* Tanzania, West Usambara Mts., Mazumbai Forest Reserve, 5♂2♀, leg. N. Scharff (ZMUC).*Diagnosis:**Males:* This species can be recognized by the following combination of features: inter-AME-PME groove and PME lobe present; paracymbium terminal part below distal clasp apically extended, which distinguish this species from *Oedothorax*, *Mitrager* and other *Callitrichia* species, except *Ca. infecta*; can be distinguished from other *Callitrichia* species by the hook-like, seta-free apophysis on the prolateral side of the palpal tibia (Fig. 18C).*Females:* The somatic features resemble those of *Oedothorax*, *Mitrager* and *Callitrichia*, but can be distinguished from *Oedothorax* and some *Callitrichia* species (which have evenly coloured opisthosoma, see generic description) by its variegated opisthosoma; can probably be distinguished from the rest of the *Callitrichia* species by the colour pattern of opisthosoma; can be distinguished from *Mitrager* by the entrance of copulatory ducts into the spermathecae ectal to the exits of fertilization ducts from the spermathecae.*Description:**Male (ZMUC):* Total length: 2.08. Prosoma: 0.93 long, 0.79 wide, with PME-lobe and a deep transversal inter-AME-PME groove, forming anterolateral sulci delimited by heavily sclerotized tegument (Fig. 19J). Eyes: AME-AME: 0.04, AME width: 0.04, AME-ALE: 0.04, ALE width: 0.08, ALE-PLE: 0, PLE width: 0.07, PLE-PME: 0.09, PME width: 0.04, PME-PME: 0.13. Clypeus: not hirsute, one sub-AME seta. Sternum: 0.55 long, 0.58 wide. Chelicerae: mastidia absent; stridulatory striae ridged, rows compressed and evenly spaced (Fig. 22J). Legs: metatarsi and tarsi of legs I and II without perpendicular lateral setae; dorsal proximal macroseta on tibia I, II, III and IV 1.46, 1.74, 2.42 and 3.41 times diameter of tibia, respectively; Tm I: 0.79. All metatarsi with trichobothrium. Pedipalp: patella prolateral proximal vertical macrosetae absent; tibia with one prolateral, two retrolateral trichobothria; TPA large, broadly rounded, glabrous, retrolateral

side with long, slender, strongly sclerotized, pointed apophysis (Fig. 18C); PC base not visible from dorsal view, distal setae close to distal clasp, distal terminal part below distal clasp extended apically (Fig. 18A); T without papillae, PT absent; TS long and slender (Fig. 18D); MSA absent; DSA wide (Fig. 18A); EM broad and flat, without papillae; ARP thick; LER absent; VRP short, with few papillae at anterior margin between ARP and VRP; TP round at tip; E short and stout, slightly retrolaterally curved (Fig. 18A, D). Opisthosoma: dorsal pattern see Fig. 24J; PMS without spigots; PLS with one FL (Fig. 18I, K).

Female (ZMUC): Total length: 2.22. Prosoma: 0.96 long, 0.77 wide. Eyes: AME-AME: 0.03, AME width: 0.04, AME-ALE: 0.04, ALE width: 0.07, ALE-PLE: 0, PLE width: 0.07, PLE-PME: 0.05, PME width: 0.06, PME-PME: 0.06. Clypeus: not hirsute, one sub-AME seta. Sternum: 0.58 long, 0.64 wide. Legs: dorsal proximal macroseta on tibia I, II, III and IV 2.75, 2.69, 2.72 and 3.24 times diameter of tibia, respectively; Tm I: 0.83. Epigyne: Clade 13 characteristic morphology (Fig. 18F–H). Opisthosoma: dorsal pattern as male; spigots as in male, PMS with one CY; PLS with two CY (Fig. 18J, L).*Remarks:* In the generic description of Jocqué & Scharff (1986), *Ophrynia* was considered as having no obvious stridulation file on the chelicerae. We found stridulation files in *Ca. juguma* and *Ca. uncata* (see Fig. 22H, I). Following the results of our phylogenetic analysis, this species is transferred to *Callitrichia*, a placement also consistent with morphological traits of the species.**CALLITRICHIA USITATA** (JOCQUÉ & SCHARFF, 1986)
COMB. NOV.(FIGS 19L, 22L, 24L, 35; SUPPORTING INFORMATION,
FIG. S2I)*Oedothorax usitatus* Jocqué & Scharff, 1986: 29, figs 86–89 (Dm).*Type material:* Holotype: **Tanzania:** Mt. Rungwe, south-west side, 1800 m, montane rain forest, ♂ 20.viii.1980 (ZMUC, not examined). Paratypes: 1♂, together with the holotype (RMCA 160.013, examined); 1♂, same locality, same date, Gallery forest, 1600 m, leg. M. Stoltze & N. Scharff (ZMUC, examined).*Diagnosis:**Males:* This species resemble *Ca. legrandi* in the vertical palpal tibial prolateral spike, but can be distinguished from the latter by the presence of ventral radical process.

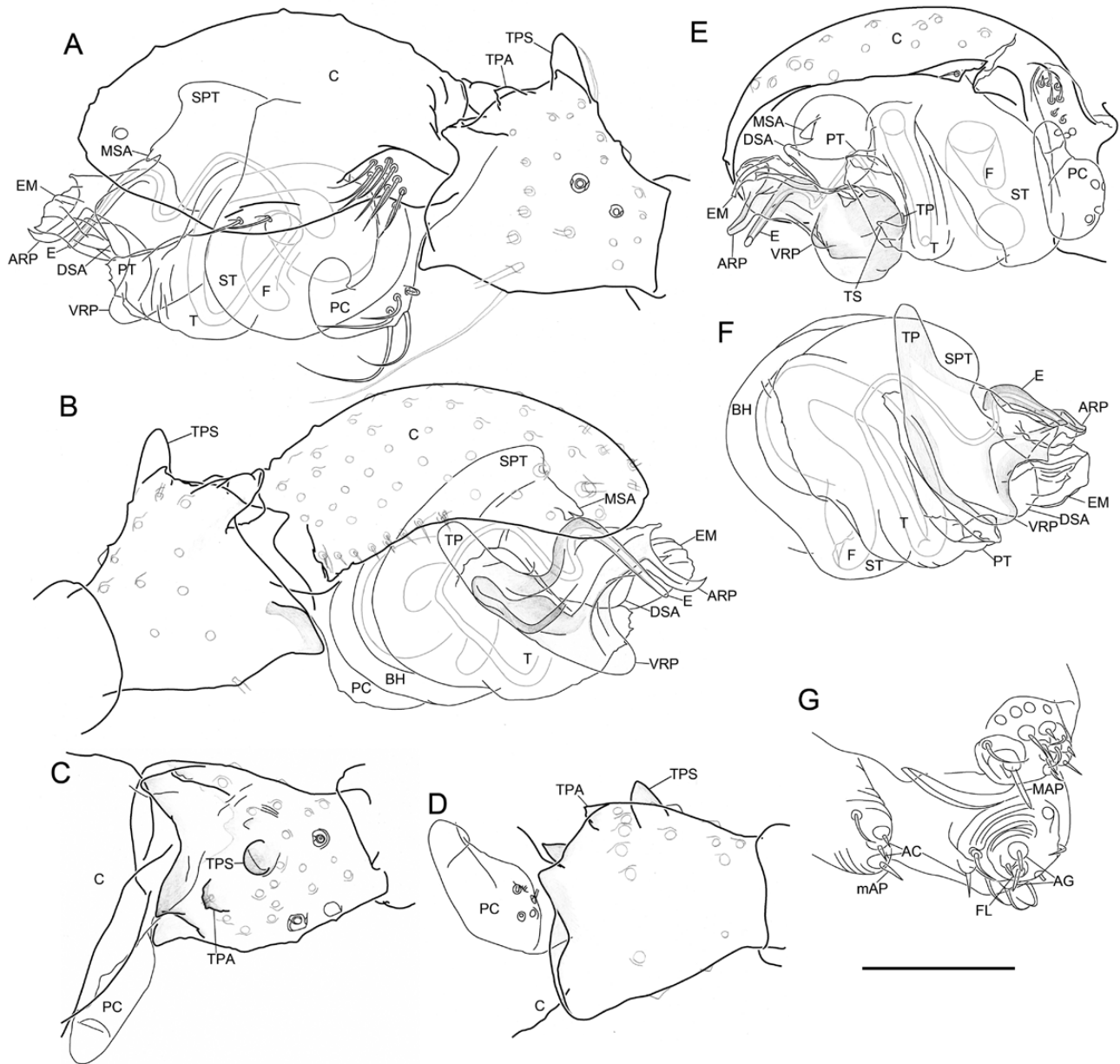


Figure 35. *Callitrichia usitata* (Jocqué & Scharff, 1986). A–D, male left palp. A, retrolateral view. B, prolateral view. C, tibia, dorsal view. D, tibia, ventral view. E, F, right palp, images flipped horizontally. E, ventroretrolateral view. F, ventroprolateral view. G, male left spinnerets. Scale bar 0.1 mm.

Description:

Male (paratype, ZMUC): Total length: 1.81. Prosoma: 0.82 long, 0.64 wide, unmodified (Fig. 19L). Eyes: AME-AME: 0.03, AME width: 0.05, AME-ALE: 0.02, ALE width: 0.06, ALE-PLE: 0, PLE width: 0.06, PLE-PME: 0.04, PME width: 0.06, PME-PME: 0.05. Clypeus: not hirsute, one sub-AME seta. Sternum: 0.49 long, 0.48 wide. Chelicerae: mastidia absent; stridulatory striae ridged, rows widely and evenly spaced (Fig. 22L). Legs:

dorsal proximal macroseta on tibia I, II and IV 2.57, 3.28 and 3.99 times diameter of tibia, respectively; Tm I: 0.63. Pedipalp: patella prolateral proximal vertical macrosetae absent; TPS directed upwards, tip round; TPA small, with one enlarged, slightly sclerotized setal base at tip (Fig. 35A, C); PC median-sized, base not visible from dorsal view, distal setae close to distal clasp, distal clasp extended apically (Fig. 35A); T without papillae, PT without papillae at tip, distal rim thin and smooth at margin; TS short; MSA present; DSA

tip straight; EM flat, without papillae, not exceeding ARP; ARP pointed; LER extended retrolaterally; VRP present; TP tip round; E retrolaterally spiral (Fig. 35E, F). Opisthosoma: dorsal pattern see Fig. 24L; PMS with mAP, two AC; PLS with triad, one AC (Fig. 35G).

Male (paratype, RMCA): Total length: 1.94. Prosoma: 0.81 long, 0.64 wide, Sternum: 0.50 long, 0.49 wide. Tm I: 0.57.

Female: Unknown.

Distribution: Tanzania, only known from type locality.

Habitat: Montane rain forests.

Remarks: Following the results of our phylogenetic analysis, this species is transferred to *Callitrichia*, a placement also consistent with morphological traits of the species.

HOLMELGONIA JOCQUÉ & SCHARFF, 2007

Type species: *Elgonia nemoralis* Holm, 1962.

Diagnosis, description and taxonomic remarks: The resemblance of *Holmelgonia* to *Callitrichia* and other related genera (i.e. *Oedothorax*, *Toschia* and *Ophrynia*) has not been mentioned in previous publications. Regarding the shape of embolic division, the enlarged terminal part of paracymbium, the vastly erected palpal tibia prolateral apophysis and the general epigyne morphology, *Holmelgonia* is similar to numerous *Callitrichia* species. Nzigidahera & Jocqué (2014) described *Holmelgonia* as characterized by the absence of cheliceral stridulatory ridges, the presence of a double ventral row of setae on the femora, the long tibial spines (two to three times as long as the diameter of the segment), tibial chaetotaxy 2-2-1-1, TmI between 0.32 and 0.7, the absence of prosomal modification and the apophysis on the dorsal side of the palpal tibia. However, all these features are not unique to the members of this genus. One potential diagnostic feature, the absence of cheliceral stridulatory ridges, is actually present in our studied species (*Ho. basalis*, Fig. 22B), and the chelicera of *Ho. disconveniensi* Nzigidahera & Jocqué, 2014 (SEM photo, figs 2–3 in Nzigidahera & Jocqué 2014) shows a scaly lateral surface without setae, which could also be interpreted as stridulatory striae (fig. 3 shows the detail of the anterior surface, instead of the lateral surface). Despite the lack of defining features for this genus, and the sister-relationship of *Ho. basalis* and *Callitrichia* shown in the present study, this genus

differs from *Callitrichia* in the lack of truncated protegulum and the presence of a central embolar apophysis (Fig. 36B, D, arrow). The latter structure is present in all species with known males, except *Ho. disconveniensi* and *Ho. afromontana* Nzigidahera & Jocqué, 2014. Due to the lack of synapomorphies defining this genus, the monophyly of *Holmelgonia* remains untested (Nzigidahera & Jocqué 2014). In our phylogenetic hypothesis (Fig. 3), *Ho. basalis* resulted sister to *Callitrichia* (Clade 40), a relationship supported by the presence of a rim at the distal area of the protegulum (Ch 38, synapomorphic) and posterior lateral spinneret with more than three aciniform gland spigots (Ch 116, homoplastic). Since only one *Holmelgonia* species was represented in our analysis, it is yet premature to decide whether the genus is a monophyletic assemblage sister to *Callitrichia*, or a paraphyletic set of taxa that should in turn require taxonomic actions. Further phylogenetic analyses with a thorough species representation of *Holmelgonia*, including the type species *Ho. nemoralis*, as well as *Callitrichia* and other related taxa, is needed.

Distribution: Ivory Coast, Cameroon, Congo, Burundi, Tanzania, Uganda, Kenya, Malawi and Mozambique.

Natural history: Species of this genus were found in lower vegetation, forest litter and by pitfall traps (Jocqué 1981; Jocqué & Scharff 1986; Scharff 1990a). Most species live at high altitude and have small endemic ranges, while some have a wide distribution at midaltitude (Nzigidahera & Jocqué 2014).

HOLMELGONIA BASALIS JOCQUÉ & SCHARFF, 1986 (FIGS 19C, 22C, 24C, 36; SUPPORTING INFORMATION, FIG. S2A)

Elgonella basalis Jocqué & Scharff, 1986: 12, figs 18–25 (Dmf).

Elgonia basalis Platnick, 1989: 232.

Elgonia basalis Scharff, 1990a: 25, figs 44–46 (mf).

Holmelgonia basalis, Jocqué & Scharff, 2007: 161.

Examined material: Tanzania, Uzungwa Mts., Mwanihana Forest above Sanje River, 1700 m, 1♂1♀ 15.viii.1982, leg. M, Stoltze & N, Scharff (ZMUC); same locality, 1800 m, pitfall trap, 1♂ 18.viii.1982, leg. M, Stoltze & N, Scharff (ZMUC); same locality, 1800 m, litter, 1♀ 15.viii.1982, leg. M, Stoltze & N, Scharff (ZMUC).

Description:

Male (ZMUC, 15.viii.1982): Total length: 1.72. Prosoma: 0.79 long, 0.61 wide, without modification

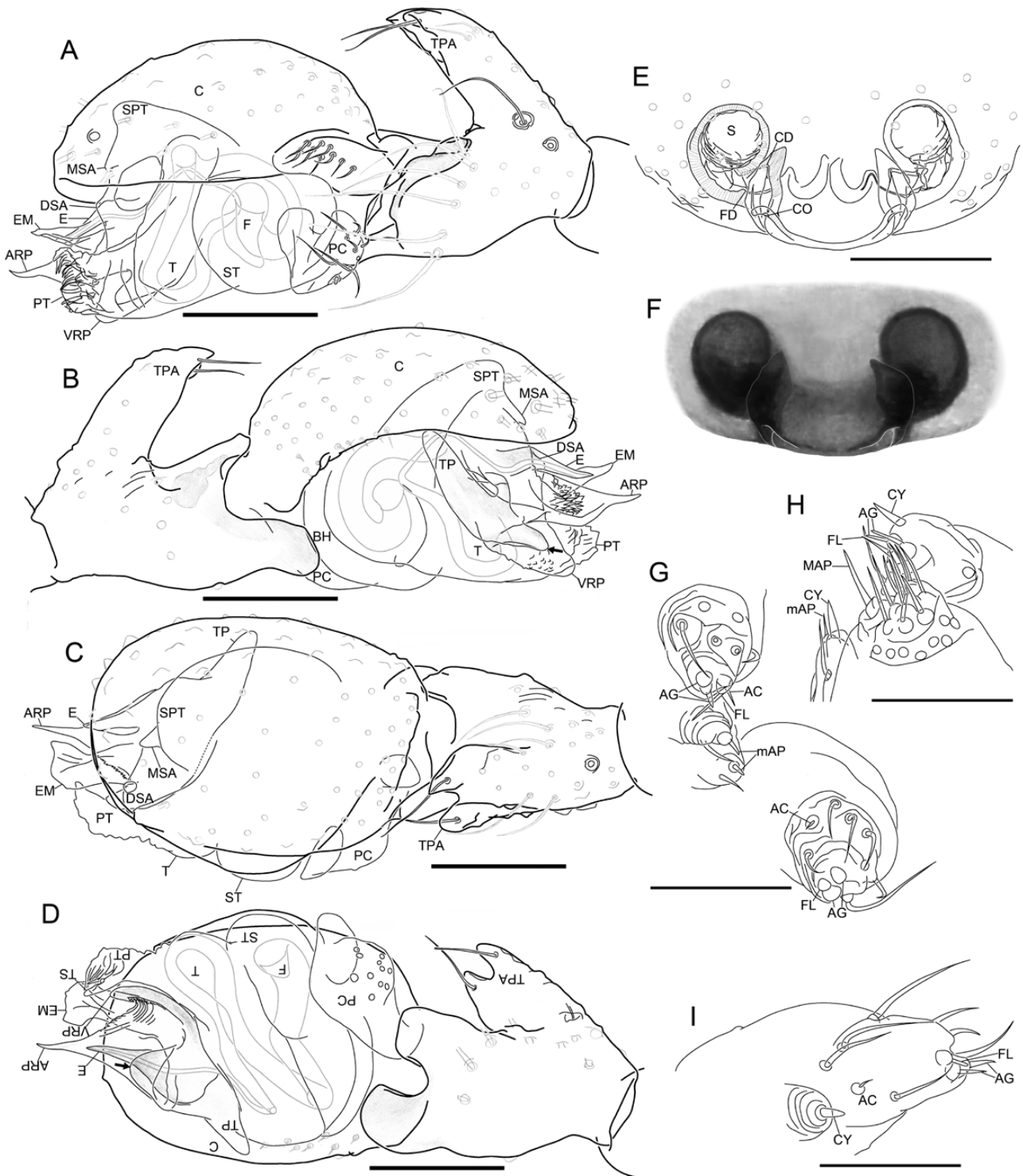


Figure 36. *Holmelgonia basalis* Jocqué & Scharff, 1986. A–D, male right palp, images flipped horizontally. A, retrolateral view. B, prolateral view. C, dorsal view. D, ventral view. E, F, epigyne. E, ventral view. F, external morphology. G, male posterior median spinnerets and posterior lateral spinnerets. H, female right spinnerets. I, female right posterior lateral spinneret. Scale bars 0.1 mm.

(Fig. 19C). Eyes: AME-AME: 0.02, AME width: 0.04, AME-ALE: 0.02, ALE width: 0.08, ALE-PLE: 0, PLE width: 0.09, PLE-PME: 0.08, PME width: 0.02, PME-PME: 0.03. Clypeus: not hirsute, one sub-AME seta. Sternum: 0.44 long, 0.48 wide. Chelicerae: mastidia absent; stridulatory striae ridged, rows widely and evenly spaced (Fig. 22C). Legs: tibia chaetotaxy 2-2-1-1; dorsal proximal macroseta on tibia II, III and IV 2.24, 4.1 and 3.85 times diameter of tibia, respectively; Tm I: 0.60. All metatarsi with trichobothrium. Pedipalp: patella prolateral proximal vertical macrosetae absent; tibia with one prolateral, two retrolateral trichobothria; TPA large, base distant from C base, distal part as wide as base, with two protuberances at tip, each with a seta below (Fig. 36A, C); PC base not visible from dorsal view, distal setae close to distal clasp, distal-setae-bearing area wide, distal clasp without striae, clasp extended apically (Fig. 36A); T without papillae, PT apical part with long papillae; TS shot, slender (Fig. 36D); MSA present; DSA wide, truncated at tip (Fig. 36A); EM broad, flat, without papillae, not exceeding ARP; ARP pointed; LER absent; central embolar apophysis present; VRP long, with papillae close to tip; TP long, round at tip; E short and slender, slightly retrolaterally curved (Fig. 36B). Opisthosoma: dorsal pattern see Fig. 24C; PMS with mAP, AC absent; PLS with triad, one AC (Fig. 36G).

Female: Total length: 2.04. Prosoma: 0.88 long, 0.62 wide. Eyes: AME-AME: 0.02, AME width: 0.04, AME-ALE: 0.02, ALE width: 0.08, ALE-PLE: 0, PLE width: 0.07, PLE-PME: 0.04, PME width: 0.07, PME-PME: 0.03. Clypeus: not hirsute, one sub-AME seta. Sternum: 0.5 long, 0.51 wide. Legs: tibia chaetotaxy 2-2-1-1; dorsal proximal macroseta on tibia I 2.85 times diameter of tibia, respectively; Tm I: 0.60. Epigyne: Clade 13 characteristic morphology, CO close to dorsal plate posterior margin (Fig. 36E, F). Opisthosoma dorsal pattern same as male; PMS with mAP, CY; PLS with triad, one AC, two CY (Fig. 36H, I).

Distribution: Tanzania.

MITRAGER VAN HELSDINGEN, 1985

Type species: *Mitrager noordami* van Helsdingen, 1985.

Diagnosis: *Mitrager* is similar to other taxa on Clade 13 in palpal and somatic features, but is characterized and can be distinguished by the following unique combination of features:

1. Paracymbium: medium- to large-sized (small in *Oedothorax*); base not visible from dorsal view

of male pedipalp (visible in *Oedothorax*); distal setae-bearing area not prominently laterally elevated (prominently laterally elevated in some *Callitrichia*); distal clasp with striae in many species (no striae in other taxa in Clade 13).

2. Copulatory bulb: embolus base protuberance absent (present in *Oedothorax*); embolus retrolaterally spiral (prolaterally spiral in *Oedothorax*), covered dorsally by lateral extension of radix (LER) in most species, except *M. elongata* and *M. tholusa*, in which it is retrolateral to the embolus (LER absent in most other species in Clade 13 except *Ca. convector*); tegular papillae absent (present in many *Oedothorax* and *Ca. macrophthalma*).
3. Palpal tibia: prolateral apophysis varies from small or absent to prominent in some species, but never elevated vertically except *M. noordami* (vertically elevated in many *Callitrichia*); scaly prolateral spike present except *M. noordami*, retrolaterally directed in most species (absent in other species in Clade 13); retrolateral apophysis short, retrolaterally curved in many species (absent in *Oedothorax* and *Callitrichia* except *Ca. convector*).
4. The general structure of the epigyne in *Mitrager* is extremely similar across species, and also similar to that of *Callitrichia*, *Holmelgonia*, *Oedothorax* and other related taxa. It can be distinguished from *Callitrichia* and *Holmelgonia* by the position of the entrance of copulatory ducts into the spermathecae, more mesal to the exits of the fertilization ducts. For a general description of epigynal conformation, see shared features defining Clade 13 above.

Monophyly: This genus is supported by the following unambiguous character transformations: the retrolateral bending of palpal tibia prolateral spike (Ch 53, synapomorphic; lost in *M. noordami*) and the wavy prolateral margin of the embolus (Ch 14, homoplastic).

Description: The genus includes medium-sized erigonines mostly with a variegated opisthosoma. Male prosoma varies in degree of modification, ranging from unnoticeable (*M. unicolor* and *M. hirsuta*) to prominent post-PME humps, post-PME grooves, PME lobe, inter-AME-PME lobe, clypeal hump, cheliceral apophysis, pre-PME groove and modified setae. Chelicerae without mastidia. Clypeus with one sub-AME seta. For palpal and epigynal feature see diagnosis.

Species included: This genus comprises 25 species (re-described below), among which 24 species are transferred from *Oedothorax*.

Distribution: Nepal, India, Indonesia (Java).

Natural history: Most species have been collected from broad-leaved or coniferous forest litter.

MITRAGER NOORDAMI VAN HELSDINGEN, 1985

(FIGS 37, 38O, 39O, 40P; SUPPORTING INFORMATION, FIG. S3C)

Mitrager noordami van Helsdingen, 1985: 353, figs 1–14 (Dmf).

Examined material: **Indonesia:** Central Java, Dijeng Plateau, near Gunung Prahau, 2580 m, sifted from litter among mosses, ferns and Ericaceae, 1♂1♀ 8.viii.1977, leg. A. Noordam (paratype, Naturalis Museum, Leiden).

Diagnosis:

Males: This species can be recognized by its unique, prominent prosomal modification (Fig. 38O).

Females: Somatic features and coloration similar to other *Mitrager* and some *Callitrichia* species, but can be distinguished by the much more convergent borders between the dorsal and ventral plates of the epigyne (Fig. 37F, G).

Description:

Male (paratype, Naturalis Museum): Total length: 2.27. Prosoma: 1.13 long, 0.77 wide, with extremely high, ballon-shaped post-PME hump, inter-PME region with a protrusion with two round lobes, anterior margin of lobes with row of light-coloured setae, interocular region with two dense, light-coloured setal tufts (Fig. 38O). Eyes: AME-AME: 0.03, AME width: 0.05, AME-ALE: 0.06, ALE width: 0.07, ALE-PLE: 0.01, PLE width: 0.08, PLE-PME: 0.1, PME width: 0.07, PME-PME: 0.35. Clypeus hirsute. Sternum: 0.6 long, 0.58 wide. Chelicerae: stridulatory striae imbricated, rows widely and evenly spaced (Fig. 39O). Legs: dorsal proximal macroseta on tibia IV 1.80 times diameter of tibia; Tm I: 0.82. Pedipalp: patella prolateral proximal vertical macrosetae absent; tibia with one prolateral, two retrolateral trichobothria; TPS absent; TPA large, conical, distal part narrow and flat, tip curved downwards; PC distal setae close to distal clasp, distal-setae-bearing area slightly wide, distal clasp without striae, clasp extended apically; T without papillae; PT median-long, with small papillae; TS median-long, slender, without papillae; MSA present; DSA wide, round at tip, ventral corner slightly more protruded (Fig. 37A); EM broad and flat, retrolateral to LER, with parallel folds extended until anterior margin, exceeding ARP; ARP flat, blunt, short; LER large, bent over E; VRP long, thick at base; R without papillae; TP long, round at tip; E median-long, retrolaterally curved,

E tip with prolateral anterior flat extension (Fig. 37A). Opisthosoma: dorsal pattern see Fig. 40P; PMS with mAP, AC absent; PLS with triad, one AC (Fig. 37H).

Female (paratype, Naturalis Museum): Total length: 2.48. Prosoma: 1.22 long, 0.84 wide. Eyes: AME-AME: 0.03, AME width: 0.05, AME-ALE: 0.03, ALE width: 0.08, ALE-PLE: 0.01, PLE width: 0.08, PLE-PME: 0.05, PME width: 0.08, PME-PME: 0.12. Clypeus: not hirsute, one sub-AME seta. Sternum: 0.67 long, 0.62 wide. Legs: dorsal proximal macroseta on tibia III 2.39 times diameter of tibia; Tm I: 0.62. Epigyne: Clade 13 characteristic morphology, border between ventral and dorsal plates largely converging toward the middle (Fig. 37F, G). Opisthosoma dorsal pattern same as male; PMS one CY, one mAP, AC absent; PLS with triad, two CY, one AC (Fig. 37I).

Distribution: Only known from the type locality in Indonesia.

Remarks: The setal tufts at interocular region and inter-PME region are aggregated setae, similar to that found in some *Callitrichia* species.

MITRAGER ANGELA (TANASEVITCH, 1998) **COMB. NOV.**

(FIGS 26A, B, 38F, 39F, 40F, 41; SUPPORTING INFORMATION, FIG. S3D)

Oedothorax angelus Tanasevitch, 1998a: 433, figs 14–18 (Dm).

Type material: Holotype: **Nepal:** Panchthar District, Dhorpar Kharka, *Rhododendron* & *Lithocarpus* forest, 2700 m, ♂13.–16.iv.1988, leg. J. Martens & W. Schawaller (SMF 38828, examined). Paratypes: **Nepal:** same locality, together with holotype, 4♂ (SMF 38853, examined) 2♂ (ZMMU), leg. Martens & W. Schawaller; Panchthar District, Paniporua, 2300 m, mixed broad-leaved forest, 4♂ (SMF 38860, examined) 2♂ (ZFMK) 1♂ (ZMMU) 16.–20.iv.1988, leg. J. Martens & W. Schawaller.

Diagnosis:

Males: Distinguished from all other *Mitrager* species (except from *M. cornuta*, *M. coronata* and *M. villosa*) by the two pairs of branched setae in the ocular region; distinguished from the aforementioned three species by the absence of postocular groove.

Description:

Male (holotype): Total length: 1.97. Prosoma: 0.91 long, 0.73 wide, PME- and postocular region elevated, posteriorly with setae bifurcated anterior-posteriorly;

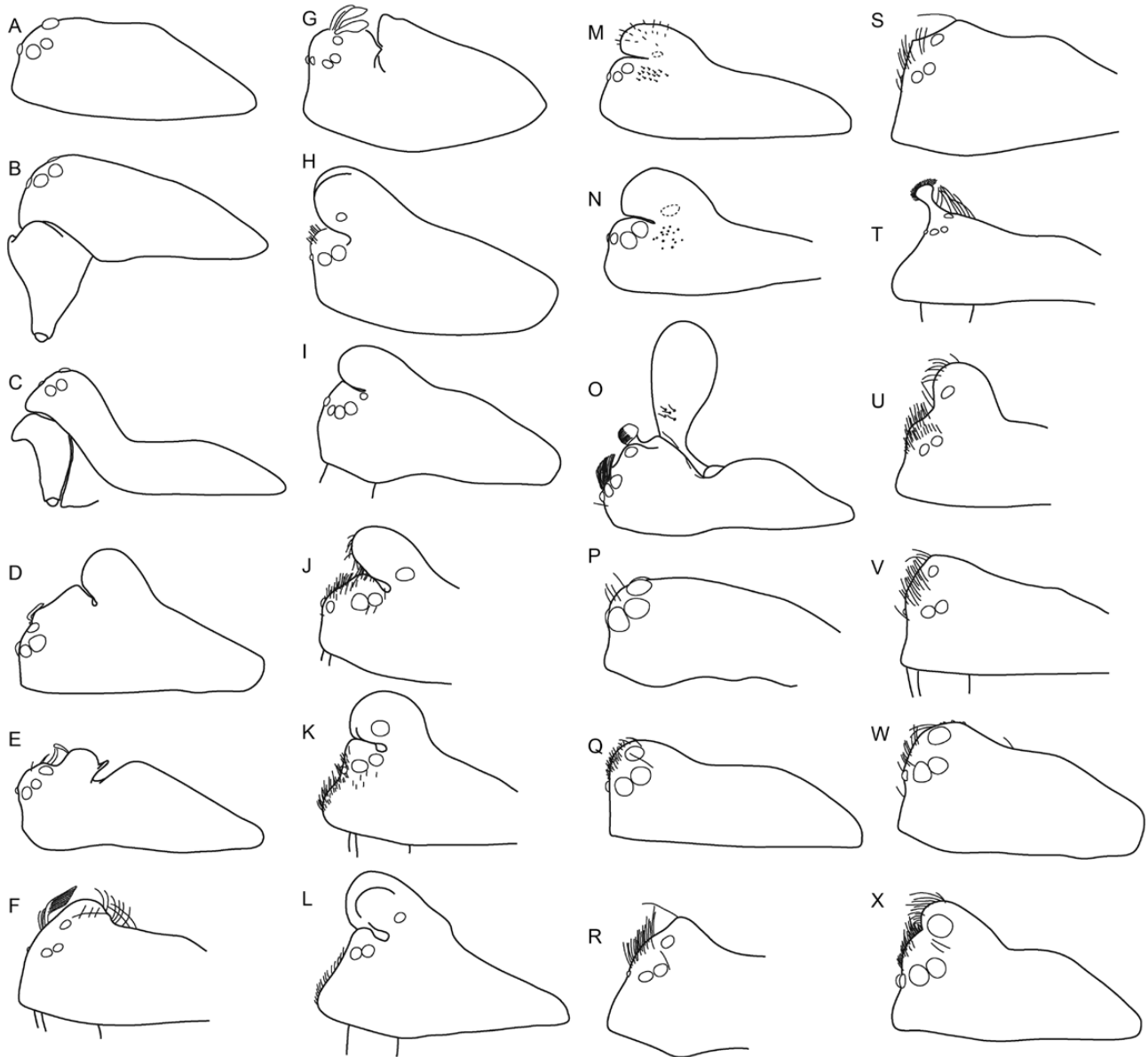


Figure 38. Male prosomal morphology of Clade 55 in [Figure 3](#), lateral. A, *Mitrager hirsuta* (Wunderlich, 1974) (Wunderlich, 1974, fig. 8). B, *M. clypeellum* (Tanasevitch, 1998) (traced from photograph). C, *M. elongata* (Wunderlich, 1974) (Wunderlich, 1974, fig. 13). D, *M. cornuta* (Tanasevitch, 2015) (Tanasevitch, 2015, fig. 16). E, *M. villosa* (Tanasevitch, 2015) (Tanasevitch, 2015, fig. 89). F, *M. angela* (Tanasevitch, 1998) (Tanasevitch, 1998a, fig. 14). G, *M. coronata* (Tanasevitch, 1998) (Tanasevitch, 1998a, fig. 6). H, *M. sexocolorum* (Tanasevitch, 1998) (Tanasevitch, 1998a, fig. 19). I, *M. globiceps* (Thaler, 1987) (traced from photograph). J, *M. lineata* (Wunderlich, 1974) (traced from photograph). K, *M. dismodicoides* (Wunderlich, 1974) (traced from photograph). L, *M. tholusa* (Tanasevitch, 1998) (Tanasevitch, 1998a, fig. 24). M, *M. lucida* (Wunderlich, 1974) (Wunderlich, 1974, fig. 30). N, *M. sexoculata* (Wunderlich, 1974) (traced from photograph). O, *M. noordami* van Helsdingen, 1985 (van Helsdingen, 1985, fig. 1). P, *M. unicolor* (Wunderlich, 1974) (traced from photograph). Q, *M. rustica* (Tanasevitch, 2015) (Tanasevitch, 2015, fig. 75). R, *M. assueta* (Tanasevitch, 1998) (Tanasevitch, 1998a, fig. 1). S, *M. malearmata* (Tanasevitch, 1998) (Tanasevitch, 1998a, fig. 50). T, *M. savigniformis* (Tanasevitch, 1998) (Tanasevitch, 1998a, fig. 40). U, *M. falcifer* (Tanasevitch, 1998) (Tanasevitch, 1998a, fig. 46). V, *M. modesta* (Tanasevitch, 1998) (Tanasevitch, 1998a, fig. 36). W, *M. lopchu* (Tanasevitch, 2015) (traced from photograph). X, *M. falciferoides* (Tanasevitch, 2015) (Tanasevitch, 2015, fig. 35).

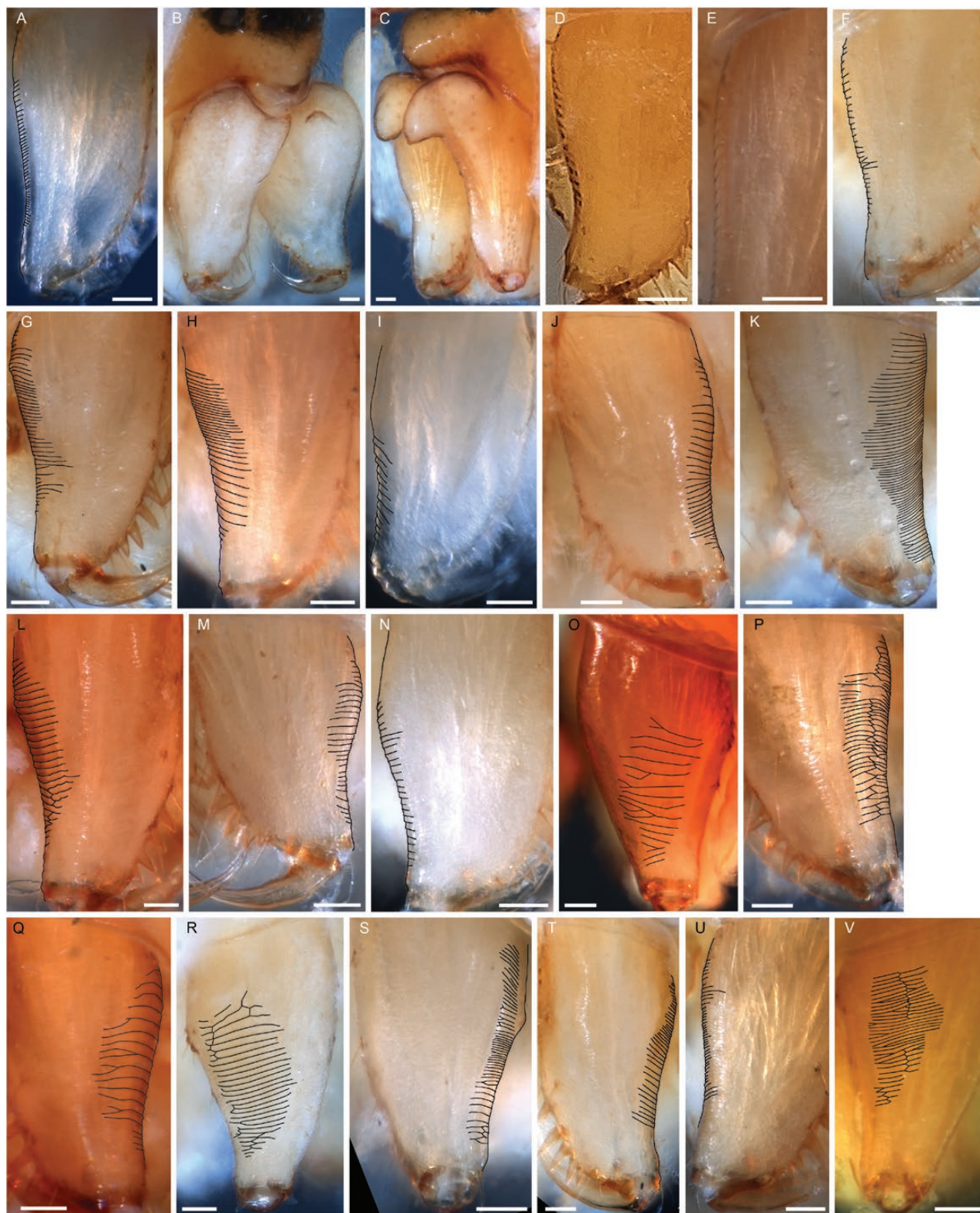


Figure 39. Male chelicerae, stridulatory striae on lateral side. A, *Mitrager hirsuta*. B, *M. clypeellum*. C, *M. elongata*. D, *M. cornuta*. E, *M. villosa*. F, *M. angela*. G, *M. coronata*. H, *M. sexoculorum*. I, *M. globiceps*. J, *M. lineata*. K, *M. dismodicoides*. L, *M. tholusa*. M, *M. lucida*. N, *M. sexoculata*. O, *M. noordami*. P, *M. unicolor*. Q, *M. rustica*. R, *M. assueta*. S, *M. savigniformis*. T, *M. falcifer*. U, *M. modesta*. V, *M. falciferoides*. Scale bars 0.05 mm.

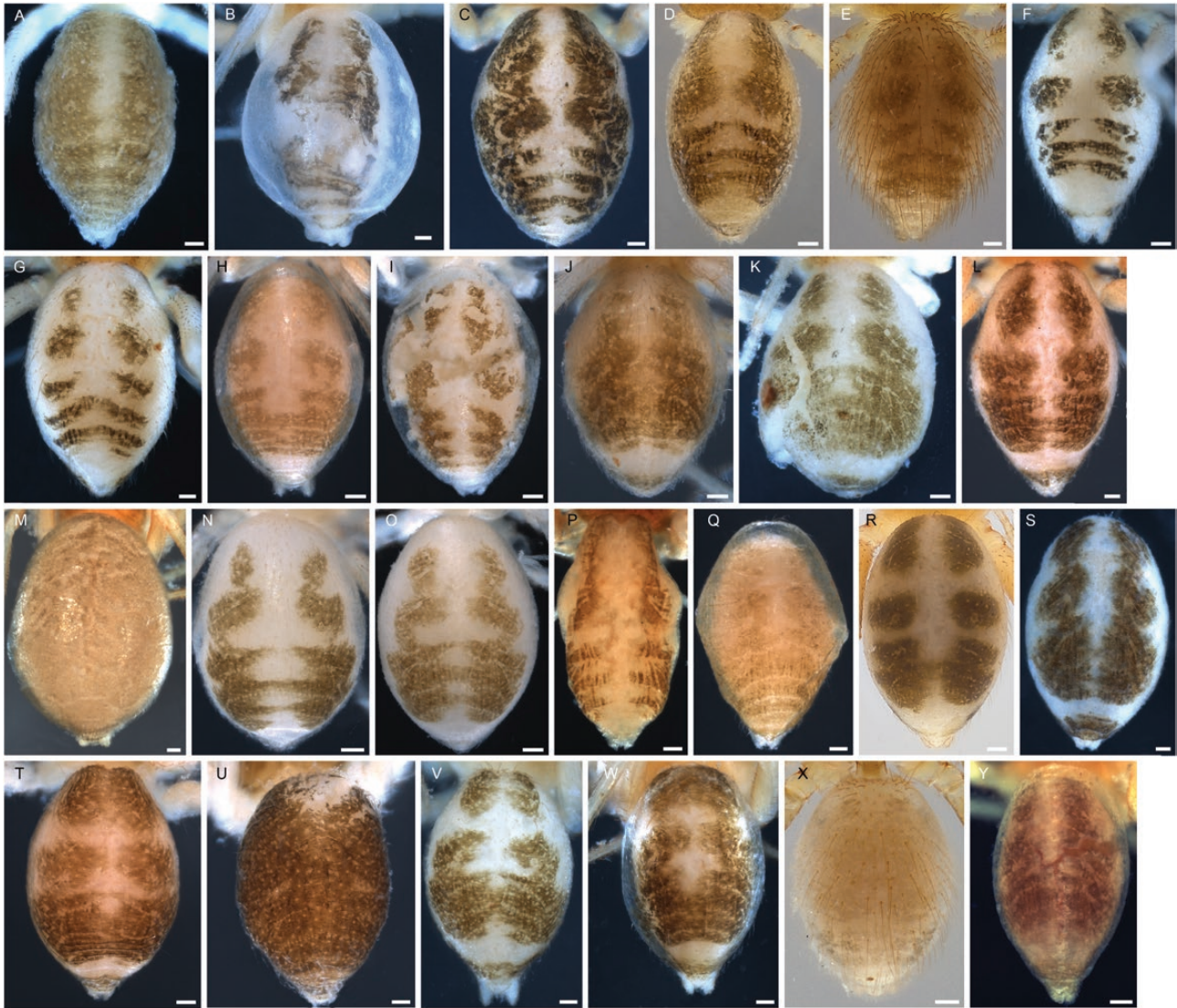


Figure 40. Opisthosoma, dorsal view. A–L, N–Y, male; D, female. A, *Mitrager hirsuta* (Wunderlich, 1974). B, *M. clypeellum* (Tanasevitch, 1998). C, *M. elongata* (Wunderlich, 1974). D, *M. cornuta* (Tanasevitch, 2015). E, *M. villosa* (Tanasevitch, 2015). F, *M. angela* (Tanasevitch, 1998). G, *M. coronata* (Tanasevitch, 1998). H, *M. sexocolorum* (Tanasevitch, 1998). I, *M. globiceps* (Thaler, 1987). J, *M. lineata* (Wunderlich, 1974). K, *M. dismodicoides* (Wunderlich, 1974). L, *M. tholusa* (Tanasevitch, 1998), holotype. M, '*M. tholusa*', paratype (not conspecific with holotype). N, *M. lucida* (Wunderlich, 1974). O, *M. sexoculata* (Wunderlich, 1974). P, *M. noordami* van Helsing, 1985. Q, *M. unicolor* (Wunderlich, 1974). R, *M. rustica* (Tanasevitch, 2015). S, *M. assueta* (Tanasevitch, 1998). T, *M. savigniformis* (Tanasevitch, 1998), paratype. U, *M. savigniformis*, holotype. V, *M. falcifer* (Tanasevitch, 1998). W, *M. modesta* (Tanasevitch, 1998). X, *M. lopchu* (Tanasevitch, 2015). Y, *M. falciferoides* (Tanasevitch, 2015). Scale bars 0.1 mm.

inter-PME region with two pairs of branched setae, posterior pair longer than anterior (Figs 26A, B, 38F). Eyes: AME-AME: 0.05, AME width: 0.04, AME-ALE: 0.05, ALE width: 0.06, ALE-PLE: 0.01, PLE width: 0.06, PLE-PME: 0.06, PME width: 0.05, PME-PME: 0.13. Clypeus: not hirsute. Sternum: 0.51 long, 0.53 wide. Chelicerae: mastidia absent, stridulatory striae imbricated, rows widely and evenly spaced (Fig. 39F). Legs: dorsal proximal macroseta on tibia I and III

0.34 and 0.35 times diameter of tibia, respectively; Tm I: 0.83. Pedipalp: patella prolateral proximal vertical macrosetae present; tibia with one prolateral, two retrolateral trichobothria; TPS without scale, retrolaterally pointed; several parallel slit organs prolateral to TPS; TPA absent; TRA bent retrolaterally (Fig. 41C); PC median-sized, base not visible from dorsal view, distal setae close to distal clasp, distal clasp with striae, directed retrolaterally, (Fig. 41A); T without

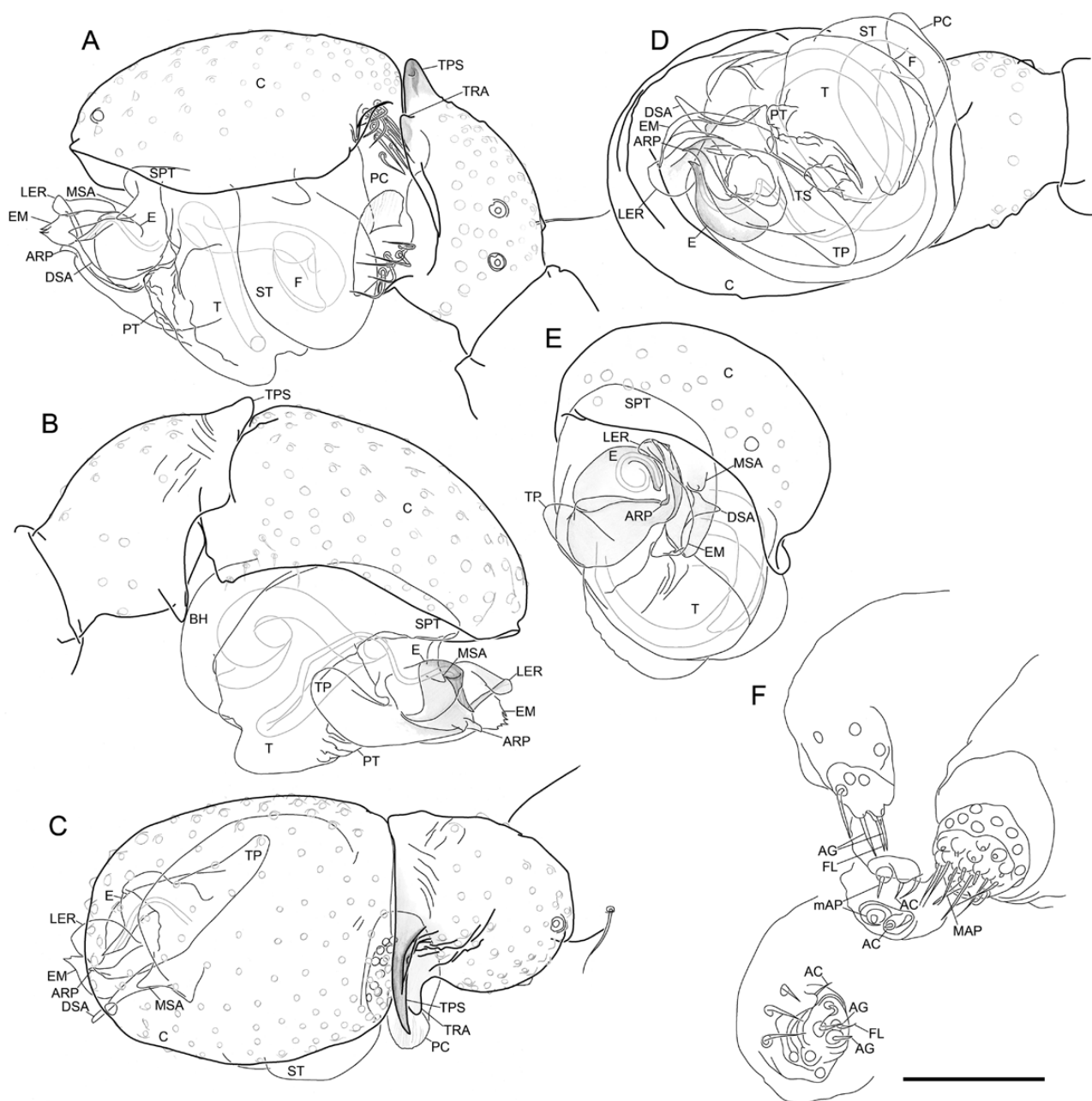


Figure 41. *Mitrager angela* (Tanasevitch, 1998). A–E, male right palp, images flipped horizontally. A, retrolateral view. B, prolateral view. C, dorsal view. D, ventral view. E, apical view. F, male spinnerets. Scale bar 0.1 mm.

papillae, PT short, TS short, without papillae (Fig. 41D); MSA present (Fig. 41A); DSA pointed, retrolaterally curved (Fig. 41D); EM flat, anterior margin with papillae, length exceeds ARP (Fig. 41B); ARP pointed, bent distally; LER without striae, extended dorsal to E; VRP absent; TP round at tip (Fig. 41B); E retrolaterally spiral, anterior margin at base slightly wavy (Fig. 41B).

Opisthosoma: dorsal pattern see Fig. 40F; PMS with mAP, one AC; PLS with triad, one AC (Fig. 41F).

Female: Unknown.

Variation: The measurements are based on examined material.

Males ($N = 9$, means in parentheses): Total length 1.97–2.26 (2.09). Prosoma: 0.91–1.00 (0.95) long, 0.69–0.77 (0.73) wide. Legs: dorsal proximal macroseta on tibia I, II, III and IV 0.24–0.37 (0.30), 0.27–0.44 (0.32, $N = 8$), 0.23–0.42 (0.33, $N = 8$) and 2.08–2.96 (2.60, $N = 5$) times diameter of tibia, respectively; Tm I: 0.75–0.84 (0.81).

Distribution: Nepal.

Habitat: broad-leaved forests at middle altitude.

MITRAGER ASSUETA (TANASEVITCH, 1998) **COMB. NOV.**

(FIGS 38R, 39R, 40S, 42, 43B; SUPPORTING INFORMATION, FIG. S4E)

Oedothorax assuetus Tanasevitch, 1998a: 431, figs 1–5 (Dm).

Type material: Holotype: **Nepal**: Kathmandu, Godawari, foot of Phulchoki Mt., 1700 m, ♂ 19.iii.1980, leg. Martens & A. Ausobsky (SMF 38848, examined). Paratypes: **Nepal**: same locality, together with holotype, 1♂, leg. J. Martens & A. Ausobsky (body: SMF 38852, palp: SMF 38841, examined).

Diagnosis:

Males: A depression between protogulum and tegulum is unique for this species. Further distinguished from most *Mitrager* species by a prosoma with a hump comprising the PME, and an ocular region bearing dense setae. Distinguished from *M. falcifer*, *M. falciferoides* and '*Oe.*' *meghalaya incertae sedis* by the smaller hump elevation; from *M. malearmata* by the longer spike prolateral to the palpal tibia prolateral apophysis; and from *M. modesta*, *M. lopchu* and *M. rustica* by the smaller body size.

Description:

Male (holotype): Total length: 2.40. Prosoma: 1.01 long, 0.77 wide, PME- and postocular region slightly elevated, with one strong seta at peak of elevation pointing forwards, interocular region with strong setae pointing upwards (Figs 38R, 43B). Eyes: AME-AME: 0.04, AME width: 0.04, AME-ALE: 0.03, ALE width: 0.08, ALE-PLE: 0, PLE width: 0.07, PLE-PME: 0.07, PME width: 0.07, PME-PME: 0.11. Clypeus: not hirsute. Sternum: 0.59 long, 0.57 wide. Chelicerae: stridulatory striae imbricated, rows widely and evenly spaced (Fig. 39R). Legs: Tm I: 0.56. Pedipalp: patella prolateral proximal vertical macrosetae present; tibia with one prolateral, two retrolateral trichobothria;

TPS scaly, retrolaterally pointed; TPA absent; TRA bent retrolaterally; PC short, base not visible from dorsal view, distal setae close to distal clasp, distal clasp without striae, directed retrolaterally (Fig. 42A); T without papillae; PT with long papillae, a depression between T and PT creates a discontinuous appearance from lateral view (Fig. 42D); MSA present (Fig. 42D); DSA not pointed, not retrolaterally curved (Fig. 42A); EM flat, anterior margin without obvious papillae, exceeds ARP (Fig. 42D); ARP pointed, angled at tip; LER with striae on distal margin, extended dorsal to E; VRP absent; TP round at tip, ventro-posterior area with round extension (Fig. 42B); E retrolaterally spiral, anterior margin at base slightly wavy (Fig. 42B). Opisthosoma: dorsal pattern see Fig. 40S; PMS with mAP, AC absent; PLS with triad, one AC (Fig. 42E).

Male (paratype): Total length: 2.39. Prosoma: 1.05 long, 0.86 wide. Legs: Tm I: 0.59.

Female: Unknown.

Distribution: Only known from the type locality in Nepal.

Habitat: Evergreen mountain or cloud forests.

MITRAGER CLYPEELLUM (TANASEVITCH, 1998) **COMB. NOV.**

(FIGS 38B, 39B, 40B, 44; SUPPORTING INFORMATION, FIG. S4B)

Oedothorax clypeellum Tanasevitch, 1998b: 436, figs 30–33 (Dm).

Type material: Holotype: **Nepal**: Kathmandu, Phulchoki Mt., pitfall traps, 2600 m, ♂ 21.iii.–14.v.1980, leg. Martens & A. Ausobsky (body: SMF 38857, palp: SMF 38835, examined).

Diagnosis:

Males: Similar to *M. elongata*, both species have elevated clypeus and anterior projections on the frontal surface of the chelicerae. Distinguished from the latter by the absence of lower stout setal group and the shape of palpal tibia apophyses.

Description:

Male (holotype, SMF): Total length: 2.54. Prosoma: 1.16 long, 0.87 wide, unmodified. Eyes: AME-AME: 0.05, AME width: 0.04, AME-ALE: 0.04, ALE width: 0.068, ALE-PLE: 0.02, PLE width: 0.07, PLE-PME: 0.06, PME width: 0.07, PME-PME: 0.07. Clypeus elevated, hirsute.

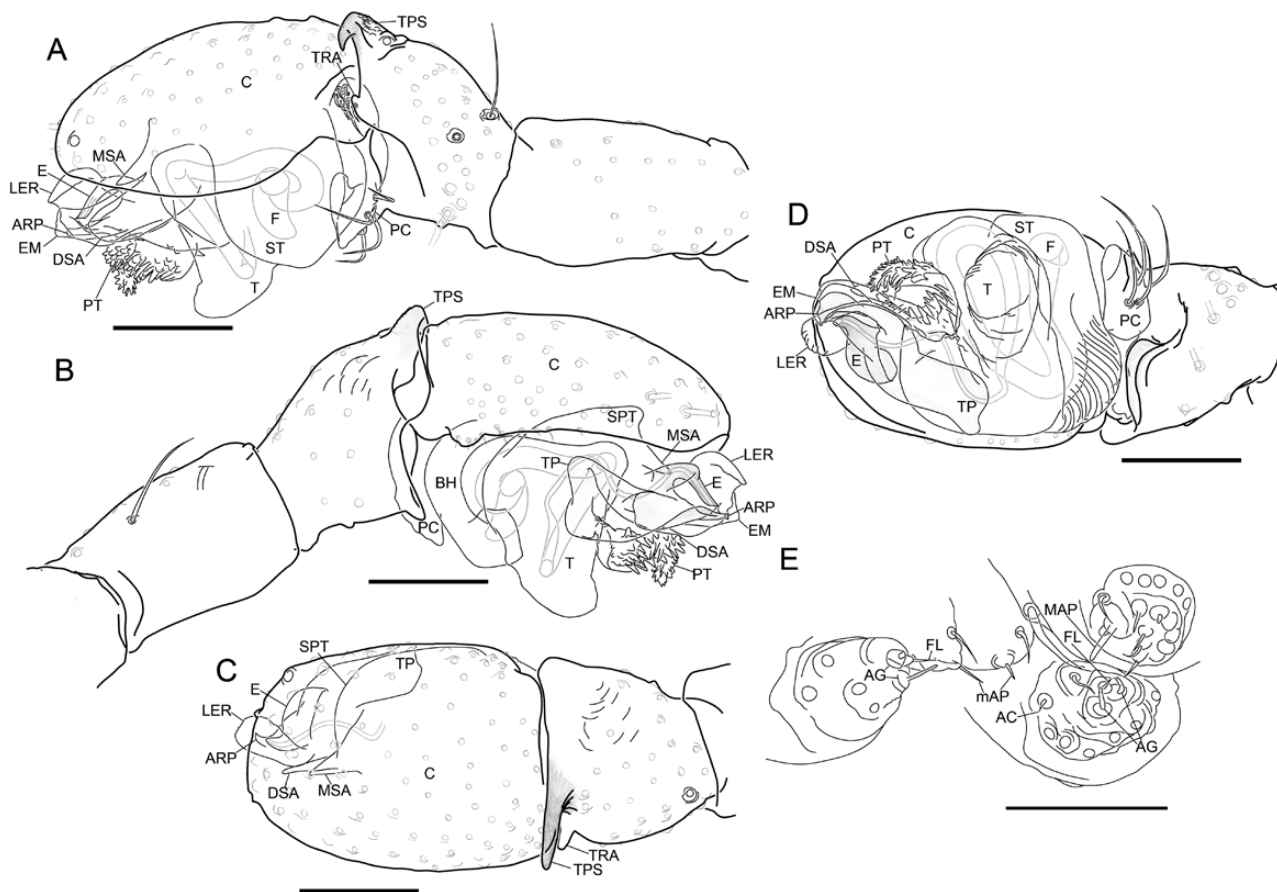


Figure 42. *Mitrager assueta* (Tanasevitch, 1998). A–D, male right palp, images flipped horizontally. A, retrolateral view. B, prolateral view. C, dorsal view. D, ventral view. E, male spinnerets. Scale bars 0.1 mm.

Sternum: 0.64 long, 0.59 wide. Chelicerae: frontally strongly elevated at base (Figs 38B, 39B); stridulatory striae absent. Legs: dorsal proximal macroseta on tibia II and IV 0.84 and 2.34 times diameter of tibia, respectively; Tm I: 0.89. Pedipalp: patella prolateral proximal vertical macrosetae present; tibia with one prolateral, two retrolateral trichobothria; TPS scaly, dorsally extended at base, distal half retrolaterally pointed; TPA arose at middle of tibia, with enlarged setal bases; TRA bent retrolaterally; PC median-sized, base not visible from dorsal view, distal setae close to distal clasp, distal clasp with striae, wider than congeners (Fig. 44A); T without papillae, PT with median-sized papillae; TS short, without papillae (Fig. 44D); MSA present; DSA broad, tip retrolaterally turned (Fig. 44E); EM flat, anterior margin without papillae, exceeds ARP (Fig. 44E); small radical papillae between ARP and E base (Fig. 44B); LER with striae on distal margin, prolateral side extended dorsal to E, retrolateral side with pointed extension (Fig. 44E); VRP absent; TP flat, narrowly round at tip; E retrolaterally

spiral, anterior margin at base slightly wavy (Fig. 44B). Opisthosoma: dorsal pattern see Fig. 40B; PMS with mAP, AC absent; PLS with triad, AC absent (Fig. 44G).

Female: Unknown.

Distribution: Only known from the type locality in Nepal.

Habitat: Evergreen mountain or cloud forests.

MITRAGER CORNUTA (TANASEVITCH, 2015) **COMB. NOV.**

(Figs 38D, 39D, 40D, 45)

Oedothorax cornutus Tanasevitch, 2015: 383, figs 16–25 (Dmf).

Type material: Holotype: **India:** Himalayas, West Bengal, Darjeeling District, Tigerhill, 2500–2600 m, near top, sifting in forest, ♂ 18.x.1978, leg. C. Besuchet

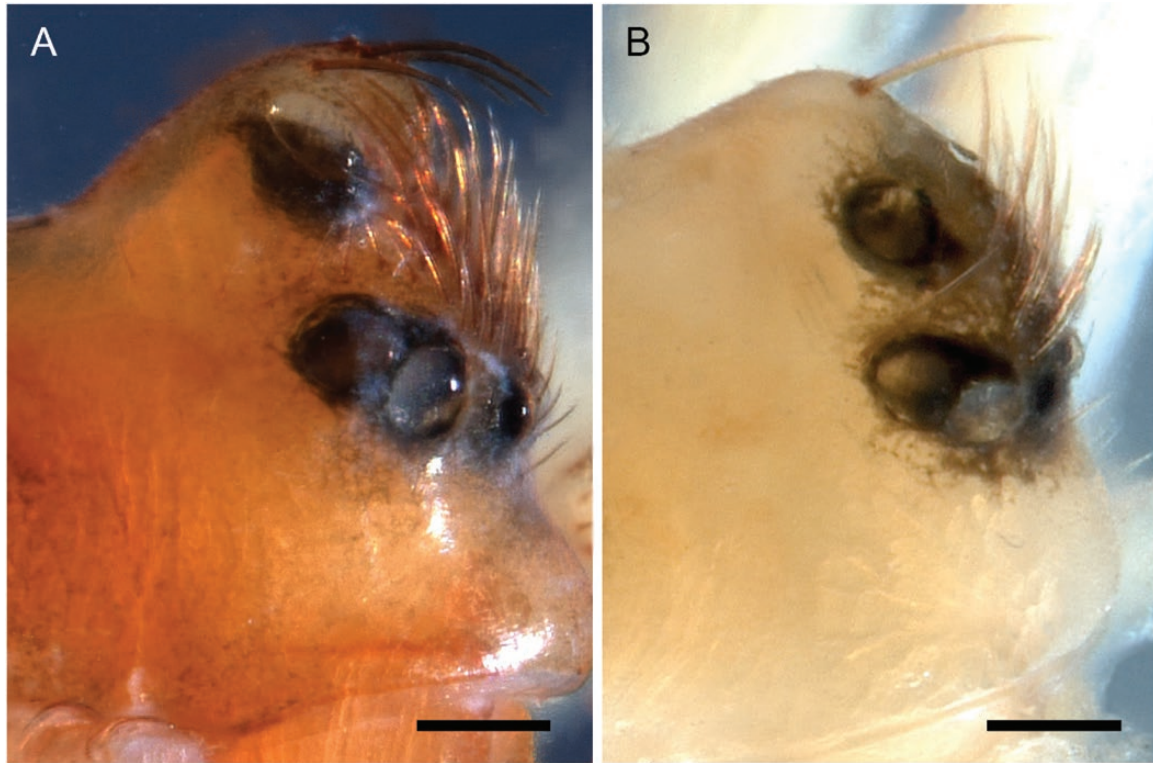


Figure 43. Interocular strong setae, lateral view. A, '*Oedothorax*' *meghalaya* (Tanasevitch, 2015). B, *Mitrager assueta* (Tanasevitch, 1998). Scale bars 0.1 mm.

& I. Löbl (MHNG, examined). Paratype: collected together with the holotype, 1♀ (MHNG, examined).

Diagnosis:

Males: Distinguished from all other *Mitrager* species (except from *M. angela*, *M. coronata* and *M. villosa*) by the two pairs of branched setae in the ocular region; from *M. angela* and *M. coronata* by the shorter branches on the branched setae between PME; from *M. villosa* by the anteriorly oriented post-ocular groove (posteriorly oriented in *M. villosa*).

Females: Similar to *M. villosa*, they can be distinguished by the shorter copulatory ducts.

Description:

Male (holotype, MHN): Total length: 1.95. Prosoma: 0.90 long, 0.70 wide, inter-PME region bearing two pairs of thick, short, appressed toward prosoma branched setae, posterior pair much longer than anterior; pale yellow rounded postocular hump separated from ocular region by deep transverse groove (Fig. 38D). Eyes: AME-AME: 0.04, AME width: 0.05, AME-ALE: 0.02, ALE width: 0.07, ALE-PLE:

0.01, PLE width: 0.06, PLE-PME: 0.07, PME width: 0.05, PME-PME: 0.11. Clypeus: not hirsute. Sternum: 0.52 long, 0.51 wide. Chelicerae: stridulatory striae rows wide, most part evenly spaced, more compressed distally (Fig. 39D). Legs: dorsal proximal macroseta on tibia I, II and III 0.13, 0.19 and 0.26 times diameter of tibia, respectively; Tm I: 0.84. Pedipalp: patella prolateral proximal vertical macrosetae absent; tibia with one prolateral, two retrolateral trichobothria; TPS scaly, retrolaterally pointed; several parallel slit organs prolateral to TPS; TPA consists of two slightly enlarged setal bases; TRA bent retrolaterally; PC median-sized, base not visible from dorsal view, distal setae close to distal clasp, distal clasp with striae, directed retrolaterally (Fig. 45A); T without papillae; PT short; TS without papillae; MSA present; DSA pointed, retrolaterally curved; EM flat, anterior margin with papillae, exceeds ARP (Fig. 45C); ARP pointed, angled on dorsal side; VRP absent; LER without striae, extended dorsal to E; VRP absent; TP round at tip; E retrolaterally spiral, anterior margin at base slightly wavy (Fig. 45C). Opisthosoma: see Fig. 40D; PMS with mAP, two AC; PLS with triad, two AC (Fig. 45G).

Female: Total length: 2.03. Prosoma: 0.96 long, 0.67 wide. Eyes: AME-AME: 0.03, AME width: 0.05,

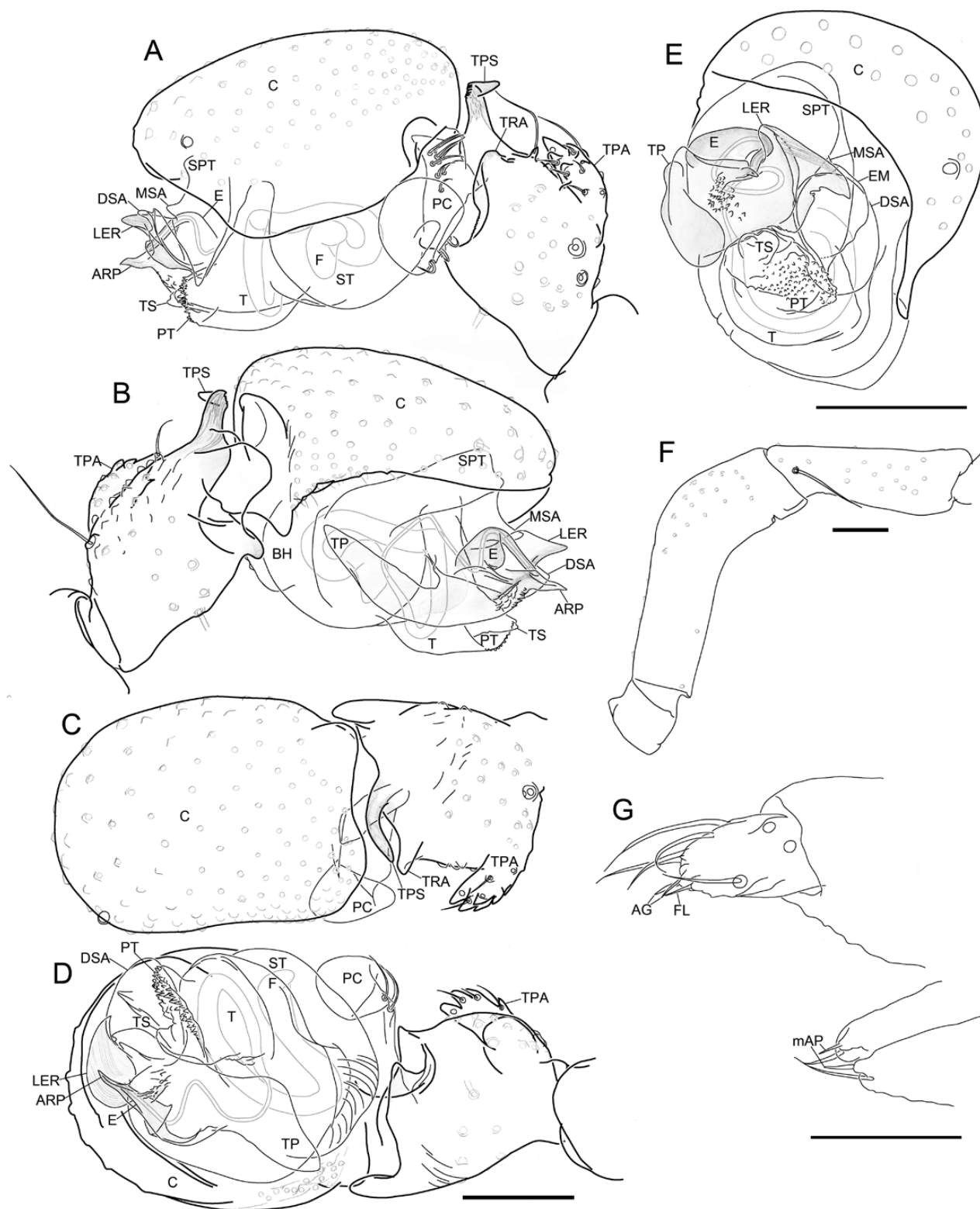


Figure 44. *Mitragrer clypeellum* (Tanasevitch, 1998). A–F, male right palp, images flipped horizontally. A, retrolateral view. B, prolateral view. C, dorsal view. D, ventral view. E, apical view. F, trochanter, femur and patella. G, male spinnerets. Scale bars 0.1 mm.

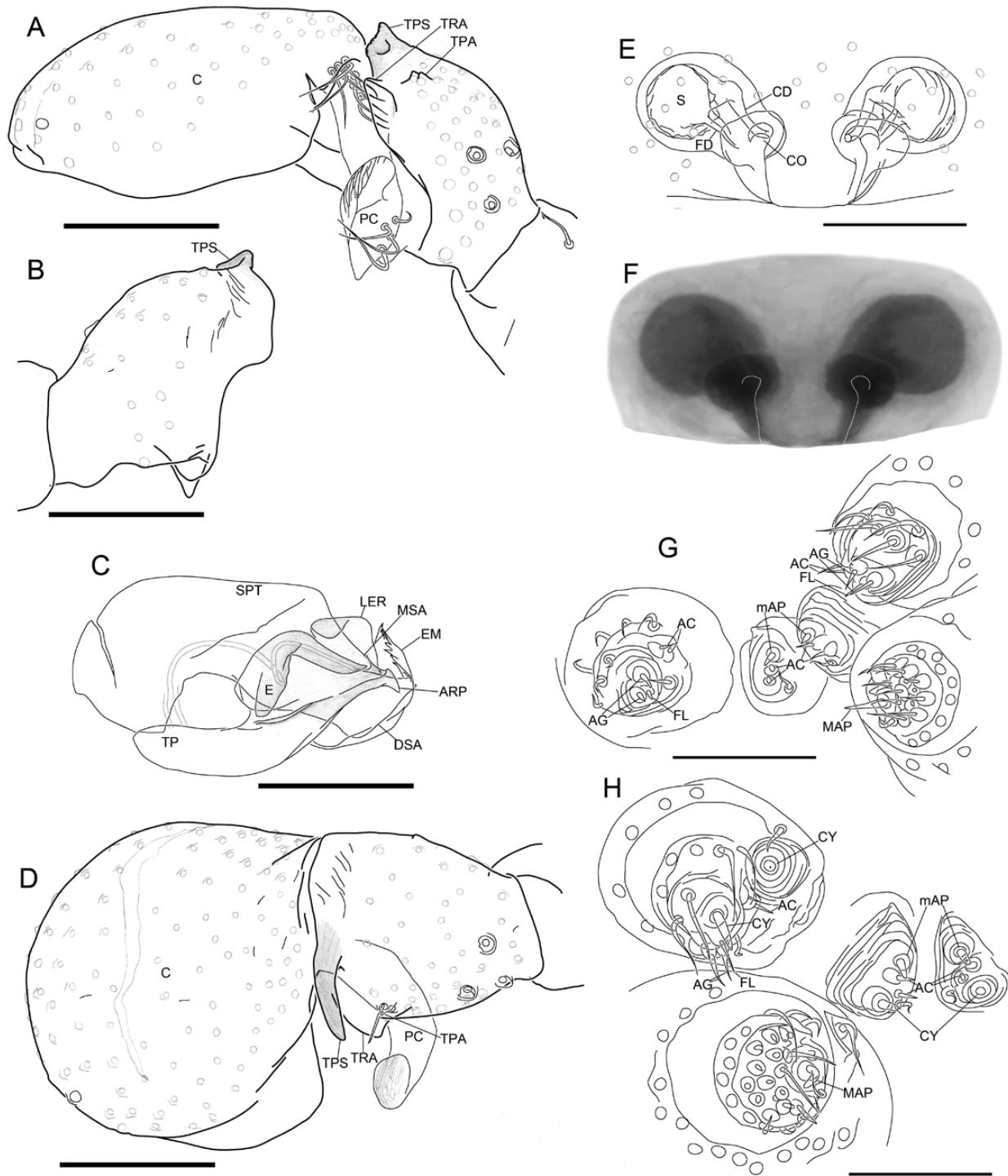


Figure 45. *Mitrager cornuta* (Tanasevitch, 2015). A–D, male right palp, images flipped horizontally. A, retrolateral view. B, tibia, prolateral view. C, embolic division, prolateral view. D, dorsal view. E, F, epigyne. E, ventral view. F, external morphology. G, male spinnerets. H, female spinnerets. Scale bars 0.1 mm.

AME-ALE: 0.02, ALE width: 0.07, ALE-PLE: 0.01, PLE width: 0.06, PLE-PME: 0.04, PME width: 0.06, PME-PME: 0.07. Clypeus: not hirsute. Sternum: 0.55 long, 0.52 wide. Legs: dorsal proximal macroseta on tibia I, III and IV 2.64, 2.47 and 3.08 times diameter of tibia, respectively; Tm I: 0.84. Epigyne: Clade 13 characteristic morphology (Fig. 45E, F). PMS with mAP, two AC, CY; PLS with triad, two AC, two CY (Fig. 45H).

Distribution: Only known from the type locality in India.

Habitat: Forest litter.

MITRAGER CORONATA (TANASEVITCH, 1998) COMB. NOV.

(FIGS 38G, 39G, 40G, 46; SUPPORTING INFORMATION, FIG. S4E)

Oedothorax coronatus Tanasevitch, 1998b: 431, figs 6–13 (Dm).

Type material: Holotype: **Nepal:** Ilam District, Mai Pokhari, 2100–2200 m, forest, ♂ 25.–27.iii.1980, leg. J. Martens & A. Ausobsky (SM 38863, examined). Paratypes: **Nepal:** Ilam District, same data as holotype, 5♂ (SMF 38839, 38831 (one male palp), examined), 2♂ (ZMMU, not examined) 25.–27.iii.1980, leg. J. Martens & A. Ausobsky; Mai Pokhari, 2100, forest, 2♂ (SMF 38859, examined) 2♂ (ZFMK, not examined) 31.iii.–1.iv.1980, leg. J. Martens & A. Ausobsky; Gitang Khola, 1900–2100 m, cultivated land, 1♂ 31.iii.1980, leg. J. Martens & A. Ausobsky (SMF 38858, examined); Mai Pokhari, 2100–2200 m, *Castanopsis* forest remains, 1♂ (SMF 38832, examined) 1♂ (ZMMU, not examined) 9.–10. iv.1988, leg. J. Martens & W. Schawaller; Panchthar District, Paniporua, 2300 m, mixed broad-leaved forest, 4♂ (carapace form b), 16–20.iv.1988, leg. Martens & W. Schawaller (SMF 38846, examined); Taplejung District, Worebung Pass, degraded broad-leaved forest, 2000, 4♂ (carapace form b) (SMF 38847, examined), 1♂ (carapace form b) (ZMMU, not examined) 21.iv.1988, leg. J. Martens & W. Schawaller.

Diagnosis:

Males: Distinguished from all other *Mitrager* species (except from *M. angela*, *M. cornuta* and *M. villosa*) by the two pairs of branched setae in the ocular region; from *M. angela* by the presence of post-ocular groove; from *M. cornuta* and *M. villosa* by the longer branches

on the two pairs of setae between PME (shorter in *M. cornuta* and *M. villosa*).

Description:

Male (holotype, SMF 38863): Total length: 2.49. Prosoma: 1.13 long, 0.91 wide, inter-PME region bearing two pairs thick, long, branched setae appressed toward prosoma, posterior pair slightly longer than anterior; pale yellow rounded postocular hump separated from ocular region by deep transverse groove (Figs 38G, 26C). Eyes: AME-AME: 0.04, AME width: 0.05, AME-ALE: 0.05, ALE width: 0.08, ALE-PLE: 0, PLE width: 0.07, PLE-PME: 0.05, PME width: 0.05, PME-PME: 0.17. Clypeus: not hirsute. Sternum: 0.63 long, 0.66 wide. Chelicerae: mastidia absent; stridulatory striae rows wide, most part evenly spaced, more compressed distally (Fig. 39G). Legs: dorsal proximal macroseta on tibia I, II, III and IV 0.47, 0.44, 0.55 and 1.29 times diameter of tibia, respectively; Tm I: 0.85. Pedipalp: patella prolateral proximal vertical macrosetae present; tibia with one prolateral, two retrolateral trichobothria; TPS scaly, retrolaterally pointed; several parallel slit organs prolateral to TPS; TPA small, with one slightly enlarged setal base; TRA bent retrolaterally (Fig. 46C). PC median-sized, base not visible from dorsal view, distal setae close to distal clasp, distal clasp with striae, directed retrolaterally (Fig. 46A); T without papillae, PT short, TS long and thick, without papillae; MSA present; DSA pointed, retrolaterally curved; EM flat, anterior margin with long papillae, length exceeds ARP (Fig. 46D); ARP pointed, with an angle on dorsal side; VRP absent; LER without striae, extended dorsal to E; TP round at tip, E retrolaterally spiral, anterior margin at base slightly wavy (Fig. 46B). Opisthosoma: dorsal pattern see Fig. 40G; PMS with mAP, two AC; PLS with triad, one AC (Fig. 46E).

Female: Unknown.

Variation: The measurements are based on examined material.

Males (N = 10, means in parentheses): Total length 2.38–2.77 (2.51). Prosoma: 1.08–1.25 (1.17) long, 0.87–0.91 (0.90) wide. Legs: dorsal proximal macroseta on tibia I, II, III and IV 0.19–0.66 (0.46, N = 9), 0.37–0.72 (0.52), 0.41–0.93 (0.62, N = 9) and 0.73–2.65 (1.41, N = 7) times diameter of tibia, respectively; Tm I: 0.81–0.85 (0.83).

Distribution: Nepal.

Habitat: Middle altitude forests.

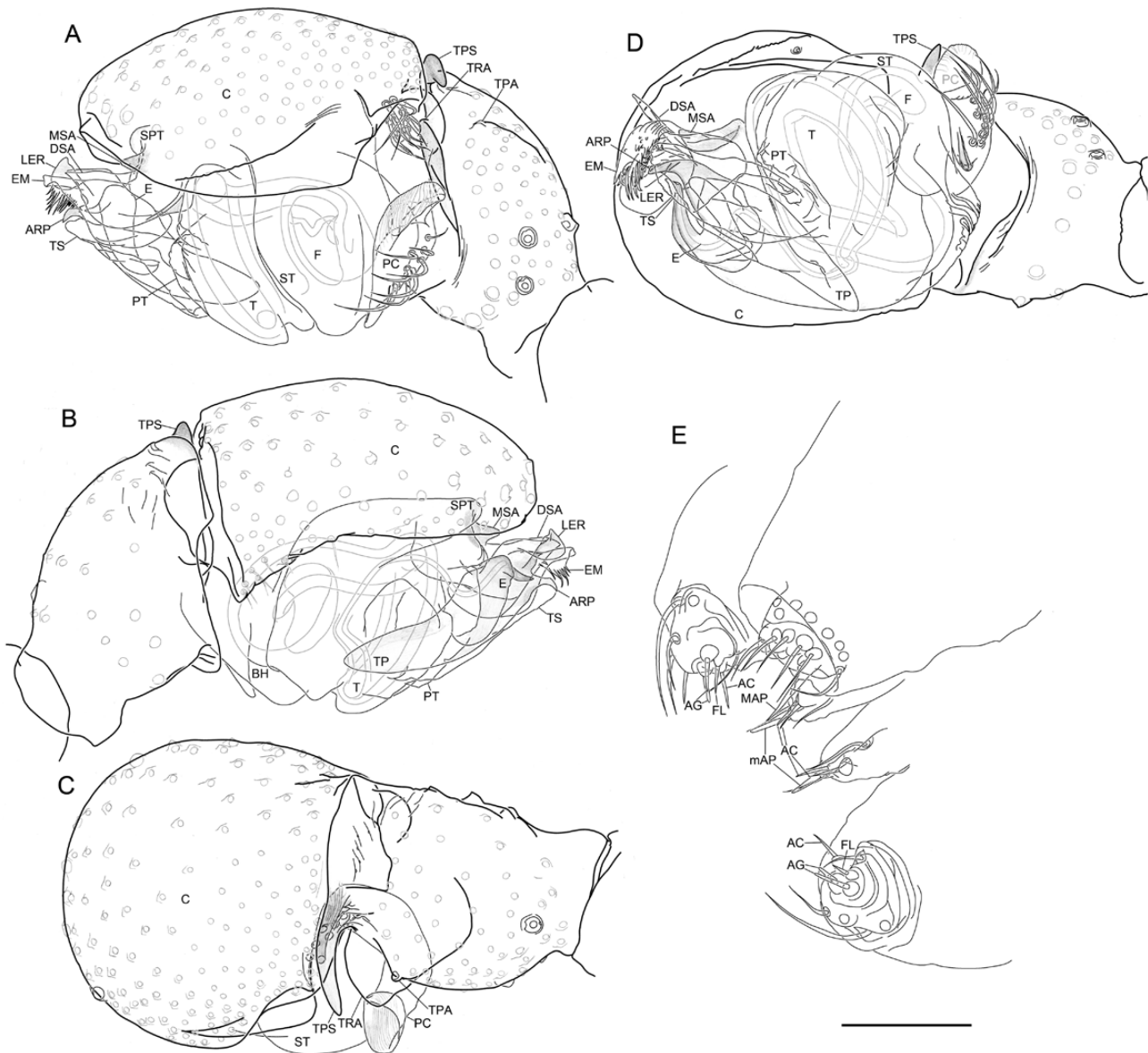


Figure 46. *Mitrager coronata* (Tanasevitch, 1998). A–D, male right palp, images flipped horizontally. A, retrolateral view. B, prolateral view. C, dorsal view. D, ventral view. E, male spinnerets. Scale bar 0.1 mm.

***MITRAGER DISMODICOIDES* (WUNDERLICH, 1974)
COMB. NOV.**

(Figs 38K, 39K, 40K, 47; SUPPORTING INFORMATION, FIG. S4I)

Oedothorax dismodicoides Wunderlich, 1974: 183, figs 42–50 (Dmf).

Type material: Holotype: **West Nepal:** down from the Gorapani saddle toward Ullcri, ravine forest, 2460 m, ♂ 15.xii.1969 (SMF 28902, examined). Paratypes: **West Nepal:** Same location and date as holotype, 2♀ (SMF 28903, examined); Thakkhola, lake next to Titi village, *Pinus*-forest, 2700 m, 1♀ 2.xii.1969 (SMF

28904, examined); Thakkhola, Lethe, 2600–2750 m, 4♀ 3.–6.xii.1969 (SMF 28905, examined).

Diagnosis:

Males: Distinguished from all other *Mitrager* species, except *M. lucida*, *M. sexoculata* and *M. tholusa*, by its prosomal modification with elevated region including posterior median eyes, a transverse groove at interocular region and an elevated and hirsute clypeus; from all other *Mitrager* species by the broader palpal tibia prolateral spike (Fig. 47B, narrower in all other species).

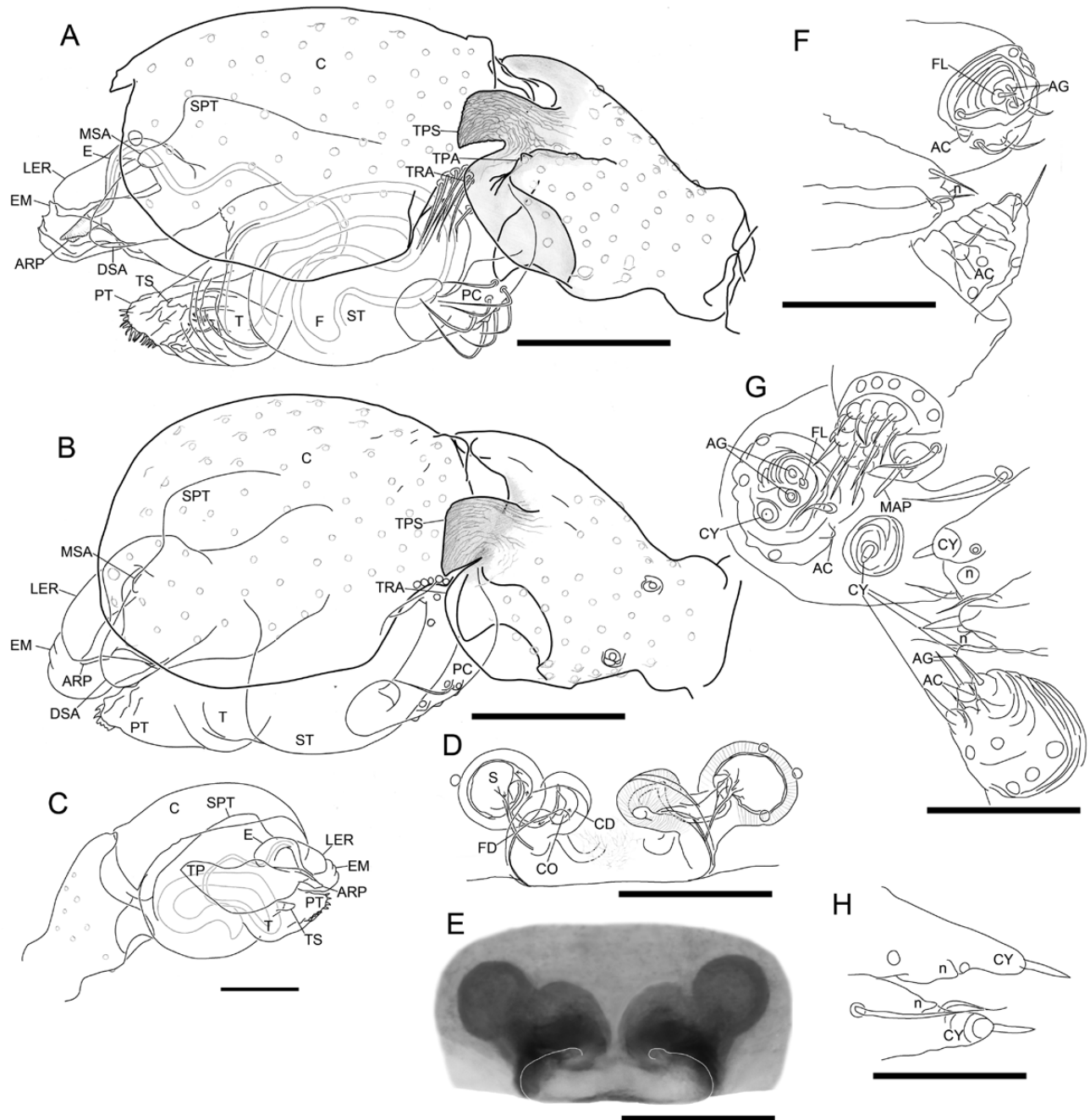


Figure 47. *Mitrager dismodicoides* (Wunderlich, 1974). A, male right pedipalp dorsoretrolateral. B, C, male left palp. B, dorsoretrolateral. C, prolateral. D, E, epigyne. D, ventral view. E, external morphology. F, male posterior median spinnerets and posterior lateral spinnerets. G, female spinnerets. H, female posterior median spinnerets, dorsal view. Scale bars 0.1 mm.

Females: Epigyne difficult to distinguish from congeners, remarkably similar to *M. lineata*.

Description:

Male (holotype, SMF 28902): Total length: 2.07. Prosoma: 1.03 long, 0.71 wide, PME-bearing region

largely elevated, frontal surface of elevation with scarcely distributed tiny setae; transverse groove between PME and other eyes; interocular region with small setae directed upwards (Fig. 38K). Eyes: AME-AME: 0.04, AME width: 0.05, AME-ALE: 0.06, ALE width: 0.08, ALE-PLE: 0, PLE width: 0.07, PLE-PME: 0.06, PME width: 0.07, PME-PME: 0.10.

Clypeus: hirsute, elevated. Sternum: 0.52 long, 0.55 wide. Chelicerae: mastidia absent, stridulatory striae rows compressed in most part, proximal and distal parts with wider rows (Fig. 38K). Legs: Tm I: 0.78. Pedipalp: patella prolateral proximal vertical macrosetae absent; tibia with one prolateral, two retrolateral trichobothria; TPS scaly, wide, retrolaterally bent; TPA slightly elevated, with one slightly enlarged setal base; TRA distally oriented; PC median-sized, base not visible from dorsal view, distal setae close to distal clasp, distal clasp without striae, distally extended; T without papillae; PT with long papillae; TS median-long, thick, with several long papillae at base; MSA present; DSA not pointed, not retrolaterally turned; EM flat, anterior margin without papillae, exceeds ARP; ARP pointed, striated, angled on dorsal side; LER without striae, extended dorsal to E (Fig. 47A); VRP absent; TP pointed at tip (Fig. 47C); E retrolaterally spiral, anterior margin at base slightly wavy (Fig. 47A). Opisthosoma: dorsal pattern see Fig. 40K; PMS without spigots, but with one nubbin (vestigial mAP); PLS with triad, one AC (Fig. 47F).

Female (paratype, SMF 28905): Total length: 2.61. Prosoma: 1.05 long, 0.83 wide. Eyes: AME-AME: 0.03, AME width: 0.05, AME-ALE: 0.07, ALE width: 0.08, ALE-PLE: 0.01, PLE width: 0.08, PLE-PME: 0.06, PME width: 0.07, PME-PME: 0.10. Clypeus not hirsute. Sternum: 0.59 long; 0.63 wide. Legs: dorsal proximal macroseta on tibia I, II, III and IV 2.10, 2.23, 2.77 and 3.08 times diameter of tibia, respectively; Tm I: 0.63. Epigyne: Clade 13 characteristic morphology, borders between dorsal and ventral plates converging anteriorly (Fig. 47D, E). Opisthosoma: dorsal pattern see fig. 44 in Wunderlich (1974); PMS one CY, mAP and AC absent, one nubbin (vestigial mAP); PLS with triad, two CY, one-two AC (Fig. 47G, H).

Variation: The measurements are based on examined material.

Females (N = 7, means in parentheses): Total length 2.16–2.61 (2.41). Prosoma: 0.95–1.08 (1.01) long, 0.74–0.83 (0.78) wide. Legs: dorsal proximal macroseta on tibia I, II, III and IV 2.20–2.41 (2.28, N = 4), 2.61–2.77 (2.73, N = 3), 2.76–3.08 (2.73, N = 4) and 2.76–3.08 (2.94, N = 4) times diameter of tibia, respectively; Tm I: 0.60–0.63 (0.61).

Distribution: West Nepal.

Habitat: Ravine forests; pine forests.

***MITRAGER ELONGATA* (WUNDERLICH, 1974) COMB. NOV.**

(FIGS 38C, 39C, 40C, 48; SUPPORTING INFORMATION, FIG. S4C)

Oedothorax elongatus Wunderlich, 1974: 176, figs 13–19 (Dmf).

Type material: Holotype: **Nepal:** Trisuli-Tal, Dunche, entrance to Gosainkund-Valley, 2000–2100 m, 1♂ 29.iv.1973, leg. J. Martens (SMF 28893, examined). Paratypes: same data as holotype, 1♂2♀ (SMF 28894, examined).

Diagnosis:

Males: This species is characterized by the anterior part of carapace with chelicerae largely elevated above the baseline of the rest of carapace, a pair of conical apophysis on the front side of chelicerae, a clypeal hump, and the particular palpal configuration.

Females: Can be identified by the dorsal pattern of the opisthosoma similar to males. Epigyne difficult to distinguish from congeners.

Description:

Male (holotype, SMF28893): Total length: 2.52. Prosoma: 1.22 long, 0.87 wide, frontal part of carapace bearing eyes and chelicerae largely elevated above baseline of margin of carapace (Figs 38C, 39C). Eyes: AME-AME: 0.04, AME width: 0.05, AME-ALE: 0.04, ALE width: 0.07, ALE-PLE: 0.01, PLE width: 0.07, PLE-PME: 0.08, PME width: 0.05, PME-PME: 0.08. Clypeus: elevated, hirsute. Sternum: 0.62 long, 0.66 wide. Chelicerae: base at frontal surface strongly elevated; stridulatory striae absent, lateral surface with short stout setal group at distal part (Fig. 39C). Legs: Tm I: 0.87. Pedipalp: patella prolateral proximal vertical macrosetae present; tibia with one prolateral, two retrolateral trichobothria; TPS scaly, broad at base, distal end retrolaterally pointed; TPA arising at middle of tibia, with slightly enlarged setal bases; TRA small, bent retrolaterally (Fig. 48D); PC median-sized, base not visible from dorsal view, distal setae close to distal clasp, distal clasp with striae, retrolateral to PC middle part (Fig. 48A); T without papillae; PT with short papillae; TS short, continuous with PT, with small papillae (Fig. 48A); MSA present; DSA broad, tip retrolaterally turned (Fig. 48B); EM absent; LER without striae, not extended dorsal to E, retrolateral side with pointed, sclerotized extension; VRP absent; TP not pointed, not turned retrolaterally; E retrolaterally spiral, anterior margin at base slightly wavy (Fig. 48F). Opisthosoma: dorsal pattern see Fig.

40C; PMS with mAP, one AC; PLS with triad, one AC (Fig. 48I, J).

Male (paratype, SMF 28894): Total length 2.65. Prosoma 1.20 long, 0.87 wide.

Female (paratype, SMF 28894): Total length: 2.88. Prosoma: 1.14 long, 0.85 wide. Eyes: AME-AME: 0.04, AME width: 0.05, AME-ALE: 0.03, ALE width: 0.08, ALE-PLE: 0, PLE width: 0.08, PLE-PME: 0.05, PME width: 0.07, PME-PME: 0.06. Clypeus: not hirsute. Sternum: 0.64 long; 0.63 wide. Legs: Tm I: 0.84. Chelicerae: stridulatory striae absent. Epigyne: Clade 13 characteristic morphology, borders between dorsal and ventral plates converging anteriorly (Fig. 48G, H). Opisthosoma: dorsal pattern as in male; PMS with mAP, AC, CY; PLS with triad, two CY, one AC (Fig. 48K, L).

Female (paratype, SMF 28894, second individual): Total length: 2.55. Prosoma: 1.18 long, 0.85 wide. Tm I: 0.85.

Distribution: Only known from the type locality in Nepal.

Habitat: No data.

MITRAGER FALCIFER (TANASEVITCH, 1998) **COMB. NOV.**

(FIGS 38U, 39T, 40V, 49; SUPPORTING INFORMATION, FIG. S3H)

Oedothorax falciferus Tanasevitch, 1998b: 440, figs 46–49 (Dm).

Type material: Holotype: **Nepal:** Ham District, Worebung Pass, degraded broad-leaved forest, 2000 m, ♂ 21.iv.1988, leg. J. Martens & W. Schawaller (SMF 38856, examined).

Diagnosis:

Males: The distinct prosomal features closely resemble *M. falciferoides* and ‘*Oe.*’ *meghalaya* in the elevated prosomal region bearing PME, with strong setae on the frontal side bent downwards, and strong setae at interocular region pointing upwards. Distinguished from the latter two species by a larger prosomal elevation; from ‘*Oe.*’ *meghalaya* by the shape of the palpal tibia apophyses; and from *M. falciferoides* by the larger body size and a more elevated retrolateral part of the palpal tibia.

Description:

Male (holotype, SMF 38856): Total length: 2.32. Prosoma: 1.10 long, 0.87 wide, PME region and postocular region

largely elevated, frontal surface of elevation with strong setae bent downwards, interocular region with strong setae directed upwards (Fig. 38U). Eyes: AME-AME: 0.05, AME width: 0.04, AME-ALE: 0.09, ALE width: 0.07, ALE-PLE: 0.01, PLE width: 0.07, PLE-PME: 0.13, PME width: 0.06, PME-PME: 0.22. Clypeus: not hirsute. Sternum: 0.62 long, 0.66 wide. Chelicerae: mastidia absent; stridulatory striae rows compressed and evenly spaced (Fig. 39T). Legs: dorsal proximal macroseta on tibia I 2.68 times diameter of tibia; Tm I: 0.57. Pedipalp: patella prolateral proximal vertical macrosetae present; tibia with one prolateral, two retrolateral trichobothria; TPS scaly, retrolaterally pointed; TPA slightly elevated; TRA bent retrolaterally; PC median-sized, base not visible from dorsal view, distal setae close to distal clasp, distal clasp with weak striae, clasp directed retrolaterally (Fig. 49A); T without papillae; PT short, apical part with small papillae; TS short and thick, without papillae (Fig. 49D); MSA absent (Fig. 49A); DSA tip round, retrolaterally curved; EM flat, anterior margin without papillae, exceeds ARP; ARP pointed, angled on ventral side; LER without striae, extended dorsal to E; radix with bulging membranous part below the junction with E; VRP absent; TP round at tip, with thicker part mesal to the tip, fitted to depression on tegulum (Fig. 49D); E retrolaterally spiral, anterior margin at base slightly wavy (Fig. 49B). Opisthosoma: dorsal pattern see Fig. 40V. PMS with mAP, one AC; PLS with triad, one AC (Fig. 49E, F).

Female: Unknown.

Distribution: Only known from the type locality in Nepal.

Habitat: Degraded broad-leaved forests.

MITRAGER FALCIFEROIDES (TANASEVITCH, 2015) **COMB. NOV.**

(FIGS 38X, 39V, 40Y, 50)

Oedothorax falciferoides Tanasevitch, 2015: 386, figs 35–43 (Dm).

Type material: Holotype: **India:** Himalayas, West Bengal, Darjeeling District, Mahanadi near Kurseong, southern slope, 1200 m, sifting in forest, ♂ 19.x.1978, leg. C. Besuchet & I. Löbl (MHNG, examined).

Diagnosis:

Males: The distinct prosomal features closely resemble *M. falcifer* and ‘*Oe.*’ *meghalaya* in the elevated prosomal region bearing PME, with strong setae on the frontal side bent downwards, and strong setae at

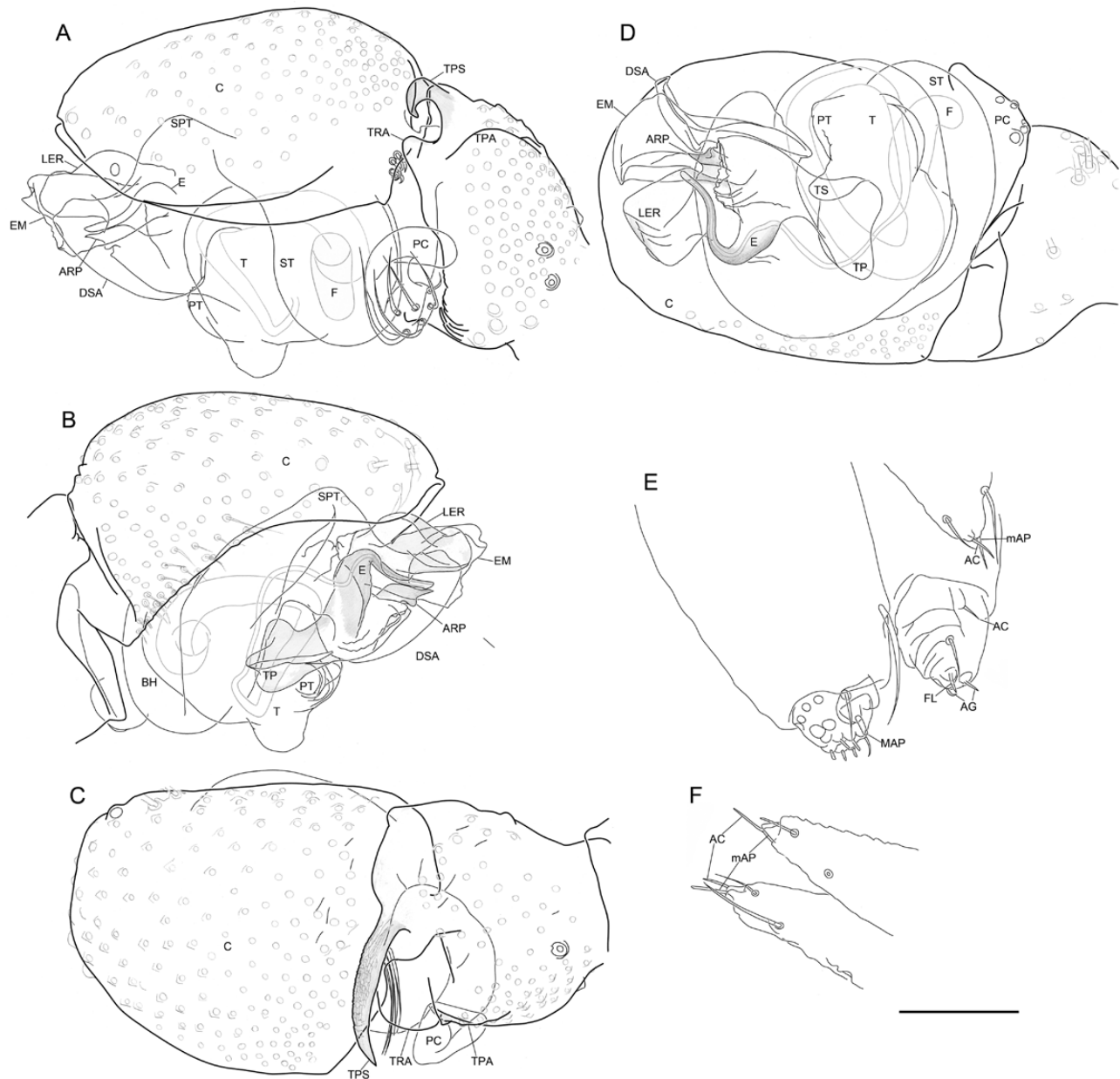


Figure 49. *Mitrager falcifer* (Tanasevitch, 1998). A–D, male right palp, images flipped horizontally. A, retrolateral view. B, prolateral view. C, dorsal view. D, ventral view. E, male right spinnerets. F, male posterior median spinnerets. Scale bar 0.1 mm.

interocular region pointing upwards. Distinguished from *M. falcifer* by the smaller prosomal elevation, the less elevated retrolateral part of the palpal tibia and the smaller body size; from '*Oe.*' *meghalaya* by the shape of the palpal tibia apophyses.

Description:

Male (holotype): Total length: 1.75. Prosoma: 0.83 long, 0.67 wide, PME- and postocular region largely

elevated, frontal surface of elevation with strong setae bent downwards, interocular region with strong setae directed upwards (Fig. 38X). Eyes: AME-AME: 0.02, AME width: 0.04, AME-ALE: 0.04, ALE width: 0.08, ALE-PLE: 0, PLE width: 0.08, PLE-PME: 0.07, PME width: 0.09, PME-PME: 0.12. Clypeus: not hirsute. Sternum: 0.47 long, 0.50 wide. Chelicerae: mastidia absent; stridulatory striae rows compressed at proximal half, wider at distal half (Fig. 39V). Legs: dorsal proximal macroseta on tibia IV 4.21 times

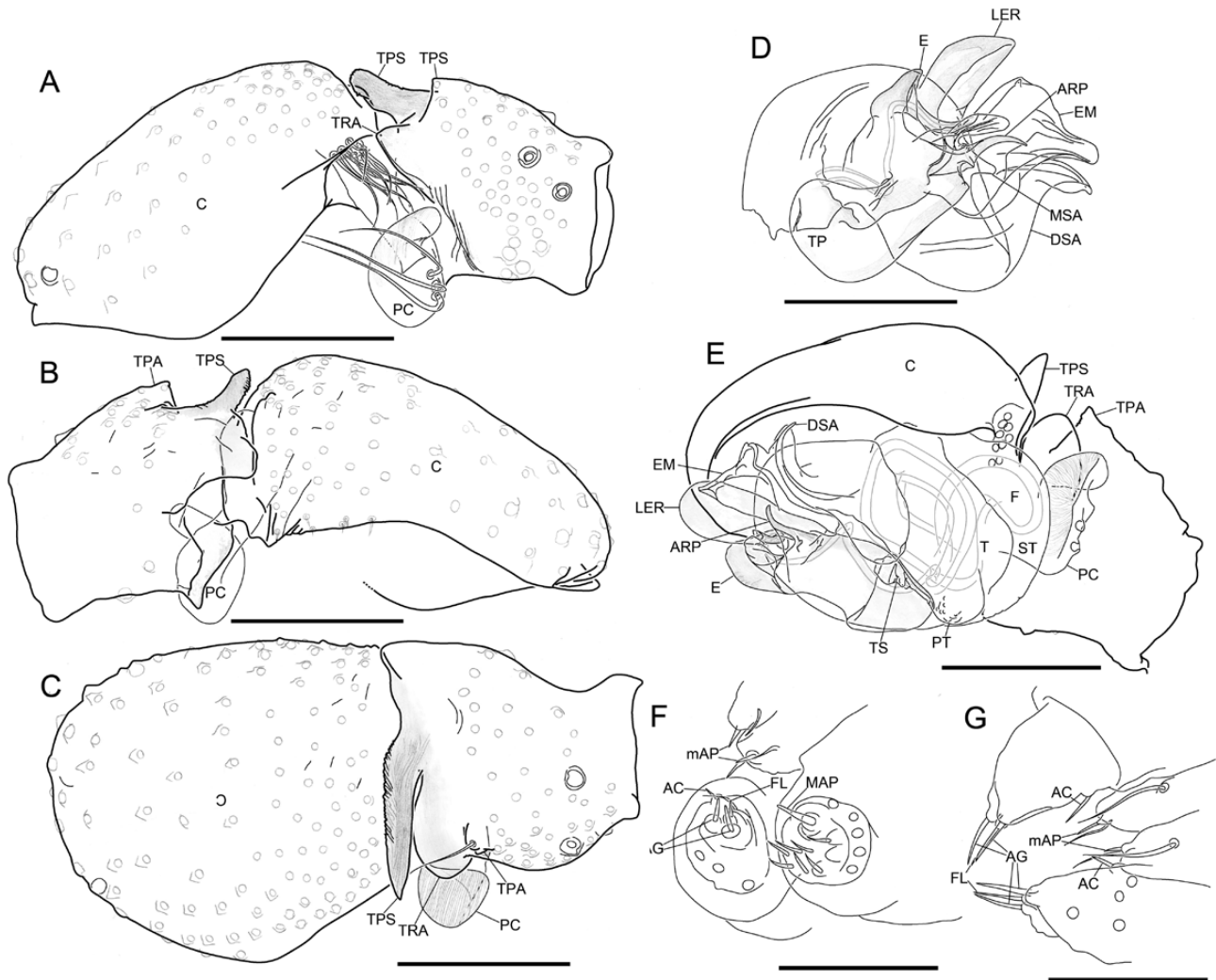


Figure 50. *Mitrager falciferoides* (Tanasevitch, 2015). A–D, male right palp, images flipped horizontally. A, retrolateral view. B, prolateral view. C, dorsal view. D, embolic division, prolateral view. E, male left palp, retrolateral view. F, male spinnerets. G, male posterior median spinnerets and posterior lateral spinnerets, dorsal view. Scale bars 0.1 mm.

diameter of tibia; Tm I: 0.50. Pedipalp: patella prolateral proximal vertical macrosetae absent; tibia with one prolateral, two retrolateral trichobothria; TPS scaly, retrolaterally pointed; TPA slightly elevated; TRA bent retrolaterally; PC median-sized, base not visible from dorsal view, distal setae close to distal clasp, distal clasp with striae, clasp directed retrolaterally (Fig. 50A); T without papillae; PT short, apical part with small papillae; TS short, without papillae; MSA present; DSA tip round, retrolaterally curved; EM flat, anterior margin without papillae, exceeds ARP (Fig. 50E); ARP pointed, angled on ventral side; LER without striae, extended dorsal to E; radix with bulging membranous part below the junction with E, protruding anteriorly; VRP absent; TP round at tip, with thicker part mesal to the tip, fitted to depression on tegulum; E retrolaterally spiral, anterior margin

at base slightly wavy (Fig. 50D). Opisthosoma: dorsal pattern see Fig. 40Y; PMS with mAP, AC absent; PLS with triad, one AC (Fig. 50F, G).

Female: Unknown.

Distribution: Only known from the type locality in India.

Habitat: Forest litter.

***MITRAGER GLOBICEPS* (THALER, 1987) COMB. NOV.**
(FIGS 38I, 39I, 40I, 51; SUPPORTING INFORMATION, FIG. S4G)

Oedothorax globiceps Thaler, 1987: 36, figs 16–21 (Dm).

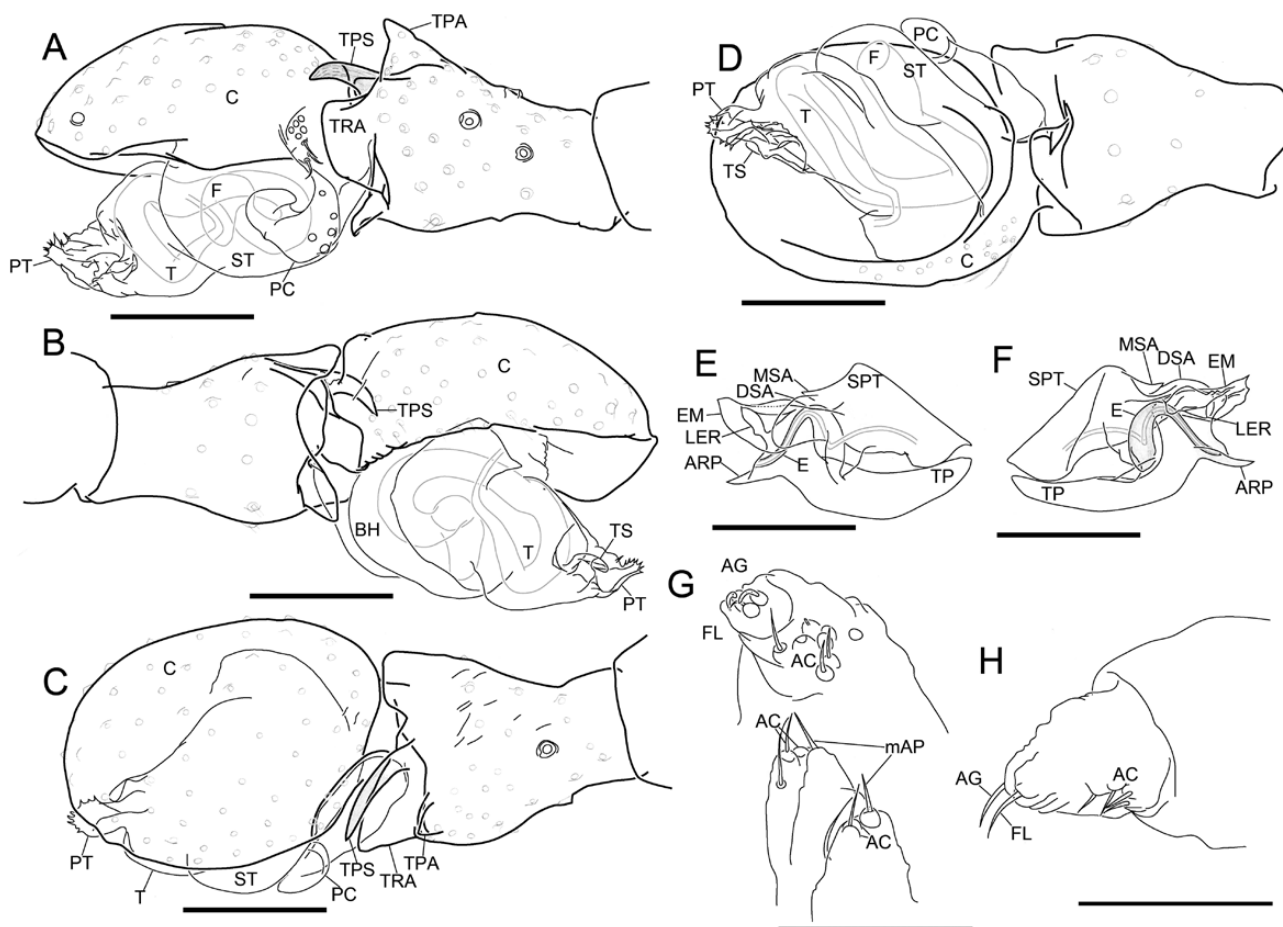


Figure 51. *Mitrager globiceps* (Thaler, 1987). A–D, male right palp, images flipped horizontally. A, retrolateral view. B, prolateral view. C, dorsal view. D, ventral view. E, F, embolic division. E, retrolateral view. F, prolateral view. G, male posterior median spinnerets and left posterior lateral spinneret. H, male left posterior lateral spinneret, dorsal view. Scale bars 0.1 mm.

Type material: Holotype: **India:** Pahalgam, coniferous forest, 2400m, ♂ 14.v.1976, leg. J. Martens (SMF 33832, examined).

Diagnosis:

Males: This species shares the prosomal post-ocular hump and transverse groove between the hump and ocular region with *M. dismodicoides*, *M. lineata*, *M. lucida*, *M. sexoculata*, *M. sexocolorum* (Tanasevitch, 1998) **comb. nov.** and *M. tholusa*, but can be distinguished by the position of the PME at the lateral side of the groove (PME above the groove in *M. dismodicoides*, *M. lineata*, *M. sexocolorum* and *M. tholusa*; PME inside the pre-PME groove in *M. lucida*, *M. sexoculata* and *M. sexocolorum*).

Description:

Male (holotype, SMF 33832): Total length: 1.98. Prosoma: 0.91 long, 0.70 wide, transverse groove

between PME, hump posteriorly (Fig. 38I). Eyes: AME-AME: 0.03, AME width: 0.04, AME-ALE: 0.04, ALE width: 0.07, ALE-PLE: 0, PLE width: 0.08, PLE-PME: 0.02, PME width: 0.06, PME-PME: 0.18. Clypeus: not hirsute. Sternum: 0.49 long, 0.52 wide. Chelicerae: mastidia absent; stridulatory striae rows widely and evenly spaced (Fig. 39I). Legs: Tm I: 0.85. Pedipalp: patella prolateral proximal vertical macrosetae absent; tibia with one prolateral, two retrolateral trichobothria; TPS scaly, distal-retrolaterally pointed; TPA median-sized; TRA apically oriented; PC median-sized, base not visible from dorsal view, distal setae close to distal clasp, distal clasp without striae, clasp directed apically (Fig. 51A); T without papillae; PT apical part with small papillae; TS short, without papillae (Fig. 51B); MSA present; DSA tip round; EM flat, anterior margin without papillae, approximately equals ARP in length; ARP pointed; LER without striae, extended dorsal to E; VRP absent; TP tip narrow; E retrolaterally spiral, anterior margin at base smoothly

curved (Fig. 51E, F). Opisthosoma: dorsal pattern see Fig. 40I; PMS with mAP, two AC; PLS with triad, 3+ AC (Fig. 51G, H).

Female: Unknown.

Distribution: Only known from the type locality in India.

Habitat: Coniferous forests.

MITRAGER HIRSUTA (WUNDERLICH, 1974) **COMB. NOV.**
(FIGS 38A, 39A, 40A, 52; SUPPORTING INFORMATION, FIG. S4A)

Oedothorax hirsutus Wunderlich, 1974: 173, figs 8–12 (Dm).

Type material: Holotype: **Nepal:** Trisuli-Valley between Ramche and Dunche, broadleaf forest, 1800–2000 m, ♂ 22.iv.1973, coll. J. Martens (SMF 28892, examined).

Diagnosis:

Males: Among the species of *Mitrager* with retrolaterally pointed TPS and minute TPA, this is the only species without external prosomal modification.

Description:

Male (holotype): Total length: 2.08. Prosoma: 0.85 long, 0.67 wide, unmodified (Fig. 38A). Eyes: AME-AME: 0.04, AME width: 0.04, AME-ALE: 0.04, ALE width: 0.07, ALE-PLE: 0, PLE width: 0.08, PLE-PME: 0.05, PME width: 0.06, PME-PME: 0.06. Clypeus: not hirsute. Sternum: 0.53 long, 0.53 wide. Chelicerae: mastidia absent; stridulatory striae rows compressed and evenly spaced (Fig. 39A). Legs: dorsal proximal macroseta on tibia IV 3.1 times diameter of tibia; Tm I: 0.34. Pedipalp: patella prolateral proximal vertical macrosetae absent; tibia with one prolateral, two retrolateral trichobothria; TPS slightly scaly, distal-retrolaterally pointed; TPA absent; TRA apically oriented (Fig. 52B); PC median-sized, base not visible from dorsal view, distal setae close to distal clasp, distal clasp without striae, clasp directed slightly apically; T without papillae, PT with small papillae, TS as long as PT, without papillae; MSA present (Fig. 52A); DSA tip anteriorly oriented; EM flat, anterior margin without papillae, exceeds ARP (Fig. 52B); ARP pointed, angled ventrally; LER without striae, extended dorsal to E; VRP absent; TP tip narrow; E retrolaterally spiral, anterior margin at base slightly wavy (Fig. 52B, C). Opisthosoma: single-coloured grey (Fig. 40A); PMS with mAP, one AC; PLS with triad, one AC (Fig. 52D).

Female: Unknown.

Distribution: Only known from the type locality in Nepal.

Habitat: Broad-leaved forests.

MITRAGER LINEATA (WUNDERLICH, 1974) **COMB. NOV.**

(FIGS 38J, 39J, 40J, 53; SUPPORTING INFORMATION, FIG. S4H)

Oedothorax lineatus Wunderlich, 1974: 181, figs 34–41 (Dmf).

Type material: Holotype: **Nepal:** Thakkhola, lake by Titi Village, Pinus-Wald, 2700 m, 1♂ 2.xii.1969, leg. J. Martens (SMF 28899, examined). Paratypes: same data as holotype, 8♀ (SMF 28900, examined); Saddle of Gorapani, *Rhododendron*-forest, at creek bank, 2750–2800 m, 2♀ 10.–14.xii.1969, coll. J. Martens (SMF 28901, examined).

Diagnosis:

Males: This species shares the prosomal post-ocular hump and transverse groove between the hump and ocular region with *M. dismodicoides*, *M. tholusa*, *M. sexocolorum*, *M. globiceps*, *M. lucida* and *M. sexoculata*. Can be distinguished from *M. sexoculata* and *M. lucida* by having externally visible posterior median eyes (inside the groove in the latter two species) and two retrolateral trichobothria (one in the latter two species); from *M. globiceps* by the larger body size and the thicker palpal prolateral spike; from *M. dismodicoides* and *M. sexocolorum* by the more posteriorly located posterior median eyes (compare Fig. 38H, J and K); from *M. tholusa* by the glabrous clypeus (hirsute in the latter species).

Females: Females of this species are indistinguishable from *M. dismodicoides*, both with an elevated region anterior to the copulatory openings.

Description:

Male (holotype, SMF 28899): Total length: 1.86. Prosoma: 0.87 long, 0.70 wide, inter-PME region with transverse, non-hirsute groove, prosomal elevation above PME region, frontal face of elevation with strong setae directed downwards, interocular region with setae directed upwards (Fig. 38J). Eyes: AME-AME: 0.03, AME width: 0.05, AME-ALE: 0.08, ALE width: 0.07, ALE-PLE: 0, PLE width: 0.07, PLE-PME: 0.10, PME width: 0.07, PME-PME: 0.26. Clypeus: not hirsute. Sternum: 0.53 long, 0.57 wide. Chelicerae: stridulatory striae rows widely and evenly spaced

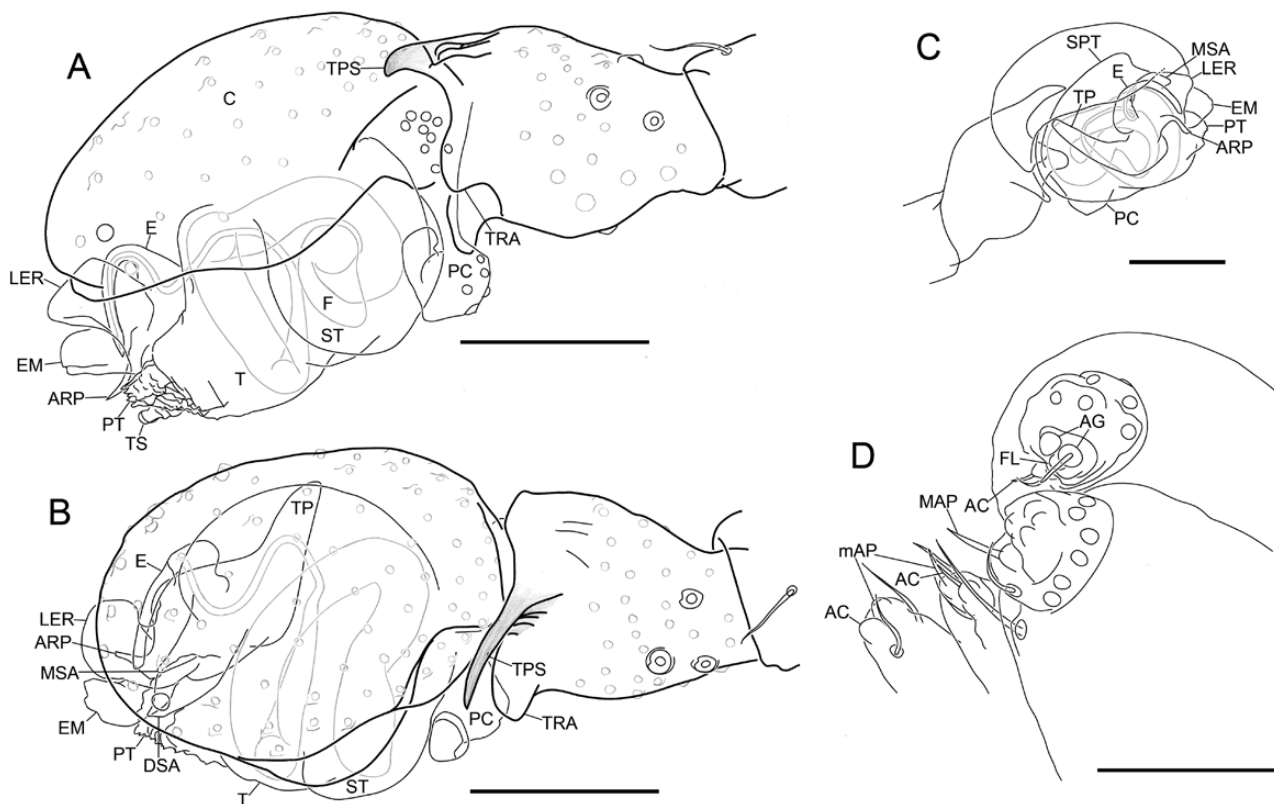


Figure 52. *Mitrager hirsuta* (Wunderlich, 1974). A–C, male left palp. A, retrolateral view. B, dorsal view. C, prolateral view. D, male spinnerets. Scale bars 0.1 mm.

(Fig. 39J). Legs: dorsal proximal macroseta on tibia I and II 0.30 and 0.46 times diameter of tibia, respectively; Tm I: 0.65. Pedipalp: patella prolateral proximal vertical macrosetae present; tibia with one prolateral, two retrolateral trichobothria; TPS scaly, wide, retrolaterally bent; TPA slightly elevated, with one slightly enlarged setal base; TRA distally oriented; PC median-sized, base not visible from dorsal view, distal setae close to distal clasp, distal clasp without striae, slightly distally extended; T without papillae; PT with papillae; TS long, slender, without papillae; MSA present; DSA not pointed, not turned retrolaterally; EM flat, without papillae, not exceeding ARP (Fig. 53A); ARP pointed, without striae, angled on ventral side; LER without striae, extended dorsal to E; VRP absent; TP slender (Fig. 53B); E retrolaterally spiral, anterior margin at base slightly wavy (Fig. 53A). Opisthosoma: dorsal pattern see Fig. 40J; PMS without spigots, with one nubbin (vestigial mAP); PLS with triad, AC absent (Fig. 53E, F).

Female (paratype, SMF 28900): Total length: 2.20. Prosoma: 0.92 long, 0.68 wide. Eyes: AME-AME: 0.03, AME width: 0.05, AME-ALE: 0.06, ALE width: 0.07, ALE-PLE: 0, PLE width: 0.07, PLE-PME:

0.04, PME width: 0.07, PME-PME: 0.08. Clypeus: not hirsute. Sternum: 0.53 long; 0.56 wide. Legs: dorsal proximal macroseta on tibia I, II, III and IV 1.98, 2.07, 2.75 and 3.05 times diameter of tibia, respectively; Tm I: 0.62. Epigyne: Clade 13 characteristic morphology, borders between dorsal and ventral plates converging anteriorly (Fig. 53C, D). Opisthosoma: dorsal pattern as in male; PMS with one nubbin (vestigial mAP), one CY; PLS with triad, two CY, three AC (Fig. 53G).

Variation: The measurements are based on examined material.

Females (N = 10, means in parentheses): Total length 2.04–2.33 (2.21). Prosoma: 0.85–1.04 (0.92) long, 0.65–0.81 (0.72) wide. Legs: dorsal proximal macroseta on tibia I, II, III and IV 1.49–2.19 (1.98), 2.02–2.46 (2.21, N = 8), 2.21–3.25 (2.67, N = 9) and 2.73–3.55 (3.12) times diameter of tibia, respectively; Tm I: 0.57–0.64 (0.62).

Distribution: Nepal.

Habitat: See collecting data of type material.

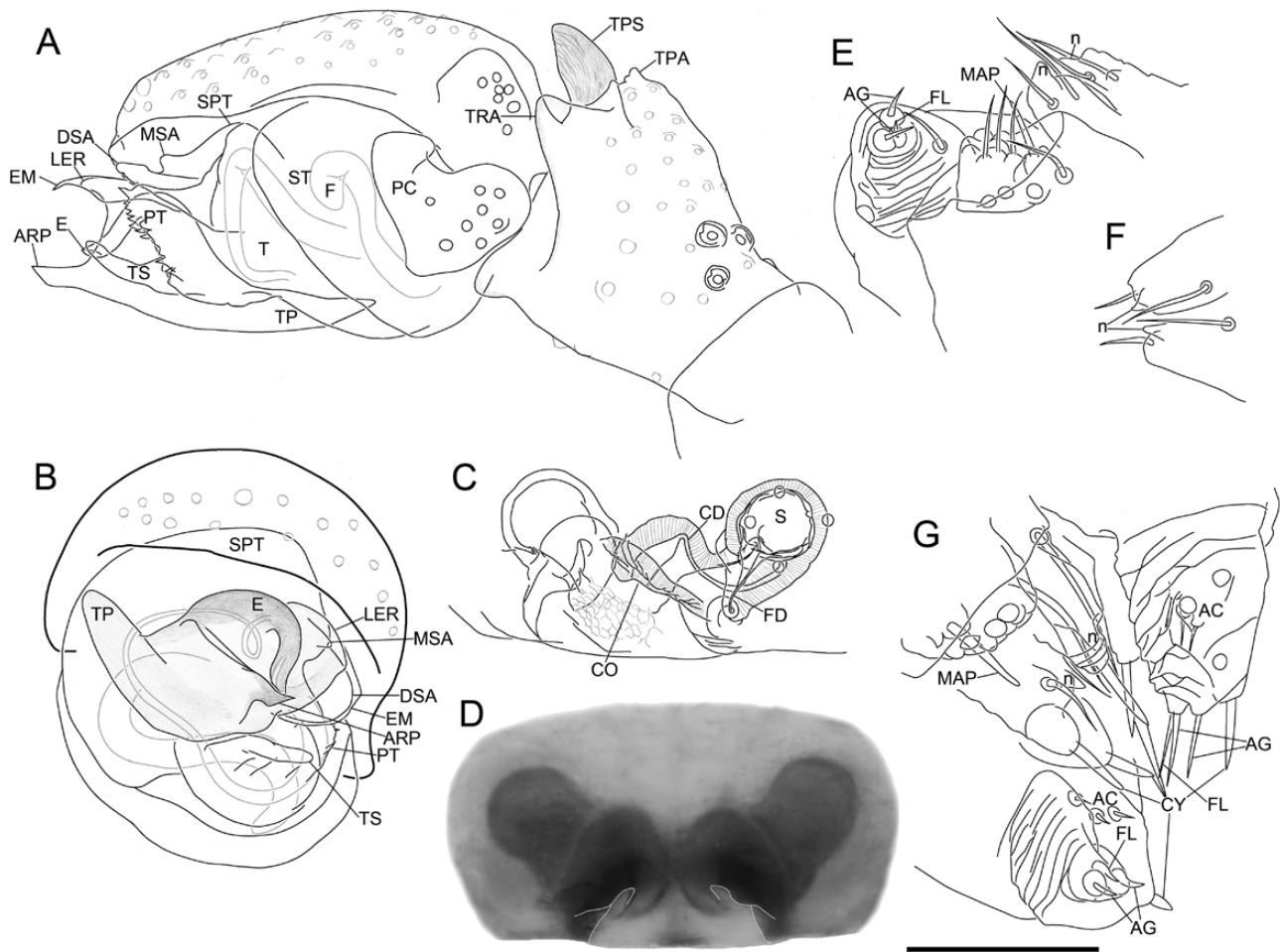


Figure 53. *Mitrager lineata* (Wunderlich, 1974). A, B, male left palp. A, retrolateral view. B, apical view. C, D, epigyne. C, ventrolateral view. D, external morphology. E, male spinnerets. F, male posterior median spinnerets, dorsal view. G, female spinnerets. Scale bar 0.1 mm.

***MITRAGER LOPCHU* (TANASEVITCH, 2015) COMB. NOV.**
(FIGS 38W, 40X, 54; SUPPORTING INFORMATION, FIG. S3J)

Oedothorax lopchu Tanasevitch, 2015: 388, figs 51–60 (Dm).

Type material: Holotype: **India:** Himalayas, West Bengal, Darjeeling District, between Ghoom and Lopchu, 13 km from Ghoom, northern slope, 2000 m, sifting in forest; ♂ 14.x.1978, leg. C. Besuchet & I. Löbl (MHNG, examined). Paratypes: collected together with the holotype; same locality, 1♂ 12.x.1978, leg. C. Besuchet & I. Löbl (MHNG, examined).

Diagnosis:

Males: This species can be recognized by its slightly elevated PME-bearing region (less elevated than species like *M. falciferoides* and *M. modesta*), the

median-long stout setae at the ocular region, and the broad-based, conical palpal tibial prolateral apophysis, which is round at tip and has no enlarged setal base.

Description:

Male (paratype): Total length: 1.95. Prosoma: 0.93 long, 0.75 wide, PME-bearing region slightly elevated, with median-long stout setae at ocular region (Fig. 38W). Eyes: AME-AME: 0.02, AME width: 0.03, AME-ALE: 0.04, ALE width: 0.08, ALE-PLE: 0.01, PLE width: 0.08, PLE-PME: 0.05, PME width: 0.07, PME-PME: 0.06. Clypeus: not hirsute. Sternum 0.50 long, 0.54 wide. Chelicerae: stridulatory striae rows widely and evenly spaced. Legs: Tm I: 0.51. Pedipalp: patella prolateral proximal vertical macrosetae absent; tibia with one prolateral, two retrolateral trichobothria; TPS scaly, retrolaterally pointed; TPA moderately elevated, without enlarged setal base; TRA bent retrolaterally

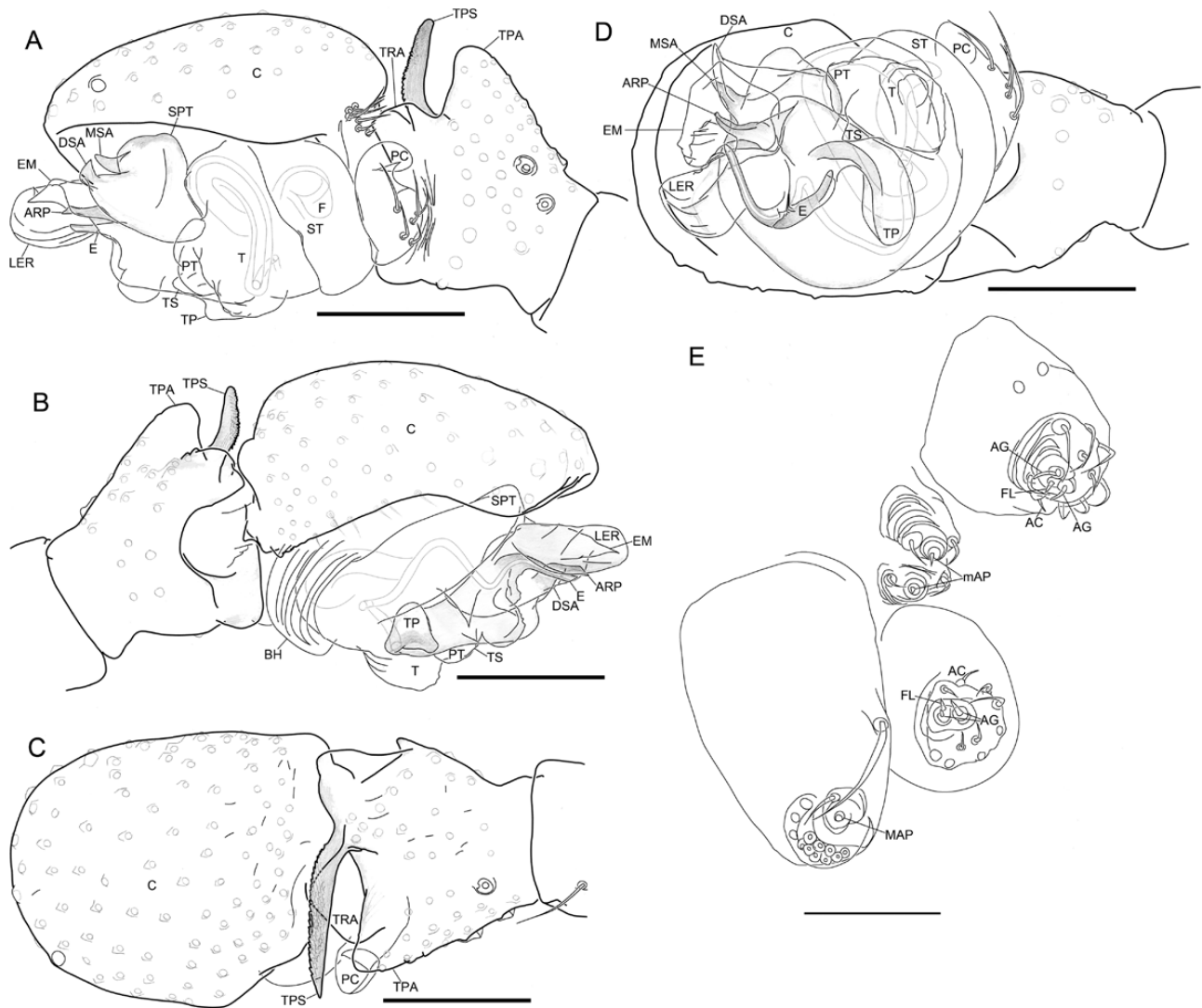


Figure 54. *Mitrager lopchu* (Tanasevitch, 2015). A–D, male left palp. A, retrolateral view. B, prolateral view. C, dorsal view. D, ventral view. E, male spinnerets. Scale bars 0.1 mm.

(Fig. 54C); PC median-sized, base not visible from dorsal view, distal setae close to distal clasp, distal clasp without striae, clasp directed retrolaterally (Fig. 54A); T without papillae; PT short, without papillae; TS short, wide at base, without papillae; MSA absent; DSA tip pointed, retrolaterally curved; EM flat, without papillae, exceeds ARP (Fig. 54D); ARP pointed, angled on dorsal side, with striae on dorsal side behind the angle; LER without striae, extended dorsal to E; radix with bulging membranous part below the junction with E; VRP absent; TP round and thick at tip, with thicker part mesal to the tip, fitted to depression on T; E retrolaterally spiral, anterior margin at base slightly wavy (Fig. 54B). Opisthosoma: dorsal pattern see Fig. 40X; PMS with mAP, without AC; PLS with triad, one AC (Fig. 54E).

Female: Unknown.

Distribution: Only known from the type locality in India.

Habitat: Forest litter.

MITRAGER LUCIDA (WUNDERLICH, 1974) **COMB. NOV.**
(FIGS 38M, 39M, 40N, 55, 56B; SUPPORTING INFORMATION, FIG. S3A)

Oedothorax lucidus Wunderlich, 1974: 180, figs 28–33 (Dm).

Type material: Holotype: **East Nepal:** Mt. Chordung at Jiri, *Abies-Rhododendron*-forest, 2900 m, 1♂

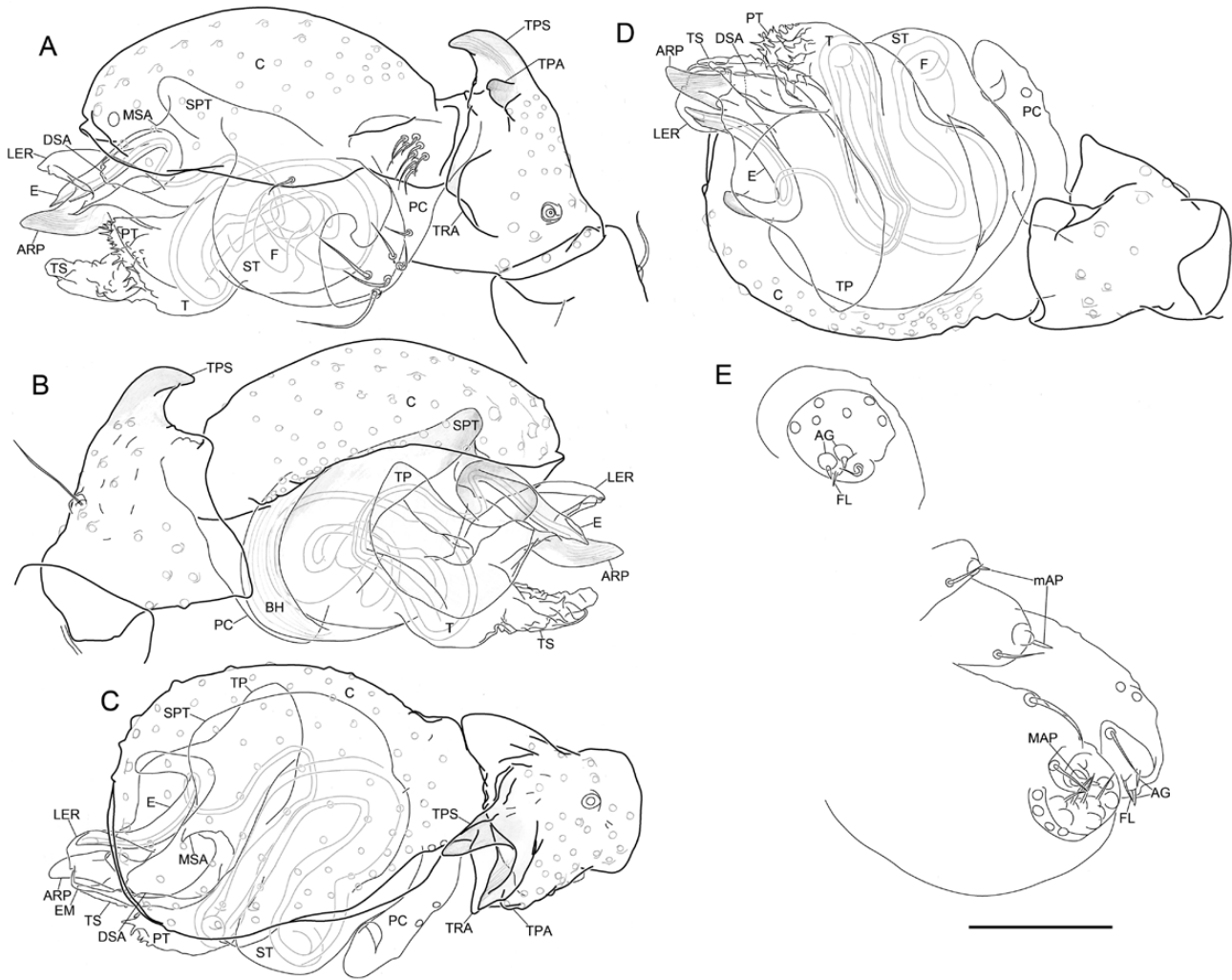


Figure 55. *Mitrager lucida* (Wunderlich, 1974). A–D, male left palp. A, retrolateral view. B, prolateral view. C, dorsal view. D, ventral view. E, male spinnerets. Scale bar 0.1 mm.

1.iv.1973 (SMF 28897, examined). Paratypes: Jiri, 1800–2000 m, 6♂ i.1970 (SMF 28898, examined).

Non-type material: 1♂ subadult collected with the paratypes (SMF 28898).

Diagnosis:

Males: This species shares with *M. sexoculata* the PME located within the transverse groove between the prosomal elevation and the remaining eyes, the highly sclerotized stump-like setae on both upper and lower surfaces within the groove, and one retrolateral trichobothrium on male palpal tibia instead of the common two. This species can be distinguished from *M. sexoculata* by the smaller TPA and the papillae-bearing PT.

Description:

Male (holotype, SMF 28897): Total length: 1.90. Prosoma: 0.94 long, 0.67 wide, region including PME elevated, transverse groove between elevation and other eyes, with highly sclerotized stump-like setae on both upper and lower surfaces within groove (Figs 38M, 56B). Eyes: AME-AME: 0.03, AME width: 0.04, AME-ALE: 0.04, ALE width: 0.05, ALE-PLE: 0.01, PLE width: 0.04; PME inside PME-lobe. Clypeus: slightly elevated, with small setae scarcely distributed. Sternum: 0.50 long, 0.47 wide. Chelicerae: stridulatory striae imbricated, rows widely and evenly spaced (Fig. 39M). Legs: dorsal proximal macroseta on tibia III 2.93 times diameter of tibia; Tm I: 0.85. Pedipalp: patella prolateral proximal vertical macrosetae absent; tibia with one prolateral, one retrolateral trichobothria;

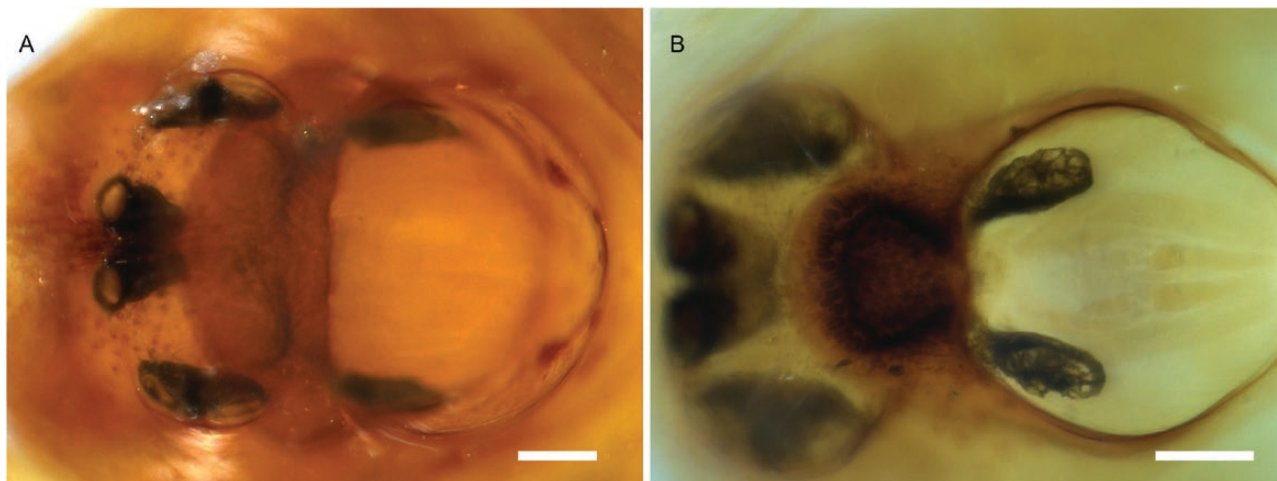


Figure 56. Setae inside inter-AME-PME groove, dorsal view, samples soaked in Eugenol. A, *Mitragrer tholusa* (Tanasevitch, 1998). B, *M. lucida*. Scale bars 0.1 mm.

TPS scaly, straight, wide at base, slightly retrolaterally directed; TPA slightly elevated; TRA distally oriented; PC median-sized, base not visible from dorsal view, distal setae close to distal clasp, distal clasp without striae, distally extended (Fig. 55A); T without papillae; PT with long papillae; TS long, thick, with several small papillae at base (Fig. 55D); MSA present; DSA not pointed, not turned retrolaterally; EM flat, without papillae, not exceeding ARP (Fig. 55C); ARP rounded at tip, striated; LER without striae, extended dorsal to E; VRP absent; TP broad (Fig. 55D); E retrolaterally spiral, anterior margin at base round (Fig. 55B). Opisthosoma: dorsal pattern see Fig. 40N; PMS with mAP, AC absent; PLS with triad, AC absent (Fig. 55E).

Female: Unknown.

Variation: The measurements are based on examined material.

Males (N = 7, means in parentheses): Total length 1.88–2.13 (1.99). Prosoma: 0.94–0.98 (0.96) long, 0.67–0.74 (0.71) wide. Legs: dorsal proximal macroseta on tibia I, II, III and IV 0.78–1.29 (1.08, N = 5), 0.77–1.24 (0.98, N = 6), 0.44–0.70 (0.59) and 1.57–2.51 (2.01, N = 3) times diameter of tibia, respectively; Tm I: 0.76–0.86 (0.82).

Distribution: East Nepal.

Habitat: Forests.

***MITRAGER MALEARMATA* (TANASEVITCH, 1998)
COMB. NOV.**

(FIGS 38S, 57; SUPPORTING INFORMATION, FIG. S3F)

Oedothorax malearmatus Tanasevitch, 1998a: 440, figs 50–52 (Dm).

Type material: Holotype: **Nepal:** Panchthar District, Paniporua, 2300 m, mixed broad-leaved forest, ♂ 16.–20.iv.1988, leg. J. Martens & W. Schawaller (SMF 38843 (palp), 38854, examined).

Diagnosis:

Males: Prosoma with hump bearing PME and ocular region bearing dense setae, similar to *M. assueta*, *M. modesta*, *M. lopchu*, *M. rustica*, *M. falcifer*, *M. falciferoides* and ‘*Oe.*’ *meghalaya*. Distinguished from the aforementioned species by a much smaller TPS (absent in ‘*Oe.*’ *meghalaya*), further distinguished from the latter three species by the much smaller hump.

Description:

Male (holotype, SMF): Total length: 1.74. Prosoma: 0.90 long, 0.71 wide, PME-bearing region elevated, one strong seta at peak of elevation anteriorly directed, interocular region with strong setae directed upwards (Fig. 38S). Eyes: AME-AME: 0.04, AME width: 0.03, AME-ALE: 0.04, ALE width: 0.07, ALE-PLE: 0, PLE width: 0.07, PLE-PME: 0.05, PME width: 0.05, PME-PME: 0.13. Clypeus: not hirsute. Sternum: 0.55 long, 0.56 wide. Chelicerae: mastidia absent; stridulatory striae rows compressed and evenly spaced. Legs: Tm I: 0.45. Pedipalp: patella prolateral proximal vertical macrosetae present; tibia with one prolateral, two retrolateral trichobothria; TPS scaly, retrolaterally pointed; TPA absent; TRA retrolaterally oriented (Fig. 57C); PC short, base not visible from dorsal view, distal setae close to distal clasp, distal clasp with striae only at tip, clasp directed retrolaterally (Fig. 57A); T without papillae; PT without papillae; TS short

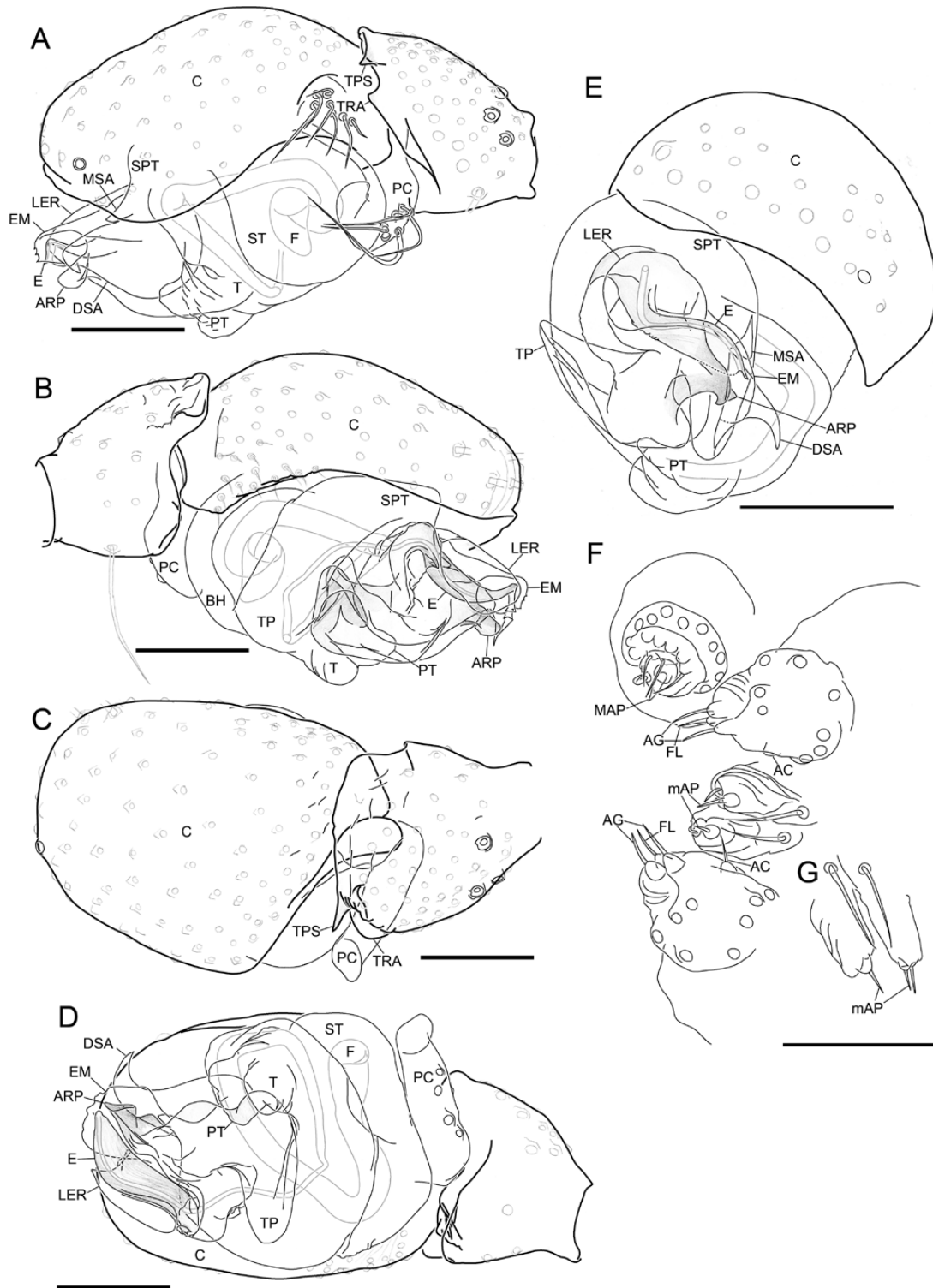


Figure 57. *Mitrager malearmata* (Tanasevitch, 1998). A–E, male right palp, images flipped horizontally. A, retrolateral view. B, prolateral view. C, dorsal view. D, ventral view. E, apical view. F, male spinnerets. G, male posterior median spinnerets, dorsal view. Scale bars 0.1 mm.

and thick, without papillae (Fig. 57C); MSA present; DSA tip pointed, retrolaterally bent (Fig. 57E); EM flat, margin with tiny papillae, exceeds ARP (Fig. 57A); ARP round at tip, angled on retrolateral side (Fig. 57E); LER without striae, extended dorsal to E; VRP absent; TP round at tip, with thicker part mesal to the tip, fitted to depression on T; E retrolaterally spiral, anterior margin at base wavy, distal half flat and broad, striated (Fig. 57B). Opisthosoma: PMS with mAP, AC absent; PLS with triad, one AC (Fig. 57F, G).

Female. Unknown.

Distribution: Only known from the type locality in Nepal.

Habitat: Mixed broad-leaved forests.

MITRAGER MODESTA (TANASEVITCH, 1998) COMB. NOV.

(FIGS 38V, 39U, 40W, 58; SUPPORTING INFORMATION, FIG. S3I)

Oedothorax modestus Tanasevitch, 1998a: 438, figs 36–39 (Dm).

Type material: Holotype: **Nepal:** Panchthar District, Paniporua, 2300 m, mixed broad-leaved forest, ♂ 16.–20.iv.1988, leg. J. Martens & W. Schawaller (SMF 38830, examined). Paratypes: 5♂ (SMF 38862, examined) 1♂ (ZMMU, not examined), collected together with the holotype.

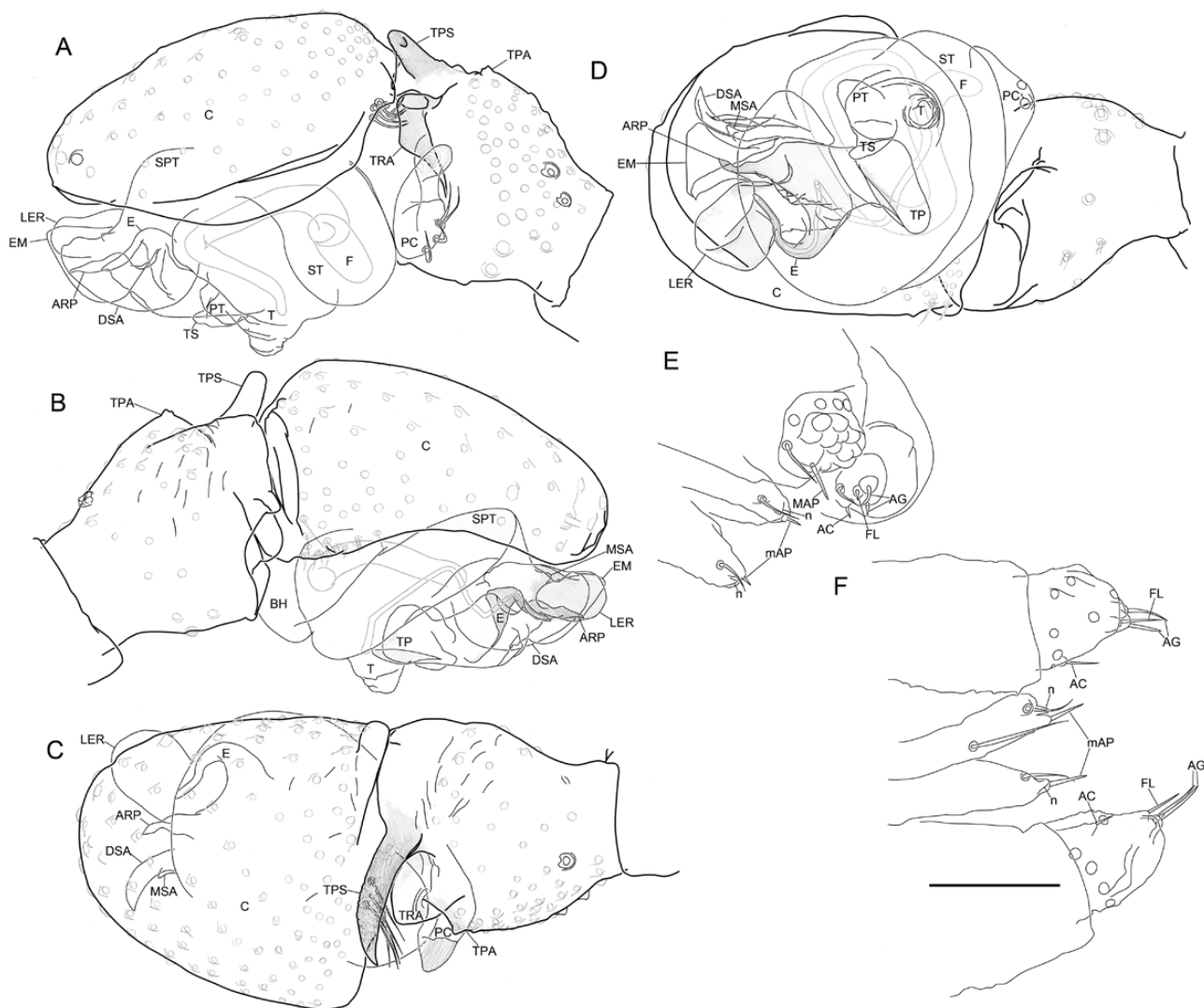


Figure 58. *Mitrager modesta* (Tanasevitch, 1998). A–D, male right palp, images flipped horizontally. A, retrolateral view. B, prolateral view. C, dorsal view. D, ventral view. E, male spinnerets. F, male spinnerets, dorsal view. Scale bar 0.1 mm.

Diagnosis:

Males: prosoma with hump bearing PME and ocular region bearing dense setae, similar to *M. assueta*, *M. malearmata*, *M. lopchu*, *M. rustica*, *M. falcifer*, *M. falciferoides* and 'Oe.' *meghalaya*. Distinguished from the latter three species by the much smaller elevation in this species; from *M. assueta*, *M. malearmata* by a much larger TPS; from *M. lopchu* by the smaller TPA; from *M. rustica* by the absence of papillae on protogulum and embolic membrane.

Description:

Male (holotype, SMF): Total length: 2.25. Prosoma: 1.01 long, 0.82 wide, PME-bearing region elevated, peak of elevation with several strong setae anteriorly directed, interocular region with strong setae directed upwards (Fig. 38V). Eyes: AME-AME: 0.05, AME width: 0.05, AME-ALE: 0.06, ALE width: 0.07, ALE-PLE: 0, PLE width: 0.07, PLE-PME: 0.09, PME width: 0.06, PME-PME: 0.13. Clypeus: not hirsute. Sternum: 0.60 long, 0.62 wide. Chelicerae: mastidia absent; stridulatory striae rows compressed and evenly spaced (Fig. 39U). Legs: dorsal proximal macroseta on tibia I, II, III and IV 1.96, unknown, 2.74 and 3.53 times diameter of tibia, respectively; Tm I: 0.53. Pedipalp: patella prolateral proximal vertical macrosetae present; tibia with prolateral, two retrolateral trichobothria; TPS scaly, retrolaterally pointed; TPA minute, with one enlarged setal base at tip; TRA bent retrolaterally (Fig. 58C); PC short, base not visible from dorsal view, distal setae close to distal clasp, distal clasp with striae, clasp directed retrolaterally (Fig. 58A); T without papillae; PT without papillae; TS short and thick, without papillae (Fig. 58D); MSA present; DSA tip round, retrolaterally bent (Fig. 58A); EM flat, without papillae, exceeds ARP (Fig. 58A); ARP pointed at tip, angled on dorsal side; LER without striae, extended dorsal to E; VRP absent; TP round at tip, with thicker part mesal to the tip, fitted to depression on T; E retrolaterally spiral, anterior margin at base wavy (Fig. 58B). Opisthosoma: dorsal pattern see Fig. 40W; PMS with mAP, AC absent, but with one nubbin (vestigial AC); PLS with triad, one AC (Fig. 58E, F).

Female: Unknown.

Variation: The measurements are based on examined material.

Males (N = 6, means in parentheses): Total length 2.05–2.25 (2.15, N = 5). Prosoma: 1.00–1.08 (1.04) long, 0.79–0.87 (0.82) wide. Legs: dorsal proximal macroseta

on tibia I, II, III and IV 1.96–2.40 (2.26, N = 4), 2.05–2.83 (2.62, N = 4), 2.74–3.39 (3.10, N = 3) and 3.53–3.81 (3.65, N = 3) times diameter of tibia, respectively; Tm I: 0.49–0.57 (0.53).

Distribution: Nepal, Only known from the type locality.

Habitat: Mixed broad-leaved forests.

MITRAGER RUSTICA (TANASEVITCH, 2015) COMB. NOV.

(FIGS 38Q, 39Q, 40R, 59)

Oedothorax rusticus Tanasevitch, 2015: 389, figs 8, 75–82 (Dmf).

Type material: Holotype: **India:** Madras, Palni Hills, Kodaikanal, 2100 m, sifting in forest above town, ♂ 11.xi.1972, leg. C. Besuchet & I. Löbl (MHNG, examined). Paratypes: 2♂7♀ (MHNG, examined) 2♂7♀ (ZMMU, not examined), collected together with the holotype.

Diagnosis:

Males: This species can be recognized by the slightly elevated PME region (less elevated than species like *M. falciferoides* and *M. modesta*), several strong setae at the interocular region, and the particular palpal configuration, including a comb-like LER margin, which is only shared with *M. noordami*, a species with distinguished prosomal structure.

Females: Females of this species can be distinguished from congeners by the PMS bearing neither AC nor mAP (also in *M. lineata* and *M. dismodicoides*), further distinguished from these two species by the opisthosomal dorsal pattern similar to male (see Fig. 59E, F).

Description:

Male (MHNG): Total length: 2.00. Prosoma: 0.90 long, 0.75 wide, PME-bearing region slightly elevated, interocular region with several strong setae directed upwards (Fig. 38Q). Eyes: AME-AME: 0.03, AME width: 0.04, AME-ALE: 0.03, ALE width: 0.08, ALE-PLE: 1, PLE width: 0.08, PLE-PME: 0.04, PME width: 0.07, PME-PME: 0.7. Clypeus: not hirsute. Sternum: 0.59 long, 0.60 wide. Chelicerae: mastidia absent; stridulatory striae rows widely and evenly spaced (Fig. 39Q). Legs: dorsal proximal macroseta on tibia I, II, III and IV 1.86, 2.31, 2.78 and 3 times diameter of tibia, respectively; Tm I: 0.68. Pedipalp: patella prolateral proximal vertical macrosetae

present; tibia with one prolateral, two retrolateral trichobothria; TPS scaly, retrolaterally pointed; TPA absent; TRA bent retrolaterally (Fig. 59C); PC median-sized, base not visible from dorsal view, distal setae close to distal clasp, distal clasp with weak striae, clasp directed slightly anteriorly (Fig. 59A); T without papillae; PT with long papillae; TS thick, median-long, without papillae (Fig. 59D); MSA present; DSA tip broad and round; EM flat, anterior margin with long papillae, slightly exceeds ARP (Fig. 59A); ARP with two angles at tip; LER margin comb-like, extended dorsal to E; VRP absent; TP tip triangular; E retrolaterally spiral, anterior margin at base slightly wavy (Fig. 59B). Opisthosoma: dorsal pattern see Fig. 40R; PMS without spigots, one nubbin (vestigial mAP); PLS with triad, AC absent (Fig. 59H).

Female (MHNG): Total length: 2.33. Prosoma: 0.98 long, 0.78 wide. Eyes: AME-AME: 0.04, AME width: 0.04, AME-ALE: 0.02, ALE width: 0.08, ALE-PLE: 1, PLE width: 0.07, PLE-PME: 0.05, PME width: 0.07, PME-PME: 0.6. Clypeus: not hirsute. Sternum: 0.59 long, 0.55 wide. Legs: dorsal proximal macroseta on tibia I, II, III and IV 2.5, 2.51, 3.01 and 3.04 times diameter of tibia, respectively; Tm I: 0.73. Epigyne: Clade 13 characteristic morphology, borders between dorsal and ventral plates converging anteriorly (Fig. 59E–G). Opisthosoma: PMS with one nubbin (vestigial mAP), one CY; PLS with triad, two CY, AC absent (Fig. 59I, J).

Distribution: India, only known from the type locality.

Habitat: Forest litter.

***MITRAGER SAVIGNIFORMIS* (TANASEVITCH, 1998)
COMB. NOV.**

(FIGS 38T, 39S, 40T, U, 60; SUPPORTING
INFORMATION, FIG. S3G)

Oedothorax savigniformis Tanasevitch, 1998a: 439, figs 40–45 (Dm).

Type material: Holotype: **Nepal:** Taplejung District, Yamputhin, ascent to pass Deorali, 2600 m, cultivated land, ♂ 16.v.1988, leg. J. Martens & W. Schawaller (SMF 38834, examined). Paratypes: **Nepal:** Panchthar District, Paniporua, 2300 m, mixed broad-leaved forest, ♂ 16.–20.iv.1988, leg. J. Martens & W. Schawaller (SMF 38849, examined).

Diagnosis:

Males: This species can be identified from all others by the club-shape of the prosomal lobe at the interocular region.

Description:

Male (holotype, SMF): Total length: 2.03. Prosoma: 1.01 long, 0.79 wide, interocular region with mushroom-shaped projection covered by dense setae at tip, inter-PME region with strong setae directed anteriorly (Fig. 38T). Eyes: AME-AME: 0.03, AME width: 0.03, AME-ALE: 0.02, ALE width: 0.05, ALE-PLE: 0.01, PLE width: 0.05, PLE-PME: 0.04, PME width: 0.04, PME-PME: 0.08. Clypeus: not hirsute. Sternum: 0.55 long, 0.58 wide. Chelicerae: mastidia absent; stridulatory striae rows compressed and evenly spaced (Fig. 39S). Legs: dorsal proximal macroseta on tibia I, II, III and IV 1.84, 2.07, 2.97 and 2.86 times diameter of tibia, respectively; Tm I: 0.65. Pedipalp: patella prolateral proximal vertical macrosetae present; tibia with one prolateral, two retrolateral trichobothria; TPS scaly, long, apical-retrolaterally pointed; TPA absent; TRA small, slightly bent retrolaterally (Fig. 60C); PC median-sized, base not visible from dorsal view, distal setae close to distal clasp, distal clasp with striae, clasp directed retrolaterally (Fig. 60A); T without papillae; PT short, apical part with small papillae; TS short, without papillae; MSA present; DSA tip pointed, retrolaterally curved; EM flat, without papillae, exceeds ARP; ARP pointed, angled on dorsal side; LER without striae, extended dorsal to E; VRP absent; TP round at tip; E retrolaterally spiral, anterior margin at base smoothly curved (Fig. 60D). Opisthosoma: dorsal pattern see Fig. 40U; PMS with mAP, AC absent; PLS with triad, one AC (Fig. 60E).

Male (paratype, SMF): Total length: 2.14. Prosoma: 0.99 long, 0.75 wide, dorsal proximal macroseta on tibia II and III 2.29 and 2.50 times diameter of tibia, respectively; Tm I: 0.70. Opisthosoma: dorsal pattern see Fig. 40T.

Female: Unknown.

Distribution: Nepal.

Habitat: Cultivated lands; mixed broad-leaved forests.

***MITRAGER SEXOCULATA* (WUNDERLICH, 1974)
COMB. NOV.**

(FIGS 38N, 39N, 40O, 61; SUPPORTING INFORMATION,
FIG. S3B)

Oedothorax sexoculatus Wunderlich, 1974: 177, figs 20–24 (Dm; possible f, figs 25–27).

Type material: Holotype: East Nepal, Jiri, 2330–2500 m, ♂ I.1970, leg. Martens, det. Wunderlich 1974 (SMF 28895, 28896 (one palp), examined).

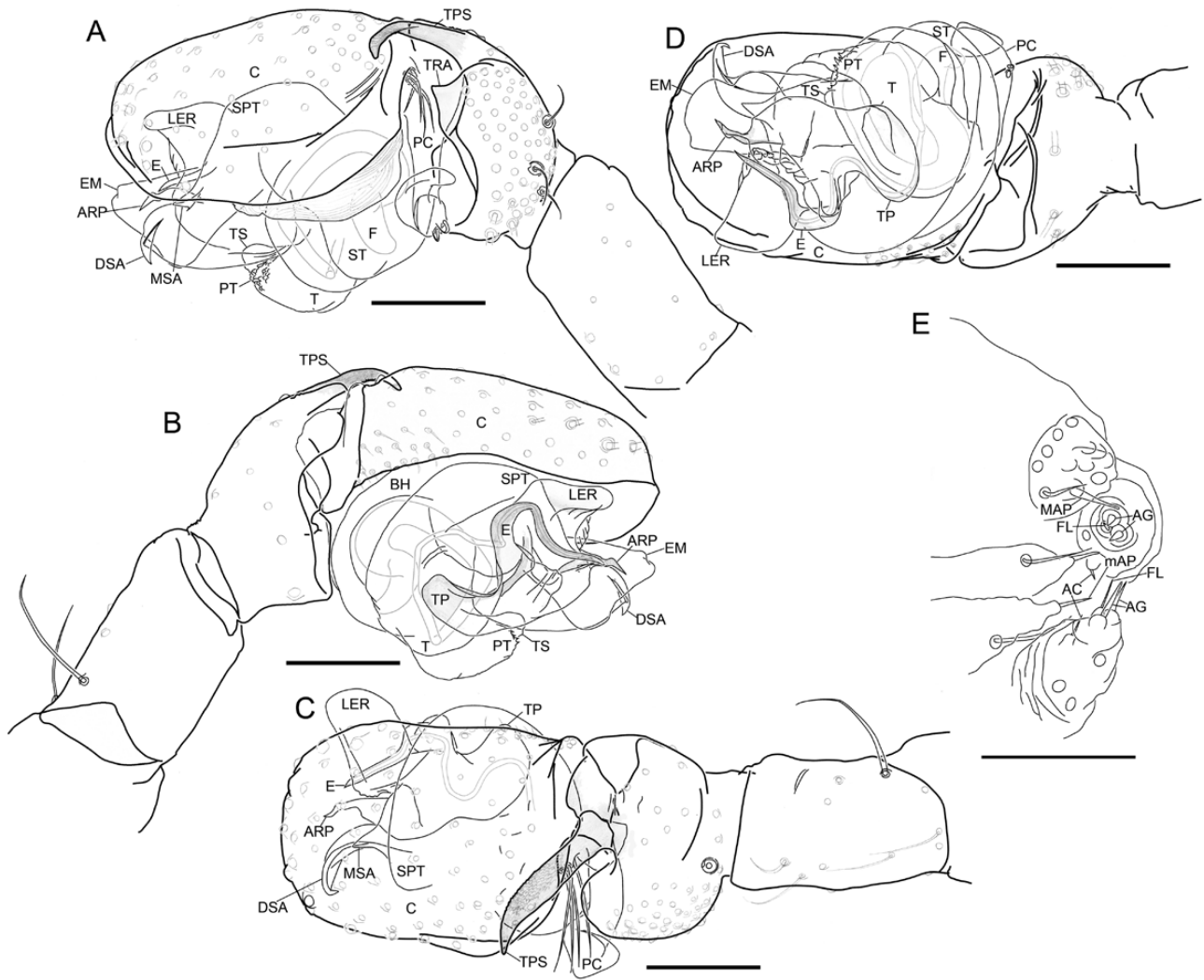


Figure 60. *Mitrager savigniformis* (Tanasevitch, 1998). A–D, male right palp, images flipped horizontally. A, retrolateral view. B, prolateral view. C, dorsal view. D, ventral view. E, male spinnerets. Scale bars 0.1 mm.

Possible female: West Nepal: pass from Gorapani, *Rhododendron*-forest, at creek bank, 2750–2800 m, xii.1969, leg. Martens [SMF 28896, examined; *Oedothorax* sp. in Wunderlich (1974), suggested to be *Oe. sexoculatus* in the original description].

Diagnosis:

Males: This species shares with *M. lucida* the PME located within the transverse groove between the prosomal elevation and the remaining eyes, the highly sclerotized stump-like setae on both upper and lower surfaces within the groove, and one retrolateral trichobothrium on male palpal tibia instead of the common two. This species can be distinguished from *M. lucida* by the larger TPA and the papillae-lacking PT.

Description:

Male (holotype, SMF): Total length: 2.02. Prosoma: 0.93 long, 0.73 wide, region including PMA elevated, transverse groove between elevation and other eyes, with highly sclerotized stump-like setae on both upper and lower surfaces within groove (Fig. 38N). Eyes: AME-AME: 0.03, AME width: 0.04, AME-ALE: 0.02, ALE width: 0.07, ALE-PLE: 0.01, PLE width: 0.08; PME not visible. Clypeus: slightly elevated, with small setae scarcely distributed. Sternum: 0.52 long, 0.52 wide. Chelicerae: mastidia absent; stridulatory striae rows widely and evenly spaced (Fig. 39N). Legs: dorsal proximal macroseta on tibia I and II 0.90 and 1.12 times diameter of tibia, respectively; Tm I: 0.80. Pedipalp: patella prolateral proximal vertical

retrolaterally spiral, anterior margin at base slightly wavy (Fig. 61B). Opisthosoma: dorsal pattern see Fig. 40O; PMS without spigots, one nubbin (vestigial mAP); PLS with triad, AC absent (Fig. 61F, G).

Possible female (SMF 28896). Epigyne: Clade 13 characteristic morphology, borders between dorsal and ventral plates parallel posteriorly, S-curved anteriorly (Fig. 61D, E). Spinnerets: PMS with CY, 2AC; PLS with triad, 2–3 AC (Fig. 61H, I). See description as '*Oedothorax* sp.' in Wunderlich (1974: 178). The absence of mAP on the PMS, a rare feature within the genus, is congruent with the male spigot configuration, further supporting the original conspecific proposition.

Distribution: Nepal, only known from the type locality.

Habitat: No data.

MITRAGER SEXOCOLORUM (TANASEVITCH, 1998)
COMB. NOV.

(FIGS 38H, 39H, 40H, 62; SUPPORTING INFORMATION, FIG. S4F)

Oedothorax sexocolorum Tanasevitch, 1998a: 434, figs 19–23 (Dm).

Type material: Holotype: **Nepal:** Terhathum District, Tinjura Dara, 2450–2850 m, species-rich mixed broad-leaved forest, Berlese funnels, ♂ 17.ix.1983, leg. J. Martens & B. Daams (SMF 38842, 38845 (one palp), examined).

Diagnosis:

Males: This species shares the prosomal PME hump and transverse groove at the interocular region with *M. dismodicoides*, *M. tholusa*, *M. lineata*, *M. globiceps*, *M. lucida* and *M. sexoculata*. Distinguished from *M. globiceps*, *M. lucida* and *M. sexoculata* by the PME at the base of the elevation, above the deepest part of the groove (directly next to the lateral ends of the groove in *M. globiceps*; situated inside the groove in *M. lucida* and *M. sexoculata*); from *M. lineata* by the shorter distance between AME and ALE and the more anterior position of the PME; and from *M. dismodicoides* and *M. tholusa* by the lack of hirsute and elevated clypeus.

Description: Male (holotype, SMF): Total length: 2.04. Prosoma: 0.93 long, 0.69 wide, region including PME elevated, transverse groove between elevation and other eyes, interocular region covered by thin setae (Fig. 38H). Eyes: AME-AME: 0.03, AME width: 0.05, AME-ALE: 0.03, ALE width: 0.08, ALE-PLE: 0.01, PLE

width: 0.08. Clypeus: not hirsute. Sternum: 0.52 long, 0.53 wide. Chelicerae: mastidia absent; stridulatory striae rows compressed proximally (Fig. 39H). Legs: dorsal proximal macroseta on tibia I, II, III and IV 0.73, 0.35, 1.89 and 2.89 times diameter of tibia, respectively; Tm I: 0.73. Pedipalp: patella prolateral proximal vertical macrosetae present; tibia with one prolateral, two retrolateral trichobothria; TPS scaly, retrolaterally pointed; TPA slightly elevated; TRA retrolaterally oriented (Fig. 62C); PC median-sized, base not visible from dorsal view, distal setae close to distal clasp, distal clasp without striae, clasp directed apically (Fig. 62A); T without papillae; PT apical part with small papillae; TS short, without papillae (Fig. 62D); MSA prominent, pointed; DSA tip pointed, anteriorly directed (Fig. 62A); EM flat, anteriorly directed; ARP horizontally flat, ventral side striated; LER without striae, extended dorsal to E; VRP absent; TP tip dorsal margin curved; E retrolaterally spiral, anterior margin at base slightly wavy (Fig. 62B). Opisthosoma: dorsal pattern see Fig. 40H; PMS with mAP, AC absent; PLS with triad, one AC (Fig. 62F, G).

Female: Unknown.

Distribution: Only known from the type locality.

Habitat: Bottom of species-rich mixed broad-leaved forests.

MITRAGER THOLUSA (TANASEVITCH, 1998) COMB.
NOV.

(FIGS 38L, 39L, 40L, M, 56A, 63; SUPPORTING INFORMATION, FIG. S4J)

Oedothorax tholusa Tanasevitch, 1998a: 435, figs 24–29 (Dmf).

Type material: Holotype: **Nepal:** Kaski District, above Dhumpus, broad-leaved forest, 2100 m, ♂ 8.–10.v.1980, leg. J. Martens & A. Ausobsky (SMF 38836, 38855 (one palp), examined). Paratypes: 1♀, collected together with holotype, leg. J. Martens & A. Ausobsky (SMF 38837, examined).

Diagnosis:

Males: Share a prosomal elevated region bearing PME, a transverse groove at interocular region and elevated hirsute clypeus with *M. dismodicoides*, *M. sexoculata* and *M. lucida*, but can be distinguished from *M. dismodicoides* by the slenderer, apically directed palpaltibial prolateral spike (Fig. 63C), and from the latter two species by having two palpal tibial retrolateral trichobothria (one in the latter two species).

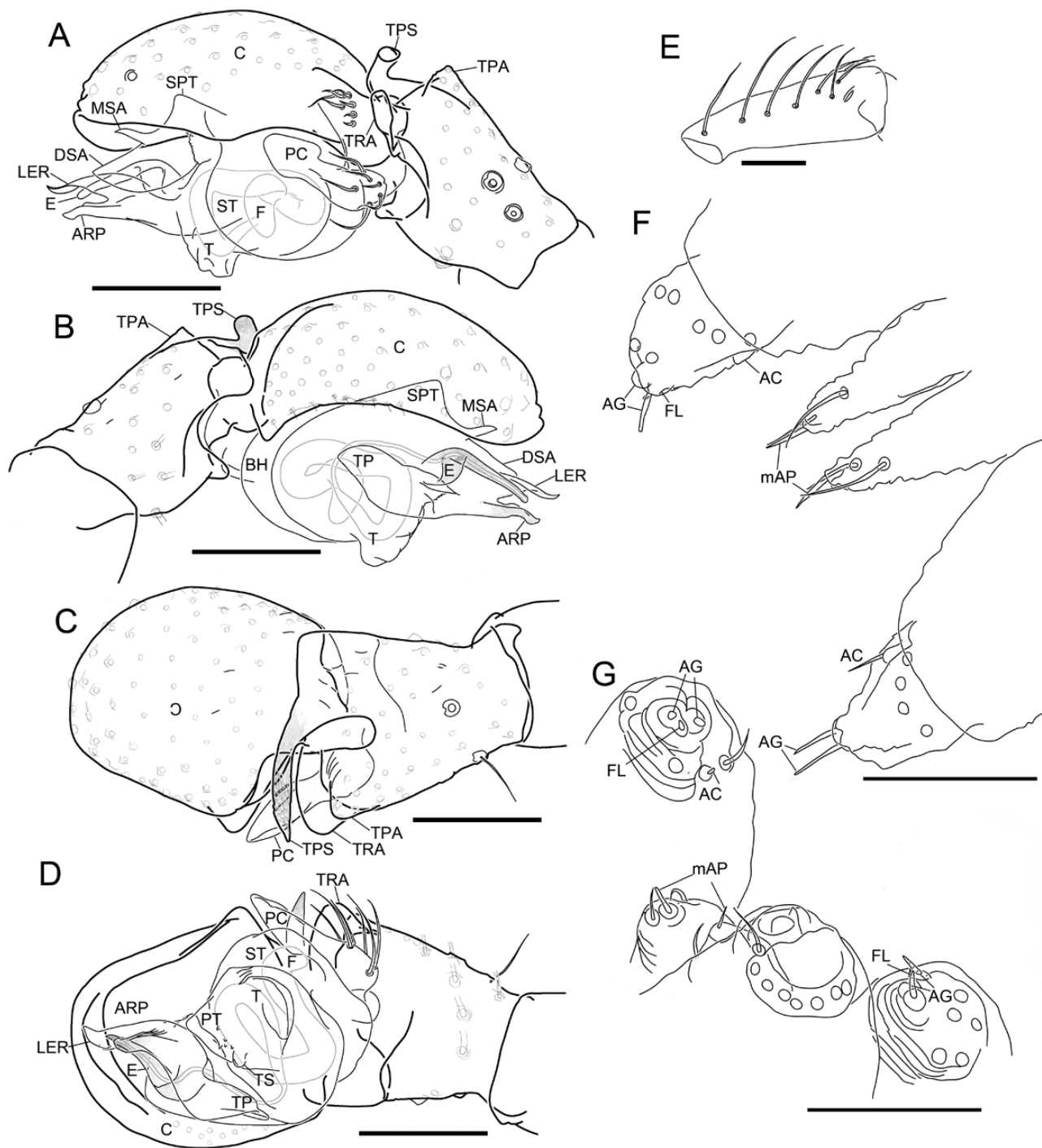


Figure 62. *Mitrager sexocolorum* (Tanasevitch, 1998). A–E, male right palp, images flipped horizontally. A, retrolateral view. B, prolatral view. C, dorsal view. D, ventral view. E, parella prolatral view. F, male posterior median spinnerets and posterior lateral spinnerets, dorsal view. G, male posterior spinnerets. Scale bars 0.1 mm.

Description:

Male (holotype, SMF): Total length: 2.74. Prosoma: 1.30 long, 0.96 wide, PME-bearing region largely elevated,

frontal surface of elevation with scarcely distributed tiny setae; transverse groove between PME and other eyes; interocular region with small setae directed upwards (Figs 38L, 56A). Eyes: AME-AME: 0.06, AME

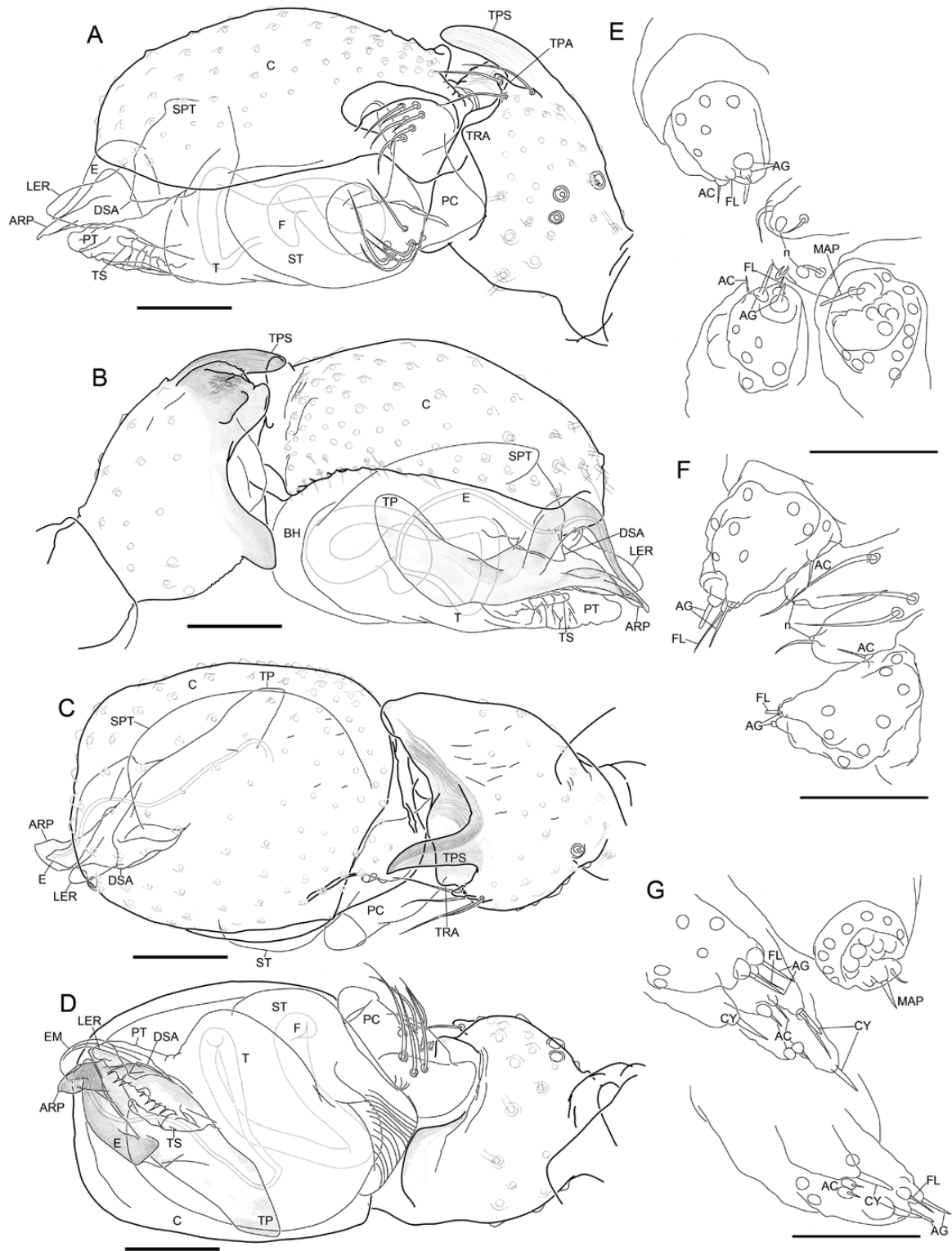


Figure 63. *Mitrager tholusa* (Tanasevitch, 1998). A–D, male right palp, images flipped horizontally. A, retrolateral view. B, prolateral view. C, dorsal view. D, ventral view. E, male spinnerets. F, male posterior median spinnerets and posterior lateral spinnerets, dorsal view. G, female spinnerets. Scale bars 0.1 mm.

width: 0.05, AME-ALE: 0.09, ALE width: 0.08, ALE-PLE: 0.01, PLE width: 0.08, PLE-PME: 0.13, PME width: 0.11, PME-PME: 0.33. Clypeus: hirsute, elevated. Sternum: 0.67 long, 0.70 wide. Chelicerae: mastidia absent; stridulatory striae ridged, rows widely and evenly spaced (Fig. 39L). Legs: dorsal proximal macroseta on tibia I, II and III 0.66, 0.76 and 1.30 times diameter of tibia, respectively; Tm I: 0.58. Pedipalp: patella prolateral proximal vertical macrosetae present; tibia with one prolateral, two retrolateral trichobothria; TPS scaly, relatively straight, tip slightly bent retrolaterally; TPA slightly elevated, with one slightly enlarged setal base at tip; TRA minute; PC large, base not visible from dorsal view, distal setae close to distal clasp, distal clasp without striae, distally extended (Fig. 63A); T without papillae; PT long, with long papillae on prolateral surface; TS median-long, thin, without papillae (Fig. 63D); MSA minute; DSA short (Fig. 63A); EM flat, without papillae, approximately equals ARP in length; ARP flat, striated on ventral surface (Fig. 63D); LER without striae, not extended dorsal to E; VRP absent; TP tip round; E retrolaterally spiral, anterior margin at base smoothly curved (Fig. 63B). Opisthosoma: dorsal pattern see Fig. 40L; PMS without spigots, one nubbin (vestigial mAP); PLS with triad, one AC (Fig. 63E, F).

Female: Unknown (see remarks).

Distribution: Nepal, only known from the type locality.

Habitat: Broad-leaved forests.

Remarks: The female paratype designated by Tanasevitch (1998) is presumably not conspecific to the male holotype in light of the following evidence: female carapace length and width much smaller than male (in all other *Mitrager* species with described female the carapace is consistently larger than males); absence of male dorsal pattern on female opisthosoma (all other recorded *Mitrager* females have patterns resembling conspecific males); female with mAP on PMS but absent in male (all other species where PMS were examined for male and female, both sexes have either absent or present mAP).

Additional morphological data taken from the paratype material:

Female (paratype, presumably not conspecific with the holotype): Total length: 2.28. Prosoma: 0.83 long, 0.66 wide. Eyes: AME-AME: 0.02, AME width: 0.04, AME-ALE: 0.03, ALE width: 0.08, ALE-PLE: 0, PLE width: 0.06, PLE-PME: 0.03, PME width:

0.06, PME-PME: 0.06. Clypeus: not hirsute, one sub-AME seta. Sternum: 0.48 long; 0.51 wide. Legs: tibia chaetotaxy 2-2-1-1, dorsal proximal macroseta on tibia I, II, III and IV 0.82, 0.69, 0.74 and 0.69 times diameter of tibia, respectively; Tm I: 0.71. Epigyne: Clade 13 characteristic morphology, see fig. 29 in Tanasevitch (1998). Opisthosoma: evenly coloured grey (Fig. 40M); PMS with mAP, one AC, one CY; PLS with triad, two CY, two AC (Fig. 63G).

***MITRAGER TRICEPS* (TANASEVITCH, 2020) COMB. NOV.**

Oedothorax Triceps Tanasevitch, 2020a: 288 (Figs 8–11, 28–30) (Dm).

Type material: Holotype: **Nepal:** Bagmati Province, Dobate Ridge northeast of Barahbise, 2800 m a.s.l., sifting rotten wood, dead leaves and moss in oak grove with *Rhododendron*, 2.v.1981, leg. I. Löbl & A. Smetana (MNHG, not examined).

Diagnosis:

Males: This species is characterized by the prominent trilobate post-ocular groove and hump, as well as the short palpal prolateral apophysis, the distally oriented palpal prolateral spike, the protegulum palpillae and the embolic division [see description in Tanasevitch (2020b)]. These features, shared with *M. tholusa*, suggest a close relationship between them, but they can be distinguished by the position of the palpal tibia prolateral apophysis, which is more distally situated in *M. tholusa* than in this species.

Females: Unknown.

Distribution: Only known from the type locality in Nepal.

Habitat: Forest litter.

Remarks: According to our re-delimitation of *Oedothorax* in the present study, this species does not belong to *Oedothorax*, but is most closely related to *M. tholusa*. We thus move this species to *Mitrager*.

***MITRAGER UNICOLOR* (WUNDERLICH, 1974) COMB. NOV.**

(Figs 38P, 39P, 40Q, 64; SUPPORTING INFORMATION, FIG. S3D)

Oedothorax unicolor Wunderlich, 1974: 172, figs 1–5 (Dmf).

Oedothorax kathmandu Tanasevitch, 2020: 286, figs 4, 18–22 (Dm), *synon. nov.*

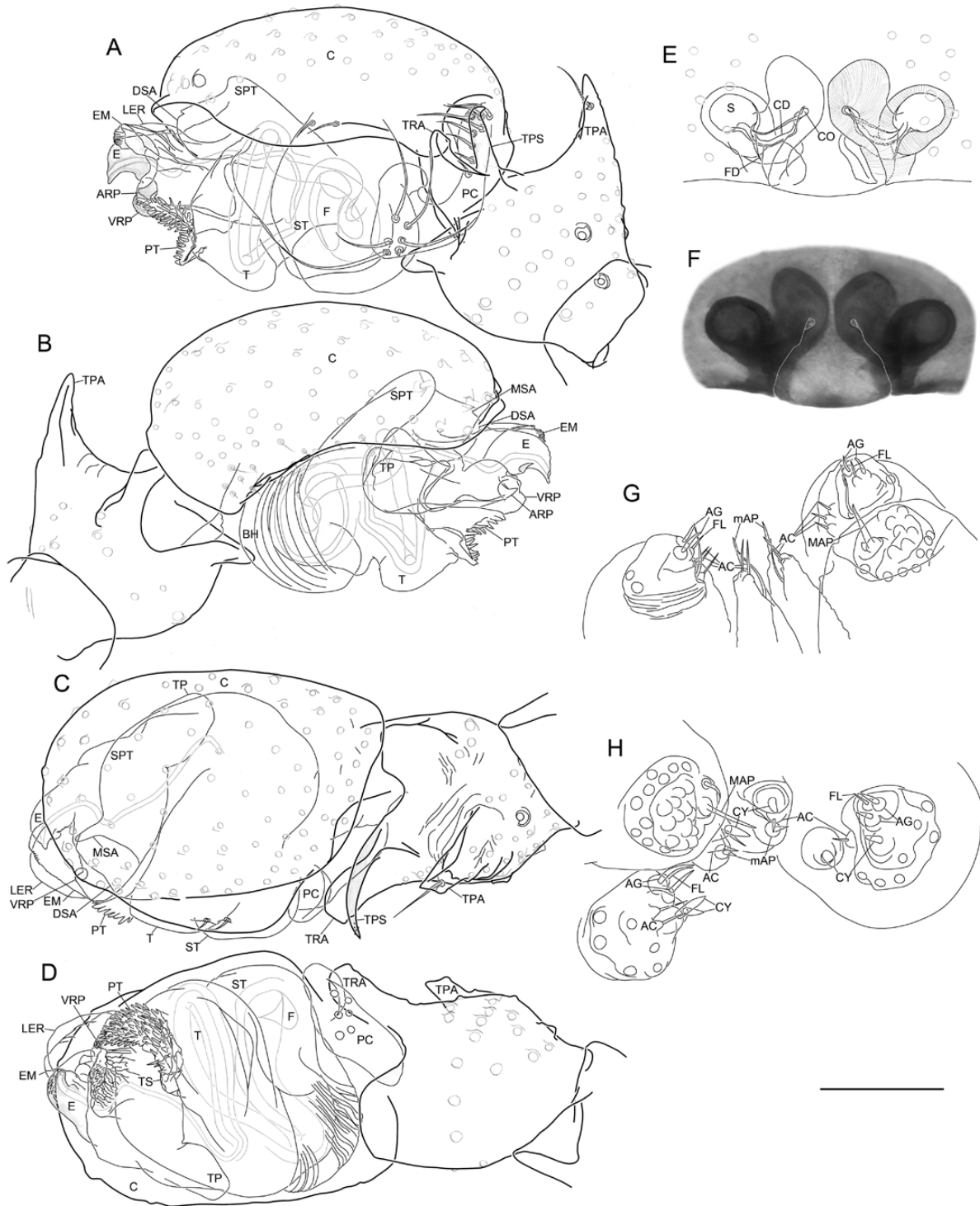


Figure 64. *Mitrager unicolor* (Wunderlich, 1974). A–D, male left palp. A, retrolateral view. B, prolateral view. C, dorsal view. D, ventral view. E, F, epigyne. E, ventral view. F, external morphology. G, male spinnerets. H, female spinnerets. Scale bar 0.1 mm.

Type material: *Oedothorax unicolor*: Holotype: **Nepal:** Kathmandu Valley, Godawari, sifted from secondary broadleaf forest, 1700 m, 1♂ i.1970, coll. J. Martens, det. Wunderlich (SMF 28889, examined). Paratypes: 1♂ (SMF 31677, examined) 1♀3 juv (SMF 28890, examined), collected together with holotype. *Oedothorax kathmandu*: Holotype: **Nepal:** Kathmandu, Balaju Park, mixed forest, 1400 m a.s.l., 17.iii.1980, leg. J. Martens & A. Ausobsky (SMF, unexamined).

Diagnosis:

Males: This species can be distinguished from congeners by the palpal tibia with the exceptionally long retrolateral apophysis, the vertically extended prolateral apophysis with an isolated setae on the ventral side of the tip and the slender prolateral spike, as well as the short, stout embolus, the scaly, ventral, radical apophysis, the lack of prosomal modification and the lack of opisthosoma dorsal pattern.

Females: Distinguished from the congeners by the especially wide cuticular region of copulatory ducts at the copulatory opening and the lack of opisthosoma dorsal pattern.

Description:

Male (holotype, SMF 28889): Total length: 2.12. Prosoma: 0.94 long, 0.76 wide, unmodified (Fig. 38P). Eyes: AME-AME: 0.02, AME width: 0.05, AME-ALE: 0.01, ALE width: 0.09, ALE-PLE: 0, PLE width: 0.10, PLE-PME: 0.03, PME width: 0.09, PME-PME: 0.07. Clypeus: not hirsute. Sternum: 0.57 long, 0.56 wide. Chelicerae: mastidia absent; stridulatory striae imbricated, rows compressed distally (Fig. 39P). Legs: dorsal proximal macroseta on tibia I and II 2.37 and 3.05 times diameter of tibia, respectively; Tm I: 0.52. Pedipalp: patella prolateral proximal vertical macrosetae present; tibia with one prolateral, two retrolateral trichobothria; TPS retrolaterally bent, tip slightly scaly; TPA prominent, with one seta at distal surface of tip; TRA long, anteriorly directed, slightly retrolaterally curved (Fig. 64C); PC median-sized, base not visible from dorsal view, distal setae close to distal clasp, distal clasp without striae, distally extended (Fig. 64A); T without papillae; PT with long papillae; TS short, without papillae (Fig. 64D); MSA present; DSA short; EM flat, with small papillae at margin, length approximately equals LER and E (Fig. 64B); ARP pointed, shorter than embolus; LER without striae, extended dorsal to E; VRP scaly, retrolaterally directed (Fig. 64A); TP tip wide; E short and thick,

slightly retrolaterally spiral, distal part above spermophore opening scaly (Fig. 64B). Opisthosoma: single-coloured grey (Fig. 40Q); PMS with mAP, two AC; PLS with triad, three AC (Fig. 64G).

Male (paratype, SMF 31677): Total length 2.04. Prosoma: 0.91 long, 0.76 wide. Legs: dorsal proximal macroseta on tibia I 2.40 times diameter of tibia; Tm I: 0.57.

Female (paratype, SMF 28890): Total length: 2.41. Prosoma: 1.09 long, 0.84 wide. Eyes: AME-AME: 0.03, AME width: 0.05, AME-ALE: 0.02, ALE width: 0.09, ALE-PLE: 0.01, PLE width: 0.09, PLE-PME: 0.04, PME width: 0.08, PME-PME: 0.06. Clypeus: not hirsute. Sternum: 0.61 long; 0.64 wide. Legs: dorsal proximal macroseta on tibia III 2.10 times diameter of tibia, respectively; Tm I: 0.53. Epigyne: Clade 13 characteristic morphology, borders between dorsal and ventral plates converging anteriorly, cuticle at CO broadly extended anteriorly, copulatory duct simple, slightly curved (Fig. 64E, F). Opisthosoma: single-coloured grey; PMS with mAP, two AC, one CY; PLS with triad, two CY, one-two AC (Fig. 64H).

Distribution: Nepal, only known from the type locality.

Habitat: Forest litter.

Taxonomic remarks: According to the type locality, the morphological data, and figs 18–22 in Tanasevitch (2020b) comparing with the description in Wunderlich (1974) and the pedipalp views in Fig. 64, *Oe. kathmandu* is identical to *M. unicolor*, thus we propose the former as a junior synonym of the latter.

MITRAGER VILLOSA (TANASEVITCH, 2015) **COMB. NOV.**
(FIGS 38E, 39E, 40E, 65)

Oedothorax villosus Tanasevitch, 2015: 395, figs 89–99 (Dmf).

Type material: Holotype: **India:** Himalayas, West Bengal, Darjeeling District, Algarah, 1800 m, sifting in forest, ♂ 9.x.1978, leg. C. Besuchet & I. Löbl (MHNG, examined). Paratypes: 2♂2♀, collected together with holotype (MHNG, examined).

Diagnosis:

Males: This species shares the two pairs of branched setae at the ocular region with *M. angela*, *F. cornuta* and *M. coronata*. The presence of a post-ocular groove distinguishes this species from *M. angela*. The branches on the two pairs of setae between PME differ from the longer branches in *M. angela* and *M. coronata*. The

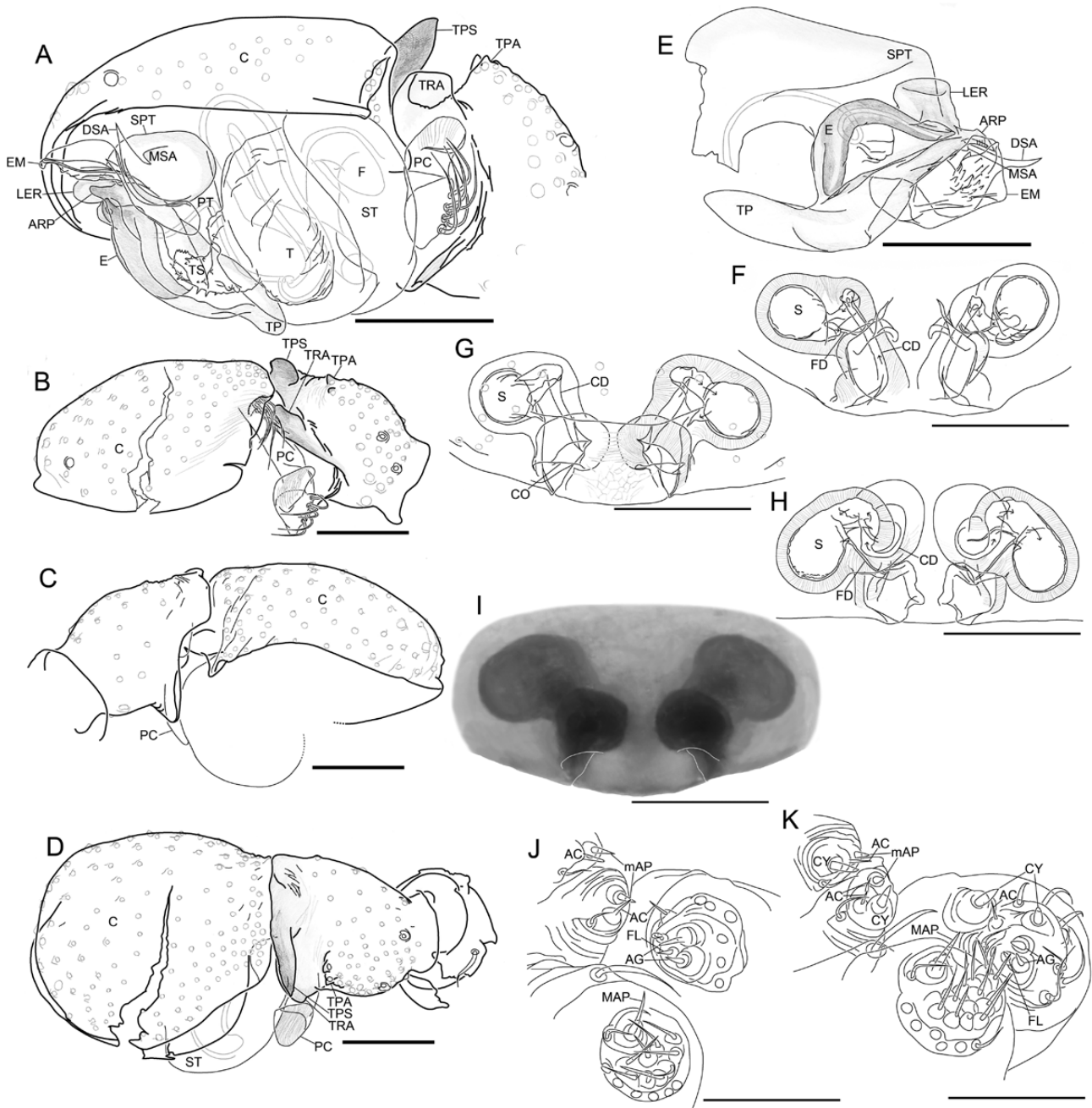


Figure 65. *Mitrager villosa* (Tanasevitch, 2015). A, male left palp, retrolateral view. B–E, male right palp, images flipped horizontally. B, retrolateral view. C, prolateral view. D, dorsal view. E, embolic division, prolateral view. F–I, epigyne. F, posterior view. G, ventral view. H, dorsal view. I, external morphology. J, male spinnerets. K, female spinnerets. Scale bars 0.1 mm.

posteriorly oriented post-ocular groove distinguishes this species from *M. villosa* (anteriorly oriented).

Females: Can be distinguished from the similar species *M. cornuta* by its more anteriorly extended path of the copulatory ducts before entering the spermathecae.

Description:

Male (paratype): Total length: 2.00. Prosoma: 0.90 long, 0.78 wide, inter-PME region bearing two pairs of thick, long, appressed-toward-head branched setae, posterior pair much longer than anterior pair; pale-yellow

rounded postocular hump separated from ocular region by deep transverse groove (Fig. 38E). Eyes: AME-AME: 0.02, AME width: 0.04, AME-ALE: 0.01, ALE width: 0.07, ALE-PLE: 0, PLE width: 0.7, PLE-PME: 0.3, PME width: 0.06, PME-PME: 0.07. Clypeus: not hirsute. Sternum 0.61 long, 0.57 wide. Chelicerae: mastidia absent; stridulatory striae imbricated, rows widely and evenly spaced (Fig. 39E). Legs: dorsal proximal macroseta on tibia II 3.61 times diameter of tibia; Tm I: 0.75. Pedipalp: patella prolateral proximal vertical macrosetae present; tibia with one prolateral, two retrolateral trichobothria; TPS scaly, retrolaterally pointed; several parallel slit organs prolateral to TPS; TPA slightly elevated, with two slightly enlarged setal base; TRA bent retrolaterally (Fig. 65C); PC short, base not visible from dorsal view, distal setae close to distal clasp, distal clasp directed retrolaterally, with striae (Fig. 65A); T without papillae; PT short, with few small papillae; TS long and thick, with small papillae; MSA present; DSA pointed, retrolaterally curved; EM flat, with small papillae, anterior margin without papillae, exceeds ARP (Fig. 65A); ARP pointed, angled on dorsal side, ventral surface striated; LER without striae, extended dorsal to E; VRP absent; TP round at tip; E retrolaterally spiral, anterior margin at base slightly wavy (Fig. 65E). Opisthosoma: dorsal pattern see Fig. 40E; PMS with mAP, one AC; PLS with triad, one AC (Fig. 65J).

Female (paratype): Total length: 2.23. Prosoma: 0.95 long, 0.75 wide. Eyes: AME-AME: 0.02, AME width: 0.04, AME-ALE: 0.02, ALE width: 0.08, ALE-PLE: 0.01, PLE width: 0.9, PLE-PME: 0.2, PME width: 0.08, PME-PME: 0.06. Clypeus: not hirsute. Sternum 0.57 long, 0.58 wide. Legs: dorsal proximal macroseta on tibia II 1.93 times diameter of tibia; Tm I: 0.75. Epigyne: Clade 13 characteristic morphology, borders between dorsal and ventral plates slightly converging anteriorly, CO wide (Fig. 65F–I). Opisthosoma: dorsal pattern as in male; PMS with mAP, one-two AC, one CY; PLS with triad, two CY, one AC (Fig. 65K).

Distribution: Only known from the type locality.

Habitat: Forest litter.

EMERTONGONE GEN. NOV.

Type species: *Lophocarenum montiferum* Emerton, 1882.

Derivatio nominis: The genus name is a combination of Emerton, in honor of the American arachnologist James Henry Emerton, the original describer of the

type species, and the ending of the generic name 'Erigone'. Genus gender feminine.

Diagnosis:

Males: Small-sized, dark-brown-coloured erigonine. This genus is characterized by its male prosomal modification comprising a post-PME groove, post-PME lobe, the anteriorly protruded hirsute clypeus and the shorter distance from PLE to clypeal lower margin compared to PME. Despite its superficial partial similarity of prosomal modification with *Oe. gibbosus*, this genus has no separate radix and embolus connected by a membranous region, and the embolic membrane is erected from distal part of distal suprategular apophysis. These characters distinguish it from all taxa in Clade 13.

Females: Can be distinguished from all other examined taxa by the shorter distance from ALE to clypeus margin compared to distance from AME to clypeus margin, the hirsute clypeus, and the transverse slit on the epigyne between the two copulatory openings (Fig. 65E, G).

Species included: ***Emertongone montifera*** (Emerton, 1882) **comb. nov.**

Phylogenetic justification: Although the prosomal modification of *Em. montifera* superficially resembles that of *Oe. gibbosus*, the palpal configuration of this species is different from that of *Oedothorax* as delimited in the present study. In the phylogeny (Fig. 2), this species is sister to Clade 12; i.e. more closely related to the *Walkenaeria* and *Gonatium* representatives than to all *Oedothorax*, *Callitrichia*, *Mitrager* and other representatives in Clade 13. The similarity in prosomal morphology is, therefore, a result of homoplasy. After a comprehensive literature research of erigonine male palpal structures, no morphologically resembling species was found that can suggest at least a preliminary (i.e. phenetic) close relatedness. Base on these findings and its resulting phylogenetic placement, this species neither belongs to *Oedothorax*, nor can it be transferred to any other established taxon. We, therefore, propose the erection of *Emertongone* gen. nov. for this unique species.

EMERTONGONE MONTIFERA (EMERTON, 1882) COMB. NOV.

(FIGS 7A, 66, 67C, 68C; SUPPORTING INFORMATION, FIG. S5B)

Lophocarenum montiferum Emerton, 1882: 47, pl. 13, fig. 2 (Dmf).

Gongylidium montiferum Simon, 1884: 500.

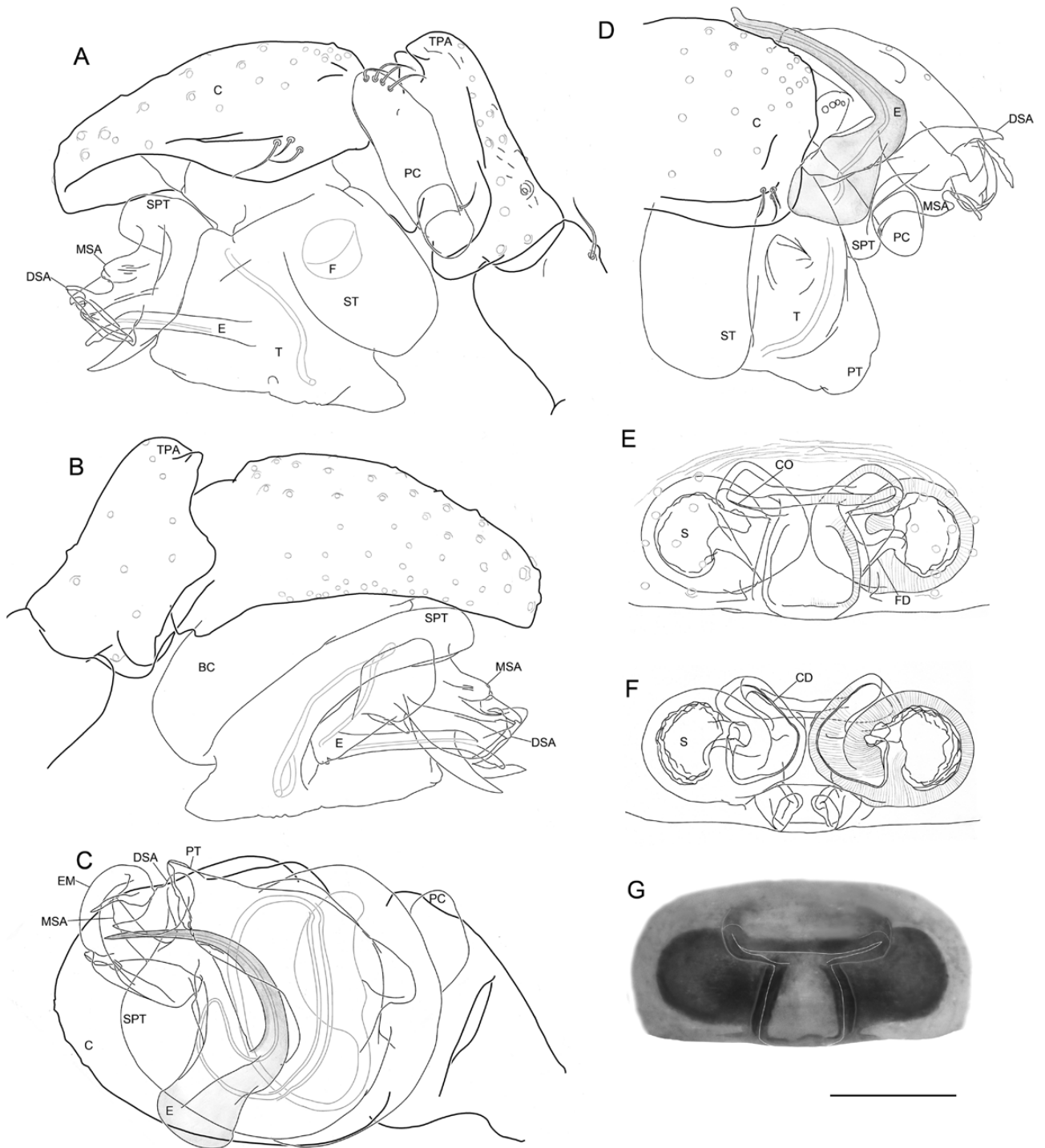


Figure 66. *Emertongone montifera* (Emerton, 1882). A–D, male left palp. A, retrolateral view. B, prolateral view. C, ventral view. D, expanded, retrolateral view. E–G, epigyne. E, ventral view. F, dorsal view. G, external morphology. Scale bar 0.1 mm.

Erigone montifera Marx, 1890: 535.

Neriene montifera Simon, 1894: 633.

Oedothorax montiferus Crosby, 1905: 312, 335.

Diplocephalus montiferus Banks, 1916: 73.

Oedothorax montiferus Bishop & Crosby, 1935: 266, pl. 22, figs 74–78 (mf).

Oedothorax montiferus Kaston, 1948: 173, figs 486–492 (mf).

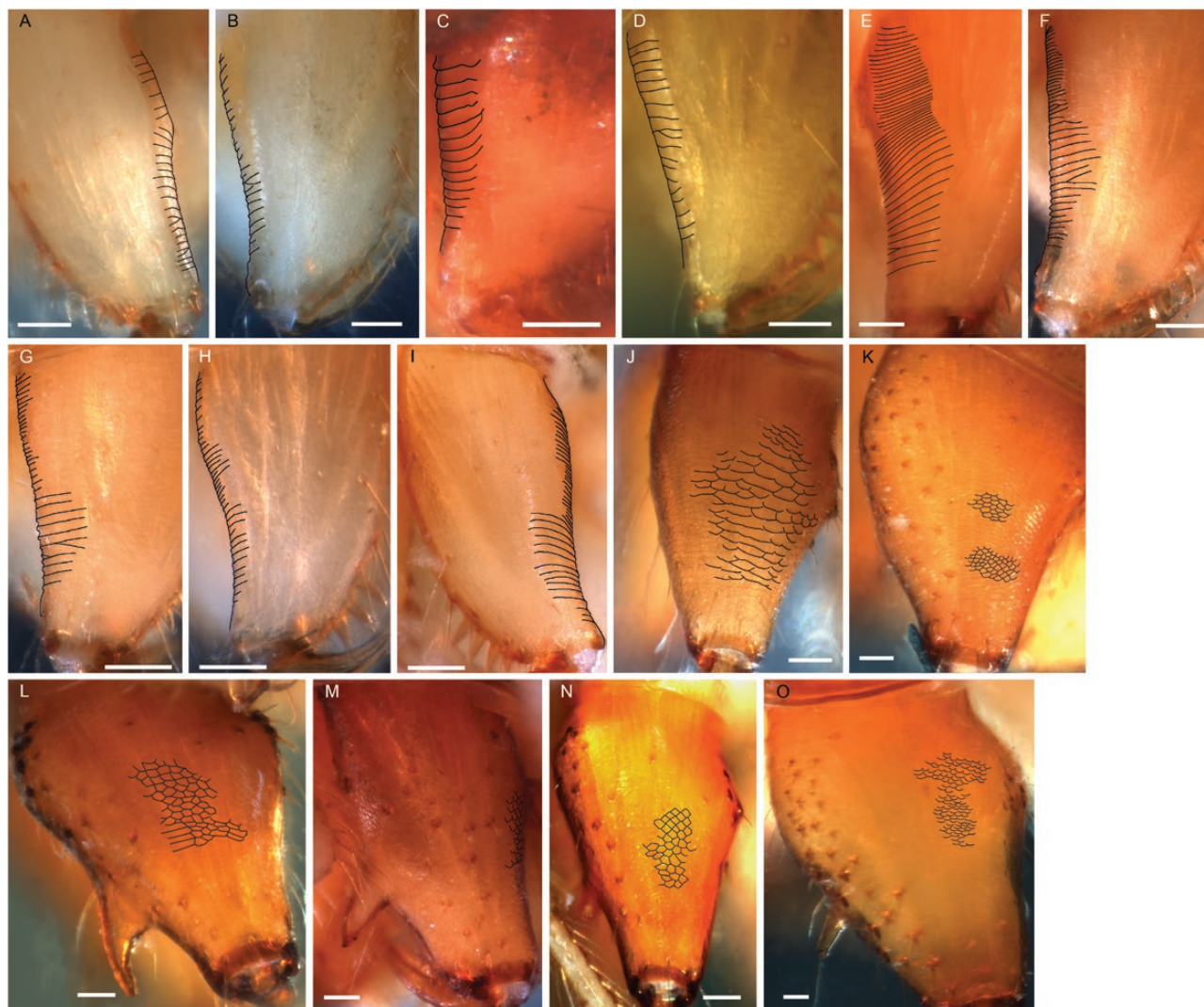


Figure 67. Male chelicerae, stridulatory striae on lateral side. A, *Jilinus hulongensis* (Zhu & Wen, 1980). B, *Cornitibia simplicithorax* (Tanasevitch, 1998). C, *Emertongone montifera* (Emerton, 1882). D, '*Oedothorax*' *paracymbialis* Tanasevitch, 2015. E, '*Oe.*' *kodaikanal* Tanasevitch, 2015. F, '*Oe.*' *cunur* Tanasevitch, 2015. G, '*Oe.*' *stylus* Tanasevitch, 2015. H, *Atypena cirrifrons* (Heimer, 1984). I, *A. formosana* (Oi, 1977). J, '*Oe.*' *nazareti* Scharff, 1989. K, *Gongylidium rufipes* (Linnaeus, 1758). L, *Ummeliata insecticeps* (Bösenberg & Strand, 1906). M, *U. esyunini* (Zhang, Zhang & Yu, 2003). N, *Hylyphantes graminicola* (Sundevall, 1830). O, *Tmeticus tolli* Kulczyński, 1908. Scale bars 0.05 mm.

Oedothorax montifer Paquin & Dupérré, 2003: 115, figs 1186–1189 (mf).

Type material: Not designated. Type locality: Brookline and Salem, Mass. (Bishop & Crosby 1935). The clear illustrations of the male prosomal and palpal structures and epigyne in the original description allow the unambiguous identification of this species.

Examined material: **USA:** Pennsylvania, Lower Friederick Township (40°16' N, 75°30' W), 4♂3♀ iii.1954, Wilton Ivie coll. & det; Massachusetts, Middlesex,

Peperell, 1♀ 24.x.1970, det. Platnick; Massachusetts, Brookline (42°19' N, 71°6' W), 1♂1♀ 10.vi.1873, coll. J. H. Emerton; Ohio, Wayne County, Neil McCoy's Woods, under rotting wood, 2♀ 25.iv.1959, J. A. Beatty.

Description:

Male (Pennsylvania): Total length: 1.70. Prosoma: 0.89 long, 0.67 wide, post-PME region largely elevated, with post-PME groove (Fig. 7A). Eyes: AME-AME: 0.02, AME width: 0.04, AME-ALE: 0.12, ALE width: 0.06, ALE-PLE: 0.01, PLE width: 0.05, PLE-PME: 0.02,

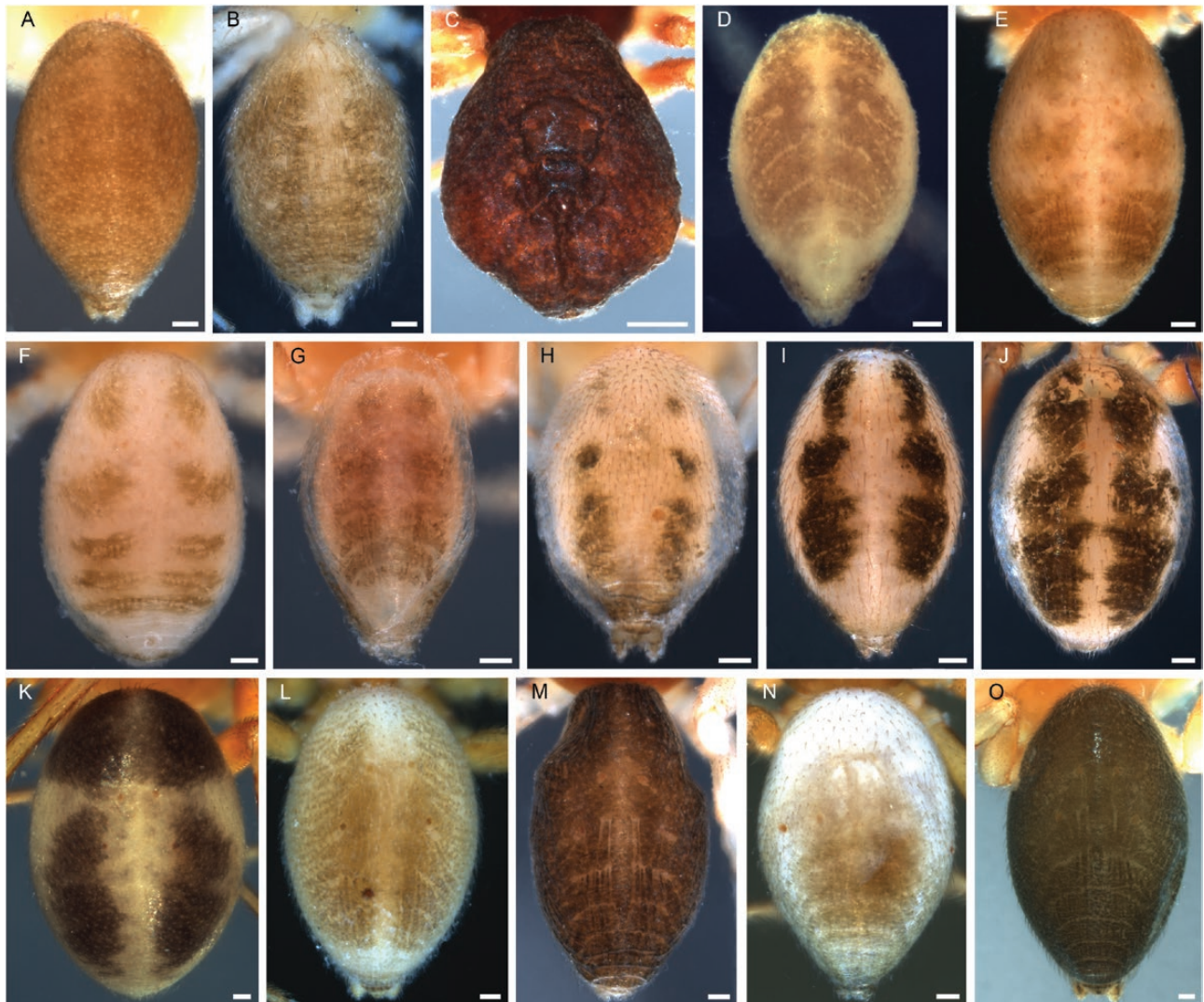


Figure 68. Male opisthosoma, dorsal view. A, *Jilinus hulongensis* (Zhu & Wen, 1980). B, *Cornitibia simplicithorax* (Tanasevitch, 1998). C, *Emertongone montifera* (Emerton, 1882). D, *'Oedothorax' paracymbialis* Tanasevitch, 2015. E, *'Oe.' kodaikanal* Tanasevitch, 2015. F, *'Oe.' cunur* Tanasevitch, 2015. G, *'Oe.' stylus* Tanasevitch, 2015. H, *Atypena cirrifrons* (Heimer, 1984). I, *A. formosana* (Oi, 1977). J, *'Oe.' nazareti* Scharff, 1989. K, *Gongylidium rufipes* (Linnaeus, 1758). L, *Ummeliata insecticeps* (Bösenberg & Strand, 1906). M, *U. esyunini* (Zhang, Zhang & Yu, 2003). N, *Hylyphantes graminicola* (Sundevall, 1830). O, *Tmeticus tolli* Kulczyński, 1908. Scale bars 0.1 mm.

PME width: 0.04, PME-PME: 0.31. Clypeus: hirsute. Sternum: 0.48 long, 0.45 wide. Chelicerae: stridulatory striae rows widely and evenly spaced (Fig. 67C). Legs: tibia chaetotaxy 2-2-1-1, dorsal proximal macroseta on tibia I, II, III and IV 0.35, 0.33, 0.33 and 0.49 times diameter of tibia, respectively; Tm I: 0.61. Metatarsi I-III with trichobothrium, IV without trichobothrium. Pedipalp: PC base visible from dorsal view, distal seta distally situated, distal clasp small; PT without papillae; TS absent; MSA round; DSA complex (Fig. 66A); EM arised from distal part of DSA; R and E

fused; E prolaterally spiral, tip retrolateral to DSA; TP, ARP, LER, and VRP absent (Fig. 66C, D). Opisthosoma: evenly coloured, dark grey (Fig. 68C).

Female (Pennsylvania): Total length: 1.70. Prosoma: 0.69 long, 0.65 wide. Eyes: AME-AME: 0.02, AME width: 0.04, AME-ALE: 0.04, ALE width: 0.06, ALE-PLE: 0.01, PLE width: 0.06, PLE-PME: 0.02, PME width: 0.05, PME-PME: 0.1. Clypeus: hirsute. Sternum: 47 long; 42 wide. Legs: tibia chaetotaxy 2-2-1-1, dorsal proximal macroseta on tibia I, II, III and IV 0.79, 0.77,

0.71 and 0.82 times diameter of tibia, respectively; Tm I: 0.56. Epigyne: dorsal plate extended anteriorly, bordering ventral plate by two lateral slits and an anterior slit, CO at lateral ends of anterior slit (Fig. 66E–G). Opisthosoma: evenly coloured, dark grey.

Variation: The measurements are based on examined material.

Males ($N = 5$, means in parentheses): Total length 1.70–1.89 (1.79). Prosoma: 0.86–0.95 (0.89) long, 0.66–0.75 (0.68) wide. Legs: dorsal proximal macroseta on tibia I, II, III and IV 0.29–0.35 (0.32), 0.25–0.33 (0.30, $N = 3$), 0.19–0.33 (0.27, $N = 4$) and 0.30–0.49 (0.42) times diameter of tibia, respectively; Tm I: 0.53–0.61 (0.56).

Females ($N = 7$, means in parentheses): Total length 1.70–2.37 (2.09). Prosoma: 0.69–0.91 (0.81) long, 0.62–0.77 (0.69) wide. Legs: dorsal proximal macroseta on tibia I, II, III and IV 0.46–0.80 (0.69, $N = 3$), 0.52–0.78 (0.66, $N = 4$), 0.44–0.71 (0.58, $N = 4$) and 0.57–0.82 (0.72, $N = 4$) times diameter of tibia, respectively; Tm I: 0.53–0.62 (0.57).

Distribution: USA.

Habitat: Maple swamps (Emerton, 1882).

CORNITIBIA GEN. NOV.

Type species: *Oedothorax simplicithorax* Tanasevitch, 1998

Derivatio nominis: The genus name refers to the tusk-like male palpal tibia apophysis of the type species. Genus gender feminine.

Diagnosis:

Males: This genus is distinguished from all other erigonines by the distinct male palpal tibia, bearing one tusk-like, seta-free apophysis rising from the proximal half of tibia and pointing apically, and several long thorns from enlarged setal bases both retrolateral and prolateral to the apophysis, as well as by the unique morphology of the embolic division (as shown in Fig. 69D). The lack of a membranous connection between the radix and the embolus and the presence of radical lateral tooth clearly distinguish this species from all taxa on Clade 13.

Females: Unknown.

Species included: *Cornitibia simplicithorax* (Tanasevitch, 1998) **comb. nov.**

Phylogenetic justification: In the original description of *Oedothorax simplicithorax* (Tanasevitch 1998), no account was given regarding the diagnostic characters used for assigning this species to *Oedothorax*, and the embolic division of this species was not clearly illustrated. Later (Tanasevitch, 2015), diagnostic characteristics of *Oedothorax* were described, including features related to the embolic division, which match most species on Clade 13. Examination of *Co. simplicithorax* revealed a greatly different embolic division configuration in this species, with an pale, ventro-prolaterally situated ‘anterior radical process’, different from that of other species examined in the present study. In the phylogeny (Fig. 2), this species is sister to a clade comprising the majority of our taxon sample (Clade 10), and not closely related to *Oedothorax*, *Callitrichia*, *Mitrager* or other taxa in Clade 13. After a comprehensive literature research of erigonine male palpal structures, no morphologically resembling species was found that can suggest at least a preliminary (i.e. phenetic) close relatedness. Base on these findings and its relatively basal phylogenetic placement, this species neither belongs to *Oedothorax*, nor can it be transferred to any other established taxon. We, therefore, propose the erection of *Cornitibia* gen. nov. for this species.

CORNITIBIA SIMPLICITHORAX (TANASEVITCH, 1998) **COMB. NOV.**

(FIGS 67B, 68B, 69; SUPPORTING INFORMATION, FIG. S5A)

Oedothorax simplicithorax Tanasevitch, 1998a: 437, figs 34–35 (Dm).

Type material: Holotype: **Nepal:** Ilam District, Gitang Khola Valley, *Alnus*-forest along river, 1750 m, ♂ 11.–13.iv.1988, leg. J. Martens & W. Schawaller (SMF 38861, examined).

Paratype: 1♂, same locality, together with holotype, leg. J. Martens & W. Schawaller (SMF 38851, examined).

Description:

Male (holotype, SMF): Total length: 2.12. Prosoma: 0.93 long, 0.78 wide, not modified. Eyes: AME-AME: 0.02, AME width: 0.05, AME-ALE: 0.02, ALE width: 0.10, ALE-PLE: 0.01, PLE width: 0.09, PLE-PME: 0.06, PME width: 0.06, PME-PME: 0.09. Clypeus: not hirsute, one sub-AME seta. Sternum: 0.56 long, 0.60 wide. Chelicerae: mastidia absent; stridulatory striae

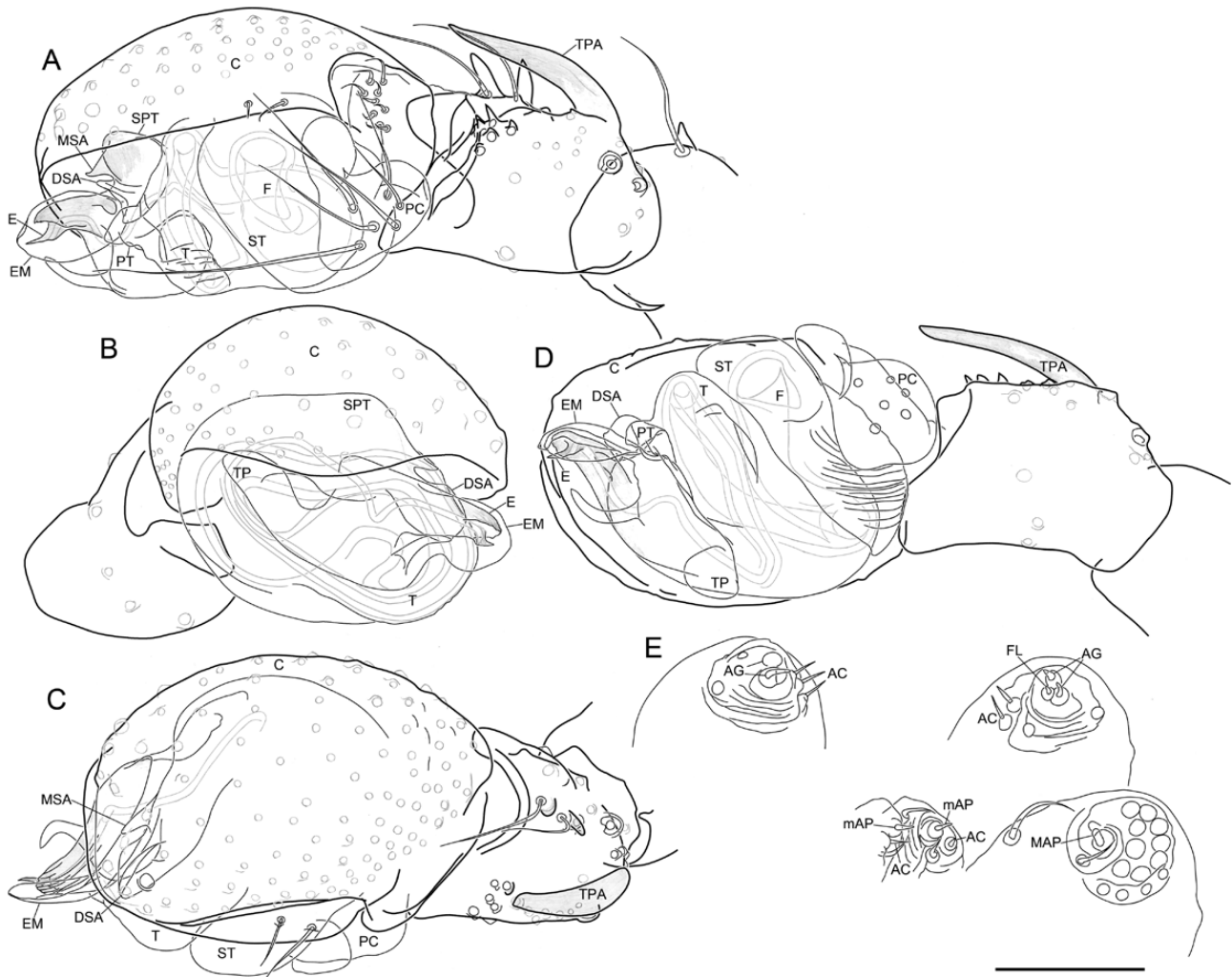


Figure 69. *Cornitibia simplicithorax* (Tanasevitch, 1998). A–D, male left palp. A, retrolateral view. B, prolateral view. C, dorsal view. D, ventral view. E, male spinnerets. Scale bar 0.1 mm.

rows widely and evenly spaced (Fig. 67B). Legs: tibia chaetotaxy 2-2-1-1, dorsal proximal macroseta on tibia I, II, and III 2.26, 2.69 and 3.06 times diameter of tibia, respectively; Tm I: 0.55. All metatarsi with trichobothrium. Pedipalp: patella prolateral proximal vertical macrosetae absent; tibia with one prolateral, two retrolateral trichobothria; TPS absent; TPA highly sclerotized, without setae, arising from middle of tibia, extended forward until above cymbium base, pointed at tip; TRA absent (Fig. 69A, C); PC large, base not visible from dorsal view, distal setae close to distal clasp, setae-bearing area wide, distal clasp without striae, clasp directed apically (Fig. 69A); T without papillae; PT short, without papillae; TS absent (Fig. 69D); MSA present; DSA short, tip behind MSA tip; EM flat, without papillae, exceeds E (Fig. 69A); ARP arising from ventro-prolateral area of R; LER and

VRP absent; TP tip round; E straight, slightly curved ventrally at tip, sharp-pointed tip extended anterior to spermophore opening, striated flat process behind E tip directed anteriorly (Fig. 69B). Opisthosoma: dorsal pattern see Fig. 68B. PMS with mAP, one AC; PLS with triad, two-three AC (Fig. 69E).

Male (paratype, SMF): Total length 1.99. Prosoma: 0.89 long, 0.77 wide. Legs: dorsal proximal macroseta on tibia I, II, III and IV of the paratype 2.41, 2.59, 3.18 and 2.50 times diameter of tibia, respectively; Tm I: 0.55.

Female: Unknown.

Distribution: Nepal, only known from the type locality.

Habitat: *Alnus*-forests along river.

JILINUS GEN. NOV.

Type species: *Oedothorax hulongensis* Zhu & Wen, 1980.

Derivatio nominis: This genus name derives from the Chinese province Jilin, where the holotype of *Jilinus hulongensis* was collected. Genus gender neutral.

Diagnosis:

Males: the embolus of his genus initiates from the distal suprategular apophysis with no membranous connection, i.e. the column is absent, which distinguishes this genus from all other erigonines.

Females: The epigyne of this genus has a particularly large chamber at each copulatory opening.

Species included: ***Jilinus hulongensis*** (Zhu & Wen, 1980) **comb. nov.**

Phylogenetic justification: In the phylogeny (Fig. 2), *J. hulongensis* appears sister to Clade 9, in a relatively basal position and not closely related to *Oedothorax*, *Callitrichia*, *Mitrager* or other taxa in Clade 13. Several palpal features indicate that this species does not share the synapomorphies with *Oedothorax* s.s.: embolus directly connected to distal suprategular apophysis without membranous region in between; anterior radical process broad and blunt; marginal suprategular apophysis absent; morphology of palpal tibial retrolateral apophysis and palpal tibial prolateral apophysis. The distinctiveness of this combination of features and its phylogenetic placement does not support transferring this species to any other known erigonine genera either. Therefore, we propose the erection of *Jilinus* gen. nov. for this species.

***JILINUS HULONGENSIS* (ZHU & WEN, 1980) COMB. NOV.**

(FIGS 67A, 68A, 70; SUPPORTING INFORMATION, FIG. S5C)

Oedothorax hulongensis Zhu & Wen, 1980: 21, fig. 4A–E (Dmf).

Oedothorax hulongensis Hu, 1984: 197, fig. 207.1–5 (mf).

Oedothorax hulongensis Zhu & Shi, 1985: 118, fig. 103a–d (f).

Oedothorax hulongensis Song, 1987: 154, fig. 115 (mf).

Oedothorax hulongensis Zhang, 1987: 131, fig. 109.1–4 (mf).

Oedothorax hulongensis Chen & Zhang, 1991: 180, fig. 177.1–4 (mf).

Oedothorax hulongensis Zhao, 1993: 192, fig. 87a, b (f).
Oedothorax hulongensis Song *et al.*, 1999: 199, fig. 113I–K (mf).

Oedothorax hulongensis Song *et al.*, 2001: 154, fig. 88A–D (mf).

Oedothorax hulongensis Zhu & Zhang, 2011: 147, fig. 97A–D (mf).

Oedothorax hulongensis Seo, 2011: 35, fig. 1–10 (mf).

Type material: Holotype: **China:** Jilin Province, Hulong Xian, riverbank, under pebbles, 1♀ 13.v.1971 (71–226, not examined). Allotype: 1♂, same location and date as holotype, not examined. Paratypes: 52♀, same location and date as holotype, not examined; Jilin Province, Huaide County, 2♀ 27.v.1972 (72–393, not examined); Liaoning Province, Chaoyang County, at riverside, 4♂89♀ 26.iii.1979 (79-2, not examined). Deposited in the Department of Cellular Biology, Norman Bethune University of Medical Science, Changchun, China.

Examined material: **China:** Hunan, 2♂2♀1985, det. Li Shuqiang (IZCAS-Ar. 417); Liaoning, Shuoyang, 1♂1♀ 9.v.1983, det. Li Shuqiang (IZCAS-Ar. 389); Hunan, 1♀ v.1985, det. Gao Jiuchun & Li Shuqiang (IZCAS-Ar. 385) (Institute of Zoology, Chinese Academy of Sciences Collection).

Unexamined literature records, South Korea: Jeollabuk-do, Mt. Naejang, 1♂1♀ 22.v.2004, leg. T. J. Kweon (Seo, 2011).

Description:

Male (IZCAS-Ar. 389): Total length: 1.90. Prosoma: 0.88 long, 0.71 wide, unmodified. Eyes: AME-AME: 0.03, AME width: 0.05, AME-ALE: 0.02, ALE width: 0.08, ALE-PLE: 0, PLE width: 0.07, PLE-PME: 0.03, PME width: 0.07, PME-PME: 0.05. Clypeus: not hirsute, one sub-AME seta. Sternum: 0.51 long, 0.52 wide. Chelicerae: mastidia absent; stridulatory striae rows widely and evenly spaced (Fig. 67A). Legs: tibia chaetotaxy 2-2-1-1, dorsal proximal macroseta on tibia I and II 1.34 and 1.41 times diameter of tibia, respectively; Tm I: 0.50. All metatarsi with trichobothrium. Pedipalp: PC median-sized, distal setae close to distal clasp, distal clasp extended distally (Fig. 70A); T without papillae; PT with long papillae; TS absent (Fig. 70D); MSA absent; DSA present; EM absent; E arising from distal part of DSA; TP small round; ARP retrolateral to DSA, broad, with small protuberances below tip (Fig. 70B). Opisthosoma: evenly coloured, grey (Fig. 68A). PMS with mAP, two AC; PLS with triad, 3+ AC (Fig. 70H).

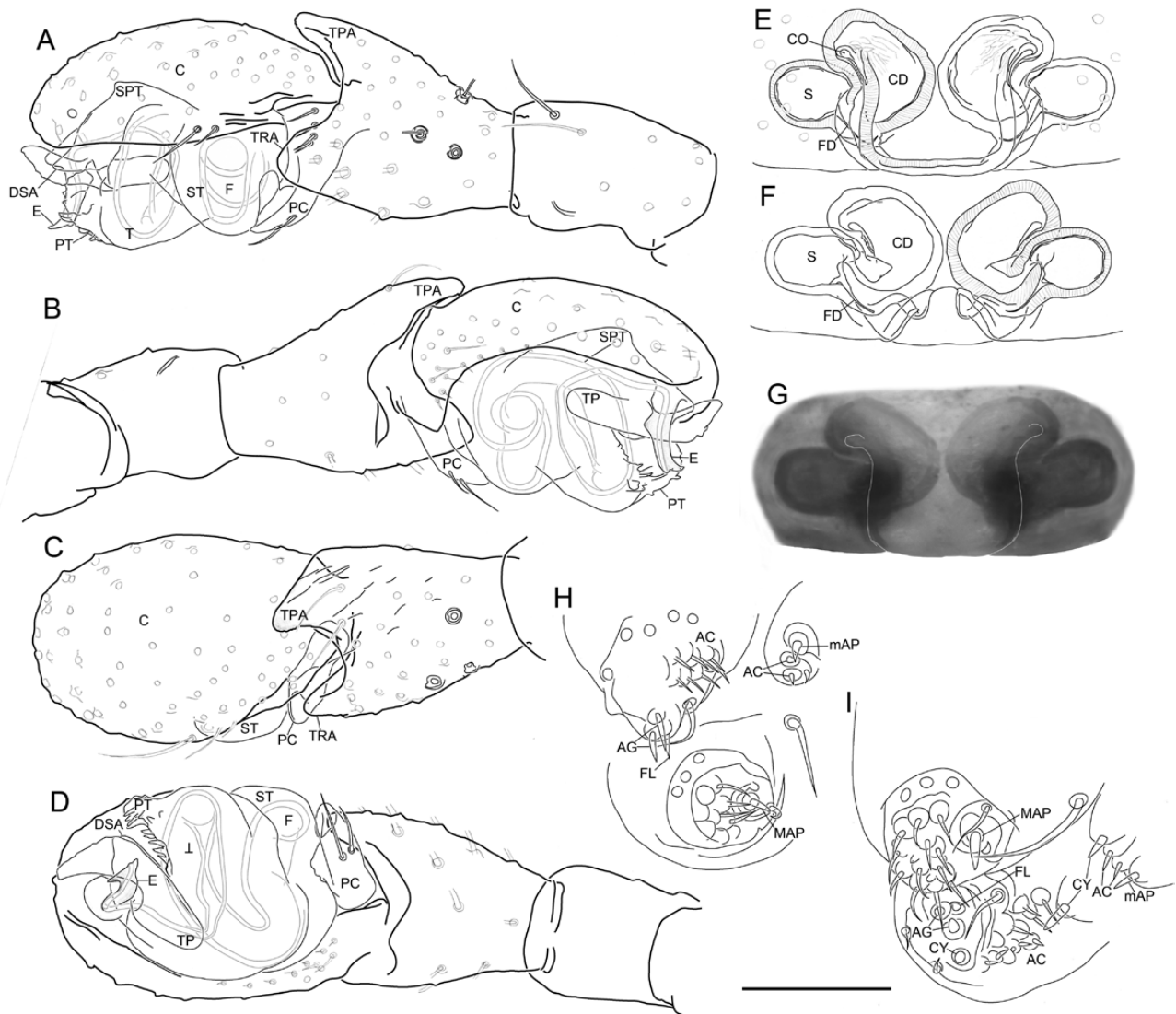


Figure 70. *Jilinus hulongensis* (Zhu & Wen, 1980). A–D, male left palp. A, retrolateral view. B, prolateral view. C, dorsal view. D, ventral view. E–G, epigyne. E, ventral view. F, dorsal view. G, external morphology. H, male left spinnerets. I, female right spinnerets. Scale bar 0.1 mm.

Female (IZCAS-Ar. 389): Total length: 2.46. Prosoma: 0.98 long, 0.76 wide. Eyes: AME-AME: 0.03, AME width: 0.06, AME-ALE: 0.02, ALE width: 0.08, ALE-PLE: 0, PLE width: 0.08, PLE-PME: 0.04, PME width: 0.08, PME-PME: 0.05. Clypeus: not hirsute, one sub-AME seta. Sternum: 0.57 long; 0.59 wide. Legs: tibia chaetotaxy 2-2-1-1, dorsal proximal macroseta on tibia I, II, III and IV 1.68, 1.69, 1.88 and 2.10 times diameter of tibia, respectively; Tm I: 0.55. Epigyne: similar to *Oedothorax*; borders between dorsal and ventral plates parallel; CO with large chambers (Fig. 70E–G). Opisthosoma: evenly coloured, grey; PMS with mAP, two AC, one CY; PLS with triad, two CY, 3+ AC (Fig. 70I).

Variation: The measurements are based on examined material.

Males (N = 6, means in parentheses): Total length 1.66–1.94 (1.79). Prosoma: 0.79–0.93 (0.85) long, 0.64–0.76 (0.69) wide. Legs: dorsal proximal macroseta on tibia I, II, III and IV 1.34–1.62 (1.46, N = 5), 1.36–1.53 (1.46, N = 5), 1.39–1.94 (1.60) and 1.52–1.75 (1.59, N = 4) times diameter of tibia, respectively; Tm I: 0.50–0.56 (0.54).

Females (N = 5, means in parentheses): Total length 2.17–1.70 (2.38). Prosoma: 0.91–1.07 (0.99) long, 0.72–0.82 (0.77) wide. Legs: dorsal proximal macroseta on

tibia I, II, III and IV 1.47–1.73 (1.60), 1.58–1.78 (1.68), 1.56–1.88 (1.68) and 1.46–2.10 (1.75) times diameter of tibia, respectively; Tm I: 0.51–0.58 (0.54).

Distribution: Russia, China, Korea.

Habitat: Riversides.

NEW COMBINATIONS

UMMELIATA ESYUNINI (ZHANG *ET AL.*, 2003) **COMB. NOV.**

(FIGS 7L, 67M, 68M, 71)

Oedothorax esyunini Zhang *et al.*, 2003: 408, fig. 2A–D (Dm).

Ummeliata xiaowutai Han & Zhang, 2014: 1, figs 1–12 (Dmf), *synon. nov.*

Type material: Oedothorax esyunini: Holotype: **China:** Hebei Province, Pingshan County, Tuoliang, 1300–1600 m (38°70' N, 113°80' E), ♂ 2.vi.1999, coll. Fengcai Zhang (Hebei University, College of life science, not examined). Paratype: Same data as holotype, 1♂ (Hebei University, College of life science, examined). *Ummeliata xiaowutai:* Holotype: **China:** Hebei Province: Yuxian County, Xiaowutai Mountains, Shanjiankou Forest Station (39°34' N, 114°53' E), 1700–2000 m, 1♂, 19.vii.2012 (not examined). Paratype: 3♀ (same data as holotype) (Museum of Hebei University, Baoding, China, not examined).

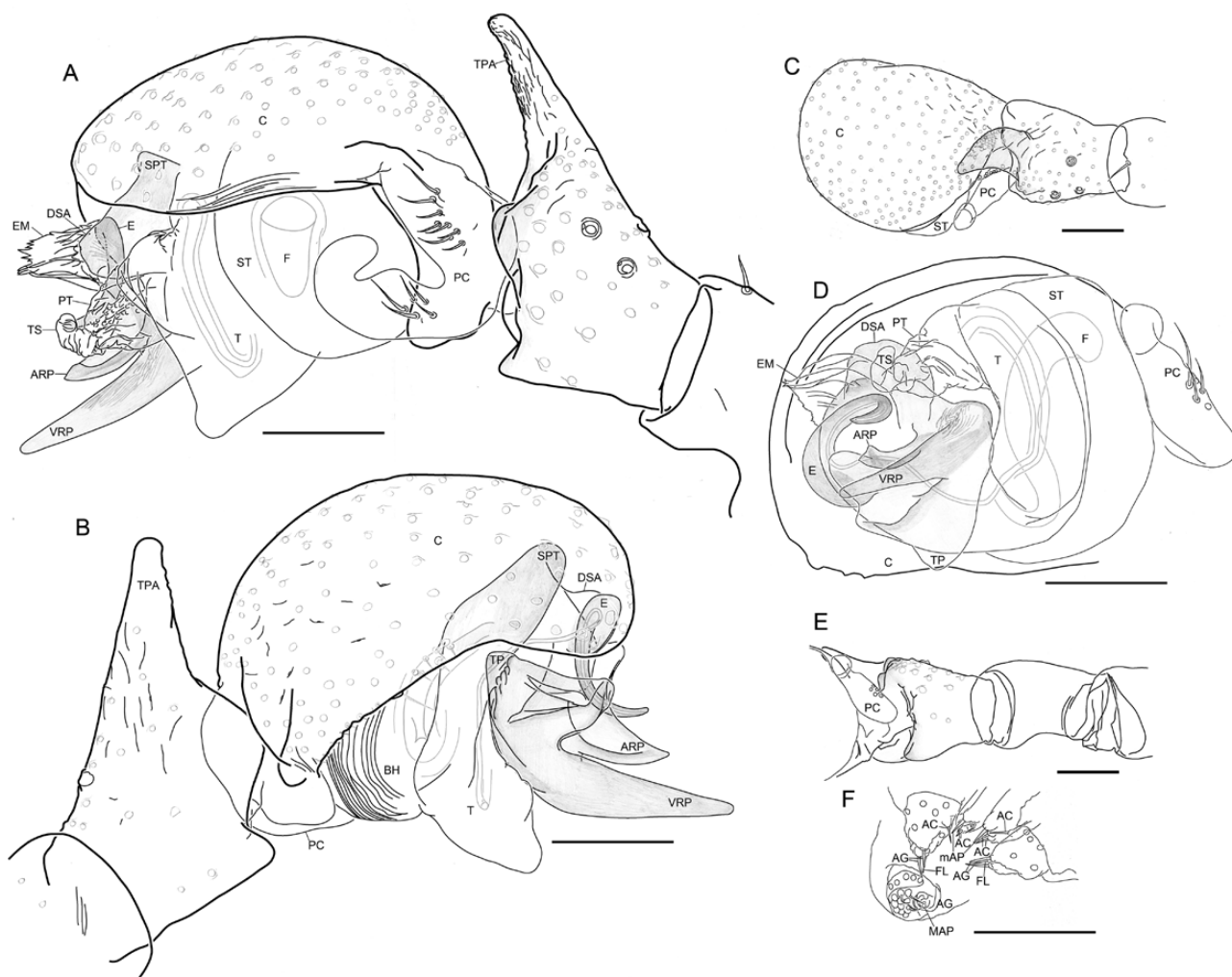


Figure 71. *Ummeliata esyunini* (Zhang *et al.*, 2003). A–E, male left palp. A, retrolateral view. B, ventroretrolateral view. C, ventral view. D, dorsal view. E, patella and tibia, ventral view. F, male spinnerets. Scale bars 0.1 mm.

Diagnosis:

Males: This species can be distinguished from all *Ummeliata* species, except *U. saitoi* Matsuda & Ono, 2001 and *U. osakaensis* (Oi, 1960), by the long palpal tibia prolateral apophysis and the configuration of the embolic division. This species can be further distinguished from the latter two species by its thin, longer and spiralling embolus (shorter, less spiral and basal part thick in the latter two) and the longer ventral radical process exceeding the apex of cymbium in lateral view.

Females: Can be distinguished from all *Ummeliata* species, except *U. saitoi*, *U. osakaensis* and *U. onoi* Saito, 1993, by the shorter copulatory ducts; can be distinguished from *U. onoi* by the depression at the area of copulatory opening; can be distinguished from *U. saitoi* by its straight margin of epigynal ventral plate over the depressed region of copulatory openings (W-shaped in *U. saitoi*; see fig. 330 in Ono et al., 2009). Comparison between *U. osakaensis* and this species requires further inspection of specimens of both species, which is beyond the scope of the current study.

Description:

Male (paratype): Total length: 2.66. Prosoma: 1.31 long, 1.03 wide, post-ocular region elevated, with non-hirsute transverse groove and relatively light-coloured hump posteriorly (Fig. 7L). Eyes: AME-AME: 0.04, AME width: 0.06, AME-ALE: 0.06, ALE width: 0.08, ALE-PLE: 0.01, PLE width: 0.07, PLE-PME: 0.08, PME width: 0.06, PME-PME: 0.08. Clypeus: not hirsute, one sub-AME seta. Sternum: 0.78 long, 0.71 wide. Chelicerae: mastidia present; stridulatory striae scaly, rows widely and evenly distributed (Fig. 67M). Legs: tibia chaetotaxy 2-2-1-1; Tm I: 0.73. All metatarsi with trichobothrium. Pedipalp: patella prolateral proximal vertical macrosetae absent; tibia with one prolateral, two retrolateral trichobothria; TPS absent; TPA long, dorsoapically extended, apical side scaly; TRA absent (Fig. 71D); PC large, base visible from dorsal view, distal setae close to distal clasp, distal clasp without striae, extended apically (Fig. 71A); T without papillae; PT with short papillae; TS long, without papillae; MSA absent; DSA present; EM flat, anterior margin with long papillae, exceeds ARP (Fig. 71A); ARP flat, slightly sclerotized; VRP long and wide, surface between VRP and ARP scaly; LER absent; TP short; E retrolaterally spiral (Fig. 71B). Opisthosoma: evenly coloured dark brown (Fig. 68M); PMS with mAP, two AC; PLS with triad, one AC (Fig. 71F).

Female: See: Han & Zhang (2014).

Distribution: China: Hebei.

Remarks: The detailed images of the male prosoma and palps of *Oedothorax esyunini* (Zhang et al., 2003) and *Ummeliata xiaowutai* (Han & Zhang, 2014), and our additional observations of the paratype of *Oe. esyunini* (Fig. 71), allow a clear determination of these species as the same. Furthermore, our phylogenetic analysis places *Oe. esyunini* as sister to *U. insecticeps*, further supporting our synonymy proposal. Since the specific epithet *esyunini* has priority over *xiaowutai*, we propose the new combination *Ummeliata esyunini*.

HYBAUCHENIDIUM MONGOLENSIS (HEIMER, 1987)
RESURRECTED COMBINATION

Hybauchenidium mongolensis Heimer, 1987: 144, figs 12–17 (Dmf).

Oedothorax mongolensis Marusik et al., 1993: 74 (Tmf from *Hybauchenidium*).

Type material: Holotype: **Mongolia:** Charchiraa Uul, forest steppe, Barber pitfall trap, ♂ 24.vii.–13.viii.1977 (not examined). Paratypes: 2♂6♀, same data as holotype (not examined).

Non-type material: 15♂17♀, same data as holotype; Ich Bogd, Barber pitfall trap, 5♂22♀ 1–21.vii.1979 (not examined). Heimer (1987) stated that all described type and non-type specimens from this species were deposited in the zoological collection at Martin-Luther-University Halle-Wittenberg. According to personal communication with the curator (Karla Schneider, 2019), these specimens are not deposited in this collection.

Diagnosis:

Males: This species can be distinguished from *Oedothorax s.s.* by the shape of paracymbium, which has an extension below the distal clasp, and the elevated clypeus, which is not elevated in *Oedothorax s.s.*, or in *Hybauchenidium cymbadentatum* (Crosby & Bishop, 1935); it can be further distinguished from other congeners by the short embolus and the shape of the palpal tibial apophysis.

Females: Can probably be distinguished from congeners by the detailed epigyne morphology, which has not been reviewed previously and is beyond the scope of the current study.

Distribution: Mongolia.

Habitat: Forest steppes.

Taxonomic remarks: In the original description of this species, Heimer (1987) stated that this species is closely related to the North-Siberian species *Hybauchenidium aquilonare* (Koch, 1879), considering the morphology of their embolic division. It is similar to *H. aquilonare* in the ventro-apically protruded protegulum and the shape of palpal tibial apophysis. The prosomal modification, with a post-ocular hump and lateral sulci and pits, are also in agreement with its congeners. Given these morphological similarities, the geographical closeness of Mongolia to Siberia and provided that no actual formal taxonomic justification has been stated for the transfer of *H. mongolensis* to *Oedothorax*, we transfer this species back to its original genus.

HALORATES ALASCENSIS (BANKS, 1900)

Gongylidium alascensis Banks, 1900: 479, pl. 29, fig. 3 (Dmf).

Oedothorax alascensis Crosby, 1905: 310.

Halorates alascensis Buckle et al., 2001: 122.

Halorates alascensis Paquin & Dupérré, 2003: 109, figs 1099–1101 (mf).

Type material: **USA:** Alaska, City and Borough of Wrangell, Berg Bay (56°36' N, 132°00'70" W), three individuals (gender not specified in Banks, 1900) (National Museum of Natural History (NMNH), not examined).

Diagnosis:

Males: This species can be identified by the thick, distally pointed, distal-retrolaterally oriented palpal tibial apophysis, and the slender, long radical process on the ventral side of the copulatory bulb (figs 1099, 1100 in Paquin & Dupérré, 2003).

Females: Can be distinguished from congeners by the more posteriorly extended parts of the epigyne lateral to the copulatory openings (fig. 1101 in Paquin & Dupérré, 2003).

Distribution: Alaska.

Remarks: Buckle et al. (2001) examined the types of *Oedothorax alascensis* in NMNH and found them identical with *Collinsia clypiella* (Chamberlin, 1920) and *Collinsia stylifera* (Chamberlin, 1949). The synonymization of *Collinsia* and *Halorates* was proposed by Millidge (1977) based on similarities in their palpal structure, but it was rejected by Eskov (1990) based on differences in their chaetotaxy and palpal features. Buckle et al. (2001), however, found that the differences cited by Eskov (1990) did not hold for the type species of these two genera, and that the

difference in chaetotaxy was not greater than found within a number of currently accepted genera. Based on these reasons, Buckle et al. (2001) accepted *Collinsia* as a junior synonym of *Halorates*. In addition, based on the synapomorphies proposed for the re-delimited *Oedothorax* in the present study, and the differences in the pedipalp of *Oedothorax alascensis* depicted in figure 3 in Banks (1900), this species does seemingly not belong to *Oedothorax*. Therefore, we accept the transfer of this species to *Halorates* by Buckle et al. (2001).

GONGYLIDIOIDES INSULANUS (PAIK, 1980) COMB. NOV.

Oedothorax insulanus Paik, 1980: 162, figs 9–21 (Df).

Oedothorax insulanus Namkung, 2002: 205, fig. 17.57A–b (f).

Oedothorax insulanus Namkung, 2003: 207, fig. 17.57A–b (f).

Gongylidioides kouqianensis Tu & Li, 2006: 59, fig. 5A–G (Dm), *synon. nov.*

Oedothorax insulanus Seo, 2011: 37, figs 11–16 (f, Dm).

Type material: *Oedothorax insulanus*: Holotype: **South Korea:** Jeonlanam-Do So Heuksan-do Island, Hang-ri, ♀ 27.vii.1979, coll. S. R. Son (not examined). Paratype: **South Korea:** So Heuksan-do Isl, Hang-ri, 2♀ 27.vii.1979, coll. S. R. Son (not examined); same location, 1♀ 27.vii.1979, coll. T. H. Jo (not examined). *Gongylidioides kouqianensis*: Holotype and paratype: **China:** Jilin Province, Kouqian County, 2♂ 29.vi.1989, Institute of Zoology, Chinese Academy of Sciences in Beijing, China (Tu and Li, 2006; not examined).

Non-type material: *Gongylidioides kouqianensis*: Gyeongsangbuk-do, Ulreung-gun, Hyeonpo, 10♂4♀ 24.viii.2006, coll. S. Y. Kim, collection of Department of Biology, Keimyung University (Seo, 2011; not examined).

Diagnosis:

Males: This species can be recognized among congeners by the combination of the following features: the lack of prominent prosomal modification; the broad, apically pointed palpal tibial retrolateral apophysis without a tooth on the inner surface; lamella characteristic extal tip horn-like, with two projections, inner one triangular in ventral view, dorsal one blunt (fig. 5F in Tu & Li, 2006).

Females: Can be diagnosed by the half-octagon-shaped dorsal plate of the epigyne (figs 16, 17 in Paik, 1980).

Distribution: South Korea; China, Jilin province.

Remarks: Tu & Li (2006) and Seo (2011) have provided informative drawings of three perspectives of the male palps of *Gongylidioides kouqianensis* and *Oe. insulanus*, respectively, and their resemblance strongly suggests that these two species are identical. Since *Oe. insulanus* was published earlier, it has priority over *Gongylidioides kouqianensis*. The palpal and epigynal morphology of *Gongylidioides insulanus* is in accordance with the generic description of *Gongylidioides* in Tu & Li (2006), and supports the placement of this species in *Gongylidioides*.

SOULGAS CORTICARIUS (EMERTON, 1909)

(FIG. 72)

Tmeticus corticarius Emerton, 1909: 194, pl. 4, fig. 4 (Dmf)

Gongylidium corticarius Banks, 1910: 29

Oedothorax corticarius Crosby & Bishop, 1928: 1050

Oedothorax seminolus Ivie & Barrows, 1935: 8, pl. 2, fig. 15 [Dm; NB: considered a junior synonym of *Soulgas corticarius* (Emerton, 1909) by Buckle *et al.*, 2001: 143] confirmed synonymy.

Soulgas corticarius Crosby & Bishop, 1936: 55, pl. 4, figs 8–10 (mf)

Soulgas corticarius Kaston, 1948: 208, figs 652, 665, 666 (mf)

Soulgas corticarius Shear, 1967: 7, figs 14, 15 (m)

Soulgas corticarius Buckle *et al.*, 2001: 143

Soulgas corticarius Paquin & Dupérré, 2003: 121, figs 1262–1264 (mf)

Type material: *Oedothorax seminolus*: Holotype: Gainesville, Florida, Gainesville (29°40' N, 82°18' W), ♂ 29.xii.1926, coll. W. M. Barrows (AMNH, examined).

Diagnosis:

Males: This species can be identified by the lack of prosomal modification, the short and wide palpal tibia,

and its long, broad, retrolaterally curved, distally rounded and incurved prolateral apophysis, and the embolic division with a direct continuation of the radix and embolus.

Females: Can be identified by the epigyne with a large, convex ventral plate and a deeply and widely emarginated dorsal plate (fig. 10 in Crosby & Bishop, 1936).

Remarks: After examining the type material of *Oedothorax seminolus* (Fig. 72) and comparing it to the descriptions of *Solugas corticarius* by Emerton (1909) and Crosby & Bishop (1936), we support the decision of Buckle *et al.* (2001) that the former is a junior synonym of the latter. Palpal features, such as the lack of membranous connection between radix and embolus, and the shape and position of the embolic membrane, indicate that this species does not belong to *Oedothorax* as delimited in the present study.

TMETICUS BREVIPALPUS BANKS, 1901

Tmeticus brevipalpus Banks, 1901: 580, pl. 33, fig. 14 (Dm).

Gongylidium brevipalpus Banks, 1910: 29.

Oedothorax brevipalpus Petrunkevitch, 1911: 261.

Oedothorax brevipalpus Roewer, 1942: 645 (unnecessary replacement name; see discussion in Buckle *et al.*, 2001: 134).

Type material: No type designated by Banks, 1901.

Diagnosis:

Males: The only reference for discerning this species is figure 14 in plate 33 in Banks (1901), which gives a rough image of its palpal tibial apophyses and the shape of the copulatory bulb, in which the

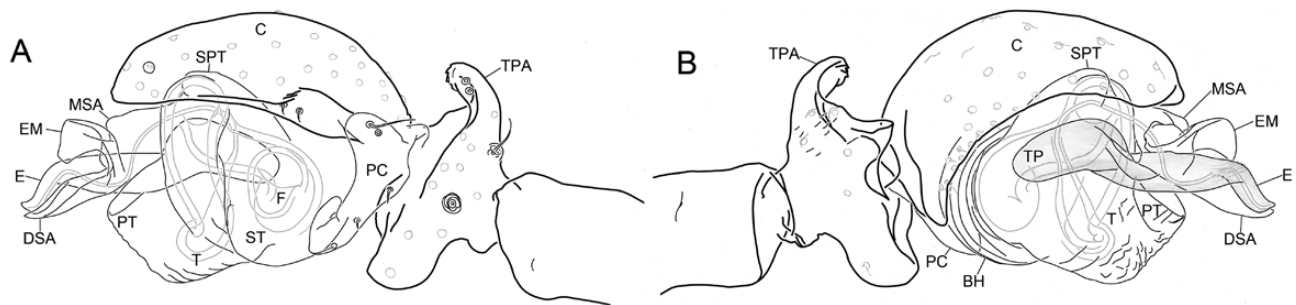


Figure 72. *Soulgas corticarius* (Emerton, 1909). A, B, male left palp. A, retrolateral view. B, prolateral view. Scale bar 0.1 mm.

complete structure of the embolic division cannot be recognized. Nevertheless, it shows no embolic division typical of *Oedothorax* and related taxa (Clade 13). In the latter taxa, the embolus has a membranous connection to a radix with an anterior radical process and a tailpiece.

Females: Unknown.

Distribution: USA, New Hampshire.

Remarks: According to the palpal structure shown in [Banks \(1901\)](#), this species does not belong to *Oedothorax* s.s.. Therefore, we propose its transfer back to *Tmeticus*, the genus to which this species was originally assigned. Its taxonomic position within Erigoninae remains unknown.

TMETICUS MAXIMUS EMERTON, 1882

Tmeticus maximus [Emerton, 1882](#): 55, pl. 16, fig. 5 (Dm).

Gongylidium maximum [Simon, 1884](#): 500.

Erigone maxima [Marx, 1890](#): 534.

Oedothorax maximu [Crosby, 1905](#): 311.

Unexamined material: **USA**: New Hampshire, Mt. Washington, half way up, in moss, 1♂ ([Emerton 1882](#)). No type was designated.

Diagnosis:

Males: This species is characterized by the large body size (nearly 3 mm long), the presence of cheliceral mastidia and the palpal morphology, including the short, rough-ended tibial apophysis and the bifurcated paracymbium tip. According to figure 5 in plate 16 in [Emerton \(1882\)](#), this species seems not to have the pointed, prolaterally spiral anterior radical process similar to *Oedothorax*, and the curvature of the embolus does not resemble that of *Oedothorax*, either. *Females*: Unknown.

Distribution: USA: Mt. Washington.

Remarks: One drawing of a male pedipalp in retrolateral view was provided in [Emerton \(1882\)](#), which shows a bifurcated tip of the paracymbium and the curvature of the embolus, both features significantly different from *Oedothorax* s.s.. We thus propose its transfer back to its original combination until further investigation is conducted. Due to the unavailability of specimens and the limited information from the original description, the relationship of this species to other erigonines remains unclear.

NERIENE FUEGIANA SIMON, 1902

Neriene fuegiana [Simon, 1902](#): 17 (Df).

Oedothorax fuegianus [Petrunkevitch, 1911](#): 262.

Oedothorax fuegianus [Miller, 2007](#): 244, fig. 186C (f, misplaced in this genus).

Neriene fuegiana [Dupérré & Harms, 2018](#): 4, fig. 4A–C (f).

Type material: Lectotype ♀ designated by [Dupérré & Harms \(2018\)](#) (Zoological Museum of Hamburg, ZMH-A0000758, not examined).

Non-Type material: **Argentina**: South Tierra del Fuego, coastline right southwest of Kap San Pio (54°15' S, 68°0' W), ♀ 'holotype' 27.xii.92, coll. Mich ([Simon, 1902](#); [Miller, 2007](#)) (not examined).

Diagnosis:

Females: This species can be identified by the epigynal morphology, with a triangular protrusion of the ventral plate in the middle over the dorsal plate (fig. 186C in [Miller, 2007](#)).

Males: Unknown.

Distribution: Chile, Argentina.

Remarks: The two epigyne drawing in [Simon \(1902\)](#) and figure 4A–C in [Dupérré & Harms \(2018\)](#) show an epigyne morphology different from that of *Oe. gibbosus* and its congeners, strongly suggesting, as also stated by [Miller \(2007\)](#), that this species is misplaced in *Oedothorax*. We thus propose its transfer back to its original combination until further investigation is conducted.

NASOONA NIGROMACULATUS GAO ET AL., 1996

Nasoona nigromaculata [Gao et al., 1996](#): 29, figs 1–5 (Dmf).

Nasoona nigromaculata [Song et al., 1999](#): 188, fig. 107D–G (mf).

Oedothorax nigromaculatus [Tanasevitch, 2018](#): 99 (transferred from *Nasoona*).

Type material: Holotype: **China**: Zhejiang Province, Mt. Putuo (30°00' N, 112°40' E), under rock, ♀ 21.viii.1992 (not examined). Paratypes: collected together with holotype, 3♂2♀ (not examined); Anhui Province, Mt. Huangshan (30°00' N, 118°10' E), 1♀ 14.viii.1992 (not examined). Deposited in the Department of Cellular Biology, Norman Bethune University of Medical Science, Changchun, China.

Diagnosis:

Males: This species can probably be identified by referring to palpal drawings in figures 1–3 in Gao *et al.* (1996), which give the outlines of the palpal tibial apophysis from three views, and a rough impression of the embolic division: it seems to have a radical tailpiece and two anterior protrusions round at the tips, one of which probably represents the embolus. Although it can not be determined which protrusion is the embolus, it is definitely not prolaterally spiral as in *Oedothorax*, and the anterior radical process, when present, is not pointed at tip. These features distinguish this species from *Oedothorax*.

Females: The only reference for identification of the females are figures 4 and 5 in Gao *et al.* (1996), which show a ventral view roughly similar to that of *Oedothorax*, but Gao depicted two stripe-like structures on both sides of the spermathecae in figure 5, which distinguishes this species from all other species examined in the current study.

Distribution: China: Zhejiang and Anhui Provinces.

Habitat: Under stones.

Remarks: Tanasevitch (2018) reasoned the transfer of this species from *Nasoona* to *Oedothorax* by stating ‘despite the poorly drawn genitals, it is obvious that the species actually belongs to *Oedothorax*’. In the light of our phylogenetic analysis, the newly delimited *Oedothorax* has a pointed anterior radical process spiral prolaterally with the embolus, and does not have the ventral-radical process-like structure in figures 1 and 2 in Gao *et al.* (1996). Due to these differences, this species presumably does not belong to *Oedothorax*. In addition, the types are lost (see remarks for ‘*Oe. collinus*’), so the relationship of this species to other taxa is unverifiable. We thus propose its transfer back to its original combination until further investigation is conducted.

ATYPENA FORMOSANA (OI, 1977)

(FIGS 7H, 67I, 68I, 73)

Callitrichia formosana Oi, 1977: 23, figs 1–5 (Dmf).

Oedothorax formosanus Brignoli, 1983: 349.

Callitrichia formosana Song, 1987: 144, fig. 104 (Tmf from *Oedothorax*).

Atypena formosana Tazoe, 1992: 212, figs 1–10 (mf); NB: generic placement following Jocqué, 1983).

Oedothorax formosanus Okuma *et al.*, 1993: 13, fig. 11A–B (f).

Atypena formosana Barrion & Litsinger, 1994: 319, figs 1673–1676 (mf).

Callitrichia formosana Song *et al.*, 1999: 160, fig. 88K–L (mf).

Callitrichia formosana Ono *et al.*, 2009: 267, figs 95–99 (mf).

Examined material: **Japan:** Okinawa, Iromotejima Island, Urauchi, 2♂3♀ 02.iv.1995, leg. A. Tanikawa, det. A. Tanasevitch (SMF 56485).

Diagnosis:

Males: This species can be distinguished from *A. cirrifrons* by the proportionally shorter distal supratregular apophysis and ventral radical process.

Females: No study of *Atypena* comparative female morphology exists to date; such diagnosis is, therefore, beyond the scope of the current study.

Description:

Male (SMF): Total length: 1.76. Prosoma: 0.78 long, 0.62 wide, PME region largely elevated, interocular region with translucent setae laterally curved (Fig. 7H). Eyes: AME–AME: 0.03, AME width: 0.06, AME–ALE: 0.05, ALE width: 0.08, ALE–PLE: 0.01, PLE width: 0.08, PLE–PME: 0.14, PME width: 0.07, PME–PME: 0.17. Clypeus: upper-half hirsute, one sub-AME seta. Sternum: 0.46 long, 0.46 wide. Chelicerae: mastidia absent; stridulatory striae imbricated, rows compressed proximally (Fig. 67I). Legs: tibia chaetotaxy 2-2-1-1, dorsal proximal macroseta on tibia I, II, III and IV 0.65, 0.82, 1.45 and 1.87 times diameter of tibia, respectively; Tm I: 0.78. All metatarsi with trichobothrium. Pedipalp: patella prolateral proximal vertical macrosetae absent; tibia with one prolateral, two retrolateral trichobothria; TPA short, pointed and sclerotized at tip; PC base not visible from dorsal view, distal setae close to distal clasp, terminal part slightly enlarged, distal clasp without striae, clasp extended apically (Fig. 73A); T without papillae; PT small, without papillae; TS long and slender, without papillae (Fig. 73D); MSA absent; DSA wide, truncated at tip, ventral corner more extended than dorsal corner (Fig. 73A); EM broad and flat, without papillae, exceeding ARP; ARP flat, unsclerotized; LER retrolateral to E; VRP long, slender; R without papillae; TP long, slender; E short and stout, slightly retrolaterally curved (Fig. 73B). Opisthosoma: dorsal pattern see Fig. 68I; PMS with mAP, three AC; PLS with triad, 3+ AC.

Female (SMF): See also Oi (1977); epigyne without prominent external modification, copulatory ducts

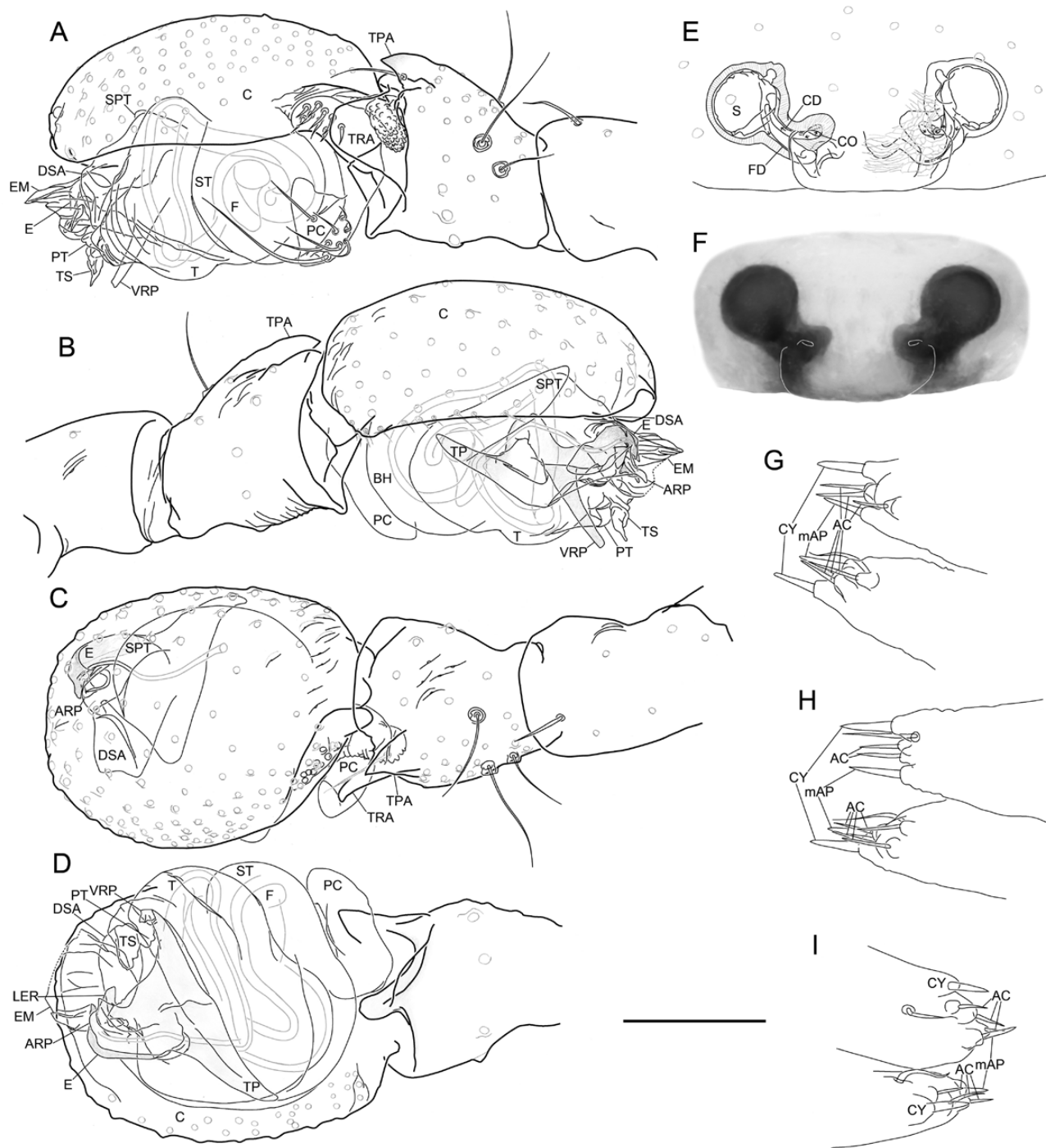


Figure 73. *Atypena formosana* (Oi, 1977). A–D, male left palp. A, retrolateral view. B, prolateral view. C, dorsal view. D, ventral view. E, apical view. E, F, epigyne. E, ventral view. F, external morphology. G, female spinnerets, first individual, dorsal view. H, female posterior median spinnerets, second individual, dorsal view. I, female posterior median spinnerets, first individual, ventral view. Scale bar 0.1 mm.

slightly curved, trojectory simple, entrances to spermathecae mesal to exits of fertilization ducts. (Fig. 73). Opisthosoma: dorsal pattern same as male; PMS with CY, mAP, 2–4 AC; PLS with triad, 2 CY, 3+ AC (Fig. 73).

Distribution: Bangladesh to Japan.

Remarks: As in *A. cirrifrons*, a scaly sac-like structure is observed at the paracymbial base (Figs 73A, C, 74A, C). According to the results of our phylogenetic analysis, and the similarities in male genital organs and prosomal modifications, this species is congeneric with *A. cirrifrons*.

ADDITIONAL MORPHOLOGICAL DATA

ATYPENA CIRRIFRONS (HEIMER, 1984)

(FIGS 7G, 67H, 68H, 74)

Paranasoona cirrifrons Heimer, 1984: 87, figs 1–8 (Dmf).

Paranasoona cirrifrons Zhu & Sha, 1992: 42, figs 1–8 (mf).

Paranasoona cirrifrons Song *et al.*, 1999: 203, fig. 114N–Q (mf).

Atypena cirrifrons Tanasevitch, 2014b: 72 (Tmf from *Paranasoona* = *Atypena*).

Atypena cirrifrons Komisarenko *et al.*, 2019: 27, figs 1, 2 (m).

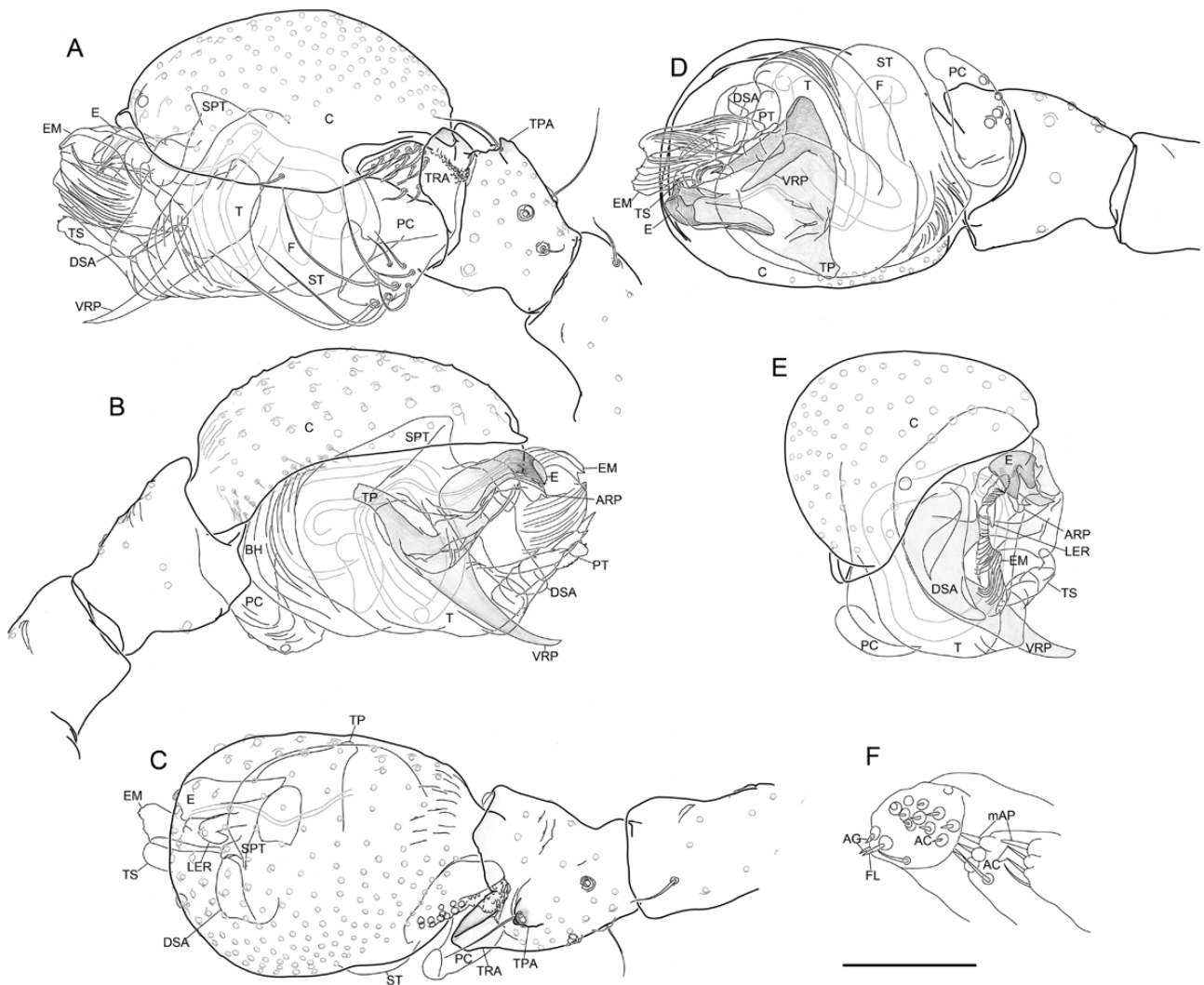


Figure 74. *Atypena cirrifrons* (Heimer, 1984). A–E, male right palp, images flipped horizontally. A, retrolateral view. B, prolateral view. C, dorsal view. D, ventral view. E, apical view. F, male right posterior lateral spinneret and posterior median spinnerets. Scale bar 0.1 mm.

Examined material: Laos: Champasak, Muang Bachiang, Pak Song (15°10.6' N, 106°14.253' E), plateau, pine forest, 1280 m, at day, sweepnet, 1♂ 27.ix.2009, coll. P. Jäger, det. A. V. Tanasevitch, 2014 (SMF 64983-124).

Diagnosis:

Males: According to available illustrations of *Atypena* species, they are all similar in regard to their prosomal and palpal morphology. According to our observation, this species can be distinguished from *A. formosana* by the proportionally longer distal suprategular apophysis and ventral radical process.

Females: No study of *Atypena* comparative female morphology exists to date; such diagnosis is, therefore, beyond the scope of the current study.

Description:

Male (SMF): Total length: 1.60. Prosoma: 0.73 long, 0.59 wide, PME region largely elevated, interocular region with translucent setae laterally curved (Fig. 7G). Eyes: AME-AME: 0.03, AME width: 0.06, AME-ALE: 0.03, ALE width: 0.07, ALE-PLE: 0.01, PLE width: 0.08, PLE-PME: 0.14, PME width: 0.07, PME-PME: 0.14. Clypeus: upper-half hirsute, one sub-AME seta. Sternum: 0.42 long, 0.43 wide. Chelicerae: mastidia absent; stridulatory striae imbricated, rows compressed proximally (Fig. 67H). Legs: tibia chaetotaxy 2-2-1-1, dorsal proximal macroseta on tibia I, II, III and IV 0.46, 0.64, 0.83 and 1.81 times diameter of tibia, respectively; Tm I: 0.79. All metatarsi with trichobothrium. Pedipalp: patella prolateral proximal vertical macrosetae absent; tibia with one prolateral, two retrolateral trichobothria; TPA short, pointed and sclerotized at tip; PC base not visible from dorsal view, distal setae close to distal clasp, terminal part slightly enlarged, distal clasp without striae, clasp extended apically (Fig. 74A); T without papillae; PT small, without papillae; TS long and slender, without papillae (Fig. 74A, C); MSA absent; DSA wide, truncated at tip, ventral corner more extended than dorsal corner (Fig. 74A); EM broad and flat, without papillae, exceeding ARP; ARP flat, unsclerotized; LER retrolateral to E; VRP long, slender; R without papillae; TP long, slender; E short and stout, slightly retrolaterally curved (Fig. 74B). Opisthosoma: dorsal pattern see Fig. 68H; PMS with mAP, three AC; PLS with triad, 3+ AC (Fig. 74F).

Distribution: India, China, Laos, Thailand, Vietnam.

'OEDOTHORAX' INCERTAE SEDIS

Oedothorax *annulatus* Wunderlich, 1974, *incertae sedis*.

Oedothorax annulatus Wunderlich, 1974: 185, figs 59–61 (Df)

Type material: Holotype: **East Nepal**, Jiri, 1800–2000 m, 1♀ i.1970, coll. J. Martens (SMF 28908, not examined).

Non-type material: 2♀, same data as holotype (SMF 28909, not examined).

Diagnosis:

Females: This species can be identified by the epigynal morphology, with spermathecae directly situated at the posterior margin of epigyne, and the copulatory ducts anterior to them (figs 60, 61 in Wunderlich, 1974).

Males: Unknown.

Distribution: Nepal.

Remarks: This species is only known by females. Given the relatively uniformity of the female internal genitalia and as also stated by Wunderlich (1974), the relationship of this species to other taxa could not be recognized before knowledge about the male occurs. The colour pattern of this species is different from that of *Oedothorax* s.s.. In addition, its distribution in Nepal is different from the Holarctic distribution of *Oedothorax* s.s.. Therefore, this species most likely does not belong to *Oedothorax* s.s..

'OEDOTHORAX' BANKSI STRAND, 1906 *INCERTAE SEDIS*
Gongylidium sp. Banks, 1900: 480.

Oedothorax banksi Strand, 1906: 445 (Df).

Type material: Bank's description (1900) was based on two females collected from Muir Glacier in 1899, but no type designation was mentioned.

Diagnosis:

Females: From original description in Banks (1900): 'the epigynum is an elliptical area with a nearly square cavity in posterior part; on middle of hind margin is a denticle projecting forward'. Although difficult to comprehend the structure solely based on this description, the presence of a cavity in the posterior part of the epigyne discriminates this species from all *Oedothorax*, *Mitrager*, *Callitrichia* species and their related genera, like *Gongylidium* and *Timeticus*.

Males: Unknown.

Distribution: USA, Alaska.

Habitat: Glacier.

Remarks: Due to the unavailability of type material and any images in the original descriptions of this species, the current status of this species is unclear.

‘*OEDOTHORAX*’ *BIANTU* ZHAO & LI, 2014 *INCERTAE
SEDIS*

Oedothorax biantu Zhao & Li, 2014: 36, figs 67A–F, 68A, B (Df).

Type material: Holotype: **China**, Yunnan: Menglun Town: Xishuangbanna Tropical Botanical Garden (21°54’38” N, 101°16’518” E), c. 627 m, bamboo plantation, fogging, ♀ 22.xi.2009 (not examined).

Diagnosis:

Females: This species differs from all *Oedothorax*, *Mitrager*, *Callitrichia* and their related genera by the tibial chaetotaxy (1-1-1-1), the knob on each side of ventral plate of the epigyne and the long slits on the ventral plate (figs 67A and 68A in Zhao & Li, 2014).

Males: Unknown.

Distribution: Known only from type locality.

Habitat: See collecting data of holotype.

Remarks: This species has tibial chaetotaxy 1-1-1-1, unlike the uniform pattern 2-2-1-1 among all other examined species in this study. The epigynal structure of this species is also prominently different from the simple composition in other *Oedothorax* species by having a knob on each side of the ventral plate and the long slits on the ventral plate of the epigyne. Therefore, this species does not belong to *Oedothorax*, and its relationship to other erigonines remains unknown.

‘*OEDOTHORAX*’ *BIFOVEATUS* TANASEVITCH, 2017
INCERTAE SEDIS

Oedothorax bifoveatus Tanasevitch, 2017a: 148, figs 31–34, 46–51 (Dmf).

Type material: Holotype: **Indonesia:** Java, Cibodas Botanical Garden, near Cipanas, c. 50 km east of Bogor, 1400 m, vegetational debris in montane *Lithocarpus* & *Castanopsis* forest, sifting; ♂ 3.–6.xi.1989, leg. D. Burckhardt, I. Löbl & D. Agosti (not examined). Paratypes: **Indonesia:** 2♂17♀, collected together with the holotype (not examined); Java, Gunung Gede-Pangrango National Park, near Cibodas (6°47’0” S, 107°01’0” E), 1450–1600 m, 1♂21♀ 4.–11.v.2005, leg. A. Schulz (not examined). **East Malaysia:** Borneo Island, Sabah, Tambunan

District, Crocker Range, near pass, 1550–1650 m, road Kota Kinabalu to Tambunan, *Lithocarpus* & *Castanopsis* forest, sifting dead wood, leaves and moss, 3♂1♀ 16.v.1987, leg. D. Burckhardt & I. Löbl (not examined).

Distribution: East Malaysia: Borneo Island; Indonesia: Java Island.

Diagnosis:

Males: This species can be identified by the shape of palpal tibia, which has a largely elevated margin on the dorsal side and a slender, setae-bearing retrolateral apophysis (fig. 49 in Tanasevitch, 2017a), and the curved shape of the radix [‘convector’ in Tanasevitch (2017a), fig. 50].

Females: Characterized by the presence of a large socket on each side of the dorsal plate of epigyne (fig. 51 in Tanasevitch, 2017a).

Habitat: Forest litter.

Remarks: Features in the male palpal configuration (e.g. paracymbium distal part massive, distal setae group distally situated; anterior radical process ending in several short, pointed processes; embolus retrolaterally spiral), as well as the epigyne (e.g. two large, rounded sockets on either side of the dorsal plate), differ significantly from *Oedothorax* s.s.. Furthermore, its Indomalayan distribution in contrast to the Holarctic distribution of *Oedothorax* also suggests that this species presumably does not belong to *Oedothorax* s.s..

‘*OEDOTHORAX*’ *CAPORIIACCOI* ROEWER, 1942 *INCERTAE
SEDIS*

Oedothorax dubius di Caporiacco, 1935: 171, pl. 1, fig. 23 (Dm; NB: preoccupied by *O. Pickard-Cambridge*, 1898, sub-*Lepthyphantes*).
Oedothorax caporiaccoi Roewer, 1942: 640 (replacement name).

Type material: No type designated.

Additional material, Mongolia: Takht-i-Suleiman, 2000 m, 1♂ 3.ix; 2♀, same locality, 5.ix (di Caporiacco, 1935) (not examined).

Diagnosis:

Males: No clear description of prosoma and palpal structures in di Caporiacco (1935).

Females: Unknown.

Distribution: Mongolia: Karakorum.

Remarks: In the description of [di Caporiacco \(1935\)](#), only one prosoma lateral view drawing was available (fig. 23 in pl. 1), not sufficient for determining its relationship with other taxa. Status unclear.

'*OEDOTHORAX*' *CASCADEUS* CHAMBERLIN, 1949
INCERTAE SEDIS

Oedothorax cascadeus [Chamberlin, 1949](#): 540, figs 77–78 (Df).

Type material: Paratype: **USA:** Idaho, Cascade, 1♀ 5.xii.1943, coll. Wilton Ivie (AMNH, not examined).

Diagnosis:

Females: This species can be recognized by the epigynal morphology: short distance between copulatory openings, triangular dorsal plate in ventral view, general appearance similar to that of *Oedothorax*.

Males: Unknown.

Remarks: The epigyne illustrated in the original description ([Chamberlin 1949](#): fig. 78) suggests a significantly elevated epigyne, not seen in any *Oedothorax* s.s. species. Taxonomic status unclear.

'*OEDOTHORAX*' *COLLINUS* MA & ZHU, 1991 INCERTAE
SEDIS

Oedothorax collinus [Ma & Zhu, 1991](#): 27, figs 1–9 (Dmf).

Oedothorax collinus [Song et al., 1999](#): 199, fig. 113F–G, N (mf).

Oedothorax collinus [Yin et al., 2012](#): 542, fig. 258a–e (mf).

Type material: Holotype: **China:** Hubei Province, Shennongjia Forestry District, Dayanwu, 1600 m, ♂ 23.vi.1986, leg. Jiuchun Gao (not examined); Allotype: ♀, same data (not examined). Paratype: 1♂4♀, same data (not examined); Hubei Province, Shennongjia Forestry District, Hongping, 1610m, 1♀ 1.viii.1986, leg. Jiuchun Gao (not examined). Deposited in the Department of Cellular Biology, Norman Bethune University of Medical Science, Changchun, China.

Non-type material: **China:** Hunan Province: Sangzhi County, Mt. Tianping, 1♀1♂ 18.vi.1981, leg. Tong Xin Wang; Shimen County, Mt. Huping, 2♂2♀ 3.viii.2002, leg. Tang Guo. Most of the specimens are deposited in animal specimens collection of Hunan Normal University, School of Life Science ([Yin et al. 2012](#)) (not examined).

Diagnosis:

Males: This species can be identified by the presence of a long, slender palpal tibial retrolateral apophysis and a shorter prolateral apophysis (figs 3–6 in [Ma & Zhu, 1991](#)), and the highly elevated post-ocular area with lateral pits (fig. 2 in [Ma & Zhu, 1991](#)).

Females: General epigynal morphology similar to that of *Oedothorax*, but the area anterior to the copulatory openings is elevated (fig. 8 in [Ma & Zhu, 1991](#)), which distinguishes it from all species examined in the current study.

Distribution: China: Hunan Province, Hubei Province.

Remarks: As inferred from the drawings of [Ma & Zhu \(1991\)](#) and [Yin et al. \(2012\)](#), this species has a long, slender palpal tibial retrolateral apophysis, an enlarged part of the cymbium above the paracymbial base, a bifurcated paracymbial tip and an embolic division extremely different from the newly delimited *Oedothorax* in the present study. We suspect that this species does not belong to *Oedothorax* s.s.. Since all specimens previously deposited in the Department of Cellular Biology, Norman Bethune University of Medical Science are lost (Shuqiang Li, Beijing, personal communication, 2017), and generic assignment based on the descriptions of this species alone is not feasible, the taxonomic state of this species remains dubious.

'*OEDOTHORAX*' *CRUCIFEROIDES* TANASEVITCH, 2020
INCERTAE SEDIS

Oedothorax cruciferoides [Tanasevitch, 2020a](#): 285, figs 1–3, 12–17 (Dm).

Type material: Holotype: **Nepal:** Ilam District, 5 km north of Sanishare, feet of Siwalik Mts, 270–300 m a.s.l., mixed *Shorea* forest, 3–5.iv.1988, leg. J. Martens & W. Schawaller (SMF, not examined).

Diagnosis:

Males: This species is characterized by the small, conical elevation between the post-ocular region, the dentiform tubercles on the palpal tibial prolateral apophysis, as well as by the morphology of the embolic division (see description in [Tanasevitch, 2020a](#)).

Females: Unknown.

Distribution: Only known from the type localities in Nepal.

Habitat: Broad-leaved forest.

Remarks: According to our re-delimitation of *Oedothorax* in the present study, this species does not belong to *Oedothorax*. Further comparison with more species to determine its taxonomic status is required. Therefore, we provisionally do not change its genus.

'*OEDOTHORAX*' *CUNUR* TANASEVITCH, 2015 *INCERTAE
SEDIS*
(FIGS 7E, 67F, 68F, 75)

Oedothorax cunur Tanasevitch, 2015: 383, figs 26–34 (Dmf).

Type material: Holotype: **India:** Madras, Nilgiri, Coonoor, 1600 m, sifting in forest below town, ♂ 22.xi.1972, leg. C. Besuchet & I. Löbl (MHNG, examined). Paratype: 1♀, collected together with the holotype (MHNG, examined).

Diagnosis:

Males: This species can be identified by the lack of prosomal modification and the distinct shapes of palpal tibia prolateral apophysis and embolic division.

Females: Epigyne simple as in *Oedothorax* s.s., *Callitrichia* and *Mitrager*.

Description:

Male (holotype): Total length: 2.10. Prosoma: 1.02 long, 0.87 wide, unmodified (Fig. 7E). Eyes: AME-AME: 0.03, AME width: 0.04, AME-ALE: 0.04, ALE width: 0.09, ALE-PLE: 0, PLE width: 0.09, PLE-PME: 0.06, PME width: 0.08, PME-PME: 0.06. Clypeus: not hirsute, one sub-AME seta. Sternum: 0.62 long, 0.59 wide. Chelicerae: stridulatory striae rows compressed proximally (Fig. 67F). Legs: tibia chaetotaxy 2-2-1-1, dorsal proximal macroseta on tibia I 1.69 times diameter of tibia; Tm I: 0.55. All metatarsi with trichobothrium. Pedipalp: patella prolateral proximal vertical macrosetae absent; tibia with one prolateral, two retrolateral trichobothria; TPS absent; TPA apical side scaly, with several setae with serrated tips on the upper margin; TRA absent (Fig. 75A, D, E); PC median-sized, base not visible from dorsal view, distal setae close to distal clasp, distal clasp with inconspicuous striae, directed retrolaterally (Fig. 75A); T without papillae; PT with long papillae; TS short, with few papillae; MSA present; DSA short, irregular ar distal margin (Fig. 75F); EM flat, anterior margin without papillae, length equals ARP; ARP flat, slightly sclerotized; LER small, without striae, not extended

dorsal to E; VRP long, anteriorly directed; TP tip narrow; E retrolaterally spiral, anterior margin at base slightly wavy (Fig. 75C). Opisthosoma: dorsal pattern see Fig. 68F; PMS with mAP, two AC; PLS with triad, 3+ AC (Fig. 75I, J).

Female (paratype): Total length: 2.22. Prosoma: 1.02 long, 0.87 wide. Eyes: AME-AME: 0.02, AME width: 0.05, AME-ALE: 0.03, ALE width: 0.09, ALE-PLE: 0.01, PLE width: 0.09, PLE-PME: 0.06, PME width: 0.08, PME-PME: 0.05. Clypeus: not hirsute, one sub-AME seta. Sternum: 0.62 long; 0.58 wide. Legs: tibia chaetotaxy 2-2-1-1, dorsal proximal macroseta on tibia II 2.09 times diameter of tibia; Tm I: 0.62. Epigyne: Clade 13 characteristic morphology, entrance of copulatory ducts into spermathecae ectal to exits of fertilization ducts (Fig. 75G, H). Opisthosoma: PMS with mAP, two AC, one CY; PLS with triad, two CY, 3+ AC (Fig. 75K).

Distribution: India, only known from the type locality.

Habitat: Lower layer of forests.

Remarks: According to the results of our phylogenetic analysis, and the lack of the distinctive characteristics of *Oedothorax* s.s., this species is more closely related to the genus *Atypena*, which is also distributed in the Oriental realm. We provisionally leave the taxonomic status of this species unchanged until further data become available.

'*OEDOTHORAX*' *HOWARDI* PETRUNKEVITCH, 1925
INCERTAE SEDIS

Oedothorax howardi Petrunkevitch, 1925: 174, pl. 8, figs 6–9 (Df).

Unexamined material: **USA:** Tennessee, Clarksville, 3♀ 1921, coll. S. E. Crumb, sent by L. O. Howard (Petrunkevitch, 1925). No type was designated.

Diagnosis:

Females: This species differs from *Oedothorax* s.s. and its related genera by the epigynal morphology seemingly without a fused middle part of the dorsal and ventral plates (fig. 6 in Petrunkevitch, 1925), as well as by the tibial chaetotaxy (1-1-1-1) (2-2-1-1 in *Oedothorax*, *Callitrichia* and *Mitrager*) and the absence of trichobothria on metatarsus I (present in *Oedothorax*, *Callitrichia* and *Mitrager*).

Males: Unknown.

Distribution: USA: Tennessee.

Remarks: The information provided in Petrunkevitch (1925) suggests that this species does not belong

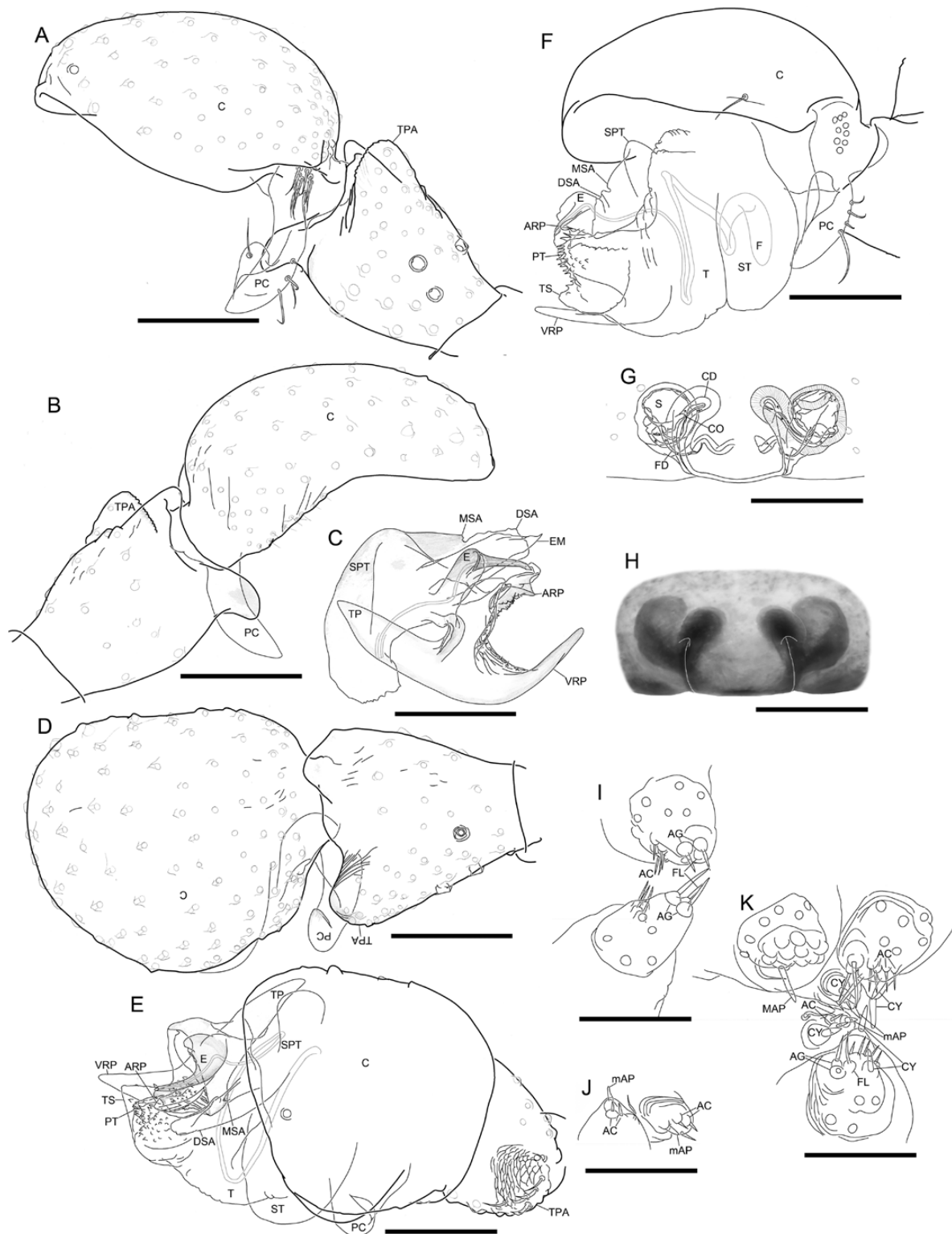


Figure 75. *Oedothorax cunur* Tanasevitch, 2015. A–D, male right palp, images flipped horizontally. A, retrolateral view. B, prolateral view. C, embolic division, prolateral view. D, dorsal view. E, F, left palp. E, dorsal view. F, retrolateral view. G, H, epigyne. G, ventral view. H, external morphology. I, male posterior lateral spinnerets. J, male posterior median spinnerets. K, female spinnerets. Scale bars 0.1 mm.

to *Oedothorax* s.s., nor is it sufficient for assigning this species to any other existing taxa. Due to the unavailability of specimens, and limited information from the original description, the relationship of this species to other erigonines remains unclear.

'OEDOTHORAX' JAPONICUS KISHIDA, 1910 *INCERTAE SEDIS*

Oedothorax japonicus Kishida, 1910: 6 (Dmf).

Unexamined material: **Japan:** Honshu, Nagaoka City, 30.v.1908, coll. Masao Nakamura (Kishida 1910). No type was designated.

Diagnosis: The original description does not provide sufficient information for the identification of this species.

Distribution: Only known from the type locality in Japan.

Remarks: No figures were provided in Kishida (1910), and according to his description, this species resembles *Paratmeticus bipunctis* (Bösenberg & Strand 1906), although no further details were provided to assert such similarity. According to the original description, the palps of *'Oe.'* *japonicus* might resemble that of *Erigonella* from Denis (1964) and Strand (1905), but both these species were also described without illustrations. Therefore, the relationship of this species to other taxa is unclear.

'OEDOTHORAX' KHASI TANASEVITCH, 2017 *INCERTAE SEDIS*

Oedothorax khasi Tanasevitch, 2017b: 331, figs 1–7 (Dm).

Type material: Holotype: **India:** Meghalaya, Khasi Hills, 16 km south-west of Mawsynram, between Mawsynram and Balat, 1000 m, sifting in forest, in ravine, ♂ 27.x.1978, leg. C. Besuchet & I. Löbl (MNHG, not examined).

Diagnosis:

Males: This species is characterized by the slightly elevated interocular region, the shape of the palpal tibial prolateral apophysis, as well as by the morphology of the embolic division (see description in Tanasevitch 2017).

Females: Unknown.

Distribution: Only known from the type locality in India.

Habitat: Forest litter.

Remarks: According to our re-delimitation of *Oedothorax* in the present study, this species does not belong to *Oedothorax*, but is probably related to *'Oe.'* *myanmar* or *'Oe.'* *kodaikanal*. Further comparison with more species to determine the taxonomic status of these *'Oedothorax' incertae sedis* species is required. Therefore, we provisionally do not change its genus.

'OEDOTHORAX' KODAIKANAL TANASEVITCH, 2015 *INCERTAE SEDIS*

(FIGS 7D, 67E, 68E, 76)

Oedothorax kodaikanal Tanasevitch, 2015: 386, figs 44–50 (Dm).

Type material: Holotype: **India:** Madras, Palni Hills, 10 km north-west of Kodaikanal, 2150 m, edge of *Rhododendron* forest with fern, sifting litter near river, ♂ 15.xi.1972, leg. C. Besuchet & I. Löbl (MHNG, examined). Paratypes: **India:** Madras, Palni Hills, 23 km west of Kodaikanal, Lake Berijam, 2150 m, *Rhododendron* forest, sifting litter, 1♂ (MHNG, examined) 1♂ (ZMMU) 14.xi.1972, leg. C. Besuchet & I. Löbl.

Diagnosis:

Males: This species can be diagnosed by the lack of external prosomal modification and the palpal features as described below.

Description:

Male (holotype): Total length: 2.27. Prosoma: 1.10 long, 0.85 wide, unmodified (Fig. 7D). Eyes: AME-AME: 0.02, AME width: 0.05, AME-ALE: 0.03, ALE width: 0.10, ALE-PLE: 0, PLE width: 0.10, PLE-PME: 0.05, PME width: 0.08, PME-PME: 0.07. Clypeus: not hirsute, one sub-AME seta. Sternum: 0.66 long, 0.60 wide. Chelicerae: stridulatory striae rows compressed at proximal end (Fig. 67E). Legs: tibia chaetotaxy 2-2-1-1; Tm I: 0.55. All metatarsi with trichobothrium. Pedipalp: patella prolateral proximal vertical macrosetae absent; tibia with one prolateral, two retrolateral trichobothria; TPS short, prolaterally situated at base of TPA; TPA long, dorsally elevated; TRA apically oriented (Fig. 76A, B, C); PC median-sized, base not visible from dorsal view, distal setae close to distal clasp, distal setae bearing area wide, distal clasp without striae, clasp extended slightly apically (Fig. 76A); T without papillae; PT without papillae; TS short, without papillae; MSA present; DSA tip straight (Fig. 76F); EM flat, anterior margin with small papillae, not exceeding ARP; ARP tip

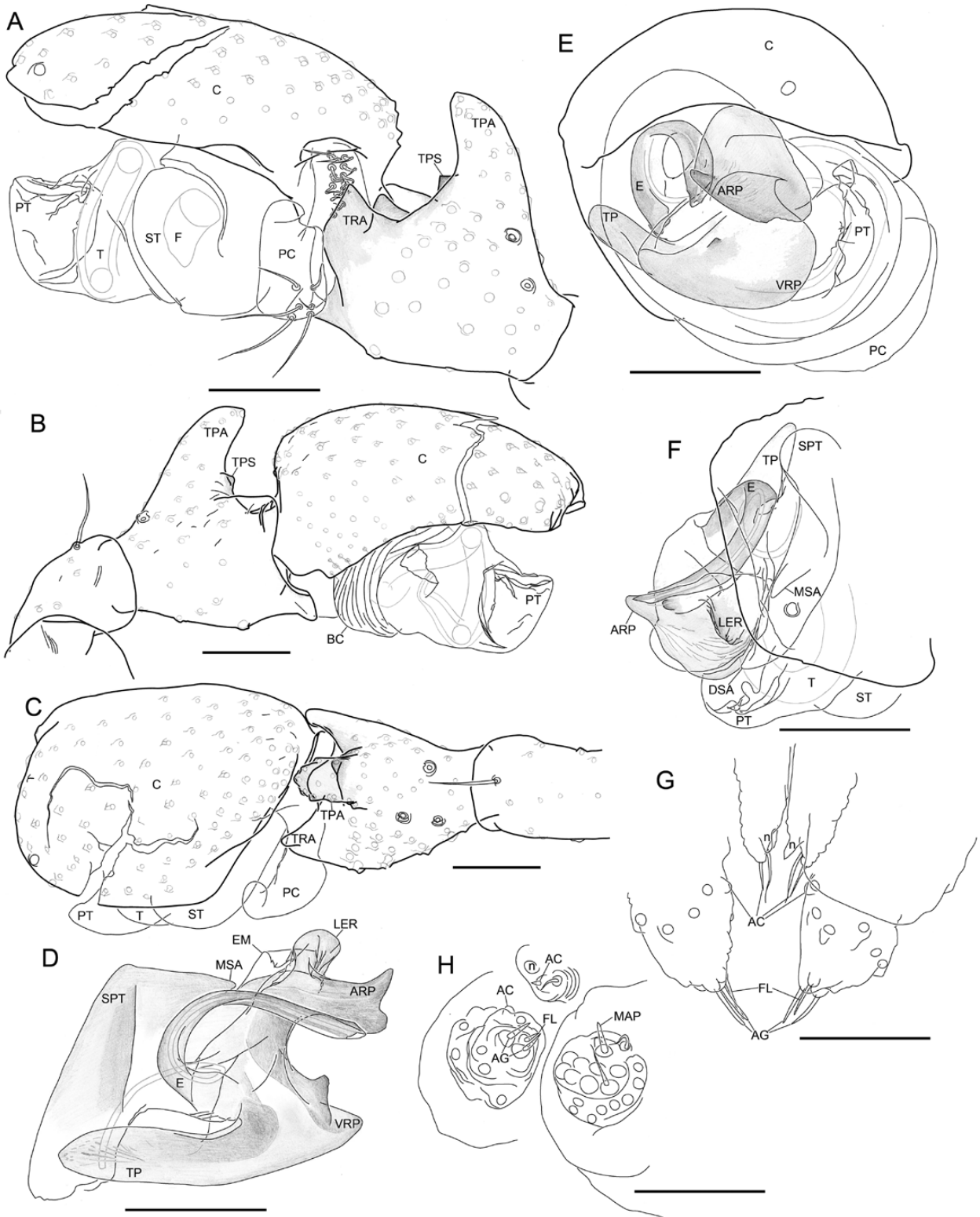


Figure 76. *Oedothorax kodaikanal* Tanasevitch, 2015. A–D, male right palp, images flipped horizontally. A, retrolateral view. B, prolateral view. C, dorsal view. D, embolic division, prolateral view. E, F, male left palp. E, apical view. F, embolic division, dorsal view. G, male posterior median spinnerets and posterior lateral spinnerets, dorsal view. H, male left spinnerets. Scale bars 0.1 mm.

blunt, with a round process ventrally; LER without striae, retrolaterally oriented; VRP with sclerotized apophysis distally; TP tip round; E retrolaterally spiral, anterior margin at base smoothly curved (Fig. 76D). Opisthosoma dorsal pattern see Fig. 68E. PMS with one nubbin (vestigial mAP), one AC; PLS with triad, one AC (Fig. 76G, H).

Male (paratype): Total length: 2.14. Prosoma: 1.02 long, 0.81 wide. Tm I: 0.54.

Female: Unknown.

Distribution: India.

Habitat: Forest litter.

Remarks: According to the results of our phylogenetic analysis, and the lack of characteristics of *Oedothorax* s.s., this species does not belong to *Oedothorax*, but is more closely related to *Atypena* and some '*Oedothorax*' *incertae sedis* species which, as in this species, are distributed in the Oriental realm. Although this species was scored in the present study as possessing TPS (the defining feature of *Mitrager*), its minute size and the position at the base of TPA in this species differ significantly from the retrolaterally bent form in *Mitrager*. In addition, the LER in this species does not bend over the embolus like in *Mitrager*. Since it shares no clear synapomorphic features with other taxa, its taxonomic affinity should be scrutinized in future studies, including other oriental erigonine species like '*Oe.*' *myanmar* Tanasevitch, 2017 and '*Oe.*' *khasi* Tanasevitch, 2017.

'*OEDOTHORAX*' *LIMATUS* CROSBY, 1905 *INCERTAE SEDIS*

Oedothorax limatus Crosby, 1905: 311, 335, pl. 29, fig. 6 (Df).

Type material: Lectotype: USA: Ithaca, NY, Nov. (AMNH, not examined).

Diagnosis:

Females: This species differs from *Oedothorax* and related taxa by the absence of trichobothrium on metatarsus IV, and by the epigynal morphology (fig. 6 in plate 29 in Crosby, 1905).

Males: Unknown.

Distribution: North America.

Remarks: The one epigyne drawing provided in Crosby (1905) is clearly different from the characteristic conformation observed in *Oedothorax* s.s..

'*OEDOTHORAX*' *MANGSIMA* TANASEVITCH, 2020 *INCERTAE SEDIS*

Oedothorax mangsima Tanasevitch, 2020a: 287, figs 5–7, 23–27 (Dm).

Type material: Holotype: **Nepal:** Kosi (= Koshi) Province, Sankhuwasawa District, Mangsima, 2200 m a.s.l, forest south of Mangsima, ravine, sifting dead leaves, mosses and rotten wood, 11.iv.1984, leg. I. Löbl & A. Smetana (MNHG, not examined).

Diagnosis:

Males: This species is characterized by the prominent post-ocular groove and hump, as well as the long, almost verticle palpal tibial apophysis and the embolic division (see description in Tanasevitch 2020a).

Females: Unknown.

Distribution: Only known from the type locality in Nepal.

Habitat: Forest litter.

Remarks: According to our re-delimitation of *Oedothorax* in the present study, this species does not belong to *Oedothorax*, but is probably related to '*Oe.*' *myanmar* or '*Oe.*' *kodaikanal*. Further comparison with more species to determine the taxonomic status of these '*Oedothorax*' *incertae sedis* species is required. Therefore, we provisionally do not change its genus.

'*OEDOTHORAX*' *MEGHALAYA* TANASEVITCH, 2015 *INCERTAE SEDIS*

(FIGS 19A, 22A, 24A, 77)

Oedothorax meghalaya Tanasevitch, 2015: 389, figs 61–69 (Dm).

Type material: Holotype: **India:** Meghalaya, above Shillong, Khasi Hills, near Shillong Peak, northern slope, 1850–1950 m, primary forest, sifting litter, ♂ 25.x.1978, leg. C. Besuchet & I. Löbl (examined). Paratypes: 1♂, collected together with the holotype (examined).

Diagnosis:

Males: This species can be recognized by the elevated PME region, the setae at inter-PME and interocular region, the structure of long, dorsally directed palpal tibial prolateral apophysis, wide distal-setae-bearing area of paracymbium and the embolic division.

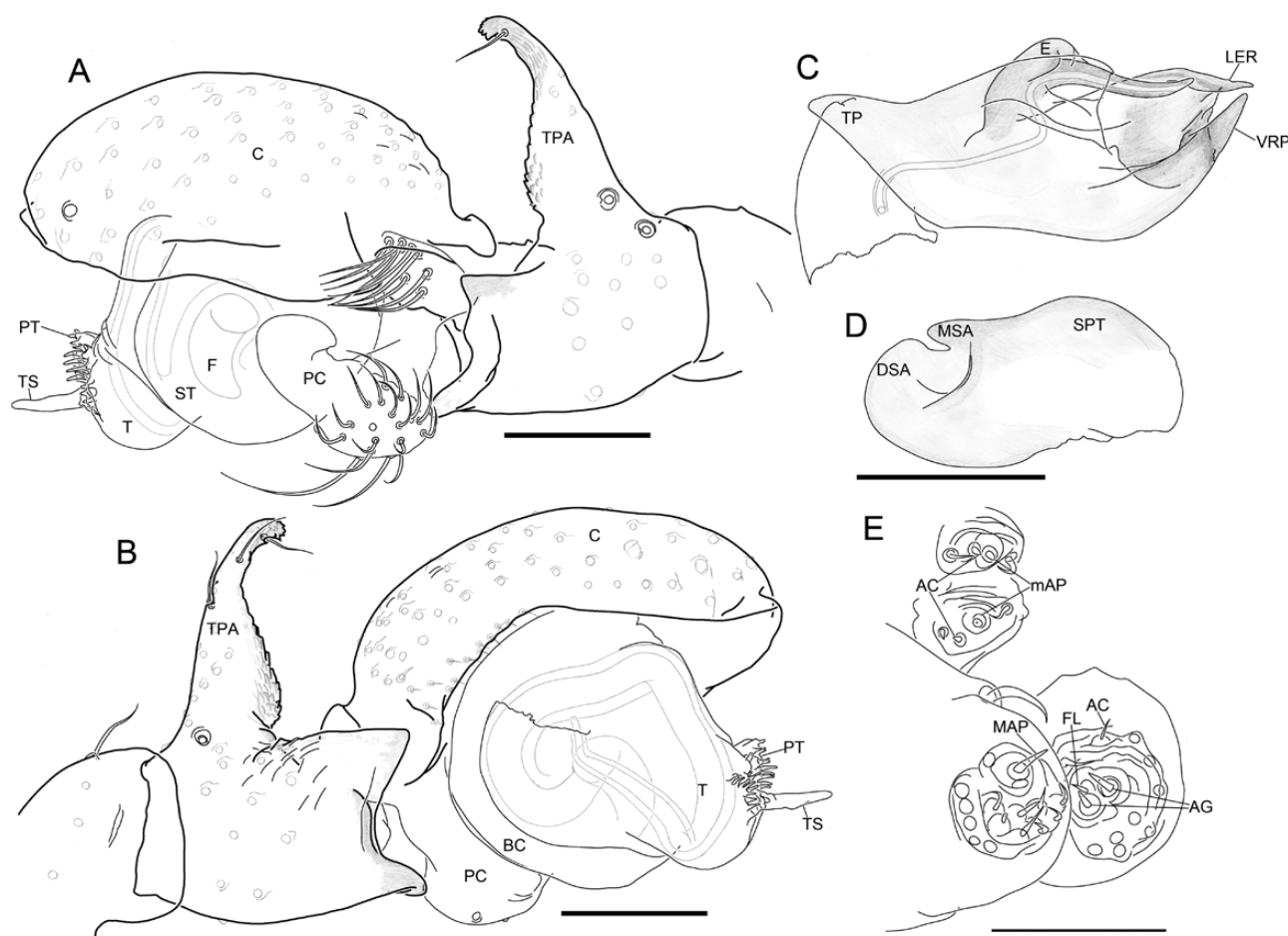


Figure 77. *Oedothorax meghalaya* Tanasevitch, 2015. A–D, male right palp, images flipped horizontally. A, retrolateral view. B, prolateral view. C, embolic division, prolateral view. D, suprategulum, retrolateral view. E, male spinnerets. Scale bars 0.1 mm.

Description:

Male (paratype): Total length: 2.15. Prosoma: 1.00 long, 0.75 wide, PME-bearing region elevated, inter-PME region with strong setae anteriorly directed, interocular region with strong setae directed upwards (Fig. 19A). Eyes: AME-AME: 0.04, AME width: 0.04, AME-ALE: 0.05, ALE width: 0.09, ALE-PLE: 0.01, PLE width: 0.08, PLE-PME: 0.09, PME width: 0.08, PME-PME: 0.15. Clypeus: not hirsute, one sub-AME seta. Sternum 0.55 long, 0.57 wide. Chelicerae: mastidia absent; stridulatory striae rows compressed and evenly spaced (Fig. 22A). Legs: tibia chaetotaxy 2-2-1-1, dorsal proximal macroseta on tibia I 2.1 times diameter of tibia; Tm I: 0.58. All metatarsi with trichobothrium. Pedipalp: patella prolateral proximal vertical macrosetae absent; tibia with one prolateral, two retrolateral trichobothria; TPS absent; TPA largely dorsally elevated, scaly at distal part and apical side; TRA small, triangular (Fig. 77A, B); PC large, base not visible from dorsal view, distal

setae numerous, distally situated, setae-bearing area largely wide, distal clasp without striae, clasp directed anteriorly (Fig. 77A); T without papillae; PT short, with long papillae; TS long, without papillae (Fig. 77A, B); MSA present; DSA tip round (Fig. 77D); EM absent; ARP absent; LER without striae, tip bent prolaterally, not extended dorsal to E; VRP bent dorsally; TP narrow at tip; E retrolaterally spiral, anterior margin at base slightly wavy (Fig. 77C). Opisthosoma: dorsal pattern see Fig. 24A. PMS with mAP, one AC; PLS with triad, one AC (Fig. 77E).

Female: Unknown.

Distribution: India, only known from the type locality.

Habitat: Forest litter.

Remarks: It is difficult to determine the homology of the two distal apophyses of the radix in this species.

According to structural similarity to those in other species, we assume homology of the upper one to LER and the lower one to VRP, and ARP is considered absent. According to the results of our phylogenetic analysis, and the lack of the distinctive characteristics of *Oedothorax s.s.*, this species is more closely related to *Atypena*, some '*Oedothorax*' *incertae sedis* species and *Mitrager*, which, as this species, are distributed in the Himalayan region and the Oriental realm. We provisionally leave the taxonomic status of this species unchanged until further data become available.

'*OEDOTHORAX*' MYANMAR TANASEVITCH, 2017
INCERTAE SEDIS

Oedothorax myanmar Tanasevitch, 2017c: 339, figs 6–7, 43–47 (Dm).

Type material: Holotype: **Myanmar**: southern Chin State, above Kampetlet, below Mountain Oasis Resort (21°11'43.6" N, 94°02'1.1" E), 1585 m, secondary forest along stream, by hand and sifting, at day, ♂ 17.v.2014, leg. P. Jäger (SMF, not examined).

Diagnosis:

Males: This species is diagnosed by the absence of prosomal modification, the small denticle on the wide, rounded darkened palpaltibial prolateral apophysis, the spoon-shaped distal suprategular apophysis, and the shape of the embolic division, which has the anterior radical process, ventral radical process and radical tailpiece (see Tanasevitch 2017, pp. 339–340).

Females: Unknown.

Distribution: Only known from the type locality in Myanmar.

Remarks: According to the drawings in Tanasevitch (2017c), the embolic division of this species resembles those of '*Oe.*' *kodaikanal*, '*Oe.*' *meghalaya*, '*Oe.*' *uncus*, '*Oe.*' *cunur*, '*Oe.*' *khasi*, '*Oe.*' *bifoveatus* and '*Oe.*' *stylus*, and is, therefore, probably closely related to these species instead of *Oedothorax s.s.*

'*OEDOTHORAX*' NAZARETI SCHARFF, 1989 INCERTAE
SEDIS; NEW FEMALE DESCRIPTION
(FIGS 7I, 67J, 68J, 78)

Oedothorax nazareti Scharff, 1989: 15, figs 7–12 (Dm).

Oedothorax nazareti Tanasevitch, 2015: 382, fig. 7 (m).

Type material: Holotype: **Ethiopia**: Shoa Administrative Province, Nazaret, under stone in

cultivated farmland, 2400 m, ♂ 22.vi.1985, leg. N. Scharff (not examined).

Examined material: Ethiopia, c. 15 km west of Debre Siwa, under stones in overgrazed woodland, 3♂10♀ 11.vi.1988, det. A. Russell-Smith (RMCA 224.501).

Diagnosis:

Males: This species can be identified by its unique conical-shaped postocular hump and setae distribution on the hump and interocular region.

Females: This species has the typical simple epigyne structures as many other *Oedothorax* species, but can be identified by the trajectory of the copulatory ducts (Fig. 78F).

Description:

Male (RMCA 224.501): Total length: 2.29. Prosoma: 1.06 long, 0.74 wide, postocular region conically elevated, covered by long, thick setae; interocular region with dense setae (Fig. 7I). Eyes: AME-AME: 0.04, AME width: 0.05, AME-ALE: 0.05, ALE width: 0.08, ALE-PL: 0, PLE width: 0.08, PLE-PME: 0.04, PME width: 0.06, PME-PME: 0.19. Clypeus: not hirsute, one sub-AME seta. Sternum: 0.63 long, 0.56 wide. Chelicerae: mastidia absent; stridulatory striae scaly, rows widely and evenly spaced (Fig. 67J). Legs: dorsal proximal macroseta on tibia I, II, III and IV 0.12, 0.13, 0.91 and 1.46 times diameter of tibia, respectively; Tm I: 0.67. All metatarsi with trichobothrium. Pedipalp: patella prolateral proximal vertical macrosetae absent; tibia with one prolateral, two retrolateral trichobothria; TPS small, ventrally situated at TPA tip; TPA long, base prolateral to palpal tibia prolateral trichobothrium, tip bent retrolaterally (Fig. 78C); PC median-sized, base not visible from dorsal view, distal setae close to distal clasp, distal clasp without striae, clasp extended apically (Fig. 78A); T without papillae; PT long, slender, without papillae; TS long, slender, without papillae; MSA absent; DSA tip straight, simple; EM absent (Fig. 78A, E); ARP with groove fitting E, round and narrow at tip; LER absent; VRP absent; TP wide, round at tip; E retrolaterally spiral at base, prolaterally spiral at tip (Fig. 78B, E). Opisthosoma: dorsal pattern see Fig. 68J. PMS with mAP, two AC; PLS with triad, 3+ AC (Fig. 78H).

Female (RMCA 224.501): Total length: 2.62. Prosoma: 1.03 long, 0.73 wide. Eyes: AME-AME: 0.02, AME width: 0.05, AME-ALE: 0.05, ALE width: 0.07, ALE-PL: 0, PLE width: 0.07, PLE-PME: 0.04, PME width:

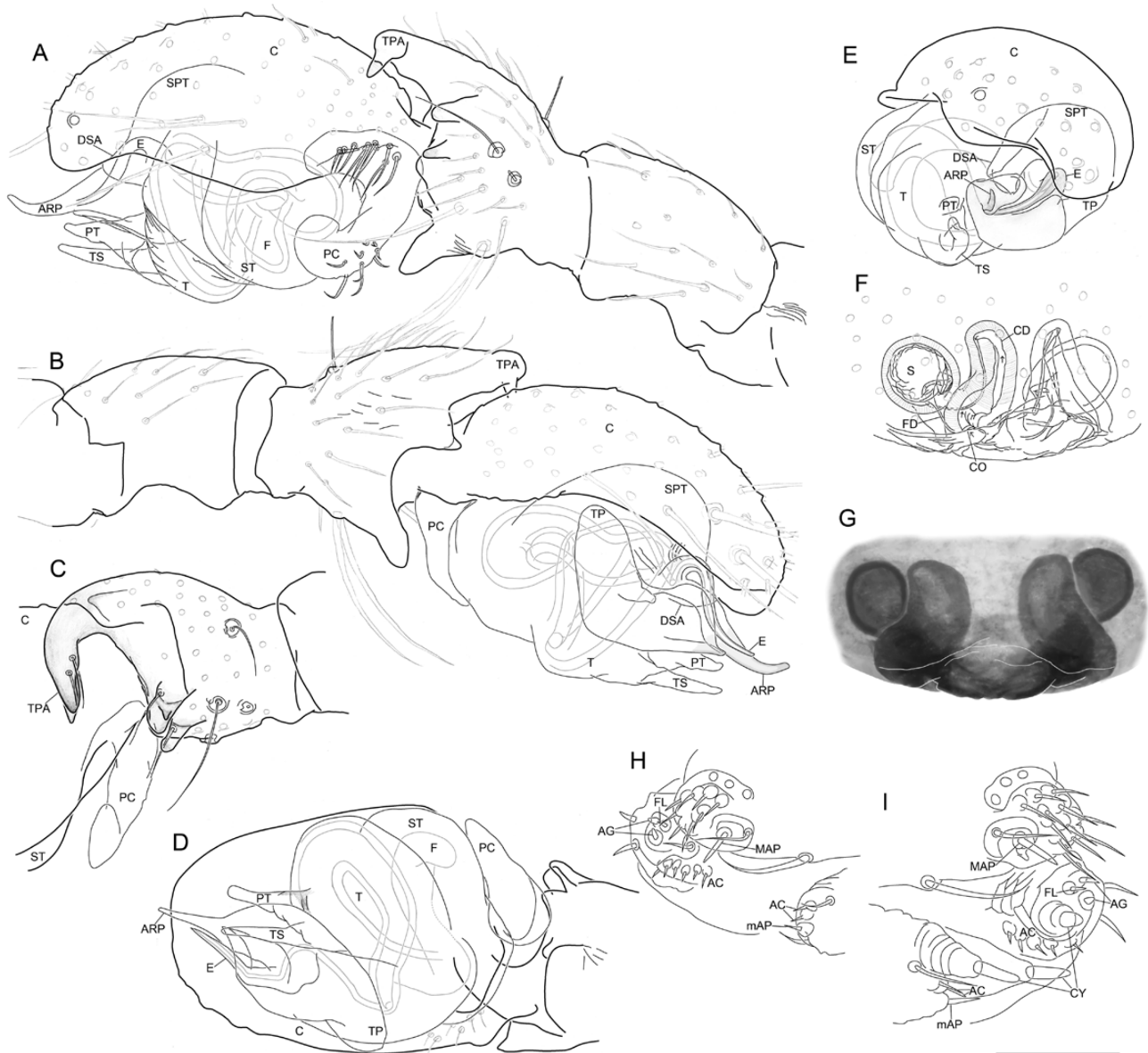


Figure 78. *Oedothorax nazareti* Scharff, 1989. A–E, male left palp. A, retrolateral view. B, prolateral view. C, dorsal view. D, ventral view. E, apical view. F, G, epigyne. F, ventrolateral view. G, external morphology. H, male right spinnerets. I, female left spinnerets. Scale bar 0.1 mm.

0.07, PME-PME: 0.07. Clypeus: not hirsute, one sub-AME seta. Sternum: 0.59 long; 0.54 wide. Legs: dorsal proximal macroseta on tibia I, II, III and IV 1.58, 1.76, 2.26 and 2.52 times diameter of tibia, respectively; Tm I: 0.60. Epigyne: CO posteriorly situated, receptacles long, wide (Fig. 78F, G). Opisthosoma: PMS with mAP, two AC, one CY; PLS with triad, two CY, 3+ AC (Fig. 78I).

Variation: The measurements are based on examined material.

Males ($N = 3$, means in parentheses): Total length 2.22–2.46 (2.33). Prosoma: 1.06–1.14 (1.09) long, 0.72–0.74 (0.73) wide. Legs: dorsal proximal macroseta on tibia I, II, III and IV 0.12–0.13 (0.12), 0.13–0.19 (0.16), 0.91–1.68 (1.28) and 1.46–2.28 (1.88) times diameter of tibia, respectively; Tm I: 0.58–0.67 (0.64).

Females ($N = 10$, means in parentheses): Total length 2.42–3.07 (2.74). Prosoma: 1.03–1.18 (1.13) long, 0.73–0.86 (0.79) wide. Legs: dorsal proximal macroseta on tibia I, II, III and IV 1.58–1.87 (1.72), 1.63–2.13 (1.90),

1.88–2.41 (2.18) and 2.15–2.68 (2.39) times diameter of tibia, respectively; Tm I: 0.60–0.69 (0.64).

Distribution: Ethiopia.

Habitat: Under stones in cultivated lands or woodlands.

Remarks: According to our phylogenetic analysis, this species lack the synapomorphic traits of *Oedothorax* s.s.. Its phylogenetic position resulted in Clade 22 sister to Clade 23. However, due to the lack of shared derived characters with other taxa in this study, its

taxonomic affinity is undetermined. Therefore, we leave its taxonomic state provisionally unchanged.

'OEDOTHORAX' PARACYMBIALIS TANASEVITCH, 2015
INCERTAE SEDIS

(Figs 7C, 67D, 68D, 79)

Oedothorax paracymbialis Tanasevitch, 2015: 389, figs 70–74 (Dm).

Type material: Holotype: **India:** Madras, Nilgiri, Hulical near Coonoor, right bank of Coonoor River,

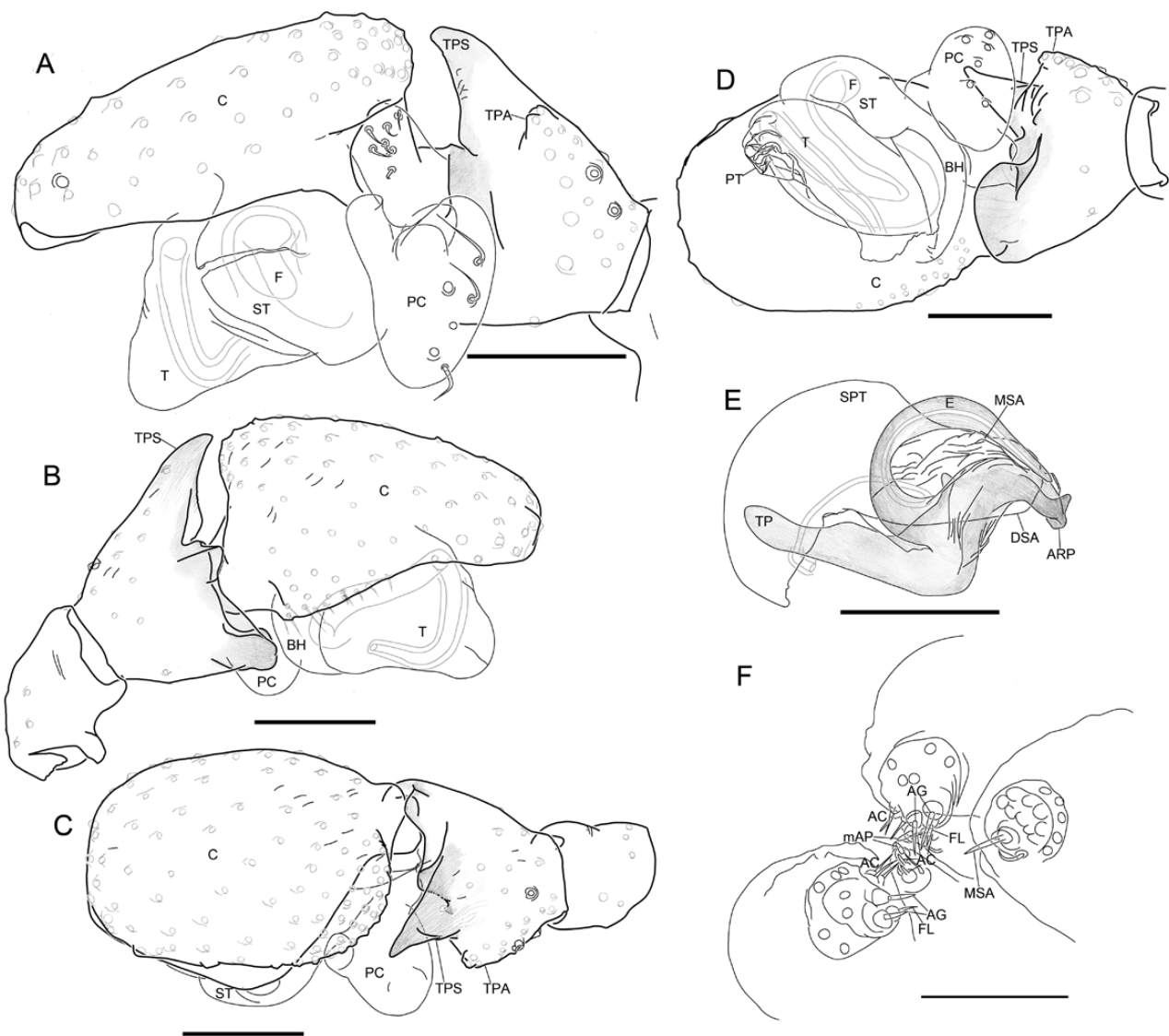


Figure 79. *'Oedothorax' paracymbialis* Tanasevitch, 2015. A–E, male right palp, images flipped horizontally. A, retrolateral view. B, prolateral view. C, dorsal view. D, ventral view. E, embolic division, prolateral view. F, male spinnerets. Scale bars 0.1 mm.

1600 m, forest in ravin, sifting, ♂ 22.xi.1972, leg. C. Besuchet & I. Löbl (MHNG, examined).

Diagnosis:

Males: This species can be diagnosed by the slightly elevated postocular region, the prominent TPS and the large distal part of paracymbium.

Description:

Male (holotype): Total length: 1.77. Prosoma: 0.77 long, 0.63 wide, postocular region slightly elevated, with curved seta directed anteriorly (Fig. 7C). Eyes: AME-AME: 0.031, AME width: 0.04, AME-ALE: 0.03, ALE width: 0.08, ALE-PLE: 0.01, PLE width: 0.08, PLE-PME: 0.03, PME width: 0.07, PME-PME: 0.06. Clypeus: not hirsute. Sternum: 0.48 long, 0.49 wide. Chelicerae: mastidia absent; stridulatory striae rows widely and evenly spaced (Fig. 67D). Legs: Tm I: 0.62. All metatarsi with trichobothrium. Pedipalp: patella prolateral proximal vertical macrosetae absent; tibia with one prolateral, two retrolateral trichobothria; TPS striped, straight, apical-retrolaterally pointed, wide at base; TPA slightly elevated; TRA absent (Fig. 79C); PC large, base not visible from dorsal view, distal setae close to distal clasp, setae-bearing region greatly enlarged, distal clasp without striae, clasp directed slightly apically (Fig. 79A); T without papillae; PT short, without papillae, distal rim thin and smooth at margin; TS absent (Fig. 79D); MSA present; DSA straight, tip round; EM absent; ARP horizontally flat, highly sclerotized; LER small, without striae, not extended dorsal to E; VRP absent; TP slender; E retrolaterally spiral, middle part wide and striped (Fig. 79E). Opisthosoma: dorsal pattern see Fig. 68D; PMS with mAP, two AC; PLS with triad, three AC (Fig. 79F).

Female: Unknown.

Distribution: Only known from the type locality.

Habitat: Forest litter.

Remarks: According to the results of our phylogenetic analysis, and the lack of the distinctive characteristics of *Oedothorax s.s.*, this species is more closely related to species in Clade 16 that, as this species, are distributed in the Oriental realm. We provisionally leave the taxonomic status of this species unchanged until further data become available.

'OEDOTHORAX' SEXMACULATUS SAITO & ONO, 2001
INCERTAE SEDIS

Oedothorax sexmaculatus Saito & Ono, 2001: 5, figs 5–9 (Dmf).

Oedothorax sexmaculatus Ono *et al.*, 2009: 284, figs 343–347 (mf).

Type material: Holotype: **Japan:** Hunshu, Fukuschima Pref., Yama-gun, Azuma-yama Mts., Jododaria, ♂, 11.vi.1986, leg. K. Kumada (NSMT-Ar 4572, not examined). Paratypes: same data as holotype, 5♂6♀ (NSMT-Ar 4573–4574, not examined); Gunma Pref., Tone-gun, Katashina-mura, Marunuma, 1♂ 1.vi.1983, leg. H. Saito (NSMT-Ar 4575, not examined).

Diagnosis:

Males: This species can be distinguished by the variegated opisthosoma, the palpal apophysis and the depiction of the bulbal structure in figures 8 and 9 in Saito & Ono (2001), in which the individual structures of the embolic division are unfortunately not clearly recognizable.

Females: This species can be identified by the dorsal pattern of opisthosoma with six dark patches, and the epigynal external morphology illustrated in figure 9 in Saito & Ono (2001).

Distribution: Japan: Honshu.

Remarks: The description of Saito & Ono (2001) is in accordance with the general combination of somatic characters of *Oedothorax*, *Mitrager* and other related taxa. Although the configuration of the embolic division is not fully recognizable in their drawings, the embolus seems to be prolaterally spiralled (fig. 8 in Saito & Ono, 2001), but the ARP tip is not pointed at tip and not spiral as in *Oedothorax*; its PC has a clearly broader distal part (fig. 6 in Saito & Ono, 2001) than in *Oedothorax*. The six distinct spots on the opisthosoma is seen neither in *Oedothorax s.s.* nor in *Mitrager*. Due to these dissimilarities, this species most probably belongs to another genus.

'OEDOTHORAX' SOHRA TANASEVITCH, 2020 *INCERTAE SEDIS*

Oedothorax sohra Tanasevitch, 2020b: 129, figs 4–6, 13–18 (Dm).

Type material: Holotype: **India:** Meghalaya, Sohra, plateau, 1320 m a.s.l., 14–26.xii.2013, leg. K. P. Tomkovich (ZMMU).

Diagnosis:

Males: The palpal morphology of this species is similar to many '*Oedothorax incertae sedis*' species from the Oriental Region, including '*Oe. kodaikanal*', '*Oe. meghalaya*', '*Oe. uncus*', '*Oe. cunur*', '*Oe. stylus*', '*Oe. myanmar*', '*Oe. khasi*', '*Oe. bifoveatus*' and '*Oe. unciger*'. It can be distinguished from '*Oe. cunur*' and '*Oe. stylus*' by the much longer, dorsally directed palpal tibial prolateral apophysis with distal dentation; from '*Oe. kodaikanal*', '*Oe. meghalaya*', '*Oe. unciger*', '*Oe. khasi*', '*Oe. bifoveatus*' and '*Oe. myanmar*' by the much longer and distally curved ventral radical apophysis; from '*Oe. uncus*' by the shorter and less curved ventral radical apophysis.

Females: Unknown.

Distribution: Only known from the type locality in India.

Remarks: From the original species description and figures (Tanasevitch 2020b: 130, figs 13–18) this species is overall most similar to '*Oe. uncus*', both in the lack of prosomal modification and the male palpal morphology, including the extensive papillae distribution on the protegulum, the long and curved ventral radical apophysis and the long, vertically pointed palpal tibial prolateral apophysis with distal dentation, etc. Therefore, this species is probably most closely related to '*Oe. uncus*' instead of *Oedothorax s.s.*

'*OEDOTHORAX*' *STYLUS* TANASEVITCH, 2015 *INCERTAE SEDIS*

(FIGS 7F, 67G, 68G, 80)

Oedothorax stylus Tanasevitch, 2015: 393, figs 83–85 (Dmf).

Type material: Holotype: **India:** Kerala, NW of Nelliampathi Hills, Kaikatty, 900 m, sifting in forest, near a spring, ♂ 30.xi.1972, leg. C. Besuchet & I. Löbl (examined). Paratypes: **India:** 1♀, collected together with the holotype; Madras, Anaimalai Hills, 18 km north of Valparai, 1250 m, forest, sifting litter, 1♂ 18.xi.1972, leg. C. Besuchet & I. Löbl (examined).

Diagnosis:

Males: This species can be diagnosed by the scaly elevation representing palpal tibial prolateral apophysis, the exceptionally long and slender ventral radical process, and the lack of prosomal modification.

Females: The general appearance of this species is *Oedothorax*-like. It can be identified by the anterior position of the copulatory ducts opening to the spermathecae.

Description:

Male (paratype): Total length: 1.70. Prosoma: 0.77 long, 0.67 wide, unmodified (Fig. 7F). Eyes: AME-AME: 0.02, AME width: 0.05, AME-ALE: 0.02, ALE width: 0.08, ALE-PLE: 0.01, PLE width: 0.08, PLE-PME: 0.03, PME width: 0.08, PME-PME: 0.03. Clypeus: not hirsute, one sub-AME seta. Sternum: 0.48 long, 0.48 wide. Chelicerae: mastidia absent; stridulatory striae rows compressed proximally (Fig. 67G). Legs: tibia chaetotaxy 2-2-1-1, dorsal proximal macroseta on tibia I 1.56 times diameter of tibia; Tm I: 0.54. All metatarsi with trichobothrium. Pedipalp: patella prolateral proximal vertical macrosetae absent; tibia with one prolateral, two retrolateral trichobothria; TPS absent; TPA short, stout, apical surface scaly; TRA absent (Fig. 80C); PC median-sized, base not visible from dorsal view, distal setae close to distal clasp, distal clasp without striae, clasp directed apically (Fig. 80A); T without papillae; PT long, with median-sized papillae; TS absent (Fig. 80D); MSA present; DSA tip slightly wavy, with a protuberance on dorsal side in front of MSA; EM flat, anterior margin with papillae, length equals ARP (Fig. 80A); ARP pointed, weakly sclerotized; LER small, without striae, not extended dorsal to E; VRP long, straight, apically directed; TP tip pointed, narrow; E retrolaterally spiral, anterior margin at base wavy (Fig. 80B). Opisthosoma: dorsal pattern see Fig. 68G; PMS with mAP, two AC; PLS with triad, 3+ AC (Fig. 80G).

Male (holotype): Prosoma: 0.77 long, 0.63 wide. Tm I: 0.54.

Female (paratype): Total length: 1.96. Prosoma: 0.85 long, 0.66 wide. Eyes: AME-AME: 0.02, AME width: 0.05, AME-ALE: 0.02, ALE width: 0.09, ALE-PLE: 0, PLE width: 0.09, PLE-PME: 0.04, PME width: 0.08, PME-PME: 0.05. Clypeus: not hirsute, one sub-AME seta. Sternum: 0.53 long; 0.51 wide. Legs: tibia chaetotaxy 2-2-1-1, dorsal proximal macroseta on tibia I, II, III and IV 2.72, 2.82, 2.60 and 3.39 times diameter of tibia, respectively; Tm I: 0.54. All metatarsi with trichobothrium. Epigyne: Clade 13 characteristic morphology, CO anteriorly oriented (Fig. 80E, F). Opisthosoma: dorsal pattern same as male; PMS with mAP, two AC, one CY; PLS with triad, two CY, 3+ AC (Fig. 80H).

Distribution: At present only known from Kerala and Madras (currently Tamil Nadu), India.

Habitat: Forest litter.

Remarks: According to the results of our phylogenetic analysis and the lack of the distinctive characteristics

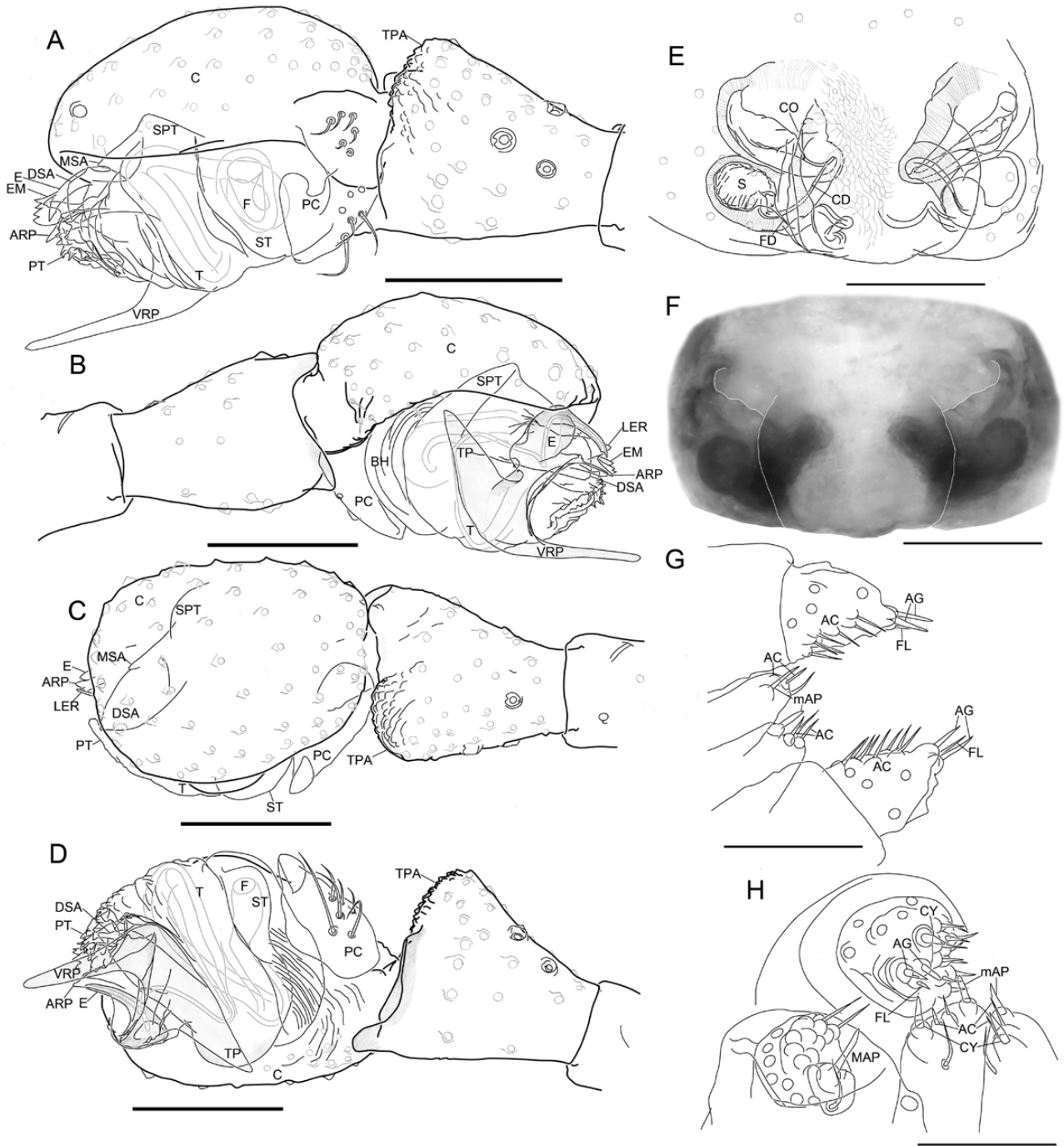


Figure 80. *Oedothorax stylus* Tanasevitch, 2015. A–D, male right palp, images flipped horizontally. A, retrolateral view. B, prolateral view. C, dorsal view. D, ventral view. E, F, epigyne. E, ventrolateral view. F, external morphology. G, male posterior median spinnerets and posterior lateral spinnerets, dorsal view. H, female spinnerets. Scale bars 0.1 mm.

of *Oedothorax s.s.* (see general description of *Oedothorax s.s.*), this species is more closely related to ‘*Oe.*’ *cunur* and *Atypena* which, as in this species,

are distributed in the Oriental realm. We provisionally leave the taxonomic status of this species unchanged until further data become available.

'OEDOTHORAX' TRILINEATUS SAITO, 1934 *INCERTAE SEDIS*

Oedothorax trilineatus Saito, 1934: 311, pl. 13, fig. 18, pl. 15, fig. 61 (Df).

Oedothorax trilineatus, Saito, 1959: 79, fig. 84a–c (f).

Material: **Japan:** Nemuro, 4♀, leg. S. Motoda, 15.vii.1931, not examined. No type material was designated.

Diagnosis:

Females: This species can be distinguished by the black prosoma, the black opisthosoma with three oblique white markings at the sides, and the white/black annulated legs and palps.

Males: unknown

Distribution: Japan: Nemuro.

Remarks: According to Saito (1934), this species has prosoma and opisthosoma uniformly black in colour, and legs are white annulated with black, different from the yellow to dark-brown coloration of *Oedothorax* and *Mitrager* species. Furthermore, according to his description, three out of four specimens have leg II as the shortest leg, in comparison to leg III as the shortest leg in Linyphiidae in general. Therefore, this species is most likely not a linyphiid.

'OEDOTHORAX' UNCIGER TANASEVITCH, 2020 *INCERTAE SEDIS*

Oedothorax unciger Tanasevitch, 2020b: 127, figs 1–3, 7–12 (Dm).

Type material: Holotype: **India:** Meghalaya, Sohra, plateau, 1320 m a.s.l., ♂ 14–26.xii.2013, leg. K. P. Tomkovich (ZMMU). Paratype: 1♂ (ZMMU), together with holotype.

Diagnosis:

Males: This species is similar to many Oriental '*Oedothorax*' species, but can be distinguished by its unique hook-shaped ventral radical process (see figs 8 and 12 in Tanasevitch 2020b).

Females: unknown.

Distribution: Only known from the type locality in India.

Remarks: According to the drawings in Tanasevitch (2020), the embolic division of this species resembles

those of '*Oe.* kodaikanal', '*Oe.* meghalaya', '*Oe.* uncus', '*Oe.* cunur', '*Oe.* myanmar', '*Oe.* sohra', '*Oe.* khasi', '*Oe.* bifoveatus' and '*Oe.* stylus' and is, therefore, probably closely related to these species instead of *Oedothorax* s.s.

'OEDOTHORAX' UNCUS TANASEVITCH, 2015 *INCERTAE SEDIS*

(FIGS 19B, 22B, 24B, 81)

Oedothorax uncus Tanasevitch, 2015: 393, figs 86–88 (Dmf).

Type material: Holotype: **India:** Meghalaya, Khasi Hills, Mawphlang, 1800 m, forest, sifting litter, ♂ 28.x.1978, leg. C. Besuchet & I. Löbl (MHNG, examined). Paratype: 1♀, collected together with the holotype (MHNG, examined).

Diagnosis:

Males: This species can be distinguished by the long, hook-shaped VRP, the long, palpal tibial apophysis with distal dentation and the lack of prosomal modification.

Females: This species can be identified by the enlarged median part of copulatory ducts.

Description:

Male (holotype): Total length: 2.20. Prosoma: 0.99 long, 0.8 wide, unmodified; interocular region with short stout setae directed upwards (Fig. 19B). Eyes: AME-AME: 0.04, AME width: 0.05, AME-ALE: 0.03, ALE width: 0.08, ALE-PLE: 0.01, PLE width: 0.08, PLE-PME: 0.06, PME width: 0.06, PME-PME: 0.08. Clypeus: not hirsute, one sub-AME seta. Sternum: 0.61 long, 0.59 wide. Chelicerae: mastidia absent; stridulatory striae ridged, rows compressed and evenly spaced (Fig. 22B). Legs: tibia chaetotaxy 2-2-1-1, dorsal proximal macroseta on tibia I, III and IV 1.35, 2.55 and 2.94 times diameter of tibia, respectively; Tm I: 0.65. All metatarsi with trichobothrium. Pedipalp: patella prolateral proximal vertical macrosetae absent; tibia with one prolateral, two retrolateral trichobothria; TPS absent; TPA prominent, dorso-retrolaterally directed, with several enlarged setal bases at tip; TRA absent (Fig. 81C); PC median-sized, base not visible from dorsal view, distal setae close to distal clasp, distal clasp without striae, clasp directed apically (Fig. 81A); T without papillae; PT median-sized papillae; TS absent (Fig. 81D); MSA present; DSA tip wavy (Fig. 81A); EM flat, length approximately equals ARP, with long papillae (Fig. 81D); ARP flat, weakly sclerotized; LER absent; VRP long, dorsally curved, tip pointed, proximally directed; TP tip round, dorsally directed; E

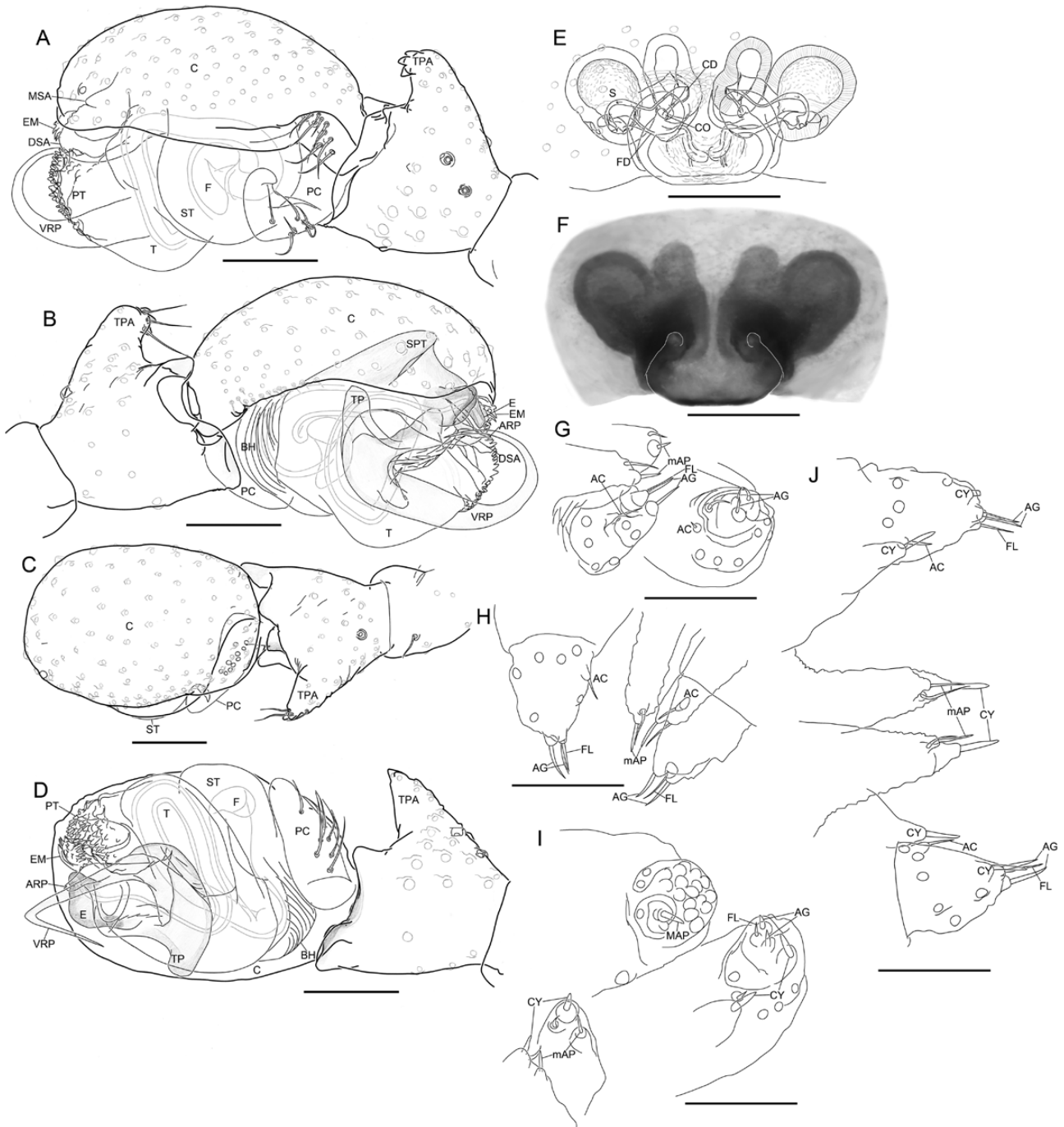


Figure 81. *Oedothorax uncus* Tanasevitch, 2015. A–D, male right palp, images flipped horizontally. A, retrolateral view. B, prolateral view. C, dorsal view. D, ventral view. E, F, epigyne. E, ventral view. F, external morphology. G, H, male posterior median spinnerets and posterior lateral spinnerets. G, lateral view. H, dorsal view. I, female spinnerets. J, female posterior median spinnerets and posterior lateral spinnerets. Scale bars 0.1 mm.

retrolaterally spiral, anterior margin at base slightly wavy (Fig. 79B). Opisthosoma: dorsal pattern see Fig. 24B; PMS with mAP, AC absent; PLS with triad, one AC (Fig. 81G, H).

Female (paratype): Total length: 2.28. Prosoma: 1.01 long, 0.78 wide. Eyes: AME-AME: 0.04, AME width: 0.04, AME-ALE: 0.02, ALE width: 0.09, ALE-PLE: 0.01, PLE width: 0.08, PLE-PME: 0.05, PME

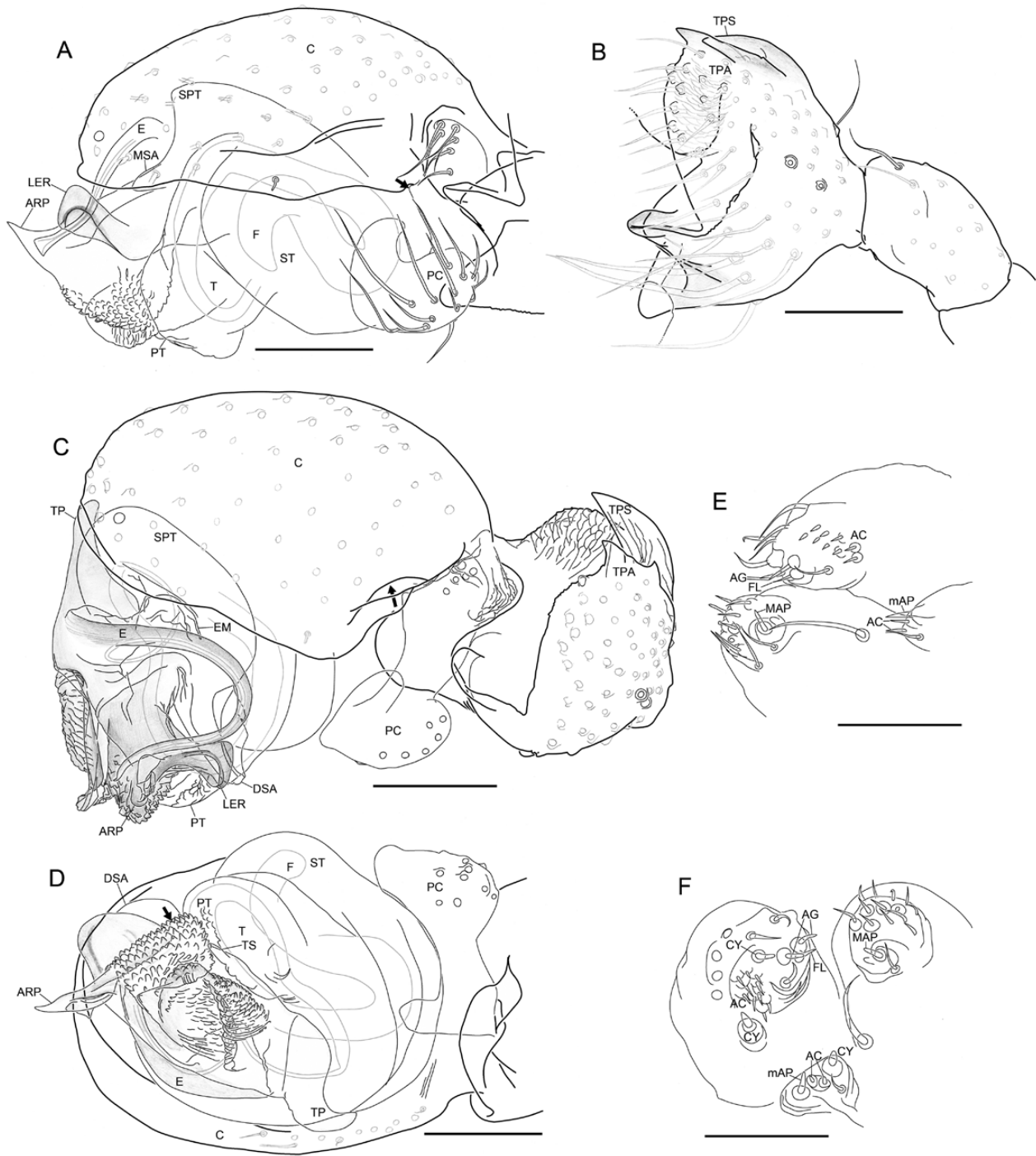


Figure 82. *Nasoona crucifera* (Thorell, 1895). A–D, male left palp. A, retrolateral view. B, tibia and patella, retrolateral view. C, retrolateral view, with copulatory bulb half-expanded. D, ventral view. E, male left spinnerets. F, female right spinnerets. Scale bars 0.1 mm.

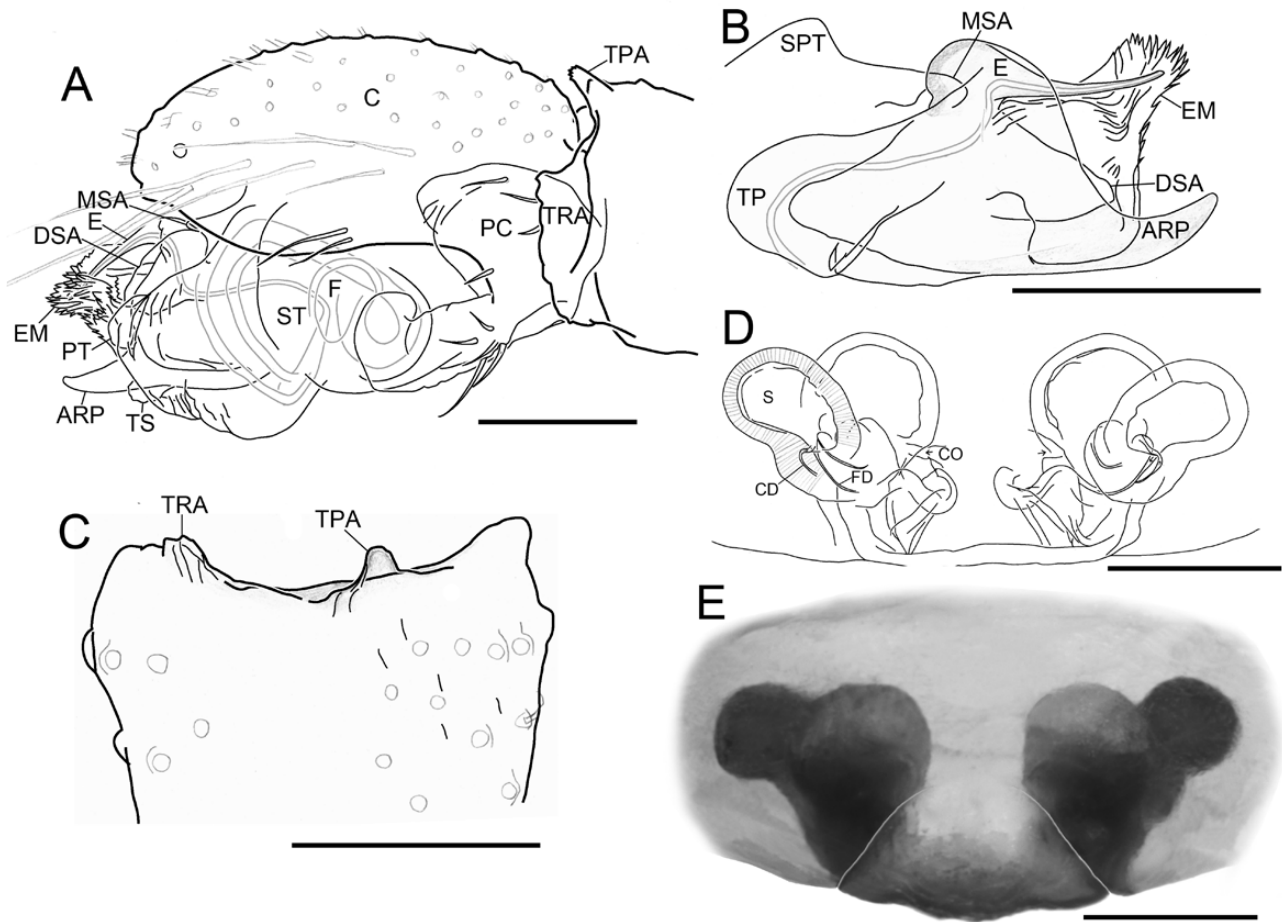


Figure 83. *Tmeticus tolli* Kulczyński, 1908. A–C, male left palp. A, retrolateral view. B, embolic division, prolateral view. C, distal part of tibia. D, E, epigyne. D, dorsal view. E, external morphology. Scale bars 0.1 mm.

width: 0.08, PME-PME: 0.06. Clypeus: not hirsute, one sub-AME seta. Sternum: 0.58 long; 0.61 wide. Legs: tibia chaetotaxy 2-2-1-1, dorsal proximal macroseta on tibia I and IV 2.28 and 3.44 times diameter of tibia, respectively; Tm I: 0.60. Epigyne: Clade 13 characteristic morphology, CO posteriorly oriented, middle part of copulatory ducts enlarged, entrances of copulatory ducts into spermathecae ectal to exits of fertilization ducts (Fig. 81E, F). Opisthosoma: dorsal pattern same as male; PMS with mAP, one CY; PLS with triad, two CY, one AC (Fig. 81I, J).

Distribution: India, only known from the type locality.

Habitat: Forest litter.

Remarks. According to the results of our phylogenetic analysis and the lack of the distinctive characteristics

of *Oedothorax* s.s., this species is more closely related to *Atypena*, some '*Oedothorax*' *incertae sedis* species and *Mitrager*, which, as in this species, are distributed in the Himalayan region and the Oriental realm. We provisionally leave the taxonomic status of this species unchanged until further data become available.

DISCUSSION

ONE STEP FORWARD IN SYSTEMATIC TAXONOMY OF ERIGONINES

Current biodiversity research on linyphiid spiders is highly biased towards Europe, with 1345 species known from Europe (Nentwig *et al.*, 2019) and only a total of 1195 species from Oriental, Afrotropical and Neotropical regions (194, 423 and 578, respectively) (Tanasevitch, 2019). This reflects the taxonomic

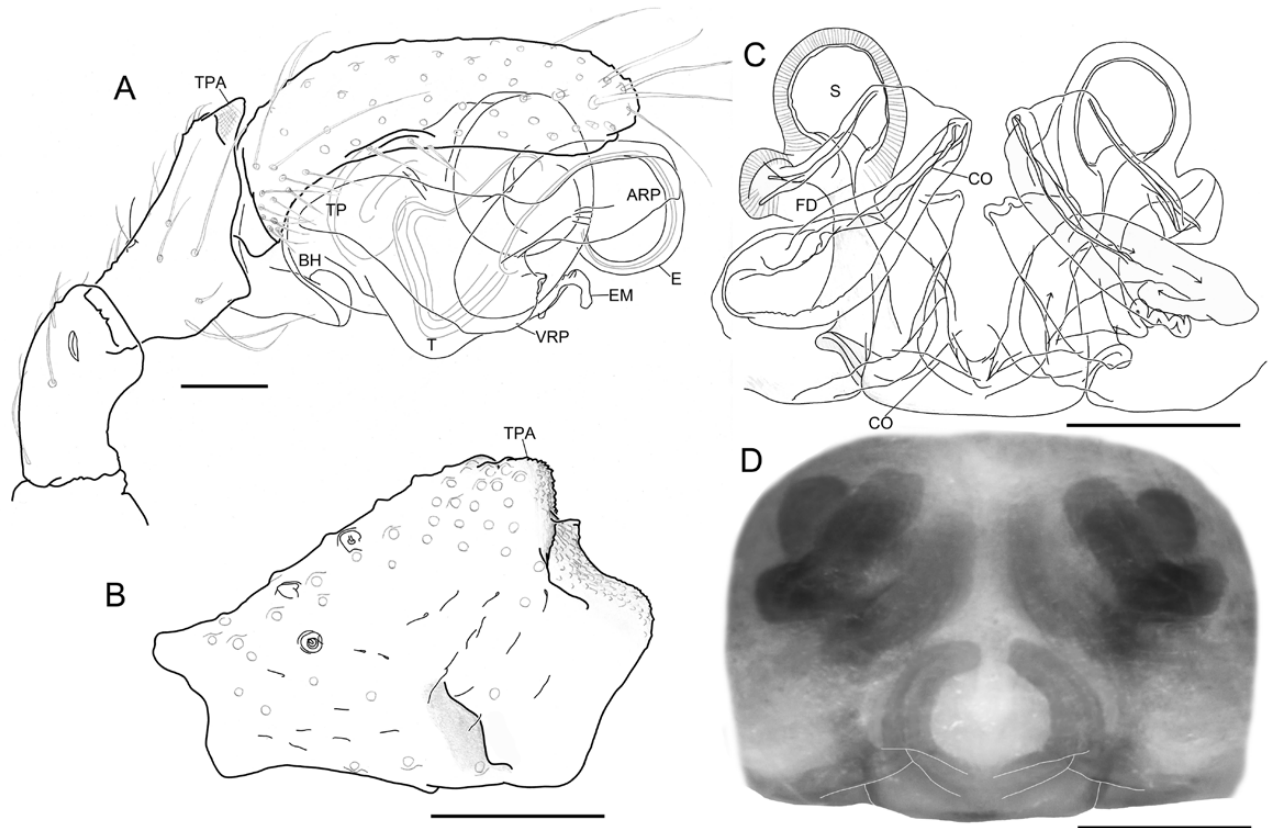


Figure 84. *Ummeliata insecticeps* (Bösenberg & Strand, 1906). A, B, male left palp. A, prolateral view. B, tibia, dorsal view. C, D, epigyne. C, ventral view. D, external morphology. Scale bars 0.1 mm.

impediment and the imbalance in collecting activity, particularly in the tropics, where the highest species diversity is usually expected. Clearly, every single description from poorly explored areas, such as South and South-East Asia (e.g. Wunderlich, 1974; Zhao & Li, 2014; Tanasevitch, 2017a, b, c), adds valuable knowledge. However, in these singleton descriptions, the newly discovered species are often assigned to existing taxa based on phenetic similarity, or new taxa are erected according to their autapomorphic features, instead of investigating shared derived features and referring to a species phylogeny. This is because a comparative approach is impeded by the small number of known species. Species descriptions often provide a set of diagnostic characters, illustrations of prosomal modifications and one or two perspectives of the male palp. These characters are useful for identification purposes, but are not necessarily informative for comparative studies, nor for providing insights about which informative characters are worth documenting when describing new species. Consequently, evolutionary questions are difficult to address in a meaningful way. Our work on the genus *Oedothorax*

also shows that the given state of classification fails to reflect the phylogenetic relationships among taxa. Designation of species to the existing taxa should entail detailed morphological characters and homology hypotheses. As suggested by the pioneering study of Hormiga (2000) on phylogenetics of erigonine spiders, we need to focus on taxon-based revisionary work and propose synapomorphies for taxa that will allow appropriate designation of new species.

RE-DELIMITED *OEDOTHORAX* AND RELATED TAXA

The results of our analysis, which is based on an expanded character matrix of Miller & Hormiga (2004) and Frick *et al.* (2010) (Matrix I), support the previous suggestion that *Callitrichia* and *Toschia* are closely related to *Oedothorax* (e.g. Holm, 1962; Wunderlich, 1978). Furthermore, our results suggest that *Holmelgonia* from Africa and *Nasoona*, *Shaanxinus* and *Ummeliata* from Asia are also closely related to *Oedothorax*. However, the relationship of these genera could not be resolved in our study. More characters and taxa might be necessary to tackle the current polytomy.

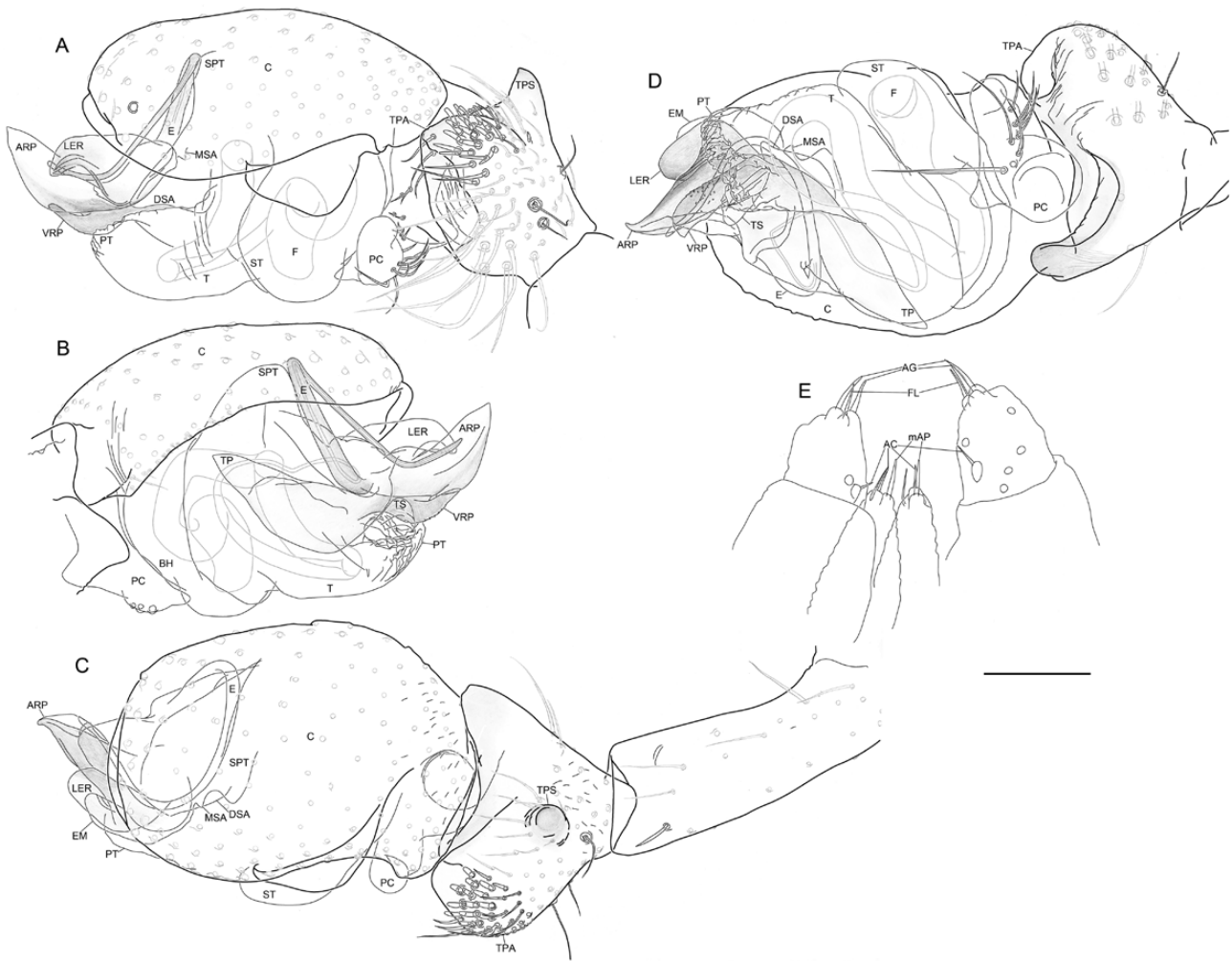


Figure 85. *Nasoona setifera* (Tanasevitch, 1998). A–, male right palp, images flipped horizontally. A, retrolateral view. B, prolateral view. C, dorsal view. D, ventral view. E, male posterior median spinnerets and posterior lateral spinnerets, dorsal view. Scale bar 0.1 mm.

The phylogenetic hypotheses generated from the EW, as well as the IW, analysis of Matrix II show species-groupings largely according to their geographical distribution: the ten species remaining in the robustly supported *Oedothorax* s.s. (Clade 27) are all distributed within the Palaearctic region, with the exception of *Oe. trilobatus* (also occurring in the Nearctic region). Additionally, all African taxa (i.e. *Callitrichia* and *Holmelgonia*), except '*Oe.*' *nazareti*, belong to Clade 39; *Ca. convector* and *Ca. usitata* are not part of this clade when analysed under implied weight with higher (2–4 for complete matrix; 2–5 for discrete character matrix) and lower concavity (5–1000 for complete matrix; 6–1000 for discrete character matrix), respectively. All five species on Clade 23 are of Palearctic distribution (*U. insecticeps* and *H. graminicola* also occur in the

continental Indomalayan region, including Taiwan); and, lastly, all *Mitrager* species (Clade 55, with the inclusion of *Ca. convector* in the analyses with implied weighting of high concavity) are of Himalayan and Indomalayan distribution. Interestingly, while Clade 39 and Clade 55 are collapsed in the consensus tree of the EW analysis of discrete characters, the implementation of implied weights to the analysis of discrete characters alone recovered these two clades and provided a grouping pattern similar to that of EW analysis of the complete Matrix II. As expected, the similarity between hypotheses generated from EW and IW analyses is at its highest (i.e. in number of recovered clades) when the homoplastic characters are only slightly down-weighted ($k = 1000$). Since the EW analysis of the discrete character matrix gave

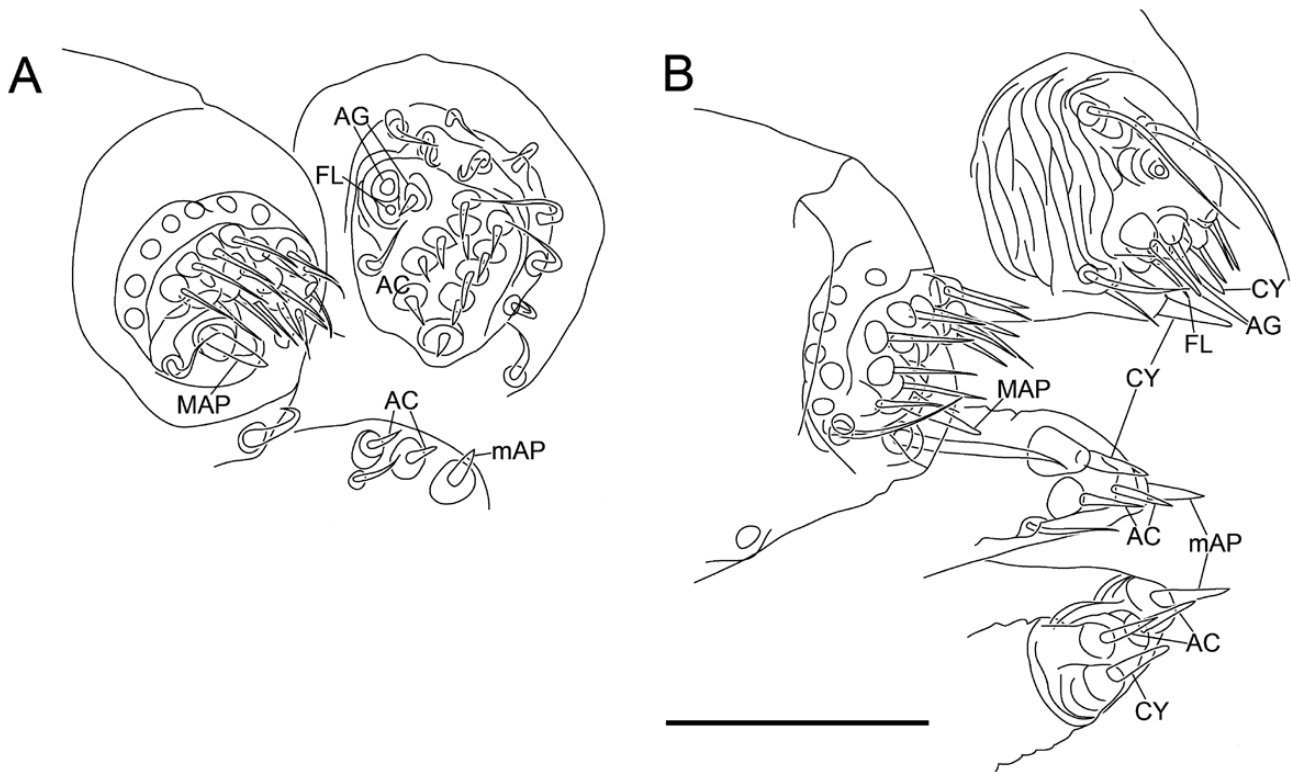


Figure 86. *Shaanxinus mingchihensis* Lin, 2019. A, male left spinnerets. B, female spinnerets. Scale bar 0.1 mm.

2472 most-parsimonious trees (MPTs), it could be questioned whether the three retained MPTs from the EW analysis of the complete Matrix II (with the continuous characters) are reliable or an artefact. However, due to the high level of congruence in its tree topology with that generated from the IW analysis of the discrete character matrix, and the independence between the discrete and the continuous characters, we regard the phylogeny from the EW analysis of the complete Matrix II as a plausible hypothesis of the relationships between our studied taxa.

The EW analysis of the complete Matrix II indicates a closer relationship between *Oedothorax* s.s. and Clade 23 (both of mainly Palearctic distribution), as well as a closer relationship between Clade 39 (Afrotropical) and Clade 55 (Himalayan/Oriental). However, the support of the deeper branches, namely the relationships between these four robust clades, are generally low. Nevertheless, when moderate to gentle k values (5–1000) were applied, the IW analyses of both discrete and discrete plus continuous characters show a closer relationship between *Oedothorax* s.s. and Clade 23, and the IW analysis of the discrete characters with $k = 1000$ shows a closer relationship between Clade 39 and Clade 55. These results coincide with the observed relationship between Afrotropical

and Himalaya/Oriental linyphiid fauna by [Tanasevitch \(2016\)](#), probably due to the connection between these continents before the Middle Jurassic break-up of Gondwana ([Besse & Courtilot, 1988](#); [Ali & Aitchison, 2008](#)).

LIMITATION OF MORPHOLOGICAL CHARACTERS IN RESOLVING INTRAGENERIC RELATIONSHIPS

In erigonines, male prosomal modifications and palpal features are highly variable, and have, therefore, provided the richest sources of somatic characters for phylogenetic analyses. Due to their involvement in courtship and copulation, these structures are probably subject to strong sexual selection, as is typically the case for animals with internal fertilization (e.g. [Arnqvist, 1998](#); [Hosken & Stockley, 2004](#); [Simmons, 2014](#)). However, under similar selective scenarios they may converge into similar features, resulting in misleading primary homology hypotheses. In addition, the different prosomal characters proposed here are unlikely to have evolved independently: the carapace being a single sclerite on which modifications vary in location across species. For instance, the different locations of glandular tissues could be the result of transformations between types of prosomal lobes,

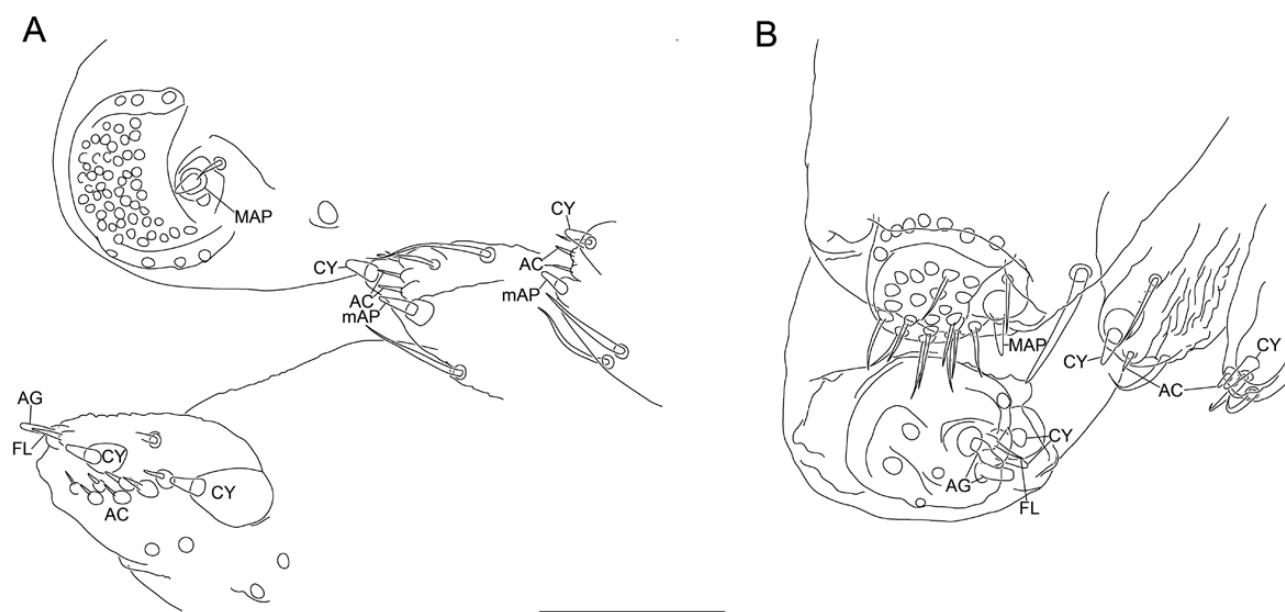


Figure 87. Female spinnerets of: A, *Linyphia triangularis* (Clerck, 1757); B, *Stemonyphantes lineatus* (Linnaeus, 1758). Scale bar 0.1 mm.

a situation observed in *Mitrager*, within which the prosomal modification transformed from post-PME lobe to PME lobe in Clade 71, from post-PME lobe to inter-PME lobe plus clypeal hump in *M. savigniformis* and to PME lobe in Clade 75. Furthermore, the degrees of elaboration of prosomal modifications within groups also varies from inconspicuous to highly pronounced. This may cause inappropriate scoring of the absence of prosomal elevations, as exemplified by *Oe. fuscus* and *Oe. agrestis*, which have internal glandular tissues in the post-PME region but barely any recognizable external modification (Michalik & Uhl, 2011). Since the internal glandular equipment is not necessarily linked to modified prosomata, scoring these species as not having a post-PME lobe will potentially result in character states that do not represent the true similarities among species. Therefore, exploration of the internal glandular tissue through histological examination or micro-computed-tomography (micro-CT) reconstruction is necessary to provide accurate scoring of prosomal character states.

In the present study, we explored the diversity of variations in palpal structures. The male palpal tibia of erigonines provides a rich source of variation that is useful for taxonomic and systematic analyses. Some specific morphological states were used for grouping species, such as the proposed synapomorphies ‘scaly margin of the palpal tibia prolateral apophysis with a retrolateral spike’ (Ch. 50) suggesting the sister-relationship of *Ca. latitibialis* and *Ca. longiductus*, or the synapomorphy ‘retrolaterally bent prolateral

spike’ (Ch. 53) for *Mitrager*. However, the characters related to the male palpal tibia are also subject to the same challenges as the prosomal characters, since the tibia is a single sclerite and the variations in size, location and shape of its apophyses are continuous and possibly evolved convergently. Therefore, primary homology hypotheses for specific apophyses observed among species are largely based on human perception of similarity, and are inherently arbitrary. In our study, the palpal tibial characters did not provide support for relationships above the genus level, except for the presence of palpal tibial apophyses for the whole erigonine branch. Incongruence among characters and their consequently high homoplasy limits the value of palpal characters for resolving intrageneric relationships, in Miller & Hormiga (2004), Frick *et al.* (2010) and the present study. All these studies investigated detailed morphological characters at a higher taxonomic level of the Erigonine subfamily and for the particular group of taxa closely related to *Oedothorax*. Henceforth, DNA sequences may be necessary for further resolving intrageneric relationships in the erigonine phylogeny. In addition, Miller & Hormiga (2004) scored six behavioural traits in their character matrix of which five characters pertained to mating and web-building. However, since behavioural data are lacking for most of their studied species, the phylogenetic information is low. As the majority of species from Afrotropical and Oriental regions are limited to museum specimens and are available only as singletons or from few type specimens,

Table 1. List of abbreviations used in the text and figures.

Male: pedipalp	
ARP	anterior radical process <i>sensu</i> Hormiga (2000)
BH	basal haematodocha
BT	palpal tibial prolateral apophysis basal thorn
C	cymbium
DSA	distal suprategular apophysis <i>sensu</i> Hormiga (2000)
E	embolus
ED	embolic division
EM	embolic membrane <i>sensu</i> Hormiga (1993)
F	fundus
LER	lateral extension of radix
MSA	marginal suprategular apophysis <i>sensu</i> Miller (1999)
PC	paracymbium
PT	protegulum <i>sensu</i> Holm (1979)
R	radix <i>sensu</i> Miller and Hormiga (2004)
SPT	suprategulum
ST	subtegulum
T	tegulum
TP	radical tailpiece <i>sensu</i> Crosby and Bishop (1925)
TPA	palpal tibial prolateral apophysis
TPS	palpal tibial prolateral spike
TRA	palpal tibial retrolateral apophysis
TS	tegular sac <i>sensu</i> Hormiga (2000)
VRP	ventral radical process
Female: Epigyne	
CD	copulatory duct
CO	copulatory opening
FD	fertilization duct
S	spermatheca
Ocular area	
ALE	anterior lateral eye(s)
AME	anterior median eye(s)
PLE	posterior lateral eye(s)
PME	posterior median eye(s)
Spinneret	
AC	aciniform gland spigot(s)
AG	aggregate gland spigot(s)
ALS	anterior lateral spinneret(s)
CY	cylindrical gland spigot(s)
FL	flagelliform gland spigot(s)
mAP	minor ampullate gland spigot(s)
n	nubbin
PLS	posterior lateral spinneret(s)
PMS	posterior median spinneret(s)
Institutions	
AMNH	American Museum of Natural History, USA

Table 1. Continued

NHM	Natural History Museum, London, United Kingdom
RMCA	Royal museum of Central Africa, Tervuran, Belgium
MHN	Muséum d'histoire naturelle de Genève, Geneva, Switzerland
MNHN	Muséum national d'Histoire naturelle, Paris, France
SMF	Senckenberg Museum, Frankfurt am Main, Germany
ZIMG	Zoological Institute and Museum, University Greifswald, Germany
ZMUC	Zoological Museum, University of Copenhagen, Denmark
ZMMU	Zoological Museum of Moscow University, Russia
Abbreviations in synonymy lists	
Dm, Df or Dmf	Original description of the male, the female or both the male and the female
f	Female epigynal illustrations are included
m	Male palpal illustrations are included
mf	Both Male palpal and female epigynal illustrations are included
Tmf or Tm	Both sexes or the male have/has been transferred from a specified genus to the one under consideration

material is not at hand for molecular approaches and behavioural observations. For the available museum specimens, the extraction of genetic material is also impeded by the small body size of the erigonines, and most of them have been preserved under room temperature for long periods.

LOSSES OF SPIGOTS AND THEIR ECOLOGICAL IMPLICATION

According to the reconstruction of character transformations on the cladograms in [Miller & Hormiga \(2004: figs 4–7\)](#) and [Frick *et al.* \(2010: figs 3–6\)](#), character state transformations in spigots within erigonines include reduction in the numbers of aggregate, flagelliform or aciniform gland spigots on the posterior lateral spinnerets, and reduction in the number of aciniform gland spigots on the posterior median spinnerets. The data of [Miller & Hormiga \(2004\)](#) and [Frick *et al.* \(2010\)](#) suggest that these changes occurred only at terminals and within genera and, therefore, provide no information on intergeneric relationships. Our results show that the losses of spigots provide support for relationships among certain

species within the genera *Callitrichia* and *Mitrager*. The absence of aciniform gland spigots in Clade 45 (i.e. *Ca. sellafontis*, *Ca. juguma* and *Ca. uncata*) suggests that these species might perform weak to no prey-wrapping, since aciniform gland spigots are used by spiders for prey-wrapping, retreat building, egg-sac building and sperm web-building (Coddington, 1989; Foelix, 2011). The smaller number of aciniform gland spigots in Linyphiidae suggests that they generally release fewer silk strands, as was shown for *L. triangularis* during prey-wrapping (Peters & Kooor, 1991). So far there is no report on other spigots taking over these functions. Furthermore, the three *Callitrichia* species mentioned above (and also *Ca. convector*) have no aggregated gland spigots. In Miller & Hormiga (2004), the presence of the posterior lateral spinneret triplet (one flagelliform gland spigot plus two aggregate gland spigots) in adult males provided ambiguous support for Linyphiidae with the reversal in Linyphiinae. In the above-mentioned four *Callitrichia* species, however, not only the adult males but also the adult females lack this triplet, as was also reported from *Drapetisca socialis*, *Neriene peltata* (Schütt, 1995) and some other dwarf spiders (Nentwig & Heimer, 2009). Aggregate gland spigots are associated with the production of sticky silk for prey capture, and the absence of these spigots in these species implies hunting strategies without sticky silk. Furthermore, the absence of minor ampullate gland spigots in *Ca. sellafontis*, *Ca. uncata*, *Ca. juguma* and some *Mitrager* species is probably connected with the reduction of web-building, since these glands are important for connecting the strands of the meshwork in linyphiid sheet webs (Peters & Kooor, 1991). In addition, silk strands from minor ampullate gland spigots, combined with silk strands from aciniform spigots, serve as bridging lines for dispersal in Araneidae (*Araneus diadematus*) (Peters, 1990). Consequently, their absence might suggest that these spiders may have reduced bridging or ballooning behaviours, which could still be carried out by major ampullate gland silks alone. Theoretically, the web reduction might indicate a strategy of actively luring prey (e.g. by chemicals, *Mastophora hutchinsoni*; Yeorgan, 1988), or by choosing an environment with abundant prey (Schütt, 1995). Prey (collembolans and other small invertebrates) might be plentiful where these particular species occur – in litter and/or low vegetation in tropical, humid areas – which might select for web reduction. The rows of long setae on the first and second pairs of legs in most *Callitrichia* species previously belonging to *Ophrynia* may serve to hold prey, similar to *D. socialis*, which holds prey with the strong, inwardly directed setae on the palps (Schütt, 1995). The webs of *Callitrichia* and *Mitrager* species have not yet been investigated, which is needed

for testing the assumption of a relationship between spigot reduction and ecological adaptation in these erigonines.

Evolution of male prosomal structures (refers to Fig. 4)

According to our phylogenetic hypothesis, the post-PME lobe is the most homoplastic prosomal feature, with nine to ten independent origins, followed by the PME lobe with eight origins. Similarly, in Miller & Hormiga (2004) and Frick *et al.* (2010), the post-PME lobe evolved six times, and the the PME lobe three and four times, respectively. On the other hand, the lateral sulci have four origins in Miller & Hormiga and Frick *et al.* (2010), whereas our study suggest that the lateral sulci and pits have evolved three times independently in different lineages. This pattern fits with the assumption of Schaible & Gack (1987) that the prosomal structures have evolved multiple times independently from species without external modifications. They hypothesized that the ancestral species already possessed nuptial-gift-producing glandular tissue, as well as the corresponding pore-bearing region on the prosoma. Due to selective advantages in transfer of secretions and female choice, secondary structures like apophyses, sulci and pits may have evolved. In *Oedothorax*, nuptial-gift-related glandular tissues were found in two species with minor or no external prosomal modification, *Oe. fuscus* and *Oe. agrestis*. However, only five species were investigated in this ultrastructural study (Michalik & Uhl, 2011). Assessing presence and absence of prosomal glandular tissue, its location and degree of complexity, requires histological and ultrastructural examination. Consequently, the current data do not suffice to reconstruct the ancestral state of the glandular equipment in *Oedothorax*, or in *Mitrager* or *Callitrichia*. However, with the current knowledge, it seems justified to assume by analogy that all modifications are associated with glandular tissue, and thus play a role in the mating process.

In Clade 72 within *Mitrager*, all species have some form of prosomal elevation. The difference in prosomal modifications might be correlated with different locations of glandular tissues across the areas on the prosoma. Since the nuptial-gift-producing area on the male prosoma is in contact with the female mouthparts during copulation in all species studied so far (see Introduction), the location of the glandular tissue is associated with the mating posture. Therefore, changes in the location and size of the glandular tissue might have evolved with minor changes in mating positions. On the other hand, changes in palpal structures might have resulted in minor changes in mating positions that

changed the contact zone between female mouthparts and the nuptial-gift-producing area slightly. Selection on the effectiveness of the interplay between prosomal shape and glandular tissue, as well as of the palpal structures, could have resulted in divergent sexual selection and, ultimately, in relatively high speciation rates. Similar changes in different lineages could have increased the probability of parallelisms, leading to the homoplastic pattern of character changes. This has also been observed in sexually dimorphic cichlid fish and sticklebacks, in which body size and colour also evolved in parallel across divergent lineages, implicating sexual selection as one of their major engines of speciation (Boughman *et al.*, 2005; Genner & Turner, 2005).

The genus *Oedothorax* was selected in this study due to its species richness and large variation in male prosomal modifications. However, the traditional delimitation of this genus was not phylogeny-based. Our revision suggests that only nine species are phylogenetically congeneric with the type species. Although the genus *Oedothorax* s.s. has had a fairly long history of faunistic and taxonomic studies in the Palearctic region, the latest species discovery was three decades ago (*Oe. meridionalis* Tanasevitch, 1987). Consequently, we consider the chances of a further discovery of new *Oedothorax* species in this region as low. In contrast to the now relatively low species diversity of *Oedothorax*, the revised *Callitrichia* and *Mitrager* comprise to date 55 and 24 species, respectively. Most of the species of *Callitrichia* and *Mitrager* were found in the Afrotropical and Oriental regions, respectively. Considering the lower degree of exploration of linyphiid spider diversity in these regions, we suggest that further studies in these areas may lead to a considerable increase in the number of described species. Both *Callitrichia* and *Mitrager* show high morphological diversity in prosomal modifications. These newly delimited taxa lay the groundwork for estimating the effect of sexual selection on speciation rate.

CONCLUSIONS

Over the course of research history on the genus *Oedothorax*, many species have been described, and speculations about their relationships to other erigonines have been proposed. The present study provides a revision of *Oedothorax* and several other taxa with similar genital structures. We re-delimited the genus *Oedothorax* based on synapomorphies, as well as the genus *Mitrager*, which includes most of the Oriental species previously described under *Oedothorax*. In addition, all but one African species previously assigned to *Oedothorax*, as well as *Typhistes gloriosus*, *Ophrynia* and *Toschia*, are transferred to the genus *Callitrichia*.

Our analysis showed that a variety of male prosomal modifications have evolved multiple times in parallel, which indicates that sexual selection has played an important role in the evolution of these sexually dimorphic features, as well as in species diversification of erigonine spiders. Due to the homoplastic property of these characters, they are not suitable as the sole defining characters of taxa above species or species-group level. We found that features on the male palps are useful characters for delimiting species. However, we might have approached the limits of potentially revealing morphological characters for phylogenetic analysis. The high probability of homoplasy of prosomal and palpal features, and the difficulty in inferring homology, limit their explanatory power for resolving intrageneric relationships within Erigoninae. This is contrary to the notion of Frick *et al.* (2010) that linyphiid genital morphology still offers many more characters to be scored for phylogenetic analyses.

Further investigations aiming at reconstructing erigonine phylogeny should incorporate DNA sequence data, which might be feasible with a combination of newly collected specimens and ancient DNA approaches (Dabney *et al.*, 2013; Tin *et al.*, 2014; Cotoras *et al.*, 2017). For addressing the evolution of nuptial-gift-related sexually dimorphic structures and its correlation with speciation rate, a focus on two groups of erigonines seems the next reasonable step in this direction. First, the genus *Callitrichia* has a relatively high species number, and contains lineages with prominent and diverse prosomal structures (species previously under *Callitrichia*, *Typhistes* and *Ophrynia*), as well as lineages without obvious external modifications (species previously under *Oedothorax* and *Toschia*). *Callitrichia* is also closely related to *Holmelgonia*, a genus in which all described species lack prosomal modifications (Nzigidahera & Jocqué, 2014). Second, the relatively well-supported Clade 24 in this study also contains one clade with (*Ummeliata*) and the other clade without (*Hylyphantes* and *Tmeticus*) prosomal modifications. These groups allow for comparisons between sister-taxa with potentially different strengths of sexual selection on prosomal modifications. Such a targeted phylogenetic analysis could include the assessment of behavioural traits involved in gustatory versus non-gustatory mating, which might yield additional revealing information on how sexual selection impacts speciation rate.

ACKNOWLEDGEMENTS

We would like to thank Nikolaj Scharff (Copenhagen, Denmark) and Holger Frick (Aarau, Switzerland) for their training in linyphiid morphology and phylogenetic analyses to SL, and their support during the construction of Matrix I. For production of images we thank Peter

Michalik and Tim Dederichs (Greifswald, Germany). For discussion on the taxonomic work we thank Michael 'Theo' Schmidt (Greifswald, Germany). For the loan of specimens we are grateful to the following people and institutions: Shuqiang Li (Institute of Zoology, Chinese Academy of Sciences, Peking, China), Nikolaj Scharff (ZMUC, Copenhagen, Denmark), Rudy Jocqué, Didier van den Spiegel and Arnaud Henrard (RMCA, Tervuren, Belgium), Andrei V. Tanasevitch (A. N. Severtsov Institute of Ecology and Evolution, Moscow, Russia), Peter Jäger and Julia Altmann (SMF, Frankfurt, Germany), Peter Schwendinger (MHNG, Geneva, Switzerland), Kirill Glebovich *Mikhailov* (ZMMU, Moscow, Russia), Peter van Helsdingen and Karen van Dorp (Leiden, Netherland), Jan Beccaloni (NHM, London, UK), Lorenzo Prendini and Louis Sorkin (AMNH, New York City, USA). This project was financed by a stipend from the Ministry of Education of Taiwan and a DAAD Stipend, both to SL. The work at the ZMUC in Copenhagen was supported by a grant from the International Office of the University of Greifswald to SL. The authors declare that they have no conflict of interests.

REFERENCES

- Aakra K. 2000.** New records of spiders (Araneae) from Norway with notes on epigynal characters of *Philodromus fuscomarginatus* (De Geer) (Philodromidae) and *Araneus sturmi* (Hahn) (Araneidae). *Norwegian Journal of Entomology* **47**: 77–88.
- Alderweireldt M. 1992.** Determinatieproblematiek van de zustersoorten van het genus *Oedothorax* (Araneae, Linyphiidae). *Nieuwsbrief van de Belgische Arachnologische Vereniging* **7**: 4–8.
- Ali JR, Aitchison JC. 2008.** Gondwana to Asia: plate tectonics, paleogeography and the biological connectivity of the Indian sub-continent from the Middle Jurassic through latest Eocene (166–35 Ma). *Earth-Science Reviews* **88**: 145–166.
- Álvarez-Padilla F, Hormiga G. 2008.** A protocol for digesting internal soft tissues and mounting spiders for scanning electron microscopy. *Journal of Arachnology* **35**: 538–542.
- Andersson M. 1994.** *Sexual selection*. Princeton: Princeton University Press.
- Arnedo MA, Hormiga G, Scharff N. 2009.** Higher-level phylogenetics of linyphiid spiders (Araneae, Linyphiidae) based on morphological and molecular evidence. *Cladistics* **25**: 231–262.
- Arnqvist G. 1998.** Comparative evidence for the evolution of genitalia by sexual selection. *Nature* **393**: 784–786.
- Austad SN. 1984.** Evolution of sperm priority patterns in spiders. In: Smith RL, ed. *Sperm competition and the evolution of animal mating systems*. London: Academic Press, 223–249.
- Banks N. 1896.** A few new spiders. *The Canadian Entomologist* **28**: 62–65.
- Banks N. 1900.** Arachnida of the expedition. In: Papers from the Harriman Alaska Expedition. XI. Entomological results: 5 Arachnida. *Proceedings of the Washington Academy of Sciences* **2**: 477–486.
- Banks N. 1901.** Some Arachnida from New Mexico. *Proceedings of the Academy of Natural Sciences of Philadelphia* **53**: 568–597.
- Banks N. 1910.** Catalogue of Nearctic spiders. *Bulletin, United States National Museum* **72**: 1–80.
- Banks N. 1916.** Revision of Cayuga Lake spiders. *Proceedings of the Academy of Natural Sciences of Philadelphia* **68**: 68–84.
- Bao M, Bai Z, Tu LH. 2017.** On a desmitracheate 'micronetine' *Nippononeta alpina* (Li & Zhu, 1993), comb. n. (Araneae, Linyphiidae). *Zookeys* **645**: 133–146.
- Barrion AT, Litsinger JA. 1994.** Taxonomy of rice insect pests and their arthropod parasites and predators. In: Heinrichs EA, ed. *Biology and management of rice insects*. New Delhi: Wiley Eastern, 13–15, 283–359.
- Becker L. 1896.** Les arachnides de Belgique, deuxième et troisième parties. *Annales du Musée Royal d'Histoire Naturelle de Belgique* **12**: 1–127.
- Bertani R. 2001.** Revision, cladistic analysis, and zoogeography of *Vitalius*, *Nhandu*, and *Proshapalopus*; with notes on other theraphosine genera (Araneae, Theraphosidae). *Arquivos de Zoologia. São Paulo* **36**: 265–356.
- Besse J, Courtillot V. 1988.** Paleogeographic maps of the continents bordering the Indian Ocean since the early Jurassic. *Journal of Geophysical Research* **93B**: 1791–1808.
- Bishop SC, Crosby CR. 1935.** Studies in American spiders: miscellaneous genera of Erigoneae, part I. *Journal of The New York Entomological Society* **43**: 217–241, 255–280.
- Blackwall J. 1834.** Characters of some undescribed genera and species of Araneidae. In: Blackwall J, ed. *Researches in zoology, illustrative of the manners and economy of animals; with descriptions of numerous species new to naturalists; accompanied by plates*. London: Simpkin and Marshall, 304–426, pl. 2–3.
- Blackwall J. 1841.** The difference in the number of eyes with which spiders are provided proposed as the basis of their distribution into tribes; with descriptions of newly discovered species, and the characters of a new family and three new genera of spiders. *Transactions of the Linnean Society of London* **18**: 601–670.
- Blackwall J. 1850.** Descriptions of some newly discovered species and characters of a new genus of Araneida. *Annals and Magazine of Natural History (2)* **6**: 336–344.
- Blackwall J. 1853.** Descriptions of some newly discovered species of Araneidea. *Annals and Magazine of Natural History* **11**: 14–25.
- Blackwall J. 1864.** A history of the spiders of Great Britain and Ireland. *Ray Society* **2**: 175–384.
- Blest AD, Taylor HH. 1977.** The clypeal glands of *Mynoglenes* and of some other linyphiid spiders. *Journal of Zoology* **183**: 473–493.
- Bond JE, Opell BD. 1997.** Systematics of the spider genera *Mallos* and *Mexitlia* (Araneae, Dictynidae). *Zoological Journal of the Linnean Society* **119**: 386–445.

- Bösenberg W. 1902.** Die Spinnen Deutschlands. II–IV. *Zoologica (Stuttgart)* **14**: 97–384.
- Bösenberg W, Strand E. 1906.** Japanische Spinnen. *Abhandlungen der Senckenbergischen Naturforschenden Gesellschaft* **30**: 93–422.
- Bosmans R. 1977.** Spiders of the subfamily Erigoninae from Mount Kenya. Scientific report of the Belgian Mt. Kenya Bio-Expedition, n° 3. *Revue Zoologique Africaine* **91**: 449–472.
- Bosmans R. 1985.** Études sur les Linyphiidae nord-africains. II. Le genre *Oedothorax* Bertkau en Africa du Nord, avec une révision des caractères diagnostiques des mâles des espèces ouest-paléarctiques. *Biologisch Jaarboek Dodona* **53**: 58–75.
- Bosmans R. 1988.** Scientific report of the Belgian Cameroon expeditions 1981 and 1983. No. 18. Further Erigoninae and Mynogleninae (Araneae: Linyphiidae) from Cameroonian highlands. *Revue Zoologique Africaine* **102**: 5–32.
- Bosmans R, Van Keer J. 2012.** On the spider species described by L. Koch in 1882 from the Balearic Islands (Araneae). *Arachnologische Mitteilungen* **43**: 5–16.
- Bosselaers J, Jocqué R. 2002.** Studies in Corinnidae: Cladistic analysis of 38 corinnid and liocranid genera, and transfer of Phrurolithinae. *Zoologica Scripta* **31**: 241–270.
- Boughman JW, Rundle HD, Schluter D. 2005.** Parallel evolution of sexual isolation in sticklebacks. *Evolution* **59**: 361–373.
- Brignoli PM. 1983.** *A catalogue of the Araneae described between 1940 and 1981*. Manchester: Manchester University Press.
- Bristowe WS. 1931.** The mating habits of spiders: a second supplement, with the description of a new thomisid from Krakatau. *Proceedings of the Zoological Society of London* **4**: 1401–1412.
- Buckle D, Carroll D, Crawford R, Roth V. 2001.** Linyphiidae and Pimoidae of America north of Mexico: checklist, synonymy, and literature. *Fabrerias, Supplement* **10**: 89–191.
- Canard A, Cruveillier M. 2016.** Rectifications nomenclaturales à apporter au catalogue mondial des araignées (1ère note). *Revue Arachnologique* **2**: 42–45.
- di Caporiacco L. 1935.** Aracnidi dell'Himalaia e del Karakoram, raccolti dalla Missione italiana al Karakoram (1929–VII). *Memorie della Società Entomologica Italiana, Genova* **13**: 161–263.
- di Caporiacco L. 1949.** Aracnidi della colonia del Kenya raccolti da Toschi e Meneghetti negli anni 1944–1946. *Commentationes Pontificia Academia Scientiarum* **13**: 309–492.
- Chamberlin RV. 1920.** New spiders from Utah. *The Canadian Entomologist* **52**: 193–201.
- Chamberlin RV. 1949.** On some American spiders of the family Erigonidae. *Annals of the Entomological Society of America* **41**: 483–562.
- Chen XE, Gao JC. 1990.** *The Sichuan farmland spiders in China*. Chengdu: Sichuan Science and Technology Publishing House.
- Chen ZF, Zhang ZH. 1991.** *Fauna of Zhejiang: Araneida*. Hangzhou: Zhejiang Science and Technology Publishing House.
- Chyzer C, Kulczyński W. 1894.** *Araneae Hungariae. Tomus II*. Budapest: Academia Scientiarum Hungaricae.
- Coddington JA. 1989.** Spinneret silk spigot morphology: evidence for the monophyly of orbweaving spiders, Cyrtophorinae (Araneidae), and the group Theridiidae plus Nesticidae. *Journal of Arachnology* **17**: 71–95.
- Coddington JA. 1990.** Ontogeny and homology in the male palpus of orb-weaving spiders and their relatives, with comments on phylogeny (Araneoclauda: Araneoidea, Deinopoidea). *Smithsonian Contribution to Zoology* **496**: 1–52.
- Costa-Schmidt LE, Carico JE, de Araújo AM. 2008.** Nuptial gifts and sexual behavior in two species of spider (Araneae, Trechaleidae, *Paratrechalea*). *Naturwissenschaften* **95**: 731–739.
- Cotoras DD, Murray GG, Kapp J, Gillespie RG, Griswold C, Simison WB, Green RE, Shapiro B. 2017.** Ancient DNA resolves the history of *Tetragnatha* (Araneae, Tetragnathidae) spiders on Rapa Nui. *Genes* **8**: 403.
- Crosby CR. 1905.** A catalogue of the Erigoneae of North America, with notes and descriptions of new species. *Proceedings of the Academy of Natural Sciences of Philadelphia* **57**: 301–343.
- Crosby CR, Bishop SC. 1925.** Studies in New York spiders. Genera: *Ceratinella* and *Ceraticelus*. *New York State Museum Bulletin* **264**: 1–71.
- Crosby CR, Bishop SC. 1928.** Araneae. In: A list of the insects of New York. *Memoirs of the Cornell University Agricultural Experiment Station* **101**: 1034–1074.
- Crosby CR, Bishop SC. 1935.** A new species of *Hybocoptus* from New York. *Entomological News* **46**: 125–127.
- Crosby CR, Bishop SC. 1936.** Studies in American spiders: Miscellaneous genera of Erigoneae. *Festschrift Embrik Strand* **2**: 52–64.
- Dabney J, Knapp M, Glocke I, Gansauge MT, Weihmann A, Nickel B, Valdiosera C, García N, Pääbo S, Arsuaga JL, Meyer M. 2013.** Complete mitochondrial genome sequence of a Middle Pleistocene cave bear reconstructed from ultrashort DNA fragments. *Proceedings of the National Academy of Sciences of the United States of America* **110**: 15758–15763.
- Dahl F. 1883.** Analytische Bearbeitung der Spinnen Norddeutschlands mit einer anatomisch-biologischen Einleitung. *Schriften des Naturwissenschaftlichen Vereins für Schleswig-Holstein* **5**: 13–88.
- Dahl F. 1886.** Monographie der *Erigone*-Arten im Thorell'schen Sinne nebst anderen Beiträgen zur Spinnenfauna Schleswig-Holsteins. *Schriften des Naturwissenschaftlichen Vereins für Schleswig-Holstein* **6**: 65–102.
- Dahl F. 1912.** Über die Fauna des Plagefenn-Gebietes. In: Conwentz H, ed. *Das Plagefenn bei Chorin*. Berlin, 339–638, Araneae, 575–622.
- Davies VT. 1998.** A revision of the Australian metaltellines (Araneae: Amaurobioidea: Amphinctidae: Metaltellinae). *Invertebrate Taxonomy* **12**: 211–243.
- Davies VT, Lambkin C. 2001.** A revision of *Procambidgea* Forster & Wilton, (Araneae: Amaurobioidea: Stiphidiidae). *Memoirs of the Queensland Museum* **46**: 443–459.

- De Keer R, Maelfait J-P. 1987.** Laboratory observations on the development and reproduction of *Oedothorax fuscus* (Blackwall, 1834) (Araneida linyphiidae) under different conditions of temperature and food supply. *Revue d'Ecologie et de Biologie du Sol* **24**: 63–73.
- De Keer R, Maelfait J-P. 1988.** *Oedothorax gibbosus* (Blackwall) and *Oedothorax tuberosus* (Blackwall): one species. *Newsletter of the British Arachnological Society* **53**: 3.
- De Lessert R. 1910.** *Catalogue des invertébrés de la Suisse. Fasc. 3, Araignées.* Geneva: Musée d'histoire naturelle de Genève.
- Denis J. 1947.** Notes sur les érigonides. XI. Les espèces françaises du genre *Oedothorax* Bertkau. *Bulletin de la Société d'Histoire Naturelle de Toulouse* **82**: 131–158.
- Denis J. 1964.** Notes sur les érigonides. XXIX. Une forme pyrénéenne d'*Erigonella subelevata* (L. Koch). *Bulletin de la Société Zoologique de France* **89**: 673–675.
- Denis J. 1968.** Notes d'aranéologie marocaine. X, Les érigonides du Maroc. *Bulletin de la Société des Sciences Naturelles du Maroc* **47**: 137–164.
- Dingerkus G, Uhler L. 1977.** Enzyme clearing of alcian blue stained whole small vertebrates for demonstration of cartilage. *Stain Technology* **52**: 229–232.
- Dupérré N, Harms D. 2018.** Raising the dead: rediscovery and redescription of some lost spider types (Araneae) described by Eugène Simon. *Evolutionary Systematics* **2**: 1.
- Emerton JH. 1882.** New England spiders of the family Theridiidae. *Transactions of the Connecticut Academy of Arts and Sciences* **6**: 1–86.
- Emerton JH. 1909.** Supplement to the New England spiders. *Transactions of the Connecticut Academy of Arts and Sciences* **14**: 171–236.
- Eskov KY. 1990.** The spider genus *Collinsia* O. Pickard-Cambridge 1913 in the fauna of Siberia and the Soviet Far East (Arachnida: Araneae: Linyphiidae). *Senckenbergiana Biologica* **70**: 287–298.
- Eskov KY, Marusik YM. 1994.** New data on the taxonomy and faunistics of North Asian linyphiid spiders (Aranei Linyphiidae). *Arthropoda Selecta* **2**: 41–79.
- Fage L, Simon E. 1936.** Arachnida. III. Pedipalpi, Scorpiones, Solifuga et Araneae (1re partie). In: Mission scientifique de l'Omo. *Mémoires du Muséum d'Histoire Naturelle de Paris* **4**: 293–340.
- Fedotov D. 1912.** K faunii Paoukow Mourmana i Nowoi Zemli. Contribution à la faune des araignées de la côte Murmane et de Novaja Zemlja. *Lejiegod Zoologicheskii Instituta Muzeya Akademii Nauk SSSR St. Petersburg* **16**: 449–474.
- Foelix RF. 2011.** *Biology of spiders, 3rd edn.* New York: Oxford University Press.
- Förster A, Bertkau P. 1883.** Beiträge zur Kenntniss der Spinnenfauna der Rheinprovinz. *Verhandlungen des Naturhistorischen Vereins der Preussischen Rheinlande und Westfalens* **40**: 205–278.
- Frick H, Scharff N. 2014.** Phantoms of Gondwana? – phylogeny of the spider subfamily Mynogleninae (Araneae: Linyphiidae). *Cladistics* **30**: 67–106.
- Frick H, Nentwig W, Kropf C. 2010.** Progress in erigonine spider phylogeny—the *Savignia*-group is not monophyletic (Araneae: Linyphiidae). *Organisms Diversity & Evolution* **10**: 297–310.
- Gao JC, Fei R, Xing SY. 1996.** A new species of the genus *Nasoona* from China (Araneae: Linyphidae: Erigoninae). *Acta Zootaxonomica Sinica* **21**: 29–31.
- Gao JC, Xing SY, Zhu CD. 1996.** Two new species of the genera *Toschia* and *Aprifrontalia* from China (Araneae: Linyphiidae: Erigoninae). *Acta Zootaxonomica Sinica* **21**: 291–295.
- Genner M, Turner GF. 2005.** The mbuna cichlids of Lake Malawi: a model for rapid speciation and adaptive radiation. *Fish and Fisheries* **6**: 1–34.
- Goloboff PA. 1993.** Estimating character weights during tree-search. *Cladistics* **9**: 83–91.
- Goloboff PA, Mattoni CI, Quinteros AS. 2006.** Continuous characters analyzed as such. *Cladistics* **22**: 589–601.
- Goloboff PA, Farris JS, Nixon KC. 2008.** TNT, a free program for phylogenetic analysis. *Cladistics* **24**: 774–786.
- Griswold CE. 1990.** A revision and phylogenetic analysis of the spider subfamily Phyxelidinae (Araneae, Amaurobiidae). *Bulletin of the American Museum of Natural History* **196**: 1–206.
- Griswold CE. 1993.** Investigations into the phylogeny of lycosoid spiders and their kin (Arachnida: Araneae: Lycosoidea). *Smithsonian Contribution to Zoology* **539**: 1–39.
- Griswold CE, Coddington JA, Hormiga G, Scharff N. 1998.** Phylogeny of the orb-web building spiders (Araneae, Orbicularia: Deinopoidea, Araneoidea). *Zoological Journal of the Linnean Society* **123**: 1–99.
- Griswold CE, Coddington JA, Platnick NI, Forster RR. 1999.** Towards a phylogeny of entelegyne spiders (Araneae, Entelegynae). *Journal of Arachnology* **27**: 53–63.
- Grube AE. 1859.** Verzeichniss der Arachnoiden Liv., Kur und Ehstlands. *Archiv für die Naturkunde Liv-, Ehst- und Kurlands* **1**: 415–486.
- Gwynee DT. 2008.** Sexual conflict over nuptial gifts in insects. *Annual Review of Entomology* **53**: 83–101.
- Han G, Zhang F. 2014.** A new species of the genus *Ummeliata* Strand 1942 (Araneae: Linyphiidae) from China. *Acta Arachnologica* **63**: 1–5.
- Heimer S. 1984.** A new linyphiid spider from Vietnam (Arachnida, Araneae). *Reichenbachia* **22**: 87–89.
- Heimer S. 1987.** Neue Spinnenarten aus der Mongolei (MVR) (Arachnida, Araneae, Theridiidae et Linyphiidae). *Reichenbachia* **24**: 139–151.
- Heimer S, Nentwig W. 1991.** *Spinnen mitteleuropas: ein Bestimmungsbuch.* Berlin: Paul Parey.
- Heinemann S, Uhl G. 2000.** Male dimorphism in *Oedothorax gibbosus* (Araneae, Linyphiidae): a morphometric analysis. *Journal of Arachnology* **28**: 23–28.
- Holm Å. 1962.** The spider fauna of the East African mountains. Part I: Fam. Erigonidae. *Zoologiska Bidrag från Uppsala* **35**: 19–204.
- Holm Å. 1968.** Spiders of the families Erigonidae and Linyphiidae from East and Central Africa. *Annales, Musée Royal de l'Afrique Centrale, Sciences Zoologiques* **171**: 1–49.

- Lewis S, South A. 2012.** The evolution of animal nuptial gifts. In: *Advances in the study of behavior*. Amsterdam: Elsevier, 53–97.
- Lewis S, South A, Burns R, Al-Wathiqui N. 2011.** Nuptial gifts. *Current Biology* **21**: R644–R645.
- Lin SW, Lopardo L, Haase M, Uhl G. 2019.** Taxonomic revision of the dwarf spider genus *Shaanxinus* Tanasevitch, 2006 (Araneae, Linyphiidae, Erigoninae), with new species from Taiwan and Vietnam. *Organisms Diversity & Evolution* **19**: 211–276.
- Locket GH, Millidge AF. 1953.** *British spiders, Vol. II*. London: Ray Society.
- Locket GH, Russell-Smith A. 1980.** Spiders of the family Linyphiidae from Nigeria. *Bulletin of the British Arachnological Society* **5**: 54–90.
- Lopez A. 1976.** Présence de glandes tégumentaires prosomatiques chez les mâles de deux Erigonidae (Araneae). *Compte Rendu Hebdomadaire des Séances de l'Académie des Sciences, Paris* **282**: 365–367.
- Lopez A, Emerit M. 1981.** Le dimorphisme sexuel prosomatique de *Walckenaeria acuminata* Blackwall, 1833 (Araneae, Erigonidae). *Bulletin de la Société Zoologique de France* **106**: 125–131.
- Ma XL, Zhu CD. 1991.** One new species of the spider genus *Oedothorax* from China (Araneae: Linyphiidae: Erigoninae). *Acta Zootaxonomica Sinica* **16**: 27–29.
- Maddison WP, Maddison DR. 2017.** *Mesquite: a modular system for evolutionary analysis*. Available at: <http://mesquiteproject.org>
- Maes L, Vanacker D, Sylvia P, Maelfait J-P. 2004.** Comparative study of courtship and copulation in five *Oedothorax* species. *Belgian Journal of Zoology* **134**: 29–35.
- Marusik YM. 1993.** A check-list of spiders (Arachnida Aranei) from Sakhalin and Kurile Islands. *Arthropoda. Selecta* **1**: 73–85.
- Marusik YM, Ryabukhin AS, Kuzminykh GV. 2010.** New data on spiders and harvestmen (Arachnida: Aranei & Opiliones) from western Koryakia, Kamchatka Peninsula. *Arthropoda Selecta* **19**: 283–293.
- Marx G. 1890.** Catalogue of the described Araneae of temperate North America. *Proceedings of the United States National Museum* **12**: 497–594.
- Matsuda M, Ono H. 2001.** A new species of the genus *Ummeliata* (Araneae, Linyphiidae) from Japan. *Bulletin of the National Museum of Nature and Science Tokyo (A)* **27**: 271–276.
- Menge A. 1868.** Preussische Spinnen. II. Abtheilung. *Schriften der Naturforschenden Gesellschaft in Danzig (N. F.)* **2**: 153–218.
- Menge A. 1871.** Preussische Spinnen. IV. Abtheilung. *Schriften der Naturforschenden Gesellschaft in Danzig, (N. F.)* **2**: 265–296.
- Merrett P. 1963.** The palpus of male spiders of the family Linyphiidae. *Proceedings of the Zoological Society of London* **140**: 347–467.
- Michalik P, Uhl G. 2011.** Cephalic modifications in dimorphic dwarf spiders of the genus *Oedothorax* (Erigoninae, Linyphiidae, Araneae) and their evolutionary implications. *Journal of Morphology*, **272**: 814–832.
- Miller F. 1970.** Spinnenarten der Unterfamilie Micryphantinae und der Familie Theridiidae aus Angola. *Publicações Culturais da Companhia de Diamantes de Angola* **82**: 75–166.
- Miller F. 1971.** Pavouci-Araneida. *Klíč zvířeny ČSSR* **4**: 51–306.
- Miller JA. 1999.** Revision and cladistic analysis of the erigonine spider genus *Sisicottus* (Araneae, Linyphiidae, Erigoninae). *The Journal of Arachnology* **27**: 553–603.
- Miller JA. 2007.** Review of erigonine spider genera in the neotropics (Araneae: Linyphiidae, Erigoninae). *Zoological Journal of the Linnean Society* **149**: 1–263.
- Miller JA, Hormiga G. 2004.** Clade stability and the addition of data: a case study from erigonine spiders (Araneae : Linyphiidae, Erigoninae). *Cladistics* **20**: 385–442.
- Millidge AF. 1951.** Key to the British genera of subfamily Erigoninae (Family Linyphiidae: Araneae): including the description of a new genus (*Jacksonella*). *Annals and Magazine of Natural History*, **12**: 545–562.
- Millidge AF. 1975.** Some new or little-known erigonid spiders from southern Europe. *Bulletin of the British Arachnological Society* **3**: 120–125.
- Millidge AF. 1977.** The conformation of the male palpal organs of linyphiid spiders, and its application to the taxonomic and phylogenetic analysis of the family (Araneae: Linyphiidae). *Bulletin of the British Arachnological Society* **4**: 1–60.
- Millidge AF. 1991.** Further linyphiid spiders (Araneae) from South America. *Bulletin of the American Museum of Natural History* **205**: 1–199.
- Müller H-G. 1983.** Zur Vorkommen von *Oedothorax agrestis* (Blackwall) (Araneida, Linyphiidae) in Hessen. *Hessische Faunistische Briefe* **3**: 64–67.
- Namkung J. 2002.** *The spiders of Korea*. Seoul: Kyo-Hak Publishing.
- Namkung J. 2003.** *The spiders of Korea, 2nd edn*. Seoul: Kyo-Hak Publishing Co.
- Nentwig W, Heimer S. 2009.** Orb webs and single-line webs: An economic consequence of space web reduction in spiders. *Journal of Zoological Systematics and Evolutionary Research* **21**: 26–37.
- Nentwig W, Blick T, Bosmans R, Gloor D, Hänggi A, Kropf C. 2019.** *Araneae v.10.2019*. Available at: <https://www.araneae.nmbe.ch>
- Nixon K. 2002.** *Winclada, program and documentation*. Available at: www.cladistics.com.
- Nzigidahera B, Jocqué R. 2014.** On the Afrotropical genus *Holmelgonia* (Araneae, Linyphiidae), with the description of three new species from the Albertine Rift. *European Journal of Taxonomy* **77**: 1–18.
- Ohlert E. 1867.** *Die Araneiden oder echten Spinnen der Provinz Preussen*. Leipzig: Engelmann.
- Oi R. 1960.** Linyphiid spiders of Japan. *Journal of the Institute of Polytechnics Osaka City University* **11**: 137–244.
- Oi R. 1977.** A new erigonid spider from Formosa. *Acta Arachnologica* **27**: 23–26.

- Okuma C, Kamal NQ, Hirashima Y, Alam MZ, Ogata K. 1993.** *Illustrated Monograph of the Rice Field Spiders of Bangladesh. Institute of Postgraduate Studies in Agriculture (Salna, Gazipur, Bangladesh) (Vol. 1).* Japan International Cooperation Agency Project Publication.
- Ono H, Matsuda M, Saito H. 2009.** Linyphiidae, Pimoidae. In: Ono H, ed. *The spiders of Japan with keys to the families and genera and illustrations of the species.* Kanagawa: Tokai University Press, 253–344.
- Ovsyannikov AG. 1937.** Contribution to the fauna of spiders of the Kursk province. *Uchenye Zapiski, Permskii Gosudarstvennyi Universitet M. Gorkogo* **3**: 89–93.
- Paik KY. 1980.** The spider fauna of Dae Heuksan-do Isl., So Heuksan-do Isl. and Hong-do Isl., Jeunlanam-do, Korea. *Kyungpook Educational Forum Kyungpook National University* **22**: 153–173.
- Palmgren P. 1976.** Die Spinnenfauna Finnlands und Ostfennoskandiens. VII. Linyphiidae 2. *Fauna Fennica* **29**: 1–126.
- Pantini P, Mazzoleni F. 2018.** I ragni de Calabria (Arachnida Araneae). *Rivista del Museo Civico di Scienze Naturali 'E. Caffi', Bergamo* **31**: 11–69.
- Paquin P, Dupérré N. 2003.** *Guide d'identification des araignées (Araneae) du Québec, Fabriques, Supplement 11.* Varennes: Association des entomologistes amateurs du Québec.
- Pérez-Miles F, Lucas SM, da Silva Jr PI, Bertani R. 1996.** Systematic revision and cladistic analysis of Theraphosinae (Araneae: Theraphosidae). *Mygalomorph* **1**: 33–68.
- Peters HM. 1990.** On the structure and glandular origin of bridging lines used by spiders for moving to distant places. *Acta Zoologica Fennica* **190**: 309–314.
- Peters HM, Kovoov J. 1991.** The silk-producing system of *Linyphia triangularis* (Araneae, Linyphiidae) and some comparisons with Araneidae. *Zoomorphology* **111**: 1–17.
- Petrunkevitch A. 1911.** A synonymic index-catalogue of spiders of North, Central and South America with all adjacent islands, Greenland, Bermuda, West Indies, Terra del Fuego, Galapagos, etc. *Bulletin of the American Museum of Natural History* **29**: 1–791.
- Petrunkevitch A. 1925.** New Erigoninae from Tennessee. *Journal of the New York Entomological Society* **33**: 170–176.
- Pickard-Cambridge FO. 1895.** List of the Araneidea of Cumberland and Lake District. *The Naturalist* **29**: 48.
- Pickard-Cambridge O. 1862.** Description of ten new species of British spiders. *The Zoologist* **20**: 7951–7968.
- Pickard-Cambridge O. 1873.** On British spiders. *Transactions of the Linnean Society of London* **28**: 433–458.
- Pickard-Cambridge O. 1879.** The spiders of Dorset. Araneidea. *Proceedings of the Dorset Natural History and Antiquarian Field Club* **1**: 1–235.
- Pickard-Cambridge O. 1882.** Notes on British spiders, with descriptions of three new species and characters of a new genus. *Annals and Magazine of Natural History (5)* **9**: 1–17.
- Pickard-Cambridge O. 1901.** Some notes on British spiders observed in 1899. *Proceedings of the Dorset Natural History and Antiquarian Field Club* **21**: 18–39.
- Platnick N. 1989.** *Advances in spider taxonomy 1981–1987: A supplement to Brignoli's A catalogue of the Araneae described between 1940 and 1981.* Manchester: Manchester University Press.
- Platnick NI, Coddington JA, Forster RR, Griswold CE. 1991.** Spinneret morphology and the phylogeny of haplogyne spiders (Araneae, Araneomorphae). *American Museum Novitates* **3016**: 1–73.
- Ramírez MJ. 2003.** The spider subfamily Amaurobioidinae (Araneae, Anyphaenidae): a phylogenetic revision at the generic level. *Bulletin of the American Museum of Natural History* **277**: 1–262.
- Reimoser E. 1919.** Katalog der echten Spinnen (Araneae) des Palaarktischen Gebietes. *Abhandlungen der Zoologisch-Botanischen Gesellschaft in Wien* **10**: 1–280.
- Roberts MJ. 1987.** *The spiders of Great Britain and Ireland, Vol. 2: Linyphiidae and check list.* Colchester: Harley Books.
- Roewer CF. 1942.** *Katalog der Araneae von 1758 bis 1940.* Bremen: Natura, Buchhandlung für Naturkunde und exakte Wissenschaften Paul Budy.
- Russell-Smith A. 2016.** Identification of females of British *Oedothorax* species. *Newsletter of the British Arachnological Society* **137**: 22–24.
- Růžička V. 1978.** Revision der diagnostischen Merkmale der Weibchen der tschechoslovakischen Arten der Gattung *Oedothorax* (Araneae: Micryphantidae). *Věstník Československé Zoologické Společnosti v Praze* **42**: 195–208.
- Saaristo MI. 1977.** Secondary genital organs in the taxonomy of Lepthyphantinae (Araneae, Linyphiidae). *Reports from the Department of Zoology, University of Turku* **5**: 1–16.
- Saaristo MI, Tanasevitch AV. 1996.** Redelimitation of the subfamily Micronetinae Hull, 1920 and the genus *Lepthyphant* Menge, 1866 with descriptions of some new genera (Aranei: Linyphiidae). *Berichte des Naturwissenschaftlich-medizinischen Vereins in Innsbruck* **83**: 163–186.
- Saito S. 1934.** Spiders from Hokkaido. *Journal of the Faculty of Agriculture, Hokkaido Imperial University, Sapporo, Japan* **33**: 267–362.
- Saito S. 1959.** *The spider book illustrated in colours.* Tokyo: Hokuryukan.
- Saito H. 1993.** Two erigonine spiders of the genus *Ummeliata* (Araneae: Linyphiidae). *Acta Arachnologica* **42**: 103–107.
- Saito H, Ono H. 2001.** New genera and species of the spider family Linyphiidae (Arachnida, Araneae) from Japan. *Bulletin of the National Science Museum, Tokyo (A)* **27**: 1–59.
- Schaible U, Gack C. 1987.** Zur Morphologie, Histologie und biologischen Bedeutung der Kopfstrukturen einiger Arten der Gattung *Diplocephalus* (Araneida, Linyphiidae, Erigoninae). *Verhandlungen des naturwissenschaftlichen Vereins in Hamburg* **29**: 171–180.
- Schaible U, Gack C, Paulus HF. 1986.** Zur Morphologie, Histologie und biologischen Bedeutung der Kopfstrukturen männlicher Zwergspinnen (Linyphiidae: Erigoninae). *Zoologische Jahrbücher. Abteilung für Systematik, Ökologie und Geographie der Tiere* **113**: 389–408.

- Thaler K. 1987.** Über einige Linyphiidae aus Kashmir (Arachnida: Araneae). *Courier Forschungsinstitut Senckenberg* **93**: 33–42.
- Thorell T. 1871.** *Remarks on synonyms of European spiders. Part II.* Uppsala: C. J. Lundström.
- Thorell T. 1873.** *Remarks on synonyms of European spiders. Part IV.* Uppsala: C. J. Lundström.
- Thorell T. 1875a.** Diagnoses Araneorum Europaeorum aliquot novorum. *Tijdschrift voor Entomologie* **18**: 81–108.
- Thorell T. 1875b.** Descriptions of several European and North African spiders. *Kongliga Svenska Vetenskaps-Akademiens Handlingar* **13**: 1–203.
- Tin MMY, Economo EP, Mikheyev AS. 2014.** Sequencing degraded DNA from non-destructively sampled museum specimens for RAD-tagging and low-coverage shotgun phylogenetics. *PLoS One* **9**: e96793.
- Toft S, Albo MJ. 2016.** The shield effect: nuptial gifts protect males against pre-copulatory sexual cannibalism. *Biology Letters* **12**: 20151082.
- Tu LH, Hormiga G. 2011.** Phylogenetic analysis and revision of the linyphiid spider genus *Solenysa* (Araneae: Linyphiidae: Erigoninae). *Zoological Journal of the Linnean Society* **161**: 484–530.
- Tu LH, Li SQ. 2004.** A preliminary study of erigonine spiders (Linyphiidae: Erigoninae) from Vietnam. *Raffles Bulletin of Zoology* **52**: 419–433.
- Tu LH, Li SQ. 2006.** A review of *Gongylidioides* spiders (Araneae: Linyphiidae: Erigoninae) from China. *Revue Suisse de Zoologie* **113**: 51–65.
- Tystshenko VP. 1971.** *Opredelitel' paukov evropejskoj casti SSSR.* Leningrad: Nauka.
- Uhl G, Busch M. 2009.** Securing paternity: mating plugs in the dwarf spider *Oedothorax retusus* (Araneae: Erigoninae). *Biological Journal of the Linnean Society* **96**: 574–583.
- Uhl G, Maelfait J-P. 2008.** Male head secretion triggers copulation in the dwarf spider *Diplocephalus permixtus*. *Ethology* **114**: 760–767.
- Uhl G, Nessler SH, Schneider JM. 2010.** Securing paternity in spiders? A review on occurrence and effects of mating plugs and male genital mutilation. *Genetica* **138**: 75.
- Uhl G, Kunz K, Vöcking O, Lipke E. 2014.** A spider mating plug: origin and constraints of production. *Biological Journal of the Linnean Society* **113**: 345–354.
- Vahed K. 1998.** The function of nuptial feeding in insects: a review of empirical studies. *Biological Reviews* **73**: 43–78.
- Vahed K. 2007.** All that glitters is not gold: sensory bias, sexual conflict and nuptial feeding in insects and spiders. *Ethology* **113**: 105–127.
- Van Hasselt AWM. 1884.** Waarnemingen omtrent anomalien van de geslachtsdrift bij spinnen-mares. *Tijdschrift voor Entomologie* **27**: 197–206.
- Van Hasselt AWM. 1885.** Catalogus araneorum hucusque in Hollandiâ inventarum. *Tijdschrift voor Entomologie* **28**: 113–188.
- Van Helsdingen PJ. 1965.** Sexual behaviour of *Lepthyphantes leprosus* (Ohlert) (Araneida, Linyphiidae), with notes on the function of the genital organs. *Zoologische Mededelingen* **41**: 15–42.
- van Helsdingen PJ. 1978.** Some synonymies in Old World spiders. *Zoologische Mededelingen* **53**: 185–197.
- Van Helsdingen PJ. 1982.** Quelques remarques sur les Linyphiidae mentionnés par Di Caporiacco. *Revue Arachnologique* **3**: 155–180.
- Van Helsdingen PJ. 1985.** *Mitrager noordami*, an erigonine novelty from Java. *Bulletin of the British Arachnological Society* **6**: 353–358.
- Vanacker D, Borre JV, Jonckheere A, Maes L, Pardo S, Hendrickx F, Maelfait J-P. 2003.** Dwarf spiders (Erigoninae, Linyphiidae, Araneae): good candidates for evolutionary research. *Belgian Journal of Zoology* **133**: 143–149.
- Vanacker D, Maes L, Pardo S, Hendrickx F, Maelfait J-P. 2003.** Is the hairy groove in the *gibbosus* male morph of *Oedothorax gibbosus* (Blackwall 1841) a nuptial feeding device? *Journal of Arachnology* **31**: 309–315.
- Vanacker D, Hendrickx F, Maes L, Verraes P, Maelfait J-P. 2004.** Can multiple mating compensate for slower development and shorter adult life in a male dimorphic dwarf spider? *Biological Journal of the Linnean Society* **82**: 269–273.
- Vogelsanger T. 1948.** Beitrag zur Kenntnis der Spinnenfauna des Kantons Graubünden. *Mitteilungen der Naturforschenden Gesellschaft Schaffhausen* **22**: 33–72.
- Vollrath F. 1977.** *Zur Ökologie und Biologie von kleptoparasitischen Argyrodes elevatus und synöken Argyrodes-Arten (Araneae, Theridiidae).* Unpublished Doctoral Thesis, University of Freiburg.
- Walckenaer CA. 1847.** Dernier Supplément. In: Walckenaer CA, Gervais P, eds. *Histoire naturelle des insectes, Vol. 4.* Paris: Aptères, 365–564.
- Wang F, Ballesteros JA, Hormiga G, Chesters D, Zhan Y, Sun N, Zhu C, Chen W, Tu L. 2015.** Resolving the phylogeny of a speciose spider group, the family Linyphiidae (Araneae). *Molecular Phylogenetics and Evolution* **91**: 135–149.
- Westring N, 1851.** Förteckning öfver de till närvarande tid Kände, i Sverige förekommande Spindlarter, utgörande ett antal af 253, deraf 132 äro nya för svenska Faunan. *Göteborgs Kungliga Vetenskaps och Vitterhets Samhälles Handlingar* **2**: 25–62.
- Westring N, 1861.** Araneae svecicae. *Göteborgs Kungliga Vetenskaps och Vitterhets Samhälles Handlingar* **7**: 1–615.
- Wiehle H. 1960a.** Spinnentiere oder Arachnoidea, XI: Micryphantidae-Zwergspinnen. *Tierwelt Deutschlands* **47**: 1–620.
- Wiehle H. 1960b.** Der Embolus des männlichen Spinnentasters. *Verhandlungen der Deutschen Zoologischen Gesellschaft* **1960**: 450–480.
- World Spider Catalog. 2020.** *World Spider Catalog. Version 21.0.* (2020, April 26). Bern: Natural History Museum Bern. Available at: <http://wsc.nmbe.ch>
- Wunderlich J. 1974.** Linyphiidae aus Nepal, II. Die Gattung *Oedothorax* Bertkau 1883 (Arachnida: Araneae). *Senckenbergiana Biologica* **55**: 169–188.
- Wunderlich J. 1978.** Zur Kenntniss der Gattung *Oedothorax* Bertkau 1883, *Callitrichia* Fage 1936 und *Toschia* Caporiacco 1949. *Senckenbergiana Biologica* **58**: 257–260.
- Wunderlich J. 1995.** Fünf gynandromorphe Baldachin-Spinnen aus Europa (Arachnida: Araneae: Linyphiidae). *Beiträge zur Araneologie* **4**: 471–477.
- Yeargan KV. 1988.** Ecology of a bolas spider, *Mastophora hutchinsoni*: phenology, hunting tactics, and evidence for aggressive chemical mimicry. *Oecologia* **74**: 524–530.

Appendix 1. Standard statistics of discrete characters in Matrix II

Ch.	St.	CI	RI	Ch.	St.	CI	RI	Ch.	St.	CI	RI	Ch.	St.	CI	RI
1	11	0.09	0.54	33	5	0.20	0.20	65	8	0.12	0.36	97	1	1.00	1.00
2	2	0.50	0	34	1	1.00	1.00	66	3	0.33	0.33	98	1	1.00	1.00
3	2	1.00	1.00	35	1	1.00	1.00	67	4	0.50	0.60	99	1	-	-
4	5	0.20	0.69	36	4	0.25	0.40	68	4	0.25	0.57	100	1	1.00	1.00
5	1	1.00	1.00	37	1	1.00	1.00	69	4	0.25	0.40	101	1	1.00	1.00
6	4	0.25	0.57	38	2	0.50	0.90	70	1	1.00	1.00	102	1	1.00	1.00
7	1	1.00	1.00	39	13	0.07	0.45	71	9	0.22	0.36	103	2	0.50	0
8	2	0.50	0.91	40	4	0.25	0.70	72	7	0.14	0.64	104	1	1.00	1.00
9	2	0.50	0	41	8	0.12	0.53	73	1	-	-	105	1	1.00	1.00
10	1	1.00	1.00	42	7	0.14	0.45	74	1	1.00	1.00	106	1	-	-
11	7	0.57	0.80	43	3/	0.66/	0.66/	75	10	0.10	0.40	107	4/	0.25	0.40
					4/	0.50/	0.33/						3/	0.33	0.60
					4	0.50	0.33						4	0.25	0.40
12	1	1.00	1.00	44	1	1.00	1.00	76	2	0.50	0.80	108	20	0.30	0.30
13	1	1.00	1.00	45	0	-	-	77	2	1.00	1.00	109	1	1.00	1.00
14	9	0.11	0.70	46	1	1.00	1.00	78	3	0.33	0.80	110	3	0.33	0.66
15	2	0.50	0.75	47	3	0.33	0.83	79	8	0.12	0.66	111	3	0.33	0.66
16	5	0.20	0.60	48	6	0.16	0.54	80	8	0.12	0.65	112	9	0.33	0.14
17	4	0.25	0.57	49	8	0.12	0.41	81	3	0.33	0.33	113	11	0.09	0.56
18	4	0.25	0.91	50	1	1.00	1.00	82	2	0.50	0.50	114	2	0.50	0
19	1	-	-	51	2	0.50	0.80	83	2	0.50	0	115	8	0.25	0.25
20	2	0.50	0.66	52	7	0.14	0.79	84	3	0.33	0.60	116	16	0.18	0.58
21	3	0.33	0.71	53	2	0.50	0.88	85	1	1.00	1.00	117	2	0.50	0.75
22	6	0.16	0.77	54	2	0.50	0.50	86	1	1.00	1.00	118	1	1.00	1.00
23	2	0.50	0.75	55	2	0.50	0.50	87	2	0.50	0.50	119	2	0.50	0.66
24	2	1.00	1.00	56	2	0.50	0.92	88	2	0.50	0.66	120	2	0.50	0
25	4/	0.25/	0	57	1	1.00	1.00	89	11	0.09	0.37	121	3	1.00	1.00
	4/	0.25/	0												
	3	0.33	0.33												
26	2	0.50	0.50	58	6	0.33	0.20	90	2	0.50	0.50	122	3	0.66	0.50
27	5	0.20	0.63	59	1	1.00	1.00	91	6	0.16	0.37	123	1	1.00	1.00
28	2	0.50	0.50	60	2	0.50	0.50	92	10	0.10	0.50	124	1	1.00	1.00
29	1	1.00	1.00	61	8	0.12	0.53	93	3	0.33	0.60	125	4	0.25	0.57
30	3	0.33	0	62	6	0.16	0.80	94	1	-	-	126	3	0.33	0.60
31	5	0.60	0.77	63	1	-	-	95	1	1.00	1.00	127	4	0.25	0.62
32	1	1.00	1.00	64	2	1.00	1.00	96	3	0.33	0.33	128	3	0.33	0.80

Appendix 2. Summarized results of the implied weights analyses using different K values. Tree lengths were calculated only by discrete characters with weight = 1.

Continuous & discrete characters										
<i>k</i>	Best score	No. of trees	No. of hits	Tree length	Cl. 23	Cl. 27	Cl. 39	Cl. 55	No. common clades with equal weight tree	
									With c & us	Without c & us
1	56.25568	1	10	489	P	P	A	A	29	29
2	46.37725	1	13	480	P	P	P – c	P + c	34	38
3	39.76465	1	12	481	P	P	P – c	P + c	34	38
4	35.01308	1	10	481	P	P	P – c	P + c	34	38
5	31.34877	1	8	468	P	P	P – us	P	45	47
6	28.40052	1	15	468	P	P	P – us	P	45	47
10	20.84077	1	8	465	P	P	P – us	P	51	53
15	15.73176	1	9	464	P	P	P – us	P	51	53
20	12.67135	1	9	464	P	P	P – us	P	51	53
30	9.14871	1	2	463	P	P	P – us	P	50	54
100	3.11914	1	8	462	P	P	P – us	P + m + un	51	53
1000	0.33026	1	1	461	P	P	P – us	P	66	70
Discrete characters only										
1	53.01254	1	2	489	P	P	A	A	30	30
2	43.62180	2	25	480	P	P	P – c	P + c	33	36
3	37.33353	5	33	481	P	P	P – c	P + c	34	37
4	32.83611	5	15	481–483	P	P	P – c	P + c	34	37
5	29.38820	4	1	476	P	P	P – c	P + c	43	46
6	26.60969	1	25	468	P	P	P – us	P	44	46
10	19.48713	2	3	468	P	P	P – us	P	45	47
15	14.69909	4	8	464	P	P	P – us	P	51	53
20	11.82697	2	7	464	P	P	P – us	P	50	52
30	8.52407	6	1	462	P	P	P – us	P	49	53
100	2.90086	6	14	462	P	P	P – us	P	58	62
1000	0.30606	2	1	461	P	P	P – us	P	62	67

A: absent; c: *Callitrichia convector*; Cl.: Clade; m: '*Oedothorax*' megalaya; P: present; un: '*Oe.*' uncus; us: *Ca. usitata*.

APPENDIX 3 CHARACTERS

Male palp

1. Cymbium (C) retrolateral margin smaller setae: 0, absent (*Oedothorax agrestis*, Fig. 5A); 1, present (*Callitrichia muscicola*, Fig. 32A). These setae are usually shorter than the neighboring setae at retrolateral side of the C, and are often separated from other C setae by a retrolateral groove. Although supporting some lower level grouping, this character is highly homoplastic among our studied species.
2. C retrolateral basal excavation: 0, absent (*Oe. agrestis*, Fig. 5A); 1, present (*Nasoona crucifera*, Fig. 82, arrow). Character 8 in Miller & Hormiga (2004). It refers to a more extensive depression beside the paracymbium.
3. Paracymbium (PC) shape: 0, triangular (*Pimoa altiocolata*, figs 303, 304 in Hormiga, 1994); 1, straight hook (*Neocautinella*, fig. 15B in Miller & Hormiga 2004); 2, spiral (*Oe. agrestis*, Fig. 5A). Character 4 (Table 1) in Coddington (1990); 8 in Hormiga (1993, 1994); 11 in Hormiga (1994b); 24 in Hormiga et al. (1995); 9 in Griswold et al. (1998); 5 in Hormiga (2000); 12 in Miller & Hormiga (2004). Except the outgroup taxa *P. altiocolata*, *Stemonyphantes lineatus* and *Linyphia triangularis*, species in this study have a spiral PC.
4. PC base: 0, covered by the cymbial base (*Mitrager angela*, Fig. 41C); 1, largely exposed, C base narrow, not retrolaterally extended (*Oe. apicatus*, Fig. 12C). Most inspected species in this study have a PC base covered by the C base, not visible from dorsal view. The narrow C base and the dorsally visible PC base is a synapomorphy of the gibbosus group, also present in *Diplocentria bidentata*, *Gongylidiellum latebricola* and *Hylyphantes graminicola*.
5. PC basal setae: 0, absent; 1, present (*Oe. agrestis*, Fig. 5A). Character 14 in Miller & Hormiga (2004). The absence of PC basal setae occurs only in two outgroup taxa and provides no additional grouping information.
6. PC distal setae: 0, absent (*Oe. apicatus*, Fig. 12A); 1 present (*Ca. muscicola*, Fig. 32A).
7. PC distal setae location: 0, distal (*Ca. muscicola*, Fig. 32A); 1, middle (*Oe. agrestis*, Fig. 5A). Most species have distal paracymbial setae, located distally near the spiral turn. In *Oedothorax* s.s. the 'distal' setae is (when present) located in the middle of the PC. In *Oe. apicatus*, *Oe. retusus* and *Oe. gibbifer*, the basal and distal PC setae are not distinctly divided and are here scored as having only basal setae (i.e. the PC distal setae is considered absent).
8. PC distal clasp lateral to base: 0, oriented forwardly (*Tmeticus tolli*, Fig. 83A); 1, not oriented forwardly (*M. coronata*-like) (*M. coronata*, Fig. 46A). In most species having spiral-shaped PC, the distal clasp of the spiral is directed forwardly, but in some Nepalese and Indian species the distal clasp is oriented laterally.
9. PC base anterior protuberance (*Shaanxinus*-like): 0, absent (*Oe. agrestis*, Fig. 5A); 1, present (*N. crucifera*, Fig. 82A, arrow; *S. curviductus* Lin, 2019, fig. 3B in Lin et al. 2019). In most of the examined species in this study, the anterior margin of the PC connects to the C in a smooth curve; in *Shaanxinus* and *N. crucifera*, there is a protuberance at the anterior margin of the PC below the joint with the C.
10. PC base spiny sac: 0, absent; 1, present (*Atypena formosana*, Fig. 73). In males of *A. cirrifrons* and *A. formosana*, a spiny, sack-like, partially sclerotized structure is located at the membranous region between PC and C, covered retrolaterally by the tibial retrolateral apophysis.
11. Embolus (E) shape: 0, retrolaterally spiral (*M. lineata*, Fig. 53B); 1, prolaterally spiral (*Oe. gibbosus*, Fig. 6E); 2, screw like (*H. graminicola*); 3, fused and integrated with radix (*Cornitibia simplicithorax*, Fig. 69D). Modified from Character 44 in Miller & Hormiga (2004). We separated the 'spiral' character state of Miller & Hormiga into retrolaterally and prolaterally spiral, since in most of our studied species the E originates dorsal to the radical part of the embolic division, and spirals retrolaterally or prolaterally related to the position of anterior apophysis of radix.
12. E base protuberance: 0, absent (*M. coronata*, Fig. 46B); 1, present (*Oe. agrestis*, arrow in Fig. 5B). A protuberance occurs on the basal part of the E in opposite direction to the E tip. Synapomorphy of *Oedothorax* s.s.
13. E base shape: 0, rounded (*O. agrestis*, Fig. 5B); 1, broad and flat (*Oe. apicatus*, Fig. 12B). The flattening and broadening of the basal part of the E is a synapomorphy of *Oe. apicatus*, *Oe. gibbifer* and *Oe. retusus*.
14. E prolateral side: 0, smooth (*Oe. agrestis*, Fig. 5B); 1, flattened and wavy (*M. coronata*, Fig. 46B). The flattened wavy prolateral extension at the base of E is present in many of the *Mitrager* species, as well as in *Mitrager* and *Atypena*.
15. E tip prolateral anterior flat extension: 0, absent, the E opens at the tip (*Oe. agrestis*, Fig.

- 5B); 1, present (*M. coronata*, Fig. 46B). In most investigated taxa in the present study, the E has its opening at the tip. The presence of flat extension on the prolateral side distal to the E opening supports the branch of *M. villosa*, *M. coronata* and *M. angela*; originating independently in *Mitrager noordami*.
16. Anterior radical process (ARP): 0, absent; 1, present (*Oe. agrestis*, Fig. 5B). Character 23 in Hormiga (2000); 55 in Miller & Hormiga (2004). Several apophyses can be found at the anteriorly on the radix. In this study, the ARP is referred to as the one with the dorsal margin continuous to the margin of both the radix and the embolus (in *Araeonus humilis* and *Co. simplicithorax*, the ARP arises from a more ventral position on the radix). According to our phylogenetic analysis, the presence of ARP supports Clade 6 and it is lost three/four times within this group according to fast/slow optimization, respectively.
 17. ARP groove fitting embolus: 0, absent (*M. villosa*, Fig. 65E); 1, present (*Oe. nazareti*, Fig. 78B, E)
 18. Lateral extension of radix (LER): 0, absent (*Oe. agrestis*, Fig. 5B); 1, present (*M. villosa*, Fig. 65E). This structure was proposed by Tanasevitch (2015) as the 'lateral extension of convector'. According to our results, this extension evolved four times: Clade 14, *Callitrichia convector*, *Ca. macrophthalma* and Clade 53.
 19. LER texture: 0, smooth (*M. villosa*, Fig. 65E); 1, striped (*M. clypeellum*, Fig. 44E). Autapomorphy of *M. clypeellum*.
 20. Lateral extension of radix (LER) margin comb-like: 0, absent (*M. villosa*, Fig. 65E); 1, present (*M. rustica*, Fig. 59D).
 21. LER orientation: 0, bent over embolus (*M. angela*, Fig. 41B); 1, not covering embolus, *A. cirrifrons*-like (*A. cirrifrons*, Fig. 80B). In the majority of *Mitrager* species, the tip of the lateral extension of radix is bent prolaterally over the embolus, but in *Atypena* and some other species it is entirely retrolateral to the embolus.
 22. Ventral radical process (VRP): 0, absent (*Oe. agrestis*, Fig. 5B); 1, present (*Ca. gloriosa*, Fig. 25B; *Ummeliata insecticeps*, Fig. 84). 'Ventral embolar apophysis' of Scharff (1990a), this apophysis originates in the radix.
 23. VRP length: 0, shorter than VRP base to TP (*Ca. sellafontis*, Fig. 20B); 1, equal or longer than VRP base to TP (*A. cirrifrons*, Fig. 80B). *A. cirrifrons*, *A. formosana*, 'Oe.' *stylus* and 'Oe.' *uncus* have especially long ventral radical process.
 24. Radix-embolus membrane: 0, absent, E and radix fused; 1, concealed; 2, clearly visible. Modified from character 51 in Miller & Hormiga (2004). In *Oedothorax*, the membranous region between E and radix extends broadly. In contrast, most other species with membrane, the two structures are seemingly overlapping (prolateral view) and the membrane is barely visible.
 25. Radical (R) anterior tooth: 0, absent; 1, present. Character 57 in Miller & Hormiga (2004). No ingroup taxa except *Co. simplicithorax* has a tooth distally above the embolus.
 26. Radical (R) mesal tooth: 0, absent; 1, present. Character 58 in Miller & Hormiga (2004). None of our investigated species have this structure, except some outgroups from the data matrix of Miller & Hormiga (2004).
 27. R papillae: 0, absent (*Oe. gibbosus*, Fig. 6B); 1, present (*Ca. picta*, Fig. 33D). *Holmelgonia basalis*, some *Callitrichia* species, two *Mitrager*, 'Oe.' *cunur* and *Ca. convector* have these papillae at the part of R, which is probably in contact with palpal tibia apophyses when the copulatory bulb is expanded in position for mating.
 28. R median highly sclerotized process: 0, absent (*A. cunur*, Fig. 75B); 1, present (*N. crucifera*, Fig. 82D, arrow). *Shaanxinus* and *Nasoona* have a highly sclerotized scaly area in the middle between E, R and TP
 29. Area between ARP and E: 0, smooth and sclerotized as surrounding cuticle (*M. villosa*, Fig. 65E); 1, *M. falciferoides*-like: membranous and irregular (*M. falciferoides*, Fig. 50D). In some *Mitrager* species, the part of R anterior to the E base is membranous and crumpled in appearance.
 30. Radical tailpiece (TP): 0, absent (*Emertongone montifera*, 66D); 1, present (*Tmeticus tolli*, Fig. 83B). Character 52 in Miller & Hormiga (2004). In the generalized system of linyphiid embolic division sclerites by Merrett (1963), the radix is attached to the base of the embolus, and often has a conspicuous plate-like tailpiece. In the description of several *Gorbothorax* species (now transferred to *Nasoona*), Tanasevitch (1998b) proposed the term 'convector' for the large, well sclerotized and elongated sclerite connected to their embolus via a short membrane, which may also apply at least to *Oedothorax*, *Gongylidium* and *Gongylidioides*. The same sclerite was coded by Hormiga (2000) for several erigonine taxa including *Oedothorax* and *Gongylidium* as lamella characteristic, a term in Merrett's system referring to a plate-like structure connected to the radix via a membrane.

- However, Hormiga's cladogram demonstrated that the lamella characteristica is not homologous in Linyphiinae and Erigoninae. In addition, in most erigonine species scored by Hormiga (2000) as having a lamella characteristica, the radical tailpiece was absent or inconspicuous. An alternative is to view this sclerite as a radical tailpiece set off by a membranous region (Miller & Hormiga 2004). In the present study, we followed the terminology of Miller & Hormiga and coded the species described by Tanasevitch as possessing radix, anterior radical process, lateral extension of radix and radical tailpiece instead of convector, distal apophysis of convector, lateral extension of convector and main body of convector, respectively.
31. TP shape: 0, flat and posteriorly extended (*Oe. gibbosus*, Fig. 6B); 1, stout and fitting onto tegulum, *M. falcifer*-like (*M. falcifer*, Fig. 49B); 2, *Stemonyphantes*-like; 3, stout, not fitting and not extended (*Hy. graminicola*, fig. 13A in Hormiga 2000) Some *Mitrager* species have an enlarged area retrolateral to the flat, outer part of the TP, which fits into a depressed area on the tegulum.
 32. TP posterior small protuberances: 0, absent (*Oe. gibbosus*, Fig. 6B); 1, present (*Oe. fuscus*, Fig. 14B). These protuberances support the clade of *Oe. fuscus*, *Oe. agrestis*, *Oe. tingitanus* and *Oe. meridionalis*, but is also present in *Oe. paludigena*.
 33. Embolic membrane (EM): 0, absent; 1, present. Character 18 of Hormiga (1993, 1994b); 22 of Hormiga (1994a); 18 of Hormiga (2000); 13 of Hormiga (2002); and 40 of Miller & Hormiga (2004). This membrane was called 'median membrane' in van Helsdingen (1965), Saaristo (1977) and Saaristo & Tanasevitch (1996). This term was originated from the obsolete idea of the linyphiids having a median apophysis, which is considered absent in later works (e.g. Hormiga 1994b). Here we refer to it as the 'embolic membrane', a term applied in most phylogenetic matrices of araneoids and linyphiids. The presence of this membrane supports Clade 2 and is lost four times in individual terminal taxa.
 34. EM shape: 0, flat (*Ca. sellafontis*, Fig. 20B); 1, cylindrical (*Oe. fuscus*, Fig. 14B). A cylindrical EM is a synapomorphy of *Oedothorax s.s.*
 35. EM: 0, large and oriented forwards; 1, small and oriented backwards (*Oe. gibbifer*, Fig. 15F). State 1 is the synapomorphy of *Oe. apicatus* and *Oe. gibbifer*, their EM is nearly invisible without the help of eugenol, which makes the column and embolic division translucent, allowing the observation of this hidden structure.
 36. Protegulum (PT): 0, absent; 1, present. Character 8 in Hormiga (2000); 16 in Miller & Hormiga (2004). Most erigonines in this study have PT, except *Ummeliata insecticeps*, *Gonatium rubellum* and *Ca. uncata*, which represent independent losses of this structure.
 37. PT shape: 0, a single structure (*Oe. gibbosus*, Fig. 6D); 1, bifurcate, one end with papillae, the other without (*O. fuscus*, Fig. 14D)
 38. PT papillae: 0, directly on the surface, without a surrounding rim (*Oe. gibbosus*, Fig. 6D); 1, surrounded by rim (*Ca. juguma*, Fig. 21D).
 39. PT papillae: 0, absent (*M. coronata*, Fig. 46D); 1, present (*Oe. gibbosus*, Fig. 6D). Character 9 in Hormiga (2000); 17 in Miller & Hormiga (2004).
 40. Area between T and PT: 0, not depressed, continuous transition between T and PT (*M. coronata*, Fig. 46D); 1, depressed, gap between T and PT (*M. assueta*, Fig. 42D). In most investigated species, the junction between T and PT is continuous, but in several *Falicitibia* species the base of PT is contracted, forming a distinct gap between T and PT.
 41. Tegular sac (TS): 0, absent; 1, present. Character 10 in Hormiga (2000); 19 in Miller & Hormiga (2004). Hormiga (2000) referred to the TS as a structure without papillae. In our current taxon sample, the sac may or may not have papillae.
 42. T papillae: 0, absent; 1, present. Character 20 in Miller & Hormiga (2004). In most species the T and PT are two continuous structures, rendering the scoring of this character arbitrary. Nevertheless, this character provides grouping information within *Oedothorax s.s.*
 43. T to subtegulum (ST) orientation in unexpanded palp: 0, T distal to ST; 1, T mesal to ST; 2, T ventral to ST. Character 21 in Miller & Hormiga (2004). In our study, this character provided no support for branches within erigonine.
 44. Suprattegulum (SPT) junction with T: 0, continuous with T; 1, with partial or complete membranous division. Character 13 (in part) in Hormiga (1993, 1994a); 15 (in part) in Hormiga (1994b); 12 in Zujko-Miller (1999); 12 in Hormiga (2000); 25 in Miller & Hormiga (2004).
 45. Distal suprattegular apophysis (DSA): 0, absent; 1, present. Character 13 in Hormiga (2000); 29 in Miller & Hormiga (2004). Uninformative. All the studied taxa have this apophysis except of *P. altiocolata*, where the SPT is absent and therefore this character is inapplicable.

46. DSA initial orientation: 0, extends distally beyond SPT; 1, extends ventrally from SPT. Character 31 in Miller & Hormiga (2004). This character supports the Erigoninae in this study.
47. DSA curvature: 0, straight (*Oe. gibbosus*, Fig. 6A); 1, ventral vertical turn and tip retrolaterally curved (*M. angela*, Fig. 41D).
48. Marginal suprategular apophysis (MSA): 0, absent (*Ca. macrophthalma*, Fig. 31A); 1, present (*Oe. gibbosus*, Fig. 6A). Character 6 in Miller (1999); 14 in Hormiga (2000); 34 in Miller & Hormiga (2004).
49. Palpal tibia prolateral apophysis (TPA): 0, absent (*M. angela*, Fig. 41C); 1, present (*Oe. apicatus*, Fig. 12C; *U. insecticeps*, Fig. 84B). Character 27 in Hormiga (1993, 1994a); 33 in Hormiga (1994b); 28 in Hormiga (2000); 27 in Miller & Hormiga (2004). As Miller & Hormiga (2004) pointed out, the establishment of homology among various apophyses on male palpal tibia in erigonines is a major problem in erigonine systematics. In *Oedothorax*, most species have two dorsal apophyses: (1) a prolateral apophysis (TPA *sensu* Miller & Hormiga, 2004) rod-shape with scaly, blunt tip (*Oe. apicatus*, *Oe. retusus*, *Oe. fuscus*, *Oe. agrestis*, *Oe. tingitanus*, *Oe. meridionalis*, *Oe. trilobatus* and *Oe. paludigena*), broad and flat (*Oe. gibbosus*) or absent (*Oe. gibbifer*); (2) a second apophysis, hereafter referred to as 'basal thorn' (BT), located closer to the C base, prolateral to the above-mentioned one. In *Mitrager* three apophyses can occur: the TPA, the retrolateral apophysis (TRA) and the prolateral spike (TPS) (see Fig. 44C). We define the TPA as the apophysis located between the retrolateral and prolateral trichobothria, the TRA as the one in the most retrolateral position, and the TPS (mostly slender, in most cases scaly) as the one arising prolaterally to the prolateral trichobothrium.
50. TPA cuticle: 0, smooth to slightly scaly (*Ca. pilosa*, Fig. 34C); 1, scaly margins and with a spike retrolaterally (*Ca. latitibialis*, Fig. 28C). Regardless the shape of the TPA, the cuticle is relatively smooth in most species. However, the TPA of *Ca. latitibialis* and *Ca. longiducta* is noticeably scaly with an additional spike at its retrolateral side.
51. Palpal tibia basal thorn (BT): 0, absent (*Oe. gibbosus*, Fig. 6C); 1, present (*Oe. apicatus*, Fig. 12C).
52. Palpal tibia prolateral spike (TPS): 0, absent; 1, present.
53. TPS retrolaterally bent: 0, straight; 1, bent.
54. Palpal tibia prolateral small apophyses: 0, absent (*Oe. fuscus*, Fig. 14C); 1, present (*Oe. agrestis*, Fig. 5C). These small apophyses without scales and bearing no setae occur in *Oe. tingitanus*, *Oe. agrestis* and *Oe. meridionalis*.
55. TPA retrolateral enlarged area with dense setae: 0, absent (*Oe. apicatus*, Fig. 12A); 1, present (*N. setifera*, Fig. 85C).
56. Palpal tibia retrolateral apophysis (TRA): 0, apically oriented (*M. savigniformis*, Fig. 60C); 1, laterally oriented (*M. angela*, Fig. 41C).
57. Palpal tibia row of parallel slit organs prolateral to prolateral spike: 0, absent (*M. falcifer*, Fig. 49C); 1, present (*M. coronata*, Fig. 46C). The presence of these parallel slit organs is synapomorphic for *M. coronata*, *M. angela*, *M. cornuta* and *M. villosa*.
58. Palpal tibia retrolateral trichobothria number: 0, four; 1, three; 2, two; 3, one. Character 13 in Griswold (1990); 48 in Platnick *et al.* (1991); 62 in Jocqué (1991); 1 in Griswold (1993); 9 in Pérez-Miles *et al.* (1996); 1 in Bond & Opell (1997); 7 in Davies (1998); 94 in Griswold *et al.* (1999); 17 in Miller (1999); 31 in Bertani (2001); 125 in Bosselaers & Jocqué (2002); 44 in Davies & Lambkin (2001); 12 in Silva Dá vila (2003); 42 in Ramírez (2003); 74 in Miller & Hormiga (2004).
59. Palpal patella (male) distal dorsal macroseta: 0, weak to moderate (i.e. thin); 1, strong (i.e. stout). Character 4 in Scharff & Coddington (1997); 78 in Miller & Hormiga (2004).
60. Palpal patella (male) ventral apophysis: 0, absent; 1, present. Character 29 in Hormiga (2000); 75 in Miller & Hormiga (2004).
61. Palpal patella prolateral proximal vertical macrosetae: 0, absent; 1, present (*M. savigniformis*, Fig. 60B).
62. Palpal femur difference in number of lyriform organ slits between prolateral and retrolateral sides: 0, more than one; 1, zero to one. All males of *Oedothorax*, *Ho. basalis* and *Callitrichia* possess five and three slits on the retrolateral and prolateral side of the distal part of the femur, respectively, although intra-specific variation occur in some species. The majority of *Mitrager* species (Clade 55 except for *M. hirsuta* and *M. sexoculata*, Clade 58 and Clade 65) have a difference in slit number of zero to one.
63. Palpal femur prolateral stout setae row (*M. elongata*-like): 0, absent; 1, present. This character is an autapomorphy of *O. elongata*.

64. Palpal femur scraper: 0, from cuticular extensions; 1, from setal bases. Except *St. lineatus*, all scrapers on the palpal femur of the investigated species are enlarged setal bases.
65. Scraper number: 0, more than one; 1, one.
66. Scraper on an elevated area: 0, absent; 1, present.

Chelicerae

67. Cheliceral setal bases on front-lateral face in male: 0, nearly flush with chelicerae to small bumps; 1, formed into distinct bumps; 2, greatly enlarged. Character 120 in Miller & Hormiga (2004). Distinct bumps support the grouping of *Ummeliata*, *Hylyphantes* and *Tmeticus* (Clade 24)
68. Cheliceral mastidia (dorsal spurs): 0, absent; 1, present. Character 39 in Miller (1999); 57 in Hormiga (2000); 56 in Hormiga (2003); 57 in Hormiga et al. (2003); 121 in Miller & Hormiga (2004). Presence of mastidia supports the grouping of *Gongylidium*, *Ummeliata*, *Hylyphantes* and *Tmeticus* (Clade 23); it also occurs independently in *O. gibbosus* within *Oedothorax* s.s., in *Gongylidium latebricola* and in *S. mingchihensis*.
69. Cheliceral fang furrow in male: 0, tapered; 1, wide and flat to concave. Character 122 in Miller & Hormiga (2004).
70. Chelicera lateral face stridulatory striae in male: 0, absent; 1, present. Character 36 in Hormiga (1993, 1994a); 52 in Hormiga (1994); 2 in Hormiga et al. (1995); 44 in Scharff & Coddington (1997); 37 in Griswold et al. (1998), 55 in Hormiga (2000), 43 in Hormiga (2002); 54 in Hormiga (2003); 55 in Hormiga et al. (2003); 116 in Miller & Hormiga (2004). Among the examined taxa, only *M. clypeellum* and *M. elongata* (Clade 58) lack cheliceral stridulatory striae.
71. Cheliceral stridulatory striae rows in male: 0, evenly spaced; 1, compressed proximally; 2, compressed distally. Modified from character 118 in Miller & Hormiga (2004). Two character states in Miller & Hormiga (2004), 'widely and evenly spaced' and 'compressed and evenly spaced' are combined to 'evenly spaced', since the width of striae rows is a continuum. Proximally compressed striae support Clade 16.
72. Chelicerae stridulatory striae scaly: 0, absent; 1, present. Modified from 117 in Miller & Hormiga (2004).
73. Chelicerae lateral lower stout setae group: 0, absent; 1, present. Autapomorphy of *M. elongata*.
74. Male cheliceral base apophysis: 0, absent; 1, present (*M. elongata*, Fig. 38C). In *M. clypeellum* and *M. elongata*, the anterior proximal part of chelicerae is elevated, forming apophyses.

Male prosoma and opisthosoma

75. Male clypeus hirsute: 0, absent; 1, present (*M. dismodicoides*, Fig. 38T).
76. Clypeus hump: 0, absent; 1, present (*M. dismodicoides*, Fig. 38T).
77. Sub-AME setae in male: 0, one; 1, two. Two sub-AME setae is a synapomorphy of Clade 18.
78. Pre-PME groove: 0, absent; 1, present (*M. lineata*, Fig. 38R).
79. PME lobe in male: 0, absent; 1, present (*M. falcifer*, Fig. 38K).
80. Inter-AME-PME strong setal group: 0, absent; 1, present (*M. falcifer*, Fig. 38K).
81. Inter AME PME hirsute region setae bend laterally: 0, absent; 1, present.
82. Inter-AME-PME lobe: 0, absent; 1, present (*M. savigniformis*, Fig. 38J).
83. Aggregated setal tuft at ocular region: 0, absent; 1, present (*Ca. sellafontis*, Fig. 7N; *M. noordami*, Fig. 38P).
84. Prosomal comb-like setae at interocular region: 0, absent; 1, present (*M. angela*, Fig. 26A, B). The branched, thus comb-like setae occur in four *Mitrager* species, *Walckenaeria acuminata* and *Ca. gloriosa*
85. Comb-like setae arrangement: 0, numerous, evenly distributed (*Ca. gloriosa*, Fig. 7L); 1, two pairs (*M. angela*, Fig. 26A, B). Two pairs of comb-like setae is a synapomorphy of *M. coronata*, *M. cornuta*, *M. angela* and *M. villosa*.
86. Pre-PME groove enlarged stout setae (*M. lucida*-like): 0, absent (*M. tholusa*, Fig. 56A); 1, present (*M. lucida*, Fig. 56B).
87. PME: 0, exposed; 1, inside PME lobe, not exposed (*M. lucida*, Fig. 38M).
88. Post-PME lobe setae bend laterally: 0, absent; 1, present.

89. Post- /inter-PME strong setal group bending forward: 0, absent (*M. assueta*, Fig. 43B); 1, present (*Oe. meghalaya*, Fig. 43A).
90. Male post-PME single macroseta strong, curved apically: 0, absent; 1, present (*N. setifera*, Fig. 19R).
91. Post PME groove: 0, absent; 1, present (*U. insecticeps*, Fig. 7K).
92. Post-PME lobe: 0, absent; 1, present (*Oe. apicatus*, Fig. 7D). Character 103 in Miller & Hormiga (2004).
93. Carapace sulci and pits: 0, absent; 1, present (*Oe. apicatus*, Fig. 7R). Character 108 in Miller & Hormiga (2004).
94. Male prosoma dorsal setae with seta-like setal base extension: 0, absent; 1, present (*M. angela*, Fig. 26B).
95. Thoracic furrow: 0, nearly smooth; 1, distinct invagination. Character 114 in Miller & Hormiga (2004).
96. Sternum-labium attachment: 0, separate; 1, fused. Character 124 in Miller & Hormiga (2004).
97. Femur I dorsal macroseta(ae): 0, absent; 1, present. Character 134 in Miller & Hormiga (2004).
98. Femur I prolateral macroseta(ae): 0, absent; 1, present. Character 135 in Miller & Hormiga (2004).
99. Tibia I distal dorsal macroseta: 0, absent; 1, present. Character 137 in Miller & Hormiga (2004).
100. Tibia I prolateral macroseta(ae): 0, absent; 1, present. Character 144 in Miller & Hormiga (2004).
101. Tibia I retrolateral macroseta(ae): 0, absent; 1, present. Character 145 in Miller & Hormiga (2004).
102. Tibia I ventral macroseta(ae): 0, absent; 1, present. Character 146 in Miller & Hormiga (2004).
103. Metatarsus I dorsal macroseta(ae): 0, absent; 1, present. Character 147 in Miller & Hormiga (2004).
104. Metatarsus I ventral macroseta(ae): 0, absent; 1, present. Character 150 in Miller & Hormiga (2004).
105. Male metatarsus and tarsus I long vertical setae: 0, absent; 1, present. The presence of these long vertical setae is a synapomorphy of *M. coronata*, *M. angela* and *M. villosa*.
106. Tibia II distal dorsal macroseta: 0, absent; 1, present. Character 139 in Miller & Hormiga (2004).
107. Tibia III distal dorsal macroseta: 0, absent; 1, present. Modified from Character 63 in Hormiga (2000); 141 in Miller & Hormiga (2004).
108. Male tibia III trichobothrial arrangement (prolateral-retrolateral): 0, three-three; 1, two-two; 2, two-three; 3, three-two; 4, four-four; 5, six-six; 6, three-four.
109. Tibia IV distal dorsal macroseta: 0, absent; 1, present. Modified from character 64 in Hormiga (2000); 143 in Miller & Hormiga (2004).
110. Metatarsus IV trichobothrium: 0, absent; 1, present. Character 65 in Hormiga (2000); 152 in Miller & Hormiga (2004).
111. Pedicel sternite and pleurites in male: 0, separated; 1, juxtaposed or fused. Character 153 in Miller & Hormiga (2004).
112. Booklung stridulatory organ in male: 0, rugose; 1, grooved; 2, squamate; 3, nearly smooth. Character 154 in Miller & Hormiga (2004).
113. Male posterior median spinneret (PMS) aciniform gland spigot (AC) number: 0, zero (*Ca. sellafontis*, Fig. 20J); 1, one (*M. angela*, Fig. 41F); 2, two (*Oe. gibbosus*, Fig. 6H); 3, three (*L. triangularis*, Fig. 87A).
114. Male PMS nubbin representing vestigial AC: 0, absent (*Ca. sellafontis*, Fig. 20J); 1, present (*M. modesta*, Fig. 58F). Males of *M. savigniformis*, *M. modesta* and *Ca. legrandi*, have a nubbin on PMS at the position corresponding to AC in other species.
115. Male PMS minor ampullate gland spigots (mAP): 0, absent (*Ca. sellafontis*, Fig. 20J); 1, present (*S. mingchihensis*, Fig. 86A); 2, nubbin (*Ca. juguma*, Fig. 21F). Six *Mitragrer* species and two *Callitrichia* species examined in this study have a nubbin on PMS at the position corresponding to the location of mAP in other species.
116. Male posterior lateral spinneret (PLS) AC number: 0, three or more; 1, two; 2, one; 3, zero. This character is analysed a additive.
117. Male and/or female PLS aggregate gland spigot (AG) number: 0, zero (*Ca. sellafontis*, Fig. 20H, J); 1, two (*A. meghalaya*, Fig. 77E), 2, one (*L. triangularis*, Fig. 87A).

Female

118. Palpal tarsus distal dorsomesal macrosetae in female: 0, absent; 1, present. Character 128 in Miller & Hormiga (2004).
119. Palpal tarsus proximal dorsoectal macrosetae in female: 0, absent; 1, present. Character 129 in Miller & Hormiga (2004).
120. Palpal tarsus distal dorsoectal macrosetae in female: 0, absent; 1, present. Character 130 in Miller & Hormiga (2004).
121. Palpal tarsus ventromesal macrosetae in female: 0, zero; 1, two; 2, three; 3, four; 4, five or more; 5, eleven to twelve. Character 131 in Miller & Hormiga (2004).
122. Palpal tarsus ventroectal macrosetae in female: 0, zero; 1, one; 2, two; 3, three; 4, four. Character 132 in Miller & Hormiga (2004).
123. Palpal tarsus claw in female: 0, absent; 1, present. Character 126 in Miller & Hormiga (2004).
124. Cheliceral teeth, retrolateral margin of fang furrow in female: 0, zero; 1, one; 2, two; 3, three; 4, four or more. Character 123 in Miller & Hormiga (2004).
125. Clypeal setae in female: 0, hirsute; 1, smooth. Character 113 in Miller & Hormiga (2004).
126. Epigynum dorsal plate orientation: 0, position of dorsal plate entirely dorsal to ventral plate; 1, dorsal plate extends anteriorly, flush with ventral plate. Character 93 in Miller & Hormiga (2004).
127. Copulatory duct encapsulation: 0, absent (*U. insecticeps*, Fig. 84C); 1, present (*Oe. agrestis*, Fig. 5E–G). Character 95 in Miller & Hormiga (2004).
128. Copulatory duct entering spermatheca: 0, mesal or dorsal to fertilization duct; 1, ectal to fertilization duct. In the current dataset, character state 1 is shared by *Ho. basalis* and *Callitrichia*, and also '*Oe. cunur*' and *Erigone atra*.

Continuous characters

129. Ratio of length of metatarsus IV to length from trichobothrium to distal end of metatarsus IV: range of measurements: 0.09–0.88 ($N = 78$). In certain *Mitrager* species, *Atypena*, *Callitrichia*, and *N. setifera*, the trichobothrium on metatarsus IV is particularly distally situated.
130. Tibia II length / tibia IV length: range of measurements: 0.69–1.22 ($N = 79$). Tibia length is measured on the dorsal side from the patella-tibia joint to the tibia-metatarsus joint.
131. Tibia III length / tibia I length: range of measurements: 0.43–0.92 ($N = 79$).
132. Palpal femur length / palpal patella length: range of measurements: 1.10–3.82 ($N = 79$). Femur length and patella length are measured on the dorsal side from the trochanter-femur joint to the femur-patella joint and from the femur-patella joint to the patella-tibia joint.

**3.4. Diversification through sexual selection on gustatory courtship traits
in dwarf spiders**

Shou-Wang Lin, Lara Lopardo and Gabriele Uhl

Manuscript published in *Frontiers of Zoology* (2021) 18: 51

RESEARCH

Open Access



Diversification through gustatory courtship: an X-ray micro-computed tomography study on dwarf spiders

Shou-Wang Lin* , Lara Lopardo and Gabriele Uhl

Abstract

Background: Sexual selection has been considered to promote diversification and speciation. Sexually dimorphic species have been used to explore the supposed effect, however, with mixed results. In dwarf spiders (Erigoninae), many species are sexually dimorphic—males possess marked prosomal modifications. These male traits vary from moderate elevations to bizarre shapes in various prosomal regions. Previous studies established that male dwarf spiders produce substances in these prosomal modifications that are taken up by the females. These substances can act as nuptial gifts, which increase the mating probability of males and the oviposition rate in females. Therefore, these dimorphic traits have evolved in the context of sexual selection. Here, we explore the evolutionary lability of this gustatory trait complex with the aim of assessing the role of this trait complex in species divergence by investigating (1) if erigonine modified prosomata are inherently linked to nuptial-gift-producing glands, (2) if the evolution of the glands evolution preceded that of the modified prosomal shapes, and by assessing (3) the occurrence of convergent/divergent evolution and cryptic differentiation.

Results: We reconstructed the position and extent of the glandular tissue along with the muscular anatomy in the anterior part of the prosoma of 76 erigonine spiders and three outgroup species using X-ray micro-computed tomography. In all but one case, modified prosomata are associated with gustatory glands. We incorporated the location of glands and muscles into an existing matrix of somatic and genitalic morphological traits of these taxa and reanalyzed their phylogenetic relationship. Our analysis supports that the possession of glandular equipment is the ancestral state and that the manifold modifications of the prosomal shape have evolved convergently multiple times. We found differences in gland position between species with both modified and unmodified prosomata, and reported on seven cases of gland loss.

Conclusions: Our findings suggest that the occurrence of gustatory glands in sexually monomorphic ancestors has set the stage for the evolution of diverse dimorphic external modifications in dwarf spiders. Differences among congeners suggest that the gland position is highly susceptible to evolutionary changes. The multiple incidences might reflect costs of glandular tissue maintenance and nuptial feeding. Our results indicate divergent evolutionary patterns of gustatory-courtship-related traits, and thus a likely facilitating effect of sexual selection on speciation.

Keywords: Nuptial feeding, Trait lability, Divergent evolution, Sexual selection, Micro-CT, Phylogeny, Araneae

Background

The great diversity of secondary sexual traits in the animal world has been the primary inspiration for Darwin's hypothesis of sexual selection [1, 2]. These dimorphic traits come in the form of coloration, ornamentation,

*Correspondence: shouwangliintaiwan@gmail.com
Zoological Institute and Museum, General and Systematic Zoology,
University of Greifswald, Greifswald, Germany



© The Author(s) 2021. **Open Access** This article is licensed under a Creative Commons Attribution 4.0 International License, which permits use, sharing, adaptation, distribution and reproduction in any medium or format, as long as you give appropriate credit to the original author(s) and the source, provide a link to the Creative Commons licence, and indicate if changes were made. The images or other third party material in this article are included in the article's Creative Commons licence, unless indicated otherwise in a credit line to the material. If material is not included in the article's Creative Commons licence and your intended use is not permitted by statutory regulation or exceeds the permitted use, you will need to obtain permission directly from the copyright holder. To view a copy of this licence, visit <http://creativecommons.org/licenses/by/4.0/>. The Creative Commons Public Domain Dedication waiver (<http://creativecommons.org/publicdomain/zero/1.0/>) applies to the data made available in this article, unless otherwise stated in a credit line to the data.

behavior, size and shape [3]. Examples of sexually dimorphic male traits evolved under mate choice or intrasexual competition, such as the feather ornaments of peacocks [4], the enlarged mandibles of stag beetles [5], and the antlers of deer [6]. Differences between populations in their mate preferences and in secondary sexual traits can lead to reproductive isolation [7]. Therefore, sexual selection has long been regarded as a driving force behind speciation [1, 8–10]. Alternatively, sexual dimorphism may also have evolved under the influence of ecological selection mechanisms. These include niche divergence between the sexes [11], such as the larger posterior salivary glands in male octopod *Eledonella pygmaea* due to intersexual vertical habitat partitioning in the water column and resulting differences in feeding habits [12]; and reproductive role division [13], like the female gigantism in many orb-weaving spiders selected for increased fecundity [14, 15].

Sexually dimorphic morphology has evolved in different spider groups several times independently, e.g., in some Theridiidae species (“cobweb spiders”) [16, 17], a pholcid (“daddy long leg spiders”) [18] and very pronounced so in the Erigoninae, a large subfamily of linyphiid spiders [19–21]. In these species, the shape and anatomy of the front body part (prosoma) of the males differ from those of the females and are highly species-specific. Moreover, in the species investigated thus far, the sexually dimorphic male prosomata play a role in nuptial feeding: females contact the specific structures and take up male glandular secretions during the mating sequence. Nuptial feeding during mating has been observed in spiders [19–22] as well as in insects [23]. In many cases, the secretions entice females to copulate and prolong copulation duration, which can increase sperm transfer [23]. There is ample evidence that these traits are involved in male-male competition, are subject to female choice, and might even represent sensory traps [24]. Therefore, it is likely that the evolution of these gustatory sexually dimorphic traits has been driven by sexual selection.

In erigonine spiders, the most speciose subfamily of Linyphiidae, which is in turn, the second-most diverse spider family [25], several morphological and behavioral studies on sexually dimorphic prosomal structures have been undertaken. In contrast to other linyphiid subfamilies, erigonines exhibit striking variations in male prosomata between and within taxa, including grooves, lobes, humps, turrets, as well as lateral sulci and pits on the prosomata [26]. Prosomal modifications are only found in adult males [27]. At least 223 among the 402 erigonine genera exhibit some degree of prosomal shape modifications, and the degree of variability differs among genera

[28, 29]. The modifications can occur anteriorly or posteriorly to the eye region of the prosoma, and are often associated with pores and modified setae [26, 30, 31]. In all species examined, the modified prosomal regions contain extensive secretory epidermal glandular tissues, with only one known exception [32–36]. Further, the cellular composition of the glandular units may vary even within a genus [36].

In all erigonines studied to date, the females contact the male prosomal structures with their mouthparts during courtship and mating and ingest the secretion [19–21, 37, 38]. The secretions released from the glandular tissue function as male mating effort through gustatory courtship, and were also shown to increase brood size [21]. Although these secretions were suspected to produce volatile substances for species recognition or female mate choice [39, 40], behavioral studies have found no indication of such pheromonal function [20, 41]. Since male prosomal structures are highly variable among species not only in position and shape but also in the degree of elaboration and secretory cell types, these male traits and the female preferences are most likely under direct selection. Since there has been no indication of ecological functions of these dimorphic male traits, the diversification is likely the result of sexual selection that is known to promote speciation [7]. Consequently, erigonine spiders are an ideal group for studying the evolution of sexually dimorphic traits and lend themselves to assessing the link between sexual selection and speciation.

Gustatory glandular tissues have also been found in erigonine species that lack pronounced prosomal modifications [32, 36]. It has thus been hypothesized that the glands may have evolved first in sexually monomorphic ancestors, followed by the independent evolution of various external modifications in different lineages [35, 40]. Indeed, recent phylogenetic studies imply parallel evolution of similar external prosomal shapes not only among erigonine genera [26, 42, 43], but also within genera [29]. However, these studies did not examine whether glandular tissues are associated with the respective prosomal structures. Consequently, the relationship between glands and prosomal shape remains to be explored, i.e., whether species without external prosomal modifications are equipped with glandular tissues, whether there are species with prosomal modifications that lack glandular tissues and whether externally similar prosomal shapes are similar in glandular equipment. Assessing the diversity of occurrence and location of glandular tissue and prosomal shape modifications within and between genera will elucidate the probability of convergence and evolvability of this trait complex.

X-ray micro-computed tomography (micro-CT) offers a non-destructive option for scrutinizing and visualizing internal morphological features and organ systems such as musculature, digestive system, nervous system, and glandular tissues [44–53]. Micro-CT has been applied to determine the location of the nuptial-gift-producing organ in a fly [54] as well as the prosomal glands in three erigonine spiders [28]. We use micro-CT to examine the presence/absence and the distribution of epidermal glands in the species included in [29]. The revision and phylogenetic analysis of [29] focused on the erigonine genus *Oedothorax* and its closely related taxa, mainly *Callitrichia* and *Mitrager*. By investigating the internal anatomy of the prosoma, we aim at elucidating the lability of this trait complex and the evolutionary patterns of both glands and prosomal structures. Instead of plotting the glandular features on the existing tree topology, we scored them as new characters and incorporated them into the character matrix, because these characters may also contain phylogenetic information. Since cheliceral and pharyngeal muscles also connect to the prosoma cuticle [28, 55–57], epidermal glands and muscle attachment are mutually exclusive. The cheliceral muscles control the movement of the chelicerae used for prey capture, grasping, chewing, digging burrows, carrying egg cases, and during courtship [58]. The pharyngeal muscles together with the sucking stomach serve to inject saliva and extract fluid from the prey [59]. There is a potential conflict between feeding and nuptial gift production caused by the limited cuticular surface space for muscle attachments and epidermal glands. We therefore also investigated the course and attachment location of these muscles.

For determining the appearances of male-specific glandular tissues in contrast to other types of tissues in the

scans, we compared the scans of female and male *Oedothorax gibbosus*, and applied the derived criteria to the identification of tissue types in other species. We also recorded cuticular structural details revealed by the scans. We assessed the variation in the glandular and muscular anatomy in species with diverse prosomal shapes, in order to address four major questions. 1) Are modified prosomata inherently linked to glands? 2) Did glands evolve before prosomal shape modifications? 3) Did similar external prosomal shapes evolve convergently and 4) are there cryptic differences in internal gland distributions among externally similar species? If prosomal structures as well as the distribution of gustatory glands show divergent evolutionary patterns between and within lineages, and similar prosomal structures evolved convergently in different lineages, we consider this strong support for a diversifying effect of sexual selection in erigonines.

Methods

Studied taxa

Among the 79 species included in the study of [29] 77 species were micro-CT-scanned for one male prosoma, except *Oedothorax gibbosus* and *Gongyliidiellum latebricola*. In *Oedothorax gibbosus*, two male morphs occur, one with strongly modified prosomal shape (*gibbosus* morph) and one without (*tuberosus* morph) [60]; consequently one male of each morph was scanned. *Gongyliidiellum vivum* was scanned instead of *G. latebricola* due to the poor preservation condition of the latter. For *Mitrager noordami* and *Oedothorax gibbosus*, the prosomata of both sexes were scanned to demonstrate the difference between the unmodified female and the modified male prosomata. Voucher information of the investigated specimens is provided in Additional File 1: Table S1.

Sample preparation, micro-CT scanning and image processing

Samples were dehydrated through a graded ethanol series (70, 80, 90, 95, 99% ethanol). To enhance tissue contrast, specimens were transferred to a 1% iodine solution (iodine, resublimated [Carl Roth GmbH & Co. KG, Karlsruhe, Germany; cat. #X864.1] in 99.8% ethanol) for 48 h [51]. Samples were washed in 99% ethanol twice, in an interval of 24-h and were subsequently mounted inside modified plastic pipette tips [28]. Micro-CT scans were performed using an optical laboratory-scale X-ray microscope (Zeiss XradiaXCT-200). Scans were performed with a 20 × objective lens unit using the following settings: 30 kV voltage/8 W power and an exposure time of 3 s. These settings resulted in scan times of about 2 h and a pixel size between 1 and 1.5 μm. Tomography projections were reconstructed using XMReconstructor (Carl Zeiss Microscopy GmbH, Jena, Germany), resulting

Table 1 Abbreviations and/or coloration of morphological structures follow mostly Wood and Parkinson (2019)

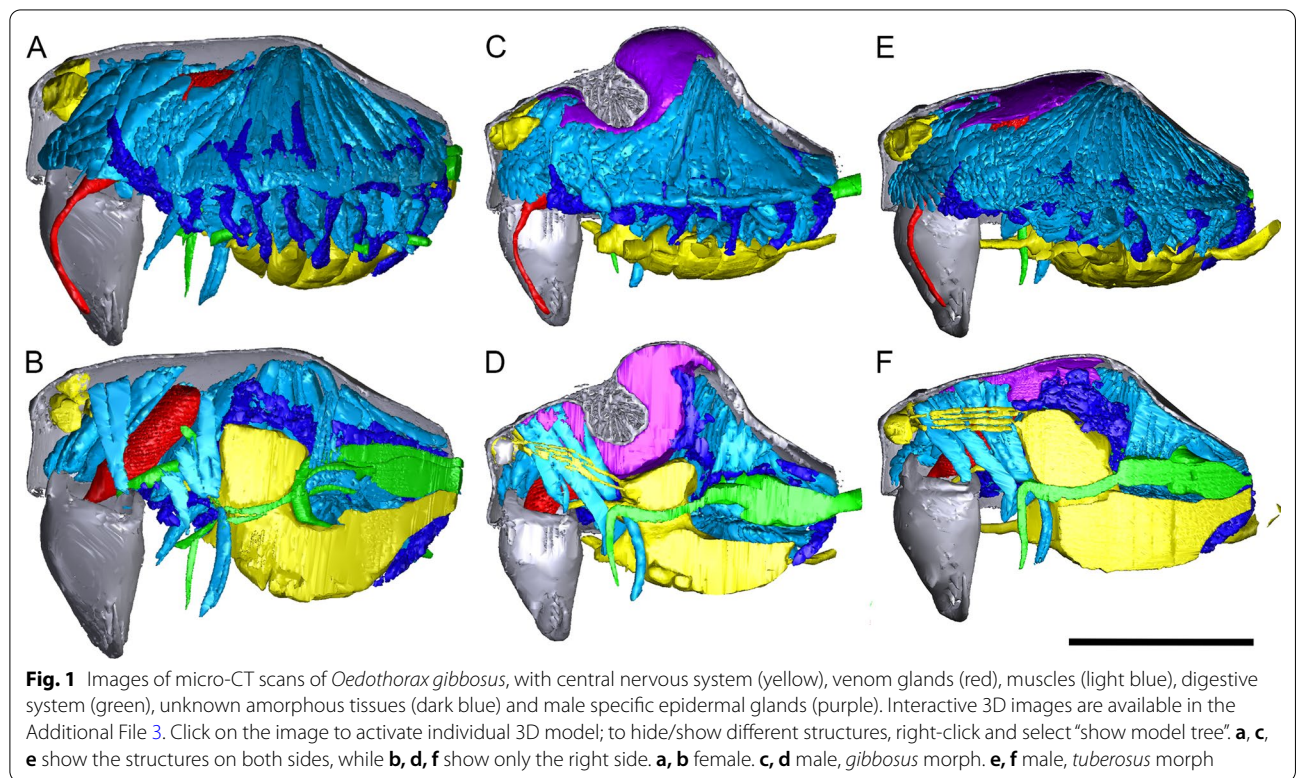
Structure and abbreviation in present paper	Color in figures
Gustatory glandular tissue	Purple
Anterior median eyes (AME)	
Anterior medial inner muscle (AMI)	Dark Blue
Anterior medial muscle (AM)	Dark purple
Anterior medial outer muscle (AMO)	Light blue
Anterior outer muscle (AO)	Red
Anterior pharyngeal dilator muscle (DA)	Light orange
Inter-cheliceral-sclerite muscle (IC)	Aqua
Lateral anterior muscle (LA)	Yellow
Lateral posterior muscle (LP)	Magenta
Posterior median eyes (PME)	-
Posterior medial muscle (PM)	Green
Posterior pharyngeal dilator muscle (DP)	Dark orange

Table 2 Summarized results of the implied weights analyses using different *k* values

<i>k</i>	Best score	No. of trees	No. of hits	Tree length	Clade 26	Clade 50	Clade 64	No. common clades with equal weight tree
1	60.52497	1	40	533	P	P	P	33
2	49.89028	1	41	526	P	M-c	P	35
3	42.88728	1	46	526	P	M-c	P	35
4	37.85770	1	50	521	P	M-c	M+n	38
5	33.96389	1	12	520	P	M-c	P	40
6	30.86829	1	3	520	P	M-c	P	40
10	22.80454	1	13	515	M	M	P	50
15	17.30398	1	2	511	M+m	M	P	47
20	13.96072	1	1	509	M	M	P	53
30	10.08356	1	5	504	M+m	M	M+n	55
100	3.43621	1	3	503	M	M+m	M+n	63
1000	0.36323	1	2	503	M	M	M	77

Tree lengths were calculated only by discrete characters with weight = 1

c: *Callitrichia convector*; M: monophyletic *m*: *Oedothorax meghalaya incertae sedis*; *n*: *Oedothorax nazareti incertae sedis*; P: polyphyletic



in image stacks (TIFF format). All scans were performed using Binning 2 (Camera Binning) for noise reduction and subsequently reconstructed with full resolution (using Binning 1). Since the microCT resolution did not allow for a cellular level identification of the tissue, we compared semi-thin histological sections of *O. gibbosus*

males (gland present in both *gibbosus* and *tuberosus* morphs) [36] and females (gland supposed to be absent) to the representation of the tissue on the virtual sections. The decision as to the presence or absence of epidermal glands in the studied species was based on this comparative assessment.

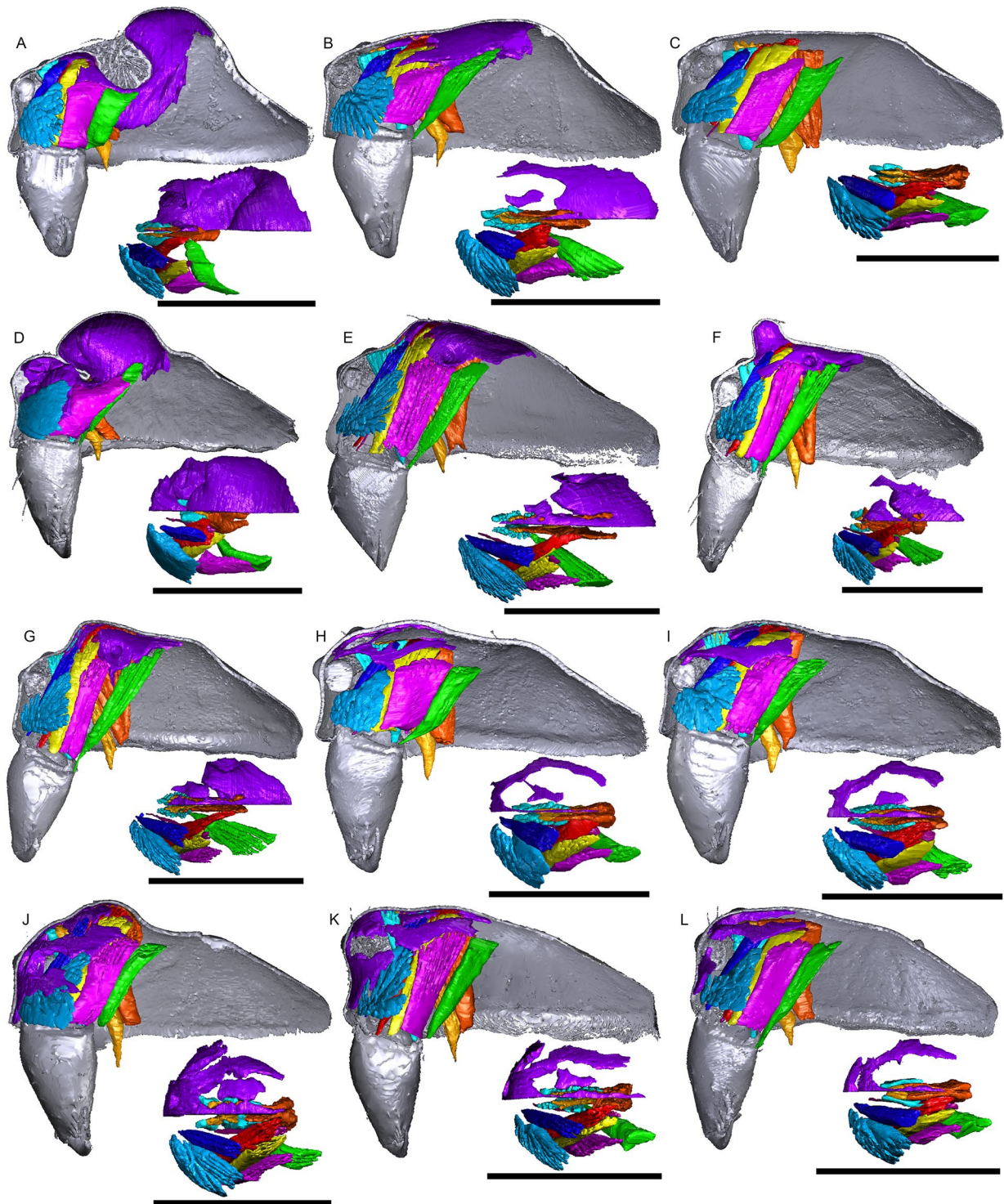
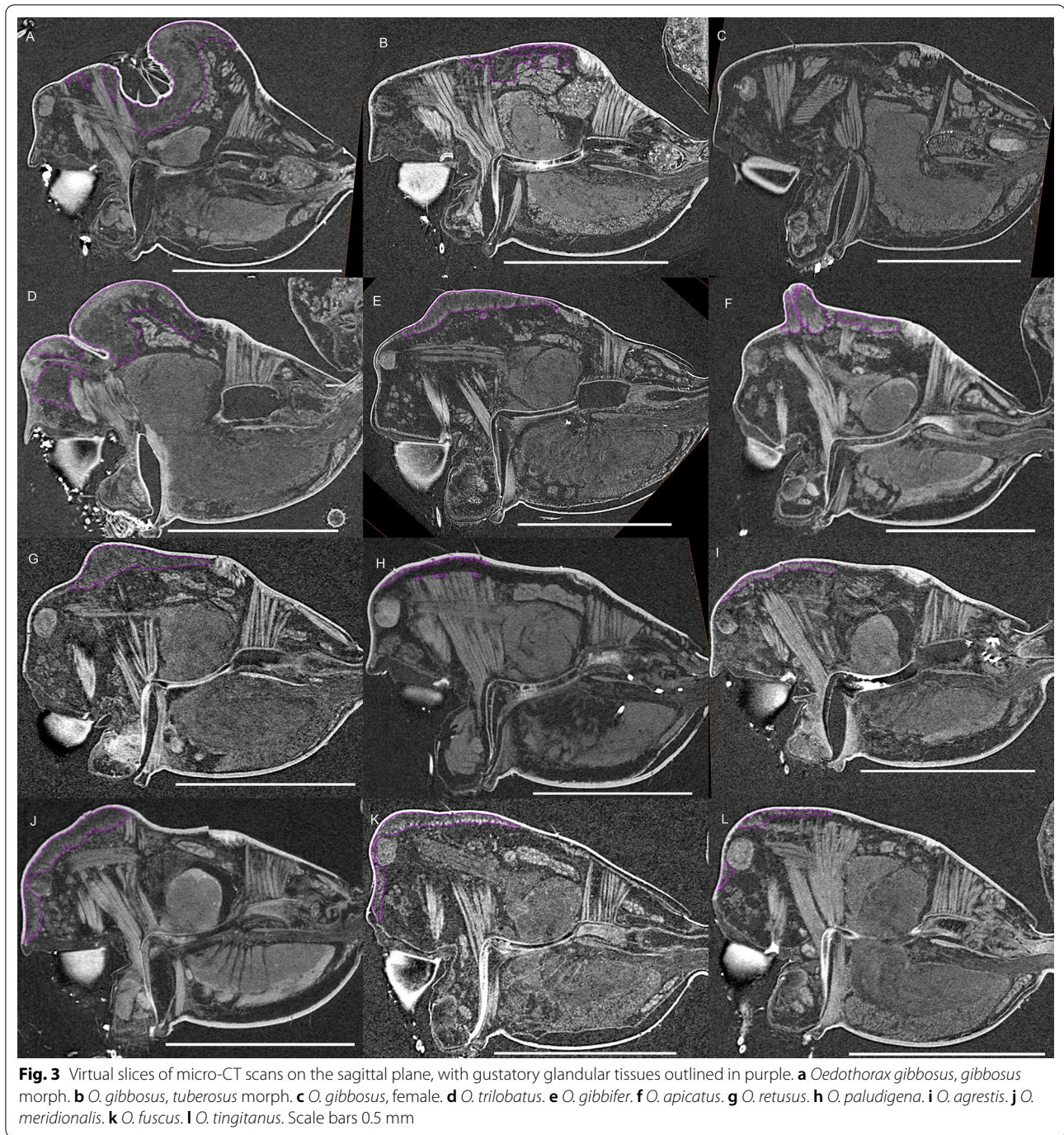
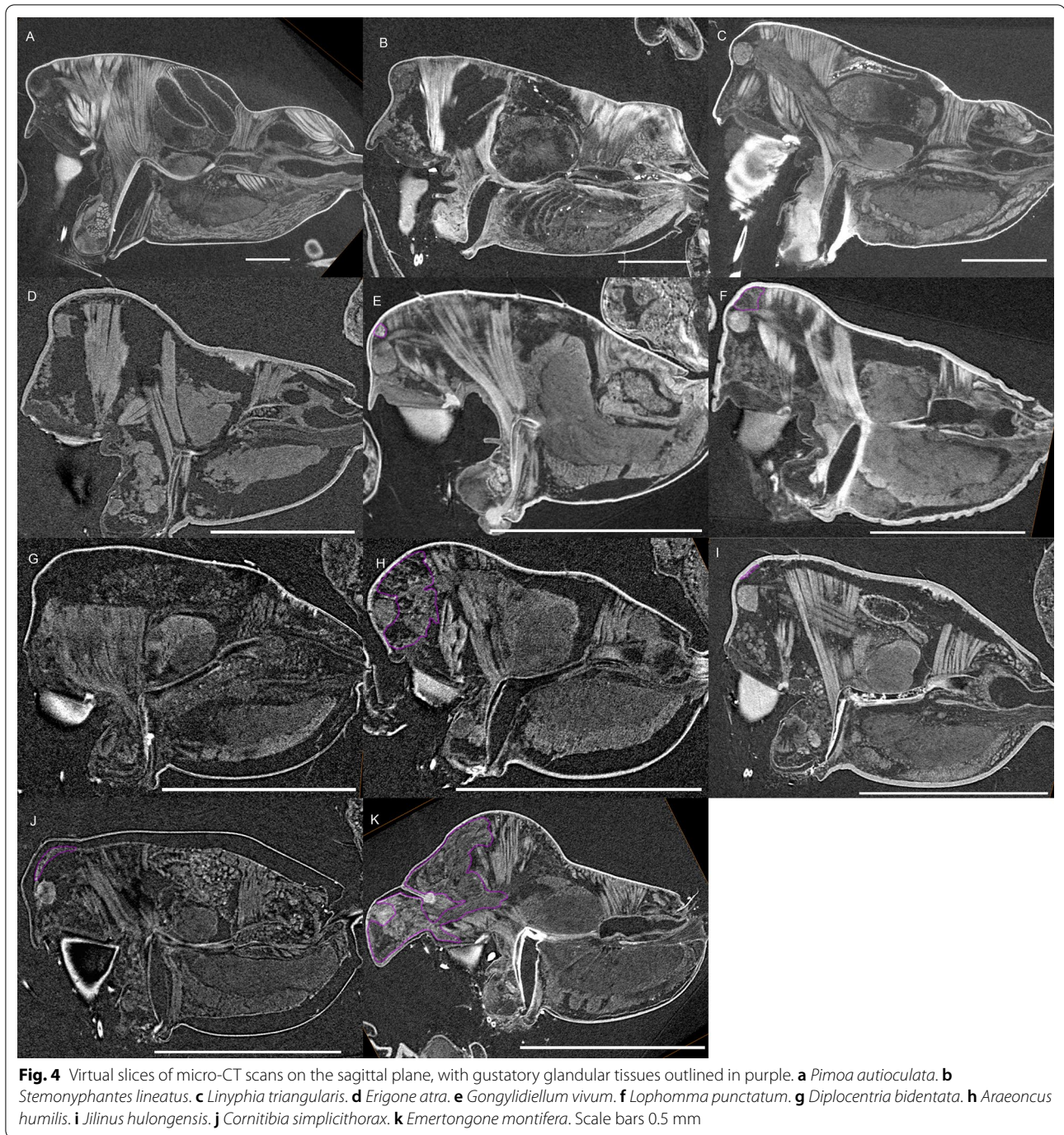


Fig. 2 Images of micro-CT scans with gustatory glandular tissues (purple), different sets of cheliceral muscles (left side), pharyngeal dilators (both sides). The right side of the prosomal cuticle digitally is segmented and color-coded following Table 1. Interactive 3D images are available in the Additional File 4. Click on the image to activate individual 3D model; to hide/show different structures, right-click and select “show model tree”. **a** *Oedothorax gibbosus*, *gibbosus* morph. **b** *O. gibbosus*, *tuberosus* morph. **c** *O. gibbosus*, female. **d** *O. trilobatus*. **e** *O. gibbifer*. **f** *O. apicatus*. **g** *O. retusus*. **h** *O. paludigena*. **i** *O. agrestis*. **j** *O. meridionalis*. **k** *O. fuscus*. **l** *O. tingitanus*. Scale bars 0.5 mm



To provide showcase examples of the internal prosomal structures, the following organ systems were digitally labeled in AMIRA 6.0.1 (Visualization Science Group, FEI) for one *Oedothorax gibbosus*-morph male, one *tuberosus*-morph male, and one female: nervous system, muscles, digestive system as well as male-specific epidermal glandular tissues, and an unknown tissue found in different areas

in the prosoma. For all examined species (except *Walckenaeria acuminata* due to low resolution caused by tissue shrinkage), the following structures were labeled: dorsal part of prosoma, chelicerae (at least the proximal part), supposed gustatory glandular tissues, and all muscles connecting the dorsal part of the prosoma with the chelicerae and the pharynx. We use the English terms for the muscle as done in



[57]. Abbreviations used in the text or figures are given in Table 1. For visualization, the labeled structures were converted to a surface mesh by Fiji [61]. These files were subsequently imported into MeVisLab (*MeVis Medical Solutions AG and Fraunhofer MEVIS*) using the “Scientific3DFigurePDFApp” module, reduced, colored, and exported as u3D files, which were subsequently inserted into the additional files in the.pdf format (Adobe Acrobat Pro).

Phylogenetic analysis and reconstruction of character state transformations

Parsimony analyses were conducted with TNT Version 1.1 [62] using a traditional search with random seed 1, 500 replications, 1000 trees saved per replication, branch swapping by TBR algorithm. Continuous characters were treated as ordered and analyzed as such [63]. For equal weight analysis, two clade support measures, Bremer



support (tree suboptimal by 17 steps during TBR retained from existing trees) and Jackknife support (removal probability = 36%), were also calculated using TNT. For implied-weighting analyses, the constants of concavity k were set for 1–6, 10, 15, 20, 30, 100, 1000 for relatively high to relatively low cost of homoplasy [64]. Character

optimization and generation of tree images were carried out using Winclada version 1.00.08 [65].

Our character matrix (Additional File 2) is based on Matrix II of [29] (79 taxa, 128 discrete and four continuous morphological characters). Seven new discrete characters were added based on findings from the micro-CT

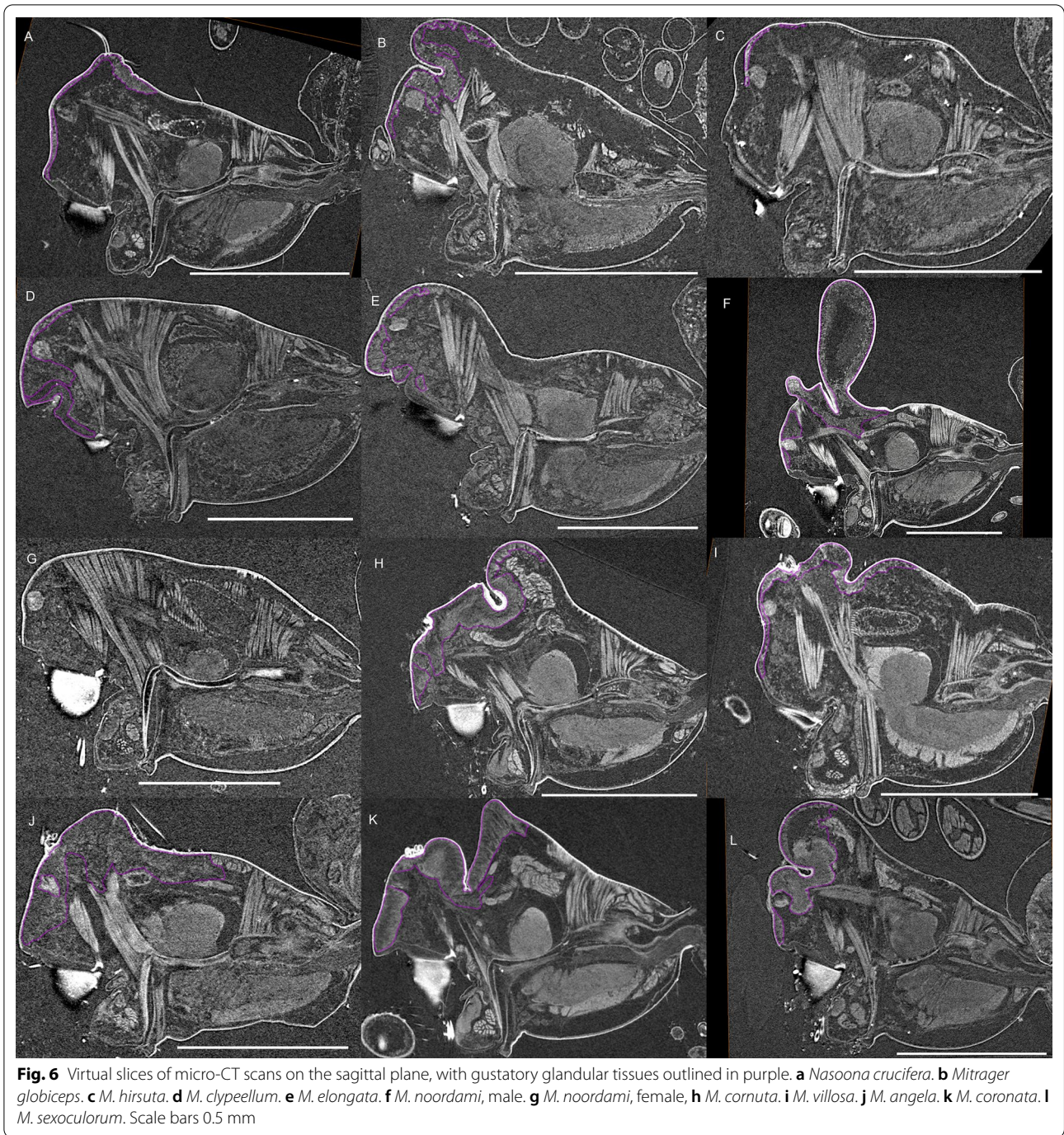
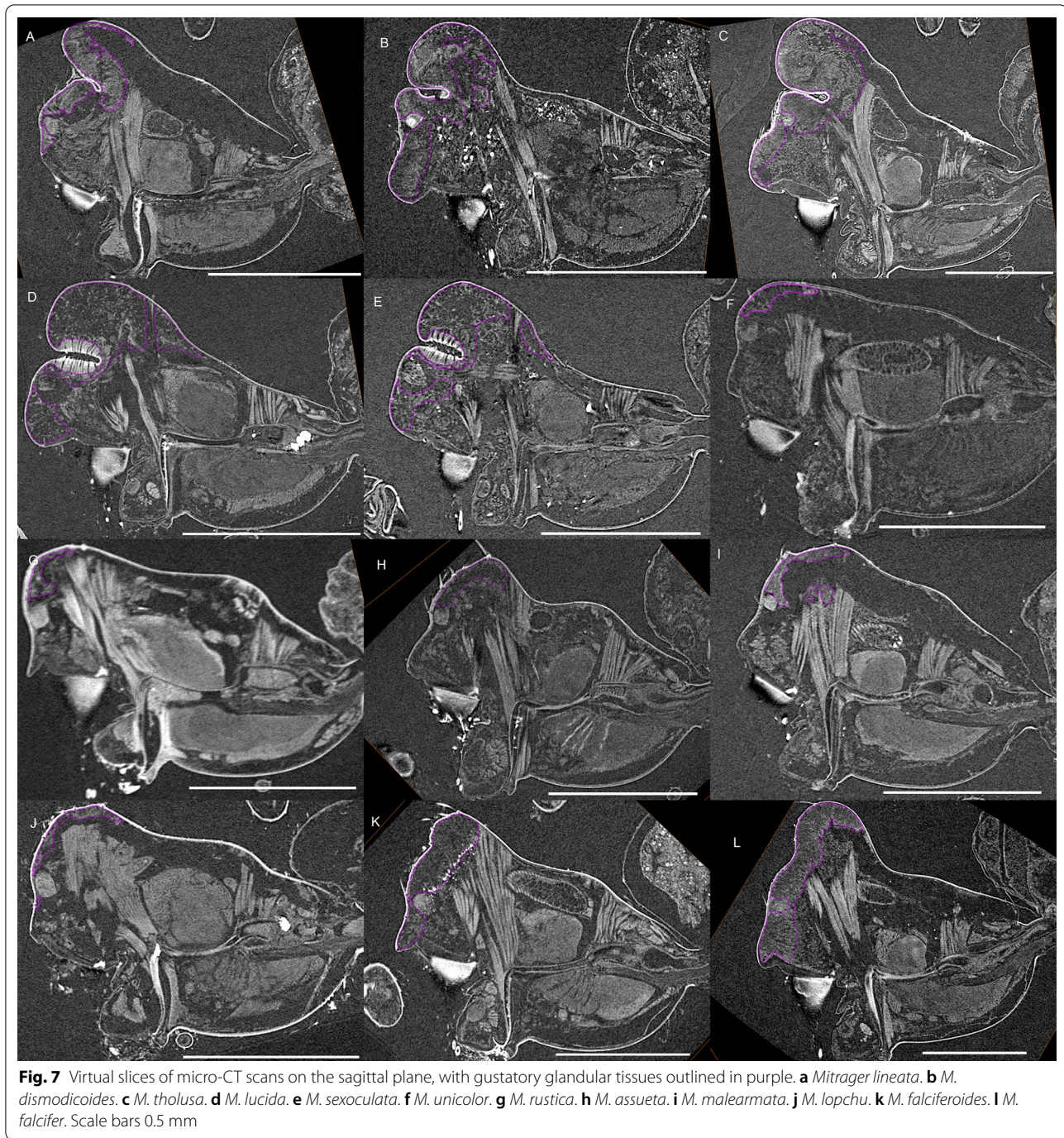


Fig. 6 Virtual slices of micro-CT scans on the sagittal plane, with gustatory glandular tissues outlined in purple. **a** *Nasoona crucifera*. **b** *Mitrager globiceps*. **c** *M. hirsuta*. **d** *M. clypeellum*. **e** *M. elongata*. **f** *M. noordami*, male. **g** *M. noordami*, female, **h** *M. cornuta*. **i** *M. villosa*. **j** *M. angela*. **k** *M. coronata*. **l** *M. sexocolorum*. Scale bars 0.5 mm

reconstruction of the internal structures (see below for description), resulting in a matrix with 135 discrete and four continuous characters: Ch. 130. gustatory epidermal gland: 0, absent; 1, present; Ch. 131. gustatory epidermal gland at before-eye region: 0, absent; 1, present; Ch. 132. gustatory epidermal gland at eye region: 0, absent; 1, present; Ch. 133. gustatory epidermal gland

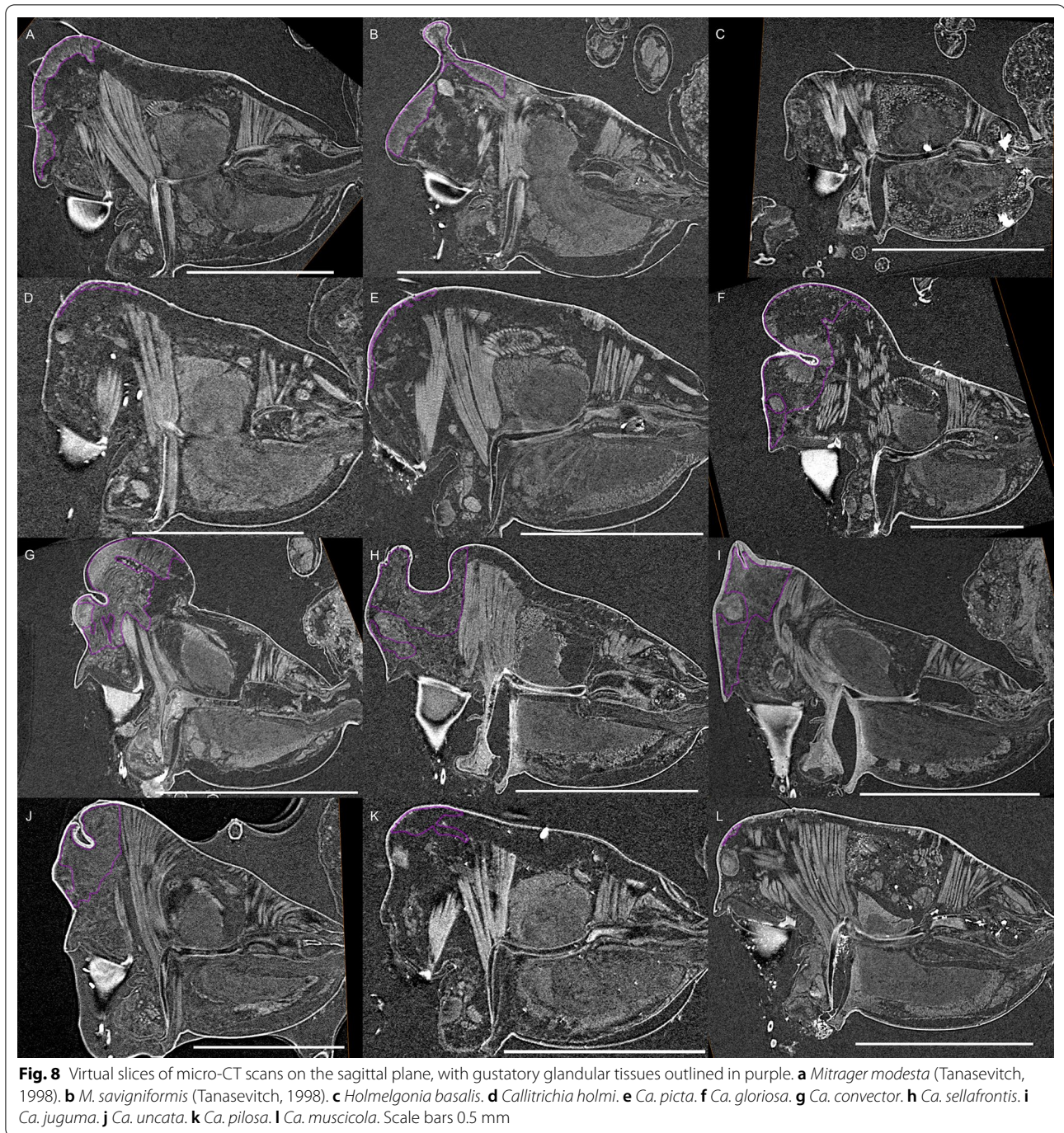
surrounded by the pharynx muscle: 0, absent; 1, present; Ch. 134. gustatory epidermal gland posterior to the pharynx muscle: 0, absent; 1, present; and 135. gland in the chelicerae: 0, absent; 1, present; Ch. 129. pre-posterior-median-eye (PME) groove muscle attachment (applicable only when the pre-PME groove is present): 0, no muscle attached to the groove; 1, inter-cheliceral-sclerite muscle



attached to the groove; 2, inter-cheliceral-sclerite muscle and anterior pharyngeal dilator muscle attached to the groove. After comparative re-examination of specimens, the previous homology interpretation of some male palpal features in two species could not be corroborated and therefore the character scoring was changed to “unknown”. The newly defined characters (Additional File

1: Table S2), other changes in the character matrix, and the observation on the cheliceral and pharyngeal muscles that differed from the previous description [57] are reported in the Additional File 1.

The micro-CT scans and reconstructions led to one character redefinition and revealed two scoring mistakes in one species in matrix II in [29]. Character 91



(i.e., absence/presence of post-PME groove) was redefined as “post-posterior-pharyngeal-dilator-muscle (-DP) groove”: i.e., the post-PME groove is located posteriorly to the posterior pharyngeal dilator muscle attachment. This redefinition rendered the scoring of this character as absent in *Emertongone montifera*, as the groove is located anteriorly to the posterior pharyngeal dilator attachment;

and as present in *Mitrager noordami*. Corrections of scoring mistakes for *Mitrager globiceps* comprise character 80 (inter-anterior-median-eye (AME) -PME strong setal group) as absent instead of present; and character 89 (post-/inter-PME strong setal group bending forward) also as absent instead of present.

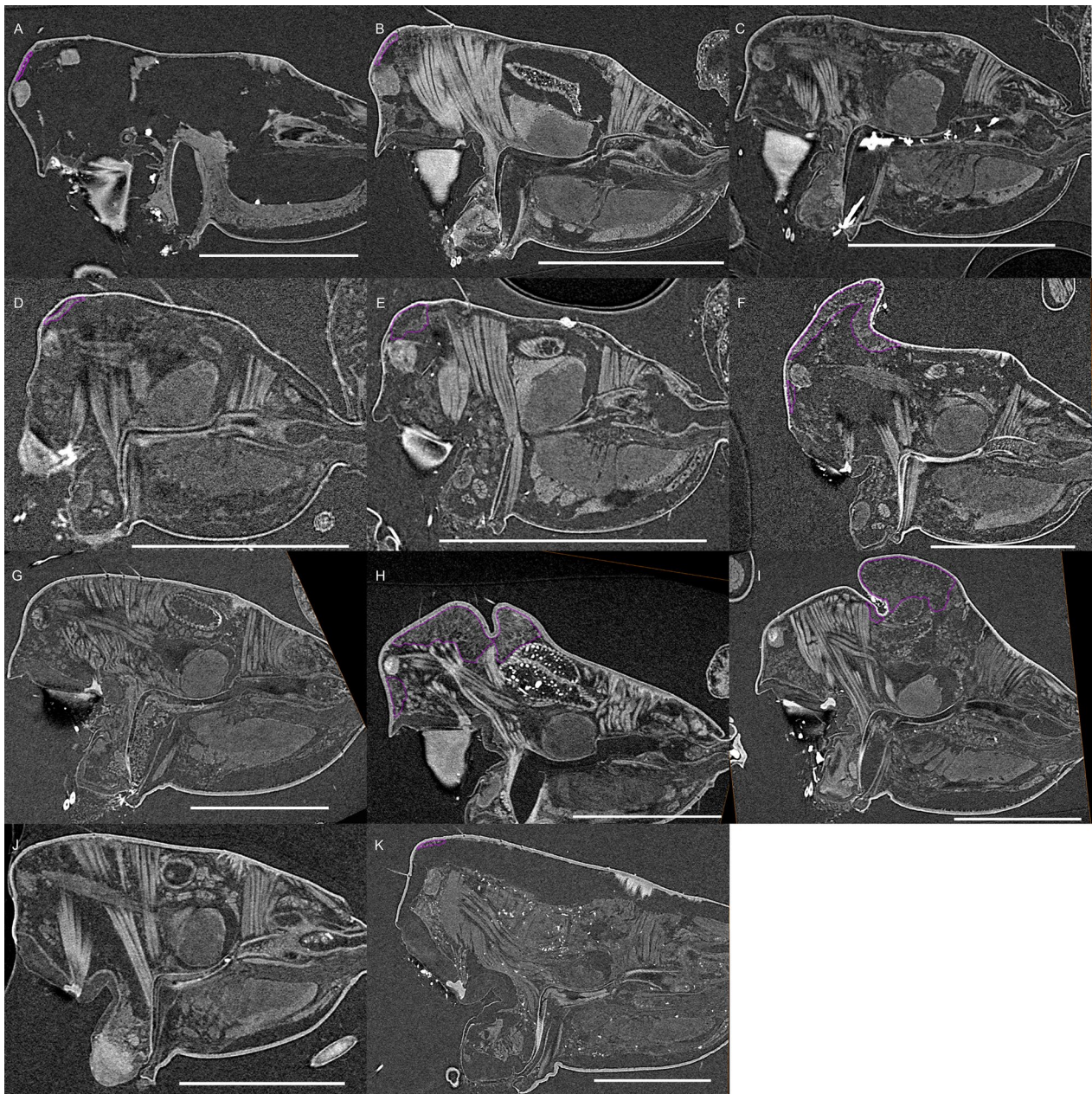


Fig. 9 Virtual slices of micro-CT scans on the sagittal plane, with gustatory glandular tissues outlined in purple. **a.** *Callitrichia latitibialis*. **b.** *Ca. longiducta*. **c.** *Ca. usitata*. **d.** *Ca. legrandi*. **e.** *Ca. macrophalma*. **f.** *Oedothorax nazareti incertae sedis*. **g.** *Gongylidium rufipes*. **h.** *Ummeliata insecticeps*. **i.** *U. esyunini*. **j.** *Hyllyphantes graminicola*. **k.** *Tmeticus tolli*. Scale bars 0.5 mm

Results

Determining male-specific glandular tissues in the scans

Figure 1 shows the internal structures of males and females of *Oedothorax gibbosus*: the glandular tissues (purple), the central nervous system (magenta), the venom glands (red), the muscles (light blue), and the digestive system (green). Epidermal tissue that appeared

homogenous was found only in the males, closely associated with the modified prosomal area (Fig. 1c–f, purple). The distribution of this type of tissue in the scans of both morphs of *Oedothorax gibbosus* male (Figs. 1c–f, 2a, b, 3a, b) is in congruence with the area marked as possessing the glandular epithelium (Figs. 7a, 9a in [36]). In this reference paper [36], the occurrence and cellular

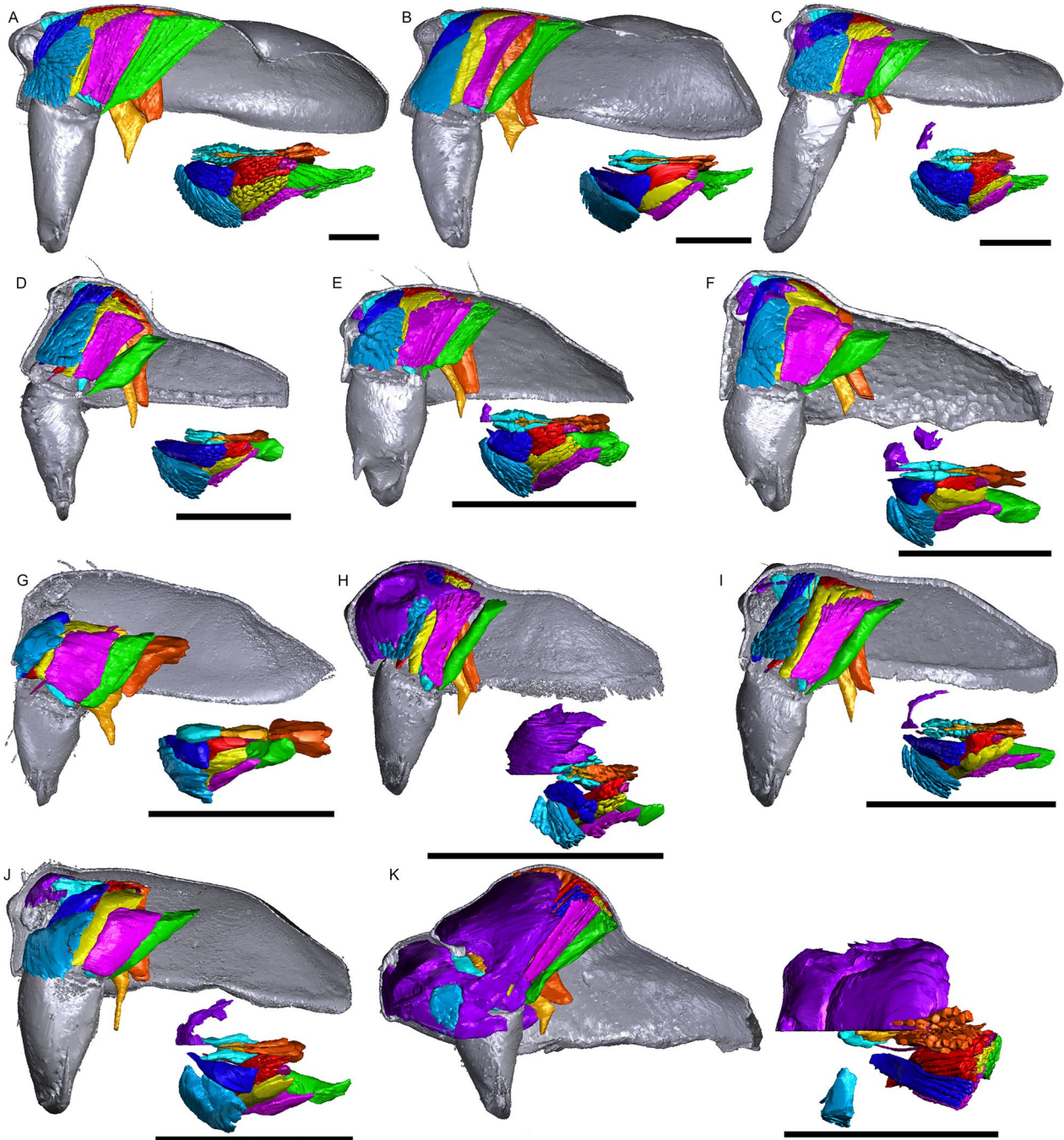


Fig. 10 Images of micro-CT scans with gustatory glandular tissues (purple), different sets of cheliceral muscles (left side), pharyngeal dilators (both sides). The right side of the prosomal cuticle is digitally segmented and color-coded following Table 1. Interactive 3D images are available in the Additional File 5. Click on the image to activate individual 3D model; to hide/show different structures, right-click and select “show model tree”. **a** *Pimoo autioculata*. **b** *Stemonyphantes lineatus*. **c** *Linyphia triangularis*. **d** *Erigone atra*. **e** *Gongyliellum vivum*. **f** *Lophomma punctatum*. **g** *Diplocentria bidentata*. **h** *Araeoncus humilis*. **i** *Jilinus hulungensis*. **j** *Cornitibia simplicithorax*. **k** *Emertongone montifera*. Scale bars 0.5 mm

(See figure on next page.)

Fig. 11 Images of micro-CT scans with gustatory glandular tissues (purple), different sets of cheliceral muscles (left side), pharyngeal dilators (both sides). The right side of the prosomal cuticle is digitally segmented and color-coded following Table 1. Interactive 3D images are available in the Additional File 6. Click on the image to activate individual 3D model; to hide/show different structures, right-click and select “show model tree”. **a** *Walckenaeria acuminata*. **b** *Gonatium rubellum*. **c** *Shaanxinus mingchihensis*. **d** *Oedothorax kodaikanal incertae sedis*. **e** *O. paracymbialis incertae sedis*. **f** *O. meghalaya incertae sedis*. **g** *Atypena cirrifrons*. **h** *A. formosana*. **i** *Oedothorax uncus incertae sedis*. **j** *O. cunur incertae sedis*. **k** *O. stylus incertae sedis*. **l** *Nasoona setifera*. Scale bars 0.5 mm

setup of the glandular tissue in several *Oedothorax* species was described with semithin histology and transmission electron microscopy. The comparison allowed us to infer from the appearance of a given tissue in the micro-CT scan to the presence or absence of gustatory epithelial glands. We then delineated the tissue as such in the erigonine males of the current study (outlined in purple; Figs. 3, 4, 5, 6, 7, 8, 9 3D reconstructions, Figs. 2, 10, 11, 12, 13, 14, 15). An amorphous tissue for unknown function occurring in both males and females was coloured in dark blue (Fig. 1). This tissue generally occurs around the organs and between muscles and does not show sexual dimorphism.

Variation in the distribution of glandular tissues and cheliceral/pharyngeal muscles

Gustatory glands were found in males of all included 46 species of erigonines with obvious sexually dimorphic prosomal shapes, except for *Erigone atra*. Gustatory glands were also found in 23 out of the 27 males of erigonine species that lack external dimorphic structures (species without external dimorphic structures are given in bold in Fig. 16). In the non-erigonine taxa included in the current study, glandular tissue is present in the eye region of *Linyphia triangularis* (Fig. 17a). However, *L. triangularis* possesses two small glandular areas, one on each side of the prosoma between the anterior median and the anterior lateral eyes. In the erigonines with gustatory glandular tissue in these areas, there is one large glandular area that spans from one side to the other. The effect of tissue shrinkage on the attachment of tissues to the cuticle is reported in the Additional File 1.

The gustatory gland distribution among the studied species varies considerably: from close to the anterior margin of the before-eye region (e.g., *Oedothorax meridionalis*, Fig. 2j) to the region adjacent to the anterior margin of the central posterior infolding of the prosoma (i.e., the fovea; e.g., *O. gibbosus*, Fig. 2a, b). In *Mitrager clypeellum* and *M. elongata*, the gustatory glands extend anteriorly and proximally into the chelicerae and seem to be connected to the gustatory glands in the before-eye and eye regions (Fig. 12d, e respectively). When gustatory glands occur in an area between attachment areas of

different muscles, there are increased intervals between these muscles. For instance, the lateral anterior muscle and the lateral posterior muscle are adjacent to each other in *Oedothorax retusus* without gustatory glandular tissue between them (Fig. 2g), while these muscles are spatially separated to different degrees in the *Oedothorax* species in Clade 74 (Fig. 2h–l). In many species, gustatory glandular tissues occur medially in the positions of the inter-cheliceral-sclerite muscle, anterior pharyngeal dilator, and posterior pharyngeal dilator, while the dorsal attachment points of these muscles are symmetrically separated in various degrees along the longitudinal axis (e.g., slightly in *Oedothorax paludigena*, Fig. 2h; strongly in *Mitrager coronata*, Fig. 12k).

In species with prosomal modifications, the extent of the dorsal attachment of the pharyngeal dilators varies along the longitudinal axis, ranging from narrow (*Oedothorax gibbosus*, Fig. 2a) to wide (*O. gibbifer*, Fig. 2e). In addition, externally similar shapes of the male prosomata may present differences in internal attachments of gustatory glands and muscles. For example, in species with a pre-PME groove, three patterns of muscle attachments related to the groove are observed (see Fig. 18): (1) no muscle attached to the groove (e.g., *Mitrager dismodioides*); (2) one branch of the inter-cheliceral-sclerite muscle attached to the groove (e.g., *M. lucida*); (3) one branch of both the inter-cheliceral-sclerite muscle and the anterior pharyngeal dilator attached to the groove (e.g., *M. sexocolorum*). In the species with the inter-cheliceral-sclerite muscle or the inter-cheliceral-sclerite muscle and anterior pharyngeal dilator attached to the groove, the PMEs are close to the upper side of the groove and not exposed. The spatial relationships between the PMEs, the inter-cheliceral-sclerite muscle, the anterior pharyngeal dilator and the central macroseta are consistent across erigonine taxa with different degrees of prosomal modification (Fig. 19). For instance, in *Mitrager tholusa* (Fig. 19c), the attachments of the inter-cheliceral-sclerite muscle, anterior pharyngeal dilator and posterior pharyngeal dilator have more anterior positions in the PME lobe, which coincide with the more anterior position of the central macroseta compared to that in *M. rustica* and *M. falciferoides* (Fig. 19a, b respectively) and

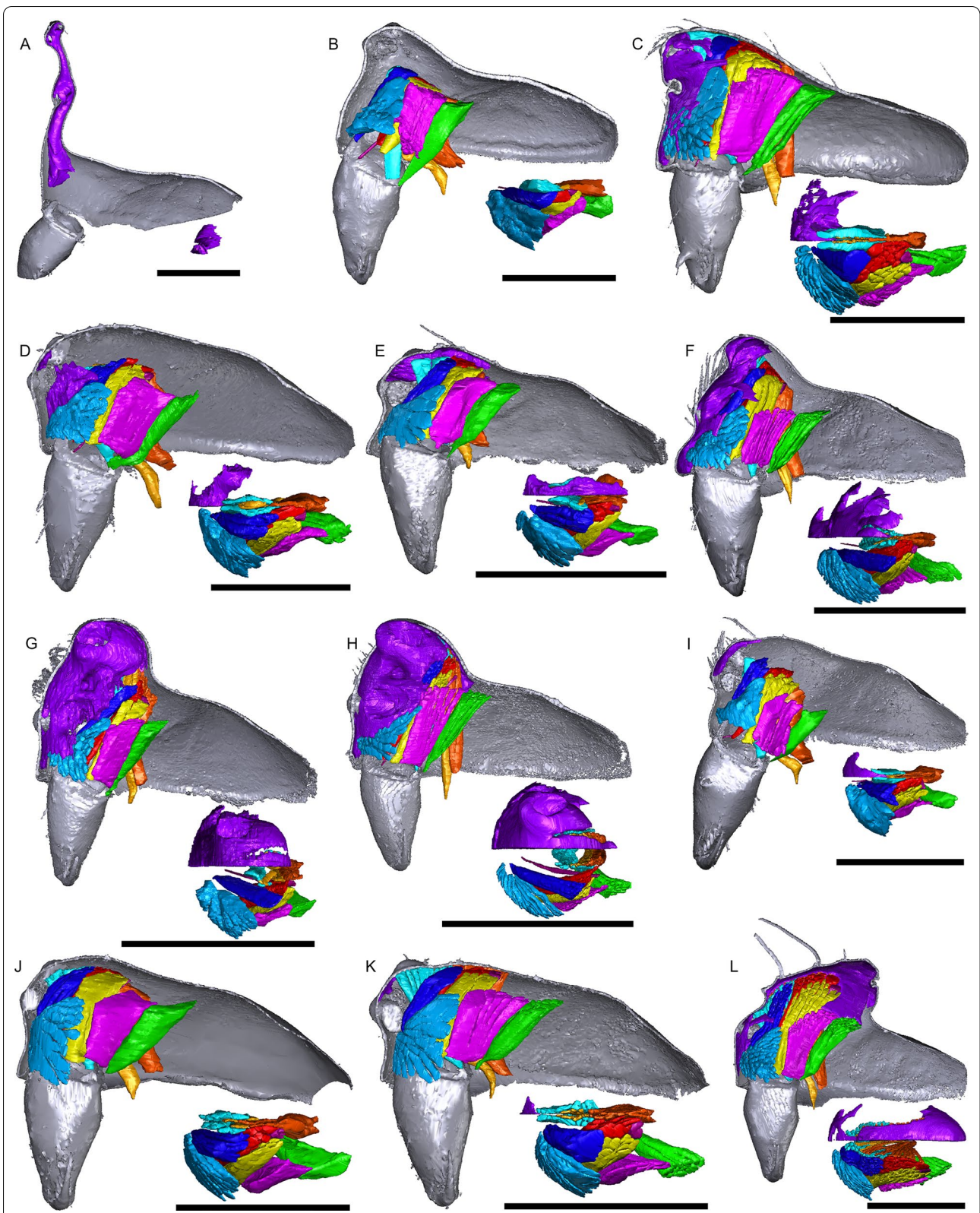


Fig. 11 (See legend on previous page.)

(See figure on next page.)

Fig. 12 Images of micro-CT scans with gustatory glandular tissues (purple), different sets of cheliceral muscles (left side), pharyngeal dilators (both sides). The right side of prosomal cuticle is digitally segmented and color-coded following Table 1. Interactive 3D images are available in the Additional File 7. Click on the image to activate individual 3D model; to hide/show different structures, right-click and select “show model tree”.

a *Nasoona crucifera*. **b** *Mitrager globiceps*. **c** *M. hirsuta*. **d** *M. clypeellum*. **e** *M. elongata*. **f** *M. noordami*, male. **g** *M. noordami*, female **h** *M. cornuta*. **i** *M. villosa*. **j** *M. angela*. **k** *M. coronata*. **l** *M. sexocolorum*. Scale bars 0.5 mm

Callitrichia gloriosa (Fig. 19f); in *M. sexocolorum* and *M. lucida*, in which the anterior filaments of the inter-cheliceral-sclerite muscle or both the inter-cheliceral-sclerite muscle and posterior pharyngeal dilator are attached to the groove, the central macroseta is located inside the groove (Fig. 19d, e respectively).

In species with a post-PME lobe, the internal attachment of the inter-cheliceral-sclerite muscle, anterior pharyngeal dilator and posterior pharyngeal dilator varies greatly among species. For instance, all three muscles are attached anterior to the post-PME groove (*Mitrager cornuta*, Fig. 20e); all three muscles are attached to the anterior side of the post-PME groove (*Oedothorax trilobatus*, Fig. 20b); only the posterior pharyngeal dilator is attached to the posterior half of the post-PME lobe, but neither the inter-cheliceral-sclerite muscle nor the anterior pharyngeal dilator (*Emertongone montifera*, Fig. 20a); all three muscles are attached to the anterior half of the post-PME lobe (*Nasoona setifera*, Fig. 20d); all three muscles are attached to most of the extent of the post-PME lobe (*O. meridionalis*, Fig. 20c); the inter-cheliceral-sclerite muscle and anterior pharyngeal dilator are attached to most of the extent of the post-PME lobe, the posterior pharyngeal dilator is attached to the posterior side of the lobe and its attachment extends further posteriorly into the prosoma (*O. nazareti incertae sedis*, Fig. 20f).

Cuticular structures revealed in micro-CT reconstruction

The resolution of our Micro-CT analysis did not allow to detect minute prosomal cuticular pores as were found using scanning electron microscopy (SEM) by [26] (see e.g. plate 20B, C, E, F in [26]). These pores are present in isolation or in groups and are not associated with other cuticular structures such as setae [26]. However, larger canals at the base of setae were discernable by micro-CT; their distribution varies among species. For instance, in the two closely related species *Mitrager clypeellum* and *M. elongata*, both of which with cheliceral apophyses, cuticular canals are present close to the junction of the clypeus and chelicerae (Fig. 17d–g): whereas they are found on the underside of the elevated clypeus in *M. elongata*, similar canals occur in *M. clypeellum* at the basal-most part of the chelicerae. Virtual sections on the sagittal plane of *Mitrager lucida* and *M. sexoculata* also

show such canals in the thickened cuticle on the upper and lower sides of their inter-AME-PME grooves (Fig. 7d, e; see virtual slice on the frontal plane in Fig. 17b). These canals are located at the bases of the modified stout setae, which so far have only been found in these two species (modified setae are reconstructed in Fig. 17c). Whether these canals function as openings for the secretion of glandular products remains to be investigated by histological methods.

Clade stability and character evolution

The equal weight parsimony analysis resulted in six most parsimonious trees (MPT, tree length = 531.37, CI = 0.312, RI = 0.637, Figs. 21, 22, 23), in which Clade 1 to Clade 13 are identical to the topologies of the MPTs from the analysis of Matrix II in [29]; three major clades (*Mitrager*, Clade 26; *Holmelgonia* + *Callitrichia*, Clade 50; *Oedothorax* (Clade 69, monophyletic) + *Gongylidium* + *Ummeliata* + *Hylyphantes* + *Tmeticus*, Clade 64) each appear to be monophyletic.

The resulting trees from different implied-weighting schemes are summarized in Table 2, reporting the monophyly/polyphyly of three major clades: *Mitrager*, Clade 26; *Holmelgonia* + *Callitrichia*, Clade 50; *Oedothorax* + *Gongylidium* + *Ummeliata* + *Hylyphantes* + *Tmeticus*, Clade 64. *Mitrager* appeared polyphyletic under strong to moderate k values (1–6); when $k = 15$ and 30, *O. meghalaya incertae sedis* occurred within a clade of *Mitrager*; *Ca. convector* was placed outside Clade 50 under strong to moderate k values (2–6), while it remained within Clade 50 under moderate to gentle k values (10–1000). With $k = 4, 30$ and 100, *O. nazareti incertae sedis* was placed in Clade 64.

Character state transformation optimization based on parsimony is summarized in Fig. 16 for both the external modifications and the internal gland distribution characters. Our evolutionary hypothesis suggests that the presence of gustatory glandular tissues in the eye region is the ancestral condition for either all erigonines or for all erigonines except *Erigone atra*. The expansion of gustatory glandular tissue from the eye region into the before-eye and/or pharynx muscle region occurred multiple times, as well as its retraction/reduction (e.g., the gustatory glands expanded into the before-eye region

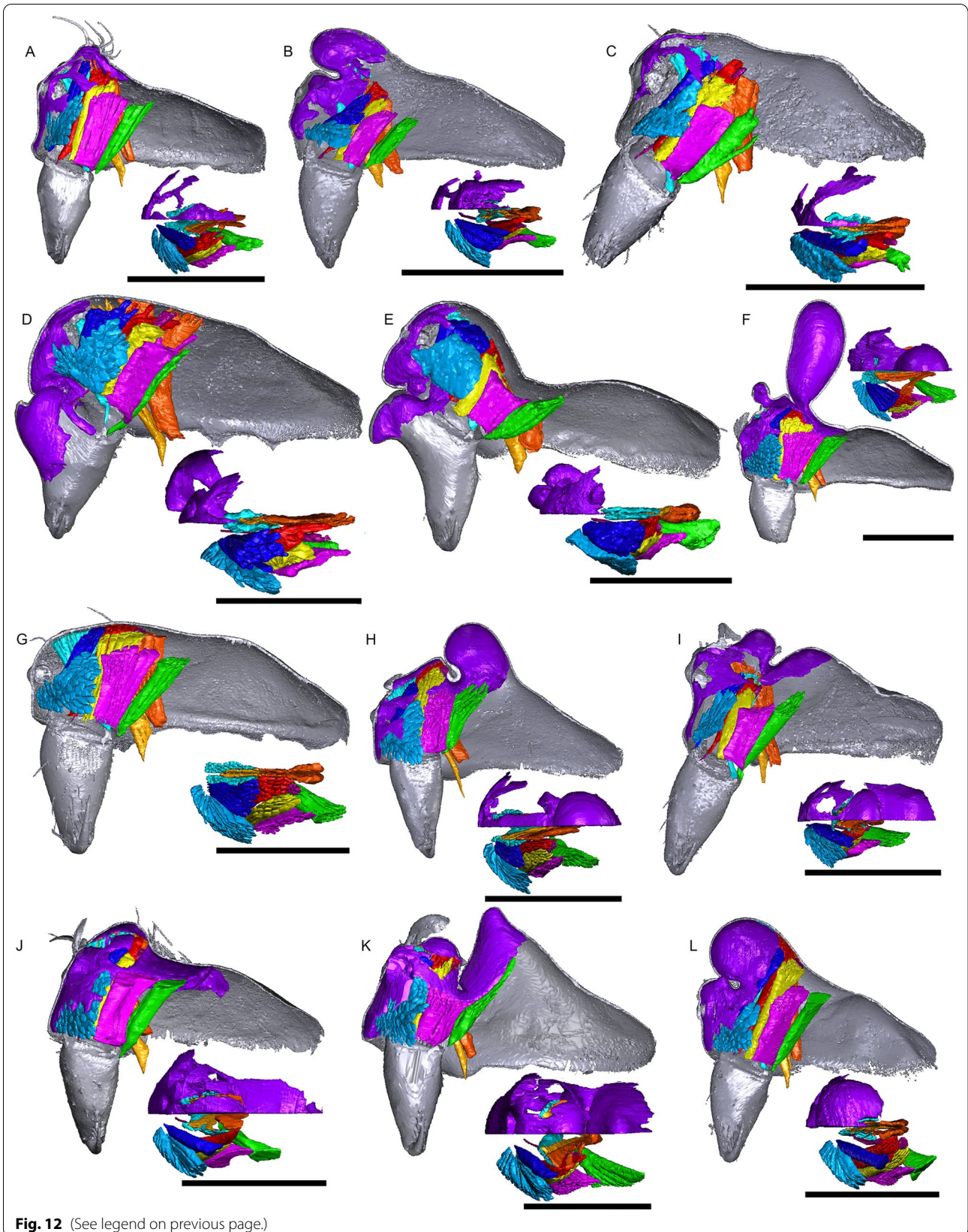


Fig. 12 (See legend on previous page.)

(See figure on next page.)

Fig. 13 Images of micro-CT scans with gustatory glandular tissues (purple), different sets of cheliceral muscles (left side), pharyngeal dilators (both sides). The right side of the prosomal cuticle is digitally segmented and color-coded following Table 1. Interactive 3D images are available in the Additional File 8. Click on the image to activate individual 3D model; to hide/show different structures, right-click and select “show model tree”. **a** *Mitrager lineata*. **b** *M. dismodicooides*. **c** *M. tholusa*. **d** *M. lucida*. **e** *M. sexoculata*. **f** *M. unicolor*. **g** *M. rustica*. **h** *M. assueta*. **i** *M. malearmata*. **j** *M. lopchu*. **k** *M. falciferoides*. **l** *M. falcifer*. Scale bars 0.5 mm

between nodes 10 and 23, then into the pharynx muscle region at node 23, and further into the post-DP region at node 25; but retracted from before-eye region at node 41 and expanded into this region again at node 45). In Clade 51, the distribution of gustatory gland shifted anteriorly at node 53 and the prosomal modifications occurred at node 54, whereas in Clade 59 the distribution reduced to only in the before-eye region (absent in *Callitrichia usitata*), and no external modification evolved. In *Oedothorax* (Clade 69), the gustatory gland distribution shifted or expanded posteriorly into the post-DP region at node 70, whereas it extended anteriorly into the before-eye region at either node 75 or 76-1. All prosomal modifications that evolved within clades are based on the presence of gustatory glandular tissues in the corresponding prosomal area at a more basal node, except for the cheliceral apophyses and the cheliceral gustatory gland. Based on the current taxon sample, it cannot be determined whether gustatory glands evolved prior to the occurrence of the apophyses in this region. Loss of gustatory glandular tissue occurred frequently during the evolution of erigonines, as seven instances of gustatory gland reduction can be inferred, all of which occur in terminal branches (indicated by the non-colored prosoma schematics in Fig. 16; loss/gain ratio = 7/1). As it was found in [29], most of the prosomal external modifications have multiple origins except the cheliceral basal apophyses. For differences in the degree of homoplasy of prosomal structures, see Additional File 1.

In Clade 36 within *Mitrager*, where all six species possess a pre-PME groove, the ancestral state of the inter-cheliceral-sclerite muscle and anterior pharyngeal dilator attachment to the internal surface of the groove is ambiguous (Fig. 18); a shift of the anterior part of the cuticular attachment of the inter-cheliceral-sclerite muscle from posterior to the groove onto the internal surface of the groove occurred in Clade 40.

Discussion

The astonishing diversity of erigonine male prosomal modifications has been the focus of many studies on this spider group [19, 29, 38]. Their function in gustatory courtship has been established in behavioral studies [20, 21], and a close association with extensive gustatory

glandular tissues has been demonstrated by previous histological studies [36, 40]. An evolutionary scenario depicting an origin of internal gustatory glandular tissues prior to the diversification of external morphologies [36, 40] has been proposed based on several erigonine phylogenetic frameworks in which external morphological characters were analyzed [26, 66, 67]. The current study provides the first phylogenetic analysis that incorporates both the external morphology and the internal gustatory gland distribution for reconstructing their evolutionary pattern and testing the aforementioned hypothesis. These results shed light on the lability of sexually selected gustatory traits and their potential to influence speciation in erigonine spiders.

Implications of differences in muscle connections to prosomal structures

We discovered the diversity of muscle connections to the pre-PME groove in the six species in Clade 36 (Fig. 18). In species with different degrees and forms of prosomal modifications (e.g., without modification, *Mitrager rustica*, and with PME lobe, *M. falciferoides*, Fig. 19a, c, respectively), the PMEs are always approximately aligned with the anterior filaments of the inter-cheliceral-sclerite muscle and the posterior pharyngeal dilator along the longitudinal axis. The connections of the anterior filaments of the inter-cheliceral-sclerite muscle and the anterior pharyngeal dilator to the pre-PME groove in species like *Mitrager sexocolorum* and *M. lucida* seem to be related to the internal position of the PMEs close to the upper side of the groove (see the positions of the eyes outlined with red in Fig. 18; Fig. 19d, e). Therefore, it seems plausible that during the ontogenesis of species that differ in muscle connections to the groove, the anchor point between the anterior and posterior elevations (i.e., the groove) differs also in the eye region (Fig. 18). In the case of *Mitrager sexocolorum* (connected to the inter-cheliceral-sclerite muscle and DA), the anchor point is located between the PMEs in a position on the longitudinal axis aligned with the posterior edge of the PMEs (Fig. 19b, upper black arrow); in *M. sexoculata* and *M. lucida* (connected to IC, Fig. 18), this point is located slightly more anteriorly, approximately in a position aligned with the center of the PMEs, not beyond the

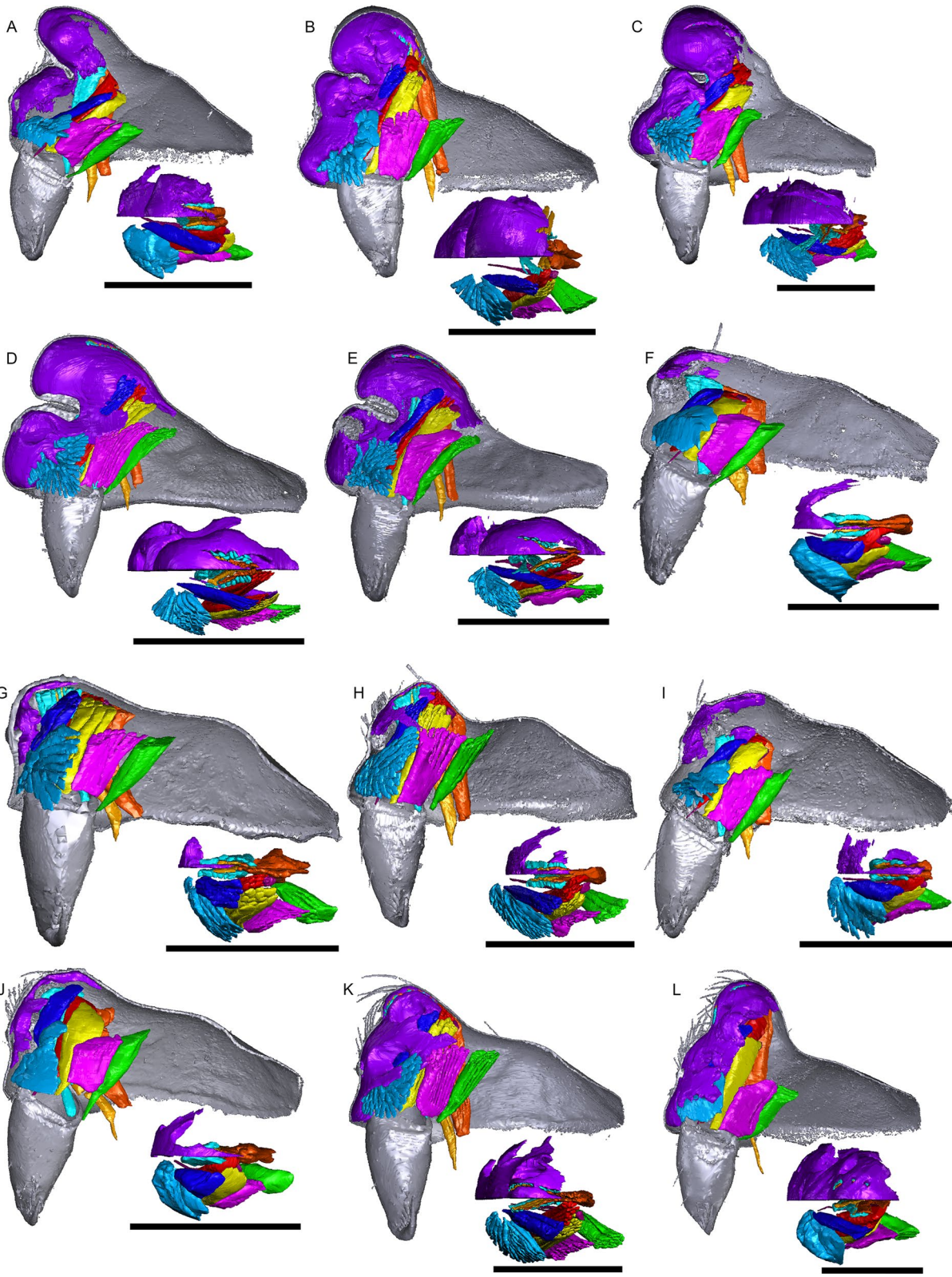


Fig. 13 (See legend on previous page.)

(See figure on next page.)

Fig. 14 Images of micro-CT scans with gustatory glandular tissues (purple), different sets of cheliceral muscles (left side), pharyngeal dilators (both sides). The right side of the prosomal cuticle is digitally segmented and color-coded following Table 1. Interactive 3D images are available in the Additional File 9. Click on the image to activate individual 3D model; to hide/show different structures, right-click and select “show model tree”. **a** *Mitragrer modesta* (Tanasevitch, 1998). **b** *M. savigniformis* (Tanasevitch, 1998). **c** *Holmelgonia basalis*. **d** *Callitrichia holmi*. **e** *Ca. picta*. **f** *Ca. gloriosa*. **g** *Ca. convector*. **h** *Ca. sellafrofrontis*. **i** *Ca. juguma*. **j** *Ca. uncata*. **k** *Ca. pilosa*. **l** *Ca. muscicola*. Scale bars 0.5 mm

anterior-most attachment of the inter-cheliceral-sclerite muscle (Fig. 19b, middle black arrow); in the case of *M. lineata*, *M. tholusa*, *M. dismodicoides* and the *Callitrichia* species in Clade 54 (no muscle attachment, e.g. *Ca. gloriosa*, Fig. 19f), the center of the groove is situated between the AMEs and PMEs, anterior to the inter-cheliceral-sclerite muscle and the anterior pharyngeal dilator (Fig. 19b, lower black arrow). We like to propose two evolutionary scenarios describing how these pre-PME grooves may have developed at different locations along the longitudinal axis. Firstly, independent (i.e., non-homologous) formations of a groove may have occurred in species with a PME lobe, like *M. falciferoides*, at different locations along the longitudinal axis (Fig. 19b, black arrows). Alternatively, shifts of the central point of the pre-PME groove along the longitudinal axis could have occurred after the evolution of this groove. Our results imply two shifts in position of the central point of the pre-PME groove in Clade 36, suggesting that the differences in its position among species do not necessarily imply independent origins of this groove (i.e., the first abovementioned scenario). A possible cause of these shifts could be changes in the positions at which female mouthparts contact the male prosomal lobe, in concert with changes of nuptial-gift-secreting areas to more anterior or posterior positions. This in turn could explain the changes in gustatory gland distribution in other erigonine groups such as *Oedothorax* (Clade 69).

Evolution of gustatory glandular tissues and external modifications

Our reconstruction of character state transformation reveals a single origin of gustatory glands, and multiple origins of various types of male prosomal external modifications (Fig. 16); the presence of glands in different prosomal areas also preceded the evolution of external structures at their corresponding positions. These findings support the hypothesis that the gustatory glands evolved in sexually monomorphic ancestors before changes in the prosomal shapes occurred [40]. We also present evidence for multiple instances of gustatory gland reduction. Interestingly, the pattern of character

state transformation on the current phylogenetic tree strongly suggests that after prosomal modifications had evolved in a clade, none of its members lost the trait complex of shapes and gustatory glands. However, in the cases of total reduction of gustatory glandular tissue, it is unlikely that the ancestral state possessed prosomal modifications. This may imply that once more elaborate male prosomal structures had evolved in a species, females became less likely to lose the preference for nuptial-gift-providing males. The benefits of nuptial feeding might exceed the costs of developing these traits, and thus they are more likely to be retained.

The cases of loss of gustatory gland suggest selective scenarios in the course of evolution that favored a decreased investment in gustatory courtship. The loss or reduction of sexually selected male traits has been demonstrated in insects and all major groups of vertebrates [68], and the loss/gain ratios can be high (5:1 for male coloration in tanagers [69]; 4:1 for colorful male ventral patches in phrynosomatid lizards [70]; 4:1 for clasping genitalia in water striders [71]). Although sexual selection may have been the primary force for the evolution and maintenance of gustatory glands and male prosomal modifications, natural selection and genetic drift might also have played a role [68]. Studies on *Oedothorax gibbosus*, in which two male morphs occur, provide insights into the costs and benefits of the male trait complex. The *gibbosus* morph, which possesses a hump and a groove and extensive gustatory glandular tissue, requires a longer developmental time and lives shorter after maturation than the less modified *tuberosus* morph [72, 73]. Individual-based simulations based on the scenario in a *Oedothorax gibbosus* population also demonstrated that males investing more in attracting females miss out on mating opportunities due to longer development, thereby opening a mating niche for less elaborate male morphs [74]. Under less stable environmental conditions, shorter mating seasons and restricted resources, males that invest less in costly traits may be at a selective advantage. When species distribution becomes patchy and gene flow between local populations is low, the probability of loss of these male traits might further increase.

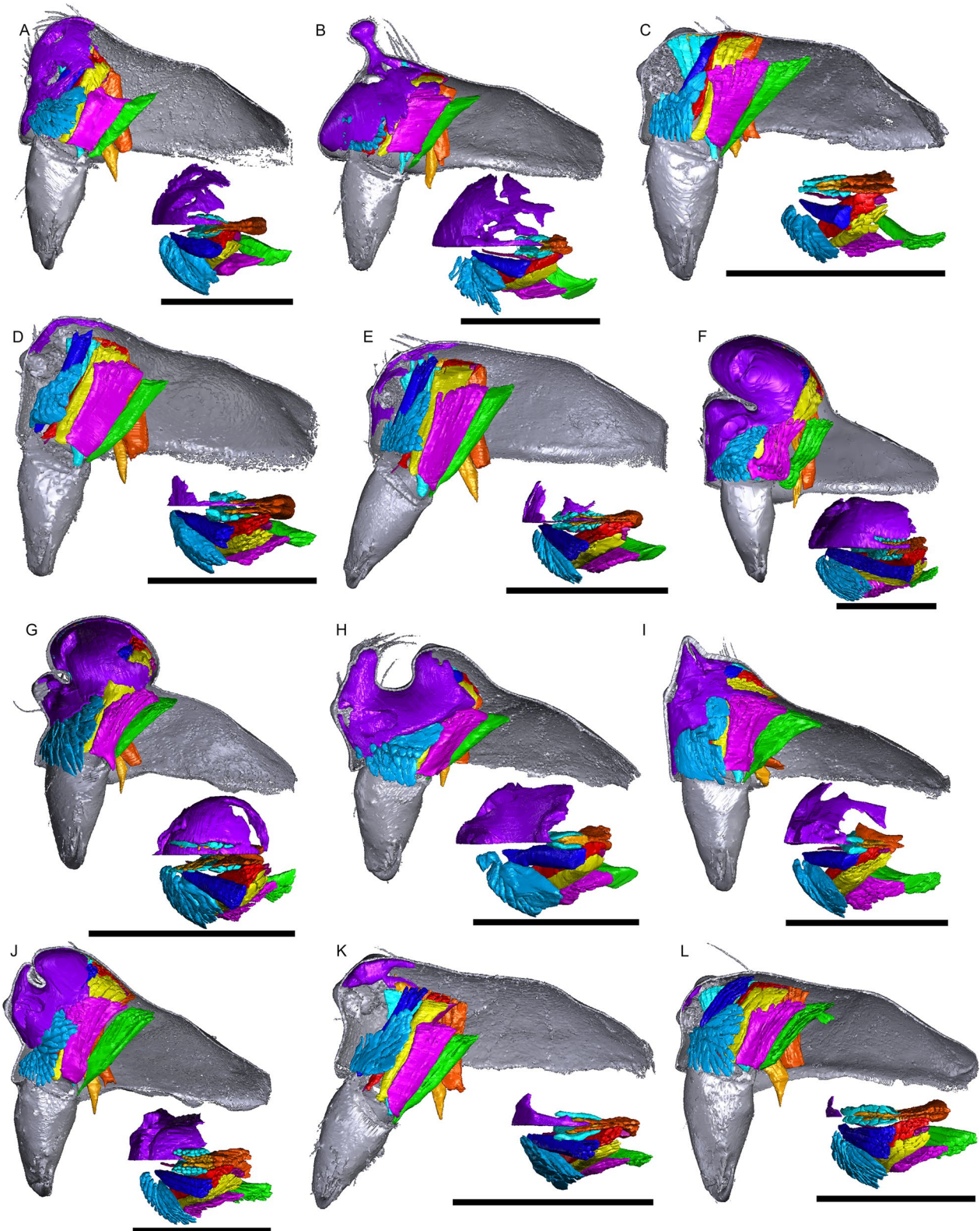


Fig. 14 (See legend on previous page.)

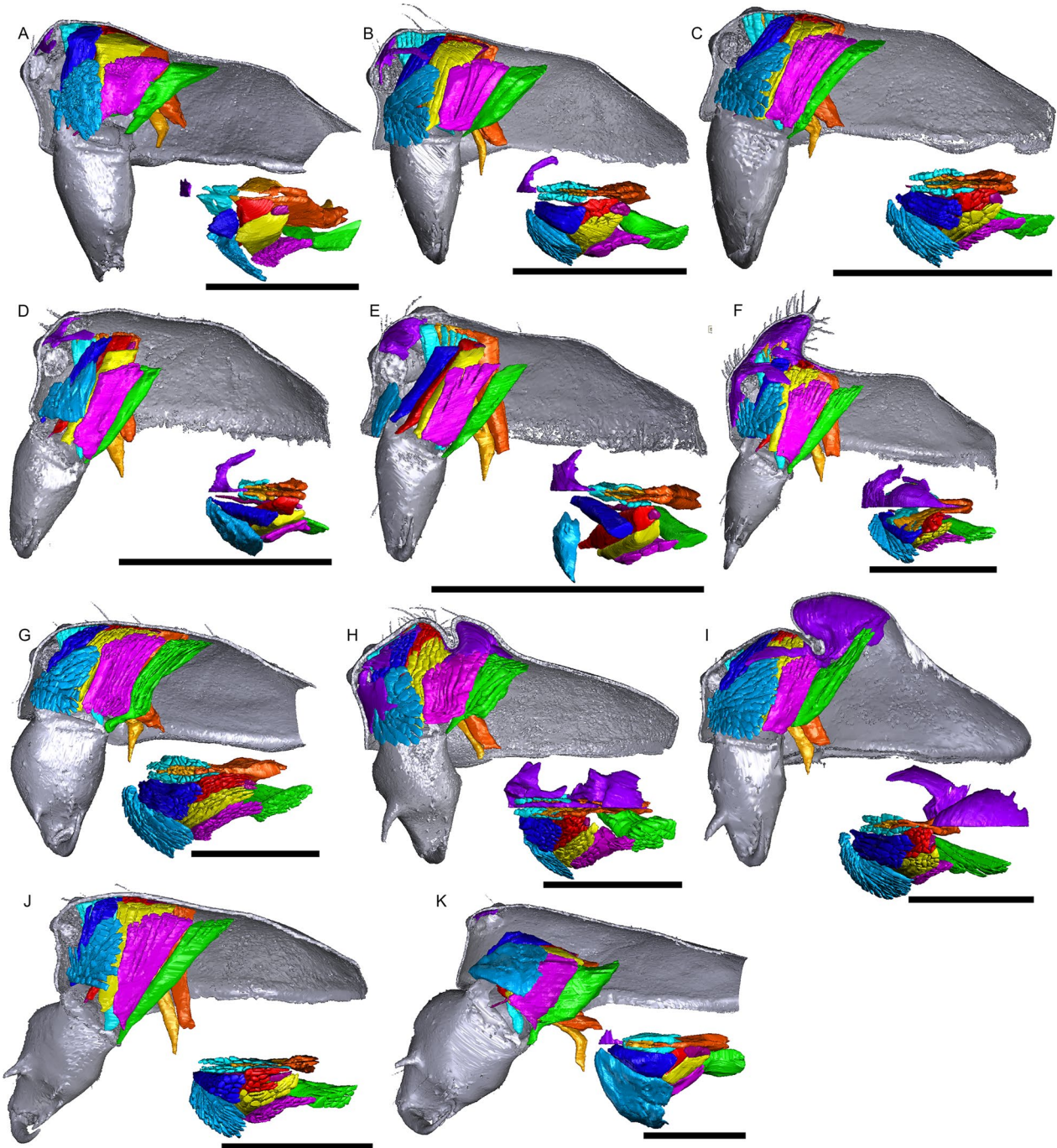
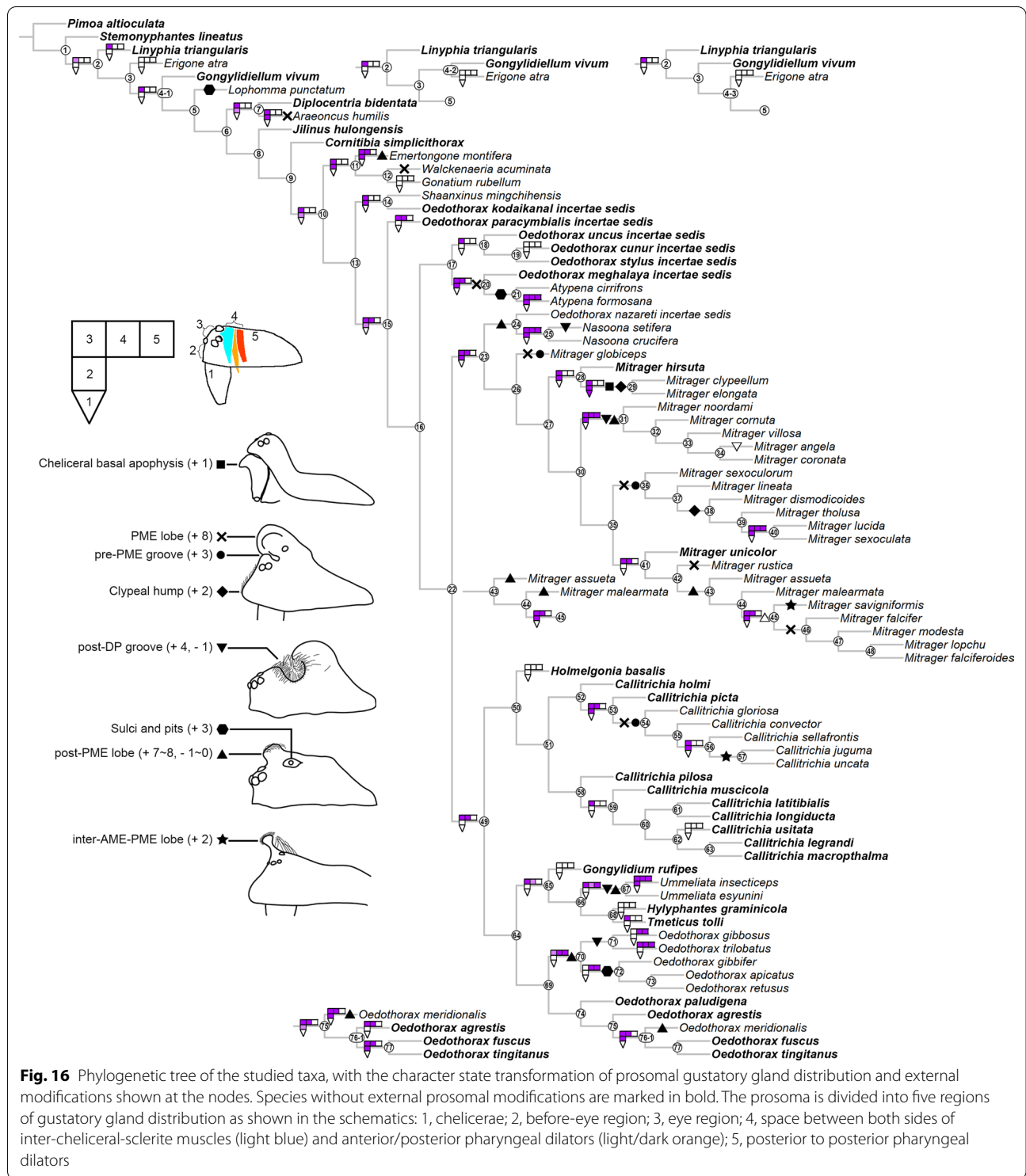
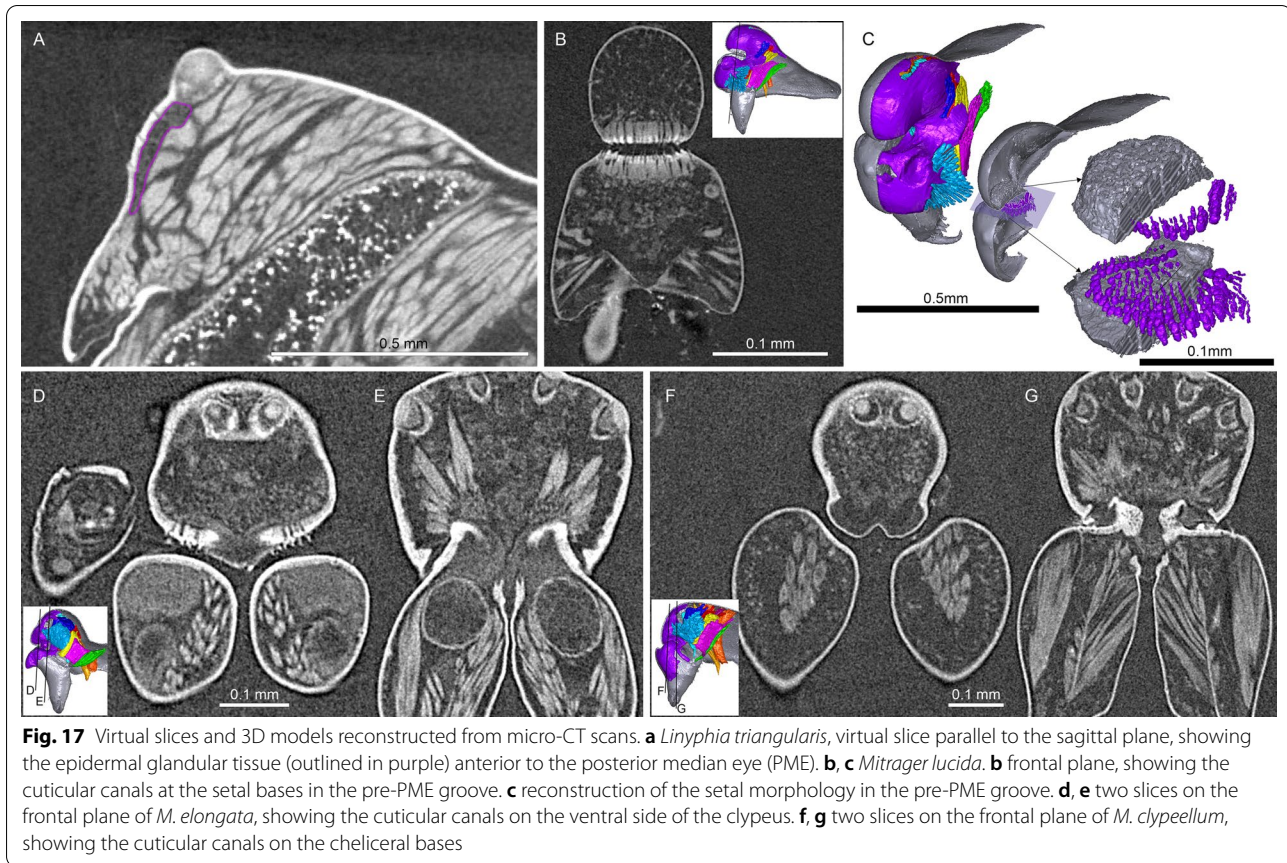


Fig. 15 Images of micro-CT scans with gustatory glandular tissues (purple), different sets of cheliceral muscles (left side), pharyngeal dilators (both sides). The right side of the prosomal cuticle is digitally segmented and color-coded following Table 1. Interactive 3D images are available in the Additional File 10. Click on the image to activate individual 3D model; to hide/show different structures, right-click and select “show model tree”. **a** *Callitrichia latitibialis*. **b** *Ca. longiducta*. **c** *Ca. usitata*. **d** *Ca. legrandi*. **e** *Ca. macrophalma*. **f** “*Oedothorax*” *nazareti*. **g** *Gongylidium rufipes*. **h** *Ummeliata insecticeps*. **i** *U. esyunini*. **j** *Hyllyphantes graminicola*. **k** *Tmetiscus tolli*. Scale bars 0.5 mm

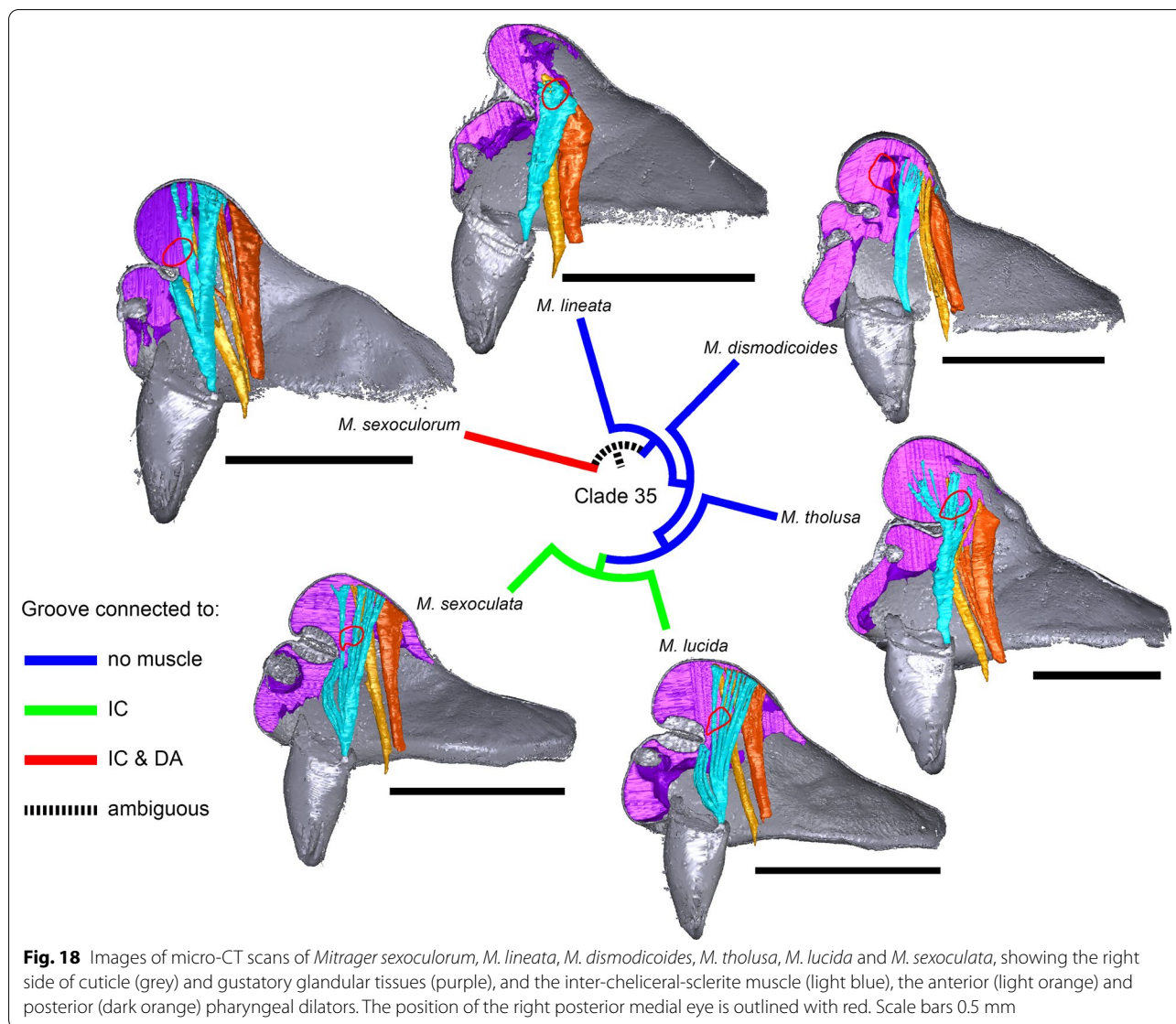




Sexual selection on dimorphic male prosomal structure and speciation

Although the effect of sexual selection on population divergence has the potential to drive speciation, disagreements exist around whether sexual selection alone influences reproductive isolation, or whether it mostly acts alongside or in the shadow of natural selection [7, 10, 75]. Comparative studies that correlate estimates of the strength of sexual selection and species richness accounting for phylogenetic relatedness do not generally support the supposed association [10]. A meta-analysis found a small but significant overall correlation between sexual selection and speciation rate and a strong dependence on methodology and proxies for sexual selection [76]. Sexual dimorphism, which is often used as a proxy for sexual selection (40 of 64 studies), yielded inconsistent results. For example, a meta-analysis examined mammals, butterflies and spiders for associations between the degree of sexual size dimorphism and variance in species richness, and found no significant association [77]. This might be because sexual size dimorphism can result from various

selective scenarios, such as intersexual competition for food resources [2, 11] and selection for larger females with higher fecundity [2, 78, 79]. In spiders, fecundity selection on females is the most likely explanation for the evolution of sexual size dimorphism [14, 15, 80, 81]. For assessing the impact of sexual selection on speciation, labile traits are required that are under sexual selection with little effect of various other sources of selection in generating trait diversity [76, 82, 83]. On the other hand, sexual selection does not necessarily accelerate diversification. For instance, when the trait optima under natural selection are more divergent than those under sexual selection, the latter may even show inhibitory effects on trait divergence among populations [84]. Female preference may drive male trait evolution, but whether it leads to species divergence depends on whether female mate preferences differ between populations [85]. Therefore, the influence of sexual selection on speciation rate lies more in its diversifying property than in its strength. The equivocal results of the comparative studies (reviewed in [9] and [76]) may partly be due to the negligence of this



aspect [7, 85]. Therefore, instead of treating sexual selection in general, comparative studies trying to address its effect on speciation should distinguish between different selective scenarios for both male traits and female preferences [7, 76].

As demonstrated by our investigation on the prosoma of erigonine spiders, the gustatory trait complex is not only externally diverse in location and shape, but the internal gland distribution also varies greatly, even across species with moderate or no external modifications. This is well exemplified by the genus *Oedothorax*, in which species with no prominent prosomal elevations have

gustatory glands located anteriorly (*O. fuscus*, Fig. 2k), medially (*O. agrestis*, Fig. 2i), or posteriorly (*O. gibbosus*, *tuberosus* morph, Fig. 2b). It is unlikely that factors other than sexual selection influence the lability of this trait complex, such as differences in niche use between sexes [11] and exposure to predation [86]. Difference in niche use between sexes are unknown in erigonines and unlikely to play a role during the major part of development since the traits are only expressed in adult males. Further, in species without external modifications, the divergent evolution in their gustatory gland distribution is even less likely to be influenced by differential niche

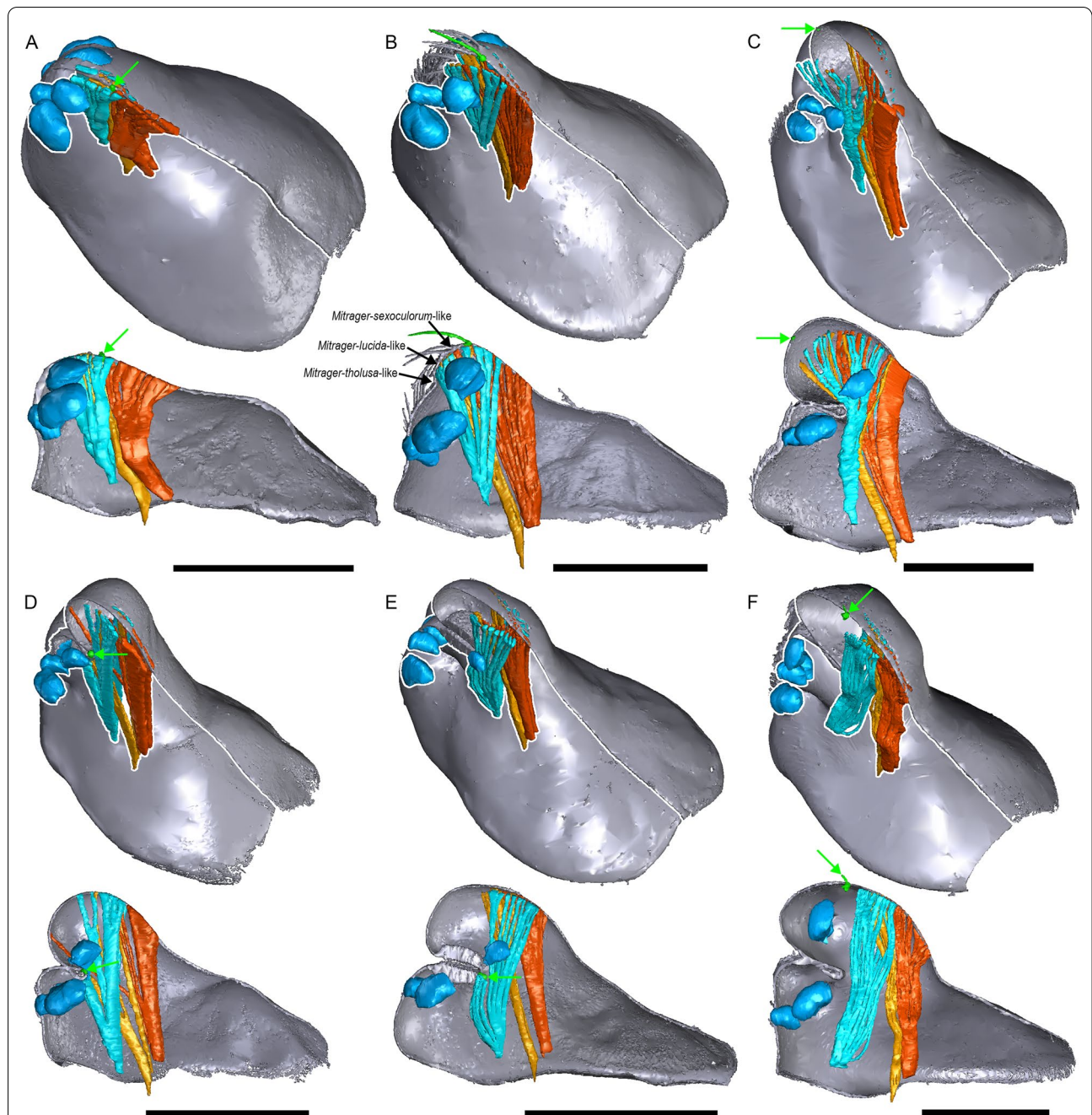
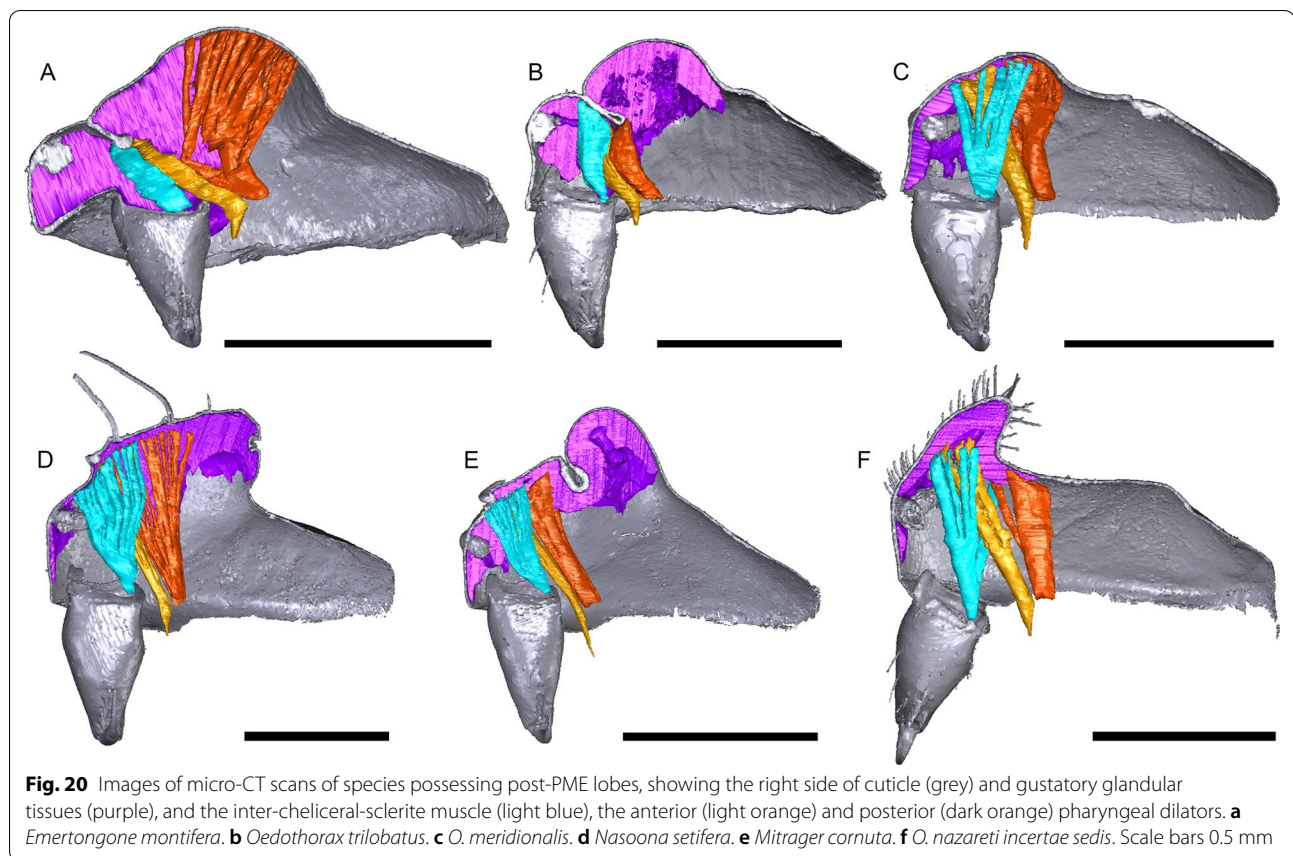


Fig. 19 Comparison between several *Mitrager* species and one *Callitrichia* species with different degrees and types of prosomal modifications. The filaments of the inter-chelical-sclerite muscle (aqua) and the anterior (light orange) and posterior (dark orange) pharyngeal dilators are extrapolated onto the cuticle surface for visually presenting the places of the muscle attachments; the macroseta on the central axis positioned behind the ocular region is marked in green and pointed at by green arrows; The black arrows in B mark the hypothesized points in the eye region, where the cuticle might have invaginated and formed the pre-PME groove in different species; the eyes are marked in light blue. **a** *M. rustica*. **b** *M. falciferoides*. **c** *M. tholusa*. **d** *M. sexocolorum*. **e** *M. lucida*. **f** *Ca. gloriosa*. Scale bars 0.5 mm



use. As for mate selectivity, which causes the isolating effects of sexual selection, it has been demonstrated in *Oedothorax gibbosus* that non-virgin females are more likely to mate with *gibbosus*-morph males, which possess more elaborated prosomal traits, whereas the *tuberosus*-morph males have higher mating probability when exposed to virgin females [73]. Male *Oedothorax retusus* that had their nuptial-gift-secreting region experimentally covered were significantly less accepted for mating compared to a control group [21]. In addition, female ingestion of male secretion continues during mating, the spatial match of the structures involved in gustation and mating is supposedly under strong selection. Given the evidence for the importance of nuptial gift to male mating success and the divergent evolutionary patterns of the position of the gustatory glands associated with various external modifications, we suggest erigonines as a suitable target group for studies on the effect of sexual selection on speciation.

Our results point out erigonine clades that are of particular interest for future studies on sexual selection and speciation. *Callitrichia* – now divided into two clades—is represented by one clade with more prominent prosomal modification and wider gustatory gland distribution (Clade 52), and another clade with reduced gustatory gland distribution and no external modification (Clade 58). In addition, *Callitrichia* (55 species) [29] is sister to *Holmelgonia* (17 species) [87], which has no prosomal modification [29, 87] and no gustatory glandular tissue. Among the 48 *Callitrichia* species for which males have been described (not including *C. celans incertae sedis*), 30 species show various degrees of prosomal modifications, while 18 species have no external modification, among some of them possess gustatory glands. Another potential target group is Clade 65, which includes *Gongylidium* (without external modification and gustatory gland, 3 species), *Ummeliata* (with both external modification and gustatory gland, 10 species), *Tmeticus* (without external modification, with

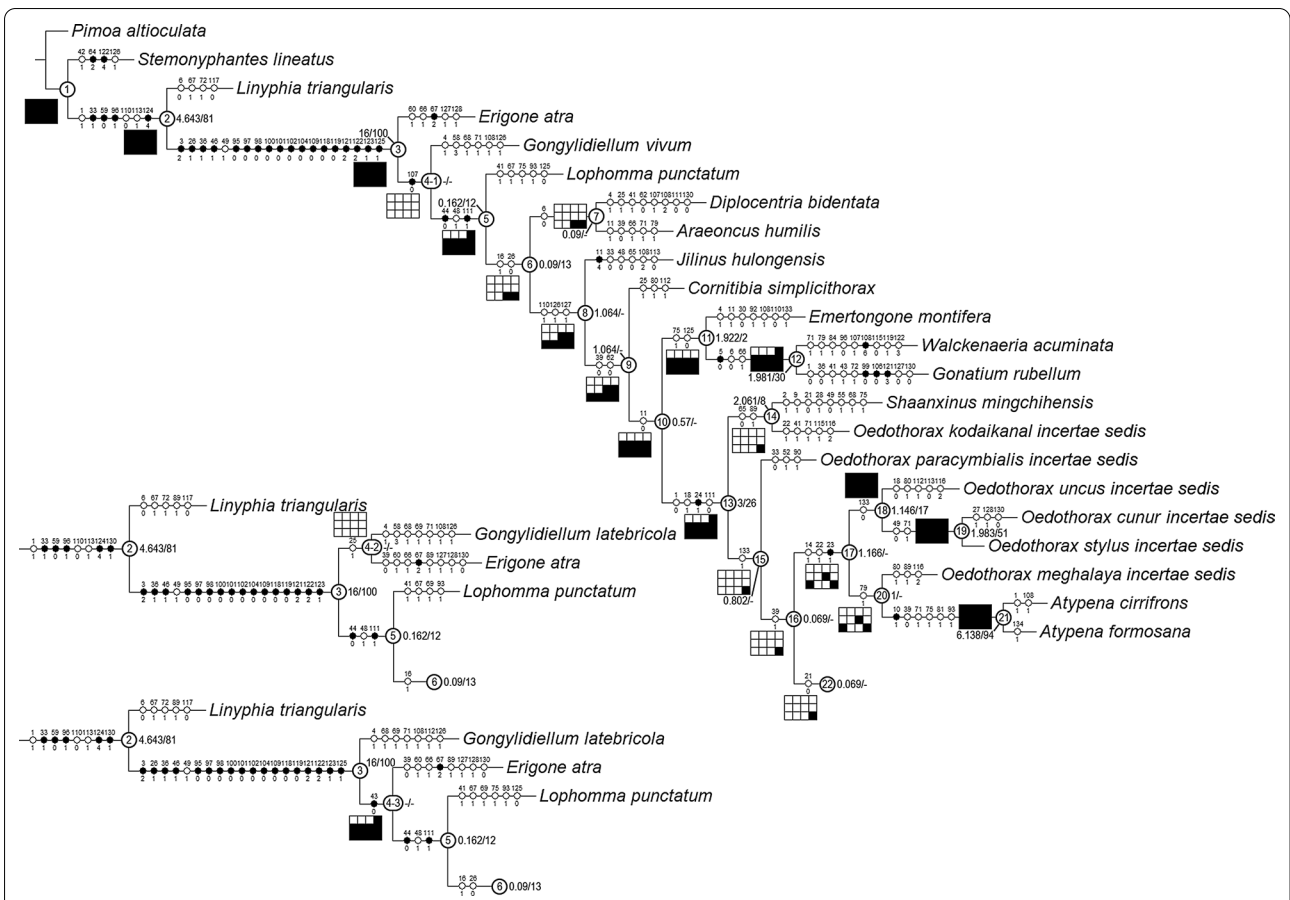
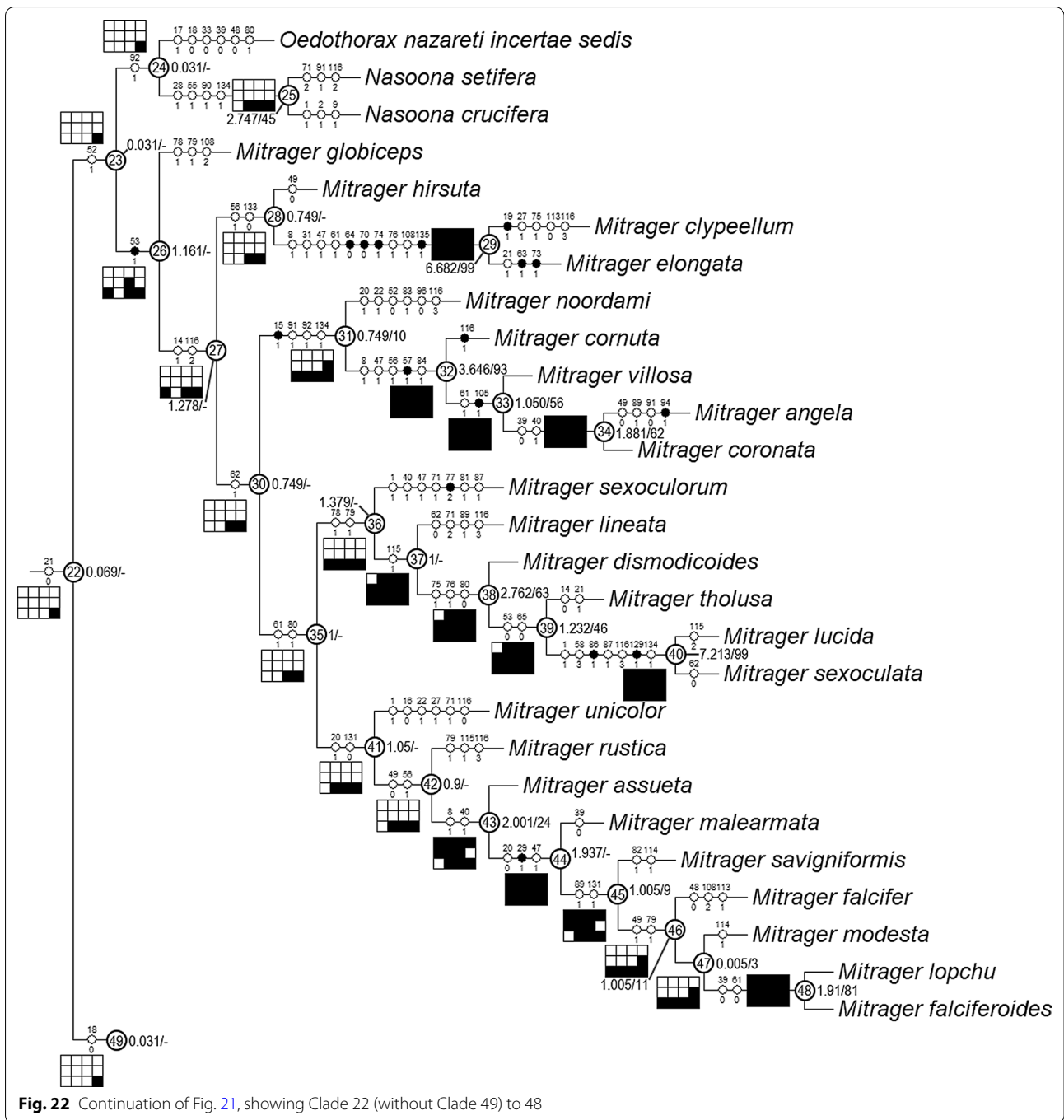


Fig. 21 The first part of the six most parsimonious trees from the phylogenetic analysis, with unambiguous character optimization (circles on branches), clade numbers (in circles on nodes) and Bremer/Jackknife support values (beside the nodes). The presence/absence of clades in the trees of the implied weights analysis with different *k* values are shown in the boxes under/above/on the branches: black for presence, white for absence

gustatory gland, 7 species) and *Hylyphantes* (without external modification and gustatory gland, 5 species) [25]. Given their species numbers and differences in their prosomal features, these taxa might lend themselves as suitable targets for comparative studies. The questions could be on the adaptive advantage of losing the gustatory glands, as well as whether lineages with more prominent prosomal modifications display higher speciation rates. Future sister group comparisons will require phylogenetic analyses with a more comprehensive taxon sampling that allows estimating speciation rates, combined with investigations of internal structures and ecological and behavioral aspects.

Conclusions

The distribution pattern of gustatory glands revealed by the micro-CT investigation provided a new set of characters for phylogenetic analyses, as well as revealing further aspects of lability of the gustatory traits in dwarf spiders. The results of our phylogenetic analyses suggest an evolutionary scenario consistent with the hypothesis that the occurrence of the glandular tissues preceded the evolution of external prosomal modifications. For most external elevations (humps, lobes, and turrets), gustatory glandular tissues in the corresponding prosomal areas occurred already



earlier in the phylogenetic tree. Incidences of glandular tissue loss indicate the cost of developing and maintaining the gustatory equipment. Even among species without obvious external prosomal modifications, differences in the distribution of gustatory glandular tissues were found. Our study provides a

glimp into the dynamics of the evolution of sexually selected gustatory structures in erigonines. We suggest several erigonine target groups for comparative studies on and the effect of sexual selection on species divergence.

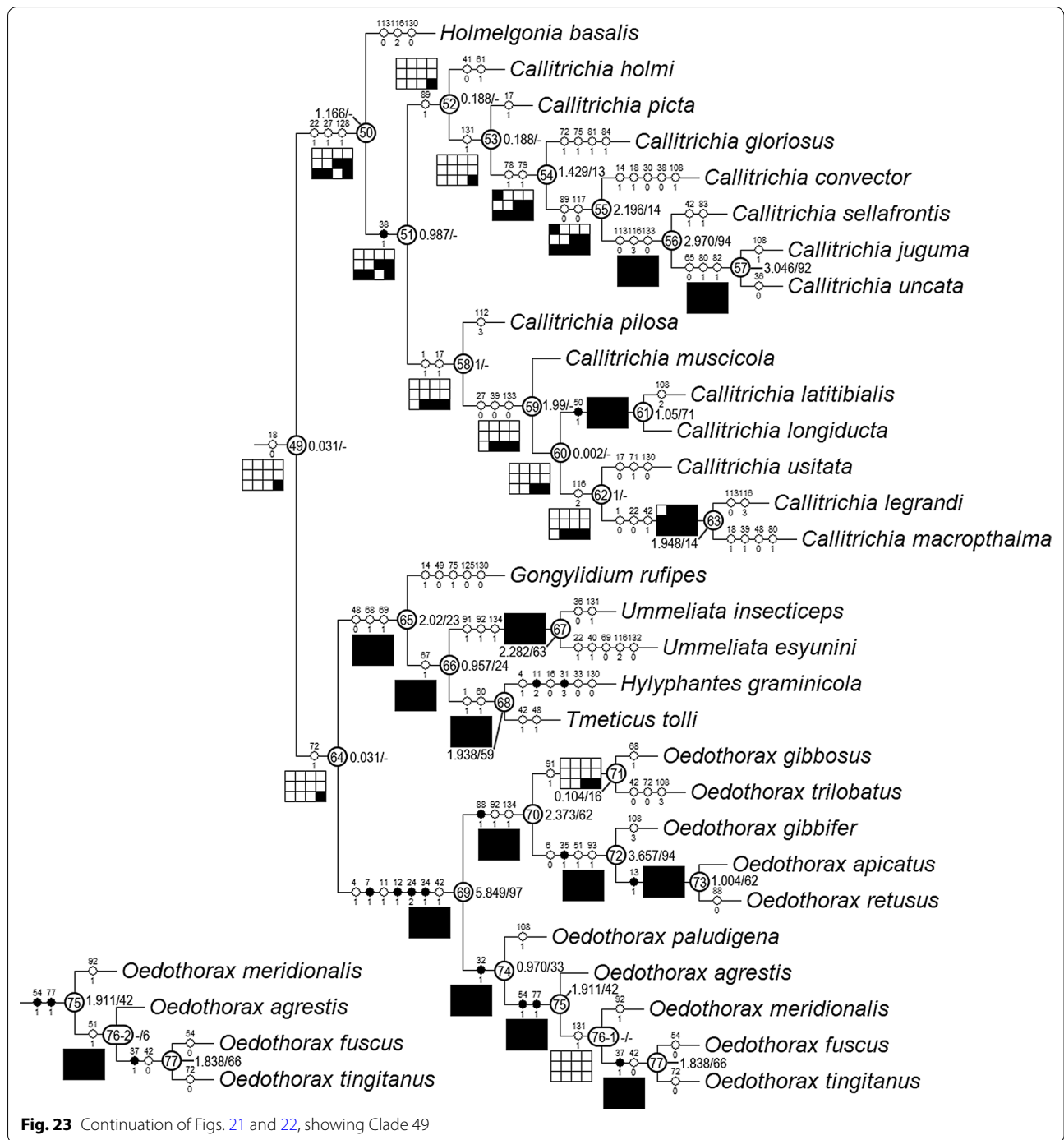


Fig. 23 Continuation of Figs. 21 and 22, showing Clade 49

Supplementary Information

The online version contains supplementary material available at <https://doi.org/10.1186/s12983-021-00435-8>.

Additional file 1. Table S1: Specimens used for microcomputed-tomography scans; differences between Matrix II in [29] and the current matrix; **Table S2:** Character matrix for the newly scored characters.

Additional file 2. Character matrix of the phylogenetic analysis.

Additional file 3. Interactive 3D images of Figs. 1A, C, E.

Additional file 4. Interactive 3D images of Figs. 2A-L.

Additional file 5. Interactive 3D images of Figs. 10A-K.

Additional file 6. Interactive 3D images of Figs. 11A-L.

Additional file 7. Interactive 3D images of Figs. 12A-L.

Additional file 8. Interactive 3D images of Figs. 13A-L.

Additional file 9. Interactive 3D images of Figs. 14A-L.

Additional file 10. Interactive 3D images of Figs. 15A-K.

Acknowledgements

We are very grateful to Jonas Wolff and Monica Sheffer for suggestions on the manuscript. For support with micro-CT imaging and reconstruction, we cordially thank Stefan Bock from the Imaging Center Biology Greifswald. For the loan of specimens we are grateful to the following people and institutions: Shuqiang Li (Institute of Zoology, Chinese Academy of Sciences, Peking, China), Nikolaj Scharff (ZMUC, Copenhagen, Denmark), Rudy Jocqué, Didier van den Spiegel and Arnaud Henrard (RMCA, Tervuren, Belgium), Andrei V. Tanasevitch (A.N. Severtsov Institute of Ecology and Evolution, Moscow, Russia), Peter Jäger and Julia Altmann (SMF, Frankfurt, Germany), Peter Schwendinger (MHNG, Geneva, Switzerland), Peter van Helsdingen and Karen van Dorp (Leiden, Netherlands), Jan Beccaloni (NHM, London, UK), Lorenzo Prendini and Louis Sorkin (AMNH, New York City, USA). We further thank two anonymous reviewers for critical suggestions on the manuscript.

Authors' contributions

SWL analyzed and interpreted the micro-CT data, constructed the character matrix, conducted the phylogenetic analyses, and was a major contributor in writing the manuscript. LL contributed to the construction of the character matrix, advised SWL on phylogenetic methods and the writing of the manuscript. GU contributed to the conceptual framework of this study and the writing of the manuscript. All authors read and approved the final manuscript.

Funding

Open Access funding enabled and organized by Projekt DEAL. This project was financed by a stipend from the Ministry of Education of Taiwan and a STIPED stipend from Greifswald (DAAD), both to S.-W. Lin. Support by the German Science foundation for co-funding the MicroCT (INST 292/119-1 FUGG, and INST 292/120-1 FUGG) is gratefully acknowledged.

Availability of data and materials

All data generated or analyzed during this study are included in this published article and its additional files.

Declarations

Ethics approval and consent to participate

Not applicable.

Consent for publication

Not applicable.

Competing interests

The authors declare that they have no competing interests.

Received: 4 June 2021 Accepted: 13 September 2021

Published online: 28 September 2021

References

- Darwin C. On the origin of species by means of natural selection. London: Murray; 1859.
- Darwin C. The descent of man and selection in relation to sex. London: Murray; 1871.
- Berns CM. The evolution of sexual dimorphism: understanding mechanisms of sexual shape differences. In: Moriyama H, editor. Sexual dimorphism. Rijeka: InTech; 2013. p. 1–16.
- Loyau A, Saint Jalme M, Cagniant C, Sorci G. Multiple sexual advertisements honestly reflect health status in peacocks. *Behav Ecol Sociobiol.* 2005;58:552–7.
- Mathieu JM. Mating behavior of five species of Lucanidae (Coleoptera: Insecta). *Can Entomol.* 1969;101:1054–62.
- Goss RJ. Deer antlers: regeneration, function, and evolution. New York: Academic Press; 1983.
- Servedio MR, Boughman JW. The role of sexual selection in local adaptation and speciation. *Annu Rev Ecol Evol Syst.* 2017;48:85–109.
- West-Eberhard MJ. Sexual selection, social competition and speciation. *Q Rev Biol.* 1983;58:155–83.
- Panhuis TM, Butlin R, Tregenza T. Sexual selection and speciation. *Trends Ecol Evol.* 2001;16:364–71.
- Ritchie MG. Sexual selection and speciation. *Annu Rev Ecol Evol Syst.* 2007;38:79–102.
- Shine R. Ecological causes for the evolution of sexual dimorphism: a review of the evidence. *Q Rev Biol.* 1989;64:419–61.
- Voight JR. Sexual dimorphism and niche divergence in a mid-water octopod (Cephalopoda: Bolitaenidae). *Biol Bull.* 1995;189:113–9.
- Hedrick AV, Temeles EJ. The evolution of sexual dimorphism in animals: hypotheses and tests. *Trends Ecol Evol.* 1989;4:136–8.
- Head G. Selection on fecundity and variation in the degree of sexual size dimorphism among spider species (Class Araneae). *Evolution.* 1995;49:776–81.
- Hormiga G, Scharff N, Coddington JA. The phylogenetic basis of sexual size dimorphism in orb-weaving spiders (Araneae, Orbiculariae). *Syst Biol.* 2000;49:435–62.
- Vollrath F. Zur Ökologie und Biologie von kleptoparasitischen *Argyrodes elevatus* und synöken *Argyrodes*-Arten (Araneae, Theridiidae) [Doctoral Thesis]. University of Freiburg; 1977.
- Knoflach B. Diversity in the copulatory behaviour of comb-footed spiders (Araneae, Theridiidae). In: Thaler K, editor. Diversity and Biology of Spiders, Scorpions and other Arachnids. Denisia (Linz); 2004. p. 161–256.
- Huber BA, Eberhard WG. Courtship, copulation, and genital mechanics in *Physocyclus globosus* (Araneae, Pholcidae). *Can J Zool.* 1997;75:905–18.
- Vanacker D, Borre JV, Jonckheere A, Maes L, Pardo S, Hendrickx F, et al. Dwarf spiders (Erigoninae, Linyphiidae, Araneae): good candidates for evolutionary research. *Belg J Zool.* 2003;133:143–9.
- Uhl G, Maelfait J-P. Male head secretion triggers copulation in the dwarf spider *Diplocephalus permixtus*. *Ethology.* 2008;114:760–7.
- Kunz K, Garbe S, Uhl G. The function of the secretory cephalic hump in males of the dwarf spider *Oedothorax retusus* (Linyphiidae: Erigoninae). *Anim Behav.* 2012;83:511–7.
- Maes L, Vanacker D, Sylvia P, Maelfait JP. Comparative study of courtship and copulation in five *Oedothorax* species. *Belg J Zool.* 2004;134:29–35.
- Vahed K. The function of nuptial feeding in insects: a review of empirical studies. *Biol Rev.* 1998;73:43–78.
- Vahed K. All that glitters is not gold: sensory bias, sexual conflict and nuptial feeding in insects and spiders. *Ethology.* 2007;113:105–27.
- World Spider Catalog (2021). World Spider Catalog. Version 22.0. Natural History Museum Bern, online at <http://wsc.nmbe.ch>. Accessed on 10.April.2021. 10.24436/2
- Hormiga G. Higher level phylogenetics of erigonine spiders (Araneae, Linyphiidae, Erigoninae). *Smithson Contrib Zool.* 2000;609:1–160.

27. Hormiga G. Cephalothoracic sulci in linyphiine spiders (Araneae, Linyphiidae, Linyphiinae). *J Arachnol.* 1999;27:94–102.
28. Lin S-W, Lopardo L, Haase M, Uhl G. Taxonomic revision of the dwarf spider genus *Shaanxinus* Tanasevitch, 2006 (Araneae, Linyphiidae, Erigoninae), with new species from Taiwan and Vietnam. *Org Divers Evol.* 2019;19:211–76.
29. Lin S-W, Lopardo L, Uhl G. Evolution of nuptial-gift-related male prosomal structures: taxonomic revision and cladistic analysis of the dwarf spider genus *Oedothorax* Bertkau, 1883 (Araneae, Linyphiidae, Erigoninae). *Zool J Linn Soc.* 2021 (in press).
30. Wiehle H. Spinnentiere oder Arachnoidea, XI: Micryphantidae-Zwergspinnen. *Tierwelt Deutschlands.* 1960;47:1–620.
31. Miller JA. Review of erigonine spider genera in the neotropics (Araneae: Linyphiidae, Erigoninae). *Zool J Linn Soc.* 2007;149:1–263.
32. Lopez A. Présence de glandes tégumentaires prosomatiques chez les mâles de deux Erigonidae (Araneae). *C R Acad Sci.* 1976;282:365–7.
33. Blest AD, Taylor HH. The clypeal glands of *Mynoglenes* and of some other linyphiid spiders. *J Zool.* 1977;183:473–93.
34. Lopez A, Emerit M. Le dimorphisme sexuel prosomatique de *Walckenaeria acuminata* BLACKWALL, 1833 (Araneae, Erigonidae). *Bull de la Soc Zool de France.* 1981;106:125–31.
35. Schaible U, Gack C, Paulus HF. Zur Morphologie, Histologie und biologischen Bedeutung der Kopfstrukturen männlicher Zwergspinnen (Linyphiidae: Erigoninae). *Zoologische Jahrbücher (Systematik).* 1986;113:389–408.
36. Michalik P, Uhl G. Cephalic modifications in dimorphic dwarf spiders of the genus *Oedothorax* (Erigoninae, Linyphiidae, Araneae) and their evolutionary implications. *J Morphol.* 2011;272:814–32.
37. Bristowe WS. The mating habits of spiders: a second supplement, with the description of a new thomisid from Krakatau. *Proc Zool Soc Lond.* 1931;4:1401–12.
38. Schlegelmilch B. Zur biologischen Bedeutung der Kopffortsätze bei Zwergspinnenmännchen (Microphantidae). *Diplomarbeit: Univ. Freiburg;* 1974.
39. Lopez A. Glandular aspects of sexual biology. In: Nentwig W, editor. *Eco-physiology of Spiders* [Internet]. Berlin: Springer; 1987. p. 121–32. https://doi.org/10.1007/978-3-642-71552-5_9
40. Schaible U, Gack C. Zur Morphologie, Histologie und biologischen Bedeutung der Kopfstrukturen einiger Arten der Gattung *Diplocephalus* (Araneida, Linyphiidae, Erigoninae). *Verhandlungen des naturwissenschaftlichen Vereins in Hamburg.* 1987;29:171–80.
41. Kunz K, Michalik P, Uhl G. Cephalic secretion release in the male dwarf spider *Oedothorax retusus* (Linyphiidae: Erigoninae): an ultrastructural analysis. *Arthropod Struct Dev.* 2013;42:477–82.
42. Frick H, Nentwig W, Kropf C. Progress in erigonine spider phylogeny—the *Savignia*-group is not monophyletic (Araneae: Linyphiidae). *Org Divers Evol.* 2010;10:297–310.
43. Miller JA, Hormiga G. Clade stability and the addition of data: A case study from erigonine spiders (Araneae: Linyphiidae, Erigoninae). *Cladistics.* 2004;20:385–442.
44. Tanisako A, Hori A, Okumura A, Miyata C, Kuzuryu C, Obi T, et al. Micro-CT of *Pseudocneorhinus bifasciatus* by projection X-ray microscopy. *J Electron Microsc.* 2005;54:379–83.
45. Betz O, Wegst U, Weide D, Heethoff M, Helfen L, Lee W, et al. Imaging applications of synchrotron X-ray phase-contrast microtomography in biological morphology and biomaterials science. I. General aspects of the technique and its advantages in the analysis of millimetre-sized arthropod structure. *J Microsc.* 2007;227:51–71.
46. Mizutani R, Takeuchi A, Hara T, Uesugi K, Suzuki Y. Computed tomography imaging of the neuronal structure of *Drosophila* brain. *J Synchrotron Rad.* 2007;14:282–7.
47. Beutel RG, Friedrich F, Whiting MF. Head morphology of *Caurinus* (Boreidae, Mecoptera) and its phylogenetic implications. *Arthropod Struct Dev.* 2008;37:418–33.
48. Friedrich F, Beutel RG. Micro-computer tomography and a renaissance of insect morphology. *Proc SPIE.* 2008;7078:70781U1–6.
49. Mizutani R, Takeuchi A, Uesugi K, Takekoshi S, Osamura RY, Suzuki Y. X-ray microtomographic imaging of three-dimensional structure of soft tissues. *Tissue Eng Part C Methods.* 2008;14:359–63.
50. Metscher BD. MicroCT for comparative morphology: simple staining methods allow high-contrast 3D imaging of diverse non-mineralized animal tissues. *BMC Physiol.* 2009;9:11.
51. Sombke A, Lipke E, Michalik P, Uhl G, Harzsch S. Potential and limitations of X-Ray micro-computed tomography in arthropod neuroanatomy: a methodological and comparative survey. *J Comp Neurol.* 2015;523:1281–95.
52. Steinhoff POM, Uhl G. Taxonomy and nomenclature of some mainland SE-Asian *Coelliccia* species (Odonata, Platycnemididae) using micro-CT analysis. *Zootaxa.* 2015;4059:257–76.
53. Sentenská L, Müller CH, Pekár S, Uhl G. Neurons and a sensory organ in the pedipalps of male spiders reveal that it is not a numb structure. *Sci Rep.* 2017;7:12209.
54. Bhandari K, Crisp P, Keller MA. The oesophageal diverticulum of *Dirioxa pornia* studied through micro-CT scan, dissection and SEM studies. *BMC Biotechnol.* 2019;19:89.
55. Palmgren P. On the muscular anatomy of spiders. *Acta Zool Fenn.* 1978;155:1–41.
56. Palmgren P. Some comments on the anatomy of spiders. *Ann Zool Fenn.* 1980;17:161–73.
57. Wood HM, Parkinson DY. Comparative morphology of cheliceral muscles using high resolution X-ray microcomputed-tomography in palpimanoid spiders (Araneae, Palpimanoidea). *J Morphol.* 2019;280:232–43.
58. Foelix RF. *Biology of Spiders.* 3rd ed. New York: Oxford University Press; 2011. p. 419.
59. Pollard SD. The feeding strategy of a crab spider, *Diaea* sp. indet. (Araneae: Thomisidae): post-capture decision rules. *J Zool.* 1990;222:601–15.
60. Vanacker D, Maelfait JP, Baert L. The male dimorphism in the dwarf spider *Oedothorax gibbosus* (Blackwall, 1841) (Erigoninae, Linyphiidae, Araneae): Results of laboratory rearing experiments. *Belg J Zool.* 2001;131:39–44.
61. Schindelin J, Arganda-Carreras I, Frise E, et al. Fiji: an open-source platform for biological-image analysis. *Nat Methods.* 2012;9:671–5.
62. Goloboff PA, Farris JS, Nixon KC. TNT, a free program for phylogenetic analysis. *Cladistics.* 2008;24:774–86.
63. Goloboff PA, Mattoni CI, Quinteros AS. Continuous characters analyzed as such. *Cladistics.* 2006;22:589–601.
64. Goloboff PA. Estimating character weights during tree-search. *Cladistics.* 1993;9:83–91.
65. Nixon K. Winclada, program and documentation. 2002. Available from: www.cladistics.com. Assessed 9 Feb 2020.
66. Arnedo MA, Hormiga G, Scharff N. Higher-level phylogenetics of linyphiid spiders (Araneae, Linyphiidae) based on morphological and molecular evidence. *Cladistics.* 2009;25:231–62.
67. Hormiga G. Cladistics and the comparative morphology of linyphiid spiders and their relatives (Araneae, Araneoidea, Linyphiidae). *Zool J Linn Soc.* 1994;111:1–71.
68. Wiens JJ. Widespread loss of sexually selected traits: how the peacock lost its spots. *Trends Ecol Evol.* 2001;16:517–23.
69. Burns KJ. A phylogenetic perspective on the evolution of sexual dichromatism in tanagers (Thraupidae): the role of female versus male plumage. *Evolution.* 1998;52:1219–24.
70. Wiens JJ. Phylogenetic evidence for multiple losses of a sexually selected character in phrynosomatid lizards. *Proc R Soc B.* 1999;266:1529–35.
71. Andersen NM. A phylogenetic analysis of the evolution of sexual dimorphism and mating systems in water striders (Hemiptera: Gerridae). *Biol J Linn Soc.* 1997;61:345–68.
72. Vanacker D, Maelfait JP, Hendrickx F. Survival differences of the two male morphs in the dwarf spider *Oedothorax gibbosus* Blackwall, 1841 (Erigoninae, Linyphiidae, Araneae). *Neth J Zool.* 2003;52:255–62.
73. Vanacker D, Hendrickx F, Maes L, Verraes P, Maelfait JP. Can multiple mating compensate for slower development and shorter adult life in a male dimorphic dwarf spider? *Biol J Linn Soc.* 2004;82:269–73.
74. Hendrickx F, Vanthournout B, Taborsky M. Selection for costly sexual traits results in a vacant mating niche and male dimorphism. *Evolution.* 2015;69:2105–17.
75. Safran RJ, Scordato ESC, Symes LB, Rodríguez RL, Mendelson TC. Contributions of natural and sexual selection to the evolution of premating reproductive isolation: a research agenda. *Trends Ecol Evol.* 2013;28:643–50.

76. Kraaijeveld K, Kraaijeveld-Smit FJL, Maan ME. Sexual selection and speciation: the comparative evidence revisited. *Biol Rev*. 2011;86:367–77.
77. Gage MJG, Parker GA, Nylin S, Wiklund C. Sexual selection and speciation in mammals, butterflies and spiders. *Proc R Soc B*. 2002;269:2309–16.
78. Williams GC. *Adaptation and natural selection*. Princeton: Princeton University Press; 1966.
79. Hughes AL, Hughes MK. Paternal investment and sexual size dimorphism in North American passerines. *Oikos*. 1986;46:171–5.
80. Kuntner M, Coddington JA. Sexual size dimorphism: evolution and perils of extreme phenotypes in spiders. *Annu Rev Entomol*. 2020;65:57–80.
81. Prenter J, Elwood RW, Montgomery WI. Sexual size dimorphism and reproductive investment by female spiders: a comparative analysis. *Evolution*. 1999;53:1987–94.
82. Badyaev AV, Hill GE. Evolution of sexual dichromatism: contribution of carotenoids- versus melanin-based coloration. *Biol J Linn Soc*. 2000;69:153–72.
83. Cardoso GC, Mota PG. Speciation evolution of coloration in the genus *Carduelis*. *Evolution*. 2008;62:753–62.
84. Servedio MR, Bürger R. The counterintuitive role of sexual selection in species maintenance and speciation. *PNAS*. 2014;111:8113–8.
85. Rodríguez RL, Boughman JW, Gray DA, Hebets EA, Höbel G, Symes LB. Diversification under sexual selection: the relative roles of mate preference strength and the degree of divergence in mate preferences. *Ecol Lett*. 2013;16:964–74.
86. Martin TE, Badyaev AV. Sexual dichromatism in birds: Importance of nest predation and nest location for females versus males. *Evolution*. 1996;50:2454–60.
87. Nzigidahera B, Jocqué R. On the Afrotropical genus *Holmelgonia* (Araeae, Linyphiidae), with the description of three new species from the Albertine Rift. *Eur J Taxon*. 2014;77:1–18.

Publisher's Note

Springer Nature remains neutral with regard to jurisdictional claims in published maps and institutional affiliations.

Ready to submit your research? Choose BMC and benefit from:

- fast, convenient online submission
- thorough peer review by experienced researchers in your field
- rapid publication on acceptance
- support for research data, including large and complex data types
- gold Open Access which fosters wider collaboration and increased citations
- maximum visibility for your research: over 100M website views per year

At BMC, research is always in progress.

Learn more biomedcentral.com/submissions



4. Eigenständigkeitserklärung

Hiermit erkläre ich, dass diese Arbeit bisher von mir weder an der Mathematisch-Naturwissenschaftlichen Fakultät der Universität Greifswald noch einer anderen wissenschaftlichen Einrichtung zum Zwecke der Promotion eingereicht wurde.

Ferne erkläre ich, dass ich diese Arbeit selbstständig verfasst und keine anderen als die darin angegebenen Hilfsmittel und Hilfen benutzt und keine Textabschnitte eines Dritten ohne Kennzeichnung übernommen habe.

Greifswald,

Student: Shou-Wang Lin

5. Curriculum Vitae

Personal data

Shou-Wang Lin, MSc

Born in 1986, 31. July in Taipei, Taiwan

Education PhD student, University Greifswald, General and Systematic Zoology, since Sep. 2014

Research topic: Evolution of Nuptial Gifts in Erigoninae: Taxonomic Revision and Phylogeny of the Spider Genus *Oedothorax*

Supervisor: Prof. Dr. Gabriele Uhl

MSc National Taiwan University, Department of Entomology, 2011

Thesis: "Life History of Two Fly Parasitoids, *Aleochara nigra* and *A. asiatica* (Coleoptera: Staphylinidae), and Its Implications in Forensic Entomology"

Supervisor: Prof. Dr. Shiu-Feng Shiao

BSc National Taiwan University, Department of Entomology, 2008

- Honors & awards
- DAAD-Prize for outstanding achievements of foreign students, University of Greifswald, 2019
 - Prize for the best poster in the study group Zoological Systematics, 111th Annual Meeting of the German Zoological Society, Greifswald, 2018
 - Prize for the best poster in the study group Zoological Systematics, 109th Annual Meeting of the German Zoological Society, Kiel, 2016
 - Stipendium STIBET des DAAD, 2016
 - 2-year government scholarship for studying abroad, Ministry of Education, Republic of China (Taiwan), 2014
 - Teaching assistant scholarship of Department of Entomology, National Taiwan University, 2009
 - Research Creativity Award, National Science Council, 2008
 - Elected as Member of Chinese Martial Arts Team, National Taiwan University, Feb. 2005 – Jun. 2008, Sep. 2008 – Jun. 2010

- Employment
- Research assistant, Zoological Institute and Museum, University of Greifswald, September – November 2020
 - Research assistant, Insect Population Laboratory, Entomology department, National Taiwan University, Taipei, August 2012 – July 2013
 - Platoon leader, military service, Army Technical Reconnaissance Group, Taiwan, Dec. 2011 – Jul. 2012
 - Part-time science teacher, Pei-Da kindergarten, Taiwan, 2004 – 2011, 2013 – 2014

- Publications
- Lin, S.-W.**, L. Lopardo, and G. Uhl. 2021. Diversification through sexual selection on gustatory courtship traits in dwarf spiders. *Frontiers in Zoology*, 18:51.
- Lin, S.-W.**, L. Lopardo, and G. Uhl. 2021. Evolution of nuptial-gift-related male prosomal structures: taxonomic revision and cladistic analysis of the dwarf spider genus *Oedothorax* Bertkau, 1883 (Araneae, Linyphiidae, Erigoninae). *Zoological Journal of the Linnean Society*, XX: 1-168.
- Lin, S.-W.**, L. Lopardo, M. Haase and G. Uhl. 2019. Taxonomic revision of the dwarf spider genus *Shaanxinus* Tanasevitch, 2006 (Araneae, Linyphiidae, Erigoninae), with new species from Taiwan and Vietnam. *Organism Diversity & Evolution*, 19, 211-276.
- Lin, S.-W.** and T. Okuyama. 2014. Hidden burrow plugs and their function in the tiger beetle, *Cosmodela batesi* (Coleoptera, Cicindelidae). *Journal of Ethology* 32, 23-27.
- Lin, S.-W.** and S. F. Shiao. 2013. Life history data on the fly parasitoids *Aleochara nigra* Kraatz and *A. asiatica* Kraatz (Coleoptera: Staphylinidae), and their potential application in forensic entomology. *Forensic Science International* 232, 46-55.

6. Other scientific contributions

Talks:

Lin, S.-W., Lopardo, L., and Uhl, G. (2016). Taxonomic study of *Oedothorax* – a hopeful dwarf spider genus for investigating the evolution of sexual dimorphic male head structures. Talk at the 29th European Congress of Arachnology, Brno (Czech Republic).

Lin, S.-W., Lopardo, L., and Uhl, G. (2016). Taxonomic study of *Oedothorax* – a hopeful dwarf spider genus for investigating the evolution of sexual dimorphic male prosomal structures. Talk at the 17th annual meeting of the Gesellschaft für Biologische Systematik (GfBS), Munich (Germany).

Lin, S.-W., Lopardo, L., and Uhl, G. (2017). Beating trees, spiders fall: fourteen new species of *Shaanxinus* Tanasevitch, 2006 (Araneae, Linyphiidae, Erigoninae) from Taiwan and Vietnam. Talk at the 110th meeting of the German Zoological Society (DZG), Bielefeld (Germany); and at the 30th European Congress of Arachnology, Nottingham (UK).

Lin, S.-W., Lopardo, L., Haase, M., and Uhl, G. (2019). Complex species history of Taiwanese *Shaanxinus* dwarf spiders implied by mitochondrial DNA sequences. Talk at the 11th Symposium of the Zoological Institute & Museum, Greifswald (Germany).

Lin, S.-W., Lopardo, L., and Uhl, G. (2021). Diversification through gustatory-courtship: An X-ray micro-computed tomography study on dwarf spiders. Talk at the 32nd European Congress of Arachnology, Greifswald (Germany).

Posters:

Lin, S.-W., Lopardo, L., and Uhl, G. (2016). Taxonomic study of *Oedothorax* – a hopeful dwarf spider genus for investigating the evolution of sexual dimorphism. Poster presentation, prize for the best poster in the study group Zoological Systematics at the 109th meeting of the German Zoological Society (DZG), Kiel (Germany).

Lin, S.-W., Lopardo, L., and Uhl, G. (2018). Implications of the newly discovered species richness of the dwarf spider genus *Shaanxinus* Tanasevitch, 2006 (Araneae, Linyphiidae, Erigoninae) from Taiwan and Vietnam. Poster presentation, prize for the best poster in the study group Zoological Systematics at the 111th annual meeting of the German Zoological Society (DZG), Greifswald (Germany).

7. Acknowledgement

First and foremost, praise and thanks to God for His grace leading me through the ups and downs all these years working on my research, and for His people, without whose support in body and spirit I would not have made it hither.

I would like to express my deep and sincere gratitude to my supervisor Prof. Dr. Gabriele Uhl, who made it possible for me to conduct my study in her department, and Dr. Lara Lopardo, who supported me with her expertise in phylogenetic systematics. Both kindhearted mentors in my research and personal life have provided invaluable guidance and practical support throughout my time in Greifswald.

Thanks to all my friends and colleagues, whom I have had the privilege to meet in the Department of General and Systematic Zoology at the University of Greifswald. My special thanks to apl. Prof. Dr. "Theo" Michael Schmitt, PD Dr. Peter Michalik and PD Dr. Carsten Müller for their precious advice, support and friendship, as well as to Dr. Monika Eberhard, Dr. Katrin Kunz, Philip Steinhoff, Monica Sheffer, Dr. Jonas Wolff, Dr. Anne-Sarah Ganske, Dr. Anja Junghanns, Dr. Pierick Mougnot, Dr. Lenka Sentenská, Heidi Land, Aileen Neumann and Birte Schadlowski, and many more. Thanks to Stefan Bock for micro-CT scans and reconstruction, and Dr. Silke Fregin for her help with molecular lab work and sequencing.

Very special thanks and greetings to all my friends and colleagues, whom I got to know during my visits in museums and congresses: Dr. Gustavo Miranda, Prof. Dr. Gustavo Hormiga, Dr. Andrei Tanasevitch, Dr. Peter Jäger, Julia Altmann, Dr. Peter Schwendinger, Dr. Jens Runge, Prof. Dr. Jutta Schneider, Prof. Dr. Yael Lubin, and many more. I want to particularly thank Prof. Dr. Nikolaj Scharff for his advice in phylogenetic methods, and Dr. Holger Frick for introducing me to the linyphiid morphology.

I am grateful to my parents for their love, prayers, caring and sacrifices for me to approach my goal. My mother has accompanied me on many field trips collecting spiders in Taiwan the year before I started my study in Germany. In her last stretch fighting the cancer, she demonstrated to me her faith and perseverance with incredible physical and mental strength from the Lord. I am truly thankful for the last few months I got to spend with her in Taiwan, a time full of mercy and grace. I also thank God's grace for Cynthia Kessler, a dear sister in Christ, a friend and a mother figure in faith, for her patience with me, her constant support from the beginning of my stay in Greifswald, and her encouragement in the times of need. The same gratitude goes to my dear friends Per and Åsa Helander, and many other brothers and sisters in the family of Christ.